UNIVERSITY OF HULL

DIPYRRIN COMPLEXES AND THEIR USES AS SELF ASSEMBLING MATERIALS

Being a thesis submitted for the Degree of Doctor of Philosophy in the University of Hull

By

Michael Benstead, MChem(hons)

December 2010

Acknowledgements

Firstly, my thanks go to my supervisors Ross Boyle and Georg Mehl for their continued help and support throughout this project. Thanks also to Julie Haley and Rob Lewis for their help with DSC, HPLC and NMR. Many thanks go to lab members of C120 and C302 both past and present for their help and interesting banter throughout my time in the lab. In particular Chris Welch, Cristina Alonso and Francesca Giuntini for their help with various reactions and NMR interpretation. Lastly, many thanks to both my parents and my lovely wife Michelle without whose support this work would not be possible as we look forward to the arrival of baby Benstead, who will have to read this at some point I'm sure.

Abstract

Several series of BODIPYs bearing mesogenic substituents were synthesised and their fluorescence and liquid crystal properties were characterized. Each compound prepared consisted of one BODIPY fluorophore and one, two or three mesogenic units based primarily on a cyanobiphenyl core. Initially, the mesogens were attached to the pyrrolic positions of the fluorophore, but it was found that mesogen attachment at the BODIPY 8-phenyl ring gave an increased preference for mesophase formation due to the molecules having a more 'rod-like' (calamitic) shape. For several of the compounds, a monotropic nematic phase was exhibited, however, no layered phase (e.g. smectic) was observed. Several linker groups between the mesogenic unit and the fluorophore were investigated and it was found that linear linker groups (e.g. ethynyl) had a greater preference for liquid crystal phase formation when compared to non-linear linker groups (e.g. triazole).

Two series of di-mesogenic compounds were prepared and a significant stabilisation of the nematic phase was observed when compared to the mono-mesogenic analogues. The compounds bearing the mesogenic units on the 8-phenyl ring were prepared by metal-catalyzed couplings and each series consisted of three compounds with increasing alkyl substitution on the bipyrrolic core of the BODIPY. This resulted in a progressive increase in fluorescence quantum yield of the compounds in each series due to increased rotational restriction of the 8-phenyl ring along with a concurrent decrease in nematic phase stability. This permitted the observation of a structure-property relationship between nematic phase stability and fluorescence intensity. A BODIPY with significantly red-shifted fluorescence was also prepared and three mesogenic units were attached to this compound. Temperature dependant fluorescence measurements were taken in order to observe any relationship between fluorescence and degree of molecular ordering (e.g. nematic phase fluorescence compared to isotropic liquid fluorescence) and several of the compounds were dissolved in a commercial nematic liquid crystal and incorporated into a twisted nematic cell in order to observe the affect that molecular alignment (induced by an electric field) had on the fluorescence.

Table of contents:

Table of figures: 7
Table of schemes: 16
Table of schemes: 16
List of abbreviations 20
List of abbreviations 20
Chapter 1: BODIPYs as components in novel light active materials 22
1. Dipyrrins 22
1.1 Structure 22
1.2 Properties of dipyrrin complexes 23
1.2.1 Fluorescence properties of dipyrrin complexes 23
1.2.2 Electrochemical properties of dipyrrin complexes 24
1.3 Synthesis 24
1.3.1 Condensation of pyrroles 25
1.3.2 Oxidation of dipyrromethanes 28
2. Borondifluorodipyrrins (BODIPYs) 29
2.1 Structure 30
2.2 Properties of BODIPYs 30
2.3 Synthesis of BODIPYs 34
2.4 Fluorescence control of BODIPYs by modification of the 8-aryl group 36
2.4.1 Photoinduced electron transfer (PeT) 36
2.5 Metal-catalyzed reactions of BODIPYs 40
2.6 Condensation reactions of 3,5-dimethyl-BODIPYs 44
2.7 Aza-BODIPYs 46
2.8 Energy transfer cassettes 48
2.8.1 Through-space energy transfer cassettes 48
2.8.2 Through-bond energy-transfer cassettes 57
2.9 BODIPY-based energy-transfer arrays as light harvesting materials in electrooptic devices 80
2.9.1 Dye-sensitized solar cells 80

2.9.2 Bulk heterojunction solar cells 85
2.10 BODIPYs as laser dyes 88
2.10.1 Laser activity of dye-doped polymeric matrices based on commercial BODIPY derivatives 92
2.10.2 Laser activity of BODIPYs in dye-doped liquid crystals 100
2.11 Polymers incorporating BODIPY fluorophores 102
2.11.1 Polymerisation through the BODIPY core 102
2.11.2 Polymerisation through F-substitution 110
2.11.3 Polymerisation through the BODIPY meso-position 112
2.11.4 Polymerisation through metal-complexation and conducting polymers . 116
3. Supramolecular assemblies 119
3.1 Principles of self-assembly 119
3.2 Self-assembly of liquid crystalline materials 120
3.2.1 Thermotropic liquid crystals 120
3.2.2 Lyotropic liquid crystals 123
3.2.3 Mesogenic BODIPYs and their self-assembling properties 124
4. Conclusions 132
Chapter 2: Aims 135
3.1. Introduction 138
3.2. Results and discussion 141
3.2.1 Synthesis 141
3.2.2 Melting behaviour 154
3.2.3 Fluorescence 159
3.3. Conclusions 161
Chapter 4: BODIPYs bearing mesogenic units attached to the 8-phenyl ring 163
4.1. Introduction 163
4.2. Results and discussion 165
4.2.1 Synthesis 165
4.2.2 Liquid crystalline behaviour 182
4.2.3 Fluorescence 190

4.2.4 Structure-property relationship between liquid crystallinity and fluorescence intensity *193*
4.2.5 Temperature dependant fluorescence measurements and BODIPY-doped nematic liquid crystal fluorescence *194*
4.3. Conclusions **199**
Chapter 5: BODIPYs bearing multiple mesogenic units **201**
5.1 Introduction **201**
5.2 Results and discussion **203**
5.2.1 Synthesis *203*
5.2.2 Liquid crystal properties *221*
5.2.3 Fluorescence *228*
5.2.4 Structure-property relationship between liquid crystallinity and fluorescence intensity *231*
5.2.5 Temperature-dependant fluorescence measurements and BODIPY-doped nematic liquid crystal fluorescence *232*
5.3 Conclusions **234**
Chapter 6: Final conclusions **236**
Chapter 7: Experimental procedures **240**
References **346**
Appendix 1: HPLC traces **380**

Table of figures:

Figure 1. 1: Dipyrromethane and dipyrromethene 22
Figure 1. 2: 2,3'Dipyrromethene and 3,3'-dipyrromethene 23
Figure 1. 3: Bis(dipyrrinato-zinc) complex 24
Figure 1. 4: BODIPY showing alternate numbering system 30
Figure 1. 5: Analogues of the core BODIPY compound 30
Figure 1. 6: 8-Aryl-BODIPYs showing effect of bulky alkyl substituents at the 1,7-positions 31
Figure 1. 7: BODIPY viscosity sensor 32
Figure 1. 8: Furanyl-BODIPY 32
Figure 1. 9: *H*- and *J*-dimers of BODIPYs 34
Figure 1. 10: *Meso*-modified BODIPY probes 36
Figure 1. 11: BODIPY where no PeT can occur 37
Figure 1. 12: Reductive PeT (a-PeT) 38
Figure 1. 13: Oxidative PeT (d-PeT) 38
Figure 1. 14: Water-soluble energy transfer cassette 44
Figure 1. 15: BODIPY-based pH sensor 45
Figure 1. 16: Aza-BODIPY 46
Figure 1. 17: Aza-BODIPY synthesis 47
Figure 1. 18: Antimony-porphyrin-BODIPY array 49
Figure 1. 19: Di-BODIPY-phthalocyanine array 50
Figure 1. 20: BODIPY-sub-phthalocyanine array 51
Figure 1. 21: BODIPY-porphyrin-fullerene array 52
Figure 1. 22: Energy level diagram showing the different photochemical processes of the BODIPY-zinc-porphyrin-crown ether triad (10) when coordinated to the fullerene unit (major processes are bold arrows) 53
Figure 1. 23: Tetra-BODIPY-perylenediimide array 55
Figure 1. 24: Tri-BODIPY array 56
Figure 1. 25: BODIPY-tetraporphyrin array 58

Figure 1. 26: BODIPY-porphyrin arrays 59
Figure 1. 27: Di-BODIPY-porphyrin array 61
Figure 1. 28: Di-BODIPY-porphyrin array with BODIPY attachment at the same phenyl ring 62
Figure 1. 29: Di-BODIPY-thiophyrin array 63
Figure 1. 30: Di-BODIPY-oxophyrin array 64
Figure 1. 31: BODIPY-bipyridyl-ruthenium complex 65
Figure 1. 32: Energy level diagram showing the various photochemical processes involved in the transfer of energy from the metal complex to the BODIPY 66
Figure 1. 33: BODIPY-oligopyridine-ruthenium complex 67
Figure 1. 34: BODIPY-terpyridine-zinc dimer 68
Figure 1. 35: BODIPY-terpyridine-platinum complex 68
Figure 1. 36: BODIPY-terpyridine-platinum complexes with differeing acceptor moieties 69
Figure 1. 37: BODIPY-ferrocene arrays 70
Figure 1. 38: BODIPY-anthracene arrays 71
Figure 1. 39: BODIPY arrays prepared by *F*-substitution 73
Figure 1. 40: BODIPY-oligopyridine arrays prepared by *F*-substitution 74
Figure 1. 41: BODIPY arrays bearing UV-absorbing donor groups 75
Figure 1. 42: BODIPY array exhibiting energy transfer efficiencies dependant on spacer length 76
Figure 1. 43: Di-BODIPY array 77
Figure 1. 44: Fluorene- and truxene-bridged arrays 78
Figure 1. 45: Tetra-BODIPY array 79
Figure 1. 46: Triphenylamine-BODIPY array for DSSCs 81
Figure 1. 47: Triphenylamine-BODIPY arrays for DSSCs bearing differing titanium dioxide binding and UV-absorbing groups 82
Figure 1. 48: BODIPYs for DSSCs with PEG arms to enhance film formation 83
Figure 1. 49: BODIPY-porphyrin array for DSSCs 84
Figure 1. 50: Light collection in a multi-dye luminescent solar concentrator 86
Figure 1. 51: BODIPY for BHJs with PEG arms to enhance film formation 87

Figure 1. 52: BODIPY-thiophene array for BHJs 88
Figure 1. 53: Core BODIPY structure for investigation into laser activity of different BODIPY derivatives 89
Figure 1. 54: BODIPY laser dyes 90
Figure 1. 55: BODIPY laser dyes with red-shifted absorption and emission 91
Figure 1. 56: BODIPY laser dyes with extended π-conjugation 92
Figure 1. 57: Commercial BODIPY dyes PM 567 and PM 597 93
Figure 1. 58: Mono-styryl BODIPY dye 96
Figure 1. 59: BODIPYs bearing polymerisable substituents 97
Figure 1. 60: 8-Phenyl analogues of PM 567 98
Figure 1. 61: Analogues of PM 597 99
Figure 1. 62: Representation of random lasing of dye molecules in a nematic liquid crystal host material (blue = nematic host molecules; red = dye molecules) 100
Figure 1. 63: Photograph showing clearly visible lasing of dye molecules dissolved in a liquid crystal host incorporated into a wedge cell (cell angled relative to the incident pump beam in order to view laser light)[190] 101
Figure 1. 64: BODIPY polymers with ethynyl or ethynyl-phenyl linker groups 103
Figure 1. 65: BODIPY polymers with short or no linker groups 105
Figure 1. 66: BODIPY polymers with differing groups on the 8-phenyl ring 106
Figure 1. 67: BODIPY polymers with different types of linker group 107
Figure 1. 68: BODIPY polymers with increasing numbers of long alkyl chains 108
Figure 1. 69: Fluorene-linked BODIPY polymers 109
Figure 1. 70: BODIPY polymer with red-shifted absorption and emission 110
Figure 1. 71: BODIPY polymers prepared *via F*-substitution 111
Figure 1. 72: Chiral BODIPY polymer 112
Figure 1. 73: BODIPY:HEMA analogue 113
Figure 1. 74: Proposed mechanisms of polymer assembly for microwave-assisted and conventional heating of BODIPY-containing hybrid polymers[205] 114
Figure 1. 75: BODIPY:HEMA polymer 115
Figure 1. 76: BODIPY polymer bearing a quaternary pyridinium moiety 116
Figure 1. 77: BODIPY-terpyridine-zinc coordination polymer 117

Figure 1. 78: Conducting BODIPY polymer 117
Figure 1. 79: Conducting BODIPY polymer with extended π-conjugation 118
Figure 1. 80: Molecular organisation in a smectic A phase[217] 121
Figure 1. 81: Molecular organisation in a nematic phase[219] 121
Figure 1. 82: Rotation of the director in a chiral nematic phase[220] 122
Figure 1. 83: Molecular organisation of discotic phases[221] 122
Figure 1. 84: Discotic liquid crystal 123
Figure 1. 85: Phospholipid bilayer[223] 124
Figure 1. 86: Discotic BODIPYs 125
Figure 1. 87: n = 16 analogue of 1.119 when viewed under crossed polarisers in the hexagonal columnar phase (left) and the same sample under irradiation and under aligned polarisers (right) 126
Figure 1. 88: Superimposed images of n = 16 analogue of 1.119 when viewed under crossed polarisers and under irradiation 126
Figure 1. 89: Discotic BODIPY which forms thin films 127
Figure 1. 90: Chemiluminescent BODIPYs 127
Figure 1. 91: Mesogenic BODIPY exhibiting nematic phase behaviour 128
Figure 1. 92: Liquid crystalline dendrimers for attachment to BODIPYs 130
Figure 1. 93: Ionic BODIPY liquid crystal formed by interactions between quaternary ammonium and sulphonate groups 131
Figure 1. 94: Ionic BODIPY liquid crystal formed by interactions between imidazole and sulphonte groups 132

Figure 3. 1: Discotic BODIPY 139
Figure 3. 2: Calamitic nematic mesogenic BODIPY 140
Figure 3. 3: First generation BODIPY LC-dendrimer 140
Figure 3. 4: 8-Phenyl-attached mesogenic BODIPYs (top) and our approach (bottom) 141
Figure 3. 5: Target compounds 142
Figure 3. 6: Mesogenic BODIPYs 145
Figure 3. 7: ^{1}H-NMR of free mesogen showing methylene units at both ends of the alkyl chain 146
Figure 3. 8: ^{1}H-NMR of mesogenic BODIPY showing down-field shift of one methylene unit of the alkyl chain due to conversion from alcohol to ester 147
Figure 3. 9: Di-mesogenic BODIPY schematic 149
Figure 3. 10: Liquid crystal properties of mesogenic units 155
Figure 3. 11: DSC thermogram of mesogenic BODIPY 4; showing heating (top line) and cooling (bottom line) 156
Figure 3. 12: DSC thermogram of mesogenic BODIPY 5; showing heating (top line) and cooling (bottom line) 157
Figure 3. 13: OPM images of the mesogenic pyrrole (14) in the nematic phase at 84.9°C (top) and 87.8°C (bottom) after annealing 158
Figure 3. 14: DSC thermogram of the mesogenic pyrrole (14); showing second heating cycle (top line) and second cooling cycle (bottom line) 159
Figure 3. 15: Fluorescence spectrum of di-mesogenic BODIPY 11 in toluene at 298K 160

Figure 4. 1: Calamitic nematic BODIPY liquid crystal 163
Figure 4. 2: Substitution on the BODIPY core, where X is the mesogenic unit and linker group 164
Figure 4. 3: Reactive site for mesogen attachment 165
Figure 4. 4: ^{1}H-NMR of mesogenic BODIPY 24 showing the multiple aromatic groups 170
Figure 4. 5: Mesogenic BODIPY prepared by Sonogashira coupling employing a less extended mesogen 173
Figure 4. 6: Mesogen used in attempted Heck reaction 181
Figure 4. 7: DSC thermogram of 23 showing second heat (top line) and second cool (bottom line) 183
Figure 4. 8: DSC thermogram of 24 showing second heat (top line) and second cool (bottom line) 184
Figure 4. 9: OPM image of 23 in the nematic phase at 142.7°C 185
Figure 4. 10: OPM image of 24 in the nematic phase at 148.6°C 185
Figure 4. 11: DSC thermogram of 30 showing second heat (top line) and second cool (bottom line) 187
Figure 4. 12: OPM image of 30 in the nematic phase at 164.1°C 188
Figure 4. 13: OPM image of nickel-(II)-dipyrrinato complex at 146.6C showing a large amount of birefringence 189
Figure 4. 14: Excitation (solid line) and emission (dashed line) of 23 (black), 24 (blue) and 25 (red); measured in toluene at 298K 190
Figure 4. 15: Excitation (solid line) and emission (dashed line) of 30 (black), 31 (blue) and 32 (red); measured in toluene at 298K 191
Figure 4. 16: Excitation (blue) and emission (pink) of 37; measured in toluene at 298K 191
Figure 4. 17: Temperature dependant fluorescence measurements of compound 23 at 10°C intervals (heated to 190°C and cooling down to 90°C - see legend); excited with a Nd:YAG laser with heating on a Mettler hot-stage 195

Figure 4. 18: Fluorescence intensity of 23 dissolved in BL024 in a twisted nematic cell (two measurements taken with an electric field applied (On) and two without an electric field applied (Off) - see legend)..... 196
Figure 4. 19: Fluorescence intensity of 25 dissolved in BL024 in a twisted nematic cell (two measurements taken with an electric field applied (On) and two without an electric field applied (Off) - see legend)..... 196
Figure 4. 20: Fluorescence intensity of 30 dissolved in BL024 in a twisted nematic cell (two measurements taken with an electric field applied (On) and two without an electric field applied (Off) - see legend)..... 197
Figure 4. 21: Fluorescence intensity of 32 dissolved in BL024 in a twisted nematic cell (two measurements taken with an electric field applied (On) and two without an electric field applied (Off) - see legend)..... 197

Figure 5. 1: Liquid crystal dendrimer-BODIPYs showing LC transitions of first, second and third generation dendrimers; m = unknown mesophase[230] 201
Figure 5. 2: Styryl-BODIPY exhibiting red-shifted fluorescence 202
Figure 5. 3: Mesogenic boronic esters for Suzuki-coupling onto dibromo-BODIPYs .. 204
Figure 5. 4: Di-mesogenic BODIPYs 53-58..... 206
Figure 5. 5: Aromatic region of the ^{1}H-NMR spectrum of 55..... 207
Figure 5. 6: Aza-BODIPY 208
Figure 5. 7: Aromatic region of the ^{1}H-NMR spectrum of 62..... 211
Figure 5. 8: Alkyl region of the ^{1}H-NMR spectrum of 64..... 215
Figure 5. 9: Aromatic region of the ^{1}H-NMR spectrum of 64..... 216
Figure 5. 10: Alkyl region of the ^{1}H-NMR spectrum of 65..... 218
Figure 5. 11: ^{1}H-NMR spectrum displaying the methylene units of the C_{11} alkyl chains of 65..... 219
Figure 5. 12: Aromatic region of the ^{1}H-NMR spectrum of 65..... 220
Figure 5. 13: Aromatic region of the ^{1}H-NMR spectrum of 65..... 221
Figure 5. 14: DSC thermogram of 55; showing second heat (top line) and second cool (bottom line)..... 222
Figure 5. 15: DSC thermogram of 56; showing second heat (top line) and second cool (bottom line)..... 222
Figure 5. 16: DSC thermogram of 57; showing second heat (top line) and second cool (bottom line)..... 223
Figure 5. 17: OPM image of 55 in the nematic phase at 138.4°C 224
Figure 5. 18: OPM image of 56 in the nematic phase at 124.7°C 224
Figure 5. 19: OPM image of 56 in the nematic phase after 1hr annealing at 118.7°C ... 225
Figure 5. 20: OPM image of 56 in the nematic phase after 3hrs annealing at 118.7°C . 225
Figure 5. 21: OPM image of 57 in the nematic phase at 89.0°C 226
Figure 5. 22: OPM image of 65 at 212.0°C..... 227
Figure 5. 23: DSC thermogram of 65; showing second heat (top line) and second cool (bottom line)..... 228

Figure 5. 24: Excitation (solid line) and emission (dashed line) of 55 (blue), 56 (black) and 57 (red); measured in toluene at 298K 229
Figure 5. 25: Excitation (red) and emission (blue) of 65; measured in toluene at 298K 230
Figure 5. 26: Temperature dependant fluorescence measuerments of 55 at 10°C intervals (heated to 190°C and cooling down to 30°C - see legend); excited with a Nd:YAG laser with heating on a Mettler hot-stage 233
Figure 5. 27: Temeprature dependant fluorescence measurements of 56 at 10°C intervals (heated to 180°C and cooling down to 30°C - see legend); excited with a Nd:YAG laser with heating on a Mettler hot-stage 233
Figure 5. 28: Fluorescence intensity of 57 dissolved in BL024 in a twisted nematic cell (two measurements taken with an electric field applied (On) and two without an electric field applied (Off) - see legend) 234

Table of schemes:

Scheme 1. 1: Synthesis of dipyrrins *via* acid-catalyzed condensation reactions 26
Scheme 1. 2: Deprotonation of *meso*-methyl dipyrrin 27
Scheme 1. 3: Synthesis of dipyrromethanes 28
Scheme 1. 4: Oxidation of dipyrromethane 29
Scheme 1. 5: Prefunctionalisation of pyrrole units 33
Scheme 1. 6: BODIPY from glutaric anhydride 34
Scheme 1. 7: BODIPY synthesis from allyl aldehyde using ytterbium (III) trifluoromethane sulphonamide as the catalyst 35
Scheme 1. 8: Mechanism of BODIPY nitric oxide probe 39
Scheme 1. 9: Oxidative functionalisation of BODIPY 41
Scheme 1. 10: Iridium- and rhodium-catalyzed reactions of BODIPYs 42
Scheme 1. 11: Palladium-catalyzed couplings of BODIPYs 42
Scheme 1. 12: Liebeskind-Srogl reaction of BODIPYs 43
Scheme 1. 13: Knoevenagel reaction of BODIPYs 44

Scheme 3. 1: Knorr pyrrole synthesis 142
Scheme 3. 2: Pyrrole hydrolysis 143
Scheme 3. 3: Vilsmeier-Haack formylation of pyrrole 143
Scheme 3. 4: Fischer esterification of dipyrrin 144
Scheme 3. 5: Mesogenic BODIPY synthesis 145
Scheme 3. 6: Pyrrole reduction and mesylation 148
Scheme 3. 7: Pyrrole acetylation and dipyrromethane synthesis 149
Scheme 3. 8: Unsuccessful dipyrromethane oxidation 150
Scheme 3. 9: Di-mesogenic BODIPY synthesis 151
Scheme 3. 10: Mesogenic pyrrole synthesis 152
Scheme 3. 11: Unsuccessful hydrogenation of mesogenic pyrrole 153
Scheme 3. 12: Mesogenic synthesis 154

Scheme 4. 1: 8-(4-Halophenyl)-BODIPY synthesis 165
Scheme 4. 2: BODIPYs bearing alkyl groups to increase the fluorescence quantum yield 166
Scheme 4. 3: Mesogenic boronic ester synthesis 167
Scheme 4. 4: Suzuki-coupling of 4-carboxyphenylboronic acid pinacol ester to 18..... 168
Scheme 4. 5: Mesogenic BODIPY preparation by Suzuki-coupling..... 169
Scheme 4. 6: 8-(4-Ethynylphenyl)-BODIPY synthesis 171
Scheme 4. 7: Mesogenic iodide synthesis..... 172
Scheme 4. 8: Mesogenic BODIPY preparation *via* Sonogashira-coupling 173
Scheme 4. 9: Mesogenic azide synthesis 174
Scheme 4. 10: Attachment of mesogen to BODIPY by 'click' chemistry..... 175
Scheme 4. 11: Unsuccessful mesogenic azide synthesis 176
Scheme 4. 12: Unsuccessful attempts to prepare azide analogues of mesogen precursors 177
Scheme 4. 13: Preparation of 5-(4-ethynylphenyl)-dipyrromethane 178
Scheme 4. 14: 'Clicked' dipyrromethane with subsequent mesylation 179
Scheme 4. 15: Mesogen attachment to dipyrromethane by 'click' chemistry with subsequent oxidation and nickel (II) complexation 180
Scheme 4. 16: Diindolylmethane synthesis 182

Scheme 5. 1: Dibromo-BODIPY synthesis 203
Scheme 5. 2: Suzuki-coupling of two mesogenic units onto a BODIPY 205
Scheme 5. 3: Dibromo-aza-BODIPY synthesis 209
Scheme 5. 4: Dihydroxy-aza-BODIPY synthesis 210
Scheme 5. 5: Aza-BODIPY ether synthesis 212
Scheme 5. 6: Di-styryl-BODIPY synthesis 213
Scheme 5. 7: Di-mesogenic di-styryl-BODIPY synthesis 214
Scheme 5. 8: Tri-mesogenic di-styryl BODIPY (65) 217

List of abbreviations

ADDP: 1,1'-(Azodicarbonyl)dipiperidine

ANT: Anthracene

BHJ: Bulk-heterojunction solar cell

BODIPY/BDP: 4.4'-Difluorobora-3a,4a-diaza-*s*-indacene

CDB: Cumyl dithiobenzoate

Col_h: Hexagonal columnar

CS: Charge separated state

DABCO: 1,4-Diazabicyclo[2.2.2]octane

DBU: 1,8-Diazabicyclo[5.4.0]undec-7-ene

DCC: *N,N'*-Dicyclohexylcarbodiimide

DCU: Dicyclohexylurea

DEAD: Diethyl azodicarboxylate

DIC: *N,N'*-Diisopropylcarbodiimide

DIEA: Diisopropylethylamine

DMAEMA: 2-(Dimethylamine)ethyl methacrylate

DMAP: *N,N'*-Dimethylaminopyridine

DSC: Differential scanning calorimetry

DSSC: Dye-sensitized solar cell

EBu: Ethyl butanoate

EDC: 1-Ethyl-3-(3-dimethylaminopropyl) carbodiimide

EDOT: 3,4-Ethylenedioxythiophene

EGDMA: Ethylene glycol dimethylacrylate

FRET: Fluorescence/Förster resonance energy transfer

FTO: Fluorinated tin oxide

HEMA: Hydroxyethylmethacrylate

HFMA: 2,2,3,3,4,4,4-Heptafluorobutyl methacrylate

HOMO: Highest occupied molecular orbital

ITO: Indium-tin oxide

LUMO: Lowest occupied molecular orbital

MeTMOS: Methyl trimethoxysilane

MLCT: Metal-ligand charge transfer state

MMA: Methyl methacrylate

OPM: Optical polarising microscopy

PCBM: [6,6]-Phenyl-C_{61}-butyric acid methyl ester

PCE: Power conversion efficiency

PDI: Polydispersity index

PDT: Photodynamic therapy

PEDOT-PSS: Poly(3,4-ethylenedioxythiophene) poly(styrenesulfonate)

PEG: Poly(ethylene) glycol

PeT: Photoinduced electron transfer

PETA: Pentaerythritol triacrylate

PETRA: Pentaerythritol tetraacrylate

PFMA: 2,2,3,3,3-Pentafluoropropyl methacrylate

PM: Pyrromethene

PMMA: Poly(methyl methacrylate)

POLICRYPS: Polymer liquid crystal polymer slices

RE: Relative efficiency

TBAF: Tetrabutylammonium fluoride

TEOS: Tetraethyl orthosilicate

TFA: Trifluoroacetic acid

TFMA: 2,2,2-Trifluoromethyl methacrylate

TMS: Tri- or tetra-methylsilane

TMSPMA: 3-(Trimethoxysilyl) propyl methacrylate

Chapter 1: BODIPYs as components in novel light active materials

1. Dipyrrins

Research into dipyrrins has traditionally been carried out by groups with the intention to synthesise porphyrins. This is due, in large part, to the advances made by Hans Fischer during the first half of the 20th century.[1] The majority of dipyrrin research currently being undertaken focuses on the synthesis of charge-neutral complexes of dipyrrins with various metals. Initially, the synthesis of dipyrrins was seen as a messy and inefficient avenue of chemical synthesis.[2] However, since the discovery and popularisation of simpler methods of dipyrromethane and dipyrrin synthesis, dipyrrin chemistry has seen some great advances. Various dipyrrinato-metal complexes have been synthesised and their geometries analyzed; and various potential applications of dipyrrins in energy transfer cassettes and photonic systems have begun to be explored.

1.1 Structure

Dipyrromethanes consist of two pyrroles attached to each other through the 2,2'-positions with a saturated methylene bridging unit. Dipyrrins are formally oxidation products of dipyrromethanes, and are structurally similar to them, but the two pyrrolic units in dipyrrins are fully conjugated.

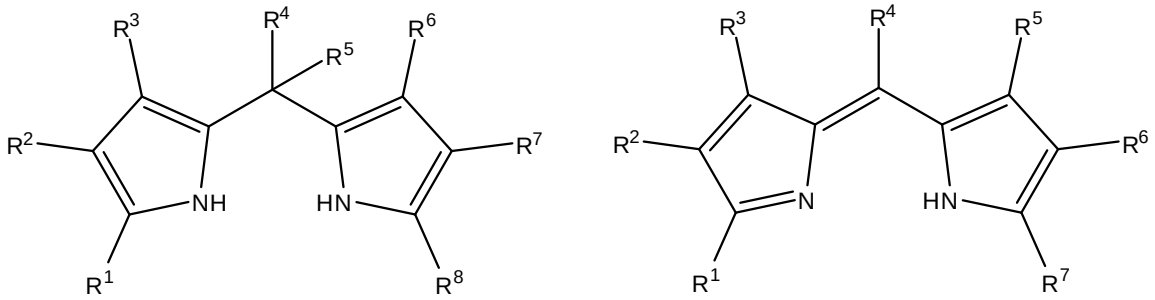

Figure 1. 1: Dipyrromethane and dipyrromethene

The fully conjugated nature of dipyrrins means that, when symmetrically substituted, the two pyrrole units are equivalent. Some examples have been reported of 2,3'- and 3,3'-dipyrrins[3] but the majority of dipyrrin research is focused on 2,2'-dipyrrins.

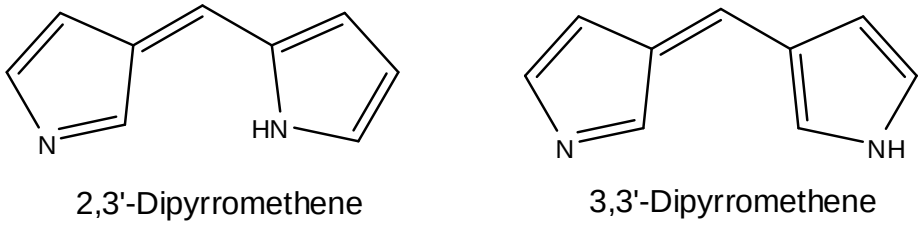

Figure 1. 2: 2,3'Dipyrromethene and 3,3'-dipyrromethene

1.2 Properties of dipyrrin complexes

1.2.1 Fluorescence properties of dipyrrin complexes

Due to the extensive conjugation present in dipyrrins and their complexes, some photoactivity would be expected. However, it was not until 2004 that dipyrrin complexes were discovered to be fluorescent. The first fluorescent dipyrrinato complex synthesised was 5-mesityldipyrrinato-zinc (II) complex. This was observed to have a fluorescence quantum yield (Φ_F) of 0.36.[4] By replacing the mesityl group with a phenyl or 4-*tert*-butylphenyl group, the fluorescence quantum yield was reduced. This was attributed to the ability of the phenyl ring to rotate, quenching fluorescence through internal conversion. The 2,6-methyl groups on the mesityl substituent prevent this rotation, limiting excited state decay processes to fluorescence. Another example of increased fluorescence by restricted rotation of the aryl substituent is shown in compound **1.1**. This heteroleptic complex has the aryl group rotation restricted not only by the 3,7-methyl groups but also by coordination of the pyridyl nitrogen to the zinc centre on the adjacent dipyrrin. This results in a fluorescence quantum yield of 0.057.[5]

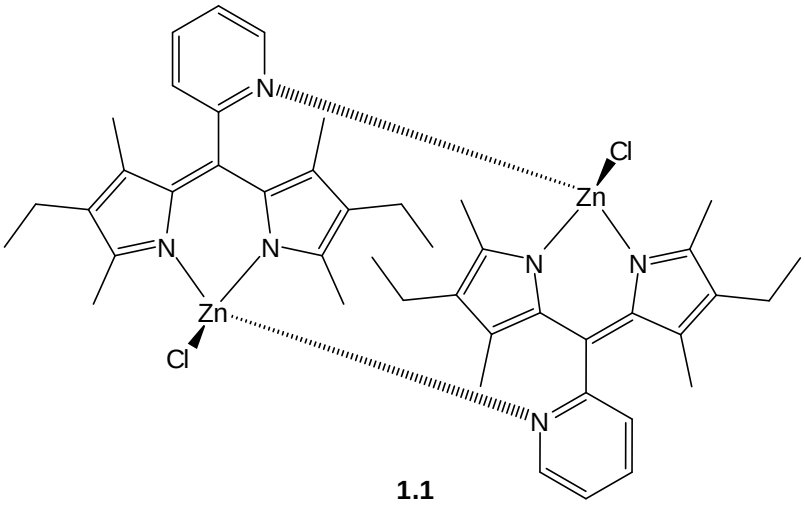

1.1

Figure 1. 3: Bis(dipyrrinato-zinc) complex

1.2.2 Electrochemical properties of dipyrrin complexes

The electrochemical properties of some dipyrrin complexes have been studied and have shown behaviour consistent with ligand-centred oxidations and reductions.[6-9] It has been shown that the redox behaviour of free-base dipyrrins is similar to that of their protonated forms. However, the protonated forms have shown lower oxidation potentials, which has been attributed to reduced electron availability. The electrochemical properties of dipyrrin complexes do exhibit differences depending on the metal to which they are coordinated.[8-10]

1.3 Synthesis

Due to the electron-rich nature of dipyrrins, fully unsubstituted dipyrrin is unstable in solutions above -40°C as it is highly susceptible to electrophilic attack.[11] By blocking the sites of attack, the dipyrrin can be stabilised. This is achieved by constructing appropriate pyrrolic precursors. 1,2,3,7,8,9-Unsubstituted dipyrrins can be isolated by incorporating an aryl group at the 5-position. The greater delocalisation of the electrons caused by the presence of an aryl group at the 5-position also means that any radical cations formed on

the dipyrrin are also stabilised making them more suitable for optoelectrochemical applications.[12]

1.3.1 Condensation of pyrroles

The most commonly used method for the synthesis of asymmetrical dipyrrins is by the condensation of pyrroles. This method proceeds *via* the acid-catalyzed condensation of a 2-formyl pyrrole with a 2-unsubstituted pyrrole to yield a 5-unsubstituted dipyrrin HX salt.[13] This method is commonly known as the MacDonald coupling in reference to the analogous reaction in the synthesis of porphyrins.[14] This procedure is usually carried out using a strong mineral acid (either hydrochloric or hydrobromic) but phosphorus (V) oxychloride has also been used with similar results.[15] 5-Unsubstituted dipyrrins are isolated as their salts due to the instability of their free-base forms, unlike the 5-phenyl dipyrrins that can be isolated as their free-bases.

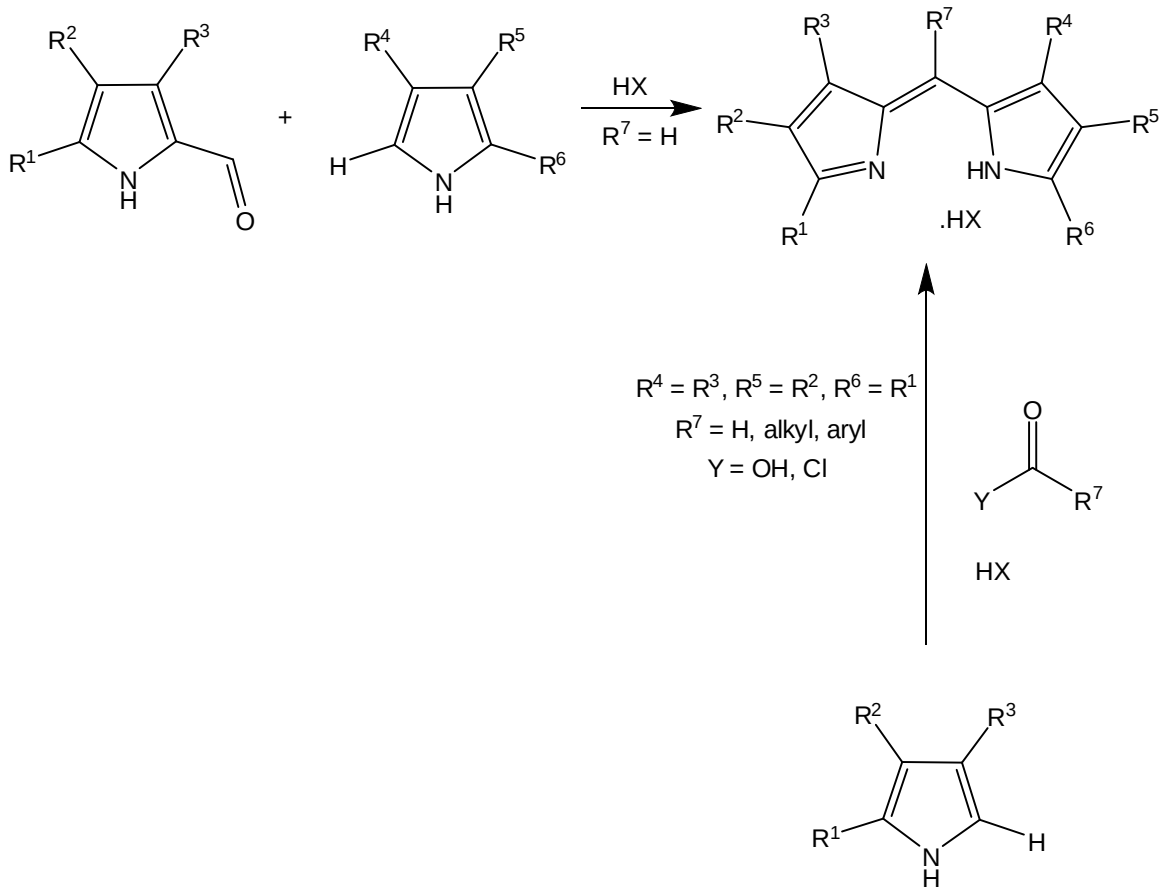

Scheme 1. 1: Synthesis of dipyrrins *via* acid-catalyzed condensation reactions

The isolation of the product dipyrrin is usually achieved courtesy of filtration, since the low solubility of the dipyrrin salt in organic solvents which renders precipitation. Yields for this reaction are reduced when 2-unsubstituted pyrroles with electron withdrawing groups are used as this leads to a lower reactivity towards the 2-unsubstituted pyrrole and an increasing preference for self-condensation of the 2-formyl pyrrole.[13] Symmetrical dipyrrins can be synthesised by a similar process (Sch. 1.1) from a 2-unsubstituted pyrrole and a carboxylic acid or acid halide. This leads to 5-substituted dipyrrins.

While there has been a great deal of chemistry carried out on dipyrrin salts as intermediates in porphyrin synthesis, there has been much less research on the chemistry of dipyrrin salts for other applications. The usual procedure is to leave the formation of the dipyrrin (or tripyrrin or tetrapyrrin) salt until it is required for the porphyrin synthesis

due to the relative instability of the dipyrrin even in its salt form. A recent report, however, showed that dipyrrin salts can be converted to vinylic dipyrroles by reaction with nBuLi (Sch. 1.2).[16] Ordinarily, dipyrrins are reacted with a comparatively mild base when they are being used for the synthesis of porphyrins, BODIPYs (borondifluoro-dipyrrins) or dipyrrin-metal complexes. This mild base deprotonates the dipyrrin to yield the monoanionic dipyrrin which is then reacted further, but in this case it has been shown that the monoanionic dipyrrin is not formed but that the nBuLi removes a proton on the methyl group at the 5-position causing tautomerization to yield the dipyrrole.

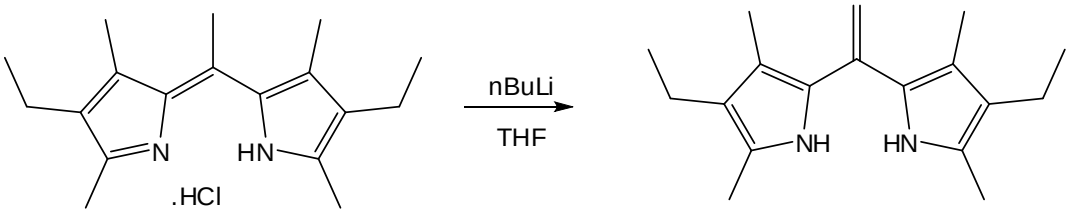

Scheme 1. 2: Deprotonation of *meso*-methyl dipyrrin

1.3.2 Oxidation of dipyrromethanes

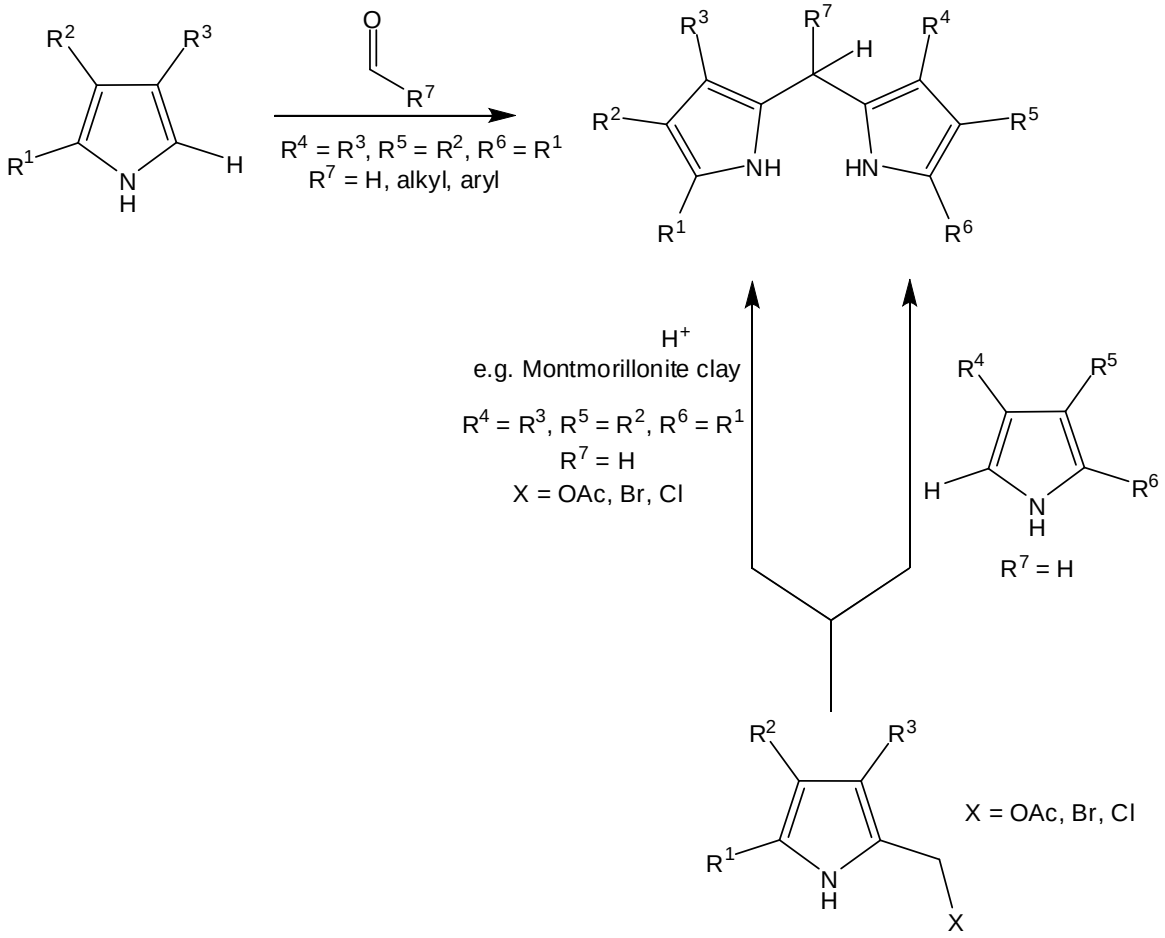

Scheme 1. 3: Synthesis of dipyrromethanes

A significantly simpler method for the synthesis of dipyrrins has become popular in recent years due to the mild conditions, ease of purification and lack of necessity for the synthesis of pyrrolic precursors. This method involves the synthesis of a dipyrromethane from the acid-catalyzed condensation of a pyrrole with an aldehyde[17] (most commonly a benzaldehyde) followed by subsequent oxidation with either DDQ or *p*-chloranil (Sch. 1.3).[18-22] The resulting 5-aryl dipyrromethanes and dipyrrins are easily purified using column chromatography (or crystallisation in some cases), and are stable in their free-base form, unlike their 5-unsubstituted counterparts. These reactions are generally carried

out using a large excess (~100 eq.) of pyrrole, but for substituted pyrroles, the number of oligomeric side-products is lower so only 2 eq. of pyrrole is generally used.[23-28]

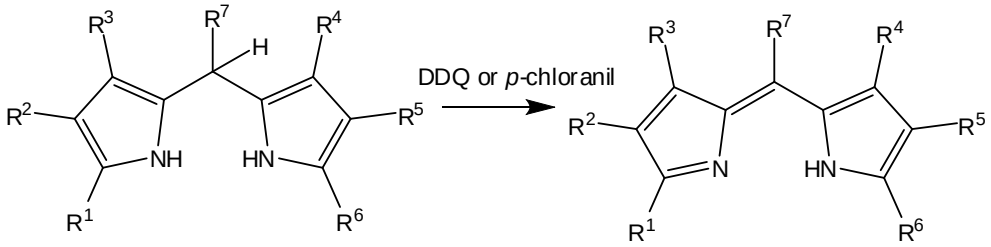

Scheme 1. 4: Oxidation of dipyrromethane

Oxidation is achieved by reacting the dipyrromethane with DDQ (2,3-dichloro-5,6-dicyano-1,4-benzoquinone) or *p*-chloranil (2,3,5,6-tetrachloro-1,4-benzoquinone) if a milder oxidizing agent is desired.[23] Although the use of DDQ or *p*-chloranil as an oxidizing agent is successful for 5-aryl dipyrromethanes, oxidation of 5-alkyl and 5-unsubstituted dipyrromethanes has been shown to consume the starting material without yielding the desired product.[29] The NMR spectra of free-base 5-substitituted dipyrrins shows rapid tautomerization, and because of this, the NH signal in the ^{1}H-NMR spectrum is not always apparent.

2. Borondifluorodipyrrins (BODIPYs)

An important group of dipyrrin complexes which has garnered a large amount of interest in recent years is the borondifluorodipyrrins (hereafter referred to as BODIPYs).[30] The primary reason for this interest is that BODIPYs are extremely fluorescent when compared to other dipyrrin-metal complexes with fluorescence quantum yields sometimes approaching unity.[31] Also, their relative stability allows a wide range of reactions to be performed on them, which has enabled a general set of guidelines about how to alter their fluorescence profiles to be generated. This stability is partially caused by the boron, nitrogen and fluorine atoms all being first row elements which allows efficient orbital overlap, promoting delocalisation of the π-system. These properties give BODIPYs the potential to be used in a range of applications such as luminescent labelling agents,[32-34] fluorescent switches,[35, 36] chemosensors[24, 37-40] and laser dyes.[41]

2.1 Structure

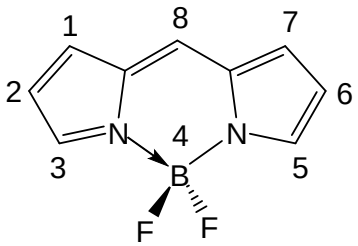

Figure 1. 4: BODIPY showing alternate numbering system

Similar to other dipyrrins, the BODIPY core is a fully delocalised system where the BF_2 unit causes an increase in the planarity of the dipyrrin, and thus an increase in fluorescence. It was thought that the core fully unsubstituted BODIPY structure (Figure 1.4) was just as unstable as the dipyrrin counterpart, until recent papers published the synthesis and characterisation of this compound.[42, 43] The BF_2 unit serves to increase the stability of the dipyrrin which makes it possible to isolate this compound as long as purification is relatively swift, so as to avoid degradation of the compound by reaction with the side-products. This core BODIPY compound was found to have a fluorescence quantum yield of 0.90 and sharp absorption and emission peaks at 503 nm and 512 nm respectively.[43] Now that this core compound has been isolated, new BODIPY dyes have an internal core compound to be measured against, and a more complete picture of the factors affecting the optical properties of BODIPYs can be developed.

2.2 Properties of BODIPYs

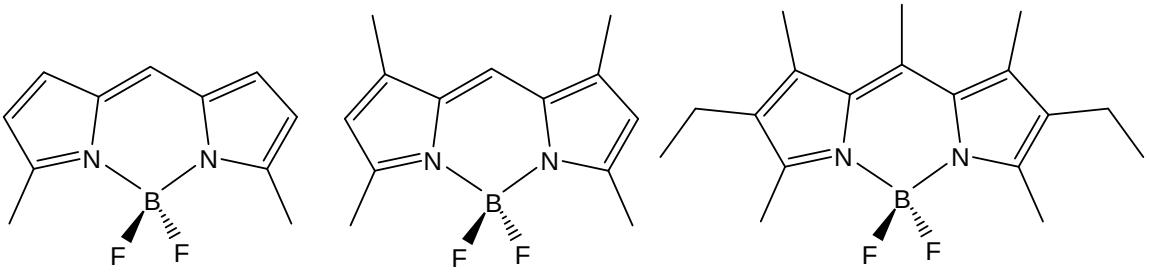

Figure 1. 5: Analogues of the core BODIPY compound

Several simple derivatives of the core BODIPY have been synthesised. Each analogue displays strong fluorescence (Φ_F = 0.70 – 0.81) and sharp absorption and emission peaks.[44, 45] It is taken as a general rule that by increasing the degree of substitution on the pyrrolic positions of the BODIPY, the absorption and emission wavelengths undergo a bathochromic shift. Substitution at the 8-position (*meso*-position) with either an alkyl or aryl group does not have a large effect on the fluorescence profile. However, a similar reduction in fluorescence is observed in BODIPYs, as in other dipyrrin-metal complexes, when a freely rotating aryl unit is attached at the 8-position. This effect can be perturbed in a similar fashion to other dipyrrin-metal complexes by restricting the rotation of the aryl unit by either attaching bulky groups to the 2,6-positions of the ring or on the 1,7-positions on the pyrrolic units (Figure 1.6).

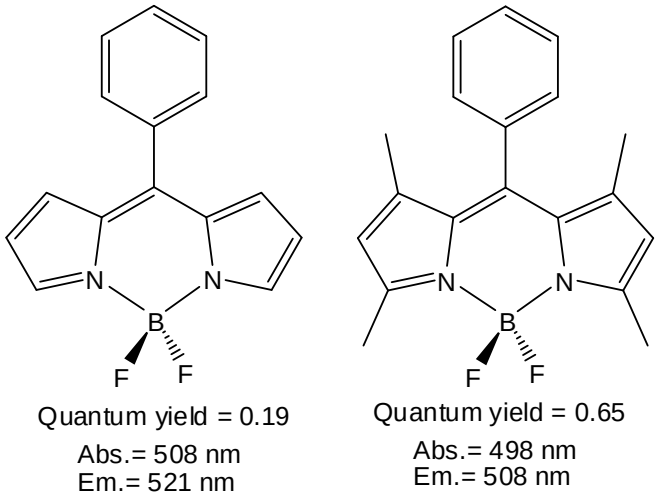

Figure 1. 6: 8-Aryl-BODIPYs showing effect of bulky alkyl substituents at the 1,7-positions

This effect has been exploited to synthesise a BODIPY viscosity probe as seen in compound **1.2 (**Fig. 1.7).[46] By attaching two BODIPY units through long alkyl chains linked together with a phenyl-1,4-dicarboxylate unit, the amount of rotation of the BODIPY 8-aryl substituent was gradually restricted with increasing solvent viscosity. A similar probe was developed which had a dodecyl chain attached *via* an ether linker to the BODIPY 8-aryl unit.[47] This restriction of rotation caused an increase in fluorescence quantum yield with increasing solvent viscosity.

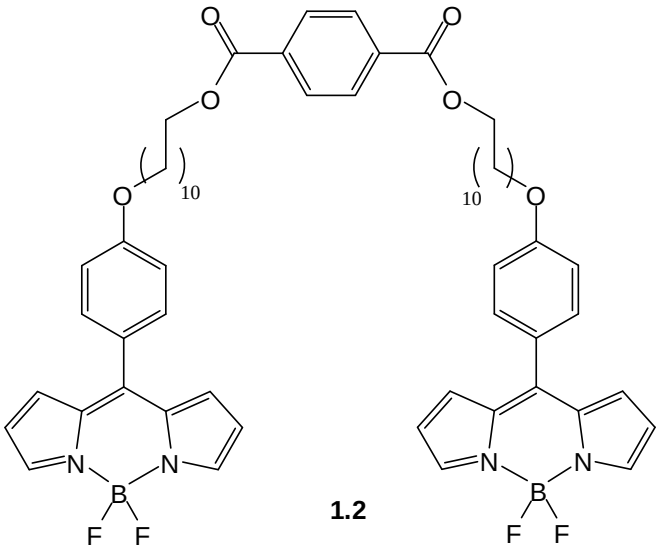

1.2

Figure 1. 7: BODIPY viscosity sensor

Various BODIPYs with fused rings attached to the pyrrolic units have been synthesised to investigate the effect of substitution on the photophysical properties of BODIPYs. These substituted BODIPYs were synthesised from preformed pyrrolic precursors specific for the desired BODIPY.

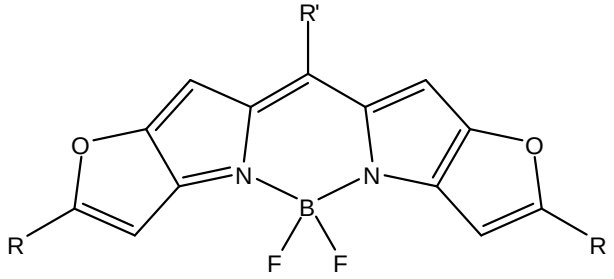

Figure 1. 8: Furanyl-BODIPY

When R = Me and R' = H, the absorption and emission maxima were red-shifted approximately 70nm, while when R = 4-methoxyphenyl and R' = CF_3, the absorption and emission maxima were shifted to 723 nm and 738 nm respectively which is in the near-IR region (Fig. 1.8).[48] These results showed that the properties of BODIPYs are highly tuneable to a variety of applications.

Various BODIPYs have been prefunctionalized from their pyrrolic precursors in order to investigate the effect of different functional groups on the photophysical properties of the

BODIPY chromophore. The general effect of extending the conjugation of the BODIPY core in this way is that the absorption and emission maxima are red-shifted.[49, 50] By attaching electron donating or withdrawing groups to different positions of these aryl groups, the photophysical properties can be greatly affected (Sch. 1.5). These pyrrolic aryl units can cause a reduction in the fluorescence quantum yield of the BODIPY by molecular motions in the same way as an 8-position aryl group.[51] This effect can be perturbed by steric interactions reducing the rotation of these aryl groups.

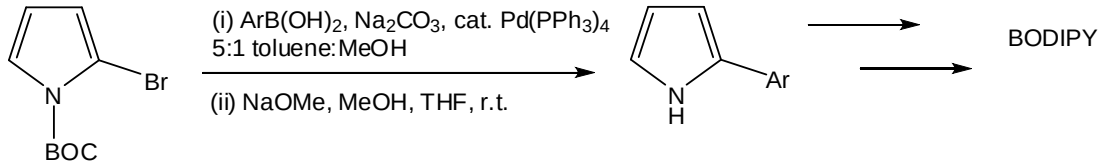

Scheme 1. 5: Prefunctionalisation of pyrrole units

Another factor that affects BODIPY fluorescence in solution is intermolecular π-stacking. BODIPYs can stack in two different ways (Fig. 1.9). The type of stacking that predominates is the almost parallel stacking known as the *H*-dimer. This consists of almost parallel $S_0 \rightarrow S_1$ transition dipoles and antiparallel electric dipole moments. The other type of stacking is where the $S_0 \rightarrow S_1$ transition dipoles are oriented in planes at 55°. This is known as the *J*-dimer. The *H*-dimer is very weakly fluorescent and exhibits blue-shifted fluorescence, absorption, and emission maxima relative to the monomer, while the J-dimer shows a red-shifted absorption and emission. The *J*-dimer is fluorescent but in highly concentrated solutions the *H*-dimer will predominate, thus making the solution less fluorescent. This effect was measured by attaching two BODIPY units to a flexible linker forcing them into close proximity, thus increasing the probability of the formation of these dimers.[52-54] A BODIPY was designed to prevent the formation of these dimers, resulting in a concentrated solution maintaining its fluorescence. This was achieved by attaching mesityl groups to the 3-, 5- and 8-positions of the BODIPY.[55]

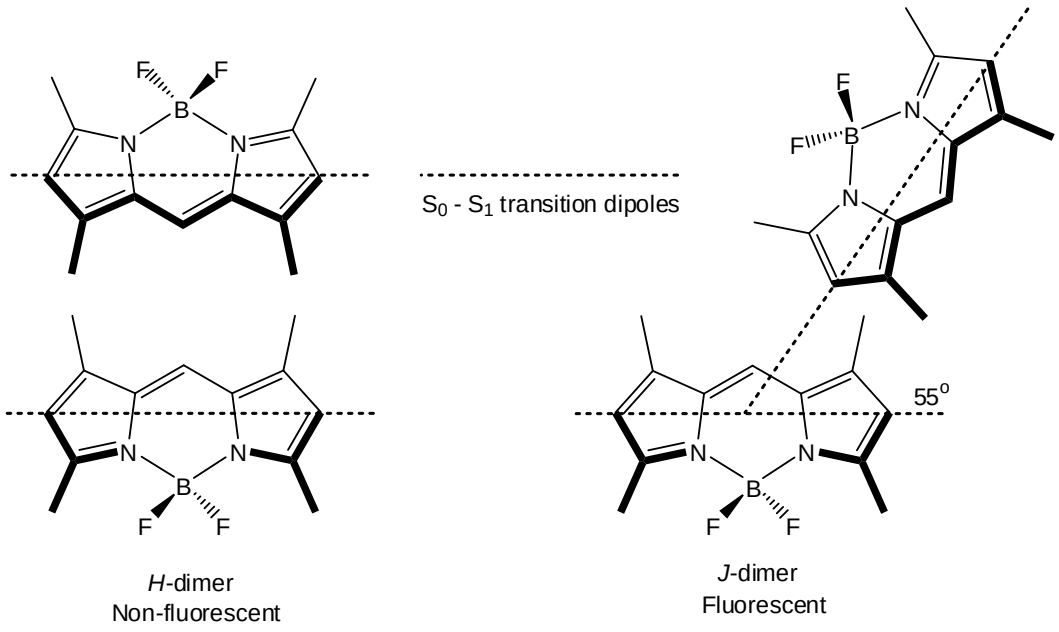

Figure 1. 9: *H*- and *J*-dimers of BODIPYs

2.3 Synthesis of BODIPYs

BODIPYs are synthesised using the same initial steps used to synthesise dipyrrins followed by treatment with an organic base (triethylamine, DIEA, DBU etc.) and boron trifluoride diethyl etherate. When seeking to synthesise a BODIPY the relatively unstable dipyrrin salts are generally not isolated. In the search for new BODIPY derivatives some specific synthetic routes have been developed.

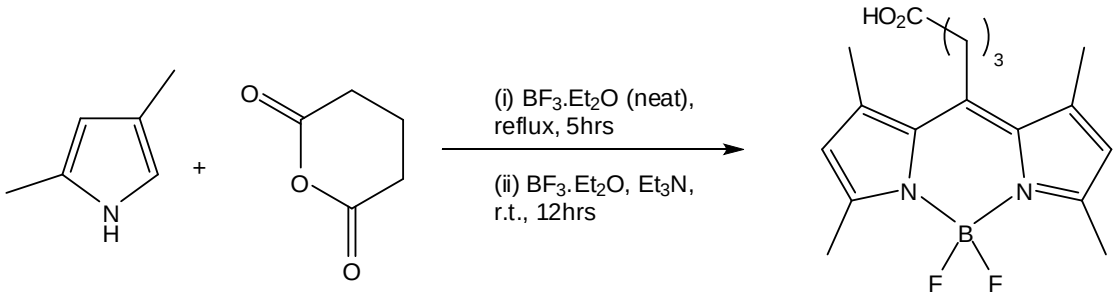

Scheme 1. 6: BODIPY from glutaric anhydride

The synthesis of a BODIPY from glutaric anhydride (Sch. 1.6) proceeds using boron trifluoride diethyl etherate as a Lewis acid to initiate the reaction to form the dipyrrin, which is then converted to the BODIPY.[56] The benefit of this reaction is that the free

carboxylic acid is produced which allows for the BODIPY to be attached to other molecules.

The synthesis of BODIPYs from 5-aryl dipyrrins is a well known and much used reaction. However, the synthesis of BODIPYs from other aldehydes has received little attention. The route presented in Scheme 1.7 shows a BODIPY synthesis from an allyl aldehyde with ytterbium(III) trifluoromethane sulphonamide as the catalyst for the condensation. This reaction, however, was found to give the product in very poor yield (2%). When compared to the thioether analogue of the same BODIPY, it was found that the allyl thioether compound (Sch. 1.7) had a fluorescence emission red-shifted by 26 nm indicating the effect of electron withdrawing groups at the 8-position.[57] Electron withdrawing groups have the effect of lowering the energy of the LUMO into which an electron is excited, thus lowering the energy required to excite the electron which causes the red-shift in the fluorescence. The fluorescence absorption and emission were also found to be red-shifted when compared to the 8-phenyl derivatives.

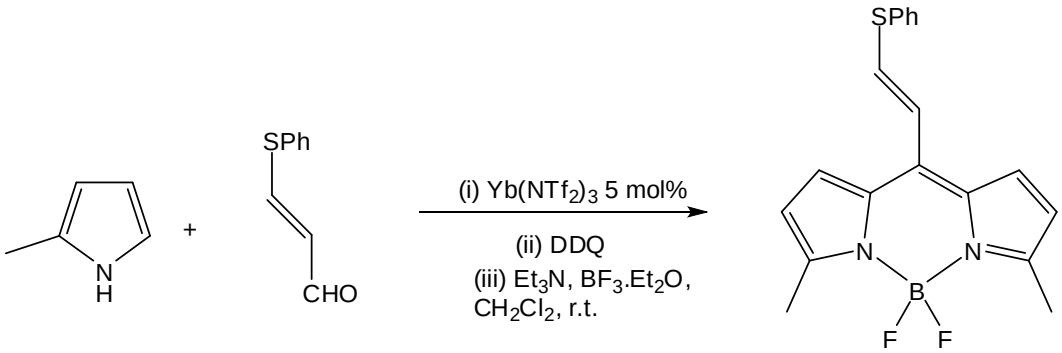

Scheme 1. 7: BODIPY synthesis from allyl aldehyde using ytterbium (III) trifluoromethane sulphonamide as the catalyst

Both of these methods can be used to prepare symmetrical BODIPYs but to prepare asymmetrical BODIPYs a different approach is required. The most commonly used method to achieve this is *via* the same route used to synthesise asymmetrical dipyrrins. An alternate approach has been developed, which involves the preparation of α-ketopyrrole intermediates with subsequent condensation with a second pyrrole unit (Lewis acid-catalyzed), followed by coordination to the boron difluoride unit.[58, 59]

2.4 Fluorescence control of BODIPYs by modification of the 8-aryl group

Due to the increased stability, when compared to other dipyrrinato-metal complexes, a large number of modifications to the BODIPY core have been achieved. The group that has received the most attention has been the aromatic group at the 8-position, which is an easily modified unit that can have a large effect on the fluorescent properties of the BODIPY. BODIPYs can also be synthesised with groups that allow *in vitro* chemical modifications to occur (e.g. metal ion complexation) promoting their use as fluorescent probes for biological systems. They can be used as sensors for redox active molecules,[37, 60-62] pH probes,[39] metal ions[63-71] and probes for conjugation to biologically active substrates.[72-74] In the examples presented in Figure 1.10, fluorescence is turned 'ON' or 'OFF' by photoinduced electron transfer (PeT) which is controlled by changes in the oxidation potentials of the 8-aryl groups when they interact with certain chemical species.

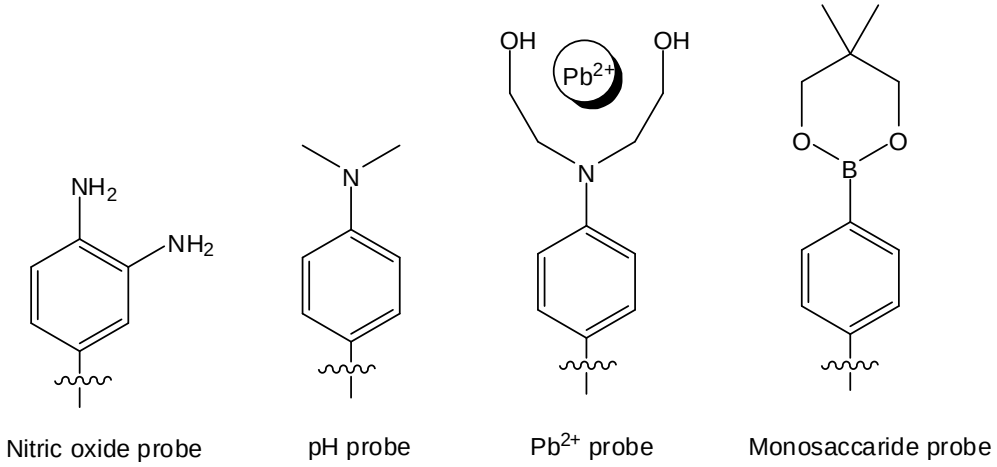

Figure 1. 10: *Meso*-modified BODIPY probes

2.4.1 Photoinduced electron transfer (PeT)

The primary factor exploited in BODIPYs to modify their fluorescence is photoinduced electron transfer. This involves the transfer of excited electrons between non-planar parts of a fluorescent molecule.[75] This transfer of excited electrons has a significant effect on the fluorescence intensity of photoactive molecules. By calculating the orbital energy levels of the two non-planar parts of a molecule, it can be predicted whether a certain change will alter the fluorescence characteristics.[76-78]

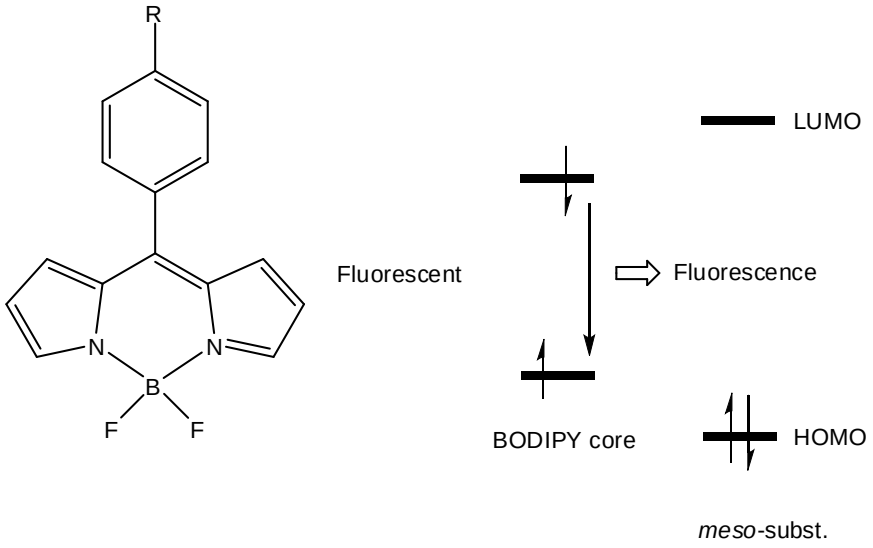

Figure 1. 11: BODIPY where no PeT can occur

For BODIPYs, the majority of substituents attached to the 8-position are aromatic groups. When this electron transfer occurs it prevents the loss of energy by fluorescence processes. It is worth noting that, during the design of new BODIPY probes that exploit this effect, that the fluorescence intensity of the BODIPY is still reduced by the effects of molecular motion. This means that the rotation would still have to be taken into account before synthesis is carried out to ensure that the target molecule's change in fluorescence intensity by PeT is large enough for it to be a suitable probe.

PeT can occur by either a reductive or oxidative process. If the substituent attached to the BODIPY core is donating electrons to the BODIPY core in the excited state, i.e. reducing it, then this is reductive PeT or a-PeT ("a" for acceptor). (Fig. 1.12)

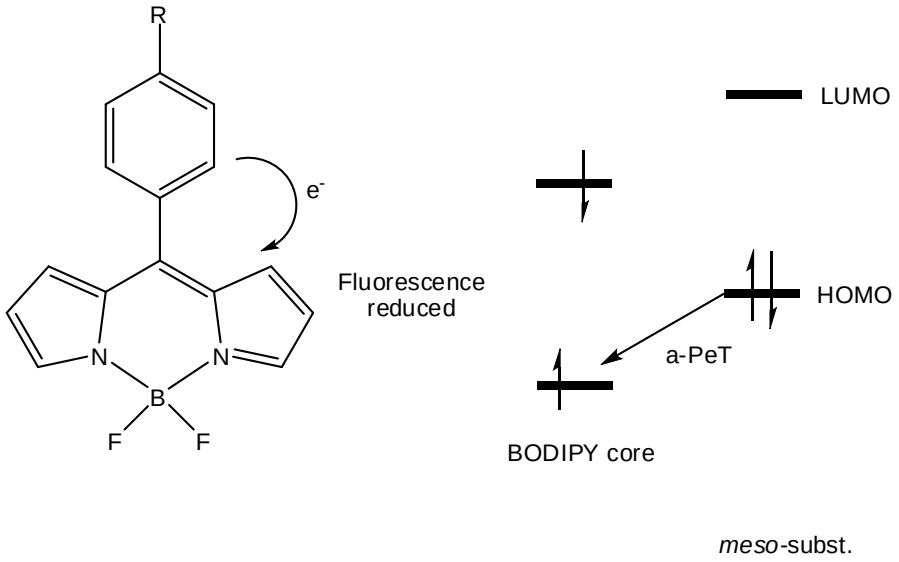

Figure 1. 12: Reductive PeT (a-PeT)

Alternatively, if the excited BODIPY core can donate electrons to the substituents LUMO then oxidative PeT, or d-PeT ("d" for donor), is occurring (Fig. 1.13).

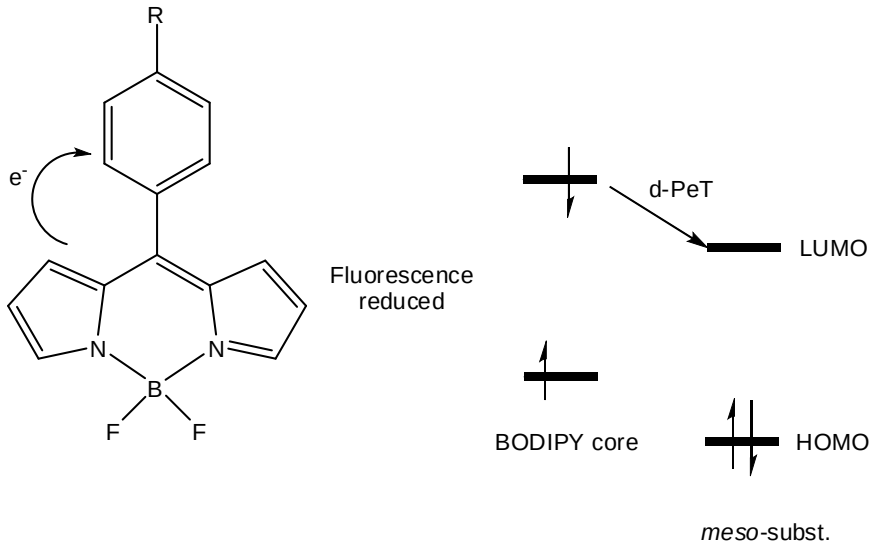

Figure 1. 13: Oxidative PeT (d-PeT)

The likelihood of electron transfer can be predicted by calculating the change in free energy (ΔG_{PeT}). This can be calculated from the Rehm-Weller equation:[79]

$$\Delta G_{PeT} = E_{1/2}(D^+/D) - E_{1/2}(A/A^-) - \Delta E_{00} - C$$

Where $E_{1/2}(D^+/D)$ is the ground state oxidation potential of the electron donor, $E_{1/2}(A/A^-)$ is the ground state reduction potential of the electron acceptor, ΔE_{00} is the excitation energy, and C is an electrostatic interaction term. The primary problem with using the approach of orbital energy level calculations is that the energy levels are calculated for the isolated *meso*-substituents. By attaching them to the BODIPY core, it is reasonable to assume that their energy levels are altered somewhat, giving this method a reasonably large margin for error. However, this approach is useful to give a reasonable prediction of the effect that certain substituents or structural changes will have on the fluorescence of this molecule.

A prime example of the use of this equation to predict PeT in BODIPY systems has been used for the development of a nitric oxide probe. For this probe, a diamine was converted *in vitro* to a benzotriazole by reaction with nitric oxide.[40]

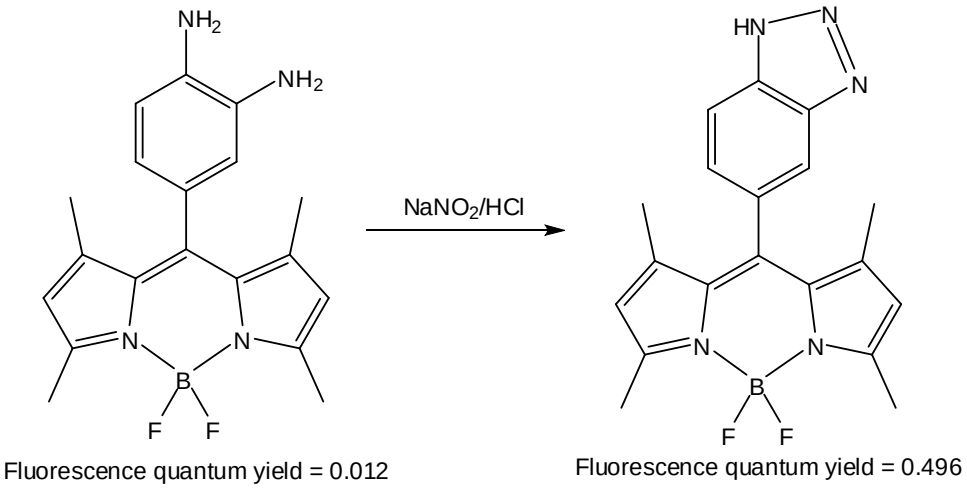

Scheme 1. 8: Mechanism of BODIPY nitric oxide probe

The HOMO energy levels of various potential *meso*-substituents were calculated including the diamine and the benzotriazole. The low fluorescence of the diamine was attributed to reductive PeT. This effect is quenched upon conversion to the benzotriazole which causes a large increase in fluorescence. This reductive PeT effect has also been exploited for zinc(II) and NO_2^+ sensors.[80, 81] In these cases, coordination to the metal or nitration makes the reduction potential of the *meso*-substituent more negative, which quenches PeT and causes the BODIPYs to become fluorescent.

This ON/OFF switching has also been investigated with regard to oxidative PeT. It has been discovered that placing strongly electron withdrawing groups on the *meso*-substituent tends to lower the LUMO of the aromatic unit. If lowered to an appropriate level, this allows the *meso*-substituent to accept electrons from the excited state of the BODIPY core. This effect was investigated by attaching nitro groups to the *meso*-substituent and by attaching acetyl groups to the 2,6-positions of the BODIPY core. While the nitro groups lower the LUMO of the aromatic substituent, the acetyl groups lower the energy level of the BODIPY orbital containing the excited electron. This brings both orbitals to a similar energy level, promoting oxidative PeT.[81] ON/OFF switching of PeT has also been observed for the phosphorylated forms of 8-(4-hydroxyphenyl) BODIPY. Phosphorylation caused PeT to switch off by lowering the HOMO energy level of the aryl substituents.[82]

2.5 Metal-catalyzed reactions of BODIPYs

Metal-catalyzed reactions can be carried out on BODIPYs either with or without the requirement for halogenation (e.g. Suzuki, Stille etc.).[83] Both methods allow the conjugation of the BODIPY to be extended producing highly fluorescent dyes and pigments with bathchromically shifted fluorescence profiles.

Metal-catalyzed reaction can take place at the 2- and 6-positions or 3- and 5-positions of the BODIPY when these positions are unsubstituted. Reaction at the 2- and 6-positions can occur by reacting a terminal alkene adjacent to an electron withdrawing group with the BODIPY in the presence of palladium(II) acetate (20 mol%) and either an oxidant, heat or in a microwave.[84]

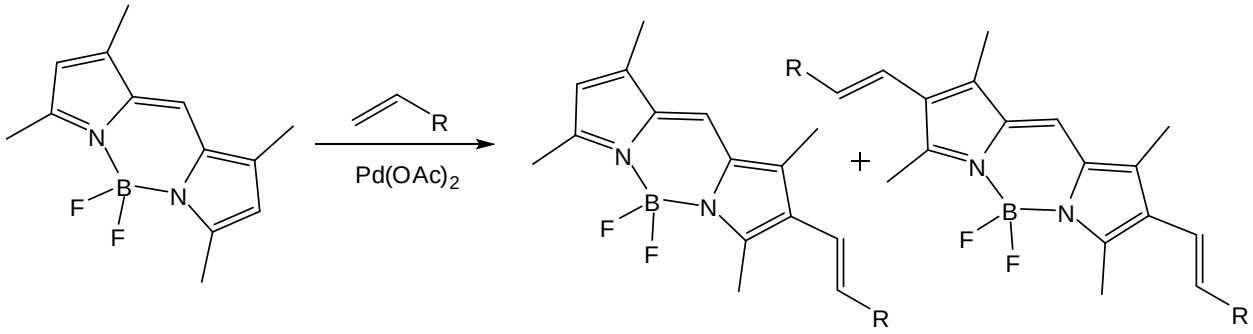

Scheme 1. 9: Oxidative functionalisation of BODIPY

The problem with this reaction is that a mixture of products is formed. The mono-substituted product predominates, but the reaction was far from selective. All the compounds synthesised had their absorption and emission maxima red-shifted by various degrees. The majority of them also had reduced fluorescence quantum yields (Φ_F values ranging 0.25-0.73) relative to the starting BODIPY (Φ_F = 0.80), presumably due to the electron withdrawing R groups.[84] The lowest value of fluorescence quantum yield was found when a sulphonate group was used as the electron withdrawing R group (Φ_F = 0.25).

Rhodium and iridium catalysts have also been used for the synthesis of new BODIPY dyes. The iridium catalyst was used to synthesise a dipyrromethane- or BODIPY-boronpinacolato species. By using 2 eq. of *bis*(pinacolato)diboron with the dipyrromethane, the reaction was selective towards the α-positions. By using 1 eq. of *bis*(pinacolato)diboron with the BODIPY, the reaction was selective towards the 2- and 6-positions. The boronpinacolato species was then reacted with a terminal alkene adjacent to an electron withdrawing group in the presence of a rhodium catalyst. The boronation reaction formed the disubstituted product primarily, but also some of the monosubstituted product. The rhodium catalyzed reaction, however, was completely selective towards the boronpinacolato groups.[85] All of the BODIPYs produced by this method were highly fluorescent (Φ_F values ranging 0.48-0.98) with absorption and emission maxima red-shifted by up to 140 nm. The fluorescence quantum yields were found to be surprisingly high for 8-aryl BODIPYs with no alkyl groups present on the fluorophore to reduce rotation of the phenyl ring. The 8-aryl group did not appear to have

a significant effect on the absorption and emission maxima of the compounds synthesised.

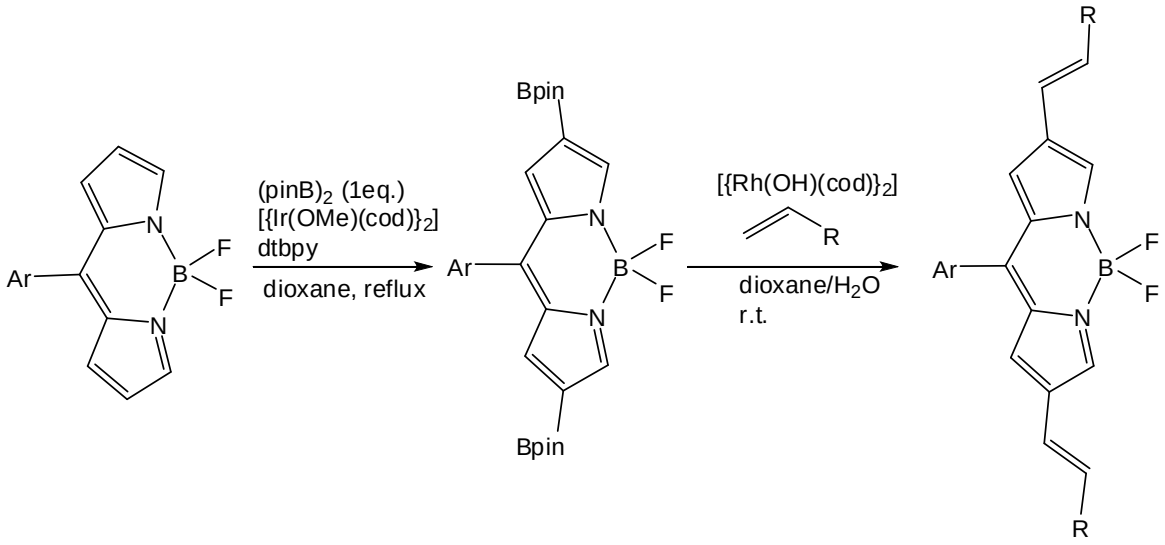

Scheme 1. 10: Iridium- and rhodium-catalyzed reactions of BODIPYs

Metal-catalyzed couplings can be carried out at C-X groups on BODIPYs, and an example is shown in Scheme 1.11. Suzuki, Stille, Heck and Sonogashira couplings have all been carried out on halogenated BODIPYs under standard conditions for these reactions.[83]

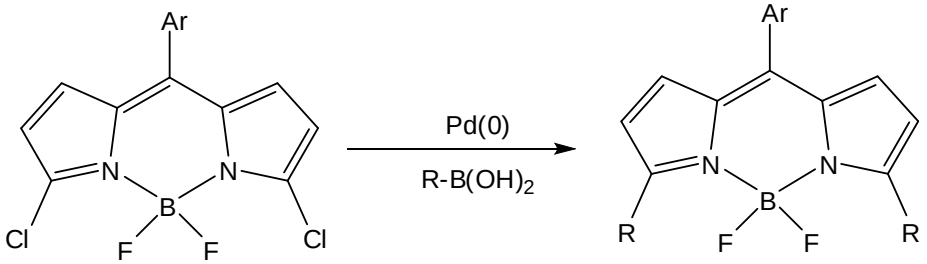

Scheme 1. 11: Palladium-catalyzed couplings of BODIPYs

The Stille ($Pd(PPh_3)_4$, $Sn(Ph)_4$), Heck (Pd^{II}/PPh_3, styrene) and Sonogashira ($Pd(OAc)_2/PPh_3$/CuI, phenylacetylene) reactions all proceeded with heating. The Suzuki ($Pd(PPh_3)_4$, 4-chlorobenzeneboronic acid) reaction however, required microwave promoted conditions. The degree of substitution could be controlled by altering the stoichiometry of the coupling reagent. For the Sonogashira, Suzuki and Stille reactions,

when 1 eq. of the coupling reagent was used, the mono-substituted product was isolated, and when ≤2 eq. of coupling reagent were used the di-substituted product was isolated. The Heck reaction required 1.5 eq. to synthesise the mono-substituted product and 2.2 eq. to synthesise the di-substituted product.[83]

A recent advance in metal-catalyzed reactions of BODIPYs is their functionalisation *via* the Liebeskind-Srogl reaction. This involved the conversion of a 3,5-dichloro-BODIPY into 3,5-dithiobutyl-BODIPY *via* a nucleophilic substitution reaction. This product was then reacted with aryl-tributyltin in the presence of a palladium(0) catalyst and copper(I) 3-methylsalicylate iodide to give mono- or di-arylated BODIPYs (Sch. 1.12).[86]

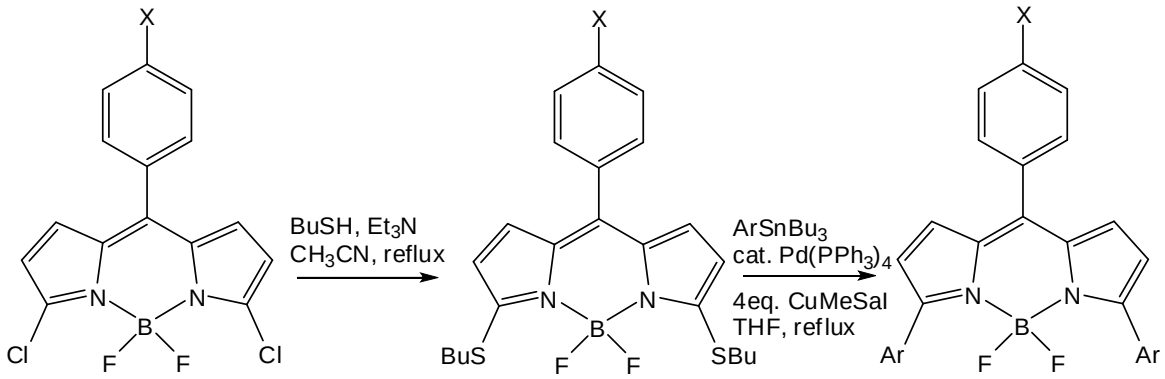

Scheme 1. 12: Liebeskind-Srogl reaction of BODIPYs

By using aryl groups that contains an electron donating group (Ar = Ph or 4-OMePh), the only product that was isolated was the di-substituted one. When an aryl unit containing an electron withdrawing group (Ar = 4-CO_2MePh) was used then a mixture of mono- and di-substituted products was obtained with the di-substituted product being the major product. The reaction was also successful when using a boronic acid instead of the tin complex.[86]

This reaction was used in the synthesis of an energy transfer cassette. By using a BODIPY where X = NO_2 and Ar = 4-methoxycarbonylbenzeneboronic acid, the di-substituted BODIPY was synthesised. The methyl ester was then hydrolyzed with subsequent reduction of the nitro group to the amine, which was then converted to the azide by reaction with sodium nitrite and sodium azide (X = N_3 and Ar = 4-

carboxybenzene). Finally, this was coupled to a BODIPY acetylene unit containing two sulphonate units *via* a 'click' reaction to produce a water soluble energy transfer cassette (**1.3**).[86]

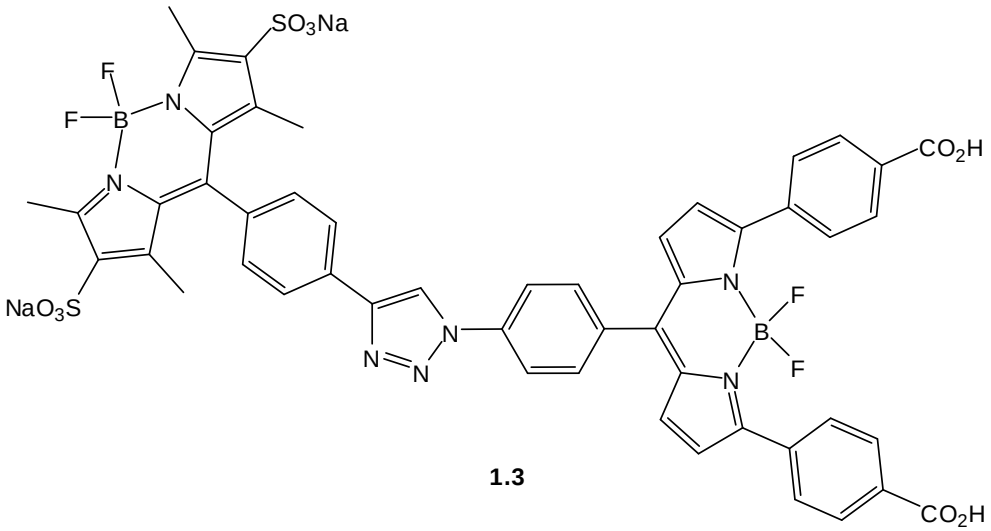

1.3

Figure 1. 14: Water-soluble energy transfer cassette

2.6 Condensation reactions of 3,5-dimethyl-BODIPYs

It has been found that the protons attached to the methyl groups of a 3,5-dimethyl-BODIPY are acidic enough to undergo some condensation reactions. In particular the Knoevenagal reaction, which allows the synthesis of styryl-BODIPYs to be carried out under relatively mild conditions. This has been achieved by reacting a 3,5-dimethyl-BODIPY with an aromatic aldehyde.[87, 88]

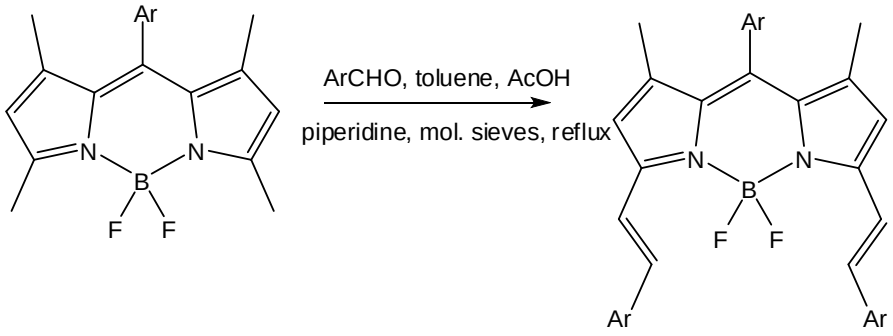

Scheme 1. 13: Knoevenagel reaction of BODIPYs

The product obtained depends on the aldehyde used and the reaction time. 4-Alkoxybenzaldehydes tend to give mixtures of products,[89] while 4-dialkylaminobenzaldehydes can give either the mono-substituted or di-substituted product. The di-substituted product was favoured by longer reaction times.[90] This reaction is a simple way to synthesise highly fluorescent BODIPYs with red-shifted absorption and emission wavelengths and a variety of functional groups. 4-Dialkylaminobenzaldehydes, for example, convey the ability for the BODIPY to behave as a pH sensor. The combination of an amino group and a phenolic group allowed the BODIPY to act as a sensor for both high and low pH (**1.4**).[91] When the phenolic group was deprotonated, the fluorescence was quenched, but the absorption and emission wavelengths remained the same, while if the amino group was protonated then the fluorescence was greatly enhanced but blue-shifted. This type of BODIPY has therefore been referred to as a 'logic gate'.

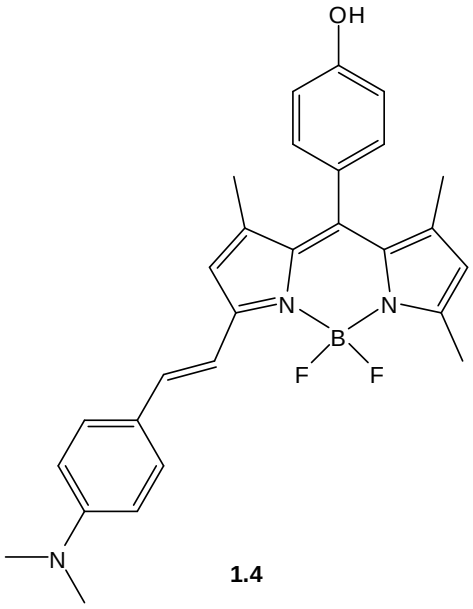

1.4

Figure 1. 15: BODIPY-based pH sensor

The reaction has obvious applications in the synthesis of BODIPY-containing energy transfer cassettes and other optoelectronic applications (e.g. solar cells). By choosing appropriate aldehydes, a series of BODIPY units can be attached together or conjugation to a porphyrin analogue can be achieved.[92-95]

2.7 Aza-BODIPYs

Aza-BODIPYs are analogues of BODIPYs in which the 8-position carbon atom has been replaced with a nitrogen atom (Fig. 1.16).

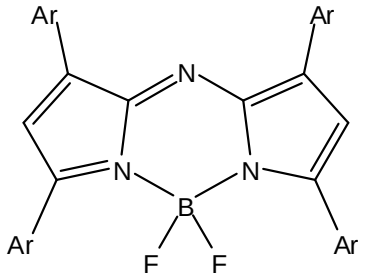

Figure 1. 16: Aza-BODIPY

The aza-dipyrromethenes can be synthesised *via* two different methods. Firstly, by converting 2,4-diarylpyrroles into their 5-nitroso derivatives followed by acid-catalyzed condensation with a second molecule of pyrrole. The second method involves the Michael addition products of chalcones reacting with an ammonia source.[96-98] Subsequent coordination to the boron centre produces the aza-BODIPY.[99] Due to the nature of the synthetic procedure (Fig. 1.17), and the instability of certain pyrrolic intermediates, aza-BODIPYs always have aryl groups at the 1-, 3-, 5- and 7-positions. Thus far, fully unsubstituted aza-BODIPY has not been synthesised.

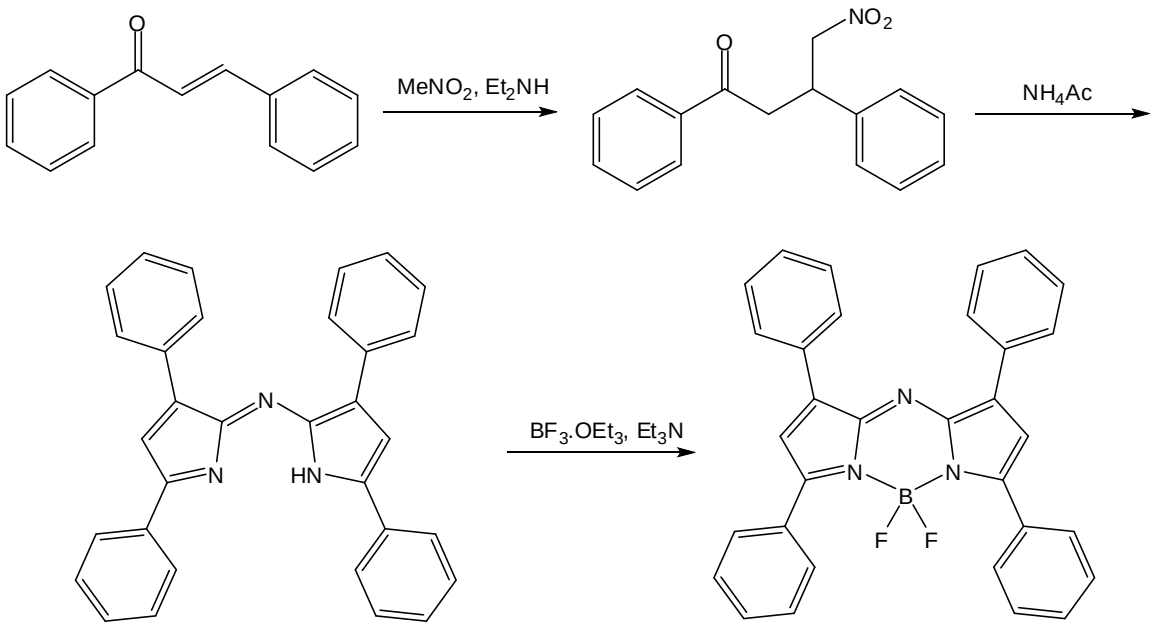

Figure 1. 17: Aza-BODIPY synthesis

The photophysical properties of aza-BODIPYs are greatly affected by the attached aryl units. Electron donating groups at the *para*-positions cause an increase in extinction coefficients and significant red-shifts in absorption maxima.[100] Electron donating groups on the 3- and 5-aryl groups have a greater effect on the absorption and emission wavelengths than the same substituents on the 1- and 7-aryl groups.[101] The extinction coefficients for simple aza-BODIPYs range between 75000-85000 M^{-1} cm^{-1} which allows them to efficiently generate singlet oxygen, the primary reactive species in photodynamic therapy, when substituted with "heavy atoms" to promote intersystem crossing to the excited triplet state.[102-105] Aza-BODIPYs have a wide range of fluorescence quantum yields just as the analogous BODIPYs do. Their photophysical properties still coincide with what would be expected of a fluorescent compound. For example, a *para*-bromo substituent on the 1- and 7-aryl groups causes no significant changes in the fluorescence properties. However, by attaching bromine atoms onto the 2- and 6-positions of the aza-BODIPY core, a reduction in fluorescence and an increase in singlet oxygen production was observed. This was attributed to the heavy atom effect.[101] While the majority of interest in aza-BODIPYs has been focused on photodynamic therapy, they have also found uses as chemosensors and pH sensors.[100, 106, 107]

2.8 Energy transfer cassettes

2.8.1 Through-space energy transfer cassettes

An energy transfer cassette consists of two or more fluorescent units attached to the same molecule. One unit acts as a donor and the other as an acceptor. The donor absorbs light and this energy is then passed to the acceptor, which emits the light at a longer wavelength. The energy can be transferred to the acceptor *via* either through-space or through-bond energy transfer.

The efficiency of through-space energy transfer depends on the spectral overlap of the donor emission with the acceptor absorbance, the distance between the donor and the acceptor, the relative orientation of donor and acceptor, and the effectiveness of other de-excitation modes (e.g. emission from donor, non-radiative processes). The energy-transfer efficiency is calculated by comparing the amount of emission from the donor with the emission from the acceptor. If no, or very little, emission is observed from the donor, it is implied that the majority of the energy is transferred from the donor to the acceptor i.e. 99+%. Through-space energy transfer has the effect of artificially enhancing the Stokes' shift of the molecule by causing emission from the acceptor in place of the absorbing (donor) fluorophore. Due to their intense fluorescence, BODIPYs have found uses in the synthesis of new energy transfer cassettes.

Due to the similarity of their structures, energy transfer cassettes containing BODIPY and porphyrin units have received a lot of attention for their through-bond energy transfer processes and subsequent applications as molecular wires. Through-space energy transfer involving porphyrinic units has been less thoroughly investigated. A simple 8-(4-hydroxyphenyl)-BODIPY has been coordinated to an antimony tetraphenylporphyrin (Sb(TPP)) *via* an alkyl chain to form a through-space energy transfer cassette. The efficiency of the energy transfer varied between 13-40%. By increasing the length of the alkyl chain spacer unit, the efficiency was found to decrease. It was found that the BODIPY acted as the donor, and therefore, no quenching of the excited state of the

porphyrin by donation of energy to the BODIPY was found. It was found that quenching did occur when a phenoxy group was coordinated to the other side of the antimony in conjunction with the BODIPY (**5**).[108]

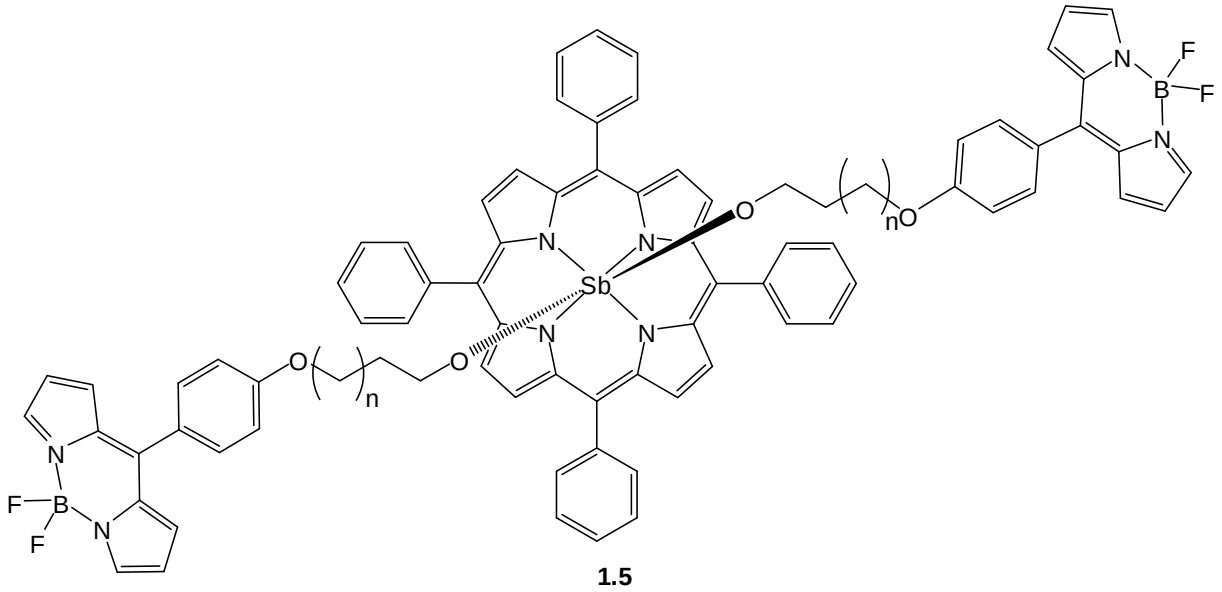

1.5

Figure 1. 18: Antimony-porphyrin-BODIPY array

A similar compound based on a silicon phthalocyanine was synthesised and found to exhibit competitive energy- and electron-transfer. Analogous to the antimony-porphyrin-BODIPY array (**1.5**), when excited at the BODIPY absorption maximum, emission was observed from the phthalocyanine core (**1.6**). The phthalocyanine emission was also observed when the compound was excited at the phthalocyanine core wavelength. However, when a styryl-BODIPY was attached to the silicon centre in the same way (**1.7**), different energy-transfer behaviour was observed. When excited at the styryl-BODIPY wavelength, very weak emission from the BODIPY and the phthalocyanine was observed. This shows that energy transfer from the BODIPY excited state to the phthalocyanine does occur, but the subsequent emission is largely quenched, presumably by an electron-transfer process. Phthalocyanine fluorescence is also very weak when the molecule is excited at the phthalocyanine excitation wavelength (613 nm). This weak fluorescence would also be due to the same electron-transfer process, as energy-transfer from the phthalocyanine to the styryl-BODIPY core is energetically unfavourable. This

showed that an electron-transfer process is switched-off for the non-styryl-BODIPY analogue upon phthalocyanine excitation, but switched-on in the styryl-BODIPY analogue.[109]

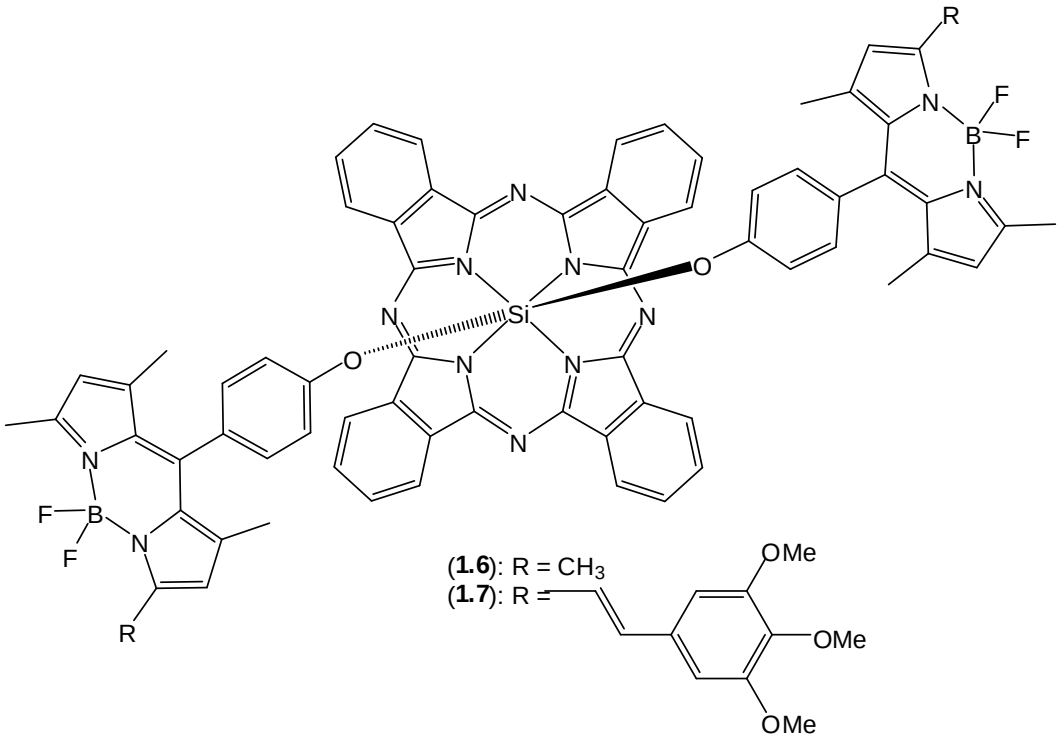

Figure 1. 19: Di-BODIPY-phthalocyanine array

Energy transfer to the BODIPY can be achieved through careful selection of both the BODIPY used and the attached fluorophore. Energy transfer from the silicon phthalocyanine to the BODIPY is energetically unfavourable due to the lower energy light that is absorbed by the silicon phthalocyanine being unable to promote an electron onto the higher energy LUMO of the BODIPY; but by using a subphthalocyanine and a di-styryl-BODIPY energy-transfer to the BODIPY was found to occur.

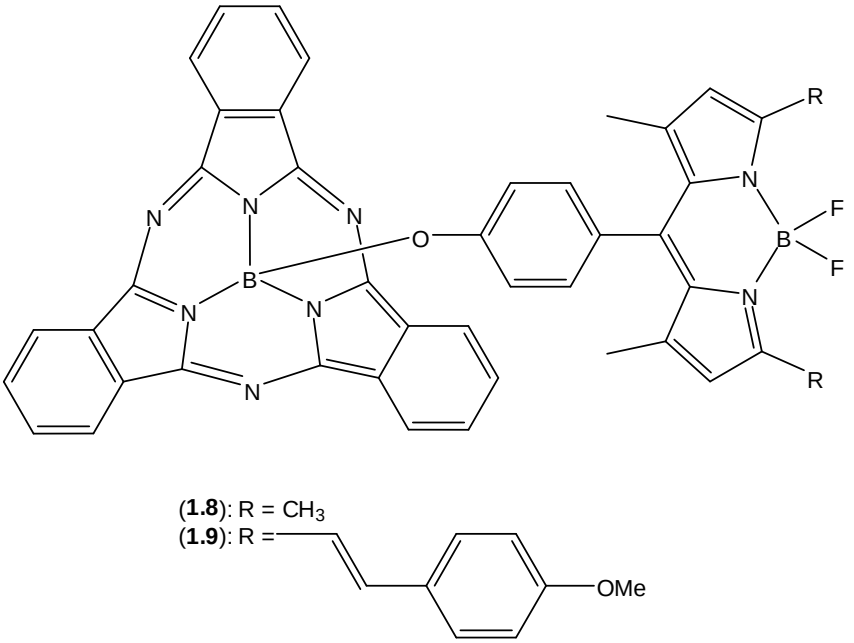

(**1.8**): R = CH_3
(**1.9**): R =

Figure 1. 20: BODIPY-sub-phthalocyanine array

For compound **1.8**, where only methyl groups are attached to the BODIPY, when excited at 470 nm (partial BODIPY excitation avoiding excitation of the boron-subphthalocyanine) energy-transfer occured onto the boron-subphthalocyanine and emission was observed at 570 nm. However, when the di-styryl-BODIPY (**1.9**) was used, excitation of the sub-phthalocyanine at 515 nm caused energy-transfer to the BODIPY and subsequent emission at 653 nm. The energy transfer quantum yield for both processes was calculated to be 98%.[94]

Through-space energy-transfer has also been shown to occur between a BODIPY-zinc porphyrin-phenanthroline and an *N*-unsubstituted imidazole-H_2-porphyrin-phenanthroline system. The imidazole appended porphyrin was tethered to the zinc-porphyrin-phenanthroline unit by hydrogen bonding between the imidazole NH and two of the phenanthroline nitrogens, as well as a coordinative bond between the zinc (II) centre and the imidazole free nitrogen.[110, 111] Despite the lack of any covalent bond between the two units, energy-transfer still occured from the BODIPY fluorophore to the H_2-porphyrin with a net efficiency of 80%. Energy transfer from the zinc-porphyrin-imidazole complex to the H_2-porphyrin occurred with an efficiency of 85%.

Both energy- and electron-transfer have been shown to occur sequentially in a BODIPY-zinc-porphyrin-crown ether triad bound to a fulleropyrrolidine.[112] In this triad (**1.10**) energy-transfer occurred from the BODIPY to the zinc porphyrin followed by electron-transfer from the zinc porphyrin to the fullerene unit. When excited at 495 nm (BODIPY excitation) both emission from the BODIPY and the zinc porphyrin was observed. The emission from the BODIPY core was partially quenched by the energy transfer to the zinc porphyrin with an efficiency of ~97%. A small anodic shift of the zinc porphyrin in the cyclic voltammogram of the triad coordinated to the fullerene, compared to the free triad, indicated interactions between the zinc porphyrin and the fullerene unit.

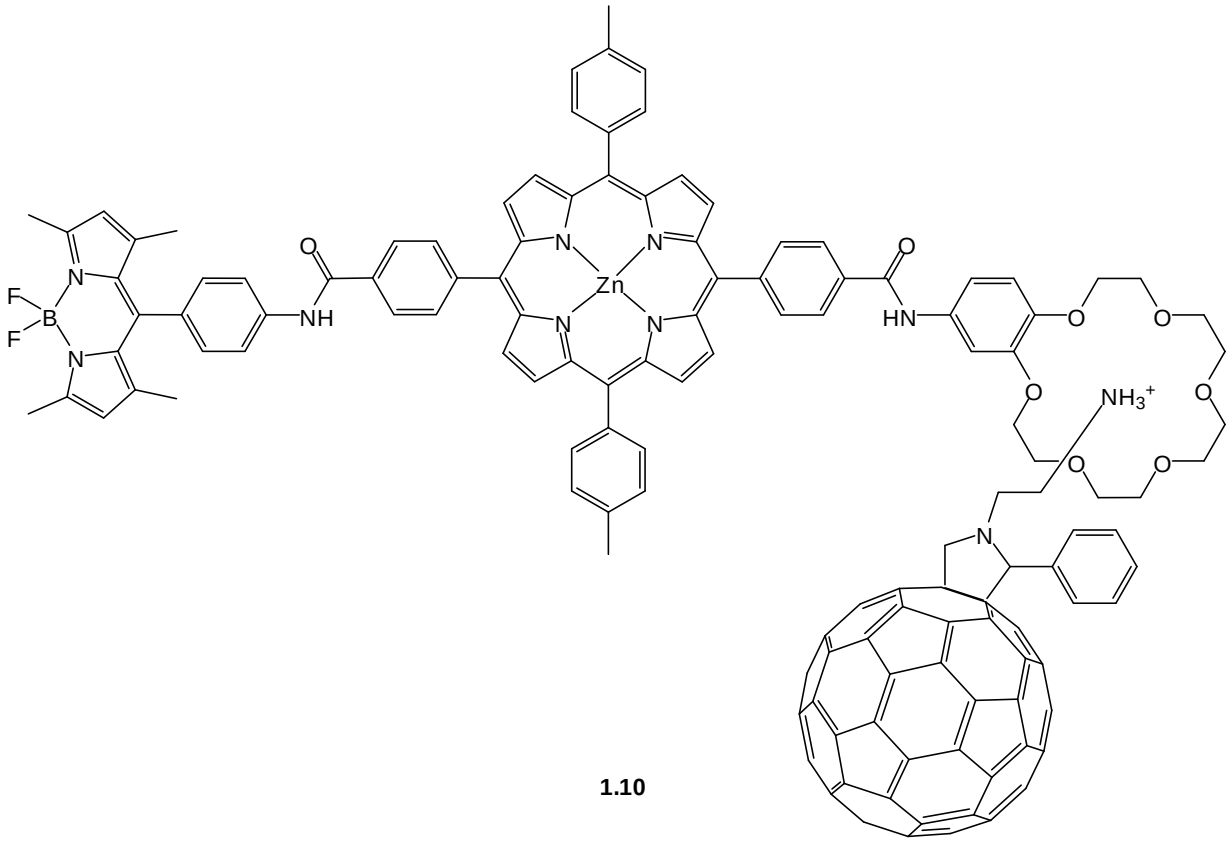

1.10

Figure 1. 21: BODIPY-porphyrin-fullerene array

An energy diagram was constructed showing the various processes involved in this triad system (Fig. 1.22). As can be seen, the initial step is either the excitation of the BODIPY followed by energy-transfer to the zinc porphyrin, or this step can be bypassed by directly exciting the zinc porphyrin. This is followed by charge separation to give the mono-

cationic zinc porphyrin and the mono-anionic fullerene, which then undergoes charge recombination to give the ground state compound again. A small amount of the singlet excited state zinc porphyrin undergoes intersystem crossing to produce the triplet excited zinc porphyrin, which can either phosphoresce or still undergo charge separation to give the charge separated species before charge recombination.

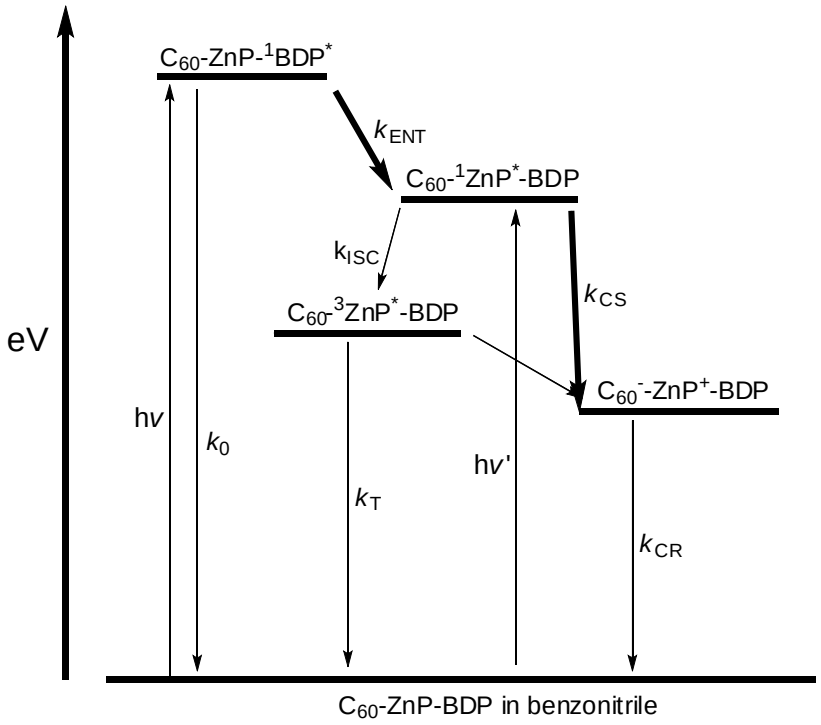

Figure 1. 22: Energy level diagram showing the different photochemical processes of the BODIPY-zinc-porphyrin-crown ether triad (10) when coordinated to the fullerene unit (major processes are bold arrows)

A similar series of compounds has been prepared which consists of one-, two- and four-BODIPYs (one attached to each phenyl ring of the zinc-porphyrin) attached by amide linkers.[113] In the case of the two-BODIPY array, the two donor units were attached in a *trans*-configuration. A fullerene terminating in an imidazole unit was then coordinated to the zinc centre (effectively forming a square-pyramidal zinc centre) to allow electron transfer to occur. The larger number of BODIPY units increased the absorption peak corresponding to the BODIPY, effectively increasing the antenna effect of this array. A similar energy diagram to the one shown in Fig. 1.22 was produced for this compound.

A simple BODIPY-fullerene dyad has also been shown to assume the triplet state by charge recombination.[114] In this array, singlet-singlet energy transfer occurred very rapidly from the BODIPY to the fullerene unit. The fullerene triplet state is then occupied by inter-system crossing. Due to the fullerene having a long triplet lifetime, triplet-triplet energy transfer occurs from the fullerene to the BODIPY despite the higher thermodynamic position. This caused an enhanced triplet yield for the BODIPY, which is usually less than a few percent, to approximately 25%. The rate of energy transfer in this dyad was found to be highly sensitive to the solvent system used, with electron transfer from the BODIPY onto the fullerene being quicker and the charge-transfer state being longer lived in a polar solvent (benzonitrile in this case when compared to toluene, dichlomethane and methyl-tetrahydrofuran).

Attachment of BODIPYs to a perylenediimide core has become increasingly common and has recently been achieved using click chemistry. This copper (0) catalyzed reaction has been utilized to attach four and six BODIPY 'arms' onto a perylenediimide core with both compounds showing energy transfer from the BODIPYs to the perylenediimide (**1.11**).[115, 116] While the absorption spectrum of the tetra-BODIPY-perylenediimide array showed absorption from the BODIPY and the perylenediimide, the emission spectrum only showed emission from the perylenediimide core, indicating efficient energy transfer (99%). The emission from the perylenediimide core was actually enhanced when excited at the BODIPY wavelength (compared to direct excitation at the perylenediimide core (588 nm)), indicating an 'antenna' effect. A similar effect was seen for the *hexakis*-BODIPY-perylenediimide. Due to the presence of additional BODIPY units, the absorption peak of these units was found to be more intense. That there was only a negligible increase in energy transfer when two additional BODIPY units are added; supports the theory that BODIPYs are very efficient energy transfer materials.

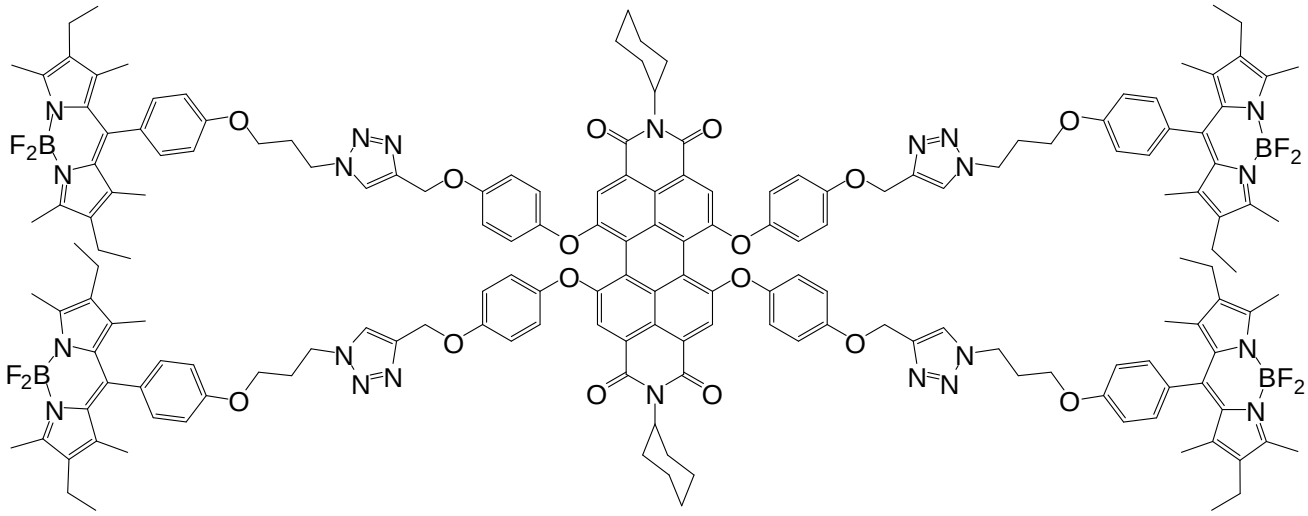

1.11

Figure 1. 23: Tetra-BODIPY-perylenediimide array

Click chemistry has also been used to connect three different BODIPYs together in an energy-transfer array (**1.12**).[95] In this array, both BODIPY 'arms' acted as donors for the central BODIPY acceptor. The styryl units on the central BODIPY had the effect of red-shifting the absorption and emission wavelengths of this unit, hence making it the acceptor. When excited at 501 nm (tetra-methyl BODIPY 'arm') and 572 nm (mono-styryl BODIPY 'arm') emission was observed at 662 nm (central di-styryl BODIPY). This emission was also observed when the central BODIPY was excited directly. The efficiency of energy transfer from both BODIPY 'arms' was calculated to be 99% in each case.

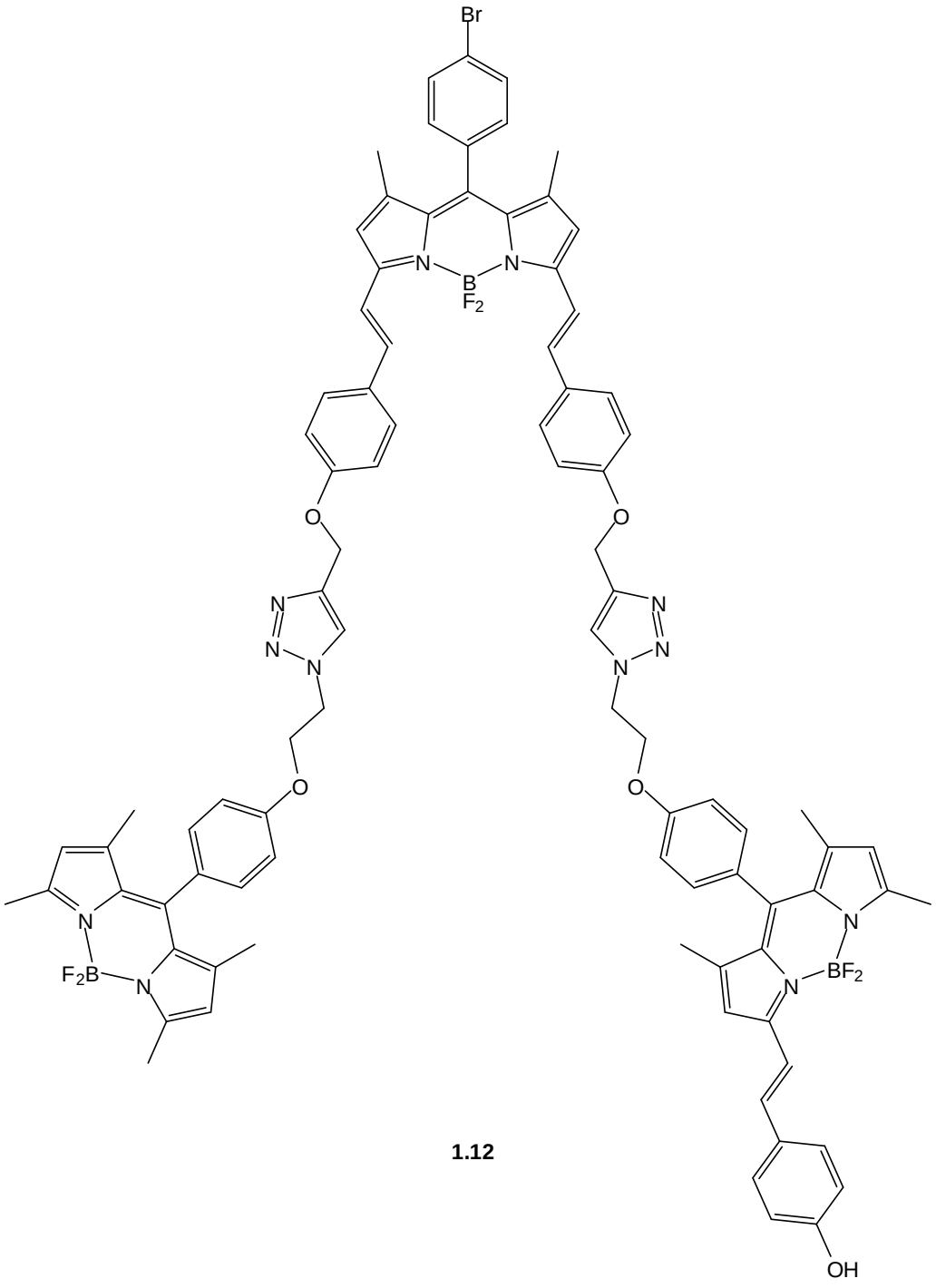

1.12

Figure 1. 24: Tri-BODIPY array

2.8.2 Through-bond energy-transfer cassettes

Förster energy transfer is the primary mechanism by which through-space energy-transfer occurs. This is mainly governed by the spectral overlap of the donor fluorescence and the acceptor absorbance. However, if the donor and acceptor are joined by a conjugated system of multiple bonds, then through-bond energy-transfer can occur. The conjugated system must be twisted or the whole molecule will act as one fluorophore. This mode of energy transfer does not follow the same rules as through-space energy-transfer. Good spectral overlap is not required, meaning that an array with a large "apparent Stokes shift" can be produced.

Lindsey made the initial studies into the efficiency of through-bond energy-transfer involving BODIPYs as donor units.[117] The main factors affecting through-bond energy-transfer were proposed as being steric interaction, characteristics of the HOMO and LUMO and the site of attachment and type of linker between the donor and acceptor. Increased rotational restriction was found to reduce both the rate and the efficiency of energy transfer. Due to the energy transfer occurring along the conjugate system, through-bond energy-transfer arrays have been described as molecular wires. Various BODIPY-porphyrin through-bond energy-transfer cassettes have been synthesised to investigate the energy transfer properties of such systems.

The multi-porphyrin array depicted in **1.13** shows an example of a linear molecular wire.[23] As in the previous examples, the BODIPY was the donor component while the free-base porphyrin was the acceptor component. Despite the distance between the donor and acceptor (90Å in this case) efficient energy transfer still occured (76%). This is an example of a through-bond energy-transfer array in which the terminal porphyrin is the acceptor component; however, there are BODIPY-porphyrin arrays in which the terminal unit is not the acceptor.

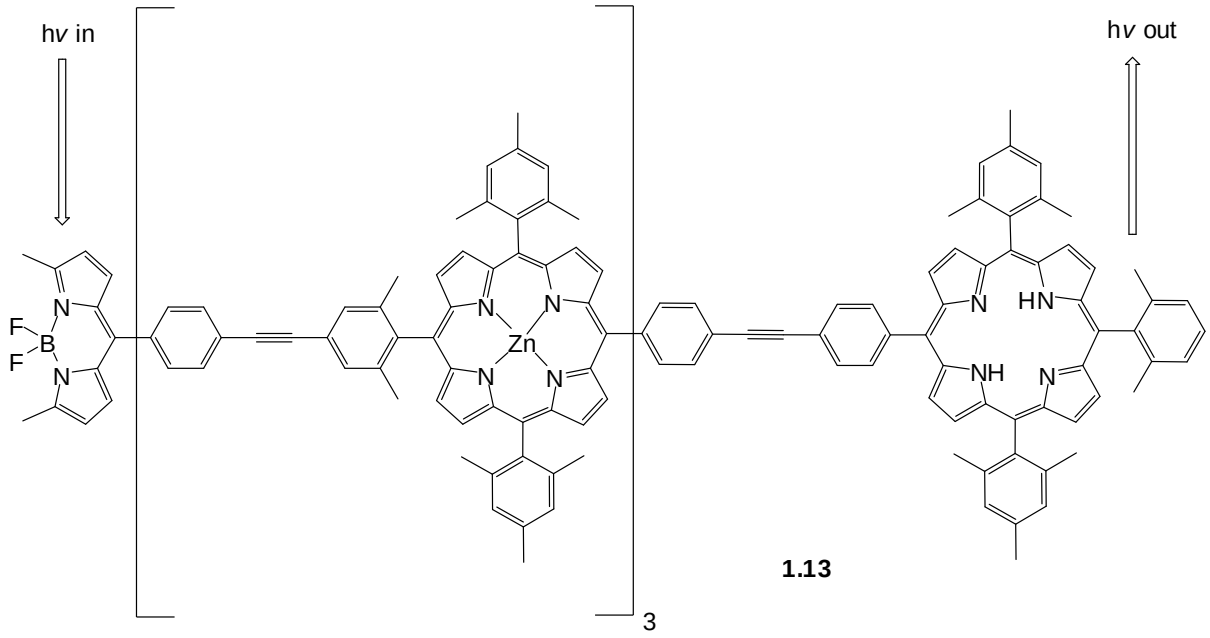

1.13

Figure 1. 25: BODIPY-tetraporphyrin array

Molecular optoelectronic linear- and T-gates have been synthesised showing fluorescence ON/OFF switching by oxidising or reducing an ancillary magnesium porphyrin (**1.14** and **1.15**).[118] When the magnesium centre was in its 2^+ state, fluorescence occured at the free-base porphyrin by through-bond energy-transfer from the BODIPY donor. When oxidized or reduced, fluorescence was quenched by intra-molecular charge transfer. Energy transfer in these compounds was also very efficient with values exceeding 80% for each array.

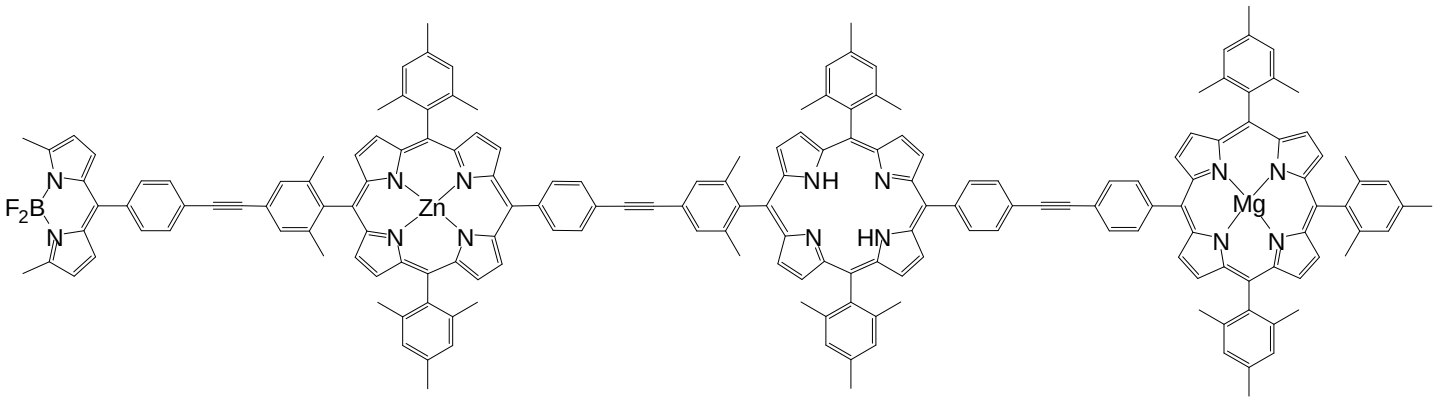

1.14

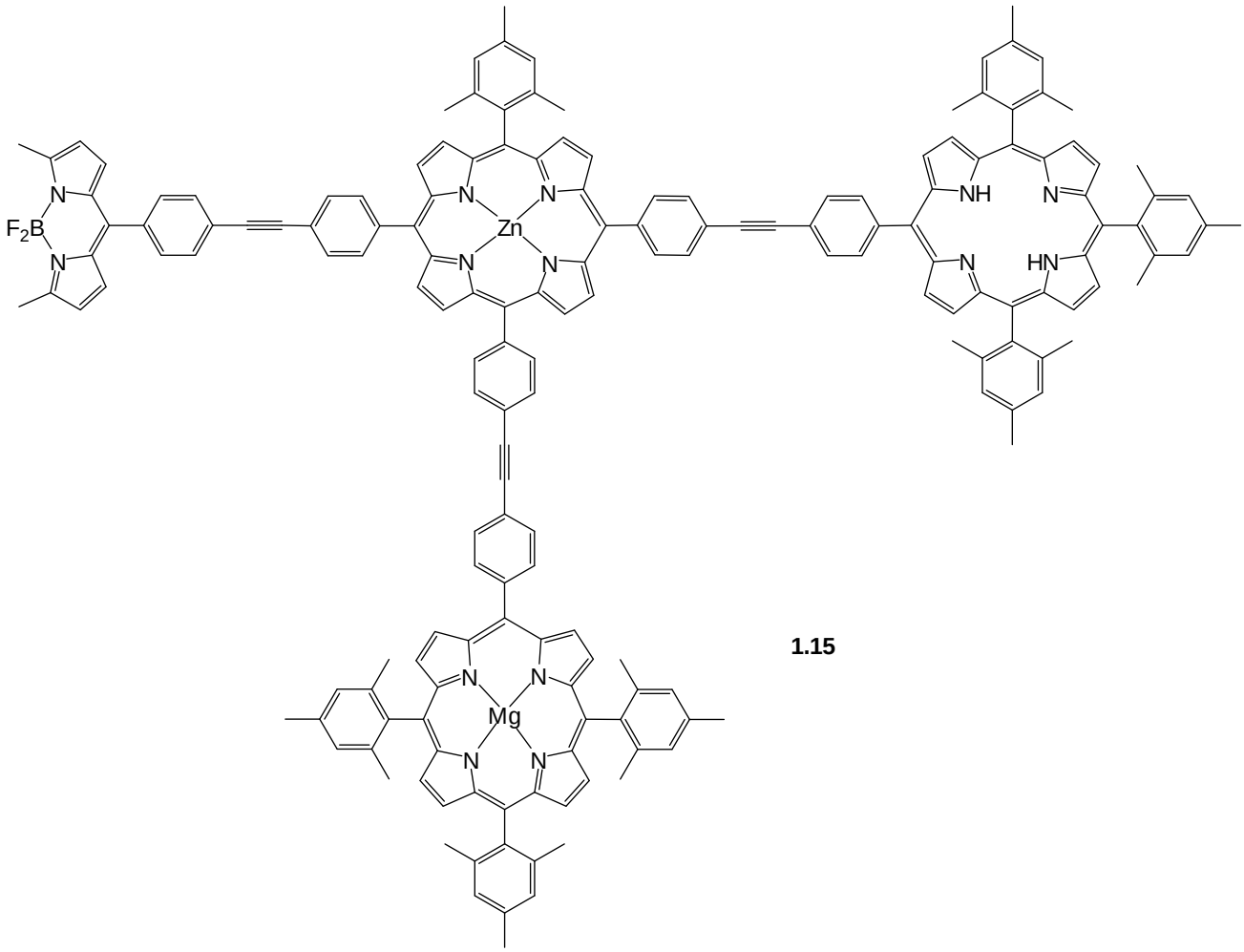

1.15

Figure 1. 26: BODIPY-porphyrin arrays

Multi-BODIPY-porphyrin arrays have also been synthesised in order to increase the antenna effect of the BODIPY units.[119] One, two (**1.16** and **1.17**), four and eight BODIPY arrays have been prepared; each using the same BODIPY fluorophore. As seen for the multi-BODIPY-perylenediimide arrays, increasing the number of BODIPY units had little effect on the energy transfer efficiency, but increased the amount of light absorbed by the compound at the BODIPY excitation wavelength. While the energy transfer efficiency of the mono- and di-BODIPY arrays was almost quantitative, the eight-BODIPY array displayed an efficiency of between 80-90%. In each case, the BODIPY was attached to the porphyrin *via* a phenyl-ethynyl linker. In this series of compounds, the eight-BODIPY array consisted of a free-base porphyrin with two BODIPY units attached to each of the four phenyl rings in the same fashion as the array depicted in **1.17**. The four-BODIPY array was similar to the eight-BODIPY array in that a BODIPY is linked to each of the four phenyl rings of the porphyrin. Interestingly, a dithiaporphyrin analogue of the four-BODIPY system showed poor electron transfer (~11%) when excited at 485 nm.[120]

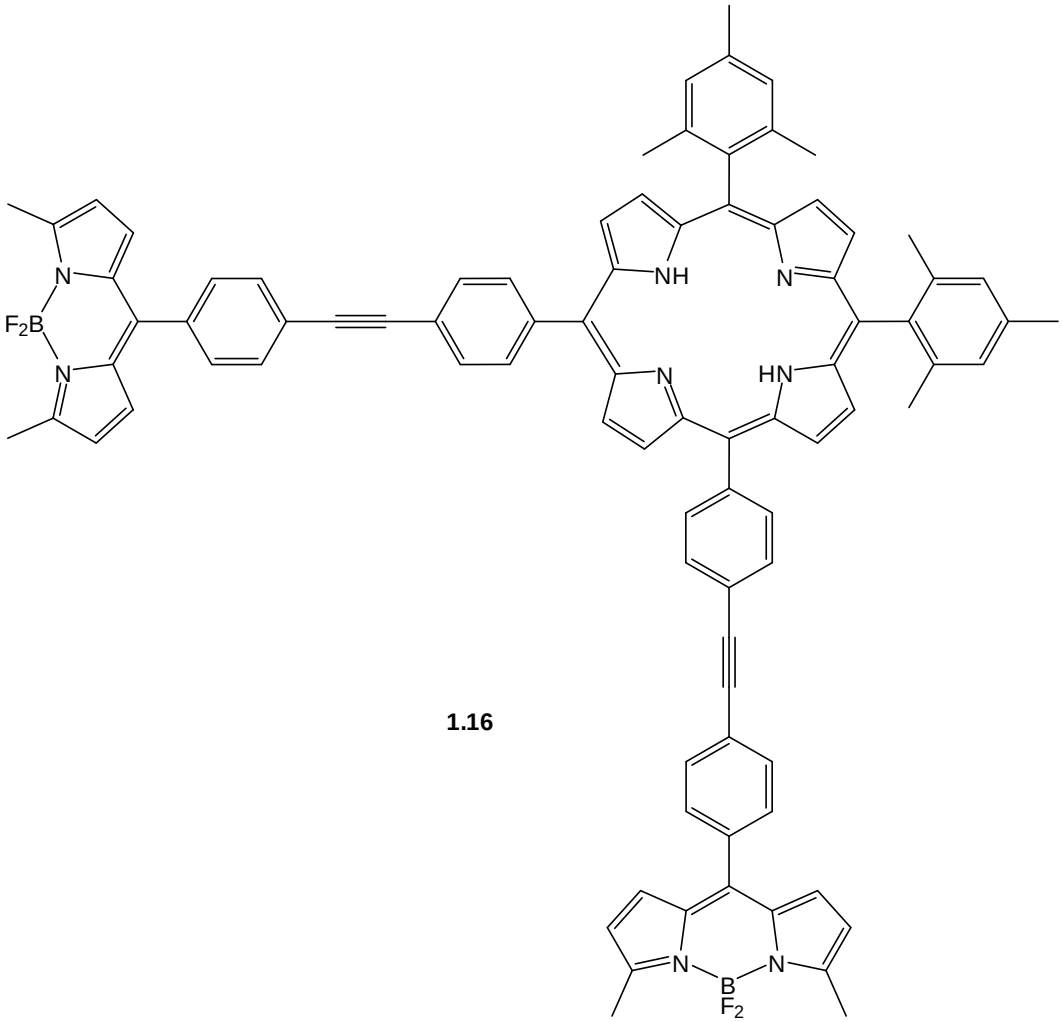

1.16

Figure 1. 27: Di-BODIPY-porphyrin array

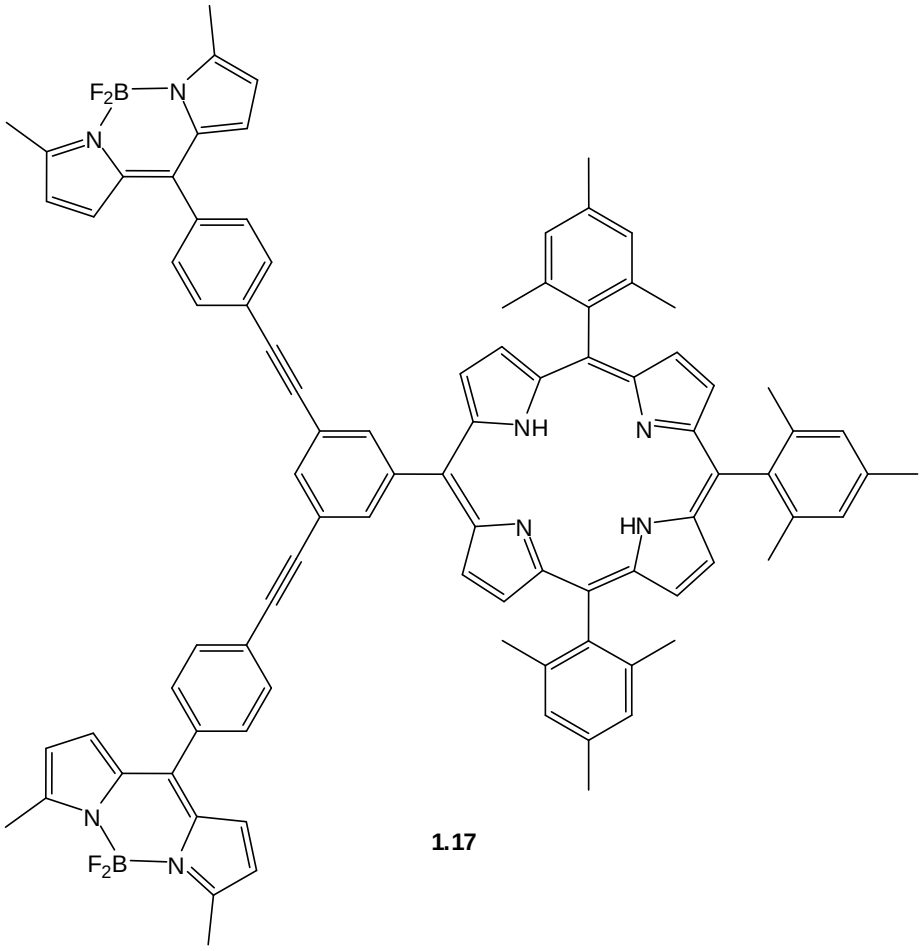

1.17

Figure 1. 28: Di-BODIPY-porphyrin array with BODIPY attachment at the same phenyl ring

Through-bond energy-transfer arrays consisting of BODIPY donors and 21-thia- or 21-oxoporphyrins have been prepared in a similar fashion to the methods used for the preparation of previous examples (**1.18** and **1.19**).[121, 122] For both of these porphyrin analogues, efficient energy transfer was observed as the porphyrin emission was enhanced when the array was excited at 485 nm. These reported energy transfer arrays are interesting, but a direct comparison is difficult as the orientations of the BODIPY units were different for each compound.

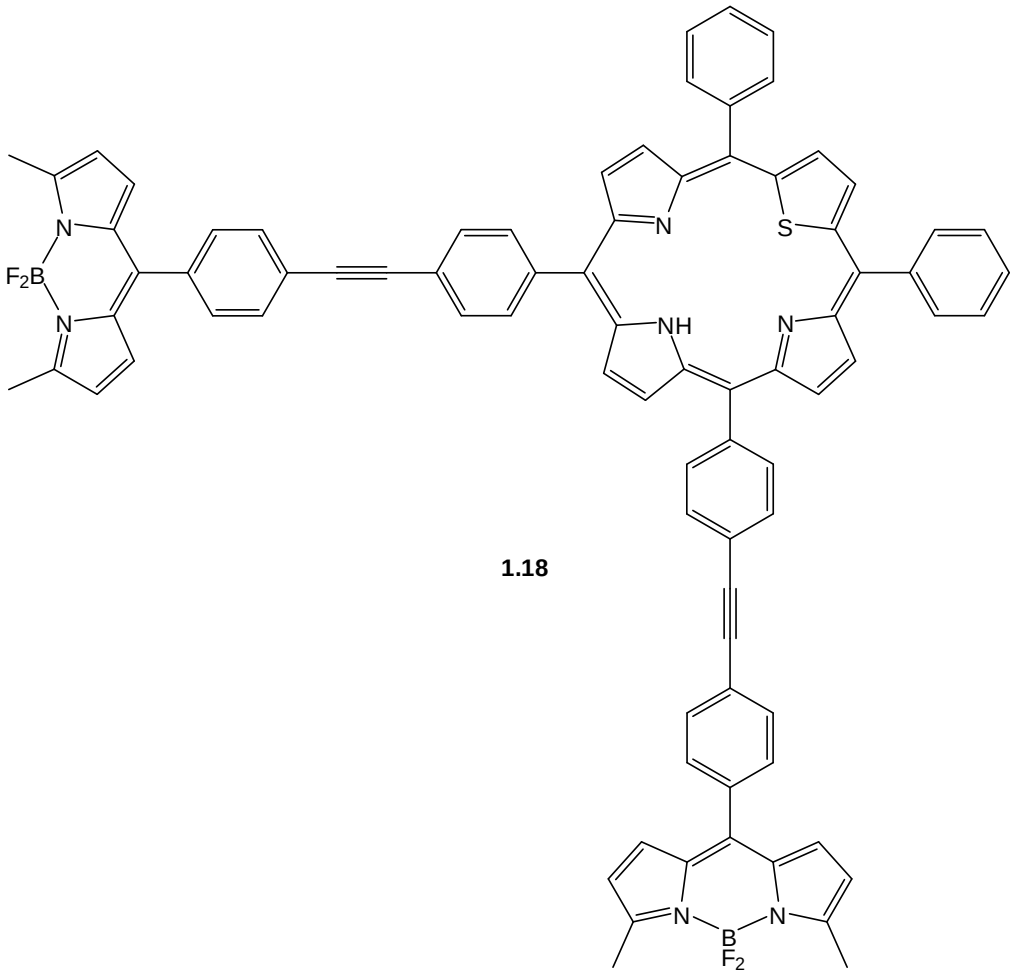

1.18

Figure 1. 29: Di-BODIPY-thiophyrin array

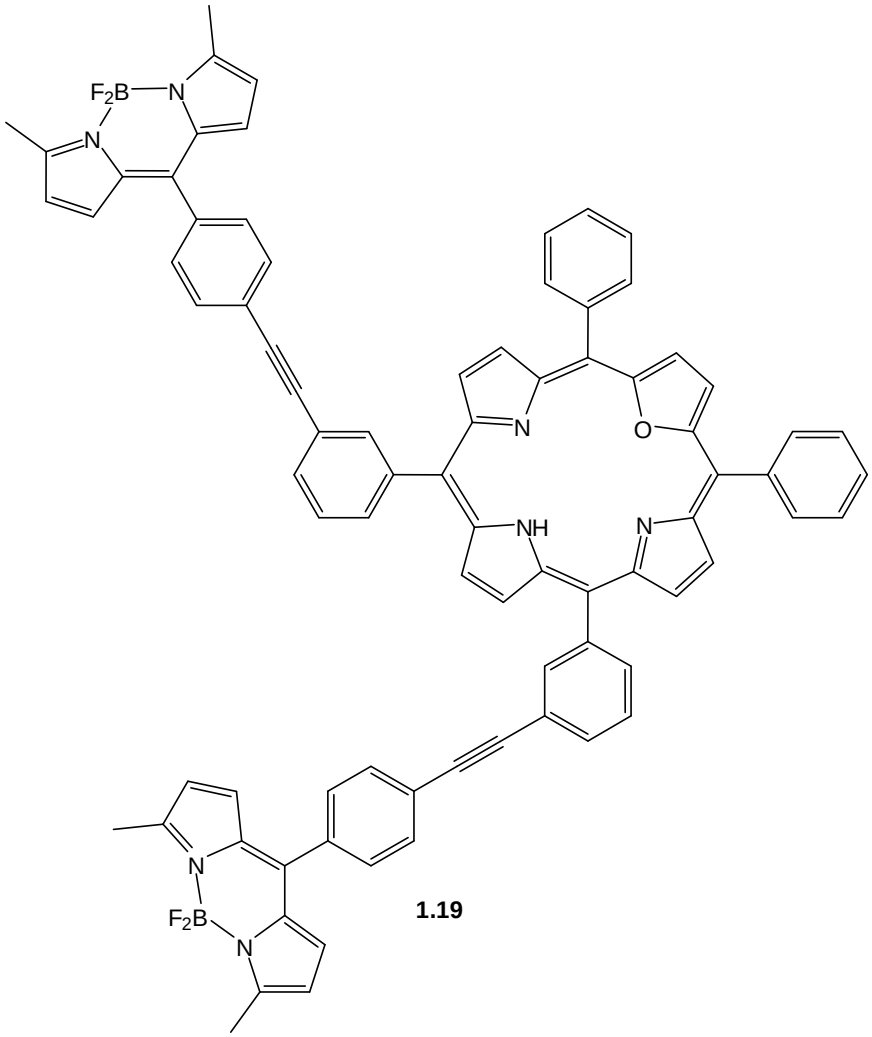

1.19

Figure 1. 30: Di-BODIPY-oxophyrin array

This highly efficient energy transfer from BODIPYs to porphyrins has been exploited for photocurrent generation.[123] In this system, a BODIPY was the terminal donor unit and was attached to a zinc-porphyrin acceptor unit, which also acted as the electron donor in a similar way to previous examples. This donor-acceptor system was then coordinated to a tri-osmium-fullerene unit, which could act as both an electron acceptor and donor. Diazabicyclooctane (DABCO) was then used to tether these arrays together by coordinating to two of the zinc-porphyrins *via* their axial positions. This ensured a high surface coverage when bound to the electrode. The supramolecular array was then exposed to indium-tin oxide (ITO) which acted as one of the electrodes, the other being platinum. Photocurrent generation was initiated by excitation of the terminal BODIPY,

which transfered its energy (through-bond) to the zinc-porphyrin. Electron transfer then occured from the zinc-porphyrin to the fullerene, and subsequently from the fullerene to the ITO electrode. A sacrificial electron donor (ascorbic acid) was also used. The photocurrent generation efficiency was calculated as being 29%. This array was also found to be highly thermally and electrochemically stable.

While it has been shown that porphyrins are useful in constructing energy transfer cassettes, this also provides a limitation on the types of arrays that can be formed. BODIPYs with metal complexes attached to them also provide an interesting class of compound that can be used as energy- and electron-transfer arrays. Several polypyridine complexes of BODIPYs have been prepared and their energy- and electron-transfer properties have been investigated. Analogues of compound **1.20** have been prepared consisting of one or two BODIPY fluorophores, *bis*- or *ter*-pyridine ligands, and various linker groups.[25-27, 124] Metal (II) polypyridine complexes were chosen because of their intense and long-lived triplet metal-to-ligand change transfer (MLCT) emission.

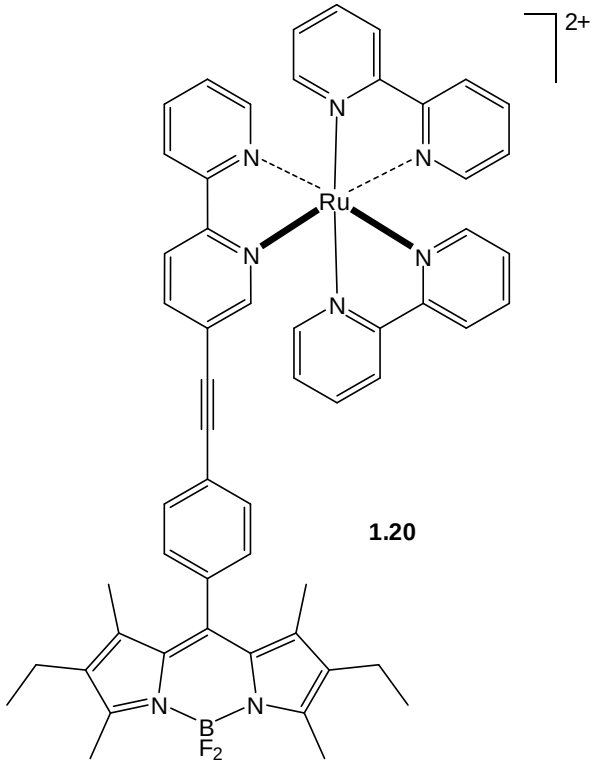

Figure 1. 31: BODIPY-bipyridyl-ruthenium complex

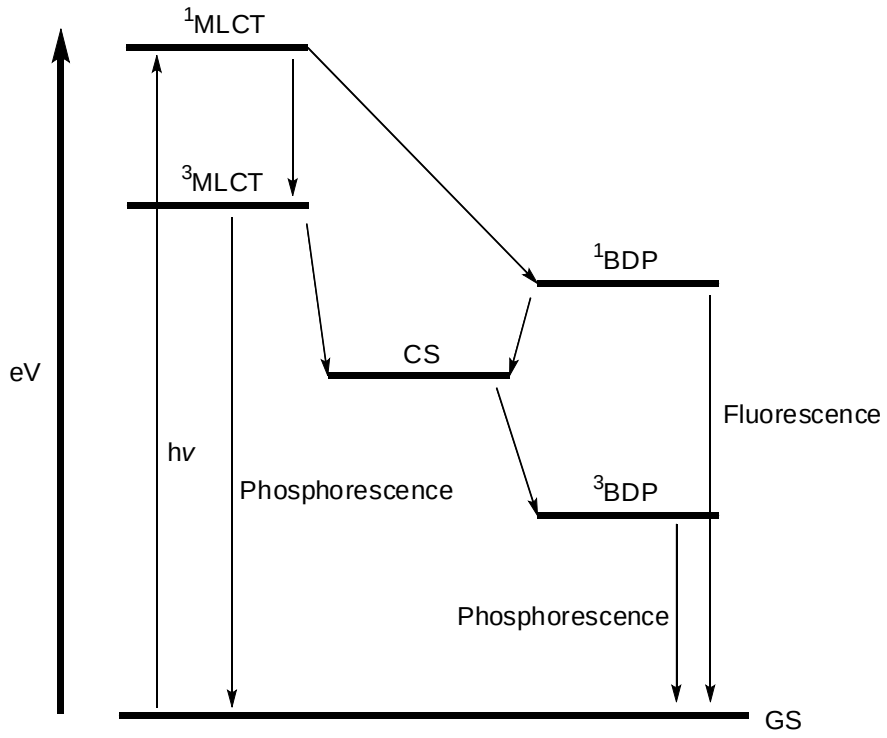

Figure 1. 32: Energy level diagram showing the various photochemical processes involved in the transfer of energy from the metal complex to the BODIPY

For the ruthenium complexes at 77K in a rigid matrix, the energy transfer mechanism appears to proceed *via* initial excitation of the ruthenium-polypyridine complex to the ^{1}MLCT state, followed by transfer of this energy to the ^{1}BDP (BODIPY singlet state) state (Fig. 1.32). This process can only proceed if the ^{1}MLCT and the ^{1}BDP energy levels are similar. The ^{3}BDP (BODIPY triplet state) state can be reached *via* a charge-separated state. Phosphorescence can occur in some of the compounds and is attributed to the presence of the ruthenium, which promotes inter-system crossing from the ^{1}BDP state to the ^{3}BDP state by the "heavy atom effect". The ^{3}BDP state can also be reached *via* energy transfer from the ^{3}MLCT state if the energy levels are close enough as this process would be spin-allowed.[125, 126] Some BODIPY-ruthenium complexes have been prepared that have the effect of quenching fluorescence *via* energy transfer.[127] In the case of compounds **1.21** and **1.22**, the ^{1}BDP state was quenched by energy transfer to the ruthenium centre with 93% and 73% efficiency respectively. This transferred energy was then lost *via* electron transfer and singlet to triplet inter-system crossing.

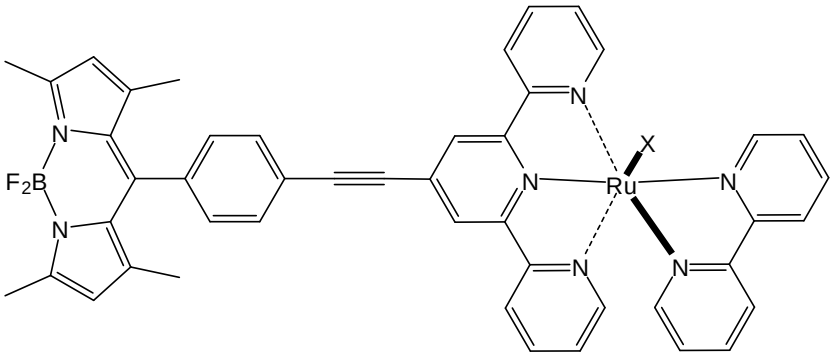

(**1.21**): X = Cl
(**1.22**): X = NCS

Figure 1. 33: BODIPY-oligopyridine-ruthenium complex

Zinc-polypyridine complexes have been incorporated into energy transfer arrays in a similar fashion to the ruthenium complexes.[128] In these complexes, the fluorescence of the BODIPY was quenched by intramolecular electron transfer (**1.23** and **1.24**). Extension of the distance between the terminal BODIPYs and the zinc centre, by incorporation of ethynyl groups, decreased the electronic coupling but electron transfer still occured to a large extent resulting in fluorescence quenching. Analogous to the ruthenium complexes, the ^{3}BDP state was at a lower energy than the charge-separated state but in this case charge-recombination occured preferentially over triplet state formation. It was proposed that charge-recombination could be enhanced by preferential localisation of the positive charge at the *meso*-carbon in the BODIPY π-radical level or by quantum mechanical effects.

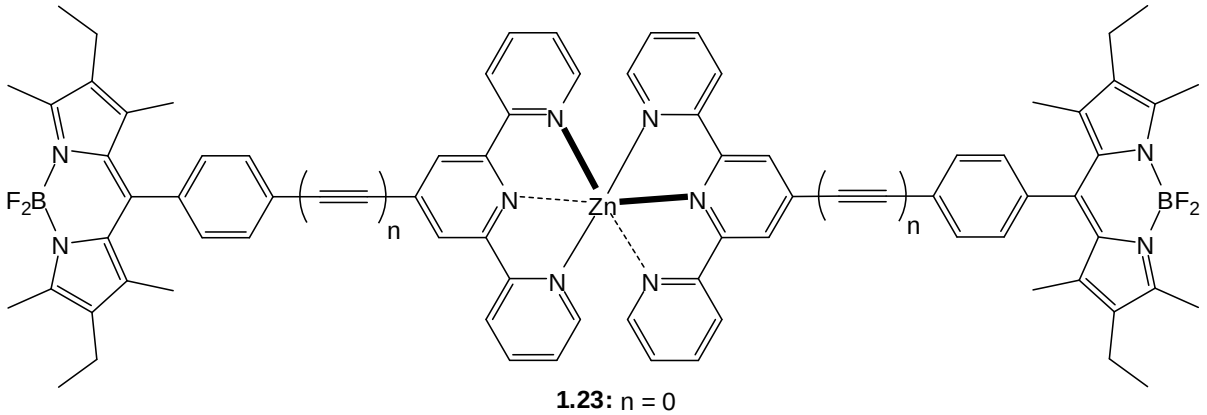

1.23: n = 0
1.24: n = 1

Figure 1. 34: BODIPY-terpyridine-zinc dimer

Platinum complexes analogous to **1.25** have been prepared and the corresponding energy transfer behaviour has been observed.[129, 130] Compound **1.25** did not exhibit any fluorescence quenching of the BODIPY compared to the zinc complex. However, luminescence from the ^{3}MLCT of the platinum centre was quenched by energy transfer to the ^{3}BDP state both at 77K and at room temperature. The heavy metal centre also promoted inter-system crossing in the BODIPY and allowed phosphorescence to occur.

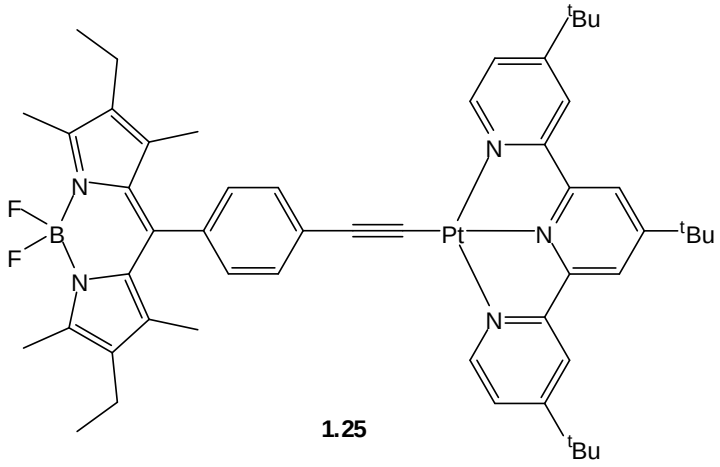

1.25

Figure 1. 35: BODIPY-terpyridine-platinum complex

Mono- and di-styryl (**1.26** and **1.27**) analogues of **1.25** have also been prepared as well as an array involving an ethynyl pyrene unit which replaced the fluorine substituents on the boron centre (**1.28**).[130] In each of these arrays, excitation to the ^{1}MLCT state lead to decay to the ^{3}MLCT state instead of the ^{1}BDP state. In the analogues **1.27** and **1.28**,

triplet-triplet energy transfer *via* a charge-separated state was found to be almost quantitative. While still efficient in **1.26** (>90%), the triplet-triplet energy transfer was less efficient due to a shorter ^{3}MLCT lifetime. In **1.28**, through-space energy-transfer occured quantitatively from the pyrenyl moieties to the BODIPY. This means that the ^{3}BDP is occupied by an electron from the charge-separated state (generated from the ^{3}MLCT), while the ^{1}BDP state is acting as an acceptor for energy from the pyrene units. When these compounds are held in a rigid matrix at 77K, this charge-separated state did not appear to be the intermediate by which the energy from the ^{3}MLCT was transferred to the ^{3}BDP state. The most likely energy transfer mechanism in this case would be through-bond energy transfer. Being held at 77K also allowed phosphorescence of **1.28** to be observed. It was assumed that phosphorescence would occur from **1.26** and **1.27**, but was more difficult to detect as it would emit in the infra-red region.

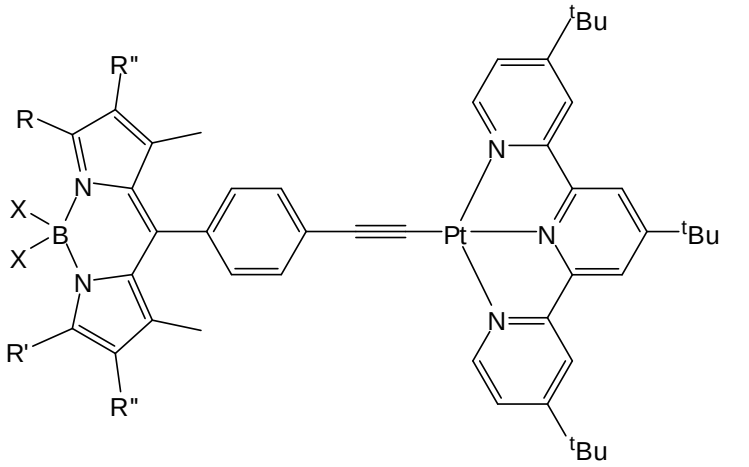

1.26: X = F; R = CH_3; R" = H; R' = OMe

1.27: X = F; R" = H; R = R' = NMe_2

1.28: R = R' = CH_3; R" = Et; X = Pyrene

Figure 1. 36: BODIPY-terpyridine-platinum complexes with differeing acceptor moieties

Due to the high stability and versatility of ferrocene derivatives, they have also been incorporated into electron transfer systems involving BODIPYs. In the case of the styryl-ferrocenyl-BODIPY (**1.29**), it was found that the molecule underwent remarkable electrochromism.[131] A clearly visible colour change occurred when the molecule went from its neutral to oxidised state (purple) and back again (blue). Compound **1.30** did not exhibit any fluorescence due to electron transfer from the ferrocene to the BODIPY.[132] Electrochemical studies showed that the ferrocene unit was difficult to oxidise, but the BODIPY unit was relatively easily reduced. A ferrocene moiety has also been used in the preparation of a ferrocene-BODIPY-fullerene triad.[133] This triad caused charge stabilisation, allowing electron transfer to occur readily. Excitation of the BODIPY causes abstraction of an electron from the ferrocene moiety, producing a BODIPY anion radical. A second electron transfer then occurs from the BODIPY onto the fullerene unit. Due to the distance between the cation and anion radicals, charge stabilisation was achieved.

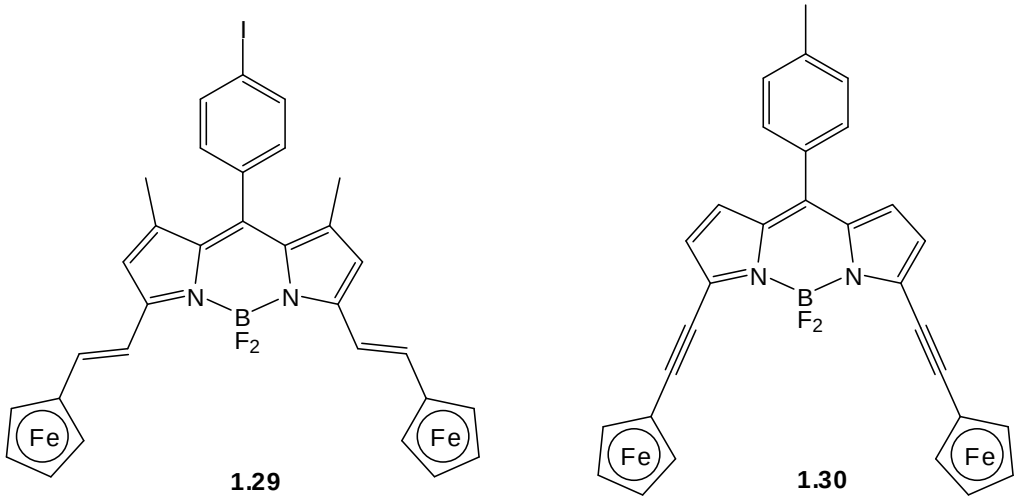

Figure 1. 37: BODIPY-ferrocene arrays

While energy transfer arrays based on porphyrins and metal complexes display remarkable potential as molecular wires and fluorescent switches, the size and synthetic routes employed to prepare these molecules precludes much of their practical use for optoelectronic applications. It seems necessary, therefore, to prepare smaller cassettes *via* simpler synthetic routes. To this end, several BODIPYs bearing anthracene moieties have been prepared and their energy transfer effects studied. Compound **1.31** had the

anthracene unit attached directly to the 5-position of the BODIPY.[134] Despite the lack of methyl groups on the BODIPY core, the anthracene unit adopted a near orthogonal geometry with respect to the BODIPY plane. This near orthogonal geometry was also observed in the 1,3,5,7-tetramethyl analogue of the same BODIPY.[78] This BODIPY appeared to undergo similar photochemical processes as those depicted in Fig. 1.22. The ^{1}BDP state can undergo charge-separation with subsequent formation of the ^{3}ANT state. This ^{3}ANT state can then decay to the ^{3}BDP state. This energy transfer (which was susceptible to changes in temperature) did not occur to any great extent, and thus made this particular compound unsuitable as an energy transfer array.

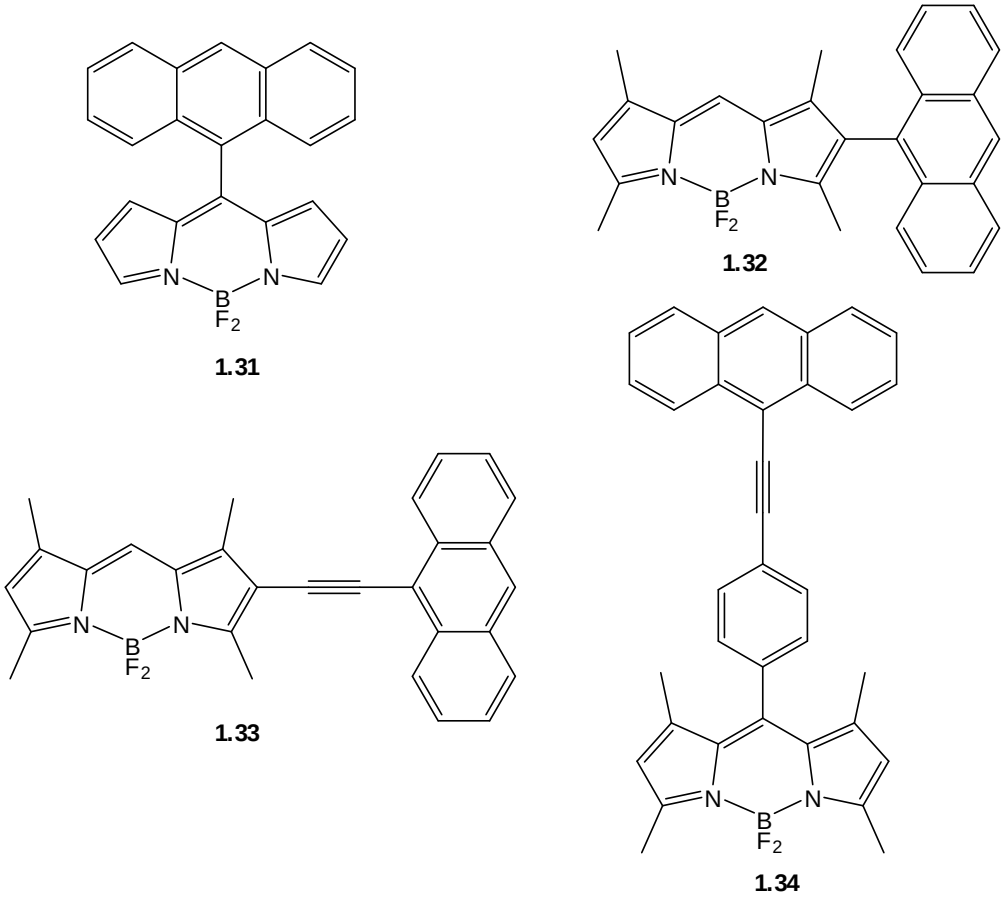

Figure 1. 38: BODIPY-anthracene arrays

A series of anthracenyl-BODIPYs were synthesised to investigate the effects of differing donor-acceptor separation and attachment position on their energy transfer properties.[15] It was shown that arrays analogous to compound **1.34** displayed energy transfer, but despite

several acceptor BODIPY units being investigated, no correlation between the structure of the acceptor and the efficiency of energy transfer was observed. In arrays such as **1.32** and **1.33**, much faster energy transfer was observed. Greater steric effects around the site of attachment to the BODIPY force the anthracenyl moiety out of the plane of the BODIPY. This, however, proved to be problematic as the energy transfer was too fast to allow measurements of the exact rate to be determined, meaning that a relationship between energy transfer and donor-acceptor separation may exist, but cannot be measured. This may, however, imply that the orientation of the BODIPY has a greater effect on the energy transfer than the BODIPY substitution.

Replacement of the fluorine substituents on the boron atom provides another route towards the preparation of energy transfer cassettes. Pyrene and perylene donors have been attached to the boron atom (**1.35-1.38**) and efficient energy transfer occured to the BODIPY acceptor; only emission from the BODIPY was observed.[135] A competing energy transfer process takes place in compound **1.36** as energy absorbed by the pyrene unit can be transferred to the perylene unit with a similar efficiency as it is transferred to the BODIPY. In particular, compound **1.36** showed potential as a light harvester due to strong absorptions in the UV region from the pyrene and perylene units. The energy transfer properties of this type of array have been used to develop an orthogonal sensor.[136] Compound **1.38** displayed efficient energy transfer from the pyrene units to the BODIPY as expected. Exposure of compound **1.38** to protons switched on an intra-molecular charge transfer process, thus decreasing the fluorescence of the BODIPY. This also caused the absorption band of the BODIPY to undergo a red-shift. As the absorption of the pyrene moieties is insensitive to cation coordination, the red-shift in BODIPY absorption caused a decrease in the rate of through-space energy transfer, thus restoring some of the pyrene fluorescence.

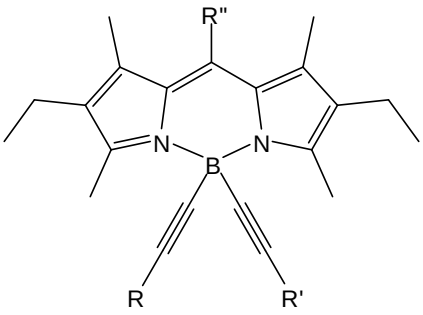

(**1.35**): R = R' = Pyrene; R" = CH_3
(**1.36**): R = Pyrene; R' = Perylene; R" = CH_3
(**1.37**): R = R' = Perylene; R" = CH_3
(**1.38**): R = R' = Pyrene; R" = 4-Pyridyl

Figure 1. 39: BODIPY arrays prepared by *F*-substitution

As an extension of this work, a BODIPY which absorbs and emits in the red region was prepared and pyrene moieties attached to the boron atom in a similar fashion.[137] In each compound of the series **1.39**-**1.43** efficient energy transfer occured from the aromatic moiety tethered to the boron atom and only emission from the BODIPY core was observed. The BODIPY itself emitted at 750 nm so there was a very large apparent Stokes' shift. Even in compound **1.43**, where two different donor groups were used, only emission from the BODIPY core was observed, indicating that even if energy transfer occurred from one donor to the other, it is still then transferred to the BODIPY core. While it would appear that energy transfer in these compounds (*F*-substituted BODIPY arrays) would proceed *via* a Förster type mechanism, poor alignment of the transition dipoles of the donors in relation to the acceptor (steric effects causing twisting of the donor units) minimizes this mechanism and through-bond energy transfer is promoted by effective electronic coupling. It is, however, important to note that through-space energy transfer in these compounds is not eliminated, merely minimized in certain cases.

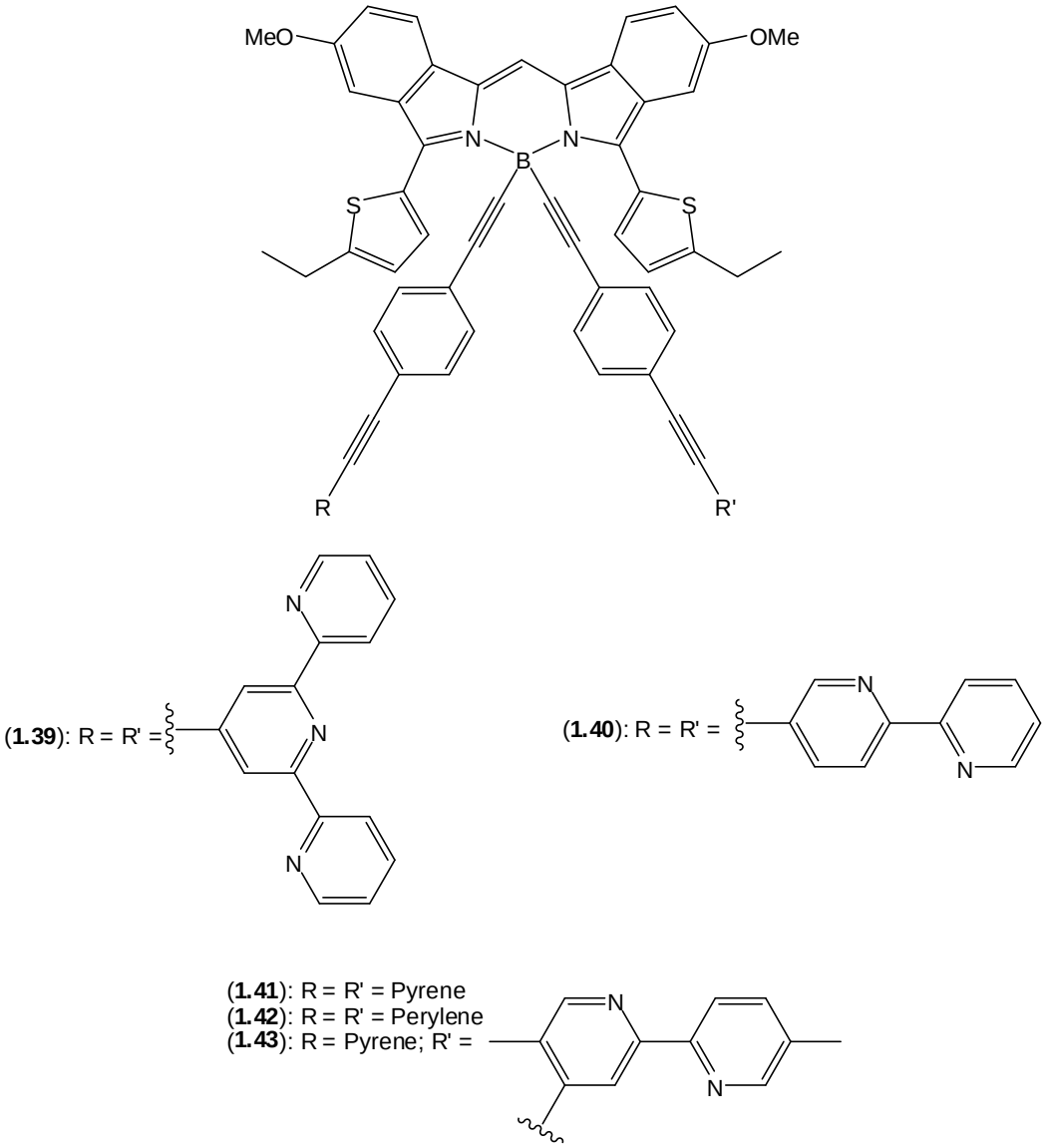

Figure 1. 40: BODIPY-oligopyridine arrays prepared by *F*-substitution

In an attempt to increase the potential for these types of molecules to be used as light harvesters in optoelectronic devices, analogues bearing three donor moieties attached to a terminal BODIPY acceptor have been synthesised (**1.44** and **1.45**),[138-140] the aim being to maximise absorption in the UV region. This feature would allow these molecules to be used as light harvesters in dye-sensitized solar cells. It was proposed, based on the studies of these compounds, that the boron centre is the main bottleneck for through-bond electron exchange. This factor could prove invaluable in the design of new arrays, BODIPY or otherwise.

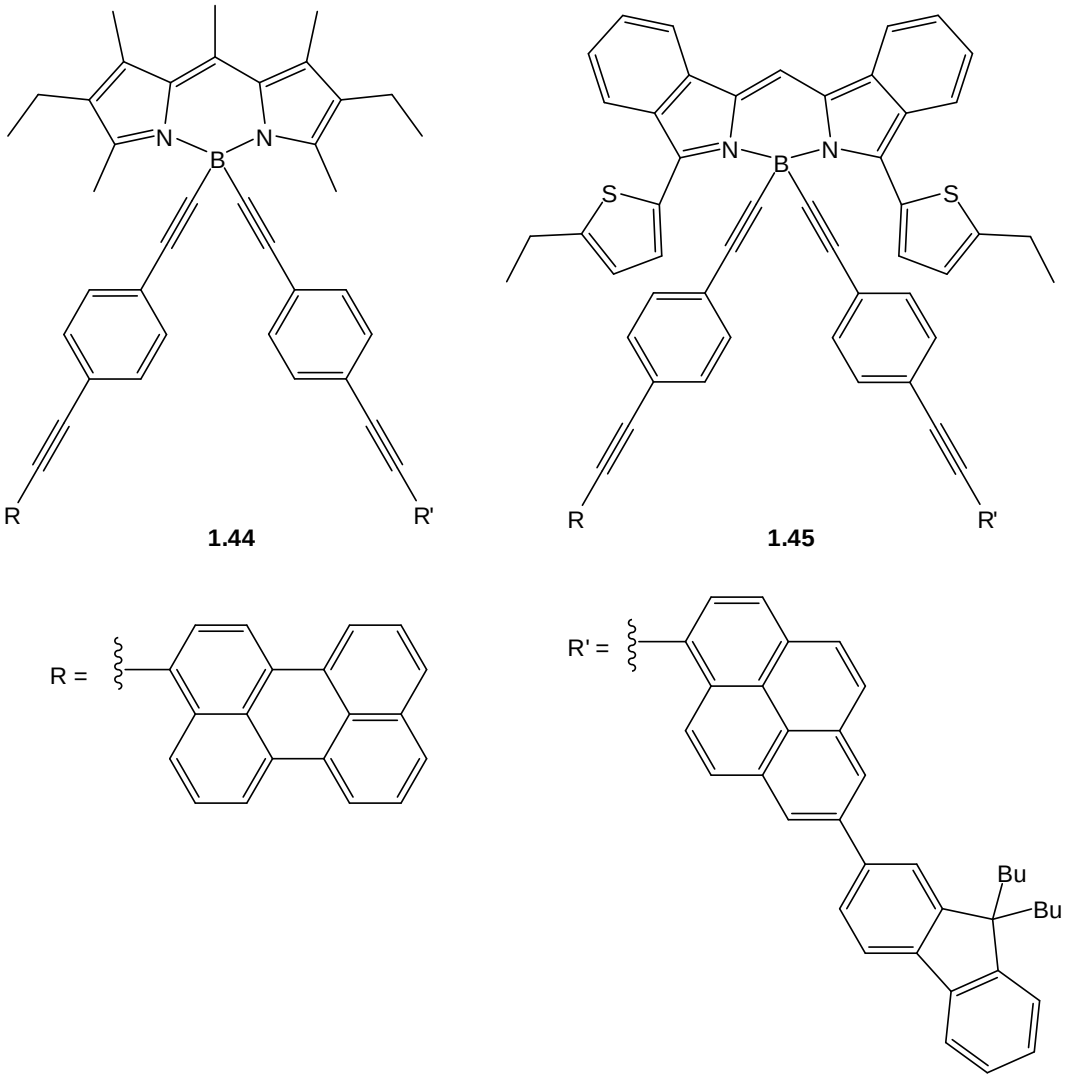

Figure 1. 41: BODIPY arrays bearing UV-absorbing donor groups

While it has been shown that different chromophores can be used to maximise absorption in a particular region of the electromagnetic spectrum, no relationship between spacer length (between donor and acceptor) and energy transfer has been determined. Using the same *F*-substitution reaction as for the previous arrays, two BODIPYs have been attached to a terminal acceptor BODIPY *via* different length aromatic linkers (**1.46**-**1.49**).[141] It was calculated that the lengths between the BODIPY acceptor and the donor was 18, 24, 31, and 38 Å for n = 0, 1, 2 and 3, respectively. Due to the polyaromatic nature of the spacer groups, these compounds absorbed at increasingly red-shifted wavelengths as the length of the spacers increases. This absorbed energy was shown to be almost quantitatively

transferred to the terminal BODIPY acceptor. Energy transfer was shown to occur from the two BODIPY units to the terminal BODIPY acceptor but with a decreasing rate as spacer length increased. Similar to compounds **1.44** and **1.45**, which contain three different donor units to maximise absorption in the UV region, compound **1.46** featured the remaining BODIPY (donor) fluorine substituents replaced with pyrene units to achieve the same effect. Again, absorption in this region showed efficient energy transfer from the pyrene unit to the terminal BODIPY acceptor. In each of these compounds, emission from the donor BODIPY could still be observed, to varying extents.

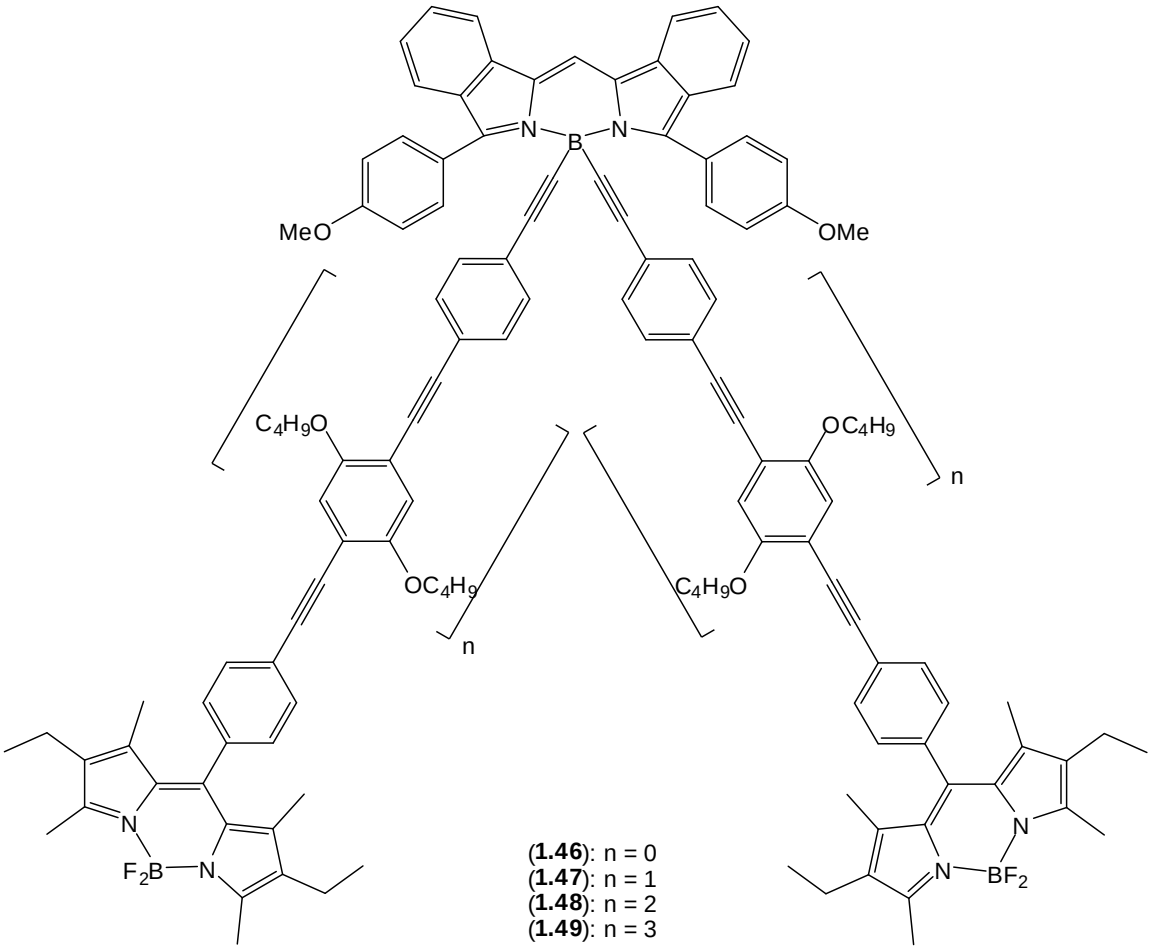

Figure 1. 42: BODIPY array exhibiting energy transfer efficiencies dependant on spacer length

The original investigations into multi-BODIPY arrays was carried out by Burgess' group.[142] This involved the preparation of a series of *bis*-BODIPY arrays connected by

different aromatic linker groups. In each case, efficient energy transfer was observed from the donor BODIPY to different acceptor *via* a through-bond mechanism. A small amount of donor fluorescence could still be observed for these arrays. This work was extended to prepare arrays consisting of two, three and four BODIPYs connected by a phenylethynyl linker.[143] The three- and four-BODIPY arrays were connected to the same single phenyl hub as in **1.50**. Efficient energy transfer occured in each of the arrays from the BODIPY donor to the styryl-BODIPY acceptor. Emission from the donor was still observed but was weaker than the emission from the acceptor (Φ_F = ≤0.1 for donor emission compared to Φ_F = 0.27-0.42 for the acceptor from the various arrays). For these arrays, direct excitation of the acceptor moiety produced fluorescence quantum yields greater than those produced by energy transfer. The energy transfer efficiency was calculated as being 99.5% and the increase in the number of BODIPY units provided the array with an increase in the antenna effect of the donor groups. It is interesting to note that despite the proximity of the BODIPY units in the four-BODIPY analogue, the donor units behaved as individual entities and there was no change in their individual photophysical characteristics.

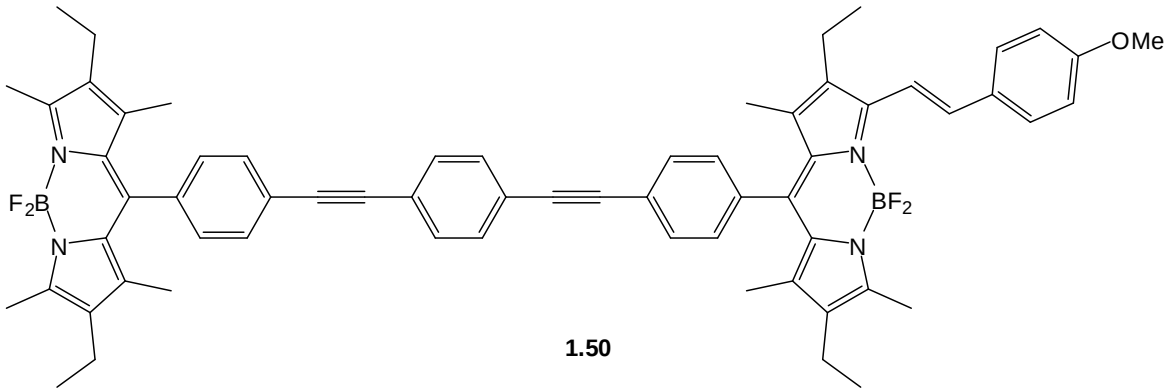

1.50

Figure 1. 43: Di-BODIPY array

Fluorene and truxene have also been used as bridging groups between different BODIPY units due to their absorption in the UV region.[144, 145] In both the fluorene and truxene array efficient energy transfer occurs from one BODIPY to the other. The fluorene was calculated to display almost quantitative energy transfer to the BODIPY, and energy transfer from the donor BODIPY to the acceptor BODIPY was calculated to have an

efficiency of more than 90%. Efficient energy transfer from the truxene core to a donor group on one of the arms occurred, but there was little control over which acceptor it transfers to. As the donor would have an absorption furthest into the blue region, and acceptor furthest into the red region, with the donor/acceptor between the two, energy transfer could occur from the donor to both the donor/acceptor and the terminal acceptor as well as from the donor/acceptor to the terminal acceptor. As energy transfer was calculated to be very efficient (>90% for each process) but not quantitative, emission from the donor (weakest emission), donor/acceptor (intermediate emission) and terminal acceptor (most intense emission) was observed. For this array, through-bond energy transfer occured from the truxene core to the BODIPY units and through-space energy transfer occured from one BODIPY to another.

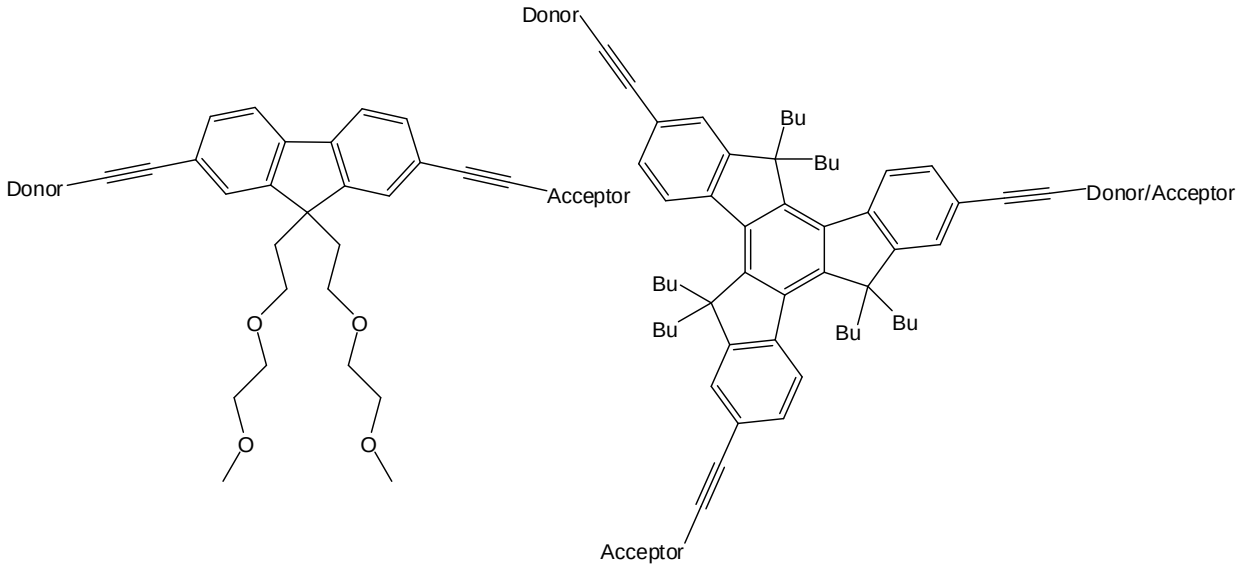

Figure 1. 44: Fluorene- and truxene-bridged arrays

A simple energy transfer system has been developed which consists of one or two BODIPY acceptor units connected by a terphenyl donor unit.[146] This system has potential applications in photovoltaic solar cells due to the terphenyl absorption in the UV region. A mono-BODIPY-terphenyl which terminated in a hydroxyl group was also synthesised and was found to act as a pH sensor, with fluorescence quenching occurring at high pH values *via* a PeT mechanism. BODIPYs connected in other simple ways have also shown efficient energy transfer properties. Simple multi-BODIPY arrays like **1.51** showed

efficient through-bond energy transfer from the three antenna donor BODIPYs onto the styryl-BODIPY, which acted as an acceptor due to the styryl groups causing a significant red-shift in the central BODIPYs absorption and emission spectrum.[92] A series of one-, two- and three-BODIPY arrays were synthesised with compound **1.51** being the latter. In compound **1.51**, emission from the three donor BODIPYs was quenched completely while the acceptor BODIPYs emission intensity was increased with increasing number of antenna BODIPY donors.

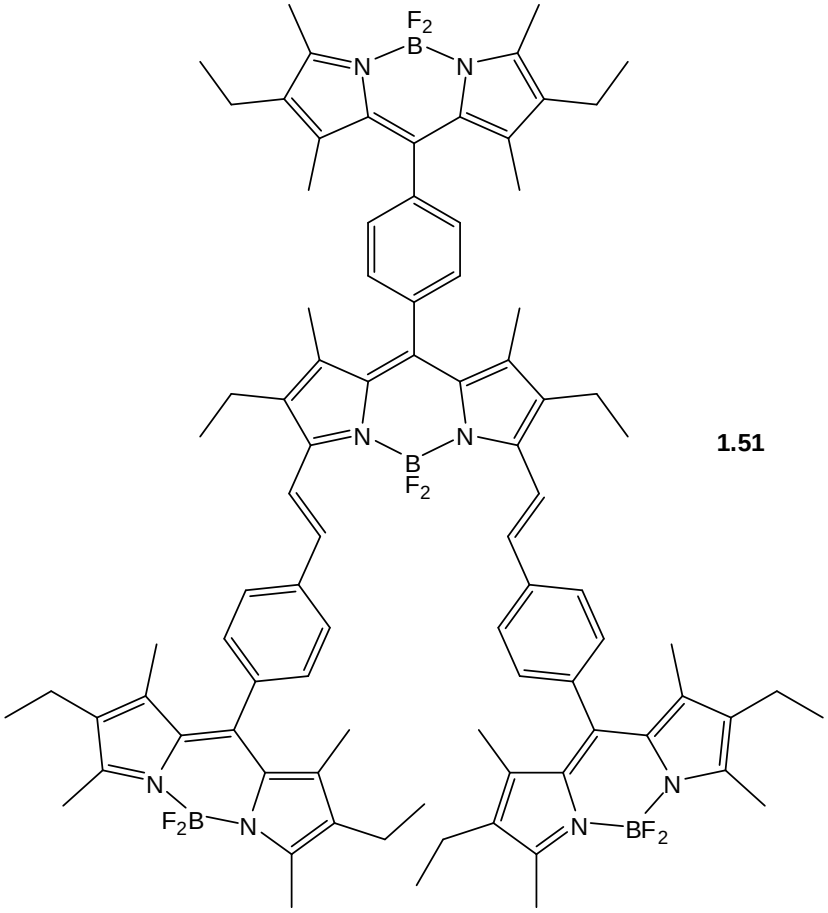

1.51

Figure 1. 45: Tetra-BODIPY array

2.9 BODIPY-based energy-transfer arrays as light harvesting materials in electrooptic devices

The versatility of BODIPYs as components of energy-transfer cassettes is quite clear, but investigations into their practical use in electrooptic devices, particularly solar cells, is now also receiving attention. Photocurrent generation for practical use in solar cells can be achieved by employing the array as a sensitizer for titanium dioxide (dye-sensitized solar cells) or by the formation of bulk heterojunction solar cells consisting of a donor/acceptor system bound between conducting surfaces (usually ITO – indium tin oxide, and another metallic electrode).

2.9.1 Dye-sensitized solar cells

Dye-sensitized solar cells (DSSCs)[147, 148] consist of a layer of dye trapped between a layer of titanium dioxide and an electrode. Such cells are held between transparent electrodes (fluorinated tin oxide – FTO glass) to allow light absorption and to receive the photogenerated current. When the dye absorbs a photon, electron transfer from the dye to the titanium dioxide conduction band occurs. This electron then moves by diffusion to the anode. Due to the dye having lost an electron, an electrolyte solution is placed below the titanium dioxide layer allowing the regeneration of the dye ground state.

The binding of organic molecules to titanium dioxide is relatively straightforward (the carboxyl group binds readily) and thus BODIPYs have been the focus of some recent research into new dye-sensitized solar cells. For these devices to be efficient, the dye must absorb in a wide range throughout the electromagnetic spectrum, which would appear to be a problem for BODIPY dyes given their relatively sharp absorption bands. However, as has been seen for some of the energy transfer cassettes, various groups can be attached to the BODIPY to maximise absorption by the dye and thus photocurrent generation. One of the earlier examples of BODIPYs as sensitizers involved a BODIPY with two triphenylamine groups attached *via* a styryl linker (**1.52**).[149] The styryl groups caused the BODIPY unit to absorb in the red region, while the triphenylamine unit

absorbed in the blue and green regions. Given that the electron density of a BODIPY moves from the BODIPY core (HOMO) to the 5-phenyl group (LUMO) upon excitation, this allows a relatively simple site for charge injection. Cyclic voltammetry of **1.52** revealed that it possesses a LUMO of 3.517eV, which allows thermodynamically favourable electron transfer into the titanium dioxide conduction band at 3.9eV. Compound **1.52** was shown to have a photon-to-current efficiency of 22%.

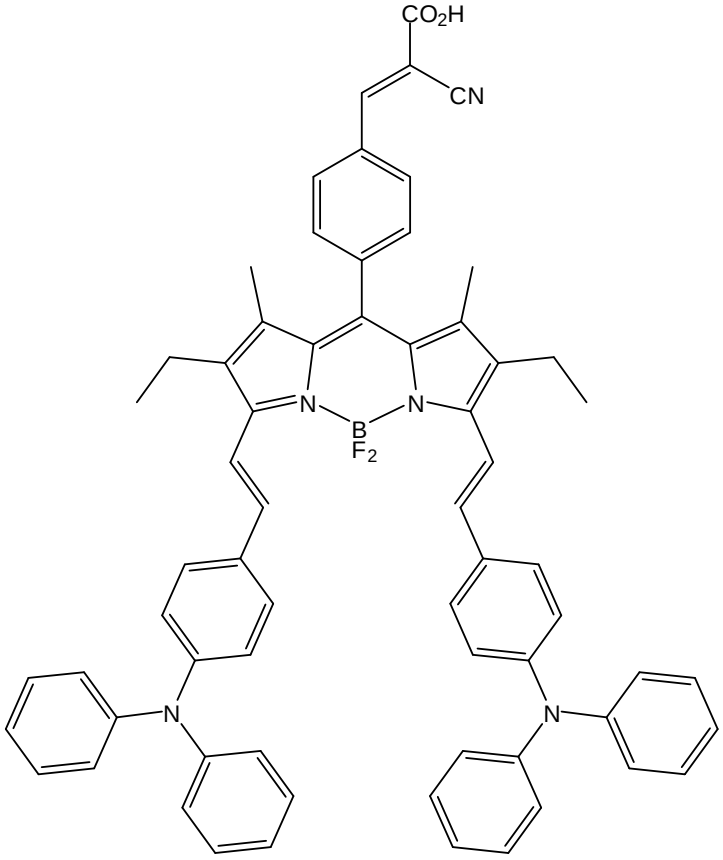

1.52

Figure 1. 46: Triphenylamine-BODIPY array for DSSCs

The use of triarylamines as donor units for DSSCs has been extended by the same group to include different substituents on the unsubstituted aryl groups, different positions for binding to titanium dioxide, and different substituents on the BODIPY core.[150] The different functional groups were used to shift the absorption maxima, as well as alter the oxidative and reductive potentials. It was observed that compound **1.53** gave the highest

photon-to-current conversion efficiency of the three compounds synthesised. A higher conversion was observed in the blue region, rather than at the BODIPY absorption in the red region. Conversion efficiencies were lower for compounds **1.54** and **1.55** indicating that position of binding to titanium dioxide as well as substituents on the BODIPY core are important factors in the preparation of DSSCs. Compound **1.53** had the highest conversion efficiency of this series of compounds at 0.68%.

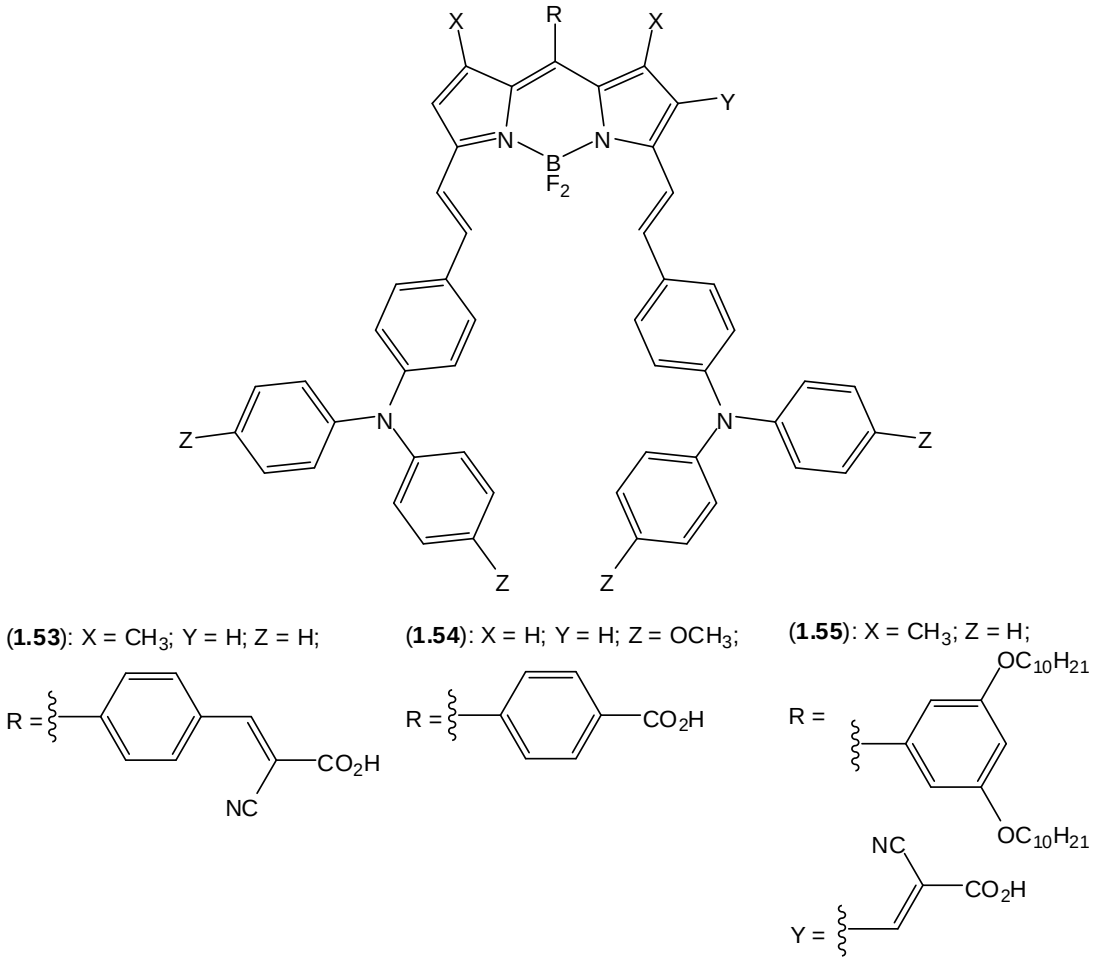

Figure 1. 47: Triphenylamine-BODIPY arrays for DSSCs bearing differing titanium dioxide binding and UV-absorbing groups

Because the synthetic route towards core BODIPYs is relatively straightforward, simple analogues of the same BODIPY core can be easily prepared and studied. This particular aspect of BODIPYs was exploited to prepare three analogues of a BODIPY containing polyethyleneglycol (PEG) arms for use in DSSCs.[151] The different BODIPY analogues

absorbed at different wavelengths in the visible region (compounds **1.56**-**1.58**). The addition of one then two styryl groups caused a progressive red-shift in the BODIPY absorption, while the increased number of aromatic groups caused an increase in the UV absorption. The PEG chains provided the molecules with enhanced film-forming properties. Photocurrent generation was measured for these compounds with excitation from 400-725 nm. As expected, compound **1.56** displayed photocurrent generation over the shortest region, due to the absorption of the BODIPY in the UV and visible regions being closer together than for **1.57** and **1.58**. Compound **1.58** displayed photocurrent generation over the entire region of the measured spectrum due to its wider absorption profile. No photon-to-current efficiencies were reported for these compounds.

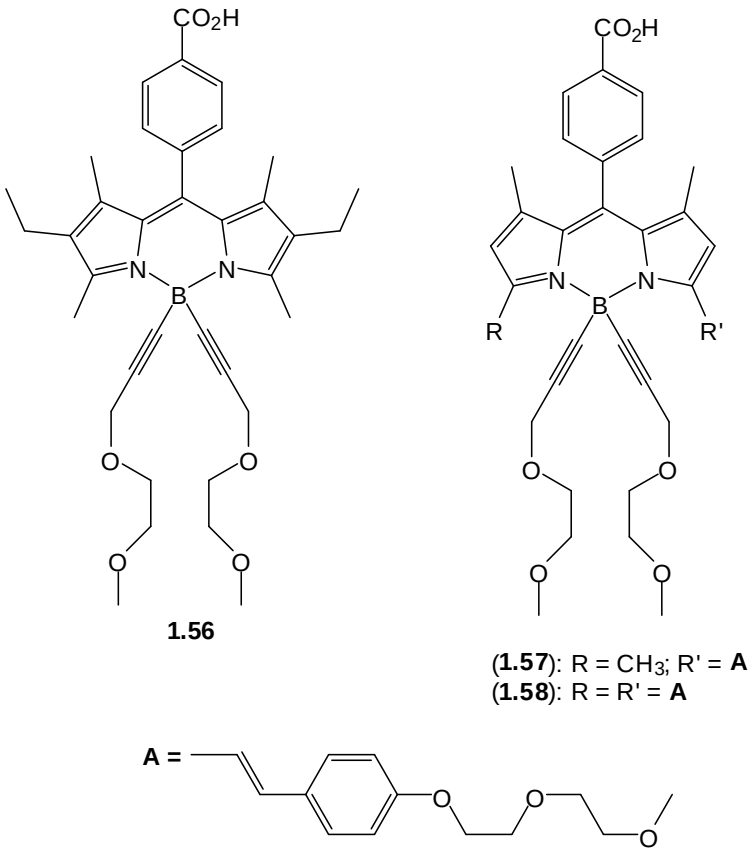

Figure 1. 48: BODIPYs for DSSCs with PEG arms to enhance film formation

Energy transfer in through-bond BODIPY porphyrin arrays has been shown to be very efficient and this effect has already been exploited in a photocurrent generation system.[123] This work has been extended to produce a BODIPY-porphyrin array bound to titanium

dioxide for use in DSSCs (**1.59**).[152] A through-bond energy transfer mechanism takes place to transfer energy from the BODIPY to the porphyrin and subsequent electron transfer occured onto the titanium dioxide. While the zinc porphyrin absorbed strongly at ~440 nm and more weakly at ~640 nm, the BODIPY absorbed at ~520 nm providing the array with three distinct absorption regions, which promoted photocurrent generation across a wide wavelength range. An analogue without the BODIPY donor was also synthesised, which showed a drop-off in photocurrent generation around 500 nm, while the array containing the BODIPY (**1.59**) maintained photocurrent generation throughout the measured wavelengths (400-700 nm). Peak photocurrent generation was centred on the strong zinc-porphyrin absorption around 440 nm with two smaller peaks at the absorptions of the BODIPY (~520 nm) and the weaker porphyrin absorption (~660 nm). This array exhibited a photon-to-current efficiency of 1.55%.

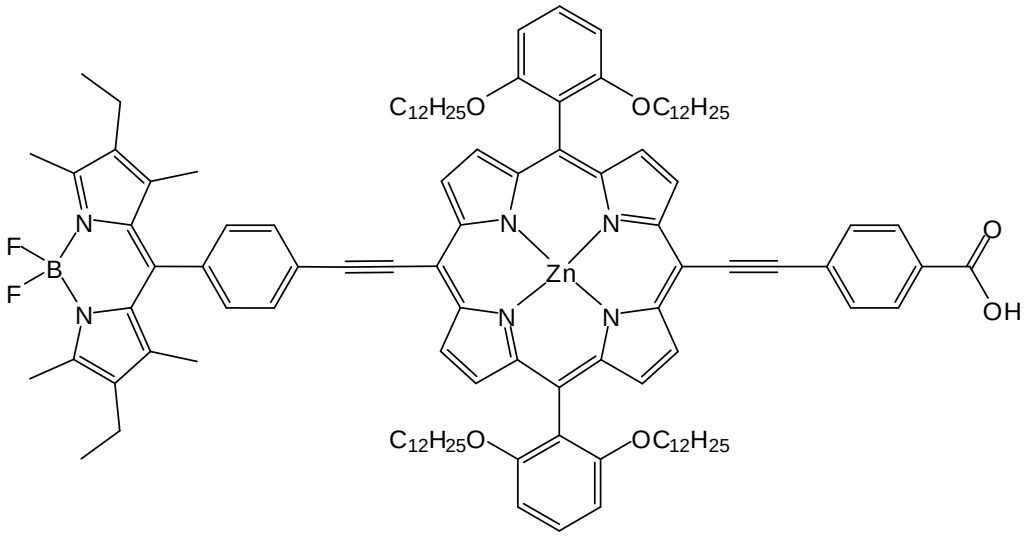

1.59

Figure 1. 49: BODIPY-porphyrin array for DSSCs

While BODIPYs display efficient energy transfer, dipyrrinato-metal complexes also exhibit strong absorptions in the UV and blue-green bends of the visible region. Although dipyrrinato-metal complexes have not yet been incorporated into DSSCs, their binding to titanium dioxide has recently been studied.[153] Rhodium, palladium and ruthenium complexes of 5-(4-carboxy)phenyl-dipyrromethene were synthesised and were shown to

bind to titanium dioxide and their absorption profiles were measured. However, no photocurrent generation experiments were reported for these compounds.

2.9.2 Bulk heterojunction solar cells

Bulk heterojunction solar cells (BHJs) consist of a charge donor and acceptor dispersed throughout a polymer matrix. Initially, the donor and acceptor are separated in a bilayer (bilayer heterojunction solar cells[154, 155]) but charge transfer was found to be inefficient. By dispersing them throughout a polymer matrix, more interfacial contact between the donor and acceptor occurs and charge transfer is more efficient.[156] Besides the increased efficiency of BHJs, their other major advantage is that, because they are a dispersed mixture of donor and acceptor, they can be fabricated by relatively simple solution-based processes, thus decreasing their production costs. Fullerene analogues have been the focus of interest in the development of BHJs due to their low LUMO energy level promoting efficient photoinduced charge transfer, highly delocalized π-system conferring stability on any charge-separated state and spherical geometry leading to isotropic electron transport through the 3D system.[156, 157] However, aromatic polymers have been the main avenue of research in the development of BHJs due to their ability to act as molecular wires, low band gap, and high electron hole mobility. Oligothiophenes in particular have attracted interest, but their synthesis, purification and electronic properties have caused some degree of difficulty in the preparation of BHJ devices.[158-160]

The initial investigation of the potential for BODIPYs as dyes for BHJs was carried out using three commercially available BODIPY dyes to dope an acrylate polymer and their effects as solar concentrators was measured.[161] Figure 1.50 shows the three different BODIPY dyes (shown as triangles, squares and circles) dispersed throughout the acrylate polymer. The first dye (A – BODIPY 494/505) absorbs the incident sunlight and then transfers the energy by FRET to the next dye (B – BODIPY 535/558) which subsequently transfers it to the final dye (C – BODIPY 564-591). 75% of the light emitted from dye C is trapped within the plate and guided to the photovoltaic cell by internal reflection. The white scattering surface reflected unabsorbed light from the first pass through back into

the plate. While efficient energy transfer was observed for this system, no photocurrent generation results were reported.

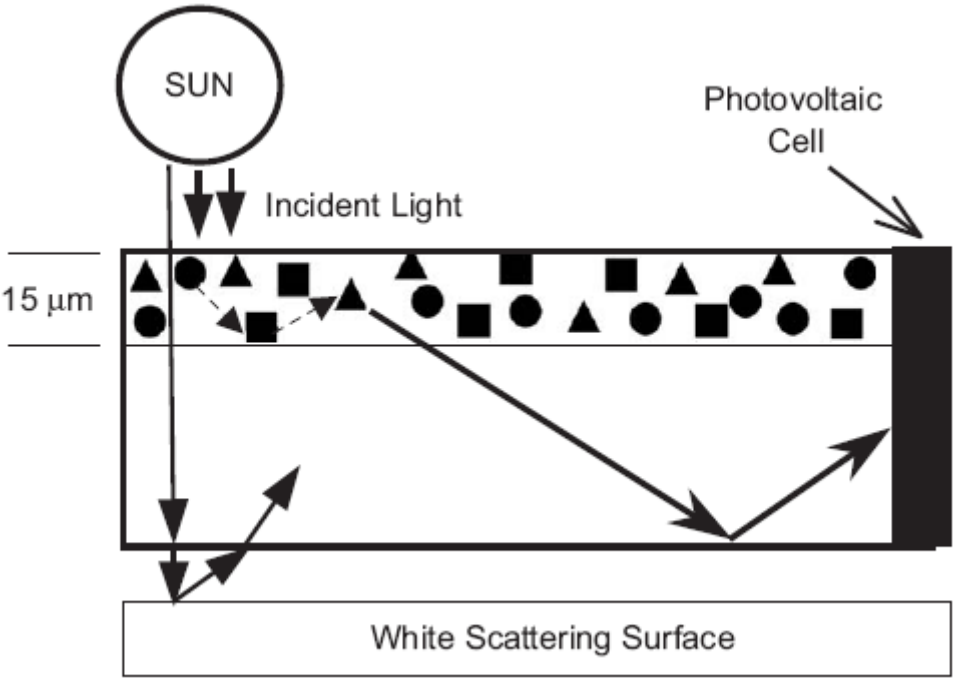

Figure 1. 50: Light collection in a multi-dye luminescent solar concentrator

Analogues of compounds **1.57** and **1.58** were prepared for use in BHJs that comprised of identical molecules other than the carboxyl group had been replaced with an iodo group (compounds **1.60** and **1.61**).[162] Compound **1.60** was found to have an excitation of 572 nm, while **1.61** had an excitation of 646 nm. When cast as thin-films on ITO-glass and bound in PEDOT-PSS (polymer support) a slight red-shift in the absorption maxima was observed. BHJs of these compounds were produced by spin-coating a mixture of BODIPY with [6,6]-phenyl-C_{61}-butyric acid methyl ester (PCBM) in a 1:2 weight ratio onto ITO-glass treated with a 40 nm thick layer of PEDOT-PSS. These cells showed distinct photocurrent generation around the major absorption peaks. An impressive power conversion efficiency[163-165] of 1.34% was calculated for these cells. The power conversion efficiency of these compounds was increased by using mixtures of both **1.60** and **1.61** with PCBM in PEDOT-PSS, and coating ITO-glass with the mixture.[166] The combination of the two different BODIPY dyes allows photons to be absorbed over a

broader spectral range. The power conversion efficiency for these mixtures was calculated to be 1.70%.

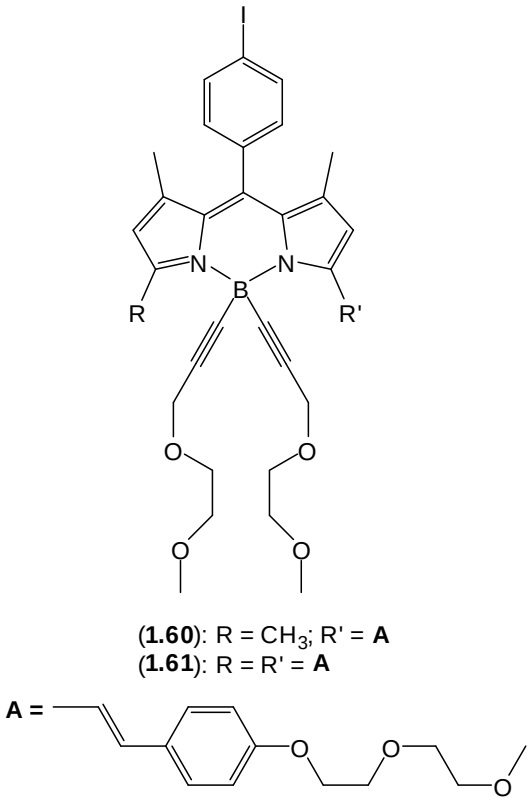

Figure 1. 51: BODIPY for BHJs with PEG arms to enhance film formation

Due to the interest in oligothiophenes as donors in BHJs, a bis(thiophene) analogue of compound **1.61** has recently been prepared that combines the light-harvesting properties of the di-styryl-BODIPY with the electron hole transport properties of an oligothiophene (**1.62**).[167] Compound **1.62** displayed strong absorption between 300-700 nm with major peaks for the BODIPY chromophore and strong absorption for the aromatic groups in the UV region. As predicted, the photocurrent generation profile matched the absorption profile and the power conversion efficiency was calculated as being 2.20% when mixed with PCBM in a PEDOT-PSS matrix.

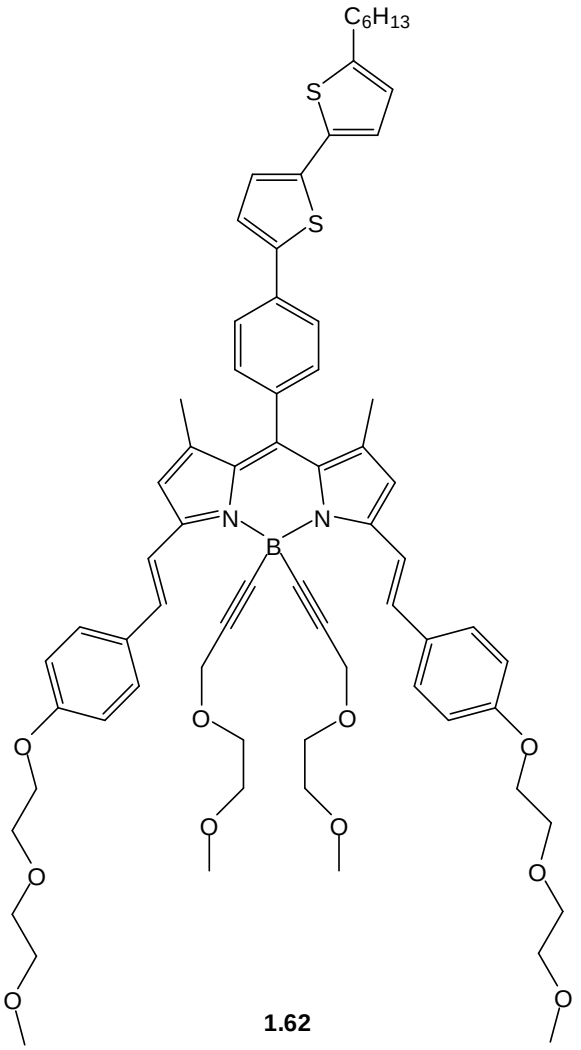

1.62

Figure 1. 52: BODIPY-thiophene array for BHJs

2.10 BODIPYs as laser dyes

Several BODIPY derivatives have been shown to exhibit laser activity. Some of the BODIPY derivatives studied exhibit relative efficiencies above that of rhodamine 6G (against which the laser activity of this series of BODIPY dyes was compared, with rhodamine 6G having a relative efficiency (RE) of 100).[168, 169] Drexhage described a simple rule governing the laser activity of fluorescent dyes which relies on π-electron distribution.[170] The rule states that "in a dye where the π-electrons of the chromophore can make a loop when oscillating between the end groups, the triplet yield will be higher than in a related compound where this loop is blocked. It may be said that the circulating

electrons create an orbital magnetic moment which couples with the spin of the electron. This increased spin-orbit coupling then enhances the rate of intersystem crossing, thus giving rise to a higher triplet yield." BODIPYs are, therefore, ideal candidates for laser dyes due to their sharp emission profiles and low rate of intersystem crossing which is kept low by the lack of conjugation through the boron atom.

In one of the initial studies of BODIPYs as laser dyes, Boyer *et al.* synthesised 28 different BODIPY derivatives and their photophysical behaviour, including relative laser efficiency, was observed.[171, 172] The range of BODIPYs they synthesised was designed to cover a wide range of relatively simple functional groups to observe their effects on the lasing properties. Different types and numbers of alkyl substituents as well as rigid cyclic motifs, aromatic units and polar groups were attached to the BODIPY core and a wide range of laser efficiencies was observed (Fig. 1.53). Several of the BODIPYs studied have since been commercialised.

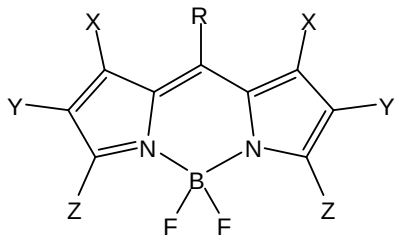

Figure 1. 53: Core BODIPY structure for investigation into laser activity of different BODIPY derivatives

The initial sub-series (seven compounds) involved the investigation into the effect that different short alkyl groups had on laser activity. A gradual red-shift was observed with increasing alkyl substitution, with tertiary butyl groups providing the largest shift (commercial BODIPY PM 597). A red-shift of ~30 nm was observed for all the BODIPYs studied in going from their emission wavelength to their lasing wavelength. This sub-series showed an odd/even effect based on the number of alkyl groups present on the BODIPY core with regard to their relative laser efficiency. BODIPYs containing an odd number of carbon atoms possessed lower relative efficiencies than those with even numbers of carbon atoms. The even derivatives had relative efficiencies of at least

100, with PM 597 having a relative efficiency of 110. Over the whole series of 28 compounds, no clear relationship between absorption wavelengths, extinction coefficient and fluorescence quantum yield and laser activity was established. Replacing the *meso*-alkyl group with a hydrogen atom caused a marked decrease in laser activity. Distortion of the planarity of the BODIPY core caused by strong steric interactions between alkyl units caused a total loss of laser activity. Phenyl groups attached to the pyrrolic positions of the BODIPY also caused low lasing activity.

This initial research has, naturally, led to various groups preparing other BODIPY derivatives in order to investigate the laser properties of the resulting dyes. Mono-amino and acetamido (**1.63** and **1.64**) derivatives of a BODIPY dye were synthesised and remarkably different laser properties were observed.[173] The acetamido derivative displayed slightly red-shifted absorption and emission compared to the amino derivative, but similar fluorescence quantum yields were observed. However, **1.64** displayed a laser efficiency of 48%, while **1.63** did not exhibit any laser emission. This lack of laser emission was not attributed to aggregation in solution but could be due to the delocalized lone pair of the amino group attached directly to the BODIPY core.

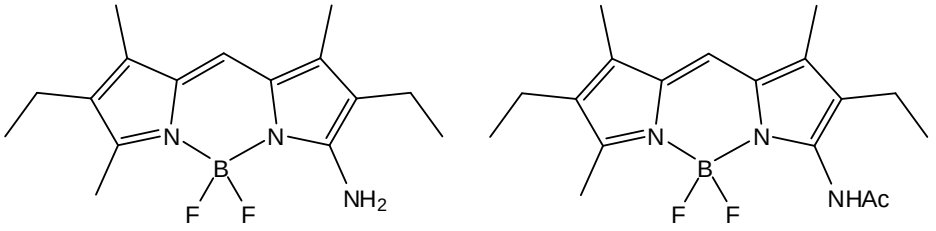

1.63 **1.64**

Figure 1. 54: BODIPY laser dyes

In order to produce laser dyes with red-shifted emissions, BODIPYs with extended conjugated π-systems have been prepared (**1.65**-**1.67**).[174] The two phenyl groups caused a red-shift in the absorption (~50 nm) and emission (~80-90 nm) of the dyes with respect to the unsubstituted dye, as well as causing much wider Stokes' shifts than is normally expected for BODIPY dyes. Despite the lack of alkyl groups restricting the rotation of the *meso*-phenyl ring, the fluorescence quantum yields were moderate (Φ_F = 0.41-0.62). This

was attributed to the efficient coupling between the electron clouds of the BODIPY core and the phenyl rings causing a restriction in their rotation. Compound **1.65** was found to possess the highest laser efficiency in several solvents, with acetone and ethyl acetate being the most suitable. Excitation at 532 nm caused a laser efficiency (in EtOAc and acetone) of 14%, while excitation at 568 nm increased this to 20%. This is likely due to the 568 nm excitation being closer to the three BODIPY dyes absorption maxima. Compound **1.66** displayed moderate laser efficiency in methanol with efficiencies of 11% and 17% for excitation at 532 nm and 568 nm respectively. Compound **1.67** displayed the weakest laser efficiency of 5% and 11% in ethanol with excitation at 532 nm and 568 nm respectively. Each of the BODIPY dyes studied appears to be photostable under laser pumping.

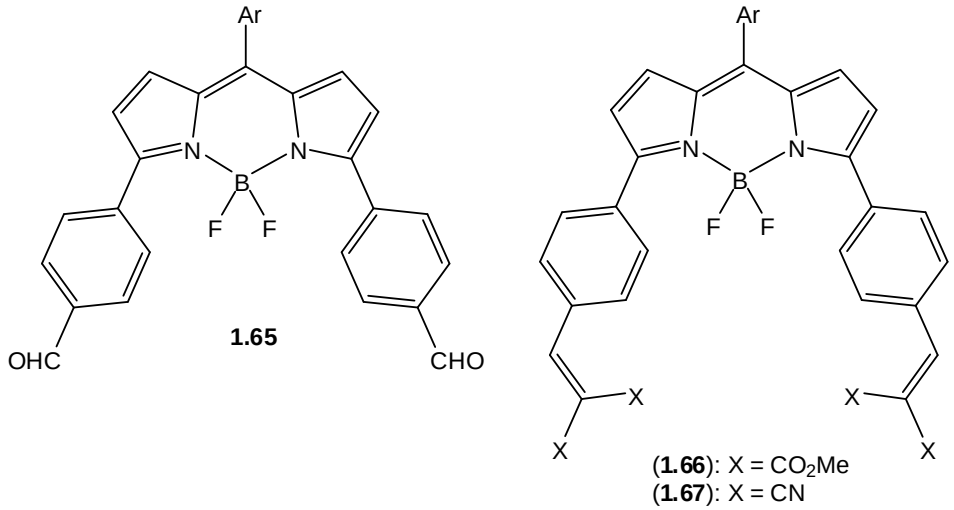

Figure 1. 55: BODIPY laser dyes with red-shifted absorption and emission

This method of red-shifting BODIPY emissions for use as laser dyes has been extended to include styryl groups and polyphenylene derivatives.[175] Compound **1.68** had the highest laser efficiency of this series (30% in THF) with compound **1.70** being similar (29% in THF). Despite having a similar core structure to **1.68**, compound **1.69** had a lower efficiency of 23% in THF. Compound **1.71** had the lowest efficiency of the series at 19% in THF, indicating that the trifluoromethyl units have the effect of increasing the laser efficiency of BODIPYs when attached to the styryl units.

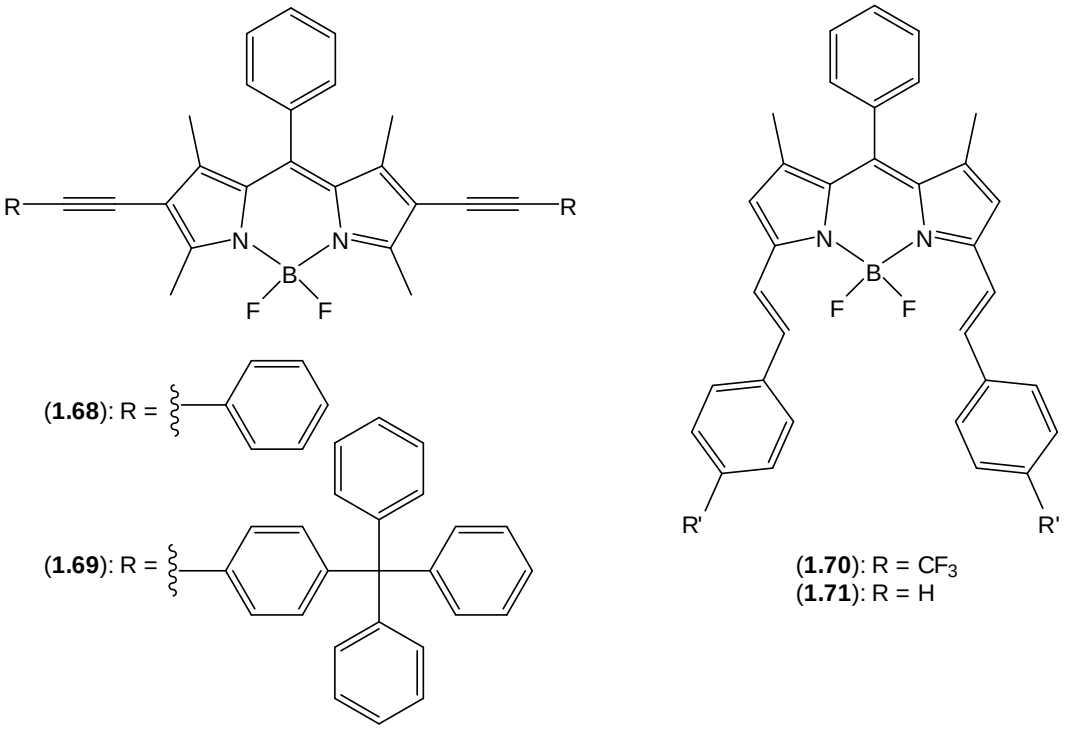

Figure 1. 56: BODIPY laser dyes with extended π-conjugation

2.10.1 Laser activity of dye-doped polymeric matrices based on commercial BODIPY derivatives

Commercial BODIPY dyes PM 567 and PM 597 have been used to dope linear and cross-linked fluorinated polymers.[176, 177] An initial investigation into the effect that increasing cross-linking in dye-doped fluorinated co-polymers has on the lasing behaviour of the dye revealed a clear relationship between laser efficiency and stability of PM 567 and degree of cross-linking. The co-polymer host was a 2,2,2-trifluoromethyl methacrylate (TFMA)/ethyleneglycol dimethacrylate (EGDMA) mixture with increasing proportions of EGDMA promoting increased cross-linking. A 99:1 TFMA:EGDMA mixture exhibited a laser efficiency of 4% and a stability of 15% after only 10000 pulses (each stability of this series of TFMA:EGDMA co-polymers was measured after 5000 and 10000 pulses; less than the usual 50000 and 100000 pulses). By increasing the amount of EGDMA to 2%, the laser efficiency was increased to 7% and the stability to 40%. The co-polymer containing 10% EGDMA was found to promote the highest efficiency and stability (18% and 55% respectively) with further increases in the amount

of EGDMA used causing a gradual decrease in both efficiency and stability (80:20 TFMA:EGDMA having an efficiency of 14% and a stability of only 12%).

In an investigation into the effect that increasing the fluorine content of the co-polymer host has on the lasing behaviour of the dye dopant, each of the polymers prepared was a methyl methacrylate (MMA) co-polymer using TFMA, 2,2,3,3,3-pentafluoropropyl methacrylate (PFMA) or 2,2,3,3,4,4,4-heptafluorobutyl methacrylate (HFMA) as the fluorinated monomers for linear polymers. The cross-linked co-polymers were prepared using MMA and EGDMA, pentaerythritol triacrylate (PETA) or pentaerythritol tetraacrylate (PETRA). Each co-polymer was prepared using two or three different proportions of monomers other than the EGDMA co-polymer which was only prepared using MMA:EGDMA 80:20. PM 597 was only bound into linear co-polymers while PM 567 was bound into both linear and cross-linked co-polymers.

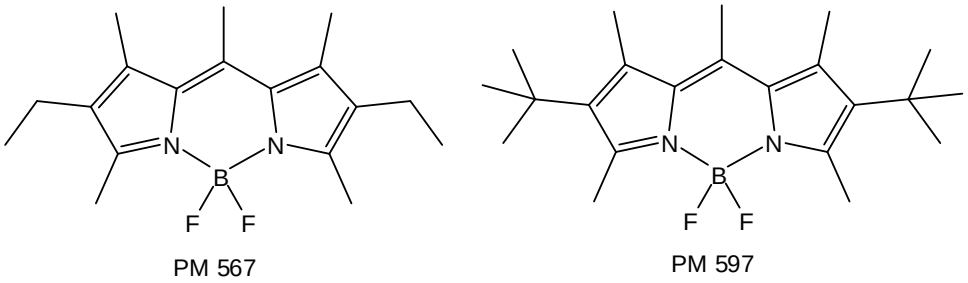

Figure 1. 57: Commercial BODIPY dyes PM 567 and PM 597

In the series of linear co-polymers, PM 567 was shown as having the highest laser efficiency when bound in MMA:TFMA 70:30. This dye-doped polymer displayed a laser efficiency of 35%, however a poor laser stability. The laser output intensity of this dye-doped polymer decreased to 26% after 100000 pump pulses at the same position of the sample at 10 Hz. This decreased to 0% when pumped at 30 Hz. When PM 567 was bound in MMA:TFMA 50:50, the laser stability was reduced to 0% when pulsed at 10Hz, with a very rapid drop in laser output by 92% after only 40000 pulses. By switching to a monomer containing a higher weight% of fluorine atoms, the laser efficiency was slightly reduced but laser stability was dramatically increased. A mixture of MMA:PFMA 70:30 was found to give the best stability of 181% when pulsed at 10 Hz and 56% when pulsed

at 30 Hz. The laser efficiency of this mixture was 22% which, although lower than the MMA:TFMA mixtures, is still moderate. By reducing the weight ratio of PFMA to 10%, a marginal increase in laser efficiency was observed (22% to 23%) but a decrease in laser stability was also seen (105% at 10 Hz, 0% at 30 Hz). This shows that the amount of fluorine attached to the co-monomer has a pronounced effect on the laser efficiency and stability. Contrary to the increase in laser stability caused by changing from TFMA to PFMA, the transition from PFMA to HFMA actually caused a reduction in laser stability along with a slight increase in laser efficiency. An MMA:HFMA 70:30 mixture showed a laser efficiency of 24% and a laser stability of 115% (10 Hz) and 31% (30 Hz). The reported efficiencies of over 100% are due to an actual increase in laser output with increased number of pulses. No definitive explanation of this effect in BODIPYs has thus far been reported but it is assumed that it is due to multiple factors.

PFMA was chosen as one of the co-monomers for the cross-linked polymers due to its moderate laser efficiency and high laser stability. The series of co-monomer mixtures for the cross-linked polymers was designed to investigate the effect that increased cross-linking had on the laser properties of PM 567. Similar laser efficiencies and emission wavelengths were observed for the cross-linked polymers, although the polymer mixtures containing PETA had slightly higher laser efficiencies. Laser stabilities were increased when going from mixtures containing 10% PETA to 20%, as well as from 10% PETRA to 20%, indicating a positive relationship between degree of cross-linking and laser stability up to a certain point. Further increases were shown to be detrimental.

The investigations of the laser properties of PM 597 were carried out using linear co-polymer mixtures of increasing fluorine weight% and cross-linking co-polymers with an increasing degree of cross-linking. The linear co-polymers were prepared from 70:30 mixtures of MMA with TFMA, PFMA and HFMA and a dramatic increase in laser stability was observed compared to PM 567. When bound in a mixture of MMA:HFMA (70:30), PM 597 showed the highest laser stability of all the series studied of 159% (10 Hz) and 105% (30 Hz) even after 500000 pulses. This mixture also displayed a laser efficiency of 36%, equal to or higher than all the PM 567 doped co-polymers. The

highest laser efficiency was observed for PM 597 in the cross-linked co-polymer PFMA:PETA 80:20 of 42% which also displayed an impressive laser stability; 94.8% (10 Hz) and 59% (30 Hz) after 250000 pulses. While PM 567 displayed higher laser stability in the cross-linked co-polymers, PM 597 displayed much higher stability in the linear co-polymers. The loss of laser activity seen upon repeated pump pulsing was attributed to a build-up of heat in the polymer which is more marked when pumped at a faster rate.

The impressive laser properties of PM 567 were also observed in silica aerogels with fluorinated co-polymers.[178] The co-polymers were 70:30 mixtures of MMA with TFMA, PFMA or HFMA with PM 567 dissolved in the co-monomer mixture which was then incorporated into a silica aerogel by adding a silica gel monolith to the solution in order for polymerization to occur within the aerogel. The MMA:TFMA mixture aerogel produced a laser efficiency of 27% (lower than PM 567 in the co-polymer alone – 35%) and a laser stability of 104% (10 Hz) and 38% (30 Hz) which is a significant increase over the stability of PM 567 dissolved in the co-polymer mixture alone (26% (10 Hz) and 0% (30 Hz)). The MMA:PFMA mixture aerogel caused an increase in the laser efficiency when compared to the free co-polymer mixture (from 22% to 32%) as well as a decrease in the laser stability at 10 Hz (from 181% to 109%) but an increase in the stability at 30 Hz (from 56% to 105%). A similar effect was observed for the MMA:HFMA mixture aerogel. While the effect that incorporating these dye-doped co-polymers into silica aerogels has on PM 567 laser efficiency appears to be unpredictable without further study, it is clear that it causes a significant increase in laser stability when pulsed at 30Hz.

PM 567 has also been incorporated into a non-fluorinated co-polymer (1:1 MMA:HEMA) including a tetraethoxysilane (TEOS) inorganic component to investigate if BODIPY laser dyes could be used in organic-inorganic hybrid materials.[179] TEOS was added to the co-monomer/BODIPY mixture before polymerization at 5, 10 and 15% proportions and a significant change in the laser stability was observed. The laser efficiency remained relatively unaffected (22, 20 and 24% for 5, 10 and 15% TEOS respectively). When only 5% TEOS was used, thermal dissipation through the polymer matrix was increased, causing an increase in laser stability of the dye (69% after 60000

pulses at 10 Hz). However, further increase in the amount of TEOS used caused a dramatic reduction in laser stability. 10% TEOS reduced the stability to 69% after only 7000 pulses and 15% TEOS reduced it even further to 69% after only 1800 pulses. While the addition of increasing amounts of TEOS caused a dramatic reduction in laser stability, it remained higher than the 1:1 MMA:HEMA mixture without any TEOS.[180-183]

An analogue of PM 567 has been prepared that possesses a styryl group (**1.68**) in order to produce a bathochromic shift in the absorption, emission and lasing wavelength.[184] The laser efficiency was determined to be as high as 18%, but varied depending on the solvent used. This styryl-BODIPY (**1.72**) was also bound in a polymer matrix and laser activity was still observed. Ethyl acetate was found to produce the highest laser efficiencies, so polymethylmethacrylate (PMMA) polymers were chosen as methyl MMA mimics the ethyl acetate solvent. Both linear and cross-linked polymers were studied, with linear polymers of two different molar proportions being prepared. Linear co-polymers MMA:TFMA 9:1 and 5:5 produced the highest laser efficiencies (18% and 16% respectively), with cross-linked MMA:EGDMA 3:2 showing the lowest (6%). PMMA showed a laser efficiency of 10% indicating that linear polymers allow the dyes to lase more efficiently than cross-linked polymers. By suspending the dyes in a solid polymer matrix, a slight red-shift (~5 nm) was observed for the emission spectrum.

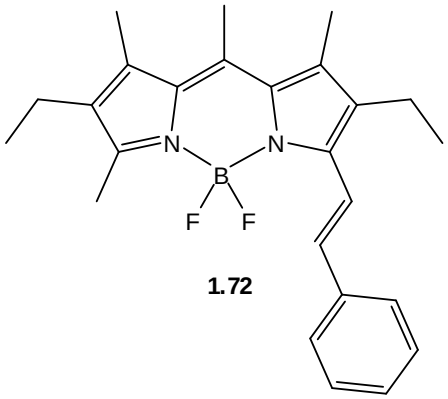

1.72

Figure 1. 58: Mono-styryl BODIPY dye

Compounds **1.73-1.76** were designed to act as dopants for polymers (**1.73** and **1.75**) and as co-monomers for polymers (**1.74** and **1.76**).[185] The laser efficiency of compounds **1.73** and **1.75** were determined in several solvents and was found to be most intense in ethanol (58% and 54% respectively). They were then made up into solid solutions in PMMA and their laser efficiency and stability was determined. Compound **1.73** exhibited a laser efficiency of 27% while the di-acetyl analogue (**1.75**) had a laser efficiency of 33%. Compound **1.75** was determined to have higher laser stability than **1.73** of 53% compared to 35% respectively. When used as co-monomers (**1.74** and **1.76**), the laser efficiency remained at a similar level (28% and 37% respectively) but the laser stability increased significantly; from 35% to 52% (**1.73** to **1.74**) and 53% to 100% (**1.75** to **1.76**). The laser stability of **1.75**:PMMA was only reduced to 67% even after 400000 pulses at 30 Hz. This indicates that covalent binding of the dye molecules to the polymer strands is an efficient way of increasing the stability of solid-state polymeric dye lasers.

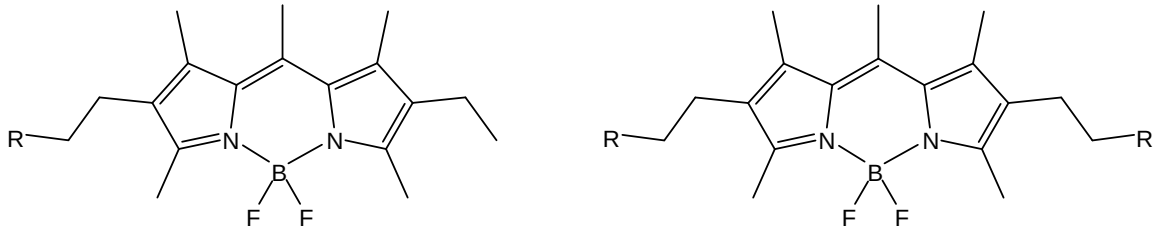

(**1.73**): R = CH_2OAc
(**1.74**): R = $CH_2OCOC(Me)=CH_2$

(**1.75**): R = CH_2OAc
(**1.76**): R = $CH_2OCOC(Me)=CH_2$

Figure 1. 59: BODIPYs bearing polymerisable substituents

Polyphenylene derivatives of PM 567 were prepared containing the same functional groups as **1.73-1.76** in order to subject them to the same experiments of polymer doping and use as co-monomers (**1.77**-**1.82**).[186, 187] Each of the derivatives had a lower fluorescence quantum yield than the parent dye PM 567, likely due to partial rotation of the phenyl ring. Compounds **1.77**, **1.79** and **1.81** showed remarkably high laser efficiencies of 42%, 66% and 80% respectively in ethyl acetate showing a significant increase in lasing efficiency with increasing number of phenyl rings. Each of the acetyl derivatives was bound in a PMMA polymer at two different concentrations (1.5 and 0.8mM) and the laser properties were observed. Each of the acetyl derivatives was found

to have a higher laser efficiency and stability than PM 567 in PMMA polymer. No significant difference in laser efficiency was observed upon increasing concentration, but the 1.5 mM mixtures displayed increased laser stability with **1.79** being the most stable (76% after 100000 pulses). The laser efficiency of compounds **1.77**, **1.79** and **1.81** in PMMA polymer was found to be 18%, 31% and 24% respectively at 1.5 mM concentration. While a moderate increase in laser efficiency was observed in increasing the number of phenyl rings from one to two, the addition of another phenyl ring caused a reduction in laser efficiency. When used as a co-monomer with MMA, a reduction in laser efficiency and stability was observed for compounds **1.80** and **1.82**, while compound **1.78**/MMA exhibited a similar efficiency but increased stability. While the reduction in laser efficiency is only slight, the decreased stability is more marked (from 82% to 67% for **1.80** and 81% to 66% for **1.82**). Compound **1.77** dissolved in PMMA was found to have the lowest stability of the series, but when used as a co-monomer with MMA was found to have the highest stability of the series (96% for 1.5 mM **1.78** in MMA). Each of these derivatives showed increased laser efficiency over PM 567 when in liquid solution, solid polymer solution and when used as a component in a co-polymer.

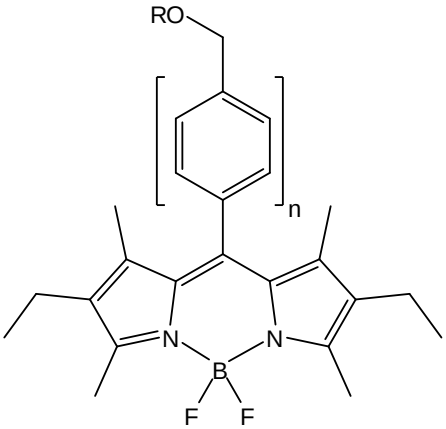

(**1.77**): n = 1; R = Ac
(**1.78**): n = 1; R = COC(Me)=CH_2
(**1.79**): n = 2; R = Ac
(**1.80**): n = 2; R = COC(Me)=CH_2
(**1.81**): n = 3; R = Ac
(**1.82**): n = 3; R = COC(Me)=CH_2

Figure 1. 60: 8-Phenyl analogues of PM 567

Similar phenyl analogues of PM 597 have been prepared which incorporate an acetyl (**1.83**) or an acrylate group (**1.84**).[188] The laser efficiency of **1.83** was calculated to be 52% in ethyl acetate, but this was reduced when dissolved in a solid polymer matrix. The highest laser efficiency for **1.83** was found for a PMMA solution (48%) with an impressive stability (98% at 10 Hz) with the stability being increased to 100% (10 Hz) in co-polymers 9:1 and 7:3 MMA:TMSPMA at the cost of further reduction in efficiency. Compound **1.86** exhibited similar behaviour in PMMA solution (efficiency of 48%) with a slightly reduced stability (85%) which was increased to 100% in 1:1 MMA:HEMA along with a decrease in efficiency to 39%. Compounds **1.84** and **1.85** were dissolved in solid PMMA and were found to have moderate laser efficiency (46% and 38% respectively) and stability (63% and 61% respectively). PM 597 dissolved in solid PMMA displays higher efficiency than all the analogues in this series (52%) and higher stability than most (88% at 10 Hz). While the laser properties were reasonable (the laser stabilities being most impressive), the interesting aspect of this study was the colour tuning of the dyes which were incorporated into the polymer matrices. Compound **1.84** emitted in the green region, PM 597 emitted in the yellow region and compound **1.83** emitted in the orange/red region.

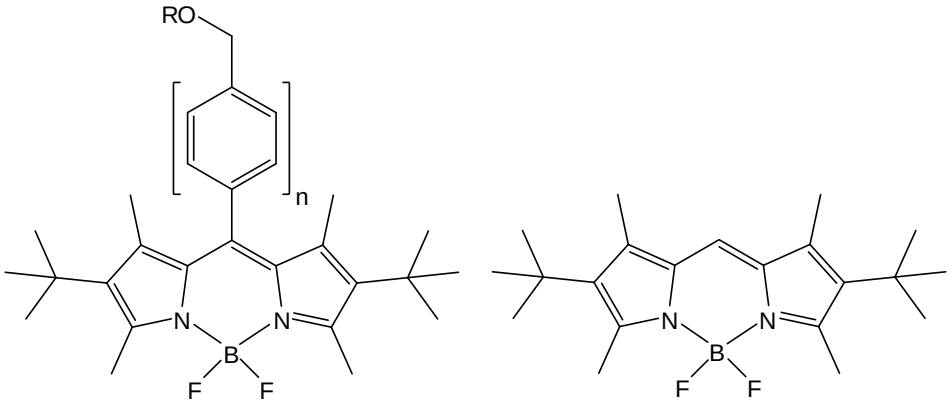

(**1.83**): n = 0; R = Ac
(**1.84**): n = 1; R = Ac
(**1.85**): R = $COC(Me)=CH_2$

1.86

Figure 1. 61: Analogues of PM 597

BODIPY emission has been shown to be promoted by electrochemical means, providing an alternative method of emission despite lacking the sharp emission band of laser emission.[189] In this study, several commercial BODIPY dyes were investigated and were found to fluoresce *via* electrochemical excitation, albeit at a much weaker intensity. Commercial BODIPYs PM 546, 567, 580 and 597 were studied and found to have fluorescence quantum yields of 0.95, 0.87. 0.85 and 0.41 respectively, when excited under conventional conditions. When excited *via* electrochemical means, a moderate red-shift in the emission was observed (19-29 nm) at a very weak intensity (Φ_{ECL} = 0.009, 0.007 and 0.003 for PM 567, 580 and 597 respectively. Electrochemical-promoted emission was not observed for PM 546).

2.10.2 Laser activity of BODIPYs in dye-doped liquid crystals

Commercially available BODIPY dyes have been used to dope nematic liquid crystals and have been shown to display laser behaviour similar to being dissolved in a solid polymer matrix. PM 597 has been used to dope BL 001 (commercially available nematic liquid crystal mixture – Merck) which has then been inserted into a wedge cell (two glass-ITO plates separated by Mylar spacers (100 μm) with the inner side of the plates being covered in rubbed polyimide alignment layers in order to induce homogeneous alignment of the nematic liquid crystal molecules).[190]

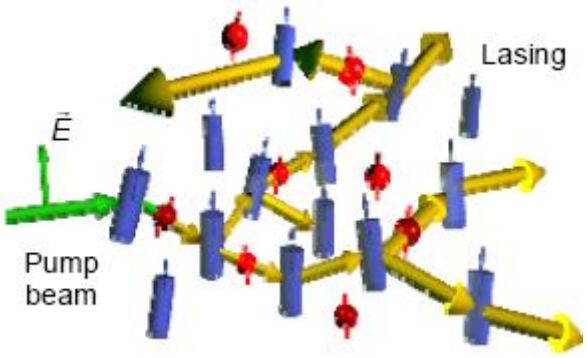

Figure 1. 62: Representation of random lasing of dye molecules in a nematic liquid crystal host material (blue = nematic host molecules; red = dye molecules)

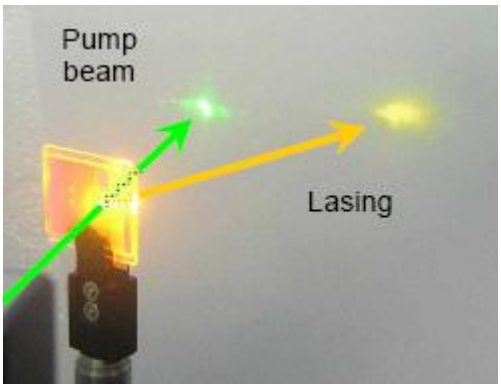

Figure 1. 63: Photograph showing clearly visible lasing of dye molecules dissolved in a liquid crystal host incorporated into a wedge cell (cell angled relative to the incident pump beam in order to view laser light)[190]

As seen in Figure 1.62, photons absorbed by the dye 'guest' molecules are spontaneously re-emitted in random directions. Due to the random nature of this spontaneous emission, a significant amount of backscattering occurs from the sample. However, due to the thickness of the sample, these backscattered photons cause the spontaneous emission from other dye molecules before they leave the sample, resulting in a coherent chain reaction. When a population inversion is achieved then the sample begins to lase. In ordinary lasers, the gain medium is suspended in an optical cavity and the pump beam is reflected back and forth through the cavity, but in this case the nematic host causes the system to act as a randomly distributed feedback laser due to backscattering of the emitted photons. Due to the partially ordered nature of the nematic host, the dye molecules adopt some of the same ordering allowing the emission to be controlled by varying the polarization of the pump beam.[191] Laser emission being most intense when the pump beam is aligned parallel to the nematic director, and least intense when perpendicular to the director. The dye-doped BL 001 was also suspended in a glass capillary tube and was shown to lase with the same intensity as the sample in the wedge cell, but at red-shifted wavelengths and with additional intense lasing modes.[192] The laser intensity also showed a decreased dependence on the polarisation of the pump beam than the aligned wedge cell sample due to the less aligned nature of the nematic host in the capillary. The laser energy output was also measured as a function of temperature and was found to require increased pump pulse energy with increasing temperature due to the decreased ordering of the nematic phase with increasing temperature. Both PM 597 and

PM 650 in BL 001 have been freely suspended in a square-comb PVC net in order to produce thin films with laser activity.[193] Efficient laser emission was observed for both BODIPYs when freely suspended.

This random lasing in dye-doped liquid crystals has been exploited to produce lasing in a chiral nematic liquid crystal in a POLICRYPS-like grating.[194] A mixture of 'guest' PM 597 and 'host' BL 088 and NOA-61 was incorporated into a POLICRYPS system in which the dye-doped chiral nematic liquid crystal is placed into narrow parallel channels long enough for several helical periods to be passed through. This is not possible with the wedge-type cells as their thickness is too short to allow any full helical periods to occur. By using a POLICRYPS system, each channel acts as a micro-cavity laser due to the channels behaving as optical resonators. Stimulated emission occurs along the channels, emerging from the end of the channels, when the incident pump beam is above a certain power. In this system the wavelength was tuneable by varying the temperature and the laser intensity by applying an electric field perpendicular to the helical axis.

2.11 Polymers incorporating BODIPY fluorophores

2.11.1 Polymerisation through the BODIPY core

BODIPYs have been incorporated into polymers through various linker groups and at various positions on the BODIPY to produce novel new fluorescent materials. The first co-polymers containing BODIPY fluorophores were prepared by Sonogashira coupling of a di-iodo-BODIPY to either a di-ethynyl-BODIPY or phenylene co-monomer (**1.87**-**1.90**).[195]

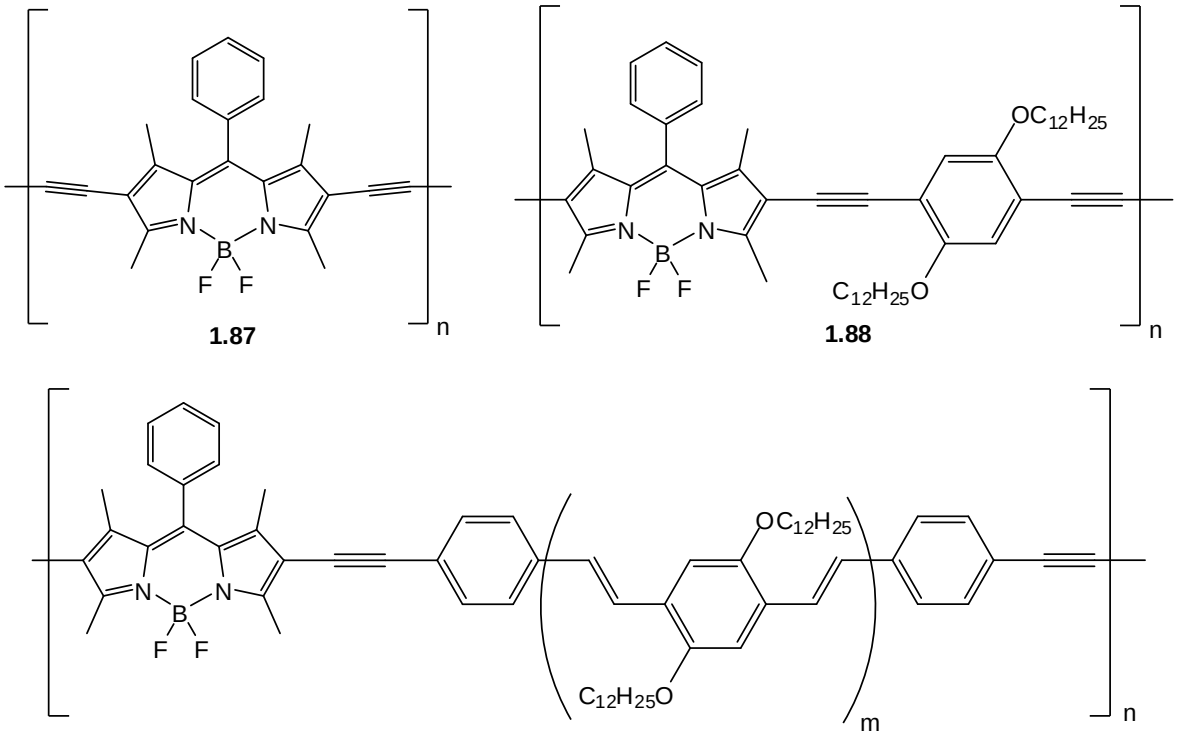

(**1.89**): m = 0
(**1.90**): m = 1

Figure 1. 64: BODIPY polymers with ethynyl or ethynyl-phenyl linker groups

The polydispersity (PDI) of compound **1.87** was the lowest of the series (1.27) while compound **1.88** was the highest (1.65). Compound **1.87** also possessed the lowest thermal decomposition temperature (200°C) and compound **1.88** the highest (240°C). The absorption and emission of this series of polymers was red-shifted relative to the BODIPY monomer, presumably due to the extended conjugation through the BODIPY core. Due to the presence of two iodo-substituents on the BODIPY monomer core, the fluorescence quantum yield for this unit was very low (0.02) but the resulting polymers all possess higher quantum yields. Of this series of polymers, compound **1.88** had the lowest quantum yield (0.08) while the other co-polymers were all very similar (0.24, 0.25 and 0.25 for **1.87**, **1.89** and **1.90** respectively). The extension of the conjugate system also had the effect of reducing the oxidation potential.

The effect that the linker group, or lack thereof, has on the photophysical properties of a BODIPY-containing polymer have been investigated by employing various metal-catalyzed cross-couplings.[196] Yamamoto, Suzuki and Sonogashira couplings were all used to prepare a series of BODIPY-containing polymers from the same starting BODIPY monomer (**1.91**-**1.93**). The PDI of these polymers were calculated to be 3.48, 3.15 and 3.02 for compounds **1.91**, **1.92** and **1.93**, respectively, and their decomposition temperatures all exceeded 310°C. Compound **1.91** displayed a remarkably high extinction coefficient of 475000 M^{-1} cm^{-1} and a relatively intense fluorescence (Φ_F = 0.57). However, as the excitation and emission maxima were approximately the same as the monomer, it was assumed that there was little interaction between adjacent fluorophores along the polymer chain. This effect is consistent with a perpendicular arrangement of the fluorophores caused by the methyl groups on the BODIPY cores forcing each adjacent fluorophore out of co-planarity. Compound **1.92** displayed an unusually hypsochromically shifted absorption and emission spectrum (λ_{ex} = 325 nm, λ_{em} = 385 nm) and a much lower fluorescence quantum yield of 0.03. Compound **1.93** displayed a moderate fluorescence intensity (Φ_F = 0.24) but a very low extinction coefficient (20000 M^{-1} cm^{-1}). It also showed broad absorption and emission bands due to aggregation of the polymer strands even in dilute solutions.

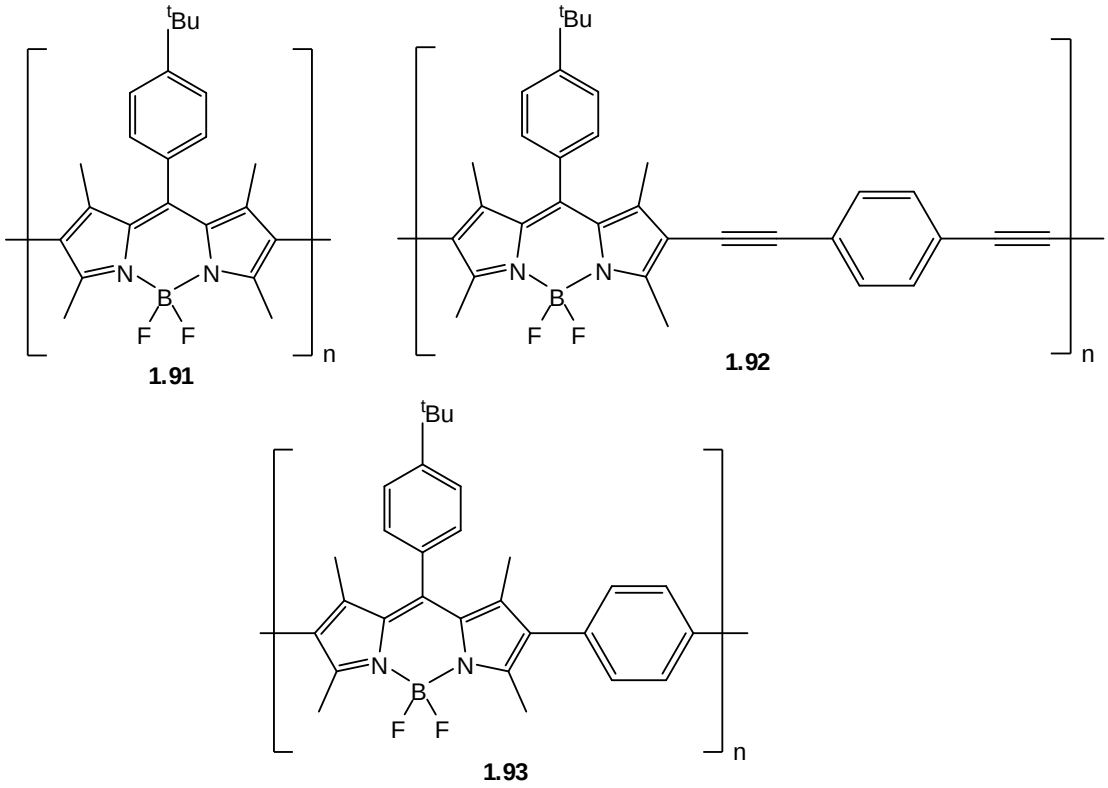

Figure 1. 65: BODIPY polymers with short or no linker groups

The effect that different groups have on the photophysical properties of a BODIPY-containing polymer have been explored by altering groups on the BODIPY phenyl ring as well as by altering the linker group between the fluorophores.[197] By separating the fluorophores with ethynyl groups (**1.94** and **1.95**), interactions between adjacent fluorophores could occur, and this caused a significant red-shift for the polymers relative to the monomers. The quantum yields were reduced upon polymerisation (0.21 and 0.23 for **1.94** and **1.95** respectively); however, compound **1.95** had a slightly higher quantum yield as well as being slightly more red-shifted than compound **1.94**.

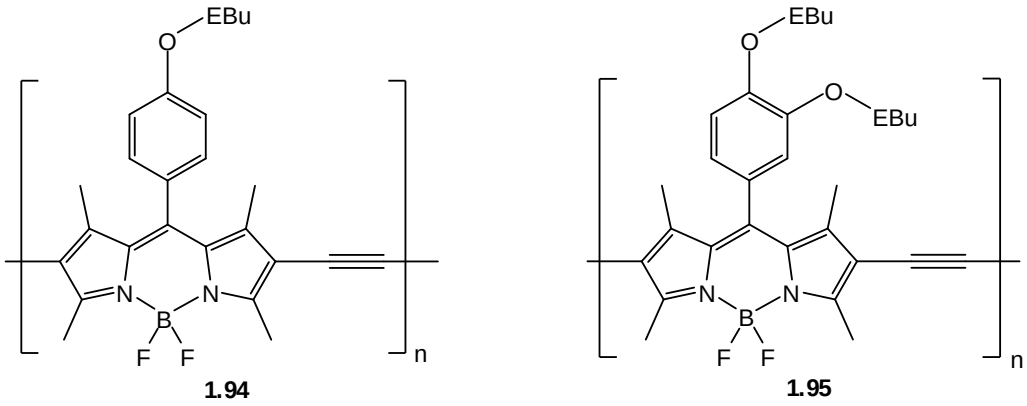

Figure 1. 66: BODIPY polymers with differing groups on the 8-phenyl ring

Interestingly, the absorption and emission spectra of compounds **1.96**-**1.98** were not as red-shifted as **1.94** and **1.95** despite having an extended conjugate system. The differences in their emission wavelengths are consistent with the band gap energy differences for the aromatic linker units. Compounds **1.96** and **1.97** were calculated to have similar quantum yields (0.25 and 0.24 respectively) but compound **1.98** had a much lower quantum yield (0.06) and fluorescence lifetime (0.23 ns). This was presumably caused by the heavy atom effect of the sulphur atom of the thiophene ring.

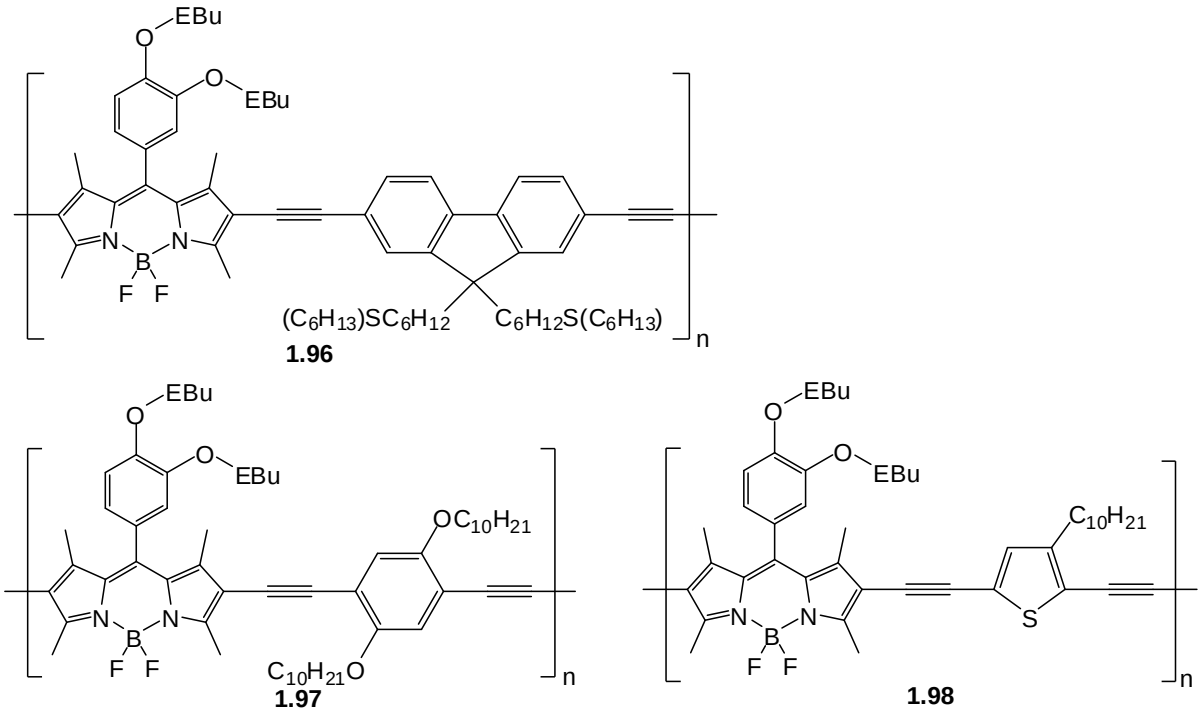

Figure 1. 67: BODIPY polymers with different types of linker group

The number of alkyloxy substituents on the BODIPY phenyl ring can have a significant effect on the photophysical properties of a BODIPY-containing polymer, particularly when cast as a thin film.[198] As would be expected, the excitation and emission spectra of polymers **1.99**-**1.101** were significantly red-shifted relative to the monomers due to extended π-conjugation, and the fluorescence quantum yields were all similar (0.13-0.15). With increasing number of alkyloxy substituents, the excitation and emission of each polymer was further red-shifted and the Stokes' shift is shortened. However, when cast as a thin film, the initial increase in the number of alkyloxy substituents caused a marked red-shift in the excitation, but only slightly for the emission. While a thin film of compound **1.99** absorbed at 680 nm and emitted at 723 nm, a thin film of compound **1.100** absorbed at 728 nm and emitted at 741 nm. However, compounds **1.100** and **1.101** had very similar excitation and emission profiles. Each of these polymers was relatively thermostable, starting to decompose only above 300°C. Polymer **1.98** and a similar analogue lacking the thiophene unit have been incorporated into a dye-sensitized solar cell device with PCBM and remarkable power conversion efficiencies (PCE) have been observed.[199] Polymer **1.98**:PCBM 1:3 was found to have the highest PCE of the series

investigated at 2.0% with a broad absorption profile due to the extended delocalized π-system along with the UV absorption of the PCBM moiety. This broad absorption spectrum resulted in a broad photocurrent generation profile.

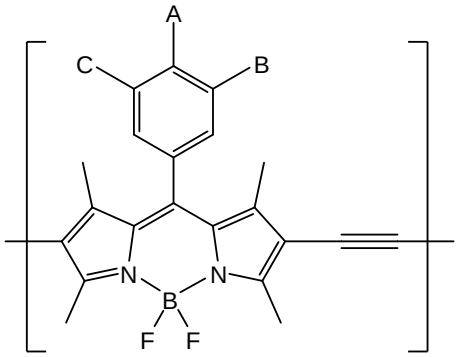

(**1.99**): A = $O(CH_2)_{11}CH_3$; B = C = H
(**1.100**): A = B = $O(CH_2)_{11}CH_3$; C = H
(**1.101**): A = B = C = $O(CH_2)_{11}CH_3$

Figure 1. 68: BODIPY polymers with increasing numbers of long alkyl chains

The effect that different substituents on the BODIPY phenyl ring have on the photophysical properties of BODIPY-containing polymers has been further investigated through the preparation of polyfluorene-BODIPY polymers (**1.102**-**1.104**).[200] As seen in previous examples, the extension of the π-system delocalisation resulted in a bathochromic shift in the polymer absorption relative to the monomer. Electron donating methoxy groups had a slight effect on the absorption but there was an even lesser effect on the emission (**1.102** and **1.103**), while the methyl groups caused an increase in fluorescence quantum yield (**1.104**). Interestingly, polymers **1.102** and **1.104** were found to be sensitive to both fluoride and cyanide anions. Both polymers displayed a decreased BODIPY absorption and emission intensity with increasing concentration of fluoride and cyanide anions, they also displayed a concurrent hypsochromic shift in the absorption wavelength. This may be due to decomposition of the BODIPY core caused by fluoride anions.[88, 201] Cyanide anions were shown to decrease the absorption peak of the BODIPY, but a new absorption band was not observed indicating that cyanide anions are not as damaging to the BODIPY core as fluoride anions. Anion size seems to play an important

role in the function of these polymers as sensors as no response was observed for chloride, bromide or iodide anions.

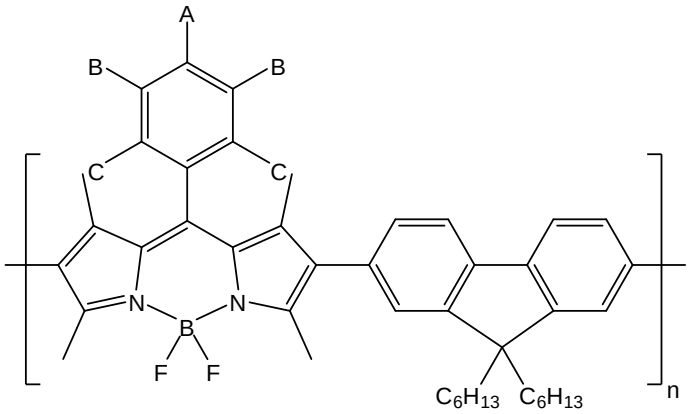

(**1.102**): A = B = OCH_3; C = H
(**1.103**): A = OCH_3; B = C = H
(**1.104**): A = B = H; C = CH_3

Figure 1. 69: Fluorene-linked BODIPY polymers

BODIPYs that display absorption and emission in the red region have also been incorporated into polymers and have been shown to undergo a further red-shift when polymerized(**1.105-1.107**).[202] While each of the polymers **1.105-1.107** absorbed and emitted in the red region, the presence and position of the methoxy group had a moderate effect on the absorption, emission and quantum yield. Polymer **1.106** was slightly hypsochromically shifted (15 nm) but displayed a more intense fluorescence relative to **1.105** (0.49 compared to 0.33), while **1.107** was bathochromically shifted (17 nm) with only a slightly increased quantum yield (0.38 compared to 0.33). Each of the polymers was red-shifted compared to their respective monomers due to extension of the π-system delocalisation. All the polymers started to decompose above 275°C.

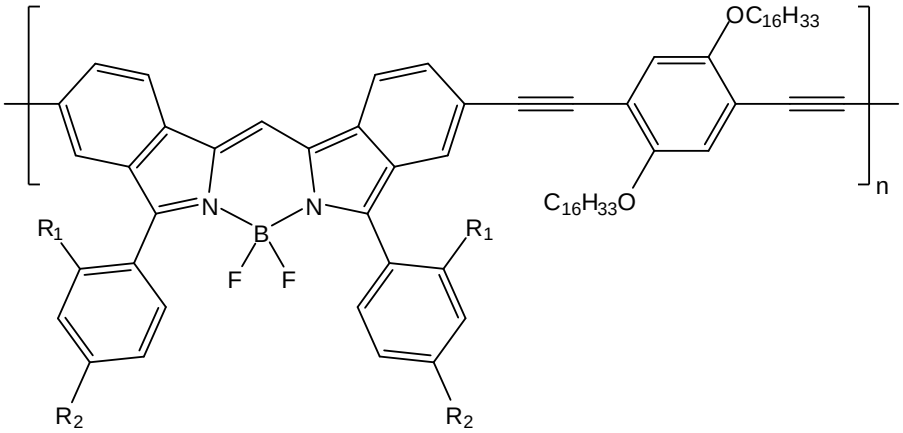

(**1.105**): $R_1 = R_2 = H$
(**1.106**): $R_1 = OCH_3$; $R_2 = H$
(**1.107**): $R_1 = H$; $R_2 = OCH_3$

Figure 1. 70: BODIPY polymer with red-shifted absorption and emission

2.11.2 Polymerisation through F-substitution

Polymerisation of BODIPYs through palladium catalyzed cross-coupling on the BODIPY core itself causes a red-shift in the fluorescence, but this effect can be tempered by polymer formation through fluorine substitution. These systems were initially investigated using relatively linear aryl groups (**1.108**-**1.110**).[203] The fluorescence quantum yields of these polymers were all relatively intense (0.80, 0.71 and 0.85 for **1.108**, **1.109** and **1.110** respectively) while the absorption and emission for each polymer was very similar to the monomer. The emission was found to red-shift and the peak broadens when the polymers were cast as thin films. The most interesting property of these polymers, however, was found to be their self-assembly behaviour. Polymer **1.108** was found to form nm-sized particles and μm-sized fibres by aggregation of the polymer strands. Polymer **1.109** was found to display a preference for particles over fibres, while polymer **1.110** displayed almost no fibre-like structures. This suggests that the fibre-like structures are a result of steric interactions of the aryl linker groups.

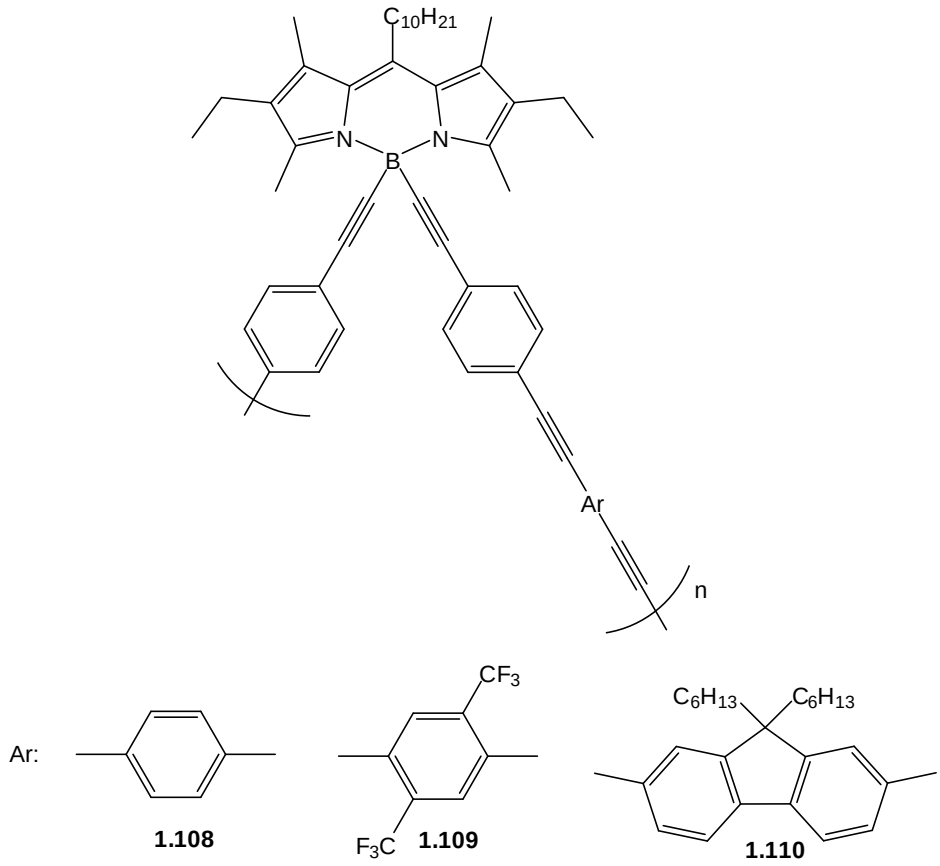

Figure 1. 71: BODIPY polymers prepared *via F*-substitution

This type of BODIPY polymerisation has been used to prepare a chiral BODIPY polymer with *S*- and *R*-6,6'-diethynyl-2,2'-dioctyloxy-1,1'-binaphthyl as the chiral linker (**1.111**).[204] The absorption and emission of each diastereomer was found to be identical, as well as to that of the monomer. Both the *R*- and *S*-polymers displayed a tendency to form fibre-like structures through aggregation of particles, but fibre formation was found to be disrupted by the addition of the other diastereomer; with 3:7 *S*-:*R*- showing complete disruption of fibre formation, and consequently only particles were observed. This was attributed to the disruption of particle aggregation caused by the presence of the opposite diastereomer.

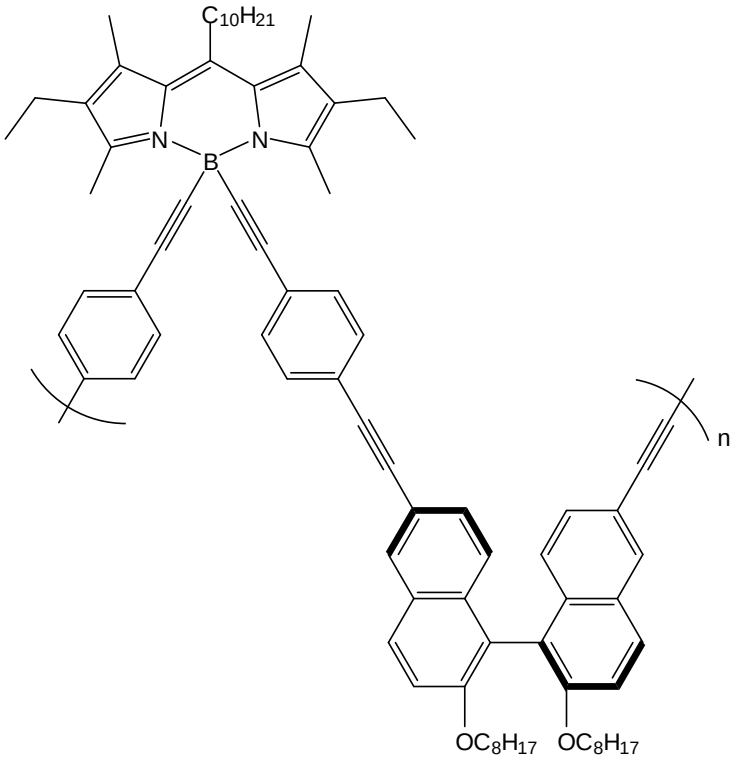

1.111

Figure 1. 72: Chiral BODIPY polymer

2.11.3 Polymerisation through the BODIPY meso-position

While polymerisation of BODIPYs through the BODIPY core itself can induce a red-shift in the absorption and emission of the resulting polymer and polymerisation *via F*-substitution can lead to interesting molecular architectures, attaching a monomer to a BODIPY through a simple linker can provide a polymer containing ancillary BODIPY fluorophores. HEMA monomer analogues have been attached to BODIPY fluorophores (**1.112**) and a hybrid polymer has been prepared by reaction with MeTMOS.[205]

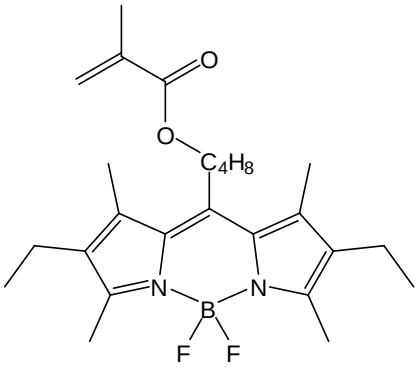

1.112

Figure 1. 73: BODIPY:HEMA analogue

Polymers of this type were prepared through both microwave and conventional heating as well as with differing molar ratios of BODIPY-HEMA:HEMA and interesting results were observed. By increasing the ratio of the BODIPY-HEMA conjugate, it was observed that the fluorescence quantum yield of the resulting polymer was lower than a less concentrated mixture. This fluorescence quenching was attributed to aggregation of the fluorophores and the formation of H-dimers. It was also observed that, on the whole, the microwave-assisted polymerisation reactions produced polymers with slightly higher quantum yields than *via* conventional heating. This led to a different mechanism of polymer assembly being proposed for each heating method (Fig. 1.74). It was observed that microwave heating discouraged aggregation of the polymer strands, and thus disrupted aggregation of the fluorophores causing a higher quantum yield. Similar to the *F*-substitution polymers, these hybrid polymers displayed very similar fluorescence to their respective monomer.

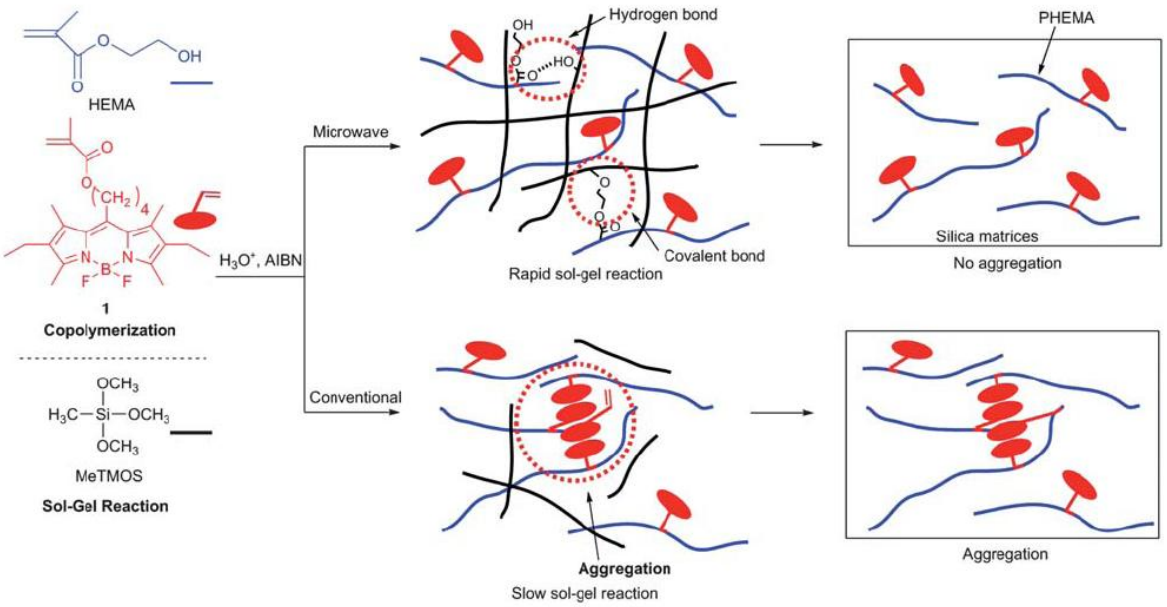

Figure 1. 74: Proposed mechanisms of polymer assembly for microwave-assisted and conventional heating of BODIPY-containing hybrid polymers[205]

Similar co-polymers have been prepared by reaction of a BODIPY:HEMA analogue with 2-(dimethylamine)ethyl methacrylate (DMAEMA) intercalated between terminal units of cumyl dithiobenzoate (CDB) (**1.113**).[206] The most useful aspect of this polymer was its solubility in water. The fluorescence intensity of these polymers was observed to increase with increasing temperature making them useful as water soluble thermometers. This fluorescence increase was thought to be due to decreasing fluorophore aggregation with increasing temperature. Polymers **1.113** as well as an analogue containing ethynyl-phenyl groups on the boron atom were found to adopt particular structures.[207]

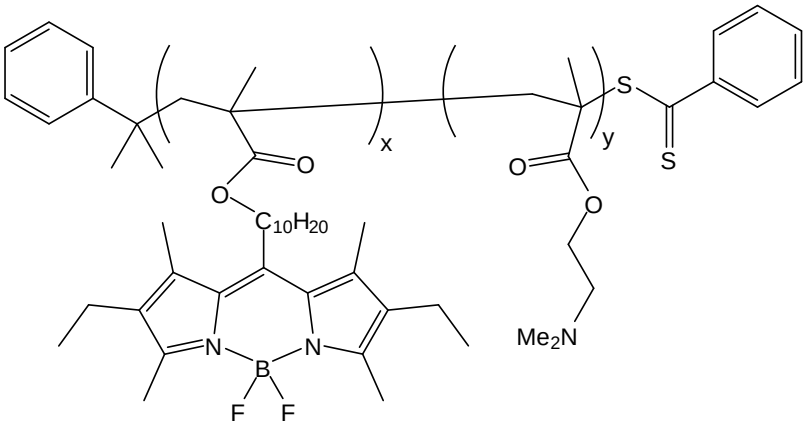

1.113

Figure 1. 75: BODIPY:HEMA polymer

The same effect was observed for a BODIPY-containing polymer formed by a quaternary pyridinium-BODIPY (**1.114**).[208] Below 23°C the fluorescence of the polymer was very weak, but a 5-fold increase in fluorescence intensity was observed upon increasing the temperature to 35°C, at which no further increase was observed (Φ_F = 0.262). This fluorescence increase was promoted by heat-induced polymer aggregation, which caused the formation of viscous microdomains, suppressing the rotation of the BODIPY pyridinium ring. This polymer was found to be stable enough to be used as a fluorescent thermometer at least ten times.

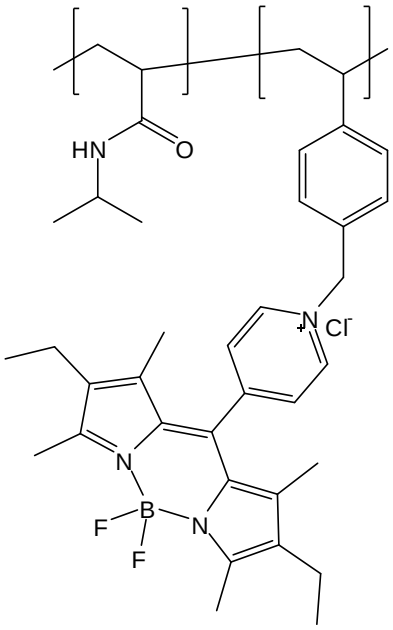

1.114

Figure 1. 76: BODIPY polymer bearing a quaternary pyridinium moiety

2.11.4 Polymerisation through metal-complexation and conducting polymers

A novel BODIPY-containing polymer was prepared by using zinc-terpyridine as a linker group (**1.115**).[209] A gradual fluorescence increase was observed upon titration of the uncomplexed form with zinc (II) triflate indicating the formation of the polymer. Two absorption peaks in the UV region also became more intense with increasing coordination polymer formation. Zinc coordination could be monitered *via* peaks in the ^{1}H-NMR spectrum becoming sharper with increasing amounts of zinc. This particular type of polymer could find use in electrochromic devices.

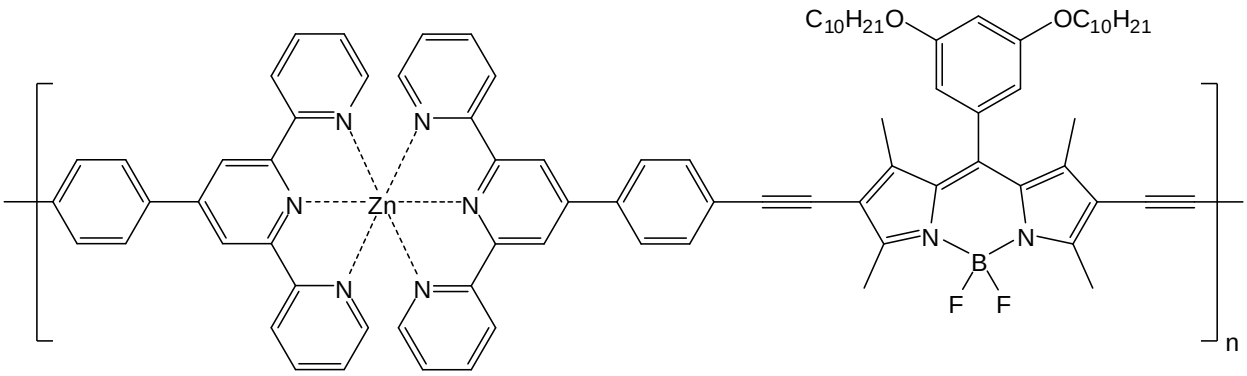

1.115

Figure 1. 77: BODIPY-terpyridine-zinc coordination polymer

As seen previously, BODIPYs can be used as components in novel photovoltaic devices. This work has been extended into the preparation of conducting BODIPY polymers. The initial investigations into conducting BODIPY polymers were carried out using a polythiophene/pyrrole-BODIPY system (**1.116**).[210] It was found that this polymer adopted 'cauliflower-like' structures in solution, indicating that polymer growth takes place after initial nucleation. Significant changes in transmittance were observed when the polymer was switched between -0.2 V and 1.2 V electric fields. A clearly visible colour change was also seen upon switching between -1.3 V and 1.1 V (red, pink, blue and green at -1.3 V, 0.0 V, 0.8 V and 1.1 V respectively).

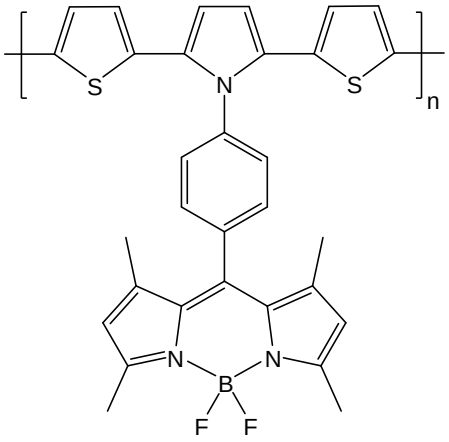

1.116

Figure 1. 78: Conducting BODIPY polymer

A donor-acceptor polymer has been prepared incorporating a BODIPY acceptor and 3,4-ethylenedioxythiophene (EDOT) donor (**1.117**).[211] As seen for the previous conducting polymer (**1.116**), a colour change was observed upon oxidation from violet (neutral) to indigo (oxidised). A clear increase in the absorption in the IR region (two-photon absorption) was seen with increasing applied voltage. A red-shift in the absorption was also observed upon conjugation of the EDOT units due to extension of the delocalized π-system.

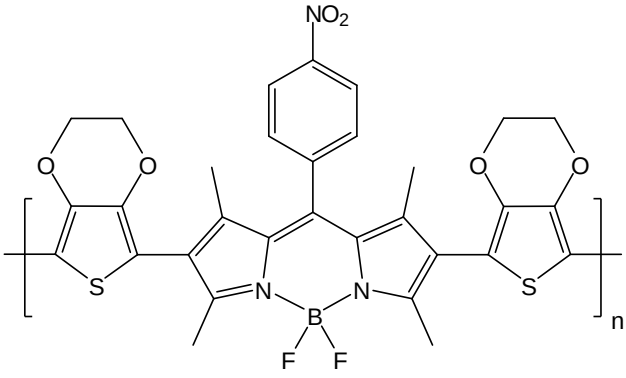

1.117

Figure 1. 79: Conducting BODIPY polymer with extended π-conjugation

An analogue of **1.117** containing thiophene units between the EDOT groups has been prepared and a slight red-shift in the absorption was observed with increasing applied potential.[212] A clear colour change from pink to blue was also observed upon oxidation. A more straightforward relationship between applied potential and absorption was observed for this analogue. A gradual decrease in BODIPY absorption with a concurrent increase in absorption in the IR region (two photon absorption) was observed with increasingly positive applied potential. Similar structures to those of **1.117** were observed under scanning electron microscopy.

3. Supramolecular assemblies

There is a large worldwide demand for self-assembling materials. One class of self-assembling material are liquid crystals. The behaviour of these, and other self-assembling materials, is altered by manipulating the intermolecular interactions that can occur in the material. This is achieved by synthetic manipulation of a molecule until it displays the desirable interactions.

3.1 Principles of self-assembly

Supramolecular assemblies are concerned with intermolecular interactions, as opposed to covalent bonds between atoms. This has led to the area as being referred to as the chemistry of molecular assemblies using non-covalent bonds.[213] The homolytic bond dissociation energy of a covalent bond is usually between 100-400kJ mol^{-1}. Non-covalent interactions are generally much weaker. Van der Waals interactions can be less than 5kJ mol^{-1} while metal-ligand interactions can have dissociation energies comparable to those of covalent bonds. Hydrogen bonding and π-π interactions are important factors to consider in the design of self-assembling materials.[214] This is because they can be manipulated to induce a limited degree of order to a material, so that it can form mesophases between being a solid and a liquid.

π-π interactions are prevalent in π-conjugated materials. The cause as well as the strength of these interactions can vary however. For example, the stacking interactions of aromatic molecules in water is mainly due to their hydrophobicity. The water molecules that are solvating the surface of the aromatic molecules have a higher energy than the rest of the water molecules. This causes the aromatic molecules to stack so that they have as little surface in contact with the water as possible. However, in solvents other than water the aromatic molecules have much less interaction with each other, so the stacking of the molecules varies depending on any solvophobic forces that occur.

Hydrogen bonds are also important in the construction of self-assembling materials. The benefit of these interactions is that they are highly selective and directional. One example of hydrogen bonds in action is between bases of DNA. Hydrogen bonds form between a donor with an available acidic proton interacting with an acceptor with a free non-bonding lone pair of electrons. The strength of these bonds depends on the solvent and the number and sequence of hydrogen bonds.[215]

3.2 Self-assembly of liquid crystalline materials

Liquid crystals have both the fluidity of a liquid and the orientational order of a crystal. The organisation of these materials is displayed in the mesophases they adopt and the temperatures at which they change phase. The number and type of phase they adopt are affected by the rigid part of the molecules, as well as their size and any peripheral side-chains that are attached. The liquid crystalline phases are not necessarily affected by temperature. Lyotropic liquid crystals occur when an appropriate molecule is in solution at a certain concentration. In this case, the solvent usually solvates part of the molecule while the rest of the molecule helps to promote aggregation, which leads to the formation of mesoscopic assemblies.

3.2.1 Thermotropic liquid crystals

Thermotropic liquid crystals form mesophases when heated to a certain temperature. When these mesophases are ordered in two dimensions they are known as *smectic* phases and when they are organized but have no two dimensional order they are known as *nematic* phases.

Smectic phases are arranged in layers that are roughly as thick as the molecules are long (Fig. 1.80). This leaves only very small interactions between layers causing the phase to display fluidity. The high degree of order in smectic phases is indicated by their greater viscosity when compared to nematic phases.[216]

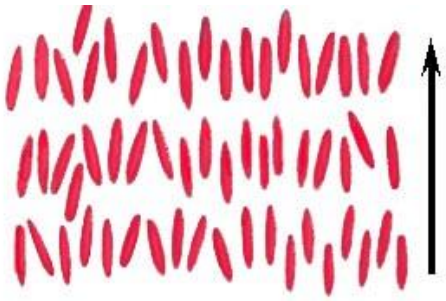

Figure 1. 80: Molecular organisation in a smectic A phase[217]

There are several different types of smectic phase, which are characterised based on the molecular ordering within each layer.[218] There are some compounds that display several smectic phases when warmed.

Nematic phases have no layers, unlike smectic phases. In these phases the molecules are ordered so that they all point in the general direction of a director (n) (Fig. 1.81). The molecules in these phases are parallel to each other and are free to move in all directions, but only to rotate about their longitudinal axis. Because of the increased mobility of the molecules in a nematic phase, they are much less viscous than smectic phases.

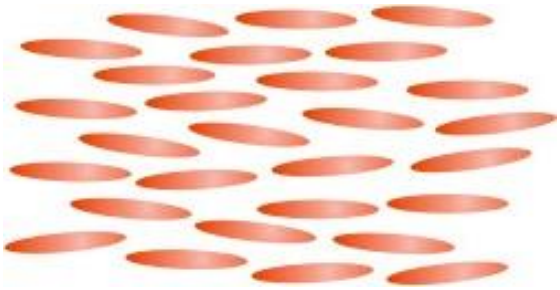

Figure 1. 81: Molecular organisation in a nematic phase[219]

There is a second type of nematic phase known as a chiral nematic (formerly referred to as cholesteric) phase. In this phase, the molecules are still arranged so that they have no two dimensional order but point in the direction of a director. However, if slices were taken of this phase while travelling down the film of liquid crystal, it would be found that the director rotates (Fig. 1.82).

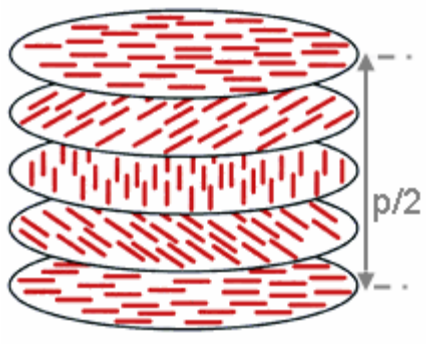

Figure 1. 82: Rotation of the director in a chiral nematic phase[220]

These phases display high optical rotation, which makes them ideal for use in liquid crystal display devices. This chiral phase can be induced by the liquid crystal molecules containing a chiral substituent or by doping the nematic phase with a chiral (but not necessarily liquid crystalline) compound.

All these examples are phases of calamitic (rod-like) molecules. However, disc-like molecules can also form liquid crystal mesophases. These are called discotic (disc-like) liquid crystals. While calamitic molecules can form smectic phases, discotic molecules form columnar phases (Fig. 1.83).

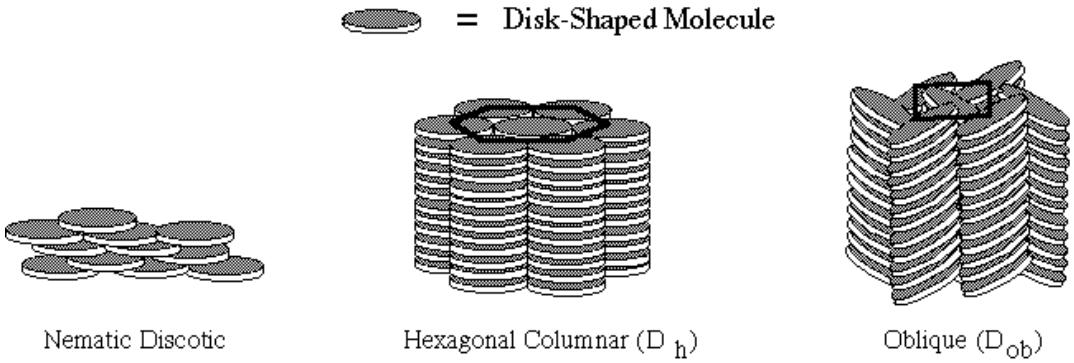

Figure 1. 83: Molecular organisation of discotic phases[221]

The first discotic molecule was discovered in 1977.[222] The columnar phase is similar to the smectic phase, in that they both have some ordering in the layers and that the layers have much weaker interactions between them than the molecules within the layers.

Discotic molecules tend to consist of an aromatic core with alkyl chains radiating out from it like spokes.

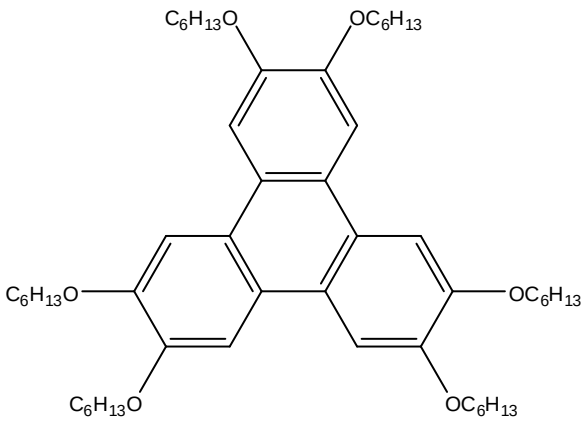

Figure 1. 84: Discotic liquid crystal

By increasing the interactions of the aromatic cores the columnar mesophases can be stabilised. This is generally achieved by increasing the size of the aromatic core to allow more π-π interactions to occur. An increased number of π-π interactions also allows for an increase in the ability of the molecules to transfer charge between them. This is also the case for calamitic liquid crystals, causing some mesophases to exhibit semi-conductive properties.

3.2.2 Lyotropic liquid crystals

Lyotropic liquid crystals display liquid crystallinity when dissolved in a solvent. They consist of a polar section and a non-polar section. Depending on the solvent being used, one part of the molecule promotes solvation, while the other part promotes aggregation. At an appropriate temperature and concentration, this causes the molecules to adopt micellar or laminar formations. One factor that can be manipulated in the design of lyotropic liquid crystals is the solvophobicity of the molecule. An increase in solvophobicity will promote aggregation of the molecules in solution. One prime example of a lyotropic liquid crystal is the phospholipid bilayer present in cells Fig. 1.85).

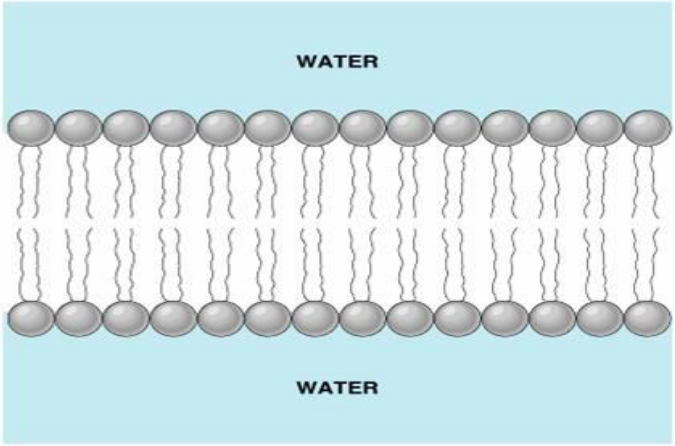

Figure 1. 85: Phospholipid bilayer[223]

In this case the molecules contain a hydrophilic phosphate 'head' and a hydrophobic lipid 'tail'. In water, the hydrophilic 'heads' line up to face the solvent, while the hydrophobic 'tails' line up to reduce their interactions with the solvent. This bilayer is fluid but clearly retains some intermolecular ordering, like all liquid crystals, hence it being known as a 'fluid mosaic'.

3.2.3 Mesogenic BODIPYs and their self-assembling properties

Because of their remarkable fluorescent properties, BODIPYs have been attracting increasing interest as self-assembling materials; particularly liquid crystals due to their increasingly common usage in display devices. BODIPYs were initially found to adopt columnar phases when appended with multiple alkyl chains.[224, 225] In this study, two discotic liquid crystals were prepared, one of which had the mesogenic unit further away from the BODIPY core (**1.118** and **1.119**). Four analogues of **1.118** were prepared where n = 1, 8, 12 and 16, while only the n = 8, 12 and 16 analogues of **1.119** were synthesised. Each of the **1.118** analogues (other than n = 1) exhibited a hexagonal columnar phase (Col_h) with gradually decreasing melting points and phase transitions, but widening columnar range with increasing chain length. The same effects were observed for the n = 12 and 16 analogues of **1.119** (the n = 8 analogue did not display a mesophase). Several of the compounds also displayed crystal-crystal transitions, and decomposition occurred when the n = 8 analogue of **1.118** was heated above 250°C.

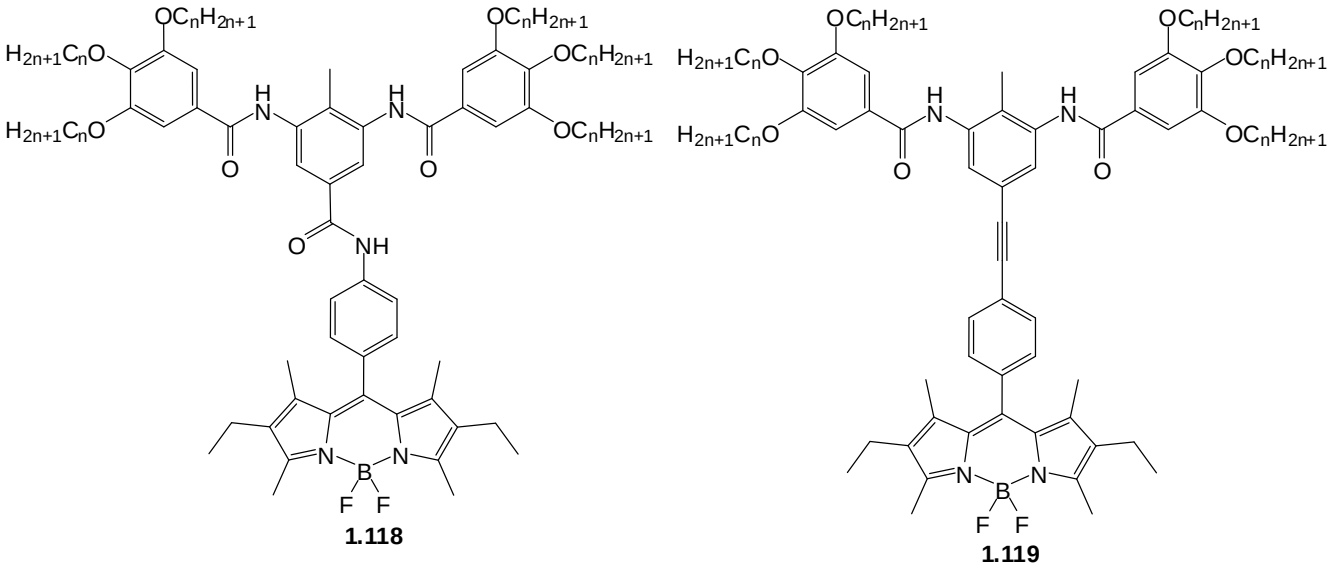

Figure 1. 86: Discotic BODIPYs

A fan-like texture was observed in the hexagonal columnar phase when viewed under crossed polarisers and this texture could still be seen when irradiated at 300-350 nm and not viewed under crossed polarisers (Fig. 1.87). Both these images were superimposed onto one another and it appeared that emission of the BODIPY in the liquid crystalline state was related to the different molecular orientations when in the mesophase (Fig. 1.88). A red-shift was also observed in the transition from the mesophase to the crystalline phase due to the formation of aggregates. These compounds were shown to undergo efficient gelation in nonane to form highly luminescent gels. An n = 17 analogue of compound **1.118** was found to exhibited electrogenerated chemiluminescence when excited with an applied electric field or with a coreactant (benzoyl peroxide).[226]

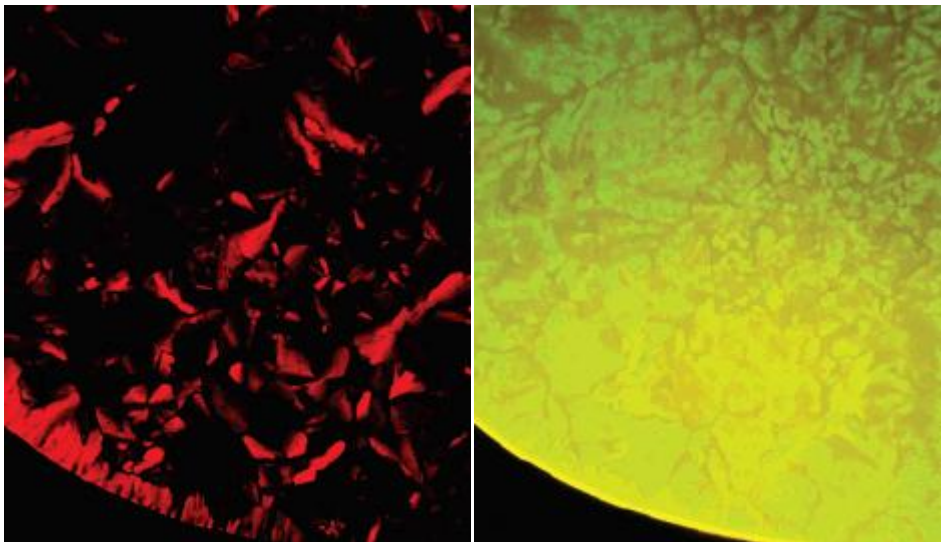

Figure 1. 87: n = 16 analogue of 1.119 when viewed under crossed polarisers in the hexagonal columnar phase (left) and the same sample under irradiation and under aligned polarisers (right)

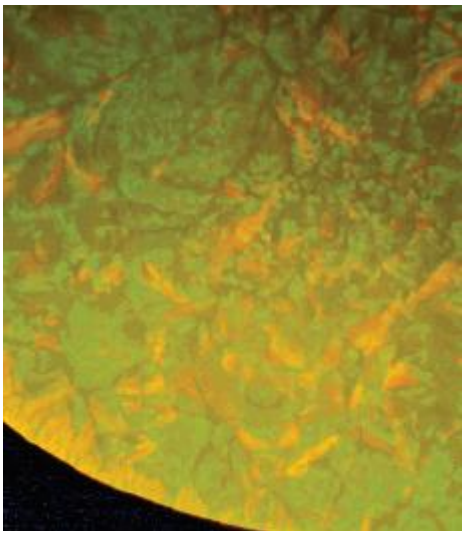

Figure 1. 88: Superimposed images of n = 16 analogue of 1.119 when viewed under crossed polarisers and under irradiation

A series of BODIPYs with similar structures to compound **1.118** have also been prepared and, while lacking mesophase formation, have been shown to readily form thin films (**1.120**).[227] As seen for several of the BODIPY-containing polymers, it was the alkyl chains that promotes this thin film formation. Electrogenerated chemiluminescence was observed for these compounds making them potentially useful in organic LEDs (OLEDs).

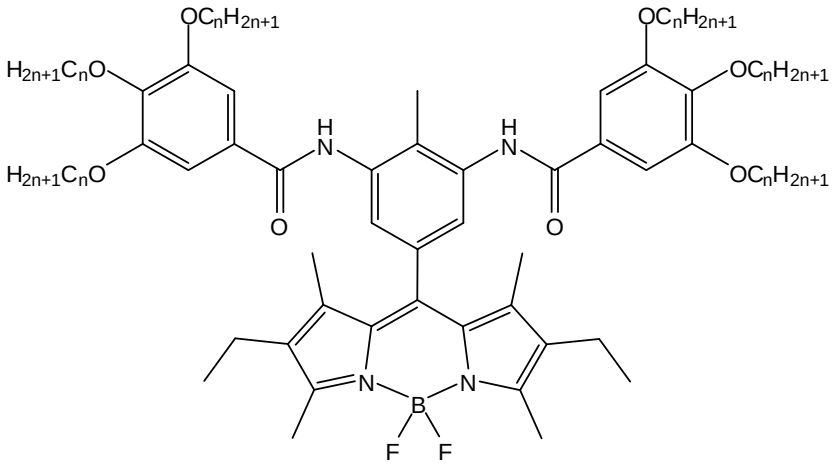

1.120

Figure 1. 89: Discotic BODIPY which forms thin films

An analogous monomesogenic BODIPY was also prepared which, despite displaying birefringence, did not exhibit any mesophase formation (**1.121**).[228] As with the analogues of compound **1.120**, analogues of **1.121** were found to form thin films and undergo electrogenerated chemiluminescence. It was observed that by using a higher voltage to generate chemiluminescence, the resulting luminescence intensity increased.

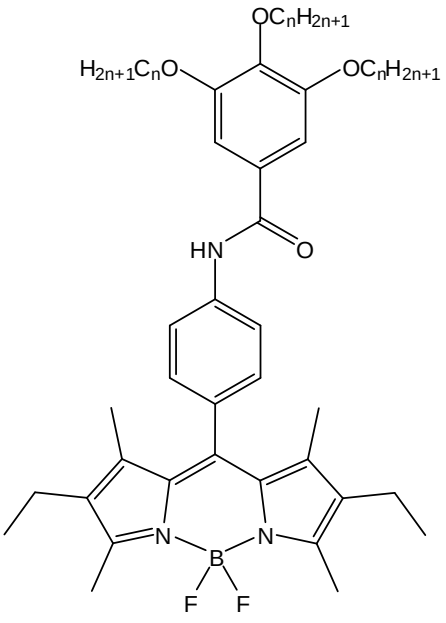

1.121

Figure 1. 90: Chemiluminescent BODIPYs

The first example of a BODIPY exhibiting the nematic phase was observed for a relatively small molecule, consisting of a BODIPY conjugated to a cyanobiphenyl by an alkyl chain (**1.122**).[229] This compound displayed a remarkably stable (90°C) enantiotropic nematic phase between 47-137°C. Interestingly, both the BODIPY and the uncomplexed mesogenic dipyrrin displayed nematic behaviour, with the BODIPY having slightly higher crystal-to-nematic and nematic-to-isotropic transition temperatures (41°C and 132°C for the uncomplexed dipyrrin and 47°C and 137°C for the BODIPY). A mesogenic bis(dipyrrinato)-nickel complex also displayed nematic behaviour, but as a monotropic phase between 134°C and 119°C.

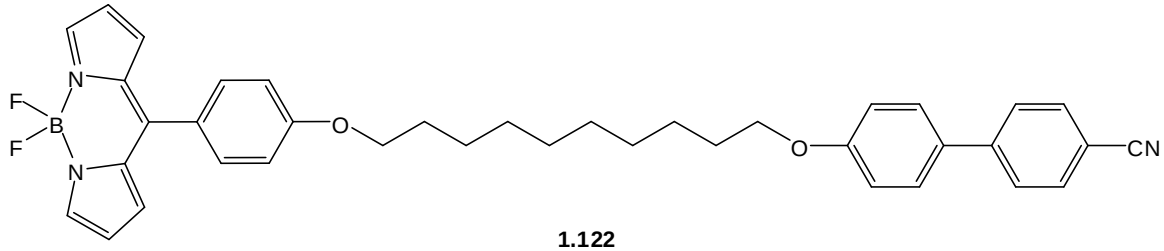

1.122

Figure 1. 91: Mesogenic BODIPY exhibiting nematic phase behaviour

Since this initial discovery, nematic behaviour has been conferred on BODIPYs by attaching them to liquid crystalline dendrimers.[230] A series of first, second and third generation liquid crystalline dendrimers were prepared and attached to a highly fluorescent BODIPY core; both nematic and smectic A behaviour was observed for the resulting mesogenic BODIPYs. The first generation BODIPY-dendrimer exhibited a nematic phase, as well as a mesophase that could not be identified. This transition from the crystal to the unknown mesophase occurred at 86°C, followed by transition into a short-lived nematic phase at 119°C before melting into the isotropic liquid at 123°C. Nematic behaviour was not observed for either the second or third generation BODIPY-dendrimers with only smectic A phases being exhibited for these compounds. The transition from the second to the third generation dendrimer caused a reduction in the crystal-to-smectic A transition temperature (100°C to 83°C) and an increase in the smectic A-to-isotropic transition temperature (155°C to 211°C), resulting in an increase in the smectic A stability. Each increase in the number of mesogens caused an increase in

the crystal-to-mesophase transition enthalpies and a concurrent increase in the enthalpy contribution per mesogenic unit. For this series of compounds, it was proposed that the BODIPY fluorophores aggregated into sublayers with the dendritic units forming layers above and below the layer of BODIPYs, with interdigitation occurring between the denritic units of adjacent layers. Like BODIPY polymer **1.114**, temperature dependant fluorescence studies were carried out on the molecules in the crystal, nematic, smectic A and isotropic liquid phases, but no significant change in fluorescence intensity was observed when going from one mesophase to the next.

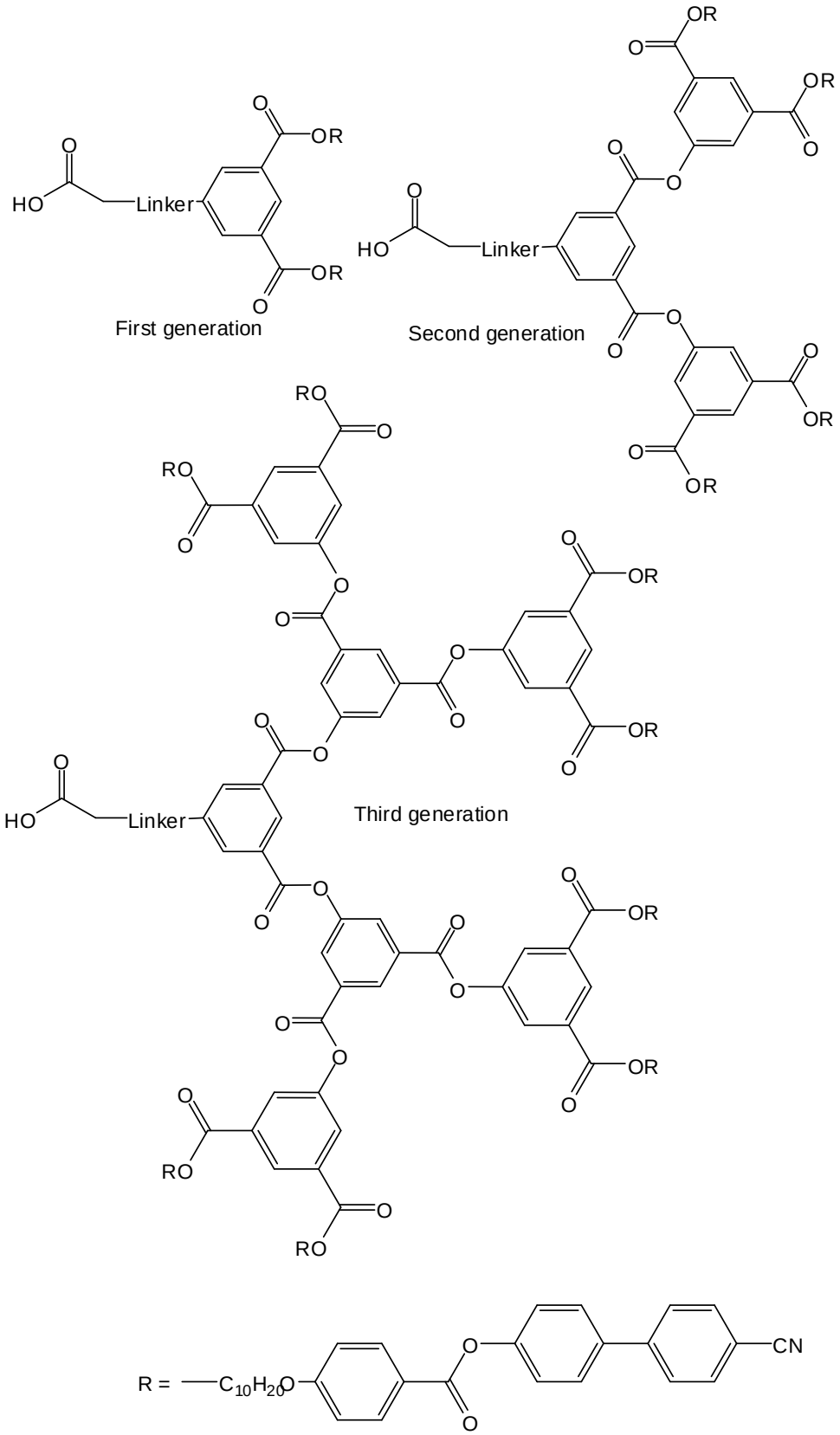

Figure 1. 92: Liquid crystalline dendrimers for attachment to BODIPYs

Ionic liquid crystals have been prepared based on BODIPYs bearing sulphonate units ionically bound to gallate-based mesogens (**1.123**) (gallic acid – 3,4,5-trihydroxybenzoic acid).[231] Three different alkyl chain lengths were employed to investigate the self-assembly behaviour of these compounds (n = 12, 14 and 16). Each analogue was found to decompose above 180°C and displayed a slightly shorter hexagonal columnar range with increasing chain length. The columnar range was still found to be very wide, being over 160°C for each compound. It was suggested that each disc in the hexagonal columnar phase consisted of centrally aggregated BODIPY units surrounded by the mesogenic units. This was the first example of a BODIPY-based ionic liquid crystal as well as the first example of a BODIPY-based liquid crystal in which the mesogenic units were not attached to the central position of the BODIPY fluorophore.

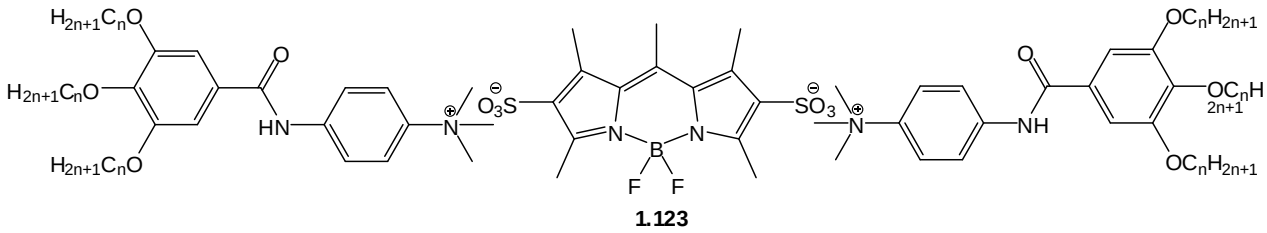

1.123

Figure 1. 93: Ionic BODIPY liquid crystal formed by interactions between quaternary ammonium and sulphonate groups

This work was extended to prepare BODIPY-based ionic liquid crystals with the same gallate-based mesogen, but coordinated to the sulphonate groups by imidazole groups (**1.124**).[232] Three analogues of compound **1.124** were prepared (n = 8, 12 and 16) and each exhibited a hexagonal columnar phase. Similar transition temperatures were determined for each of the analogues with a fan-like texture being observed when viewed under crossed polarisers. As for compound **1.123**, it was proposed that the BODIPY units aggregate together and the mesogenic units form a disc-like shape around them. An n = 12 analogue was prepared which terminated in a methacrylate group and was polymerized *via* a photoinduced mechanism. The resulting polymer was found to form thin films and to be highly chemically stable.

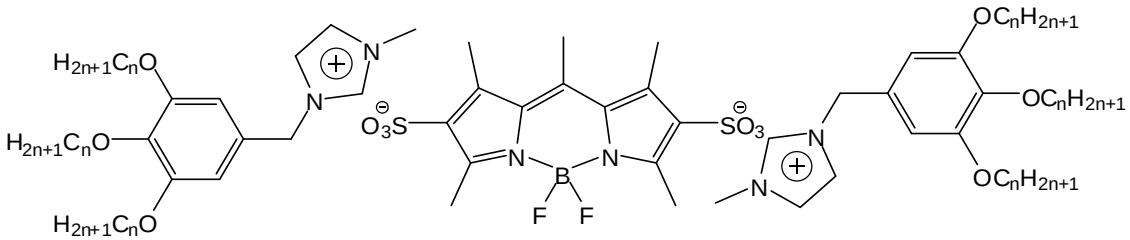

1.124

Figure 1. 94: Ionic BODIPY liquid crystal formed by interactions between imidazole and sulphonte groups

A polymer dispersed nematic liquid crystal host has been doped with a simple BODIPY dye to study the alignment of the dye molecules relative to the host material.[233] Reorientation of the dye molecules was proposed to occur by interactions with both the host material and directly with the electric field. The two reorientation mechanisms cause a rotation of the dye alignment axis, thus causing a change in the fluorescence intensity due to rotation of the dye transition dipole moment. This rotation of the dye transition dipole moment caused a reduction in the fluorescence intensity when the electric field was switched on. The drop in fluorescence intensity was not a clear ON/OFF switching, but rather a reduction by approximately 60 counts when the electric field was on. Due to the dye molecules being a very dissimilar shape to the nematic host material, they only align with the host weakly; so while this initial study lays the groundwork for further research, BODIPYs that align more strongly with the host material may display very different properties.

4. Conclusions

The remarkable fluorescence properties of BODIPYs give them great potential as photoactive materials. Increasing interest in the chemistry of BODIPYs is helping to fuel the number of applications they can be used for, including non-materials based applications, such as chemosensors[234-238] and as imaging agents.[239-244] BODIPYs have even started to find applications as photodynamic therapy agents,[245-247] usually considered to be the primary application of porphyrins and phthalocyanines.

The high efficiency of energy transfer from and to BODIPY dyes has allowed them to find applications in energy transfer arrays and hence solar cells. They exhibited surprisingly high power conversion efficiencies in both bulk heterojunction solar cells as well as dye-sensitized solar cells. While BODIPYs for BHJs display efficient photocurrent generation, they tend to require groups that promote film formation (e.g. PEG) in order for them to be dispersed throughout the heterojunction, BODIPYs for titatium dioxide sensitisation, however, just require a group that enables binding to the inorganic material (e.g. carboxyl). While this would seem to make dye-sensitizing agents a more attractive prospect for photocurrent generation, the increasing use of organic materials like BHJs promotes further research into BODIPYs as BHJ components.

Due to their intense fluorescence and high photostability, BODIPYs can also be used as laser dyes with remarkably high efficiencies in some cases. This laser activity has prompted several groups to dissolve the dyes in a solid polymer matrix, in which the dyes lase with a lower efficiency than in liquid solution but with a higher stability. The BODIPYs remain laser active even when dissolved in a semi-ordered material like a nematic liquid crystal. The dye molecules have been shown to align weakly with the host material and lasing has been observed when the dye-doped material is incorporated into an optical cell, capillary tube, and when freely suspended. Due to the prevalence of the polymer and liquid crystal host materials, and the commercial availability of a range of BODIPY dyes, laser activity studies of this type are the most easily accessed area of materials research for BODIPYs.

While commercial BODIPY dyes can be readily dissolved in a polymer matrix, the incorporation of BODIPY fluorophores into the polymer backbone itself requires greater synthetic consideration. It has been shown by several groups that BODIPYs can be incorporated into a polymer chain by attachment through the BODIPY core, by fluorine substitution, or through the BODIPY *meso*-position. This leads to a wide variety of polymers with a range of self-assembling and photophysical properties. These polymers can also be cast as thin films which possess different photophysical properties to the BODIPY polymer in solution, allowing colour tuning to take place even after the

synthesis of the molecule is complete. Polymerisation has even been shown to occur through metal complexation when the appropriate ancillary ligands are attached. Due to the delocalised π-system and efficient energy transfer processes that can occur in BODIPYs, conducting polymers can be prepared which show high sensitivity to an applied electric field (electrochromism), making them potentially useful as molecular switches.

More recently, attempts have been made to incorporate the BODIPY fluorophore into a liquid crystalline molecule. Initially, discotic type molecules were prepared, some of which exhibited hexagonal columnar phases, while others could be cast as thin films but did not display any mesophase behaviour. The first example of a BODIPY-containing nematic liquid crystal was reported by Boyle *et al.* and consisted of a BODIPY fluorophore conjugated to a cyanobiphenyl mesogen. Despite being a relatively simple mesogen, the resulting mesogenic BODIPY exhibited a wide range nematic phase at moderate temperatures. Liquid crystal dendrimers terminating in cyanobiphenyl units have also been employed to induce liquid crystallinity onto a BODIPY quite effectively but require additional synthetic steps for dendrimer synthesis. Ionic liquid crystals have also been prepared which exhibited hexagonal columnar phases with each disc being formed from aggregated BODIPYs surrounded by mesogenic units. These results illustrate that BODIPYs have promise as fluorescent liquid crystals; however, this particular area of research is still in its infancy and further work is required before BODIPY-based liquid crystals find their way into optoelectronic devices.

There are a growing number of reactions that can be carried out on BODIPY dyes, with each one affecting the photophysical properties of the dye in reasonably specific ways, and these reactions are being exploited in the preparation of new BODIPY-based materials. The recent synthesis of the core BODIPY dye (fully unsubstituted) finally allows each new BODIPY and BODIPY-based material to be compared to a relevant standard. These factors, plus the increasing interest in organic materials, are fuelling the preparation of new, novel photoactive materials based on BODIPY dyes, primarily for the production of highly sensitive optoelectronic devices and more efficient solar cells.

Chapter 2: Aims

The self-assembly properties of BODIPYs are still relatively unexplored, with BODIPYs exhibiting a nematic phase being the most recent development.[229, 230] In each of these examples, the nematic phase was found to be moderately stable due to the BODIPYs tendancy for aggregation being overcome by the attached mesogenic unit. The mesogenic BODIPY prepared by Boyle *et al.* is of a relatively small molecular size compared to the mesogenic BODIPYs prepared by Ziessel *et al.* which incorporated a liquid crystal dendrimer. In each of these BODIPYs, the mesogenic unit was attached at the 8-aryl substituent in order to give the molecule a 'rod-like' structure.

Our first objective was to move the position of mesogen attachment onto one of the pyrrolic positions in order to observe the effect this had on the self-assembly behaviour. Attachment of the mesogenic units to the pyrrolic positions using ionic bonding has been previously reported.[231, 232] Our approach however, was to attach the mesogens *via* a covalent linker. The BODIPYs prepared would incorporate a moderately flexible linker group between the mesogen and the fluorophore. As the BODIPY would be 8-unsubstituted, the fluorescence quantum yield would be very large compared to unsubstituted 8-aryl BODIPYs. Our aim was to prepare a BODIPY that exhibited a nematic phase as this mesophase is required when designing a liquid crystal display device. Due to cyanobiphenyl mesogens having a greater preference for nematic phase behaviour, they would be expected to be better at conferring the desired liquid crystallinity onto the BODIPY due to the polar nature of the nitrile group; however, a mesogen with the alkyl chain in the terminal position can also be attached to investigate this effect. In order to increase the preference for mesophase formation, one approach to attach two mesogenic units to a similar fluorophore. The mesogens chosen for this would be those that provided the mono-mesogenic BODIPY with the greatest preference for mesophase formation.

In an attempt to fine-tune the self-assembly properties of previously reported 8-aryl BODIPYs,[229, 230] several series of mesogenic 8-aryl BODIPYs can be prepared with varying linker groups between the mesogen and the fluorophore. Each series would consist of three BODIPYs with increasing alkyl substitution on the BODIPY core in order to produce a gradual increase in fluorescence quantum yield through the series. These alkyl groups can also have an effect on the preference of the mesogenic BODIPYs for mesophase formation. This would provide some information about whether a structure-property relationship exists between fluorescence intensity and liquid crystal phase stability. In order to investigate the effect of increasing the molecular length on the self-assembly properties of the molecules, mesogenic BODIPYs incorporating an ethynyl group can be prepared. The effect that a non-linear molecular shape has on the self-assembly properties of BODIPYs is currently unknown. Thus far, no nematic BODIPYs incorporating a bent-core structure have been reported. In order to investigate this, a BODIPY incorporating a triazole linker group between the mesogen and the fluorophore is required. It was anticipated that a triazole linker group between the mesogen and the fluorophore would cause the molecule to have a 'kink' in its shape.

It was expected that any mesophases exhibited by the mono-mesogenic BODIPYs would be stabilised by the attachment of a second mesogenic unit. In order to investigate this, a series of di-mesogenic BODIPYs is required. This can be achieved by preparing BODIPYs with two reactive sites for mesogen attachment at the 8-aryl group. This series would allow investigate any structure-property relationship between fluorescence quantum yield and liquid crystal phase stability by increasing alkyl substitution on the BODIPY core through the series to be identified. Similar mesogens can be used for this series as for the previous mono-mesogenic BODIPYs in order to effectively compare the two classes of compound.

Due to recent attempts to prepare BODIPYs with significantly red-shifted fluorescence,[87, 248] the synthesis of a mesogenic BODIPY with red-shifted fluorescence is of major interest. This is due to all the previously reported mesogenic BODIPYs having very similar fluorescence profiles. It was anticipated that this could be achieved by extending

the conjugation of the BODIPY core by attached aryl or styryl groups. An aza-BODIPY bearing four aryl units and a BODIPY with attached styryl groups may provide the desired properties. Due to the increased size of the aza- and styryl-BODIPYs compared to their non-extended analogues, it was expected that multiple mesogenic units would be required to induce liquid crystallinity. This can be investigated by attaching increasing numbers of mesogens onto various positions on the fluorophore. Due to increased interest in the potential uses of BODIPYs in optoeletronic devices, the temperature- and alignment-dependant fluorescence of several of the prepared BODIPYs by measuring the fluorescence at various temperatures and when dissolved in a commercial liquid crystal and incorporated into a twisted nematic cell was identified as one of the major aims of this work. Alignment-dependant fluorescence measurements are of particular interest in the field of liquid crystal display devices.

Chapter 3: BODIPYs bearing mesogenic units attached at the pyrrolic positions

3.1. Introduction

4-Difluoro-4-bora-3a,4a-diaza-*s*-indacene (BODIPY) derivatives are attracting increasing attention, primarily due to their remarkable photophysical properties, high fluorescence quantum yields, sharp absorption spectra, large molar extinction coefficients and excellent photostability[32] have prompted several research groups to search for applications in both biological and materials fields.[249-251] Fluorescent chemosensors,[252] laser dyes,[172, 253] fluorescent labels,[254] photodynamic therapy[255] and electro-chemiluminescent materials[189, 256, 257] are some of the areas in which BODIPYs have been found to have potential use.

One class of materials of particular interest are liquid crystals, as they are able to exhibit various mesophases with differing degrees of molecular ordering. It is these mesophases that allow this extraordinary class of molecule to find applications in the expanding field of nanotechnology.[258] The use of BODIPYs as liquid crystalline materials, however, remains relatively unexplored.[224, 225, 228-232] Due to liquid crystal mesophases being intermediates between crystals and isotropic liquids, the structure of any potential liquid crystalline molecule must be carefully designed in order to control the strength of the intermolecular interactions. The effect that the attachment of the fluorescent BODIPY core has on the liquid crystalline behaviour of a mesogen has not, to the best of our knowledge, been systematically investigated.

The initial research into liquid crystalline/self-assembling BODIPYs involved the synthesis of discotic (‘disc-like’) liquid crystals using a branched structure, formed by the attachment of long alkyl chains to an aromatic unit attached to the 8-phenyl group by amide linkages.[224, 225, 231] This allowed the molecules to stack on top of each other, forming columnar phases. Additionally, the branched structure allowed the molecules to form gels in some cases (Fig. 3.1).

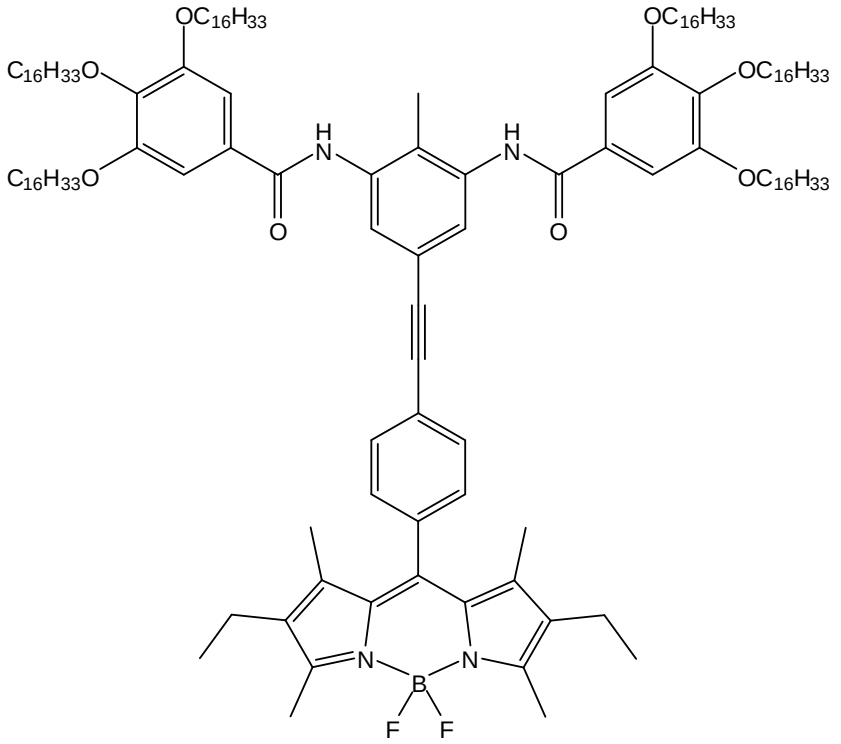

Figure 3. 1: Discotic BODIPY

The initial breakthrough in the incorporation of the BODIPY fluorophore in calamitic (‘rod-like’) mesogens was made by Boyle *et al.*[229] in which a cyanobiphenyl unit was attached to the 8-phenyl ring of a dipyrrin, and a nickel and boron-difluoro complex (Fig. 3.2) was subsequently synthesised, producing two calamitic nematic liquid crystals. This was also the first example of a BODIPY and dipyrrin complex that could adopt a nematic mesophase, indicating that this new class of molecule could find use in display devices or other areas of nanotechnology. A zinc complex of the same mesogenic dipyrrin was also synthesised, but it was found that this complex did not display a mesophase. This was attributed to the increased distortion from planarity of the dipyrrin ligands around the zinc centre.

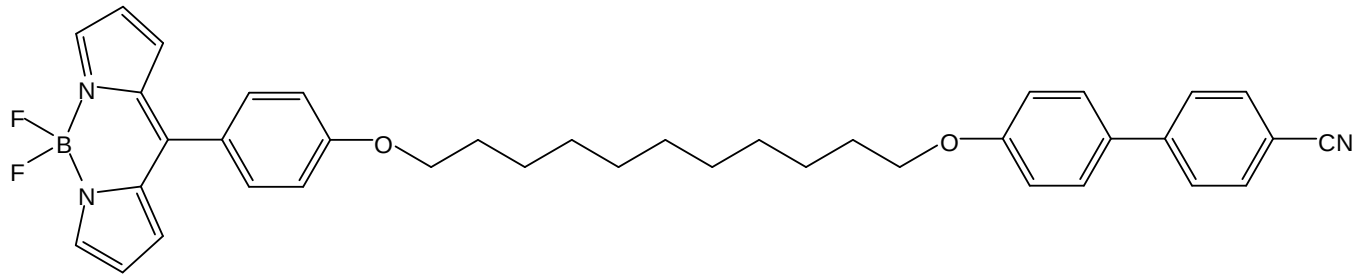

Figure 3. 2: Calamitic nematic mesogenic BODIPY

First, second and third generation liquid crystalline dendrimers have also been attached to the BODIPY core, also on the 8-phenyl ring, to induce liquid crystalline behaviour.[230] Despite the branched structure of these liquid crystalline dendrimers, the BODIPY-dendrimer conjugates adopt calamitic nematic phases (Fig. 3.3). Thus far, however, there has been no investigation into the effects of moving the position to which the mesogenic units are attached to a BODIPY fluorophore.

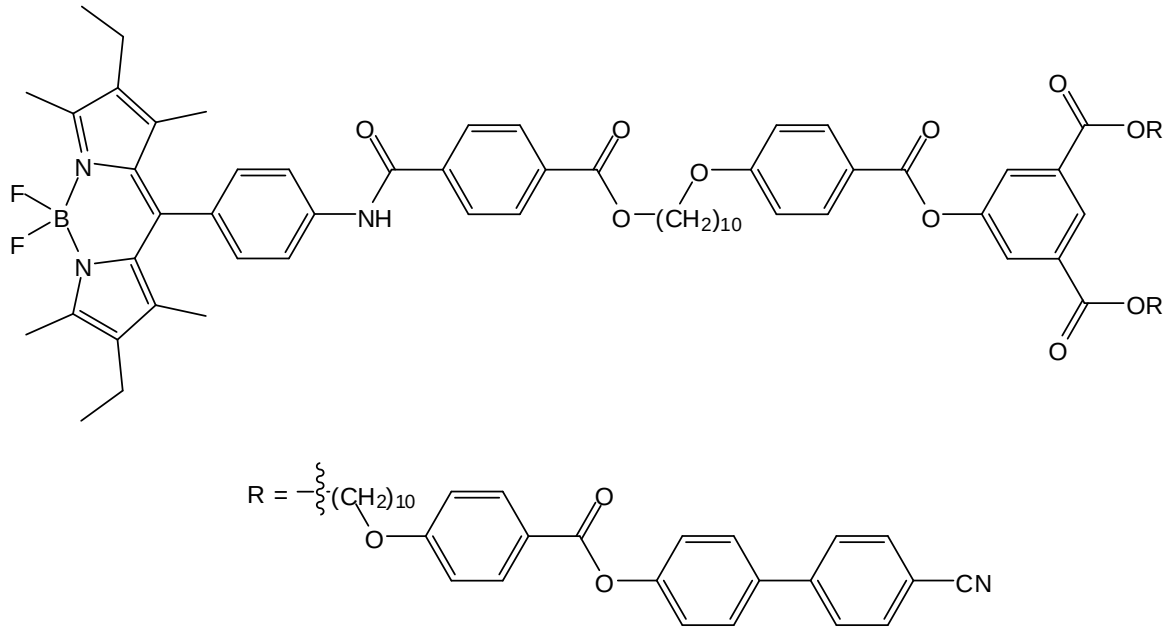

Figure 3. 3: First generation BODIPY LC-dendrimer

Thus far, all mesogenic BODIPYs have consisted of a dipyrrin core containing a phenyl substituent at the 8-position. This provides a convenient reactive site for mesogen attachment and a simple synthetic route to the core fluorophore. In the case of the

calamitic liquid crystals, the mesogen (including the long alkyl chain spacer) provides a long and relatively thin shape to the molecule, while the fluorophore appears to disfavour this rod-like shape due to its larger width. The size of the fluorophore would appear to disrupt the packing of the long molecules, while in the case of the discotic BODIPYs it would appear to enhance columnar packing due to its tendency towards aggregation. With this in mind we attempted to utilize the width of the BODIPY core to extend the linear length of the molecule as a whole (Fig. 3.4). This would potentially cause a reduction in the width-to-length ratio, presumably reducing the disruption of the molecular packing in any potential liquid crystalline mesophase.

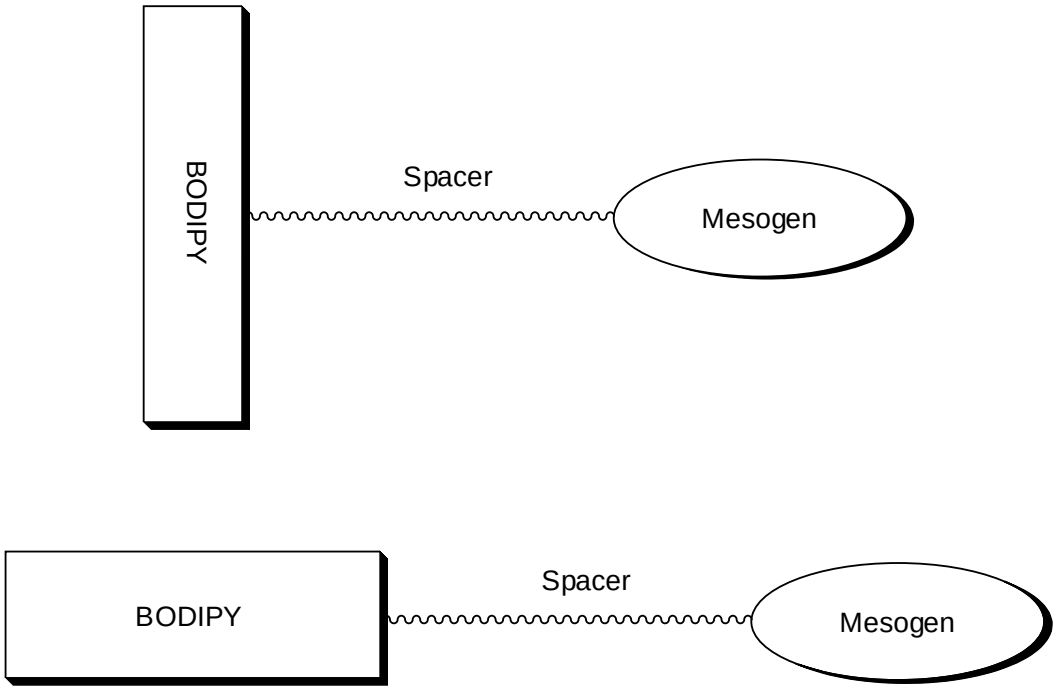

Figure 3. 4: 8-Phenyl-attached mesogenic BODIPYs (top) and our approach (bottom)

3.2. Results and discussion

3.2.1 Synthesis

In order to attain the desired shape of mesogenic BODIPY, we attached the mesogens to one of the pyrrolic positions of the fluorophore (Fig. 3.5). For this we chose an ester group as the linker between mesogen and fluorophore due to the ease of mesogen

attachment and ready incorporation into the BODIPY, owing to its presence on the initial Knorr pyrrole.

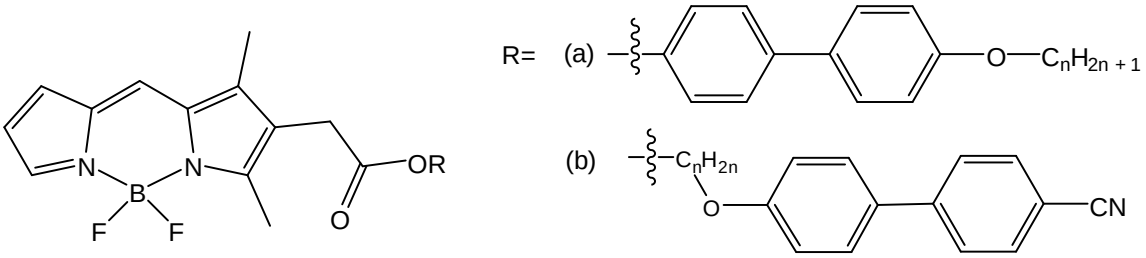

Figure 3. 5: Target compounds

The synthesis of side-attached mesogenic BODIPYs was achieved by first synthesising the pyrrolic precursors. These were synthesised *via* a Knorr pyrrole synthesis to give a pyrrole containing two ester groups (Sch. 3.1), one of which would ultimately be removed completely, while the other would be hydrolyzed to the carboxylic acid.

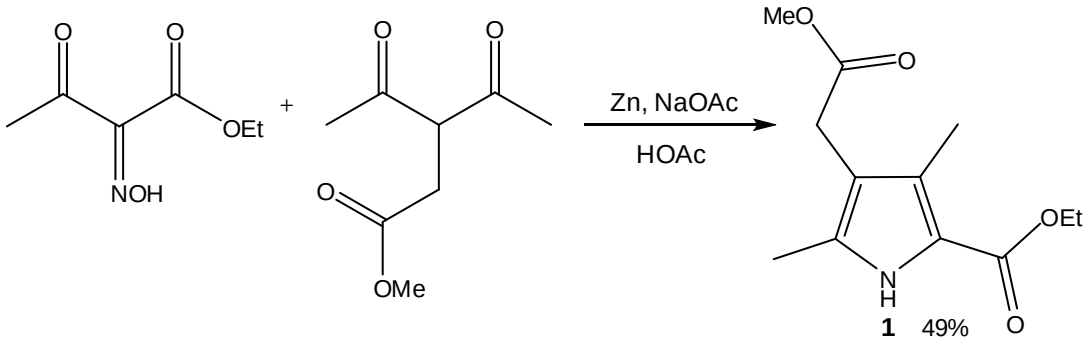

Scheme 3. 1: Knorr pyrrole synthesis

Firstly, the ketoester was synthesised by reacting methyl bromoacetate with 2,4-pentanedione in the presence of potassium carbonate. The resulting oil was partially purified by distillation under reduced pressure. The Knorr pyrrole synthesis was carried out under standard conditions,[259] using sodium acetate and zinc powder in hot glacial acetic acid, followed by precipitation by pouring the hot solution into cold water. Purification was achieved by recrystallisation from ethanol. Hydrolysis of the Knorr pyrrole was achieved by heating the pyrrole at reflux temperature in ethanolic sodium hydroxide (Sch. 3.2) with subsequent precipitation by acidification.

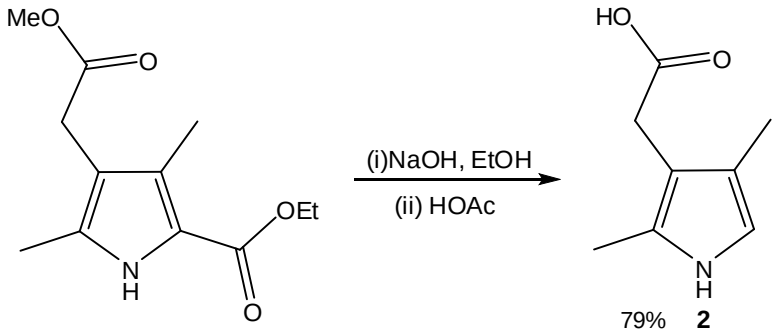

Scheme 3. 2: Pyrrole hydrolysis

2-Formylpyrrole was then synthesised *via* a Vilsmeier-Haack formylation carried out on pyrrole (Sch. 3.3). The formylation was carried out under standard conditions and the 2-formylpyrrole (**3**) was purified using column chromatography. The crude product was an oil so could be loaded directly onto the top of the column allowing for easy purification.

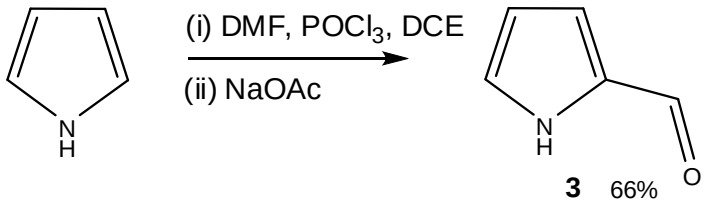

Scheme 3. 3: Vilsmeier-Haack formylation of pyrrole

The 2-formylpyrrole (**3**) and the hydrolyzed pyrrole (**2**) were then combined in glacial acetic acid with a catalytic amount of hydrobromic acid to synthesise the dipyrrin hydrobromide salt. The dipyrrin hydrobromide salt intermediate was not isolated due to its solubility in acetic acid making precipitation difficult, if not impossible. The acetic acid was then removed *in vacuo* and the residue dissolved in dry dichloromethane before triethylamine and boron trifluoride diethyl etherate were added to produce the BODIPY. The large number of side-products and high polarity of the BODIPY carboxylic acid meant that purification was exceedingly difficult using chromatography so an adequate ^{1}H-NMR spectrum could not be obtained. Due to the success of the subsequent mesogen attachment *via* DCC-coupling, it was presumed that the free BODIPY carboxylic acid was formed albeit in a low yield.

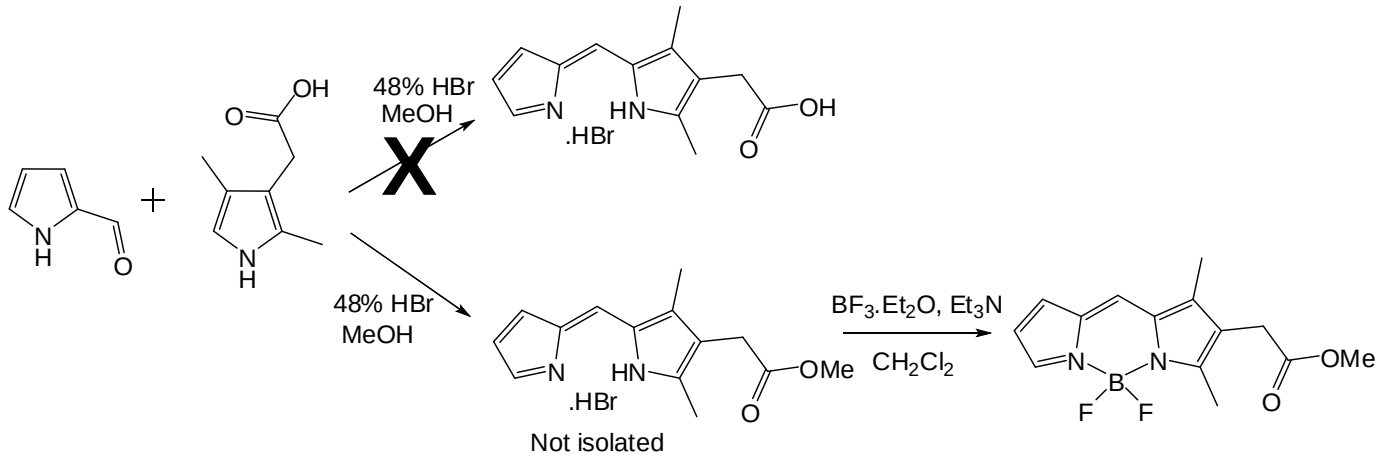

Scheme 3. 4: Fischer esterification of dipyrrin

While methanol or ethanol are normally used for the dipyrrin synthesis, it was observed that the free carboxylic acid group of the pyrrole allowed for Fischer esterification to occur when using these solvents, yielding the methyl or ethyl esters instead of the free carboxylic acid (Sch. 3.4). Hydrolysis of the BODIPY methyl ester was attempted to isolate the free carboxylic acid, but decomposition of the BODIPY occurred, despite the reaction being carried out in ethanolic lithium hydroxide at room temperature. An extraction into mild basic solution followed by precipitation/extraction using mild acid was also attempted, but again caused decomposition of the product. In each case, the fluorescence of the BODIPY was seen to reduce significantly. TLC analysis of the reaction mixture showed the decomposition of the BODIPY, possibly *via* deboronylation with regeneration of the dipyrrin. Due to the solubility of the dipyrrin salt in water, it was impossible to determine if hydrolysis of the methyl ester had occurred as aqueous extraction was carried out. The mesogenic unit was then attached *via* a DCC-coupling in THF using a catalytic amount of DMAP to yield the mesogenic BODIPY, which was purified using column chromatography (Sch. 3.5).

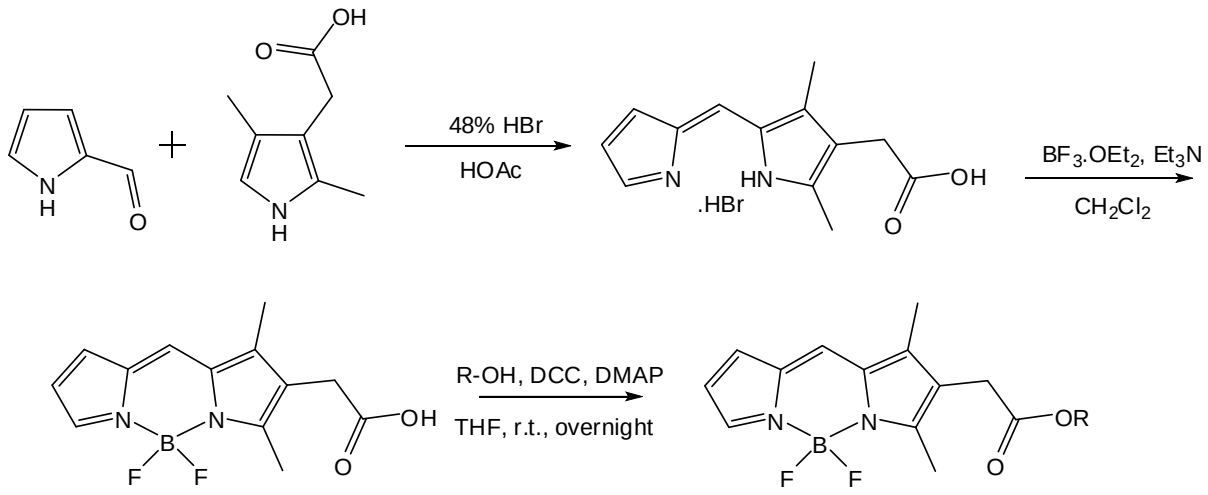

Scheme 3. 5: Mesogenic BODIPY synthesis

Three different mesogenic units were attached to the same BODIPY core *via* this DCC-coupling; a biphenyl unit which terminated in a C_{11} chain (**4**), followed by two cyanobiphenyl units with a C_8 (**5**) and C_{11} (**6**) spacer between the BODIPY and the cyanobiphenyl unit (Fig. 3.6). The two different chain lengths were used to investigate if there was any effect on the melting point or mesophase formation caused by a slightly longer chain.

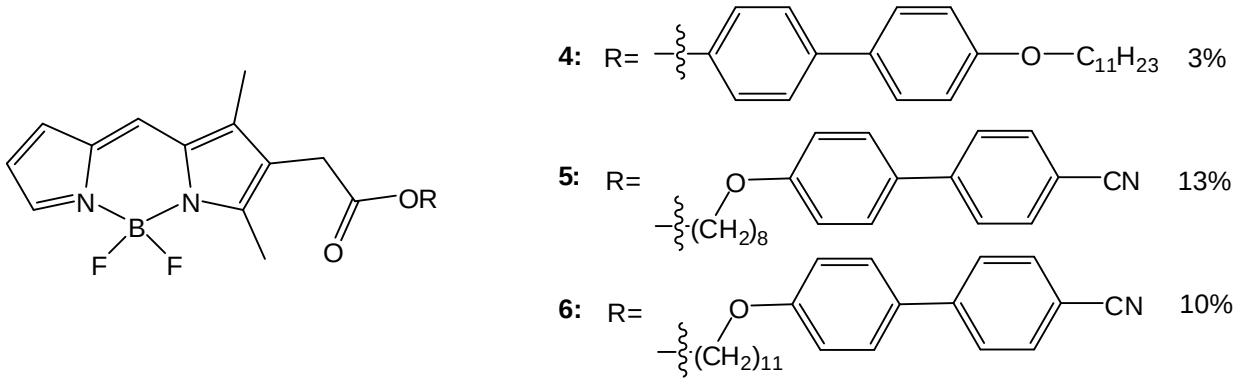

Figure 3. 6: Mesogenic BODIPYs

While dipyrrin and BODIPY syntheses tend to give moderate to low yields, in this case yields for the final compounds (3, 13 and 10% overall for **4**, **5** and **6** respectively) were so low because of the high polarity of the intermediates and the lack of purification until the final step. In each case the products were bright red/orange solids.

^{1}H-NMR spectroscopy shows the attachment of the mesogens to the BODIPY by the down-field shift of one of the methylene units of the alkyl chain. In the free mesogen, the terminal methylene unit is adjacent to a hydroxyl group, but attachment to the BODIPY makes it adjacent to a carboxyl group causing a down-field shift in the corresponding triplet in the ^{1}H-NMR spectrum (Fig. 3.7 and 3.8).

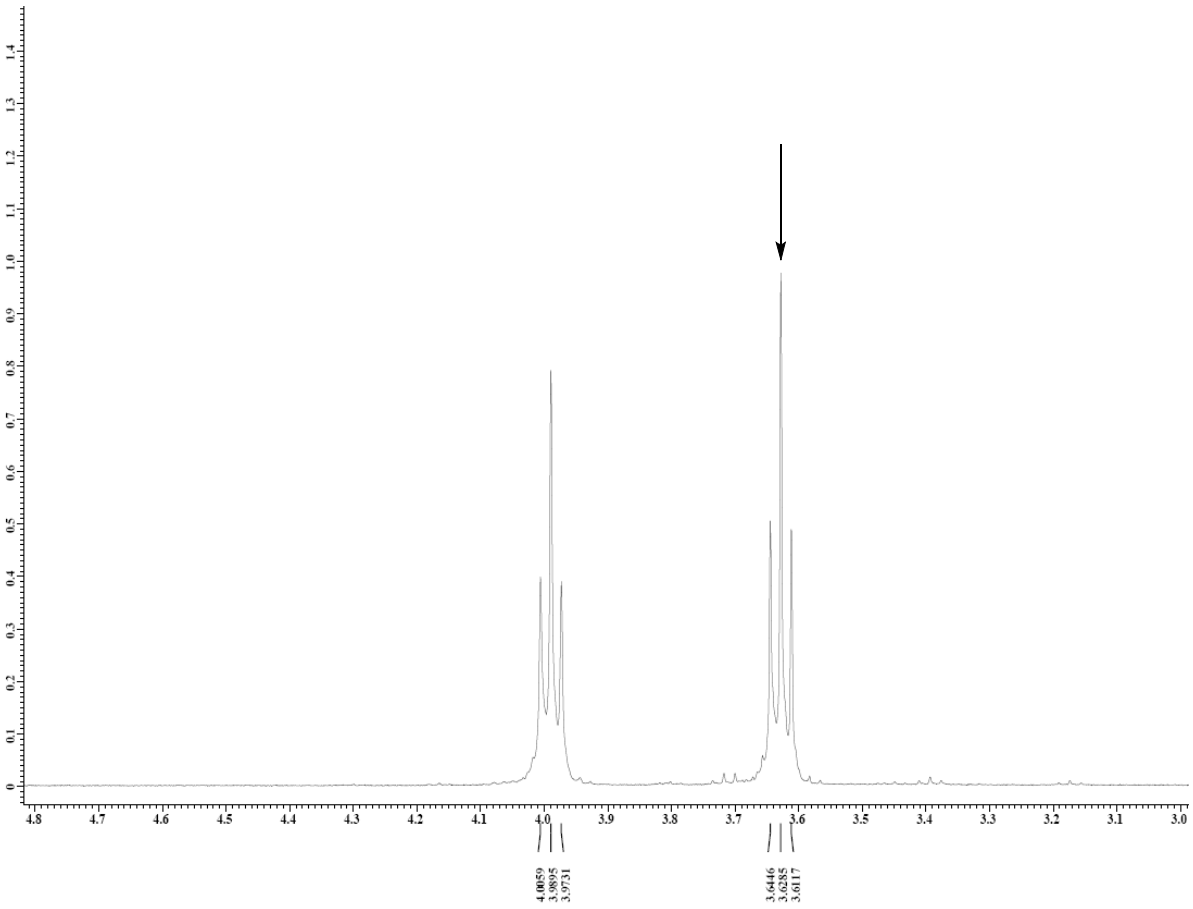

Figure 3. 7: ^{1}H-NMR of free mesogen showing methylene units at both ends of the alkyl chain

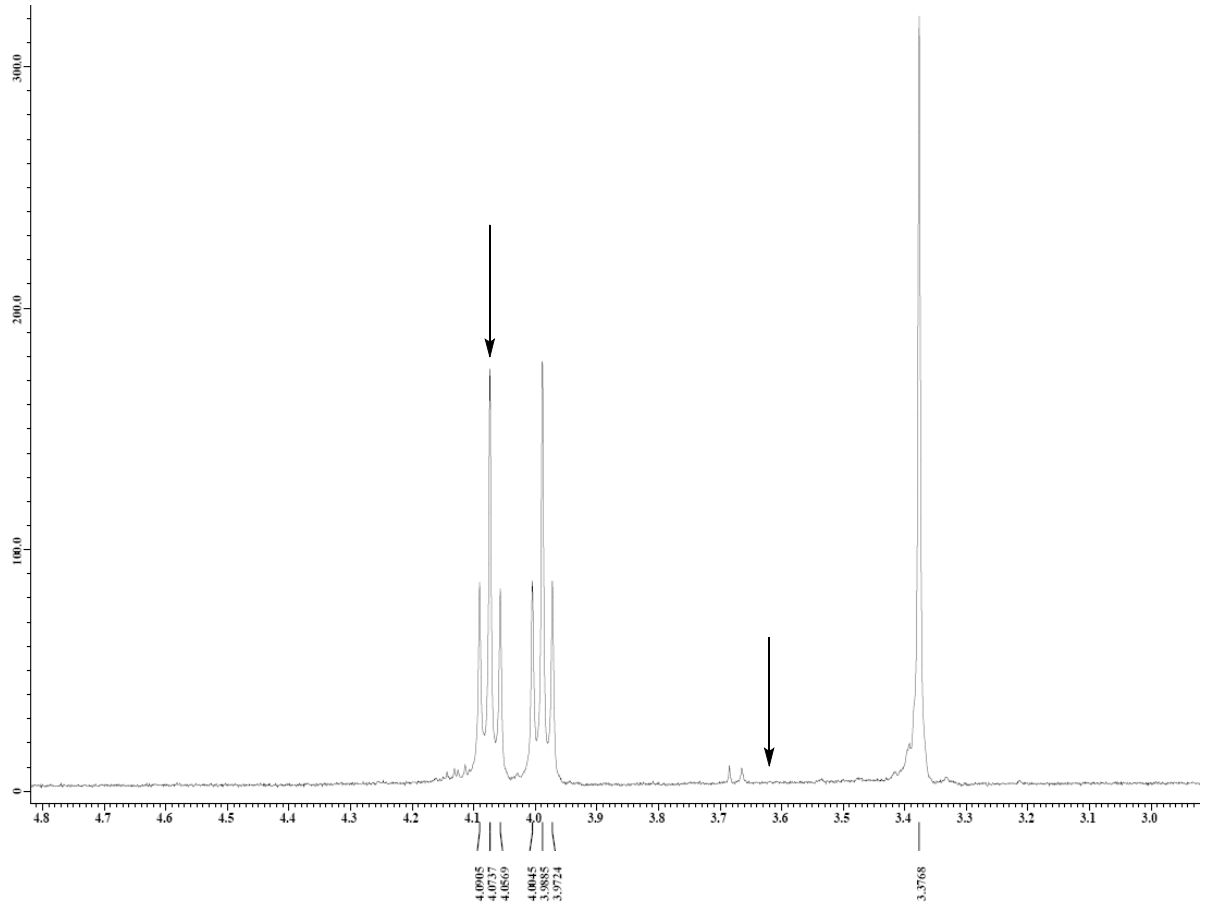

Figure 3. 8: ^{1}H-NMR of mesogenic BODIPY showing down-field shift of one methylene unit of the alkyl chain due to conversion from alcohol to ester

Following the synthesis of the mesogenic BODIPY esters, an attempt was made to synthesise mesogenic BODIPY ethers. Due to the increased flexibility of ether linkers as well as their more linear nature, we hypothesised that the resulting mesogenic BODIPY would have a stronger preference for liquid crystalline behaviour. An ether group would also be more stable to the acidic conditions of dipyrrin formation. Due to ethers also being stable to basic conditions, it would allow the mesogen to be attached followed by subsequent hydrolysis of the ethyl ester before this was reacted with 2-formylpyrrole (**3**) to produce the dipyrrin. Starting from the same Knorr pyrrole (**1**), a reduction was carried out using diborane (generated from boron trifluoride diethyl etherate added to sodium borohydride in THF) to produce the pyrrole alcohol (Sch. 3.6).

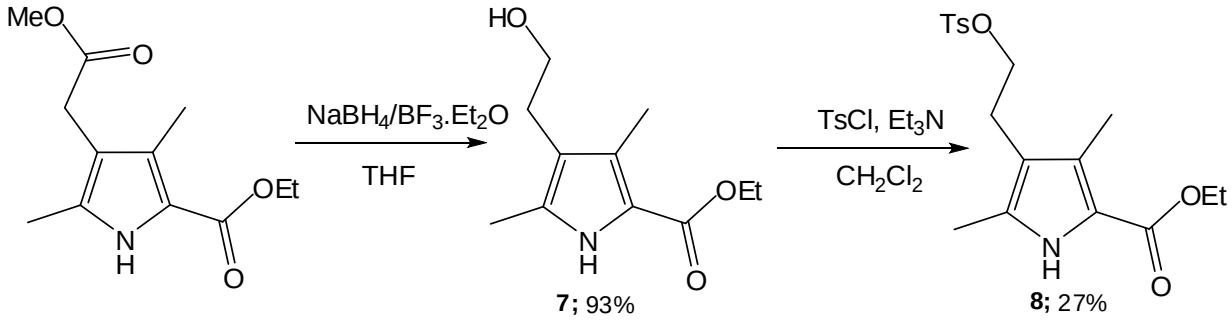

Scheme 3. 6: Pyrrole reduction and mesylation

An attempt was made to react the pyrrole alcohol (**7**) with a short chain alkyl iodide *via* a Williamson ether synthesis, however we found that the alcoholic proton was not acidic enough to undergo etherification without using a very strong base (e.g. sodium), which caused decomposition of the pyrrole, possibly *via* hydrolysis of the ethyl ester with subsequent deprotonation of the pyrrole. In order to allow the etherification reaction to occur with the pyrrole as the electrophile and using a separate nucleophile, a tosylate group was attached to the hydroxy group (**8**). While the test reaction of the pyrrole mesylate with *p*-cresol gave the desired product, the yields were poor and any mesogens to be attached to this pyrrole would be restricted to having phenolic hydroxy groups. An attempt was made to hydrolyse the reduced pyrrole in order to ultimately synthesise a BODIPY containing a free hydroxy group which would be easier to chromatograph due its lower polarity. However, the hydrolysis only resulted in decomposition of the pyrrole, possibly *via* a similar mechanism as when sodium metal was added to the pyrrole alcohol (**7**), yielding only intractable by-products.

Despite the successful synthesis of the previous mesogenic BODIPYs, we still had not addressed the issue of the fluorophore merely being attached on the end of the mesogen. We therefore decided to incorporate the fluorophore into the mesogen as a whole by attaching two mesogenic units to the BODIPY core in a symmetrical fashion. The two alkyl spacer units could enable the molecules to pack more efficiently. The cyanobiphenyl mesogen was chosen as it is a more powerful nematogen than the mesogen terminating in a C_{11} chain due to the nitrile groups causing repulsion between the molecules promoting the formation of liquid crystalline mesophases.

Figure 3. 9: Di-mesogenic BODIPY schematic

In order to avoid the problems encountered with the asymmetrical mesogenic BODIPYs (inability to isolate intermediates, difficult purification and harsh conditions), an attempt was made to synthesise a dipyrromethane *via* an alternative route. This route would also allow the mesogens to be attached to the pyrrole first, before dipyrromethane and subsequent BODIPY synthesis.

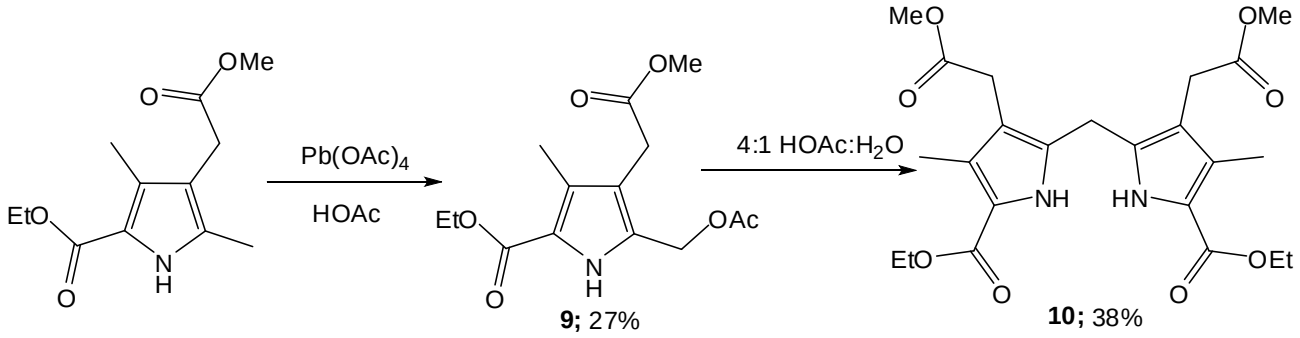

Scheme 3. 7: Pyrrole acetylation and dipyrromethane synthesis

The same Knorr pyrrole (**1**) was used as for the previous BODIPYs as the starting material (for an initial test reaction) which was mono-acetylated with lead (IV) acetate (**9**). This pyrrole was then reacted with itself in a glacial acetic acid/water mixture to yield the desired dipyrromethane (**10**). Yields for these steps were moderate (for pyrrole reactions), giving 27% and 38% for the acetylation and dipyrromethane synthesis respectively (Sch. 3.7).

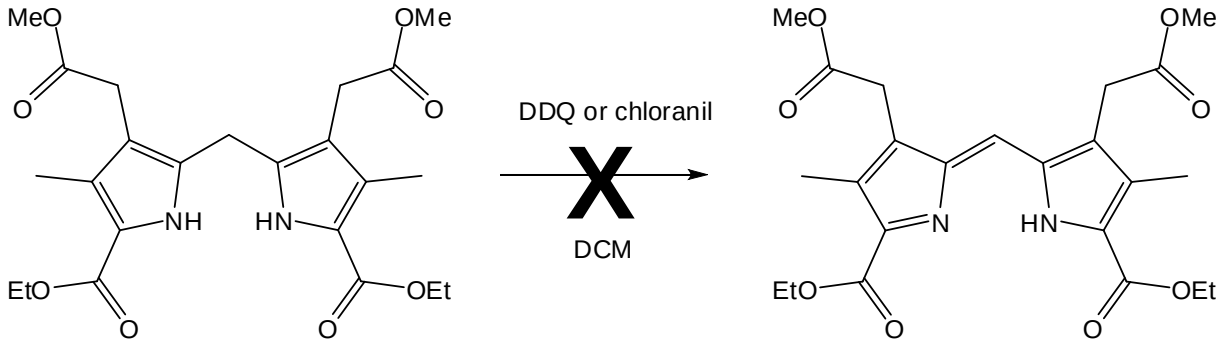

Scheme 3. 8: Unsuccessful dipyrromethane oxidation

Despite the success of the dipyrromethane synthesis, the subsequent oxidation did not yield the desired product. The oxidation was attempted with both DDQ and chloranil, but was unsuccessful in both cases, possibly due to the free-base dipyrrin being unstable (Sch. 3.8). An attempt was also made to carry out the oxidation with DDQ and then reacting this with triethylamine and boron trifluoride diethyl etherate to produce the BODIPY. Ideally, the BODIPY would be more stable than the free-base dipyrrin out of solution and thus, potentially easier to isolate. This proved not to be the case and this reaction also produced intractable by-products.

A symmetrical dimesogenic BODIPY was then synthesised starting from the same Knorr pyrrole (**1**). The symmetrically substituted dipyrrin was synthesised by reacting the Knorr pyrrole with formic acid (which acts as the bridging methylene unit) in the presence of hydrobromic acid. The dipyrrin salt precipitated out upon cooling and was filtered off as a bright red solid. The BODIPY was synthesised in the same fashion as the asymmetrical BODIPY and was not isolated due to difficulties in purification caused by the high polarity. The mesogen attachment was achieved by a DCC-coupling and the final product was purified by column chromatography to give the pure product as a bright red solid (**11**). The overall yield for the di-mesogenic BODIPY was in a similar region (5%) to the mono-mesogenic analogues due to the difficulty in purification of the BODIPY carboxylic acid leading to large amounts of side-products (Sch. 3.9). Diisopropylethylamine was used as the base for boron complexation due to it producing fewer by-products than triethylamine. Due to the low solubility of the dipyrrin

hydrobromide salt the boron complexation solution was refluxed for 18hrs instead of simply being stirred, as for the previous BODIPYs.

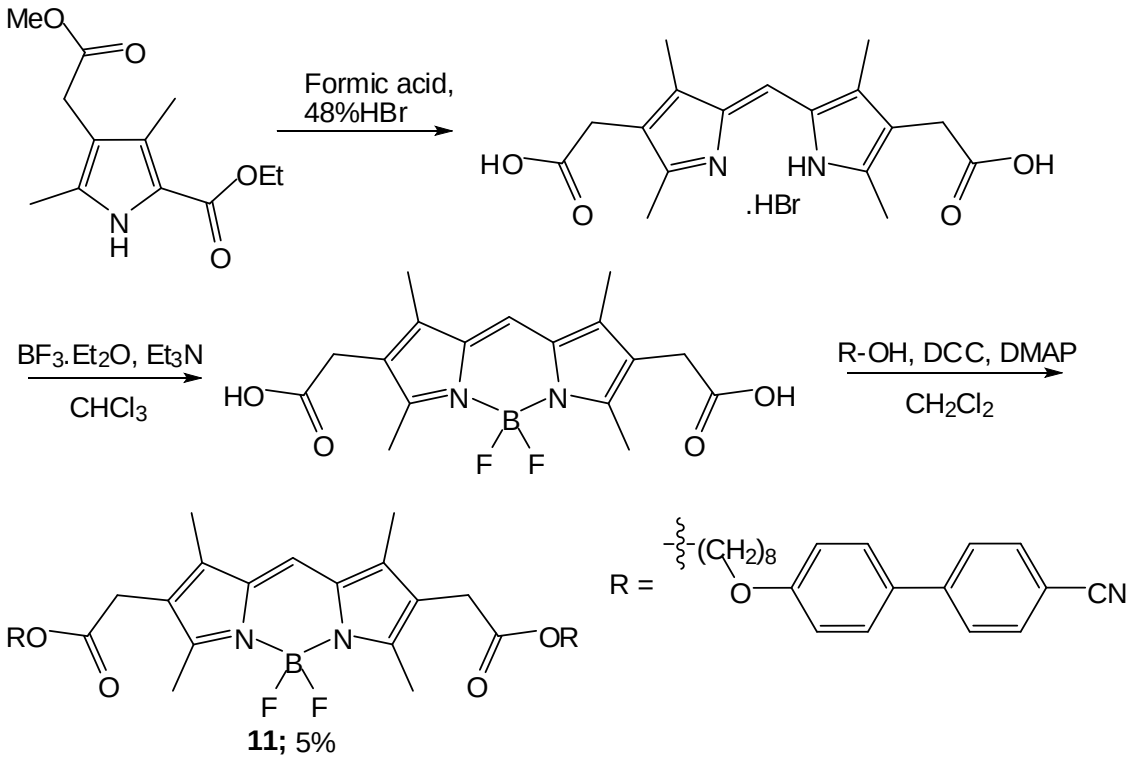

Scheme 3. 9: Di-mesogenic BODIPY synthesis

In order to provide a more efficient route to the dimesogenic BODIPY, a different Knorr pyrrole was synthesised, containing a benzyl ester (**12**) instead of an ethyl ester. The pyrrole was synthesised *via* the same reaction as the previous pyrrole however the product oiled out when poured into water and had to be extracted into dichloromethane before being crystallized with methanol followed by recrystallisation from ethanol.

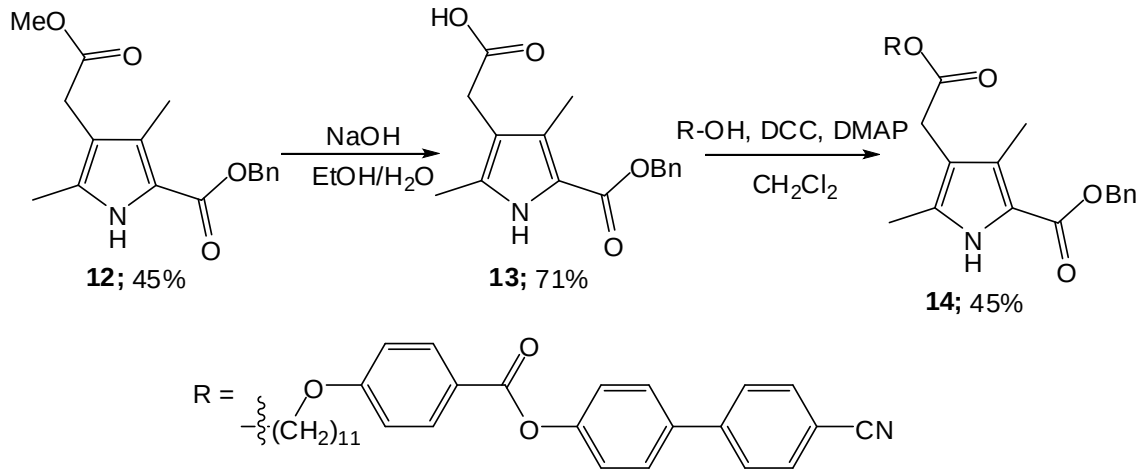

Scheme 3. 10: Mesogenic pyrrole synthesis

The methyl ester was selectively hydrolyzed (**13**) before the mesogen was attached *via* a DCC-coupling (**14**). A triphenyl type mesogen was used due to it being a more powerful nematogen and better able to induce liquid crystallinity on the BODIPY. However, while the DCC-coupling was achieved in reasonable yield (45%), the attempted hydrogenation of the benzyl ester was unsuccessful (Sch. 3.11). Test hydrogenation reactions on pyrrole **12** were also carried out but were found to be unsuccessful. The reaction was performed both in a hydrogenator (being shaken under a hydrogen atmosphere) and with hydrogen being bubbled through the solution, but both reactions yielded only starting material. Longer reaction times (4 hrs, 8 hrs, 1 day, 2 days and 3 days were attempted) and increasing percentages of palladium on carbon (10, 20 and 30% palladium on carbon were attempted with multiple batches of each percentage being employed – nine different batches from various suppliers were used in total) were used as well as increased molar proportions of catalyst (5, 10, 20 and 30 mol% were attempted) but still only starting material was obtained. Several different solvents were also employed (THF, EtOAc, acetic acid and dioxane were attempted) but they appeared to have little effect on the reaction. Due to hydrogenation of a benzyl group on a pyrrole generally considered to be facile, the reasons for these reactions being unsuccessful are unclear. The catalysts used could have been poisoned due to over-exposure to oxygen or other materials, or possibly some small impurity in the starting material caused a poisoning of the catalyst. A tertiary butyl group could have been used as a protecting group for the ester as it could be

efficiently removed with a catalytic amount of TFA, but the harsh conditions of dipyrrin synthesis (strong acid and heat) could still have caused problems for the deprotected pyrrole. The strong acid could have hydrolyzed the mesogen ester producing the dipyrrin carboxylic acid that was produced in the previous mesogenic BODIPY syntheses (Sch. 3.5). For these reasons, these synthetic routes were discarded and an alternative approach was developed (see Ch. 4).

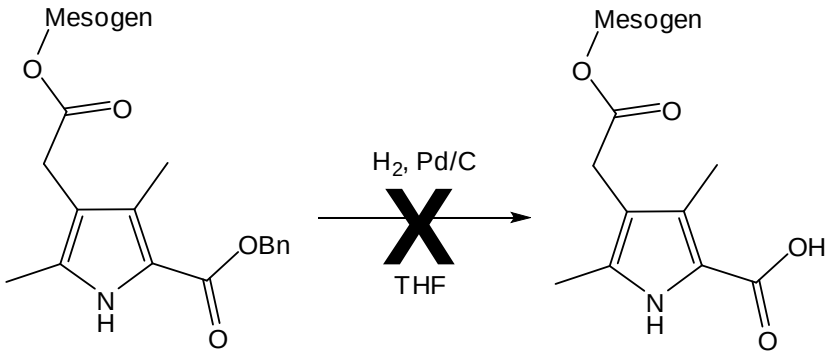

Scheme 3. 11: Unsuccessful hydrogenation of mesogenic pyrrole

The triphenyl mesogen (**16**) was synthesised in a two step procedure. An etherification reaction with a subsequent DCC-coupling exploiting the higher nucleophilicity of the phenolic hydroxy group over the alkyl hydroxy group yielded the desired product. The product of each of these reactions was purified using recrystallisation. The other mesogens were synthesised *via* one-step Williamson ether reactions and purified by recrystallisation.

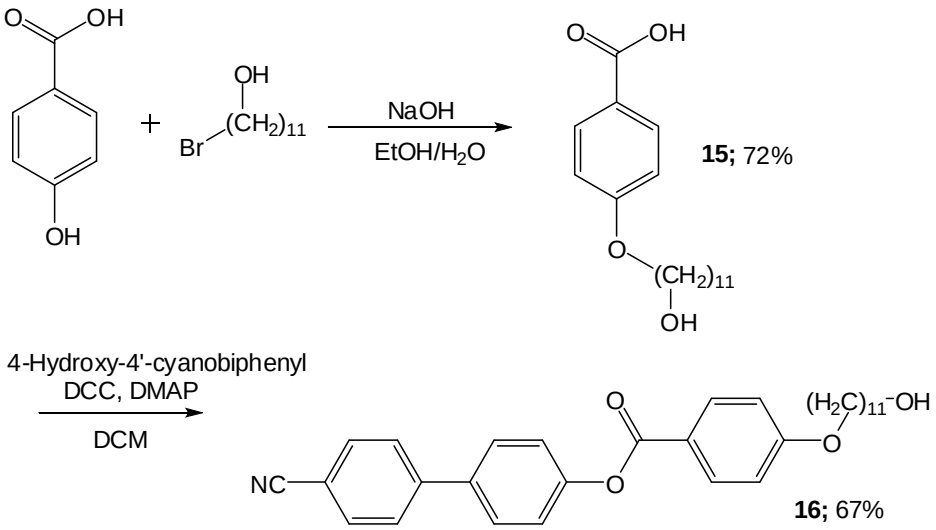

Scheme 3. 12: Mesogenic synthesis

3.2.2 Melting behaviour

The two cyanobiphenyl type mesogens were chosen because of their preference for adopting nematic behaviour when attached to other molecules. The additional benzoic ester group on the larger mesogen confers stronger nematic behaviour, while also raising the melting point of the mesogen. This is due to the polarisable core being extended allowing increased weak (relatively) inter molecular interactions between the aromatic sections of the molecules. While the non-cyanobiphenyl mesogen is not inherently liquid crystalline, the presence of a polarisable biphenyl core and a long alkyl chain could potentially allow the BODIPY to adopt a mesophase (possible smectic due to the lack of a highly polar group). Both cyanobiphenyl type mesogens adopt smectic A mesophases, with the larger mesogen only exhibiting a nematic phase over 1°C (Fig. 3.10)[260-263]. This is due to the long alkyl chains present on each mesogen greatly increasing the lateral intermolecular interactions to a large enough degree to allow layers to form. Shorter alkyl chains tend to increase the preference for nematic behaviour. This effect can be seen for the C_8 cyanobiphenyl, which exhibits a nematic phase over 13.2°C as well as a smectic A phase, while the C_{11} analogue only displays smectogenic behaviour. As can be seen from Fig. 2.10, the additional phenyl ring increases the stability of the smectic phase while also causing a very short nematic phase to be exhibited.

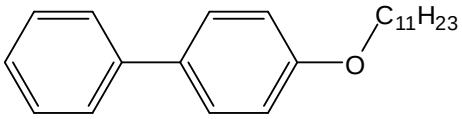

Non-liquid crystalline

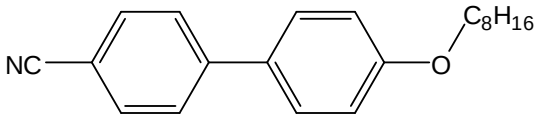

Cr 53.8 Sm_A 67 N 80 I

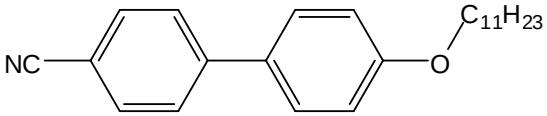

Cr 71.5 Sm_A 87 I

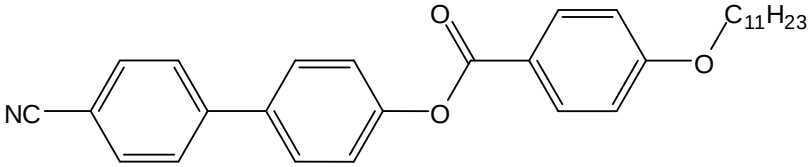

Cr 104 Sm_A 224 N 225 I

Figure 3. 10: Liquid crystal properties of mesogenic units

Once the hydroxyl group is present on the terminal position of the mesogens, the liquid crystalline properties change dramatically. The non-cyanobiphenyl mesogen obviously remains thus, while the cyanobiphenyl type mesogens only display nematic behaviour. Based on the reported mesogenic BODIPYs[229], we would predict that this nematic behaviour would be conferred on the resulting mesogenic BODIPYs that were synthesised.

The non-cyanobiphenyl mesogen did not confer any unusual melting behaviour on the BODIPY to which it was attached (**4**). No mesophase formation of the mesogenic BODIPY was observed. We attribute this to the mesogens' lack of any strongly polarisable groups (e.g. nitrile) and the position of the biphenyl section causing a preference for normal crystalline behaviour over any mesogenic behaviour. This is shown in the DSC curve for this compound (Fig. 3.11). A crystal to isotropic liquid transition is

shown at 133°C and the molecule could be supercooled to 120°C before recrystallizing. This indicates a slight mesogenic effect, likely from the long flexible alkyl chains intertwining with each other once in the isotropic liquid.

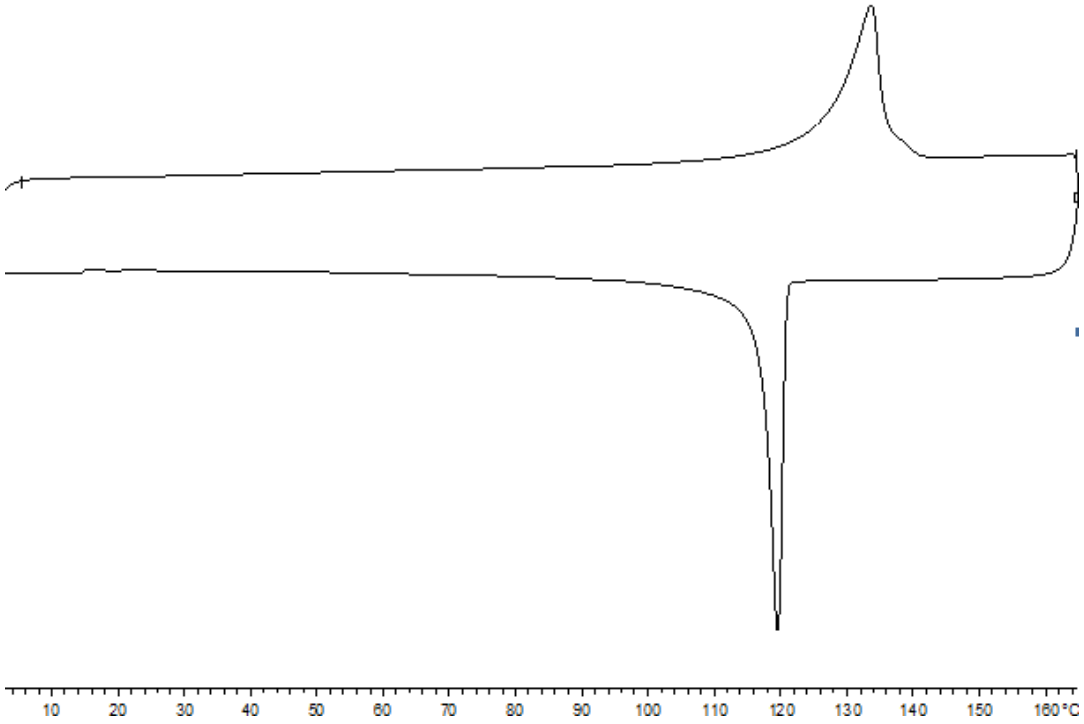

Figure 3. 11: DSC thermogram of mesogenic BODIPY 4; showing heating (top line) and cooling (bottom line)

The cyanobiphenyl analogue (**5**) did not exhibit liquid crystalline behaviour, as was observed for the non-cyanobiphenyl BODIPY. The DSC heating curve (Fig. 3.12) shows some initial melting (double hump at ~20-35°C) then some slight recrystallisation (smooth trough between ~60-95°C) before fully melting into the isotropic liquid at 101°C. The cooling curve shows the compound being supercooled to 32°C before crystallizing.

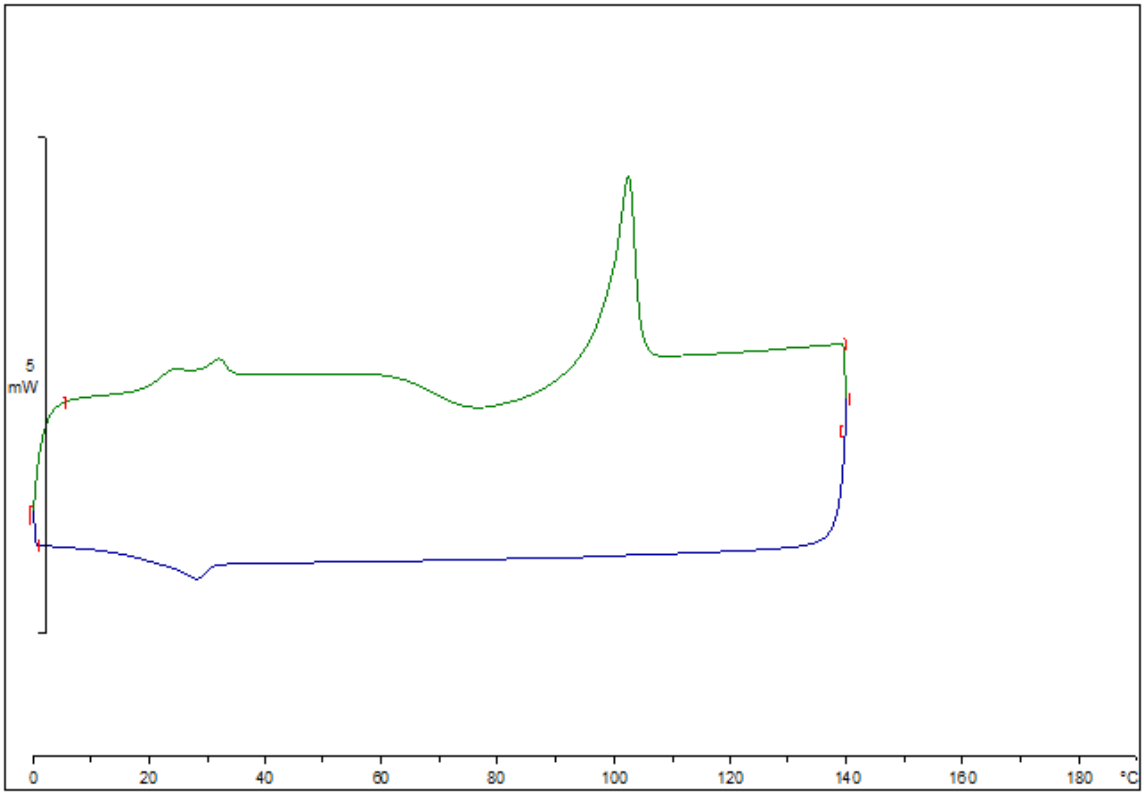

Figure 3. 12: DSC thermogram of mesogenic BODIPY 5; showing heating (top line) and cooling (bottom line)

The mesogenic pyrrole (**14**), however, exhibited a nematic phase due to the strong mesogen attached to it overcoming the pyrroles tendency for crystalline behaviour. It can be seen from the microscopy pictures that the mesogenic pyrrole exhibits a schlieren texture typical of nematic liquid crystals when viewed under crossed polarisers (Fig. 3.13). Due to the failure of the hydrogenation of this compound, an efficient route to the subsequent dimesogenic BODIPY was not realised.

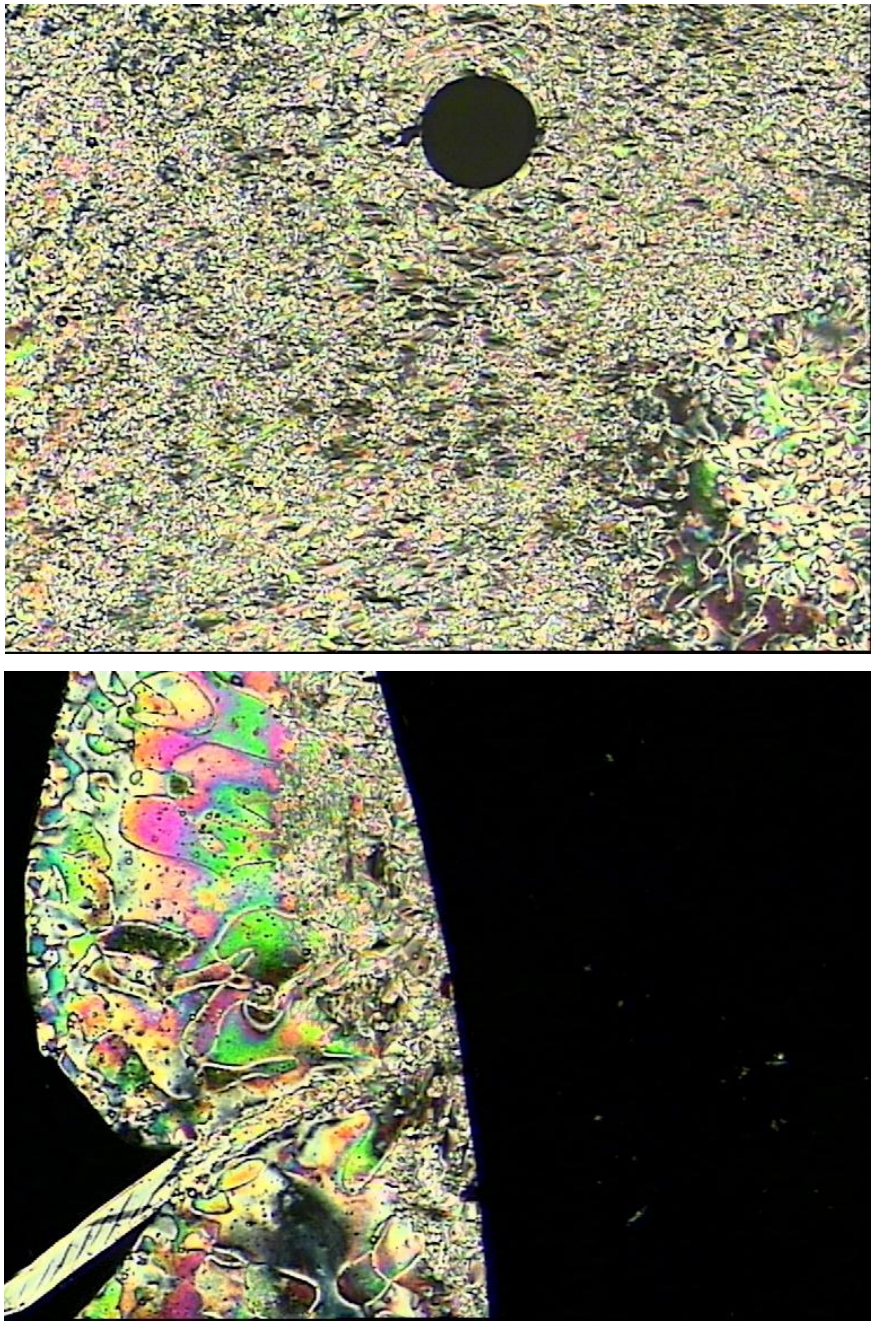

Figure 3. 13: OPM images of the mesogenic pyrrole (14) in the nematic phase at 84.9°C (top) and 87.8°C (bottom) after annealing

The DSC curve of the mesogenic pyrrole shows the presence of a wide nematic range from 10-85°C (Fig. 3.14). Despite the appearance of the curve, the nematic phase is only monotropic as the nematic phase is not observed on the initial heat from the crystalline solid. Upon cooling the nematic phase is adopted and as the compound is cooled further it solidifies as a glass rather than a crystalline solid. Given the wide nematic range, it is

clear that the nematic phase of this compound is quite stable, indicating that the pyrrole unit does not override the preference for mesophase formation of the mesogenic unit.

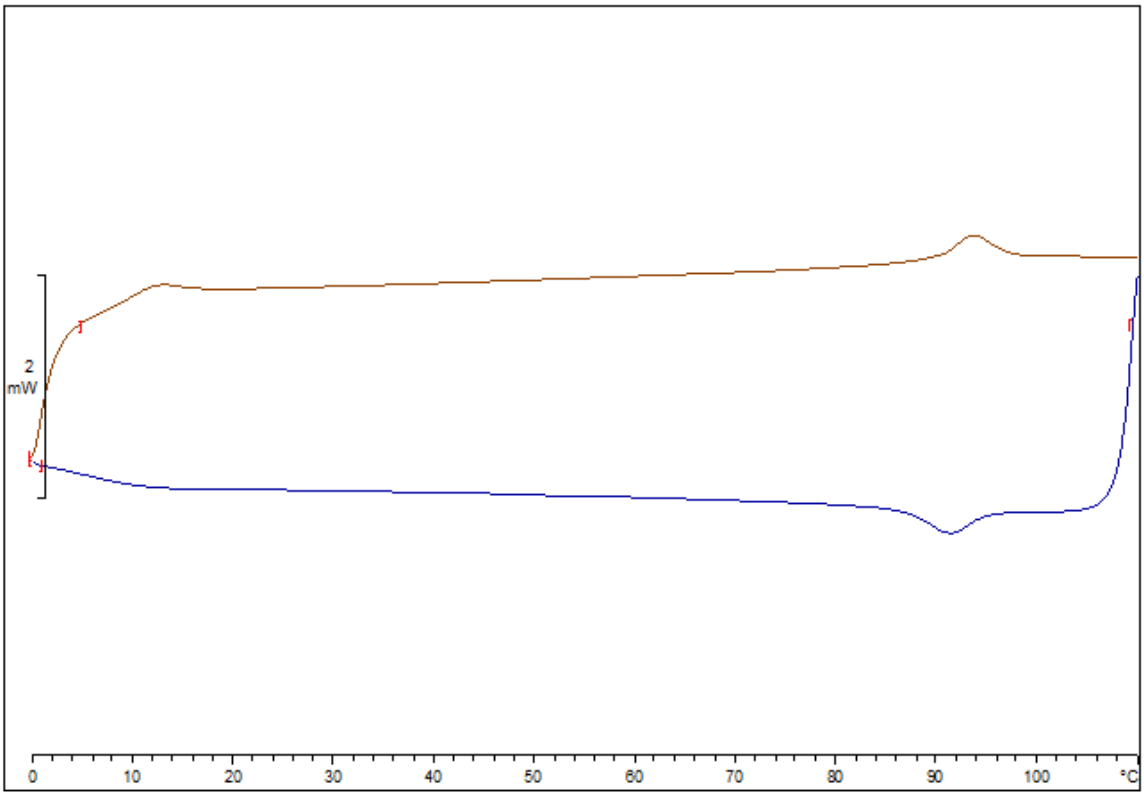

Figure 3. 14: DSC thermogram of the mesogenic pyrrole (14); showing second heating cycle (top line) and second cooling cycle (bottom line)

3.2.3 Fluorescence

All of the mesogenic BODIPYs (both mono- and di-mesogenic) exhibited an intense fluorescence. The dimesogenic BODIPY (**11**) was chosen as a representative example of the series to measure the photophysical properties. Due to the lack of strongly electron withdrawing or donating groups attached directly to the BODIPY core, the side-attached mesogenic BODIPYs synthesised would not be expected to display any significant change in wavelength (excitation and emission), fluorescence quantum yield or lifetime in relation to each other.

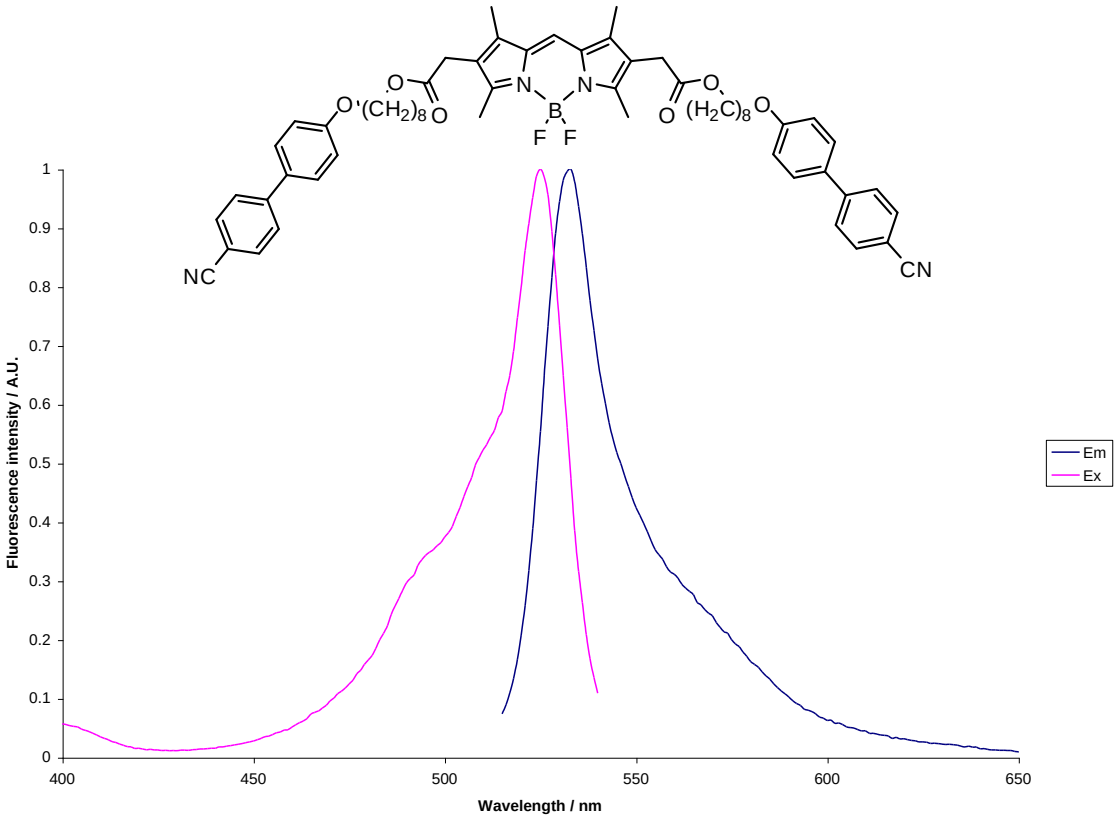

Figure 3. 15: Fluorescence spectrum of di-mesogenic BODIPY 11 in toluene at 298K

λ_{ex} / nm	λ_{em} / nm	Stokes shift / nm	Φ_F	τ_{fl} / ns	k_r / 10^8 s^{-1}	k_{nr} / 10^8 s^{-1}	ε / M^{-1} cm^{-1}
525	533	8	0.95	5	1.9	0.1	92000

Table 3. 1: Photophysical data for di-mesogenic BODIPY (11)

All of the observed fluorescence appeared to be from the BODIPY core (Fig. 3.15) implying that there is no, or little, fluorescence resonant energy transfer (FRET) that occurs between the biphenyl unit of the mesogen and the BODIPY core. A short Stokes shift is observed; an effect similar to other reported BODIPYs lacking any electron withdrawing or aromatic substituents on the BODIPY core. The absorption coefficient indicates a moderately strong absorbance but the calculated value is comparable to previously reported BODIPYs. It can be clearly seen that this dimesogenic BODIPY has a large radiative decay constant (k_r) when compared to its non-radiative decay constant (k_{nr}). These constants were calculated using the equations:

$$k_r = \Phi_F / \tau_F$$
$$k_{nr} = (1 - \Phi_F) / \tau_F$$

Equation 3. 1 and 3. 2: Radiative and non-radiative decay constants

The large fluorescence quantum yield (and thus radiative decay constant) of this compound is partially caused by the lack of phenyl ring at the 8-position. Other BODIPYs with an 8-phenyl ring tend to have smaller quantum yields due to the rotation of the phenyl ring. Even in BODIPYs where this rotation is restricted it still occurs to a small degree and those compounds will, in general, have lower quantum yields. The lack of 8-phenyl ring means that the absorbed energy is much less likely to be lost *via* non-radiative molecular motions, thus increasing the quantum yield of this compound.

3.3. Conclusions

These studies show that mesogenic BODIPYs with the mesogens attached to a linker group on a pyrrolic position can be prepared. However, the synthetic route used gave low yields and made isolation and purification of the intermediates and products excessively difficult. It was observed that none of the mesogenic (both mono- and di-mesogenic) BODIPYs presented here exhibited any liquid crystal mesophase, but could be supercooled to varying degrees. A mesogenic pyrrole was found to display a nematic phase from 93-105°C, but the subsequent hydrogenation reaction failed and this promising intermediate could not be converted into a dipyrrin complex. The lack of liquid crystallinity was surprising as the previously reported nematic BODIPY[229] employed a similar mesogen but exhibited a relatively stable mesophase. These results imply that the lack of an 8-aryl substituent promotes crystallisation of the BODIPY, possibly by increased aggregation of the fluorophores. The intense fluorescence of the dimesogenic BODIPY was observed, but due to the lack of liquid crystalline behaviour, the practical use of this type of compound would be severely limited. The fact that mesogenic BODIPYs have been previously reported[224, 225, 229, 230, 232] and their interesting liquid crystalline/self-assembling and photophysical behaviour have been observed indicates that mesogenic BODIPYs could have potential use in optoelectronics and display

devices; however, a different approach would be required in the synthesis of these molecules.

Chapter 4: BODIPYs bearing mesogenic units attached to the 8-phenyl ring

4.1. Introduction

Due to the difficulties in synthesising the side-attached mesogenic BODIPYs, as well as their lack of mesophase formation, the design of an alternative synthetic route to the mesogenic BODIPY was required that would allow versatility in the type of mesogen and the nature and position of linker group between the mesogen and BODIPY. As the preparation of an 8-phenyl BODIPY is relatively facile, simple reactive sites can be incorporated onto the central phenyl ring to which mesogens can be attached. As mesogenic 8-phenyl BODIPYs have been shown to adopt liquid crystalline mesophases despite terminating in a relatively large fluorophore[229, 230], it is to this position that our attention turned.

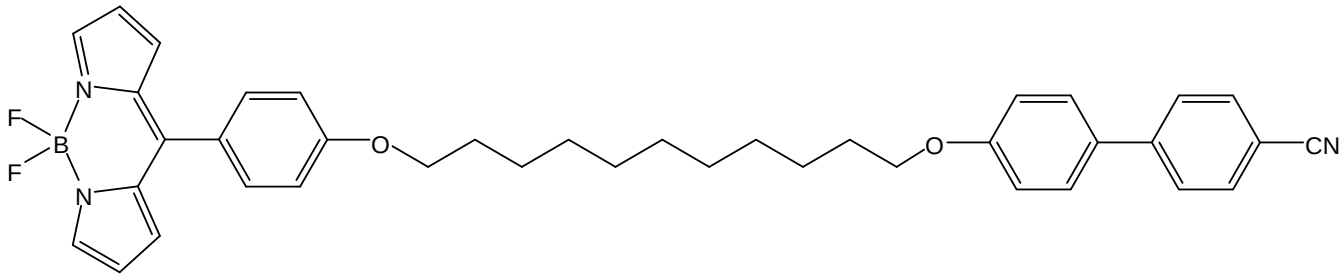

Figure 4. 1: Calamitic nematic BODIPY liquid crystal

As the restriction of the rotation of the BODIPY 8-phenyl ring causes an increase in the fluorescence intensity of the fluorophore, a series of mesogenic BODIPYs was designed with varying degrees of alkyl substitution on the BODIPY core (Fig. 4.2). Increasing alkyl substitution on the BODIPY core will increase the fluorescence quantum yield but the effect that the alkyl groups will have on the liquid crystallinity of the molecules has, thus far, not been systematically investigated.

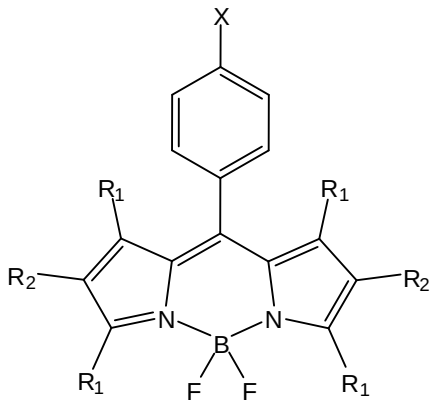

Figure 4. 2: Substitution on the BODIPY core, where X is the mesogenic unit and linker group

Different linker groups between the mesogen and the BODIPY are expected to have a significant effect on the liquid crystallinity of the resulting mesogenic BODIPY due to the changing molecular length and the angle between the fluorophore and the mesogen (e.g. ethynyl = linear, triazole = bent). In order to increase the mesogenic BODIPYs' propensity for liquid crystalline behaviour, only cyanobiphenyl type mesogens were used as they appeared to provide the side-attached mesogenic BODIPYs with more unusual melting behaviour than the non-cyanobiphenyl mesogen.

Metal-catalyzed couplings were chosen as the primary method of mesogen attachment to allow both linear and non-linear linker groups to be prepared. To this end Suzuki, Sonogashira and 'click' reactions were employed to form aryl-aryl, ethynyl-aryl and triazole linker groups. The reason these specific reactions were chosen is because the reactive sites on the BODIPY core are easily incorporated into the fluorophore as they can all be attached onto the benzaldehyde precursor (Fig. 4.3).

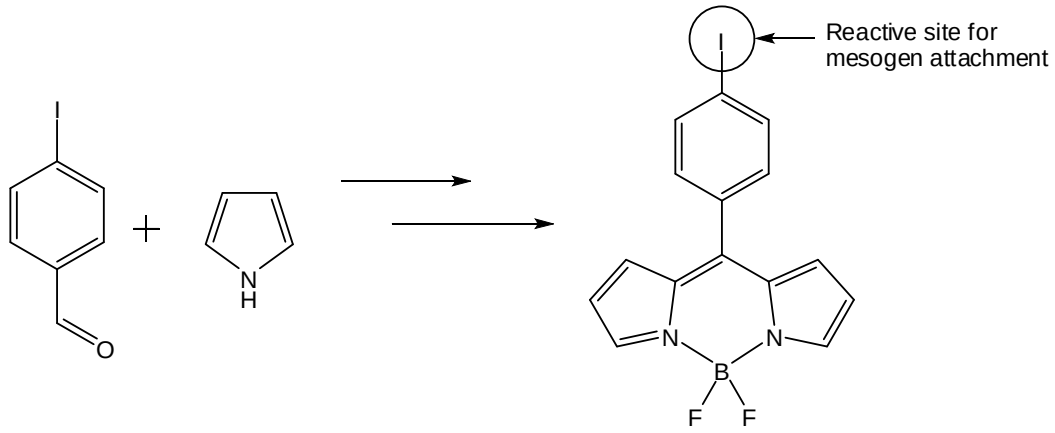

Figure 4. 3: Reactive site for mesogen attachment

4.2. Results and discussion

4.2.1 Synthesis

The BODIPYs for Suzuki coupling reactions were synthesised by the generally accepted standard method from either the benzaldehyde or the benzoyl chloride.[35, 264] The pyrrole-unsubstituted BODIPYs had to be synthesised from the benzaldehyde due to potential problems with polymerisation if the benzoyl chloride was used. Bromide (**17**) and iodide (**18**) analogues were prepared in 6% and 18% overall yield respectively without isolation of the dipyrromethane intermediate of the bromide analogue or dipyrrin intermediates of either analogue (Sch. 4.1). Due to the bright colour and moderate fluorescence of the BODIPYs, column chromatography was relatively straightforward.

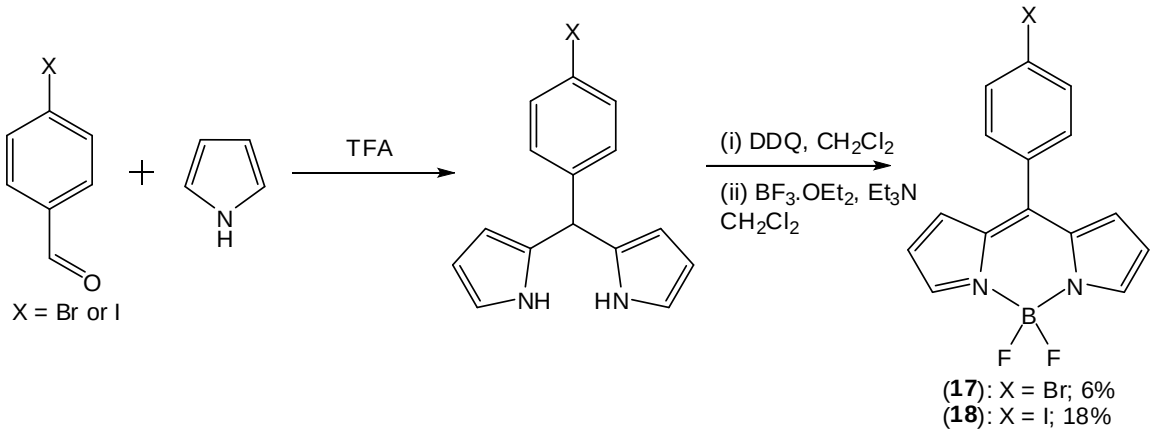

Scheme 4. 1: 8-(4-Halophenyl)-BODIPY synthesis

The tetramethyl and tetramethyl-diethyl analogues of the 4-iodophenyl BODIPY were prepared from the respective pyrrole and 4-iodobenzoyl chloride in dry dichloromethane. Due to the elimination of the dipyrromethane formation step and the intense fluorescence of the products, purification of these compounds was even more straightforward than the unsubstituted analogues. This facilitated the preparation of larger amounts of these BODIPYs in a shorter amount of time. **19** and **20** were prepared in 35% and 36% yields, respectively (Sch. 4.2).

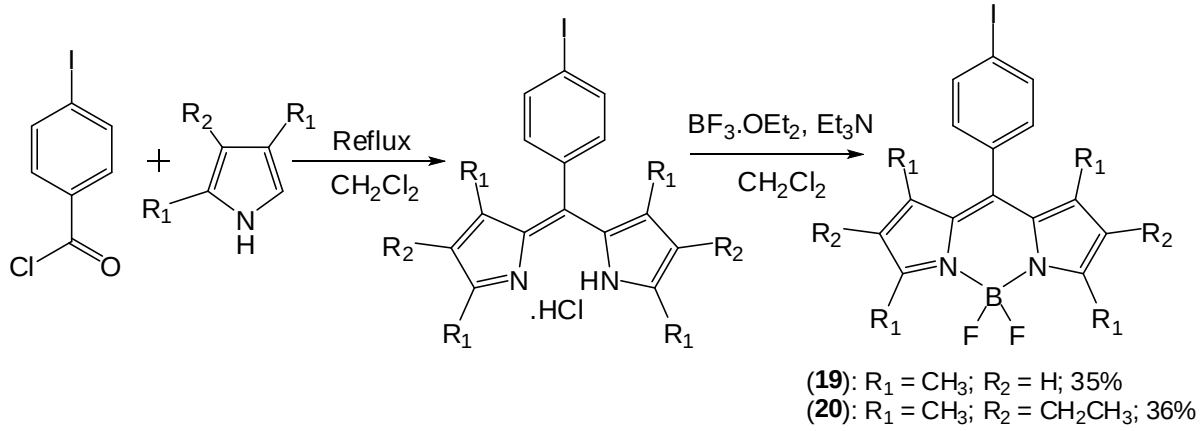

Scheme 4. 2: BODIPYs bearing alkyl groups to increase the fluorescence quantum yield

The mesogen prepared for attachment to the BODIPY was the same one attached to the mesogenic pyrrole from the previous chapter. In order to attach it to the BODIPY, the mesogen was appended with a boronic acid pinacol ester (**21**), *via* a DCC-coupling in reasonable yield. The synthesis and purification of this compound was straightforward due to the precipitation of the DCU (dicyclohexylurea), allowing it to be filtered off, and the product requiring only recrystallisation from ethyl acetate (Sch. 4.3). DIC was also employed as a coupling reagent but DCC was preferred due to the precipitation of DCU helping to drive the reaction towards the desired product.

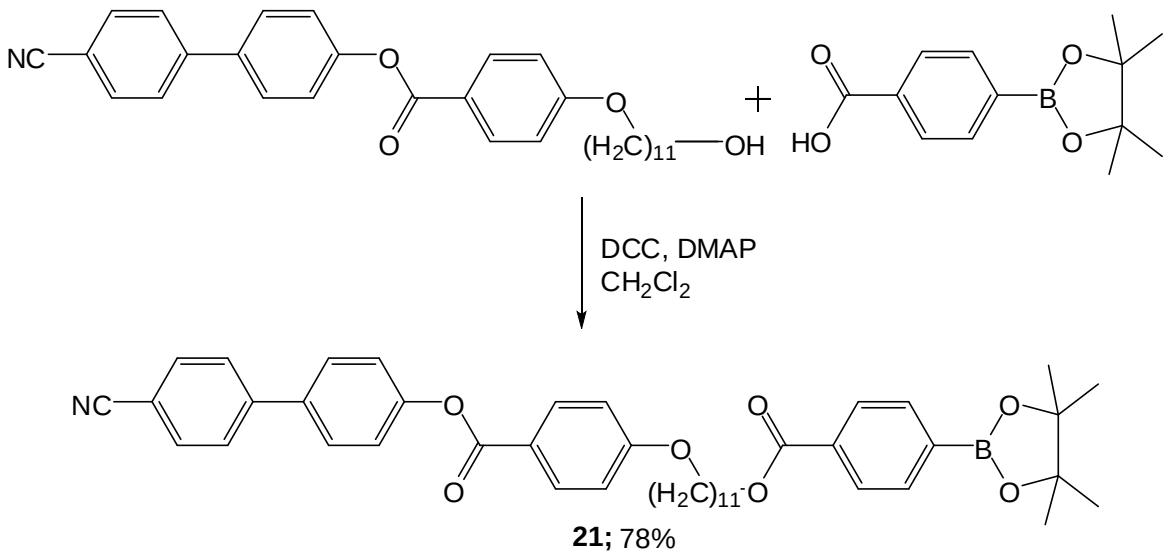

Scheme 4. 3: Mesogenic boronic ester synthesis

Initially, a Suzuki coupling was carried out between the 4-iodophenyl-BODIPY (**18**) and 4-carboxyphenylboronic acid pinacol ester in order to allow subsequent mesogen attachment *via* a DCC-coupling (Sch. 4.4). Whilst yielding the product in moderate yield (49%), the reaction was slow (50 hrs) and not all the starting materials were consumed. Chromatography required increasing amounts of methanol due to the polar carboxyl group. Subsequent attachment of the mesogen, however, was found to be unfeasible due to a very small amount of product isolated (<5%) and seemingly a large amount of decomposition of the BODIPY carboxylic acid. The large size of the mesogen and weak nucleophilicity of the mesogen hydroxyl group could have caused the slow reaction rate. This prompted us to change our strategy and use the mesogenic boronic acid pinacol ester in a final convergent step.

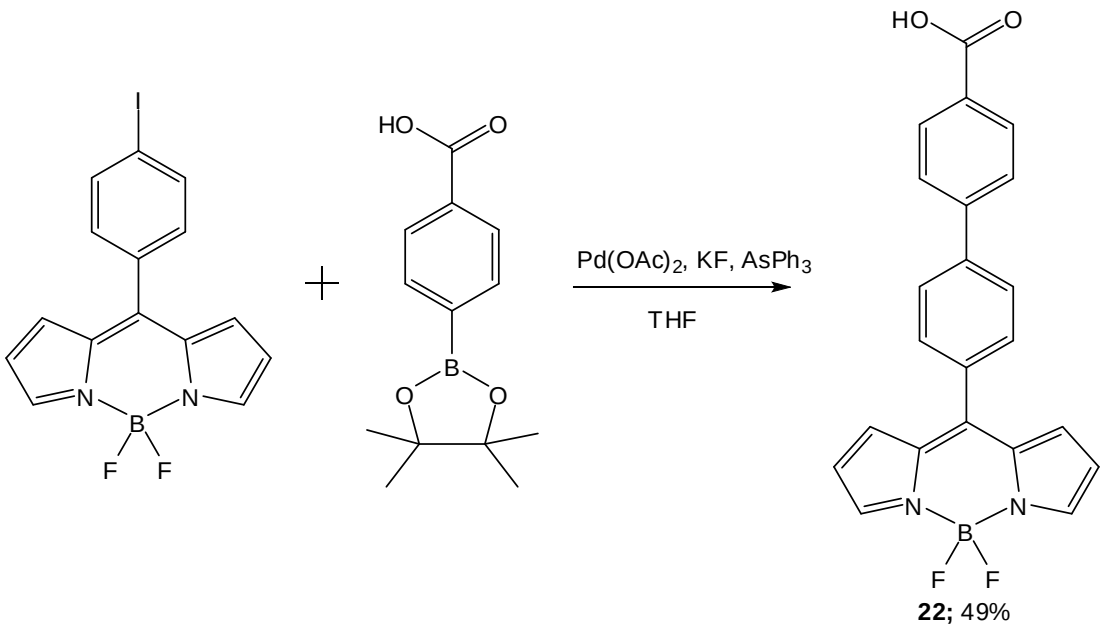

Scheme 4. 4: Suzuki-coupling of 4-carboxyphenylboronic acid pinacol ester to 18

The Suzuki coupling was attempted under the same conditions as with 4-carboxyphenylboronic acid pinacol ester but was found to be much slower. We attributed this to the increased size of the mesogen causing increased steric effects around the palladium, reducing the rate of reaction. Several palladium catalysts ($Pd(OAc)_2$, $Pd(PPh_3)_4$, dibenzylideneacetone dipalladium (II) and $Pd(PPh_3)_2Cl_2$), bases (KF, K_2CO_3 and Na_2CO_3) and ligands ($AsPh_3$, PPh_3 and (2-biphenyl)di-*tert*-butylphosphine) were used in an attempt to increase the reaction rate, but none were particularly successful. We, therefore, hypothesised that changing the heating method might increase the rate of reaction so attempted a microwave-assisted reaction. As dibenzylideneacetone dipalladium (II) was found to be the best catalyst and (2-biphenyl)di-*tert*-butylphosphine the best ligand, these reagents were chosen for the microwave-assisted reaction. Potassium carbonate was chosen as the base and DMF as the solvent due to the high solubility of the reagents in this medium and the high boiling point, viscosity and microwave translucency of DMF. The reaction was carried out at 65°C at 75W for five minutes before thin layer chromatography was carried out, which showed that the reaction was complete. No washing was carried out to remove the base or catalyst as these were easily removed during column chromatography. The DMF was removed by evaporation *in vacuo* and the residue was subjected to column chromatography eluting

with toluene:hexane or dichloromethane:hexane. It was found that, after chromatography, a small amount of unreacted mesogen eluted with the product, so the isolated mixture was redissolved in dichloromethane and cooled in an ice-bath. Cold methanol was then added to the solution to precipitate the pure product which was isolated using filtration and then washed with methanol to yield orange or red solids in 20%, 49% and 42% yields for **23**, **24** and **25**, respectively.

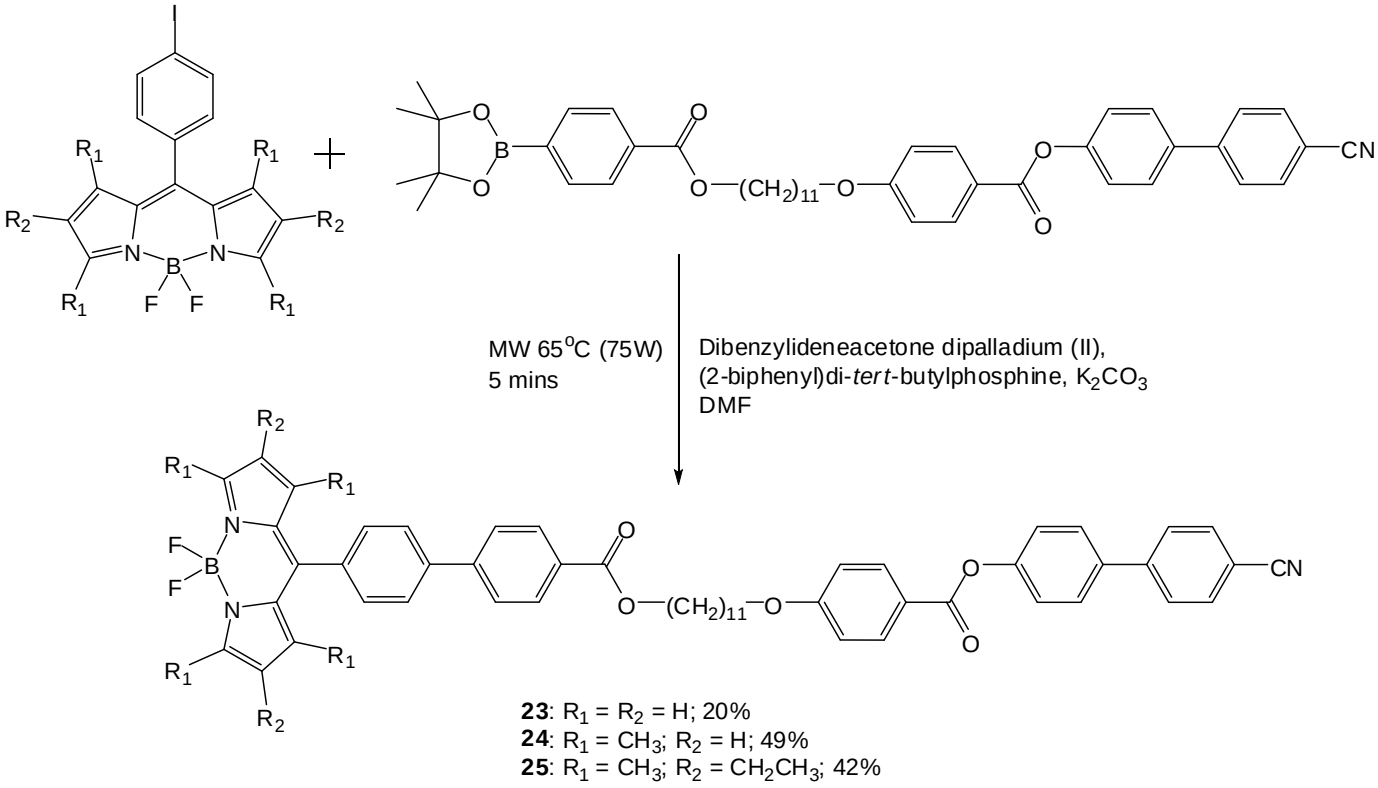

Scheme 4. 5: Mesogenic BODIPY preparation by Suzuki-coupling

Due to the presence of five different 1,4-disubstituted phenyl rings on the product molecules, ^{1}H-NMR spectroscopy did not enable the assignment of each of the protons on their respective phenyl ring. Despite the aromatic peaks being very close together, the integrations of the aromatic peaks (Fig. 4.4) supported the presence of the desired product, along with the easily assignable alkyl peaks. The aromatic region of the ^{1}H-NMR spectra did not change significantly through the series as the only difference in the three structures was the number of alkyl groups attached to the BODIPY core, which

caused a decrease in the number of pyrrolic signals and an increase in the number of alkyl signals.

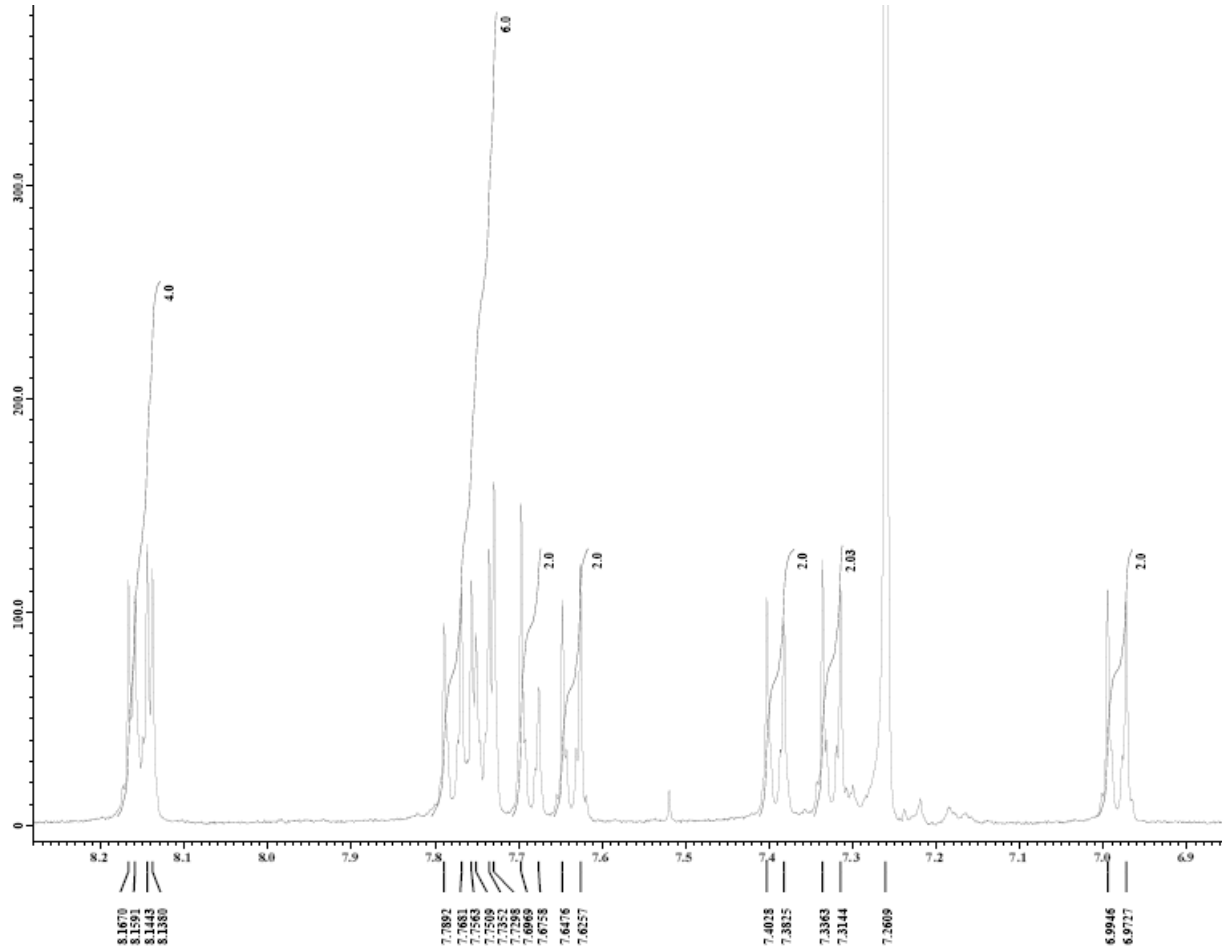

Figure 4. 4: ^{1}H-NMR of mesogenic BODIPY 24 showing the multiple aromatic groups

In order to synthesise a series of mesogenic BODIPYs with an extended molecular axis, BODIPYs bearing terminal ethynyl substituents were prepared (Sch. 4.6). These BODIPY intermediates were prepared *via* a similar method as the previous 4-iodophenyl analogues. The TMS-protected intermediates were isolated for the unsubstituted and tetramethyl BODIPYs and were then deprotected with either potassium carbonate or TBAF. TBAF was found to cause a moderate amount of BODIPY decomposition and the R_f values for the TMS-protected and deprotected BODIPYs were found to be very similar. The TMS-protected analogue of **28** was not isolated due to facile deprotection

during chromatography, so deprotection was carried out on the impure mixture before purification of **28**.

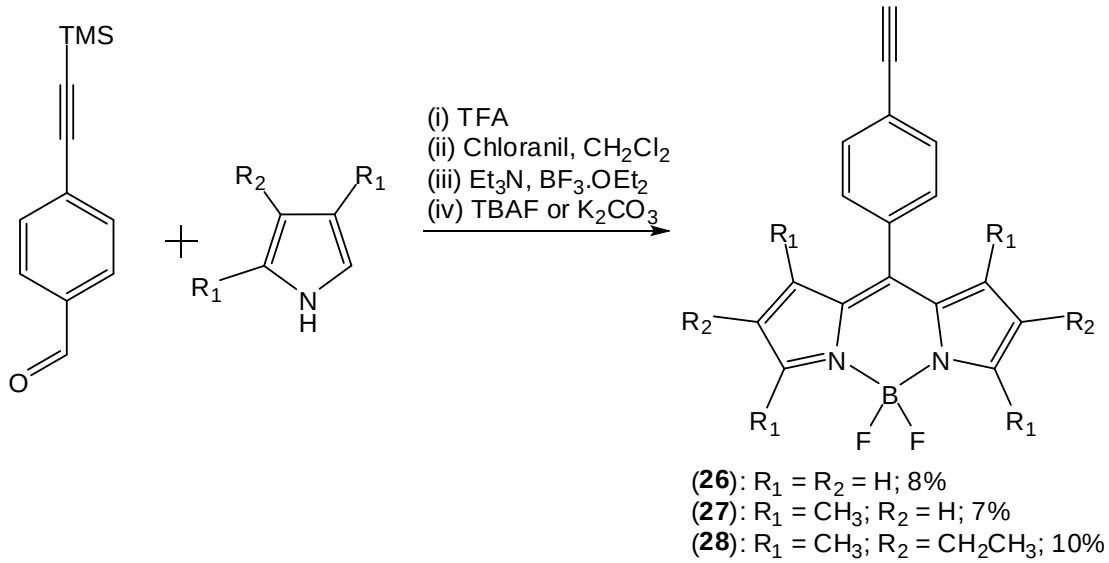

(**26**): $R_1 = R_2 = H$; 8%
(**27**): $R_1 = CH_3$; $R_2 = H$; 7%
(**28**): $R_1 = CH_3$; $R_2 = CH_2CH_3$; 10%

Scheme 4. 6: 8-(4-Ethynylphenyl)-BODIPY synthesis

Subsequent mesogen attachment was achieved by microwave-assisted Sonogashira coupling involving the ethynyl-BODIPY and a mesogen terminating in an aryl iodide. The mesogen was prepared *via* the same reaction as the boronic ester mesogen using 4-iodobenzoic acid and the product was purified by recrystallisation from ethyl acetate (Sch. 4.7).

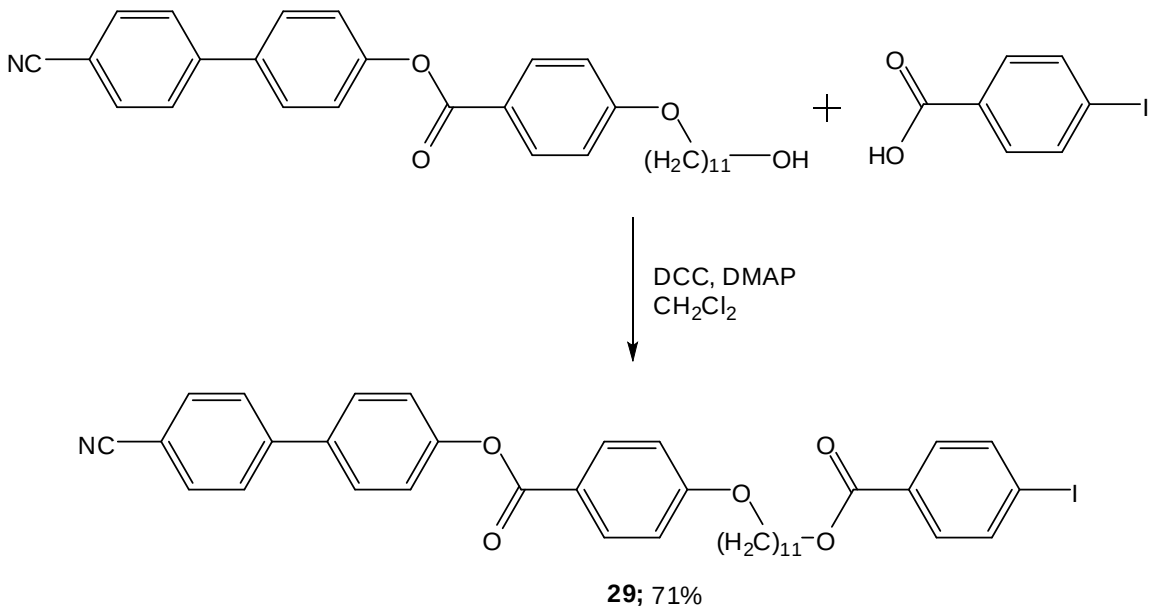

Scheme 4. 7: Mesogenic iodide synthesis

The mesogen attachment was carried out at the same temperature and heating time as the Suzuki couplings (Sch. 4.8), but bis(triphenylphosphine)palladium (II) chloride was used as the catalyst in place of dibenzylideneacetone dipalladium (II) as it was found to give improved yields. Copper iodide and triethylamine was chosen as co-reagents based upon standard Sonogashira conditions.[83] The yields were comparable to those for the Suzuki couplings and were similar throughout the series. Purification was achieved using column chromatography eluting in toluene with small proportions of ethyl acetate followed by precipitation from dichloromethane with cold methanol. A mesogenic BODIPY bearing a cyanobiphenyl mesogen (as attached to the side-attached mesogenic BODIPYs) was also prepared by the same method to investigate whether a less powerful mesogen would induce liquid crystalline behaviour (Fig. 4.5).

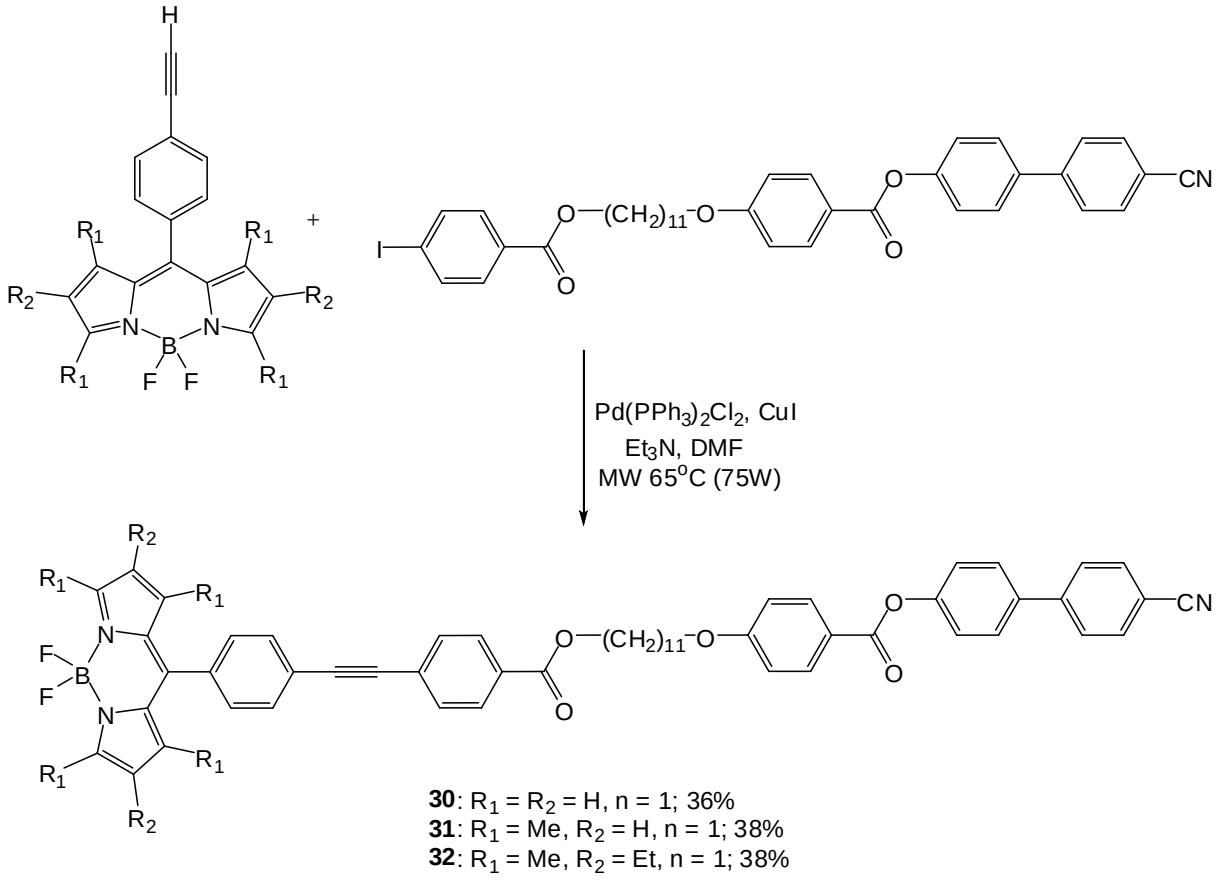

Scheme 4. 8: Mesogenic BODIPY preparation *via* Sonogashira-coupling

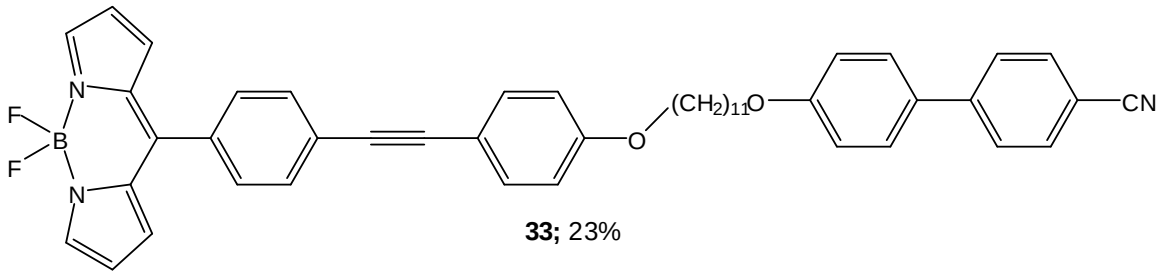

Figure 4. 5: Mesogenic BODIPY prepared by Sonogashira coupling employing a less extended mesogen

While the ethynyl groups causes an extension in the molecular length, the triazole group would cause a kink in the molecular shape as well as an extension in the molecular length. To prepare a mesogenic BODIPY incorporating the triazole group, a BODIPY bearing an ethynyl group (**26**) and a mesogen terminating in an azide were prepared (Sch.

4.9). The preparation of the mesogen was achieved in three straightforward, high yielding steps. Firstly, attachment of a C_{11} chain to the cyanobiphenyl unit was carried out under Williamson ether synthesis conditions. The product was purified using recrystallisation from ethanol before drying *in vacuo*. A methanesulfonate group was then attached *via* reaction of the alcohol with methanesulfonyl chloride in the presence of triethylamine (to neutralize the hydrochloric acid formed) and DMAP (catalyst) with purification by recrystallisation from ethanol. The azide was prepared by reacting the mesylate mesogen with sodium azide in DMSO at 60°C for 16 hrs. After thorough extraction of the DMSO using several water washes, purification of the product was achieved using recrystallisation from ethanol.

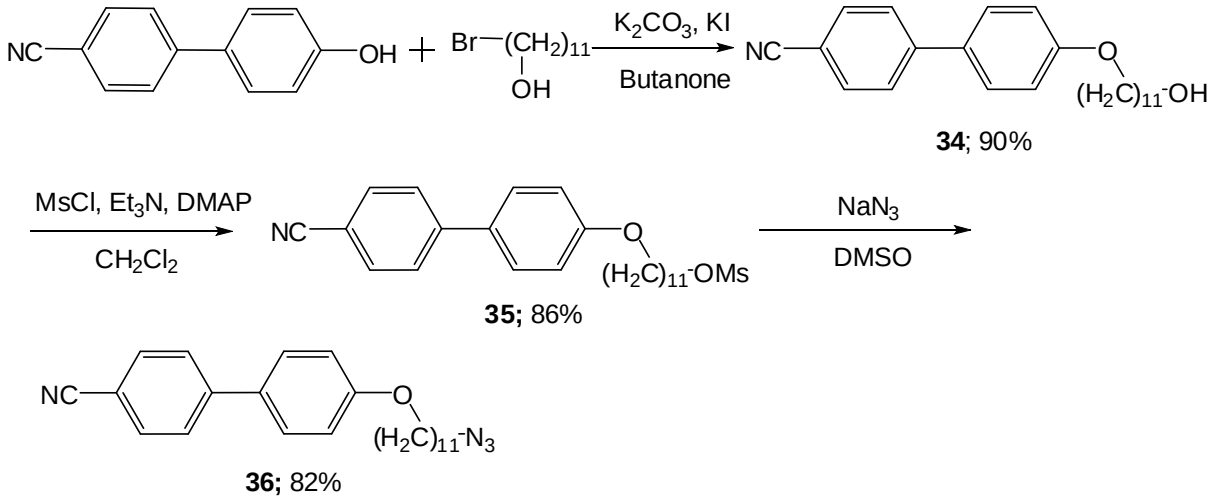

Scheme 4. 9: Mesogenic azide synthesis

The attachment of the mesogen to the BODIPY was achieved using a copper (I) catalyzed 1,3-Huisgen dipolar cycloaddition (commonly referred to as 'click' chemistry). A mixture of copper (0) nanopowder and copper (II) sulphate with sodium ascorbate as the co-reductant was found to yield the desired product in a similar yield to the Suzuki and Sonogashira reactions, but without the need for microwave heating (Sch. 4.10). This reaction was carried out at 50°C for 20 hrs due to the reaction being relatively slow. Purification was carried out using column chromatography eluting with a toluene:ethyl acetate mixture, but subsequent precipitation from dichloromethane was not required as the product was already pure.

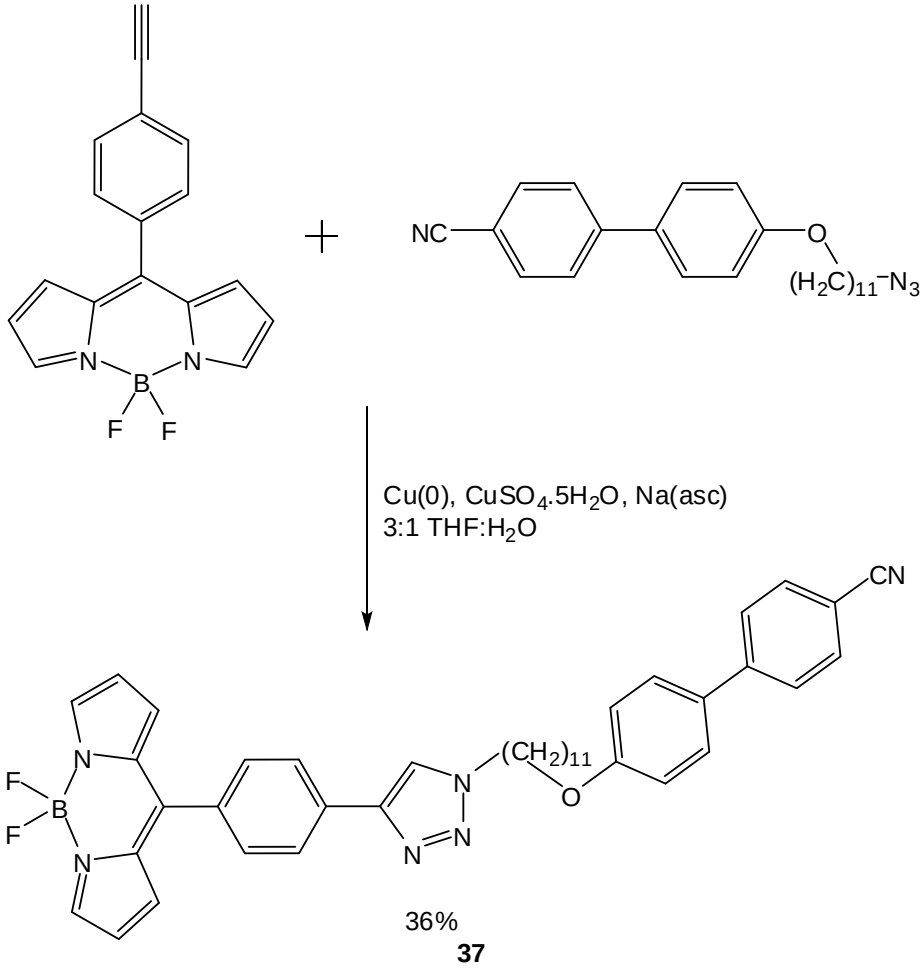

Scheme 4. 10: Attachment of mesogen to BODIPY by 'click' chemistry

As can be seen, the mesogen used in this reaction is less nematogenic than the mesogens used for the Suzuki and Sonogashira reactions as it lacks the additional ester and phenyl ring in the polarisable part of the mesogen. This was due to difficulty in synthesising the azide of the mesogen containing three phenyl rings. Mesylation of the mesogenic alcohol was successful, but subsequent reaction with sodium azide caused decomposition of the starting material and/or product and neither was isolated even under mild heating conditions (Sch. 4.11). ^{1}H-NMR experiments carried out on the isolated white solid showed the presence of two double doublets, possibly indicating the presence of 4-hydroxy-4'-cyanobiphenyl, which could be produced *via* hydrolysis of the mesogen mesylate.

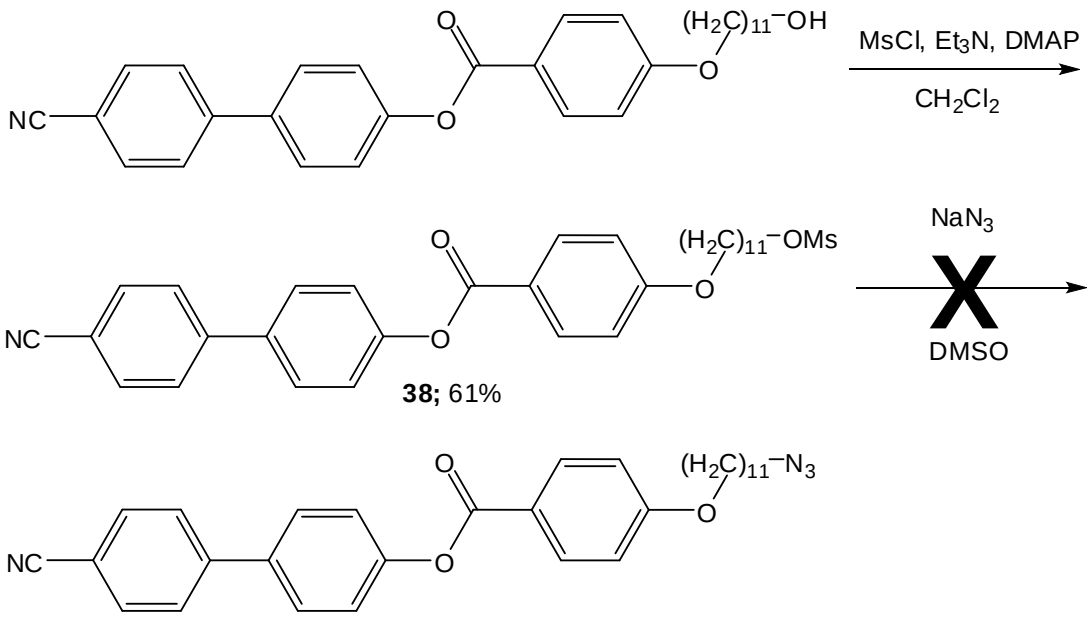

Scheme 4. 11: Unsuccessful mesogenic azide synthesis

In order to overcome this problem, attempts were made to prepare azide analogues of the mesogen and BODIPY precursors. 11-Bromoundecan-1-ol was reacted with sodium azide to yield 11-azidoundecan-1-ol in quantitative yield but subsequent mesylation was unsuccessful. Mesylation of the alkylated 4-hydroxybenzoic acid compound was achieved *via* a similar reaction with methanesulfonyl chloride (**39**). Subsequent reaction with sodium azide, however, was unsuccessful, resulting in decomposition of the starting material (Sch. 4.12).

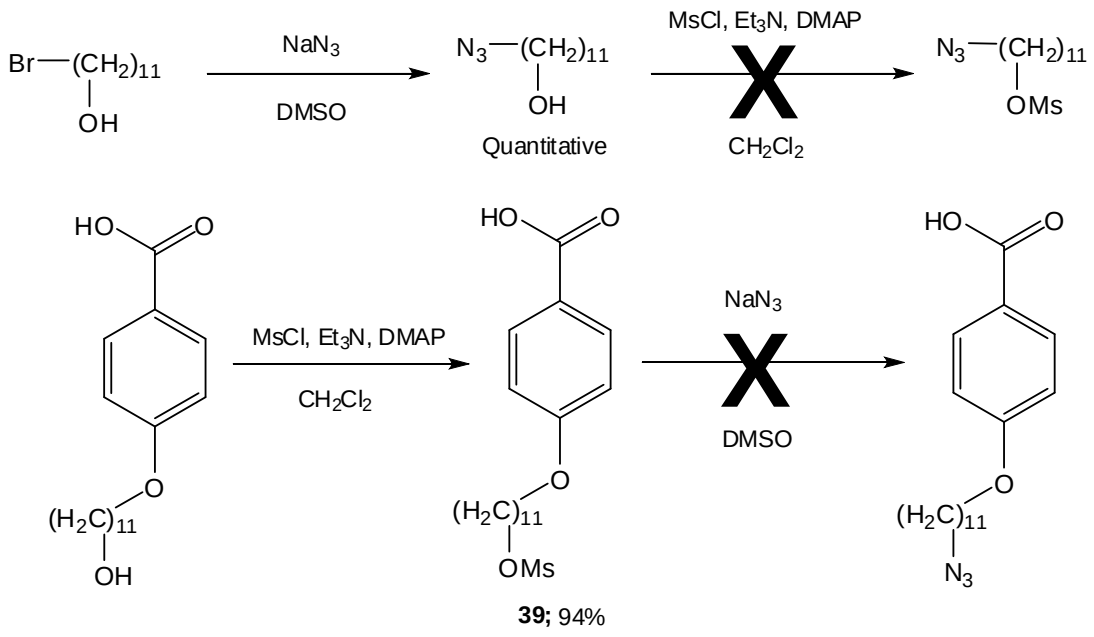

Scheme 4. 12: Unsuccessful attempts to prepare azide analogues of mesogen precursors

Due to the lack of success in preparing the mesogenic azide, BODIPY precursors bearing functional groups for mesogen attachment were prepared. Firstly, 5-(4-ethynylphenyl)-dipyrromethane (**40**) was prepared *via* reaction of pyrrole with 4-trimethylsilylethynylbenzaldehyde followed by deprotection of the TMS group with potassium carbonate (Sch. 4.13). Column chromatography was carried out on the TMS-protected dipyrromethane, but crystallisation was not achieved so deprotection was carried out before finally purifying using column chromatography eluting with dichloromethane:hexane.

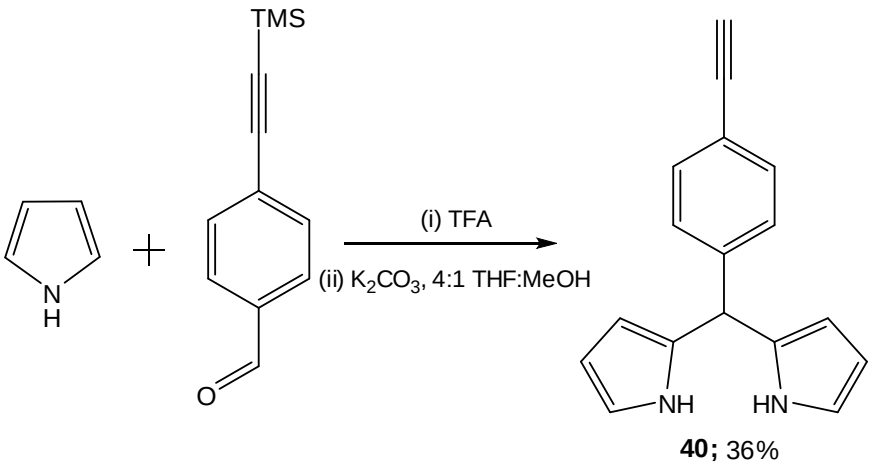

Scheme 4. 13: Preparation of 5-(4-ethynylphenyl)-dipyrromethane

The dipyrromethane was reacted with 11-azidoundecan-1-ol in DMF with copper (II) sulphate as the catalyst and sodium ascorbate as the co-reductant to yield the triazole-containing dipyrromethane (**41**) terminating in a C_{11}-OH unit in 48% yield. This was then successfully mesylated (**42**) under the same conditions in quantitative yield (Sch. 4.14). The initial 'clicked' dipyrromethane was purified by passing it through a short silica column while the mesylate did not require purification beyond washing with 2% hydrochloric acid and water. Subsequent reaction with 4-hydroxybenzoic acid under Williamson ether synthesis conditions was unsuccessful, causing decomposition of the starting material.

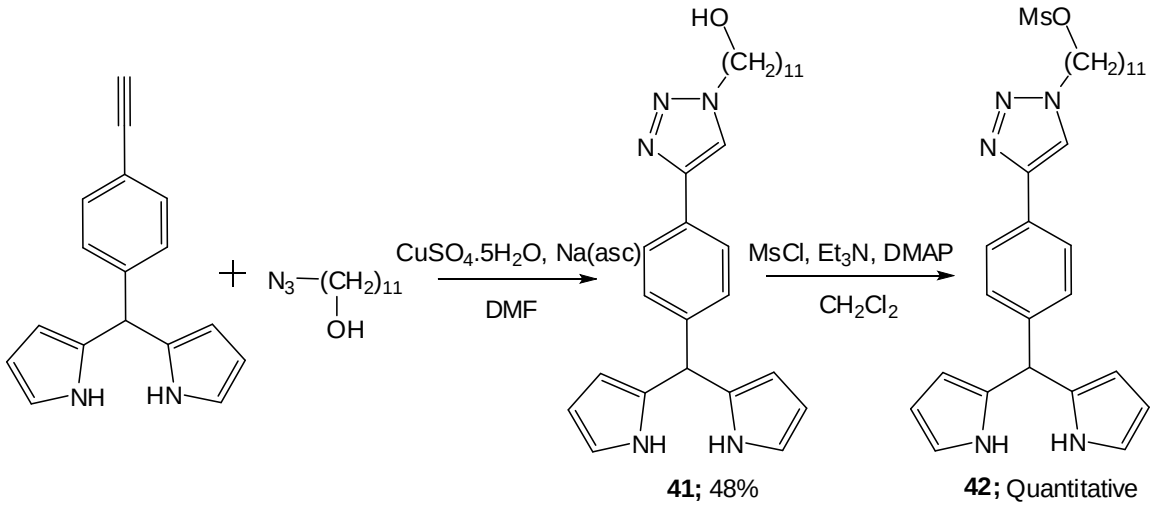

Scheme 4. 14: 'Clicked' dipyrromethane with subsequent mesylation

Due to the lack of success in attaching a more nematogenic mesogen to the BODIPY *via* either of these approaches, the same cyanobiphenyl mesogen used for the 'click' reaction in Scheme 4.10 was attached to the dipyrromethane to investigate whether any liquid crystallinity was conferred on the resulting molecule. The primary aim of this approach was to synthesise a mesogenic dipyrrin-metal complex containing two mesogenic units. 5-(4-Ethynylphenyl)-dipyrromethane (**40**) was reacted with the azide mesogen under the same 'click' conditions as depicted in Scheme 4.14, but with an alternate solvent system. This reaction proceeded at room temperature to yield the pure product (**41**), after column chromatography, in 49% yield. Subsequent oxidation of the dipyrromethane with DDQ was successful (**42**), but with a very low yield (7%), despite being carried out using the generally accepted methodology.[18-22] There is no obvious reason why this reaction proceeded with such a low yield, but as the effect that a triazole group has on the DDQ oxidation of a dipyrromethane has not been thoroughly investigated, the presence of a triazole group could be significant. A nickel-(II)-dipyrrinato complex (**43**) was prepared using nickel (II) acetate in dichloromethane, with purification being achieved by passing the residue through a short silica column yielding the product in 49% yield. A nickel (II) complex was chosen over a zinc (II) complex as it has been reported that zinc complexes adopt a more tetrahedral geometry around the metal centre while the nickel complex adopts a distorted square planar geometry.[265]

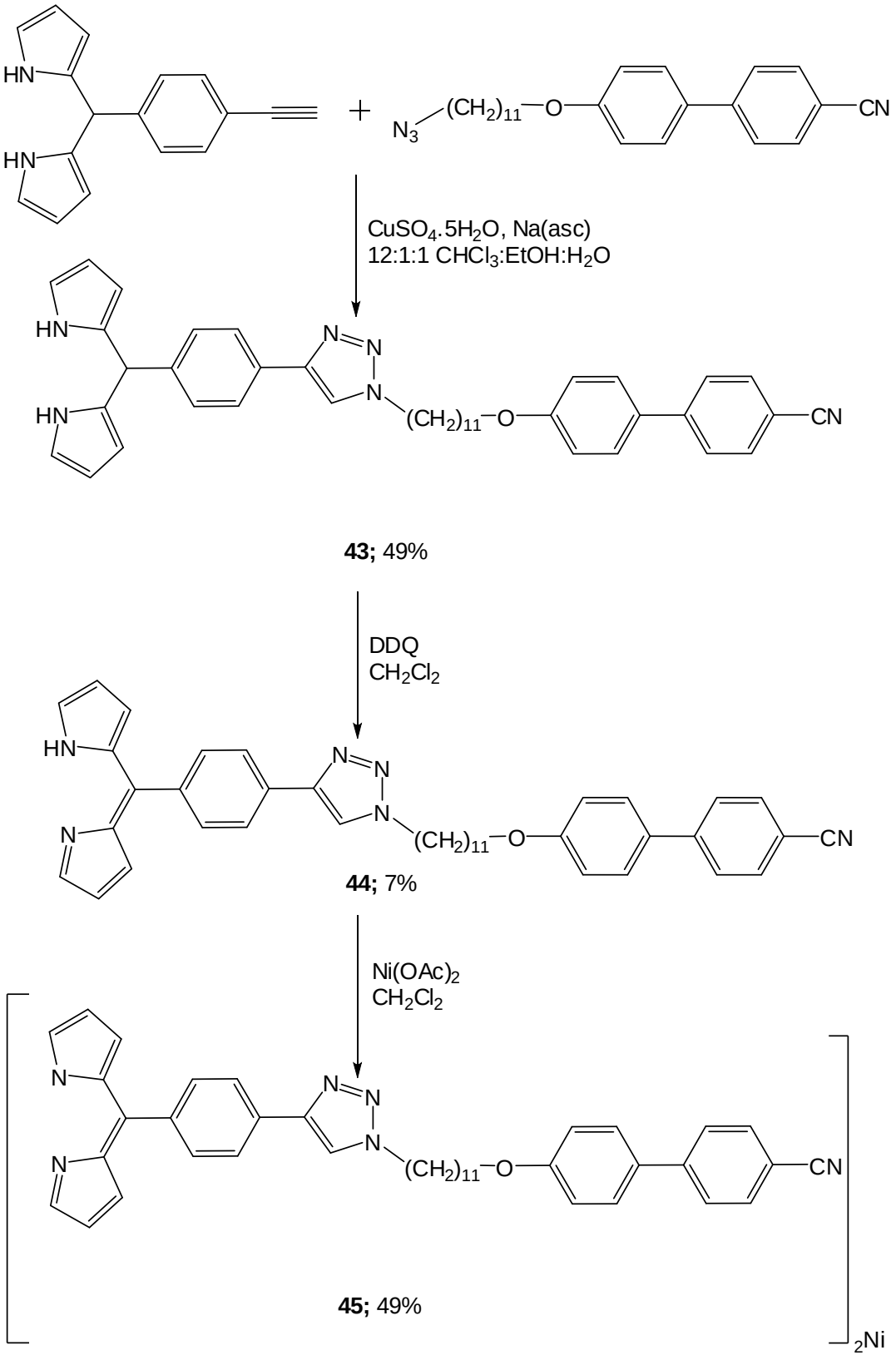

Scheme 4. 15: Mesogen attachment to dipyrromethane by 'click' chemistry with subsequent oxidation and nickel (II) complexation

A Heck reaction was also attempted on the 4-iodo-BODIPY (**18**) to investigate whether an allyl linker group and different type of mesogen could induce liquid crystallinity onto the BODIPY. The mesogen chosen for this reaction would have an alkyl spacer group attached side-on. (Fig. 4.6) The reaction was carried out under the same conditions as the Suzuki couplings but was found to be unsuccessful, with only a small amount of starting BODIPY being recovered (~7%).

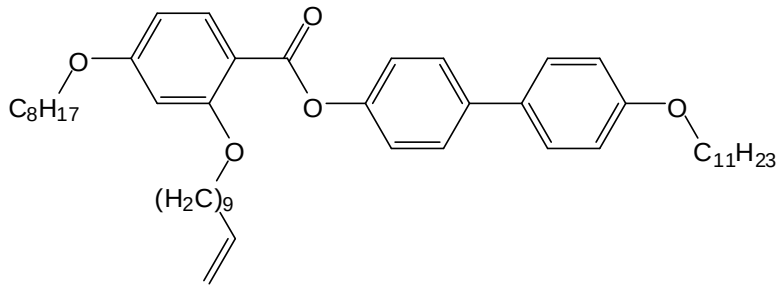

Figure 4. 6: Mesogen used in attempted Heck reaction

An attempt was next made to prepare a mesogenic BODIPY which displayed red-shifted fluorescence relative to the previously prepared BODIPYs. To achieve this, a diindolylmethane was prepared *via* an analogous route used for dipyrromethane preparation. This method used concentrated hydrochloric acid in place of TFA and no purification was required beyond neutralisation with sodium hydroxide and precipitation with water to yield the product in 12% yield (Sch. 4.16). Subsequent oxidation with DDQ or chloranil was unsuccessful as was reaction of the crude mixture, resulting from the attempted oxidation, with boron trifluoride diethyl etherate.

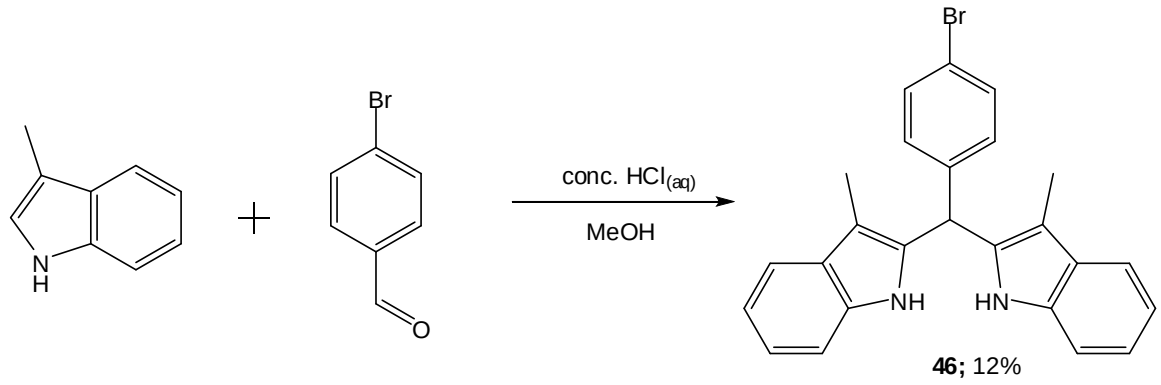

Scheme 4. 16: Diindolylmethane synthesis

4.2.2 Liquid crystalline behaviour

Of the series of BODIPYs prepared by Suzuki couplings, **23** and **24** exhibit liquid crystalline mesophases, with a monotropic nematic phase being observed for each compound. As can be seen from the DSC curves (Fig. 4.7 and 4.8) of these compounds, the nematic range is shortened and the clearing temperature is increased upon addition of the four methyl groups to the BODIPY core. The increased bulkiness of the BODIPY core also requires the material to be supercooled by 58ºC below its melting point before adopting the nematic phase. These effects were attributed to the increased bulk of the BODIPY core causing a disruption in the molecular packing of the nematic phase, with the restricted rotation of the 8-phenyl ring causing an increase in the rigidity of the BODIPY core, increasing the preference for crystalline behaviour by increasing intermolecular π-π interactions. These effects are further reinforced in **25** by the two ethyl groups increasing the bulk of the fluorophore even further. The molecular packing is disrupted enough for the mesophase to disappear completely and only crystalline behaviour is observed, however, the ethyl groups cause a reduction in the melting point compared to **24**. This liquid crystalline behaviour is markedly different from that displayed by previously reported nematic BODIPYs, with the additional phenyl ring at the 8-position disrupting nematogenicity to the extent that the nematic range is relatively short even when a more powerful mesogen is used. The increase in steric bulk around the fluorophore also causes an increase in the transition enthalpy from the isotropic liquid to the nematic phase. As the four methyl groups induce an increased preference for

crystalline behaviour over liquid crystalline behaviour, the transition enthalpy must increase to overcome this. The ΔS/R values were calculated to provide a unitless figure to compare the compounds (with R being the ideal gas constant).

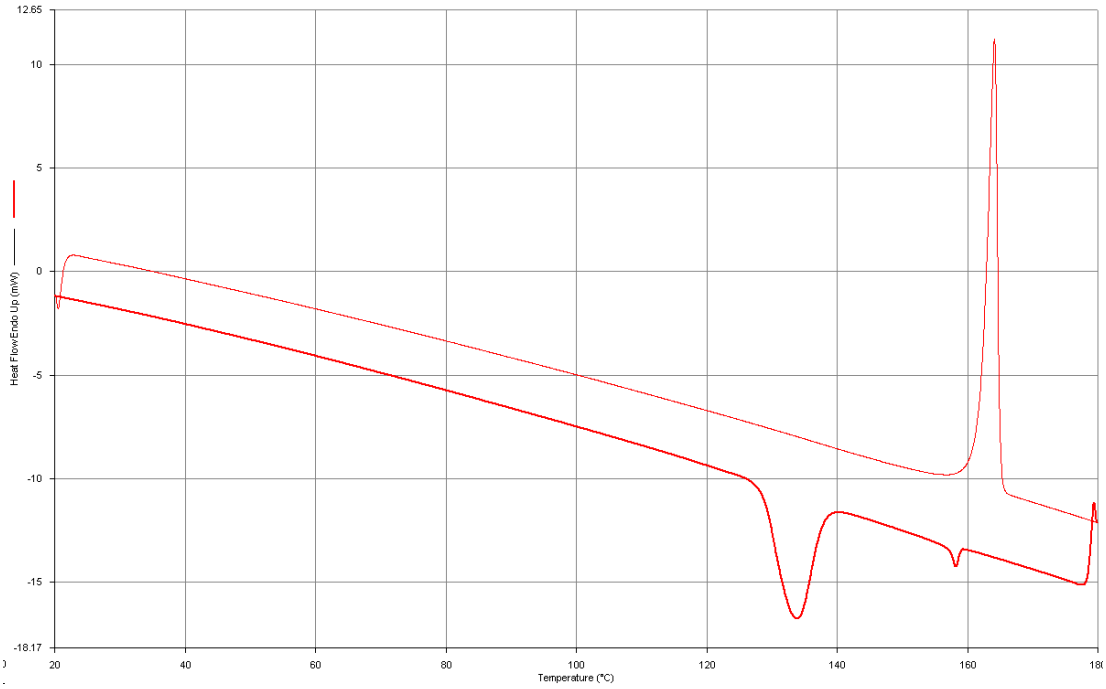

Figure 4. 7: DSC thermogram of 23 showing second heat (top line) and second cool (bottom line)

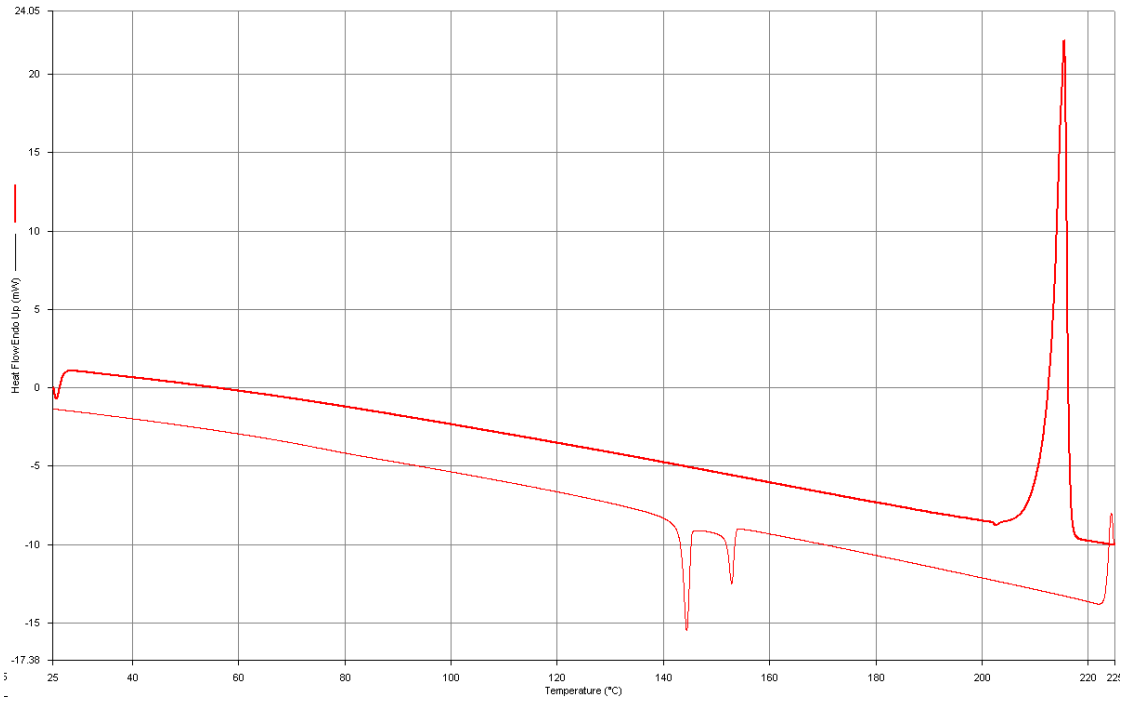

Figure 4. 8: DSC thermogram of 24 showing second heat (top line) and second cool (bottom line)

The optical polarising microscopy (OPM) images show **23** and **24** in the nematic phase with the schlieren texture clearly visible, especially for **23**, typical of a nematic phase (Fig. 4.9 and 4.10). The orange colour is due to the colour of the compounds and not a birefringent effect.

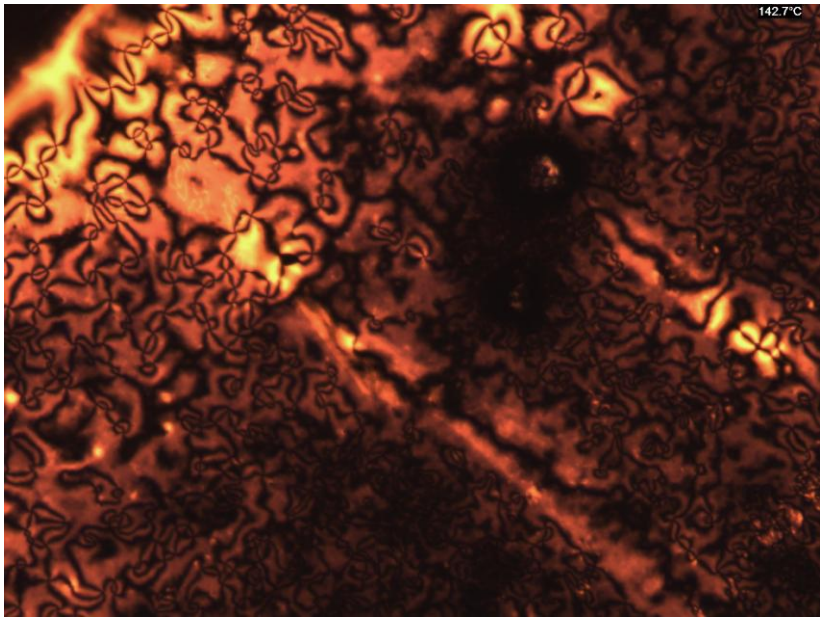

Figure 4. 9: OPM image of 23 in the nematic phase at 142.7°C

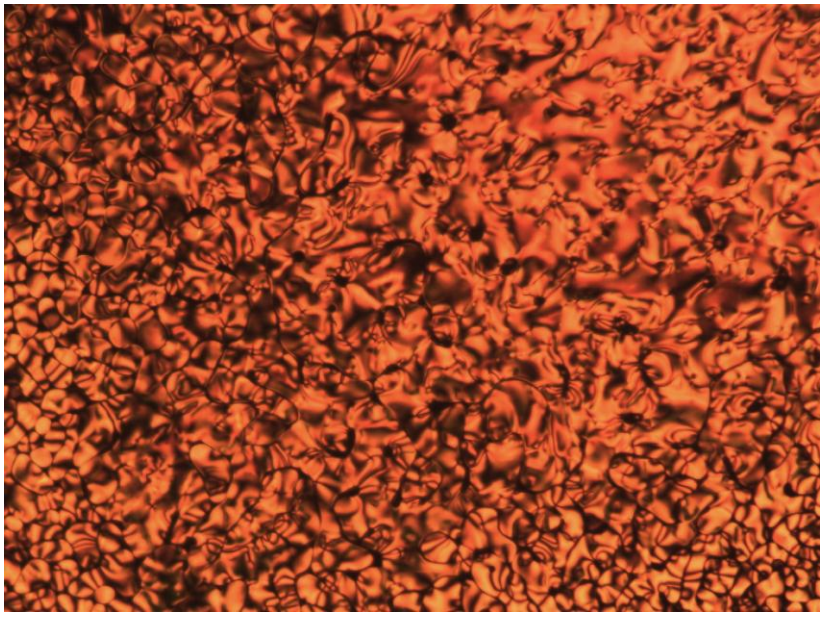

Figure 4. 10: OPM image of 24 in the nematic phase at 148.6°C

Compound	LC transitions (ºC)	Nematic range (ºC)	ΔH (kJ mol^{-1}) (Iso-N transition)	ΔS_{mol} / R (Iso-N transition)
23	Cr (N 159) 162 I	21	1.54	0.43
24	Cr (N 153) 211 I	8	4.12	1.15
25	Cr 194 I	-	-	-

Table 4. 1: Liquid crystal transitions, nematic ranges, Iso-N enthalpies and Iso-N reduced entropies for compounds 23-25

The increased molecular axis in the mesogenic BODIPYs prepared by Sonogashira reactions causes a further reduction in the liquid crystallinity of the molecules by increasing the intermolecular interactions. The DSC curve for **30** (Fig. 4.11) is similar to the DSC curve for **24** as they both have short nematic ranges and some degree of supercooling is required before the nematic phase is adopted. Due to the very short nematic range of **30**, the nematic phase is eliminated in **31** by the four methyl groups and remains thus for **32**. The OPM image shows the schlieren texture of **30** in the nematic phase (Fig. 4.12). Due to the very short nematic phase, some crystallisation can be seen in the lower right of the image.

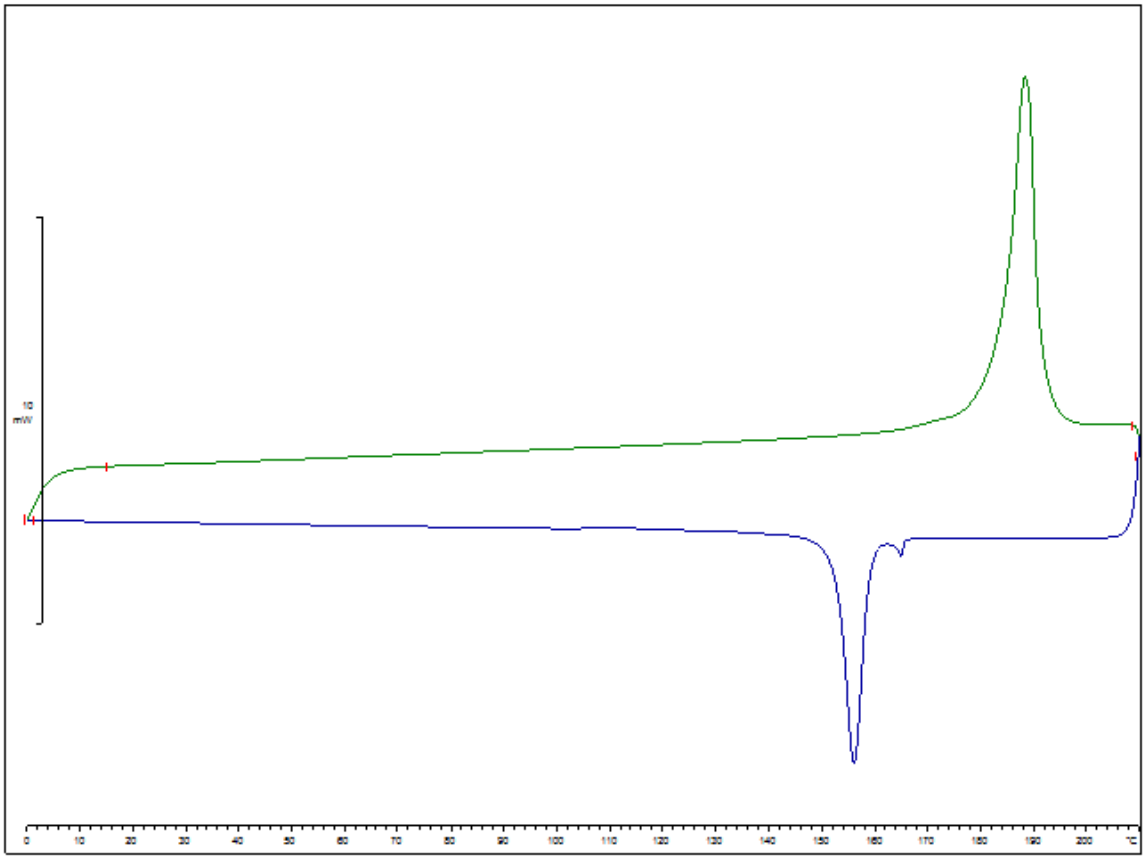

Figure 4. 11: DSC thermogram of 30 showing second heat (top line) and second cool (bottom line)

The transition enthalpy of **30** is relatively low when compared to the enthalpies for **23** and **24**. Increased intermolecular interactions also cause an increase in the clearing temperature of **30**. Analogous to the mesogenic BODIPYs prepared by Suzuki couplings, the four methyl groups cause an increase in clearing temperature which is then reduced by the two ethyl groups of **32**.

Figure 4. 12: OPM image of 30 in the nematic phase at 164.1°C

The dipyrromethane (**43**), dipyrrin (**44**), BODIPY (**37**) and nickel-(II)-dipyrrinato complex (**45**) were all observed under the optical polarising microscope but, despite the nickel-(II)-dipyrrinato complex displaying some birefringence (Fig. 4.13), no liquid crystalline mesophase was observed. This was attributed to the triazole causing the overall molecular shape to be non-linear as well as the cyanobiphenyl mesogen being less nematogenic than the mesogen used in the Suzuki and Sonogashira reactions.

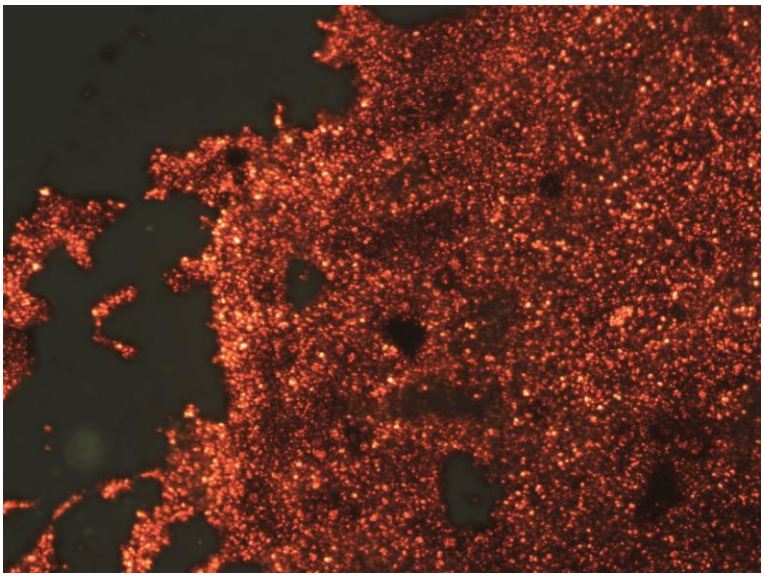

Figure 4. 13: OPM image of nickel-(II)-dipyrrinato complex at 146.6C showing a large amount of birefringence

Compound	LC transitions (°C)	Nematic range (°C)	ΔH (kJ mol^{-1}) (Iso-N transition)	ΔS_{mol} / R (Iso-N transition)
30	Cr (N 166) 183 I	7	0.86	0.24
31	Cr 200 I	-	-	-
32	Cr 185 I	-	-	-

Table 4. 2: Liquid crystal transitions, nematic ranges, Iso-N enthalpies and Iso-N reduced entropies for compounds 30-32

By comparing the reduced entropies of compounds **23**, **24** and **25** it can be seen that the four methyl groups cause a larger entropy change in cooling from the isotropic liquid to the nematic phase. This indicates a lesser degree of order in the tetramethyl analogue (**23**) over the mesogenic BODIPYs bearing no substituents on the pyrrolic positions (**23** and **30**). This is caused by the increased rigidity due to the rotational restriction induced by the methyl substituents on the central phenyl ring disrupting the molecular packing in the nematic phase. Due to the extended long molecular axis in compound **30** compared to **23**, increased intermolecular interactions promote a greater degree of ordering, thus reducing the value of the reduced entropy.

4.2.3 Fluorescence

The two series of mesogenic BODIPYs prepared by palladium-catalyzed couplings exhibit increasingly intense fluorescence with increasing alkyl substitution on the BODIPY core. Very low quantum yields and fluorescence lifetimes are exhibited by the unsubstituted mesogenic BODIPYs **23**, **30** and **37** due to relatively unrestricted rotation of the 8-phenyl ring. The attachment of four methyl groups causes a dramatic increase in fluorescence intensity by restricting the 8-phenyl ring rotation, which is increased further by the additional two ethyl groups. The unsubstituted and tetramethyl BODIPYs absorb at approximately the same wavelength but the tetramethyl BODIPYs have a shorter Stokes' shift, presumably because they possess fewer vibrational modes due to restriction of the 8-phenyl ring rotation. The tetramethyl-diethyl BODIPYs have slightly red-shifted absorption and emission relative to the other BODIPYs due to all the pyrrolic positions on the BODIPY core being occupied. They also have similar, but slightly longer Stokes' shifts compared to the tetramethyl BODIPYs (Fig. 4.14, 4.15 and 4.16).

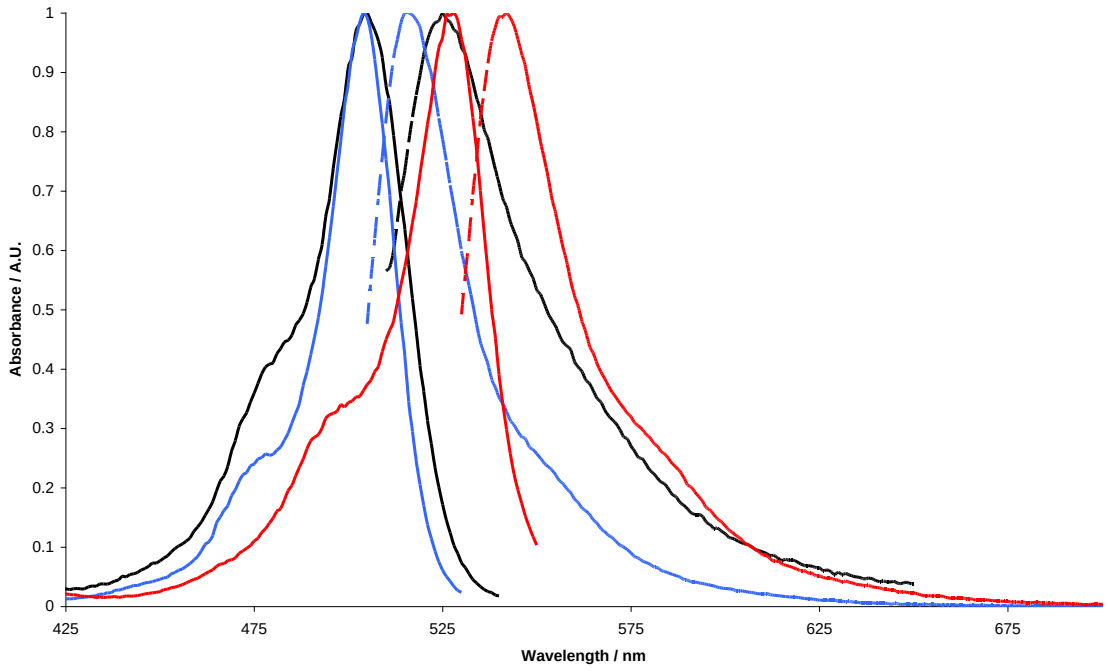

Figure 4. 14: Excitation (solid line) and emission (dashed line) of 23 (black), 24 (blue) and 25 (red); measured in toluene at 298K

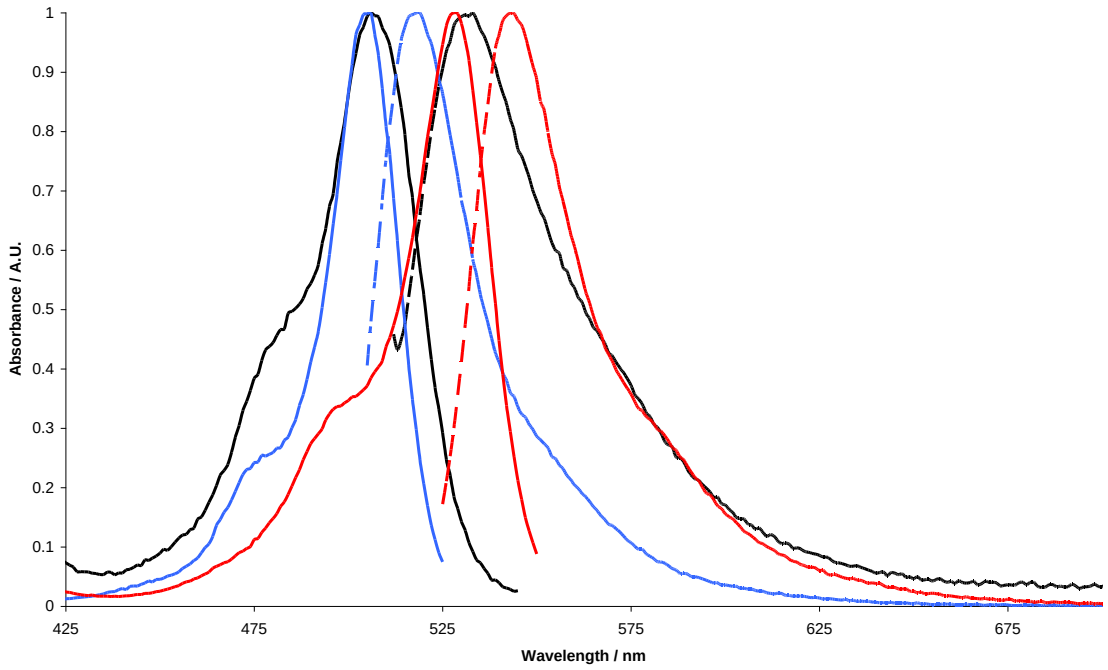

Figure 4. 15: Excitation (solid line) and emission (dashed line) of 30 (black), 31 (blue) and 32 (red); measured in toluene at 298K

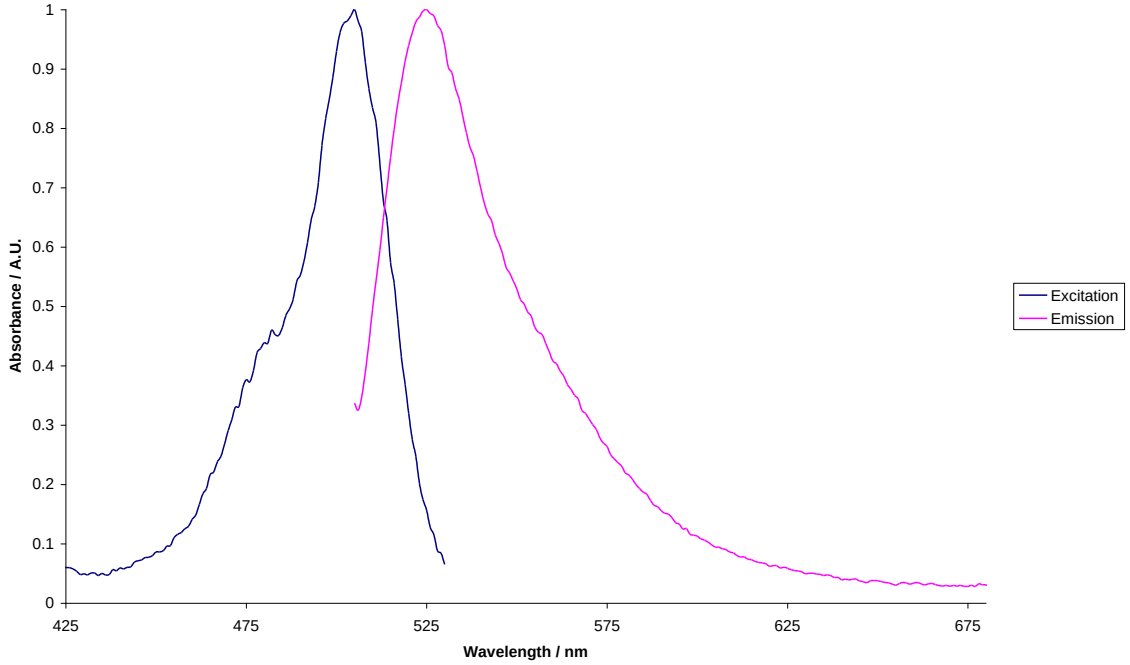

Figure 4. 16: Excitation (blue) and emission (pink) of 37; measured in toluene at 298K

The alkyl substituted BODIPYs all have longer fluorescence lifetimes than the unsubstituted BODIPYs due to stabilisation of the excited singlet state by the alkyl groups. As would be expected from the quantum yields, the less fluorescent BODIPYs have smaller radiative constants while the more fluorescent BODIPYs have higher radiative constants. There is a gradual increase in absorption coefficient with increasing alkyl substitution for the mesogenic BODIPYs attached by Suzuki couplings, but the reverse occurs for the mesogenic BODIPYs attached by Sonogashira couplings. There is only a marginal red-shift in the fluorescence profiles of the ethynyl-containing BODIPYs as the extension of the π-conjugation does not pass through the BODIPY core as the 8-phenyl ring (and the aromatic groups attached to this ring) is not co-planar with the bipyrrolic core. The 8-phenyl ring is free to rotate in the unsubstituted BODIPYs meaning that only partial overlap of the π-orbitals occurs, while in the alkylated analogues, the alkyl groups force the 8-phenyl ring out of co-planarity with the BODIPY core minimizing any overlap of the π-orbitals. Despite the presence of a triazole ring in **37**, the fluorescence profile is very similar to those of **23** and **30**.

Compound	λ_{ex} **(nm)**	λ_{em} **(nm)**	Φ_F	**ε (M^{-1} cm^{-1})**	**ΔS (nm)**	k_r **(10^8 s^{-1})**	k_{nr} **(10^8 s^{-1})**	τ_{fl} **(ns)**
23	505	526	0.032	57000	21	1.8	54	0.18
24	505	517	0.48	89000	12	1.8	2.0	2.66
25	528	543	0.63	103000	15	2.9	1.7	2.18
30	508	533	0.01	116000	25	10	9.9 (x 10^{10})	0.01
31	506	519	0.37	92000	13	1.6	2.8	2.27
32	529	544	0.78	82000	15	2.0	0.55	4
37	504	523	0.047	64000	19	2.0	9.3 (x 10^{10})	0.23

Table 4. 3: Photophysical data of 23-25, 30-32 and 37; measured in toluene or CH_2Cl_2 at 298K

4.2.4 Structure-property relationship between liquid crystallinity and fluorescence intensity

These results show a clear inverse relationship between the tendency of the molecules to mesophase formation and their fluorescence intensity. While increasing alkyl substitution on the BODIPY core has a very predictable effect on the fluorescence intensity, the effect it has on any liquid crystalline behaviour is not as obvious due to lack of investigation in this particular aspect of BODIPYs.

Compound	LC transitions (°C)	Nematic range (°C)	Φ_F
23	Cr (N 159) 162 I	21	0.032
24	Cr (N 153) 211 I	8	0.48
25	-	-	0.63
30	Cr (N 166) 183 I	7	0.01
31	-	-	0.37
32	-	-	0.78

Table 4. 4: Structure-property relationship between liquid crystallinity and fluoresccence intensity of 23-25, 30-32 and 37

Due to the BODIPY being in a terminal position on the molecule, increasing the number of alkyl groups on the BODIPY fluorophore only increases the size of one terminal while the mesogenic terminal remains the same size. The incorporation of four methyl units on the BODIPY fluorophore causes a significant increase in the clearing/melting temperature along with a shortening of the nematic range. The nematic range of compound **30** is short enough that the attachment of four methyl units eliminates the nematic phase completely. Due to rotational restriction of the BODIPY 8-phenyl ring caused by the 1- and 7-methyl groups, the fluorescence quantum yield of the BODIPY is increased.

The same effect is observed in compounds **25** and **32**, where the nematic range of **24** is shortened enough to eliminate the nematic phase. As the nematic phase is already eliminated in compound **31**, a reduction in the melting point is observed with increased

size of the fluorophore. A further increase in fluorescence intensity is also observed due to a longer range steric effect of the ethyl groups on the 8-phenyl ring.

4.2.5 Temperature dependant fluorescence measurements and BODIPY-doped nematic liquid crystal fluorescence

Compound **23** was chosen to carry out temperature dependant fluorescence measurements due to it exhibiting the widest nematic range of the compounds prepared in these series' (Fig. 4.17). It has been previously reported that the fluorescence of a liquid crystalline BODIPY increases with decreasing temperature,[230] which is an effect observed in this case also. However, no marked increase in fluorescence was reported upon transition from the isotropic liquid to the nematic phase or from the nematic to the crystalline phase. In the case of compound **23**, while no significant increase in fluorescence intensity is observed in the transition from the isotropic liquid to the nematic phase, a noticeable increase in fluorescence intensity occurs when cooling from 150°C to 140°C. As can be seen from the DSC thermogram of compound **23** (Fig. 4.7), crystallisation from the nematic phase into the crystalline phase starts to occur around 140°C and a short time annealing the sample allows almost complete crystallisation to occur. This causes the molecules to adopt a much more rigid conformation, presumably greatly restricting the rotation of the 8-phenyl ring while also causing a reduction in other molecular motions causing an increase in fluorescence intensity. Decreasing the temperature in the crystalline phase causes an increase in fluorescence intensity from a second emission maximum at approximately 620 nm, corresponding to the increased formation of *J*-dimers as the molecules pack closer together. This peak is only slight when in the isotropic or nematic phase due to the more diffuse nature of the molecular packing. The formation of *J*-dimers does occur to a certain extent as evidenced by the red-shift in the fluorescence compared to the solution-based measurements but is much more pronounced when crystallisation occurs. It was expected that the transition from the isotropic to the nematic phase would also cause an increase in fluorescence intensity due to increased 8-phenyl ring rotational restriction but this was not observed, presumably

due to the more diffuse nature of a nematic phase over a layered phase e.g. smectic, or the crystalline phase.

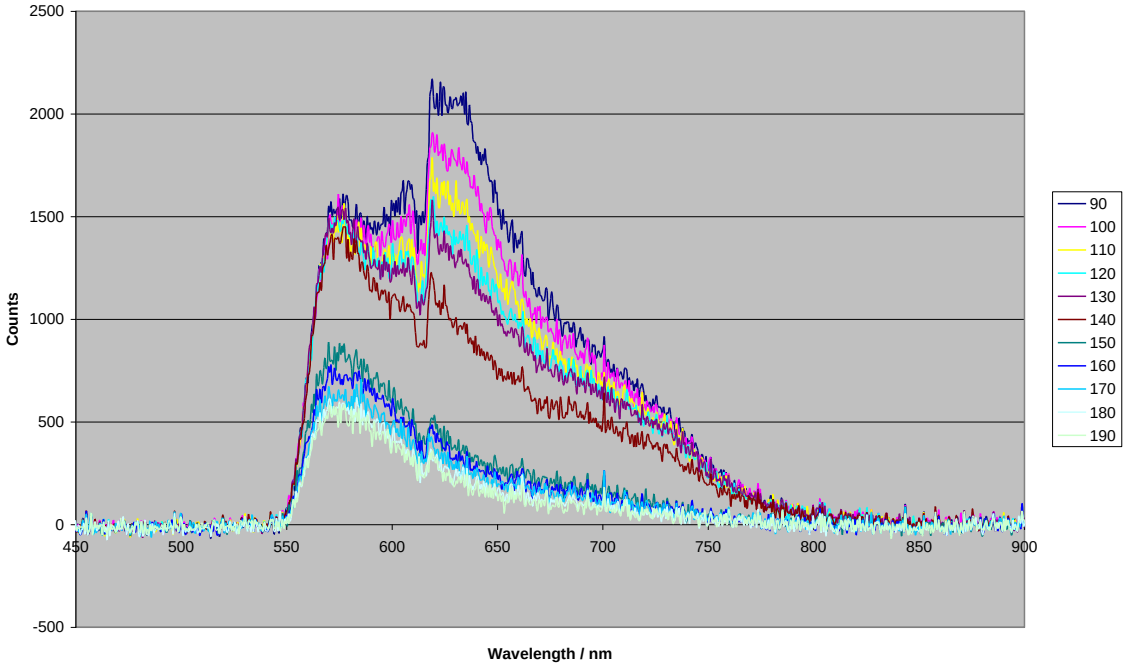

Figure 4. 17: Temperature dependant fluorescence measurements of compound 23 at 10°C intervals (heated to 190°C and cooling down to 90°C - see legend); excited with a Nd:YAG laser with heating on a Mettler hot-stage

In order to investigate the effect that the alignment of the BODIPY molecules has on their fluorescence, four of the mesogenic BODIPYs (**23**, **25**, **30** and **32**) were dissolved in a commercial nematic liquid crystal (BL024 – Merck) and incorporated into a twisted nematic cell (inner top plate aligned perpendicular to the bottom plate). The sample was excited with a UV laser and the fluorescence intensity was measured when an electric field was applied. Compounds **23**, **25**, **30** and **32** were chosen as they were the most and least fluorescent compounds of their respective series. Compounds **30** and **32** were studied to investigate if the increased molecular length had any effect on the alignment with the host material.

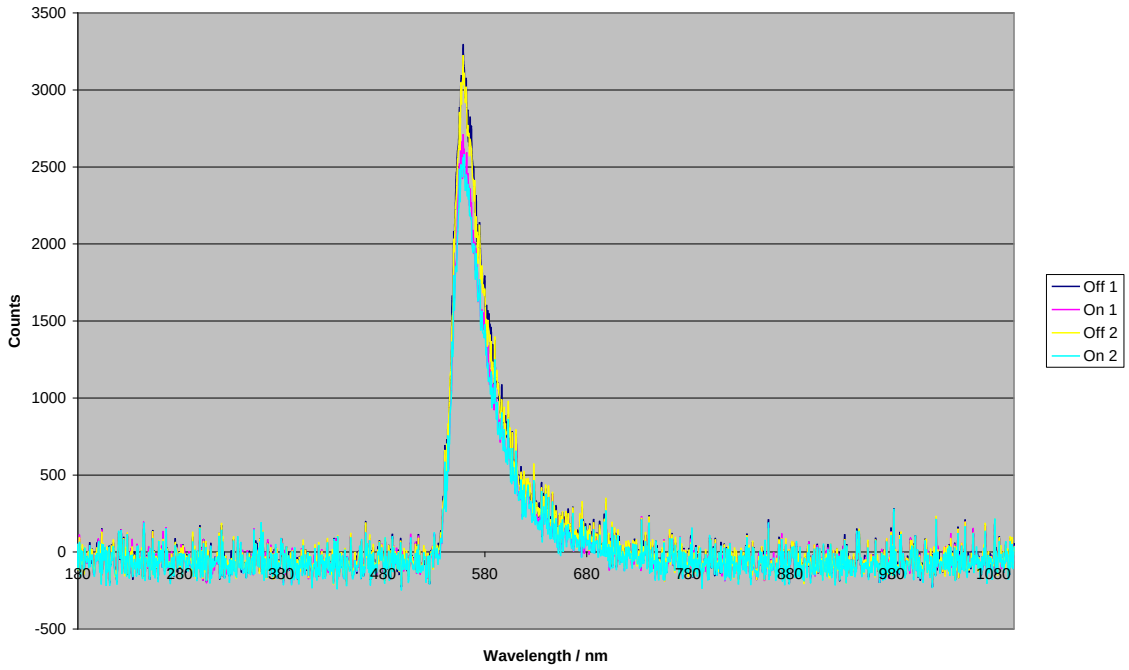

Figure 4. 18: Fluorescence intensity of 23 dissolved in BL024 in a twisted nematic cell (two measurements taken with an electric field applied (On) and two without an electric field applied (Off) - see legend)

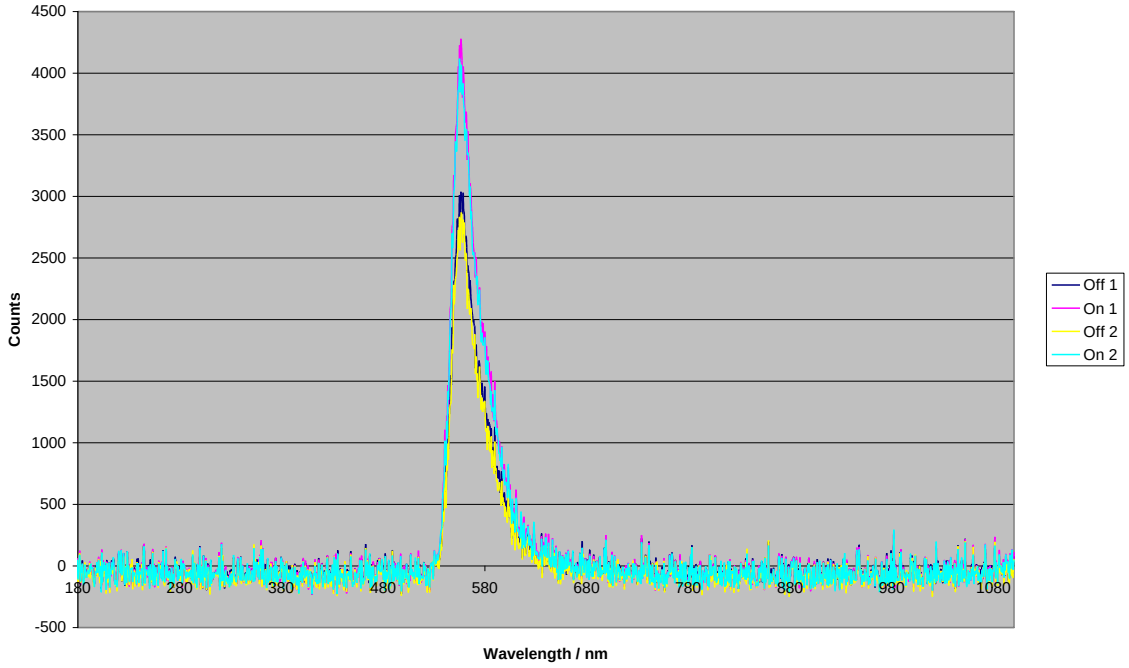

Figure 4. 19: Fluorescence intensity of 25 dissolved in BL024 in a twisted nematic cell (two measurements taken with an electric field applied (On) and two without an electric field applied (Off) - see legend)

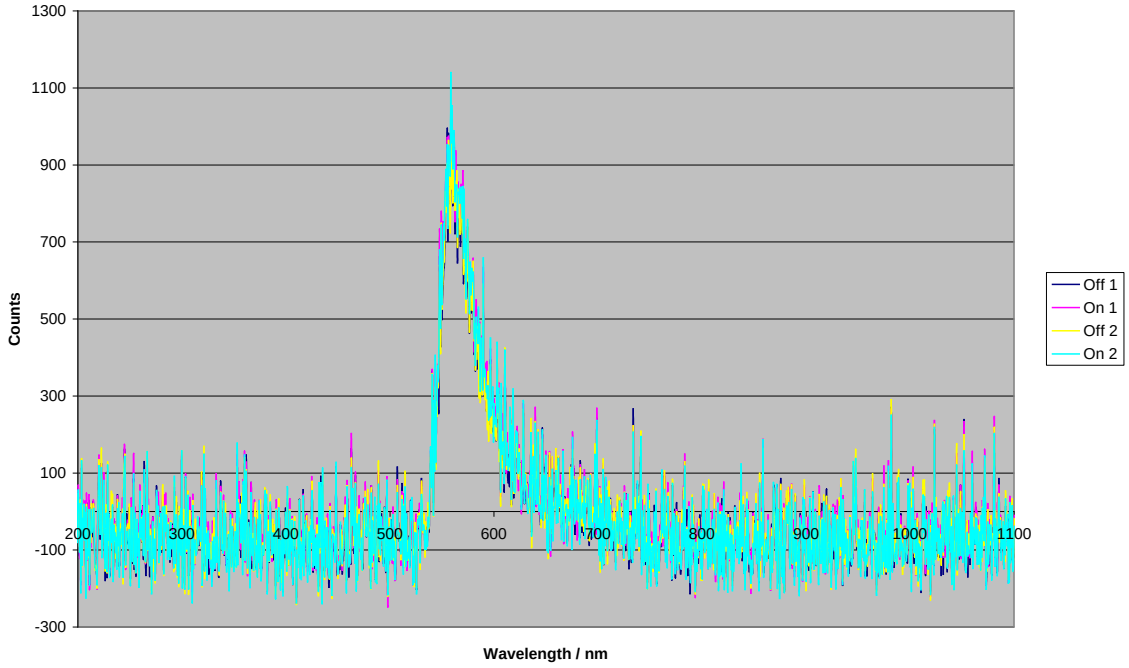

Figure 4. 20: Fluorescence intensity of 30 dissolved in BL024 in a twisted nematic cell (two measurements taken with an electric field applied (On) and two without an electric field applied (Off) - see legend)

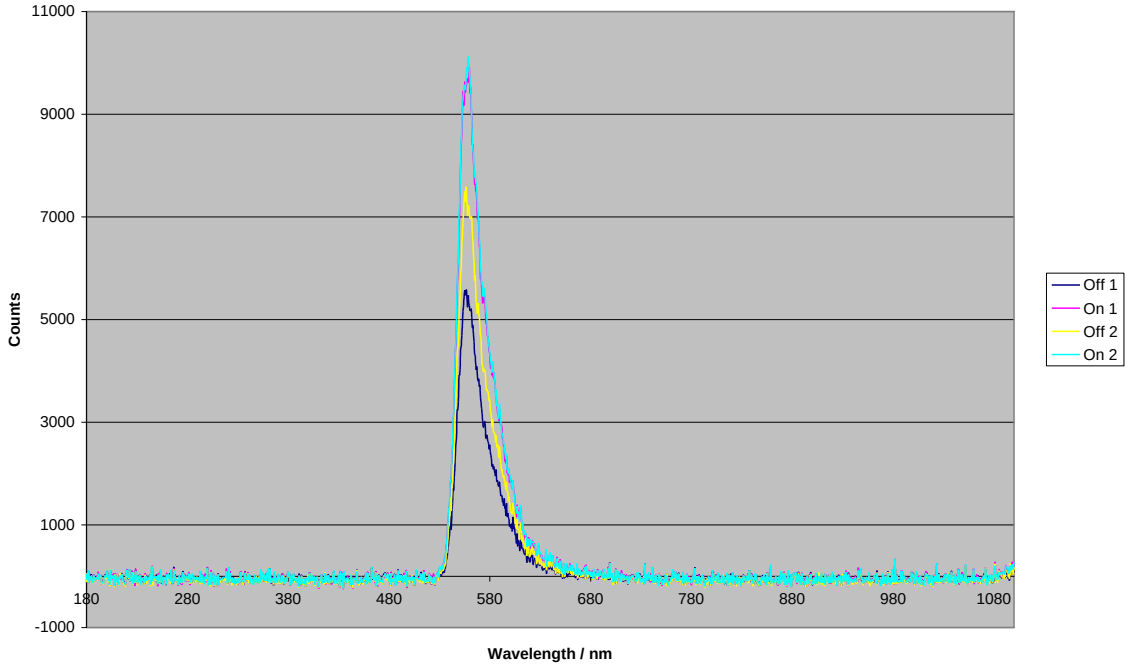

Figure 4. 21: Fluorescence intensity of 32 dissolved in BL024 in a twisted nematic cell (two measurements taken with an electric field applied (On) and two without an electric field applied (Off) - see legend)

The core-unsubstituted mesogenic BODIPYs only displayed a minor change in fluorescence intensity when the electric field was applied. In particular, the mixture of compound **30** displayed no obvious change in fluorescence intensity (Fig. 4.20). The mixture of compound **23**, however, displayed a small, but noticeable, reduction in fluorescence intensity when the electric field was applied (Fig. 4.18). The changes in fluorescence intensity were attributed to an increase or decrease in the number of BODIPY transition dipole moments aligned parallel or non-parallel to the exciting laser beam. In order for the BODIPY to absorb a photon efficiently, its transition dipole moment (which is across the bipyrrolic core) must lie parallel to the electric field of the incident photon. Therefore, from the spectra presented in Figures 4.18-21, it would be assumed that mixtures of compounds **25** and **32** would have more BODIPY transition dipole moments aligned parallel to the incident beam when an electric field is applied to the cell, while the mixture of compound **23** would have slightly less BODIPY transition dipole moments aligned parallel to the incident beam. Due to the negligible change in fluorescence intensity for the mixture of compound **30** neither of these situations can be assumed. In the twisted nematic cell, the long axes of the host molecules lie parallel to the planes of glass that make up the cell (i.e. perpendicular to the incident beam), while the long axes lie perpendicular to the planes of glass when an electric field is applied (i.e. parallel to the incident beam). This is the case for all the host molecules in the cell except for those in close proximity to the rubbed polyimide inner surfaces at the top and bottom of the cavity. The rubbed polyimide surfaces will force some of the BODIPY molecules to align with the host, while those further away from these surfaces will not necessarily align with the host molecules quite so efficiently due to differences in molecular size and shape.

Due to the smaller size of the BODIPY core in compound **23**, it would be expected that the molecules would align with the host material more efficiently. If this is the case, then it would be expected that the fluorescence intensity of compound **23** would decrease when an electric field is applied due to the molecules reorienting themselves perpendicular to the planes of glass in the cell, and thus making the transition dipoles perpendicular to the incident beam. The larger size of the BODIPY core in compounds **25**

and **32** would presumably cause the mesogenic BODIPY molecules to align with the host material less efficiently. This would cause the BODIPY molecules to align non-perpendicular to the planes of glass in the cell when an electric field is applied, meaning more of the transition dipole moments of the fluorophores would align parallel to the incident beam, causing an increase in fluorescence intensity. While both these effects were observed in these experiments, without carrying out further experiments on the dye-doped liquid crystal samples this is not enough evidence to prove this mechanism of molecule alignment definitively.

4.3. Conclusions

The results presented here show that mesogenic BODIPYs can be prepared *via* microwave-assisted palladium catalyzed couplings as well as by 'click' chemistry reactions in reasonable yields. It has been observed that the attachment of large mesogenic units to the fluorophore causes a very slow reaction rate under conventional heating conditions which promoted the use of microwave-assisted heating. Each of the compounds prepared was synthesised *via* more straightforward and higher yielding reactions than the side-attached mesogenic BODIPYs. The resulting mesogenic dipyrrins and BODIPYs displayed varying degrees of fluorescence intensity and nematic phase stability. A monotropic nematic phase was observed in three of the compounds synthesised and an inverse relationship between nematic range and fluorescence intensity was observed. This is due to the fluorescence intensity being attributed to increasing alkyl substitution which causes an increase in the size of the fluorophore, disrupting the molecular packing thereby reducing the nematic range. The linker group between the mesogen and the fluorophore was found to have a profound effect on the nematic stability due to extension of the molecular axis and distorting the molecules linearity. These factors cause a reduction in the nematic phase stability, sometimes to the extent that the nematic phase is eliminated.

Temperature dependant fluorescence measurements were carried out on compound **E** and a noticeable increase in fluorescence intensity was observed upon crystallisation from the

nematic phase. This was attributed to fewer molecular motions causing an increase in the radiative decay rate constant. A dramatic increase in the formation of *J*-dimers was also observed due to the closer proximity of the molecules in the crystalline phase. Four of the BODIPYs prepared were dissolved in a commercial nematic liquid crystal (BL024) and this mixture was incorporated into a twisted nematic cell. A change in fluorescence intensity was observed in three of the mixtures when an electric field was applied to the cell. These changes were attributed to changes in the alignment of the BODIPY transition dipole moments relative to the incident beam. The efficiency of the molecular packing of the mesogenic BODIPYs with the host material significantly affects the alignment of the fluorophores relative to the incident beam. It was hypothesised that BODIPYs with a larger core align with the host material less efficiently due to steric interactions while smaller BODIPY fluorophores align more efficiently due to less significant steric interactions. Due to increasing interest in using BODIPYs as dopants for commercial liquid crystals, several of the mesogenic BODIPYs synthesised in this chapter are currently under investigation as potential laser dyes. This is due to the host material being better able to accommodate a fluorophore of a similar shape.

Chapter 5: BODIPYs bearing multiple mesogenic units

5.1 Introduction

Due to the relatively facile synthetic routes employed for the preparation of mono-mesogenic BODIPYs with the mesogen attached through the 8-position, similar procedures were predicted to enable the preparation of BODIPYs bearing multiple mesogenic units. The BODIPYs bearing liquid crystalline dendrimers reported by Ziessel *et al.* exhibited a short nematic phase or relatively wide smectic A ranges,[230] so it was hypothesised that increasing the number of mesogenic units in smaller molecules could produce a similar effect. As can be seen (Fig. 5.1), the increasing number of mesogenic units (as well as dendrimer size) causes the elimination of the nematic phase due to an increased preference for the more ordered smectic A mesophase.

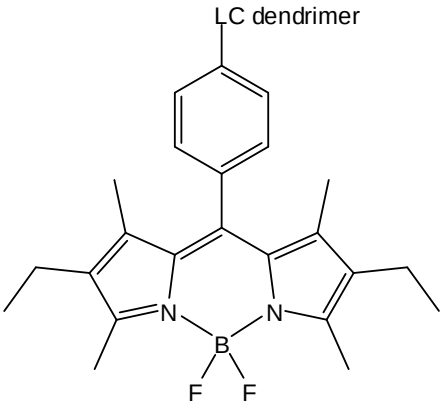

First generation: Cr 86 M 119 N 123 I
Second generation: Cr 100 S_A 155 I
Third generation: Cr 83 S_A 210 I

Figure 5. 1: Liquid crystal dendrimer-BODIPYs showing LC transitions of first, second and third generation dendrimers; m = unknown mesophase[230]

In a similar way to the BODIPYs prepared in the previous chapter, the effect that increasing alkyl substitution has on the fluorescence intensity and liquid crystallinity of the molecules was investigated. The increasing alkyl substitution of the BODIPY core was expected to display a similar effect on the fluorescence intensity and liquid crystalline properties. In each series of compounds the linker groups remained constant

and two mesogens of a similar type (both containing a cyanobiphenyl unit but with one a stronger mesogen – see Chapter 3 for a comparison of their liquid crystalline behaviour) were employed. Palladium-catalyzed coupling was also employed due to the successful reactions detailed in the previous chapter.

Due to the unsuccessful preparation of a red-shifted BODIPY from the previously synthesised diindolylmethane, an alternative route to a red-shifted BODIPY was also sought. The generally accepted method of producing a bathochromic shift in the fluorescence of a BODIPY is to extend the π-conjugate system. This has been achieved by several methods but the most facile and generally applicable appears to the attachment of styryl groups to the 3- and 5-methyl groups *via* a Knoevenagel condensation. This reaction has been used in the preparation of pH sensors,[87, 90] ion probes[234, 266-268] and even PDT.[255] By selection of an appropriate reagent for the condensation, additional sites for mesogen attachment can be incorporated on to the BODIPY while also providing the desired bathochromic shift in fluorescence.

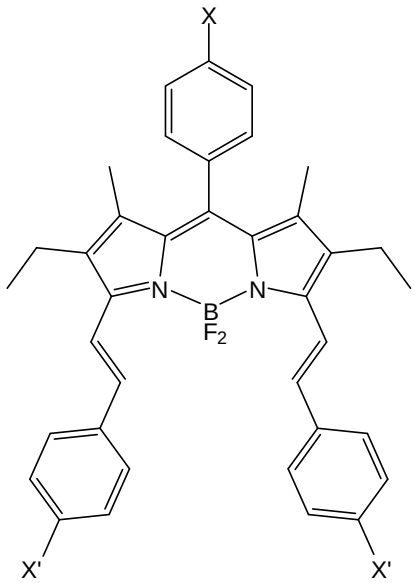

Figure 5. 2: Styryl-BODIPY exhibiting red-shifted fluorescence

5.2 Results and discussion

5.2.1 Synthesis

As palladium-catalyzed reactions were to be used as the method of mesogen attachment, 3,5-dibromobenzaldehyde was chosen as the precursor to the three BODIPYs to which the mesogens would be attached (Sch. 5.1). These three BODIPYs were prepared using the accepted methodology[35, 264] in 29%, 7% and 13% yields for **47**, **48** and **49** respectively. Yields for the BODIPYs bearing alkyl substituents were found to be lower than that of the unsubstituted BODIPY. While chloranil was used for the oxidation step to produce **47**, DDQ was used to oxidise **48** and **49** which may have caused partial decomposition of the dipyrrin intermediate due to DDQ being a stronger oxidant. The mesogens employed were reacted with 4-carboxyphenylboronic acid pinacol ester in preparation for attachment *via* Suzuki coupling.

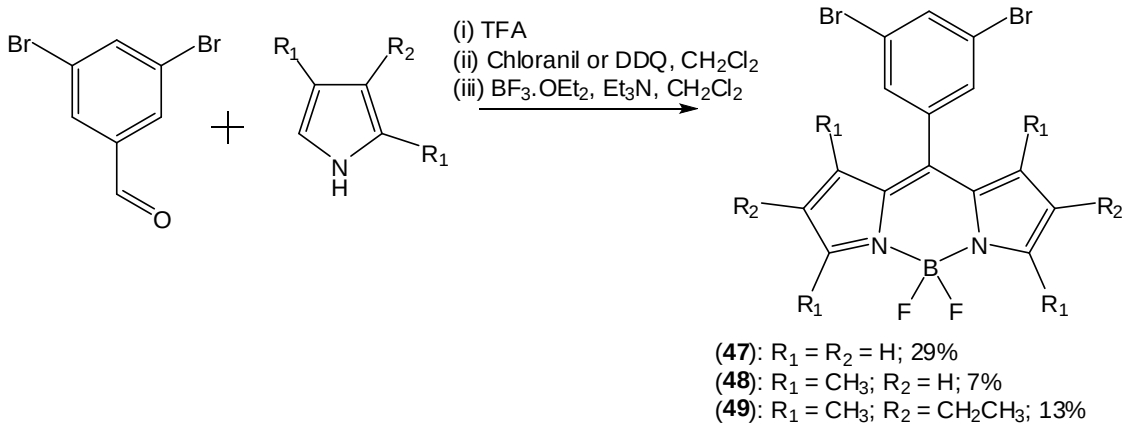

Scheme 5. 1: Dibromo-BODIPY synthesis

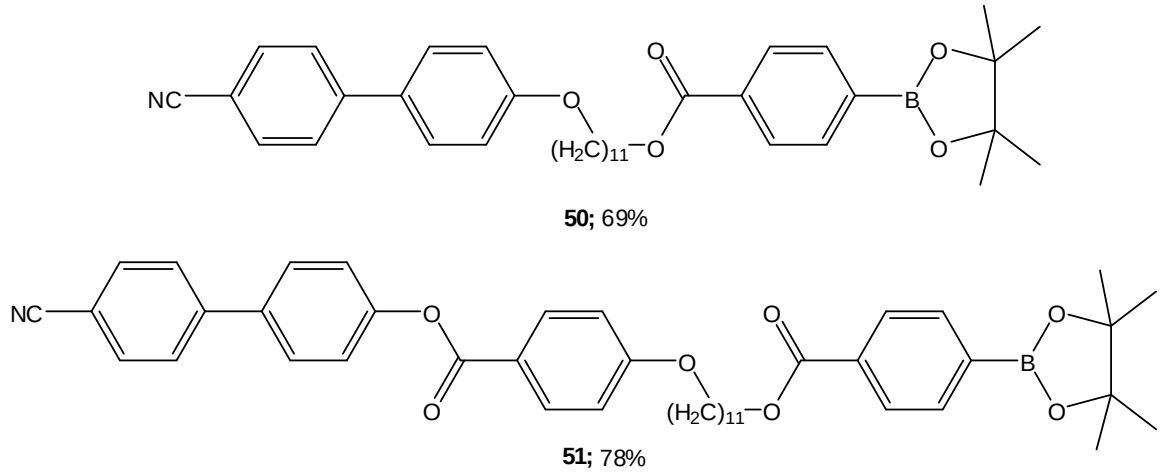

Figure 5. 3: Mesogenic boronic esters for Suzuki-coupling onto dibromo-BODIPYs

The Suzuki coupling was carried out using the same conditions as for the previous Suzuki couplings albeit with greater proportions of mesogen, catalyst, base and phosphine ligand (Sch. 5.2). Similarly to the mono-mesogenic BODIPYs, purification was achieved using column chromatography (eluting with toluene:EtOAc mixtures) followed by precipitation from dichloromethane with cold methanol to yield the pure product. Yields for the reactions were moderate, ranging from 25-69%, with compounds **53** and **56** being isolated in surprisingly low yields. The presence of alkyl groups on the BODIPY core should promote higher yields due to lower by-product formation (which is the case for compounds **54** and **57**).

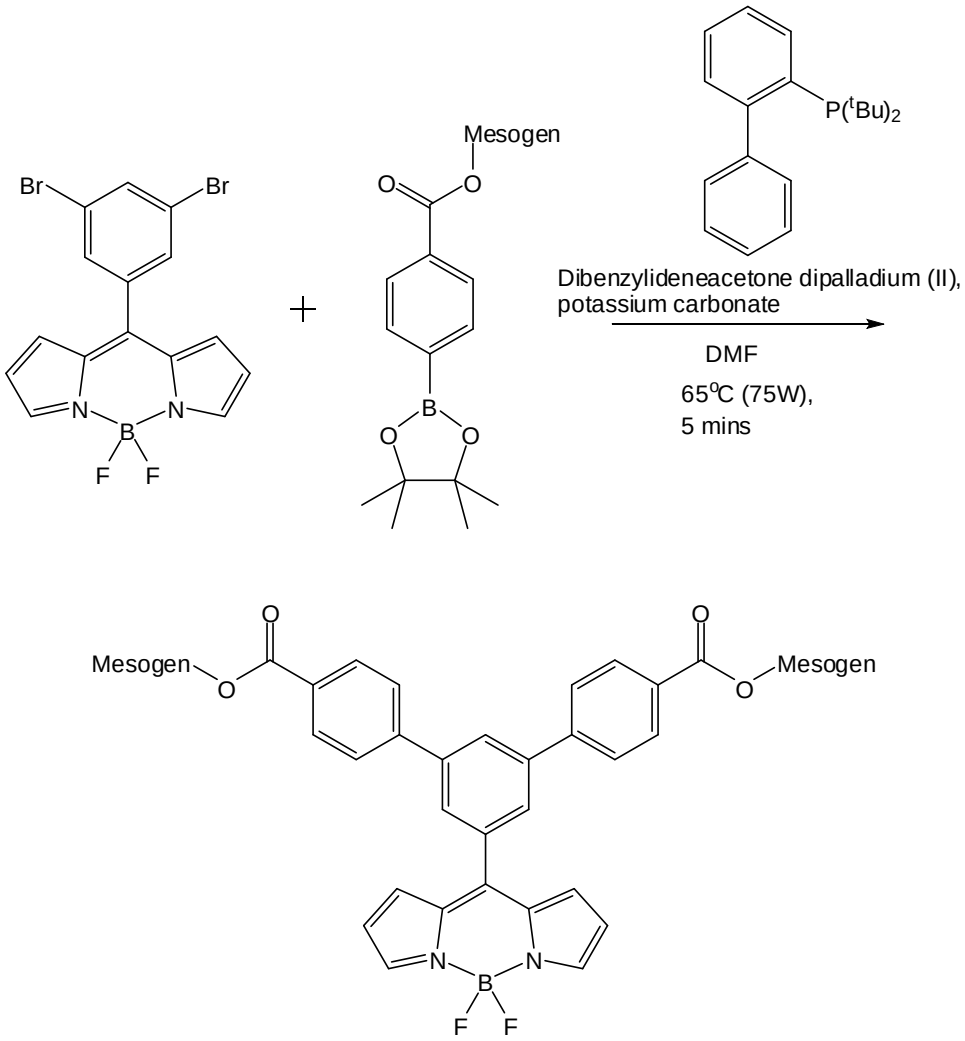

Scheme 5. 2: Suzuki-coupling of two mesogenic units onto a BODIPY

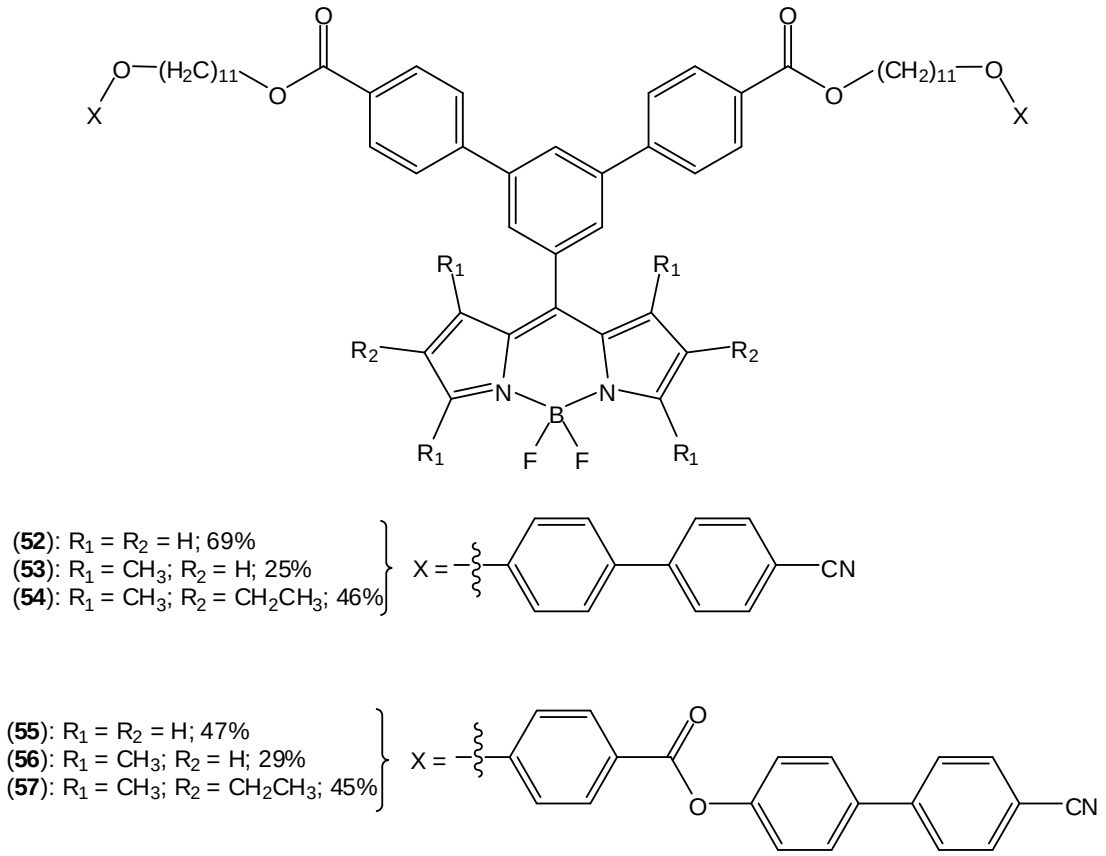

Figure 5. 4: Di-mesogenic BODIPYs 53-58

The ^{1}H-NMR spectra of these compounds were relatively similar to those of the mono-mesogenic BODIPYs aside from the respective integrals and the presence of a 1,3,5-trisubstituted phenyl ring (not always visible amongst other aromatic peaks). Inspection of the aromatic region of the ^{1}H-NMR of compound **55** shows the presence of two multiplets due to overlaying phenyl peaks, as well as distinct doublets and the clearly visible 1,3,5-trisubstituted signals arising from the presence of the ring protons (Fig. 5.5).

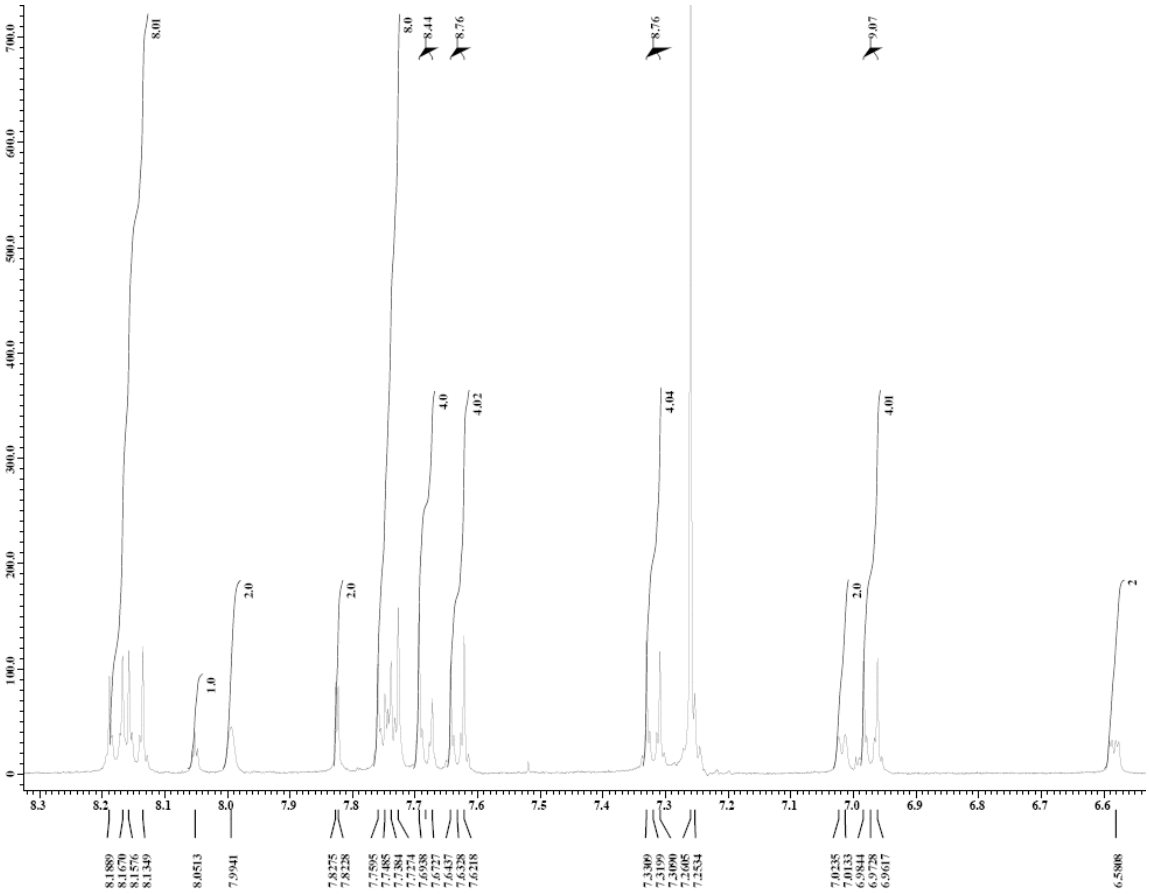

Figure 5. 5: Aromatic region of the ^{1}H-NMR spectrum of 55

In order to prepare a BODIPY with a red-shifted fluorescence and with the capacity for several functional groups to be attached, attempts were made to synthesise an aza-BODIPY. This class of molecule has been shown to display remarkably red-shifted fluorescence due to the four aromatic moieties and the bridging nitrogen as seen in phthalocyanines.[248, 269-272] Aza-BODIPYs are prepared from the reaction of benzaldehydes and acetophenones to form chalcones which are then nitrated. These nitrated chalcones are then reacted with a large excess of ammonium acetate to yield the aza-dipyrrin, to which the boron trifluoro group is coordinated.

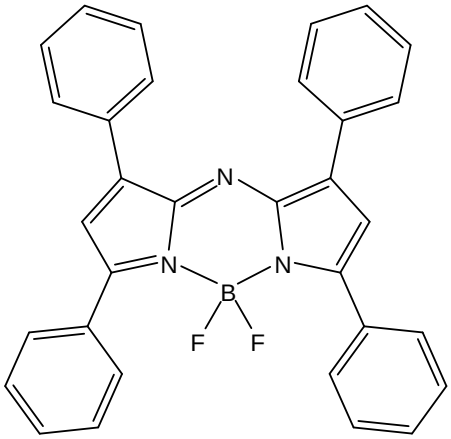

Figure 5. 6: Aza-BODIPY

Due to the success of the palladium-catalyzed reactions employed in the attachment of mesogenic units to BODIPYs, attempts were made to synthesise an aza-BODIPY bearing bromo- or iodo-groups (Sch. 5.3). Firstly, 4-bromoacetophenone was reacted with benzaldehyde in the presence of potassium hydroxide to yield the corresponding chalcone (**58**) in 67% yield. Purification of this compound was achieved using recrystallisation from ethanol. The chalcone was then nitrated (**59**) using methyl nitrate in the presence of diethylamine and purified by recrystallisation from methanol in 69% yield. Synthesis of the aza-dipyrrin was then achieved *via* reaction of the nitrated chalcone with 35 eq. of ammonium acetate in refluxing ethanol. Upon cooling, the product precipitated out as a blue/black solid which was washed with ethanol. Due to the very low solubility of the aza-dipyrrin in ordinary or deuterated solvents (chloroform, acetone, THF, methanol, dichloromethane, DMF, DMSO), NMR experiments could not be carried out. The same problem occurred when attempting to dissolve the subsequent aza-BODIPY for purification by column chromatography and NMR experiments. An iodo- and tetra-bromo analogue (a bromo substituent on the 4-position of each phenyl ring) were also prepared but the same solubility issues were encountered.

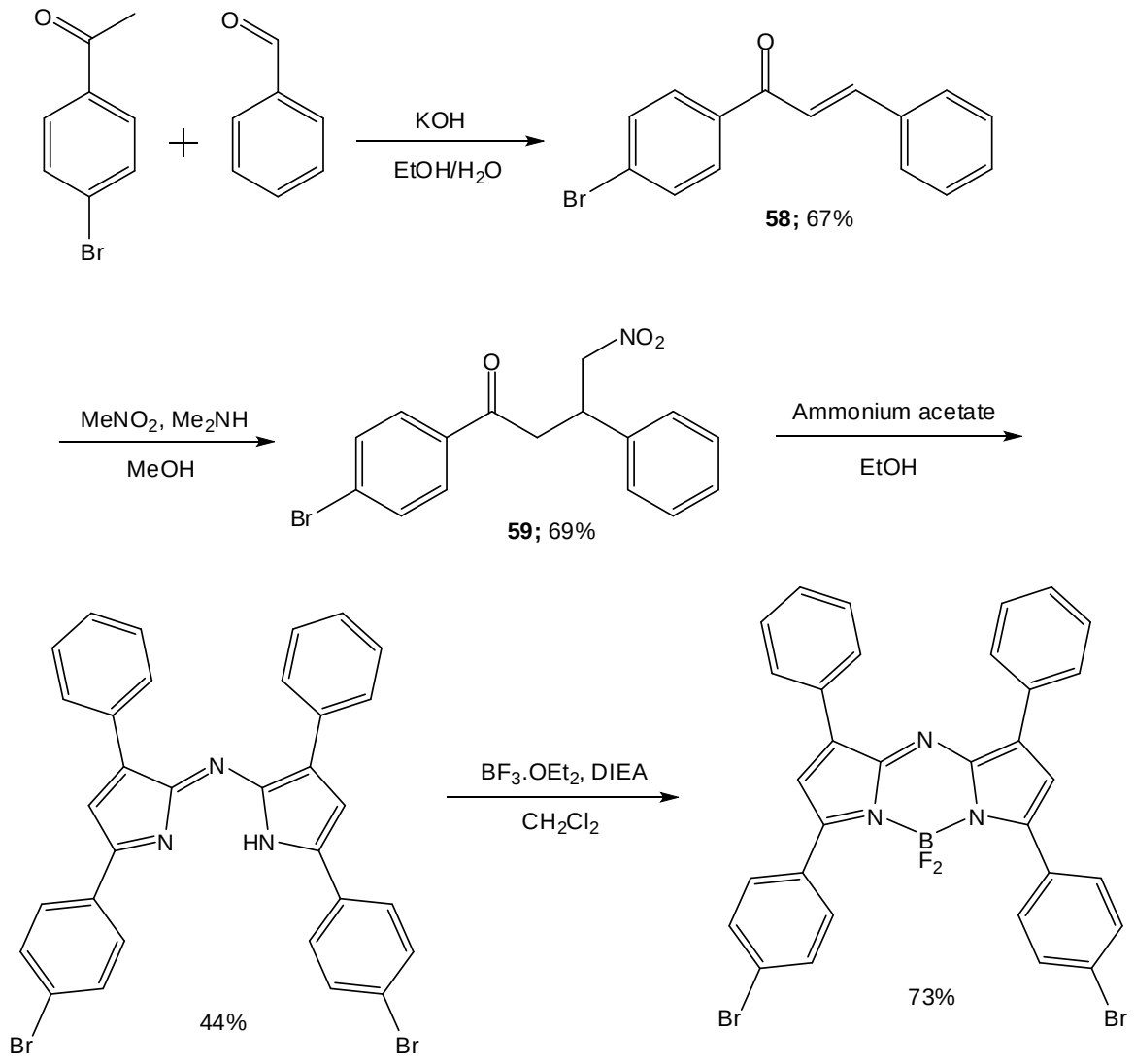

Scheme 5. 3: Dibromo-aza-BODIPY synthesis

In order to circumvent the solubility problems encountered with the aza-dipyrrins and aza-BODIPYs bearing halide substituents, an aza-BODIPY with hydroxyl functionalities was prepared (Sch. 5.4). The chalcone (**60**) was prepared by an acid-catalyzed condensation due to the presence of the acidic phenolic hydroxyl group. The reaction was carried out using concentrated sulphuric acid and the product precipitated out of solution upon cooling. Purification was achieved by recrystallisation from ethanol to yield the product in 57% yield. The nitration was carried out using the same conditions as the halide containing chalcones but upon removal of the solvent, crystallisation did not occur and a tan coloured oil was isolated. This oil was carried through to the aza-dipyrrin (**61**)

synthesis, as purification could be achieved by precipitation. Butan-1-ol was used as the solvent for the aza-dipyrrin synthesis due to its higher boiling point. The product was soluble enough for identification *via* ^{1}H-NMR spectroscopic analysis, but too insoluble for an adequate ^{13}C-NMR spectrum to be obtained. Complexation of the boron difluoro unit was carried out under the same conditions as the previous BODIPY syntheses, with the product (**62**) being soluble enough for column chromatography and ^{1}H-NMR (Fig. 5.7) and ^{13}C-NMR experiments to be carried out. The aza-BODIPY was isolated in 55% yield from the aza-dipyrrin. Unlike the previously synthesised BODIPYs, no obvious colour change was observed upon complexation to give the boron difluoro derivative.

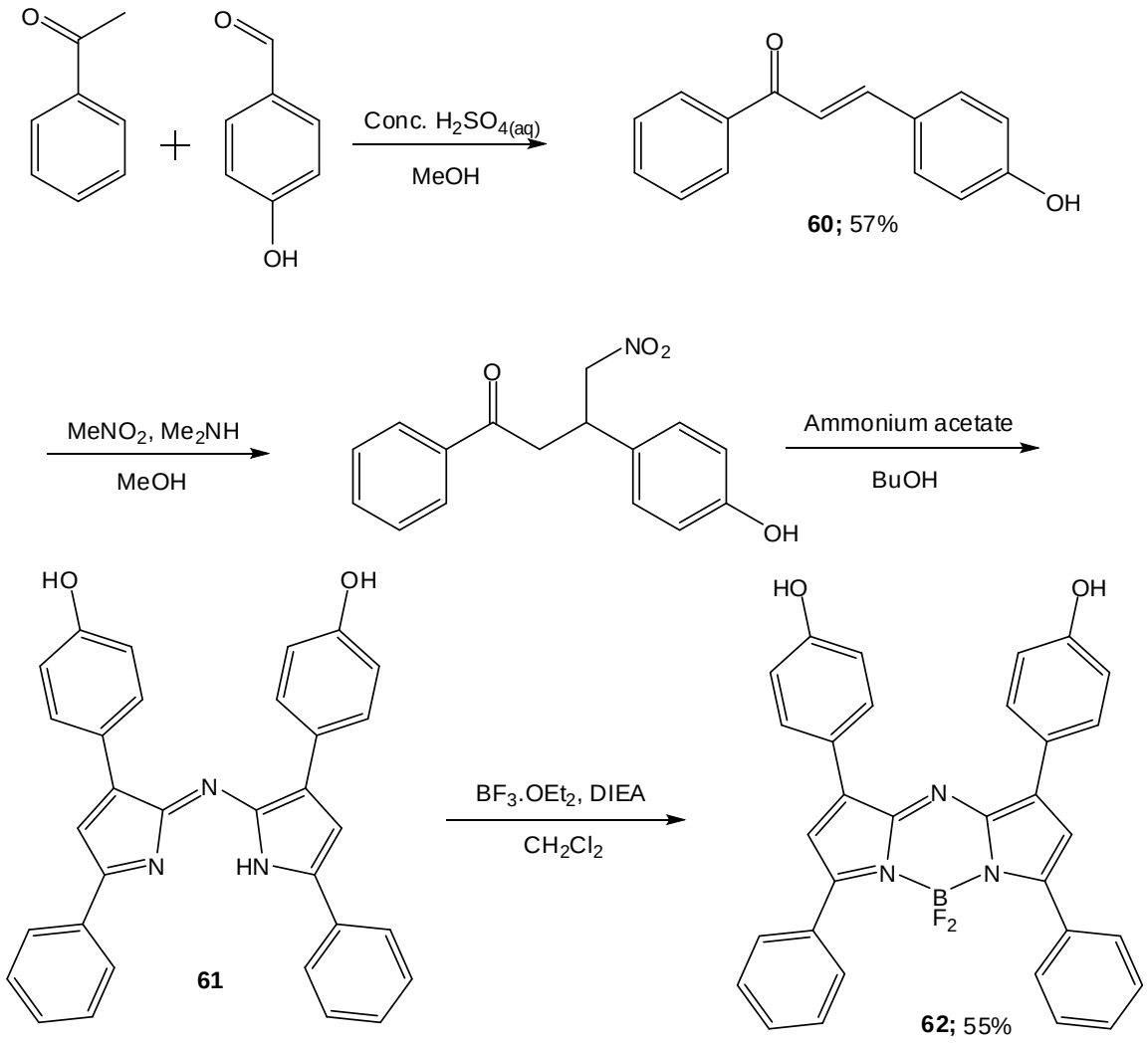

Scheme 5. 4: Dihydroxy-aza-BODIPY synthesis

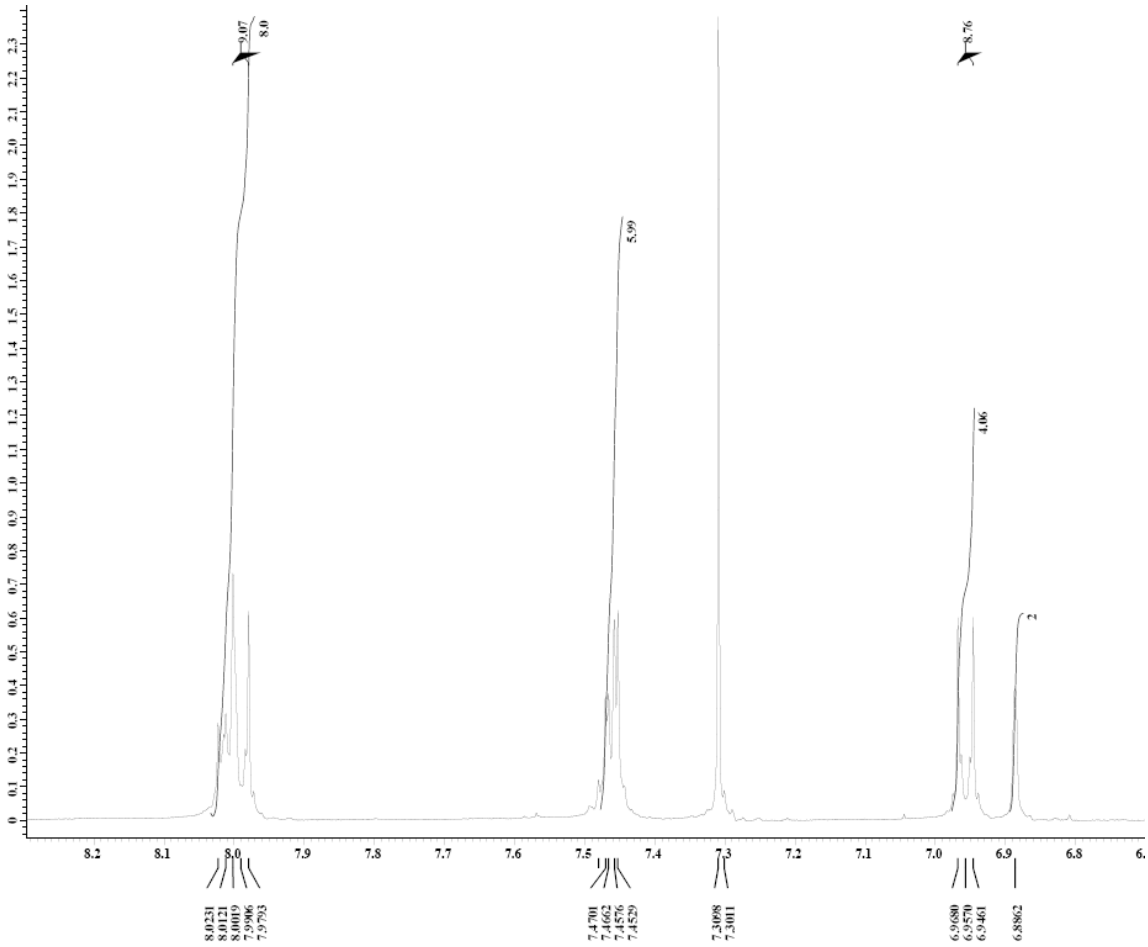

Figure 5. 7: Aromatic region of the ^{1}H-NMR spectrum of 62

While the solubility problems of the aza-BODIPY were overcome, carrying out successful reactions on the hydroxyl groups proved to be more problematic. Carbodiimide couplings and Mitsunobu reactions using both carboxylic acids and alcohols were attempted, but a large amount of decomposition occurred and no product formation was observed. Several different reagent combinations were attempted (DCC, DIC, EDC, DEAD, ADDP) but each reaction produced the same result. An etherification was achieved *via* a Williamson ether synthesis using benzyl bromide in the presence of potassium carbonate and potassium iodide (Sch. 5.5) but was found to be unsuccessful when using an aliphatic halide despite using a stronger base (NaH). Due to the restrictive nature of using benzyl halides to attach mesogens to the aza-BODIPY *via* Williamson ether syntheses, this avenue of investigation was abandoned.

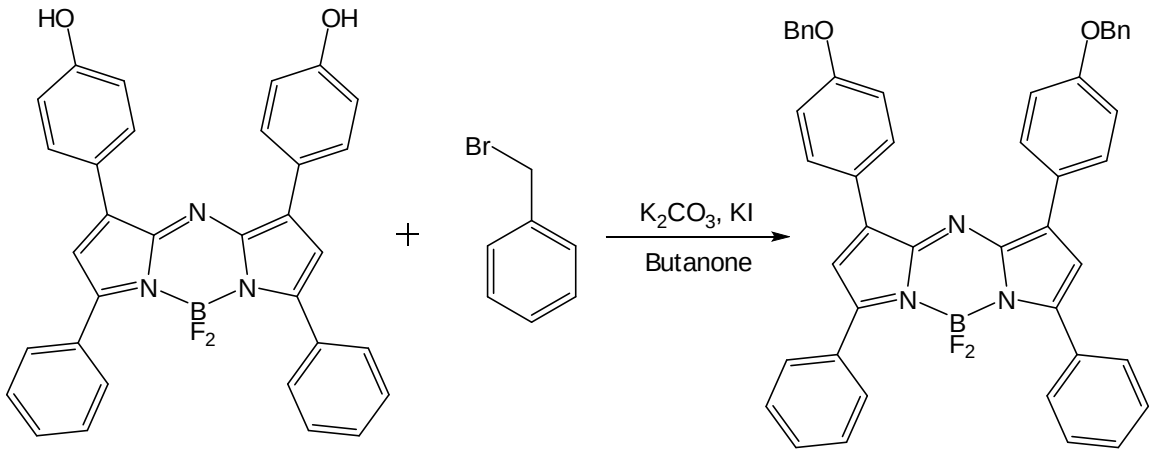

Scheme 5. 5: Aza-BODIPY ether synthesis

Due to the unsuccessful attempt to synthesise a BODIPY exhibiting red-shifted fluorescence from a diindolylmethane or an aza-BODIPY, an effort was made to extend the BODIPY π-conjugate system by the attachment of styryl groups. This was achieved by reacting **20** with 4-hydroxybenzaldehyde in the presence of piperidine, glacial acetic acid and a catalytic amount of magnesium perchlorate in dry toluene (Sch. 5.6). Molecular sieves were added to bind the water molecules produced during the condensation. Purification was achieved using column chromatography followed by washing with hexane. In order to facilitate the attachment of the more extended mesogen, the condensation reaction was attempted with methyl-4-formyl benzoate (for attachment by carbodiimide coupling) and 4-iodobenzaldehyde (for attachment by palladium-catalyzed coupling) but both were found to be unsuccessful despite promising initial thin layer chromatography analysis. It was found that both product and starting material decomposed rapidly when piperidine was used without the acetic acid. However, the reaction was found not to proceed when both piperidine and acetic acid were used despite the electron withdrawing groups present on the benzaldehyde. An attempt was made using DBU as the base in an effort to increase the rate of reaction, but this was again found to be unsuccessful. Due to the fact that styryl-BODIPYs had previously been prepared using benzaldehyde bearing a functional group with a delocalised lone pair of electrons (e.g. *N,N'*-dimethylamine[87, 90]), 4-hydroxybenzaldehyde was chosen as the co-reagent. This also offered the opportunity for mesogens to be attached *via* a Williamson

ether synthesis using the phenolic groups. The reaction was carried out over 3 days using five molar equivalents of 4-hydroxybenzaldehyde in order to acquire the di-styryl-BODIPY (**63**) as the major product. A small amount of the mono-substituted compound was isolated, but no subsequent reactions were carried out on it as it was presumed that the attachment of two mesogens (one on each hydroxyl group) would cause the molecule to have a greater tendency for liquid crystalline behaviour.

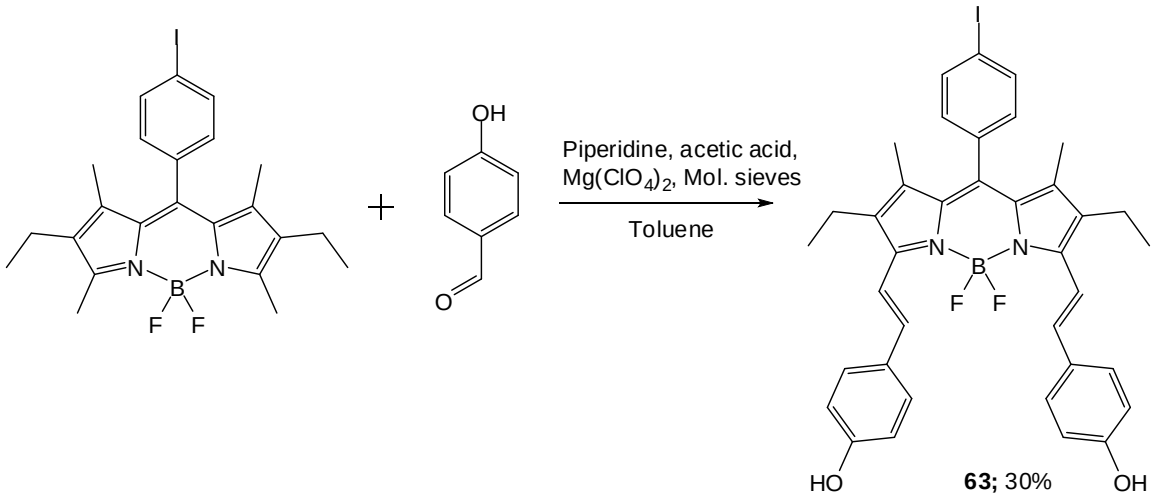

Scheme 5. 6: Di-styryl-BODIPY synthesis

The mesogens were then reacted with the di-styryl-BODIPY under Williamson ether synthesis conditions (potassium carbonate) to yield the di-mesogenic product (**64**) after 2 days in moderate yield (Sch. 5.7). The presence of the desired product was indicated by a dramatic increase in R_f on a thin layer chromatography plate. Purification was achieved by column chromatography eluting in a THF:hexane mixture followed by washing the resulting solid with cold acetone, hexane and methanol.

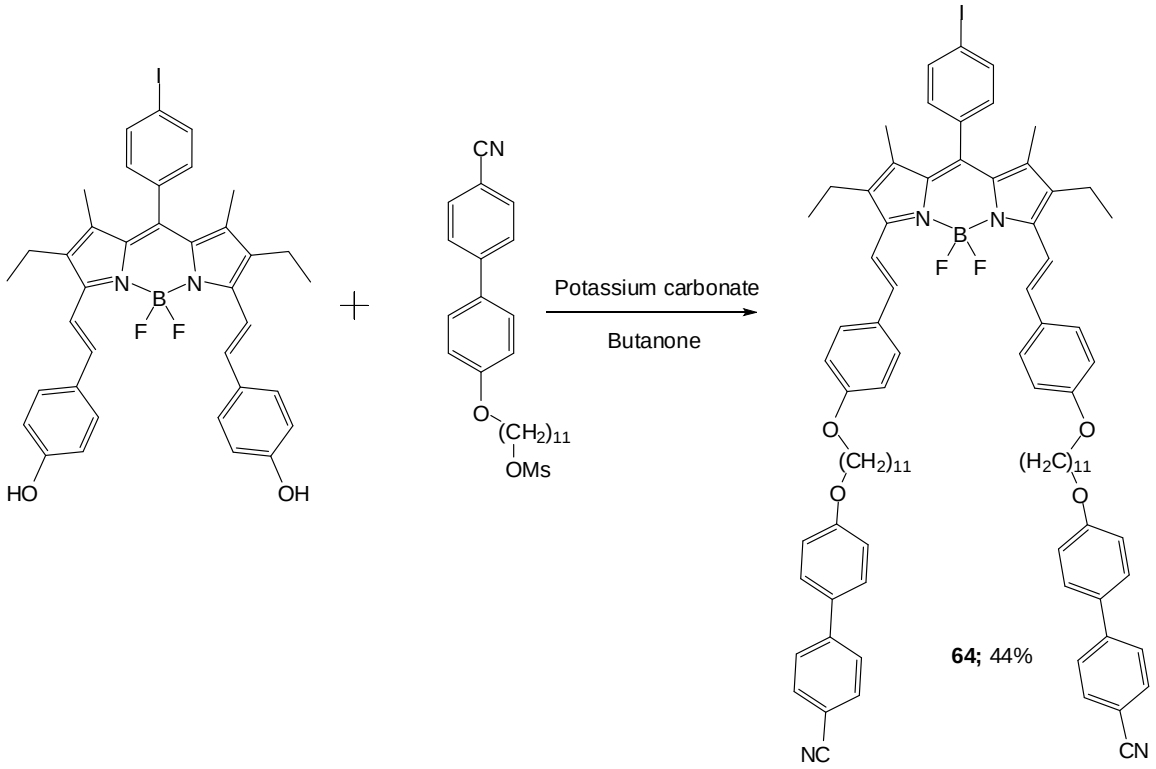

Scheme 5. 7: Di-mesogenic di-styryl-BODIPY synthesis

The resulting di-mesogenic BODIPY (**64**) was readily soluble in deuterated chloroform so an accurate ^{1}H-NMR could be obtained. The alkyl region showed the BODIPY methyl and ethyl groups as well as the mesogen alkyl chains (Fig. 5.8). The triplet at ~4.0 ppm corresponds to the methylene units adjacent to the oxygen atoms. The aromatic region shows several well-defined doublets along with some overlapped multiplets (Fig. 5.9). The doublet at 7.20 ppm corresponds to the alkenic protons however; the second alkenic doublet appears to align with one of the multiplets between 7.6 and 7.7 ppm. The 4-iodophenyl doublets are observed quite clearly despite a wide separation.

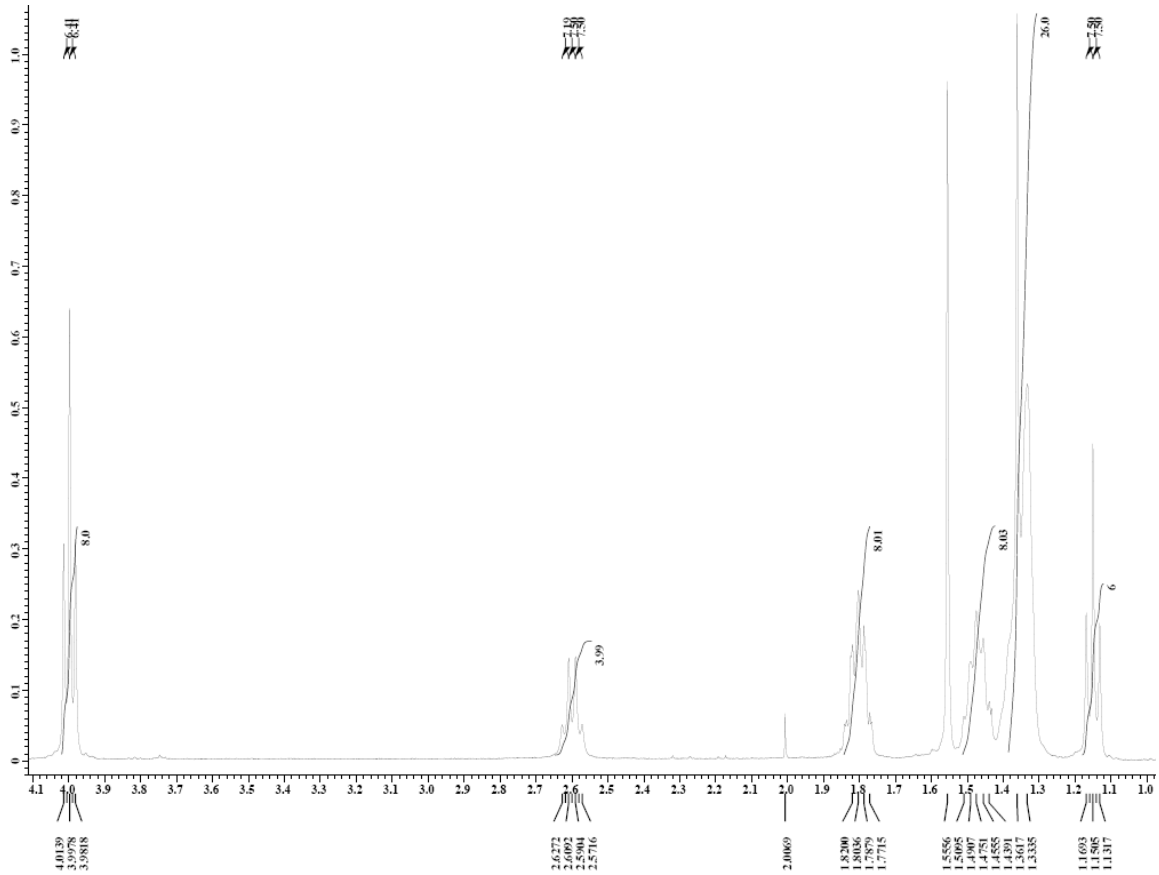

Figure 5. 8: Alkyl region of the ^{1}H-NMR spectrum of 64

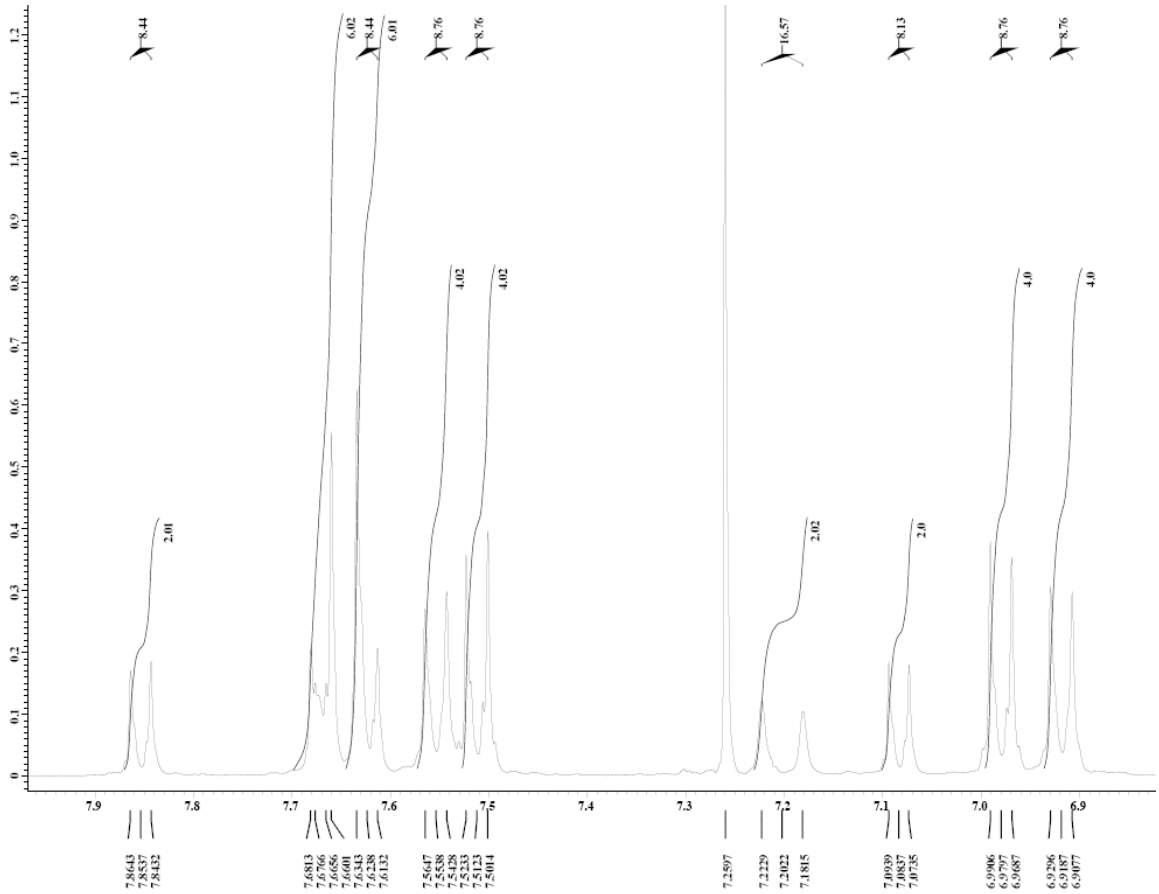

Figure 5. 9: Aromatic region of the ^{1}H-NMR spectrum of 64

Attachment of a third mesogen was achieved *via* Suzuki coupling of phenyl iodide in the 8-position under similar conditions to the previous Suzuki couplings (**65**) (see previous chapter) (Sch. 5.8). However, due to the increased size of this molecule compared to the previous mesogenic BODIPYs the reaction was carried out for ten minutes instead of five minutes. This is due to some of the unreacted starting material still being present after five minutes microwave heating (determined by TLC analysis). Purification was achieved using column chromatography eluting with a dichloromethane:hexane mixture followed by precipitation from dichloromethane with cold methanol. The yield for this reaction was moderate despite the size of the fluorophore and mesogenic components.

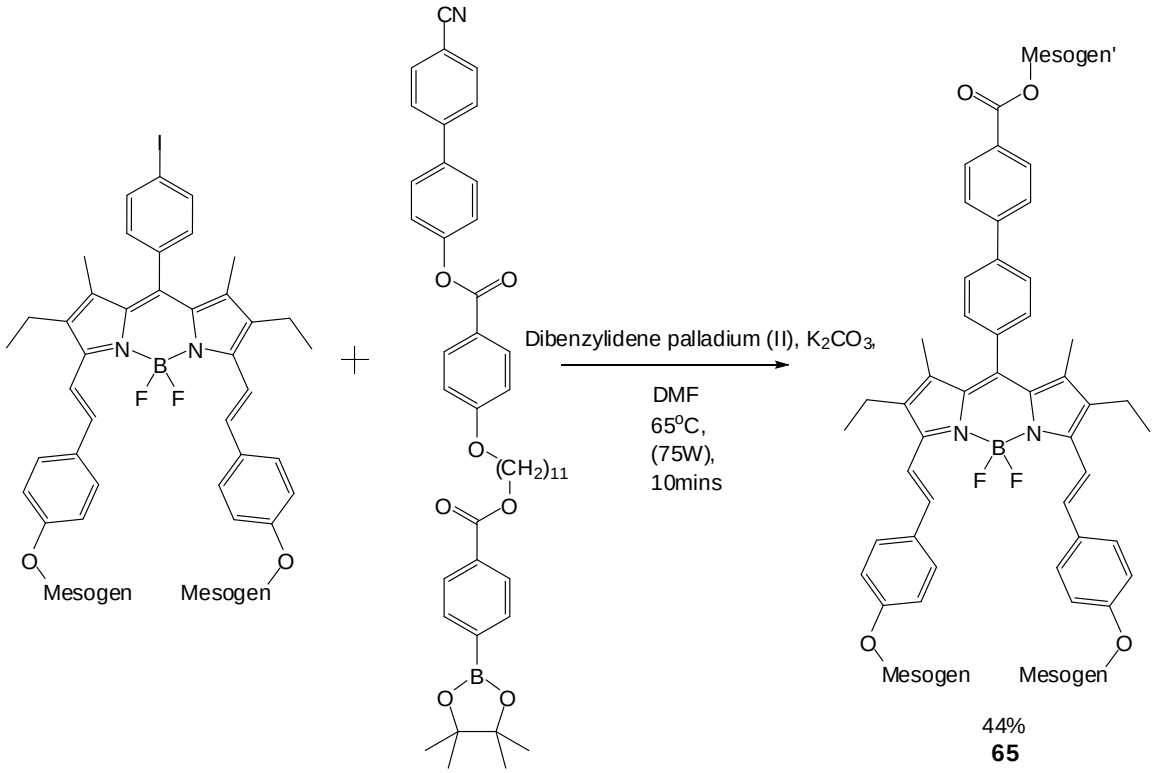

Scheme 5. 8: Tri-mesogenic di-styryl BODIPY (65)

This compound was only sparingly soluble in deuterated solvents with chloroform being used to carry out the NMR experiments. Due to this sparing solubility, ^{13}C-NMR was difficult to obtain and only ^{1}H-NMR was acquired. The alkyl region of this spectrum was straightforward to assign due to little overlap of the relevant peaks (Fig. 5.10). The triplets corresponding to the end methylene units of the two mesogens attached to the styryl groups were found to overlap but not quite to the same degree as in Fig. 5.8 (Fig. 5.11). A large amount of overlap was observed in the aromatic region due to the large number of aromatic groups in addition to the alkenic protons (Fig. 5.12 and 5.13). This made assignment of the individual peaks difficult (other than one alkene doublet); however, the integrals amount to the correct number of protons.

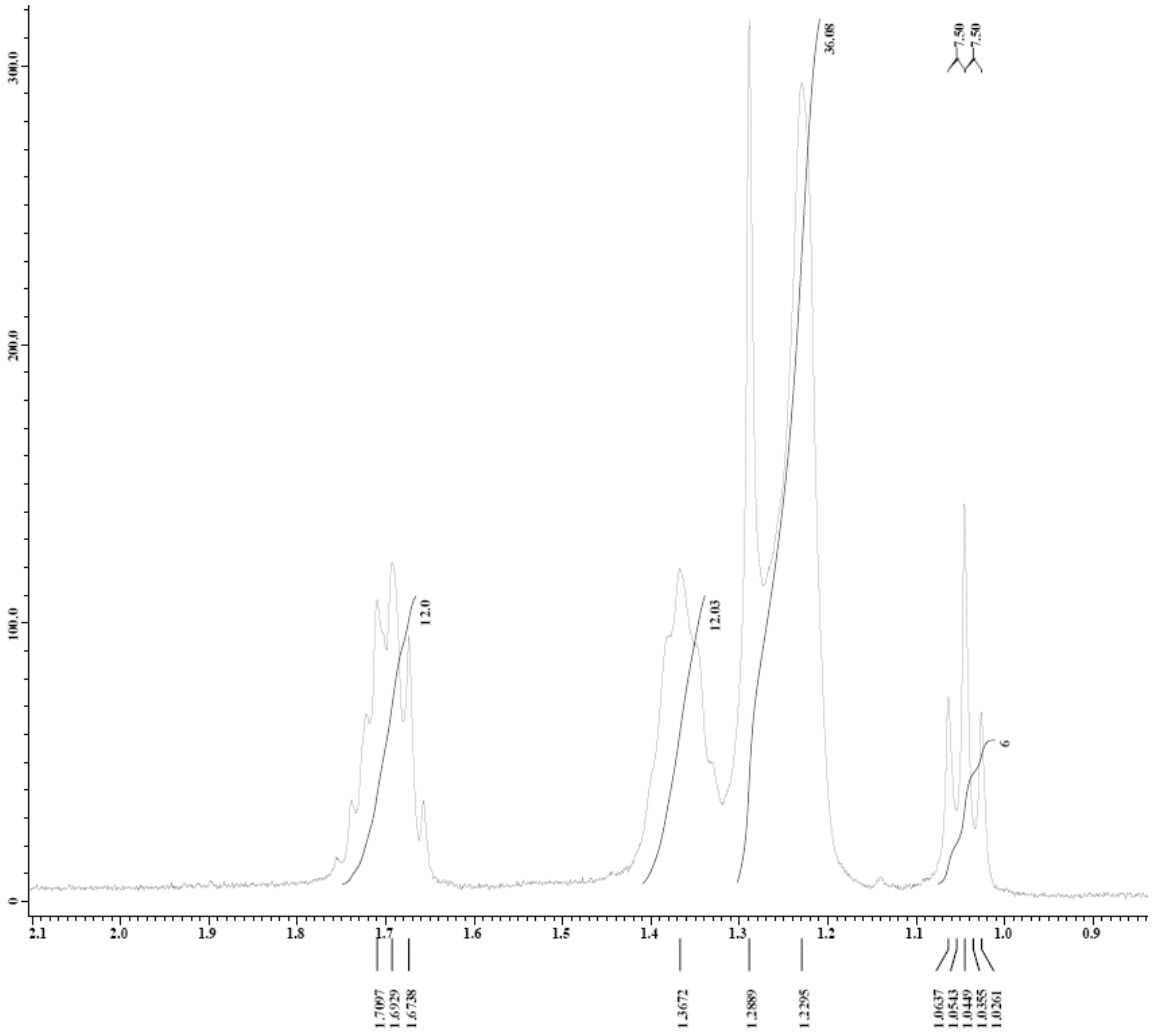

Figure 5. 10: Alkyl region of the ^{1}H-NMR spectrum of 65

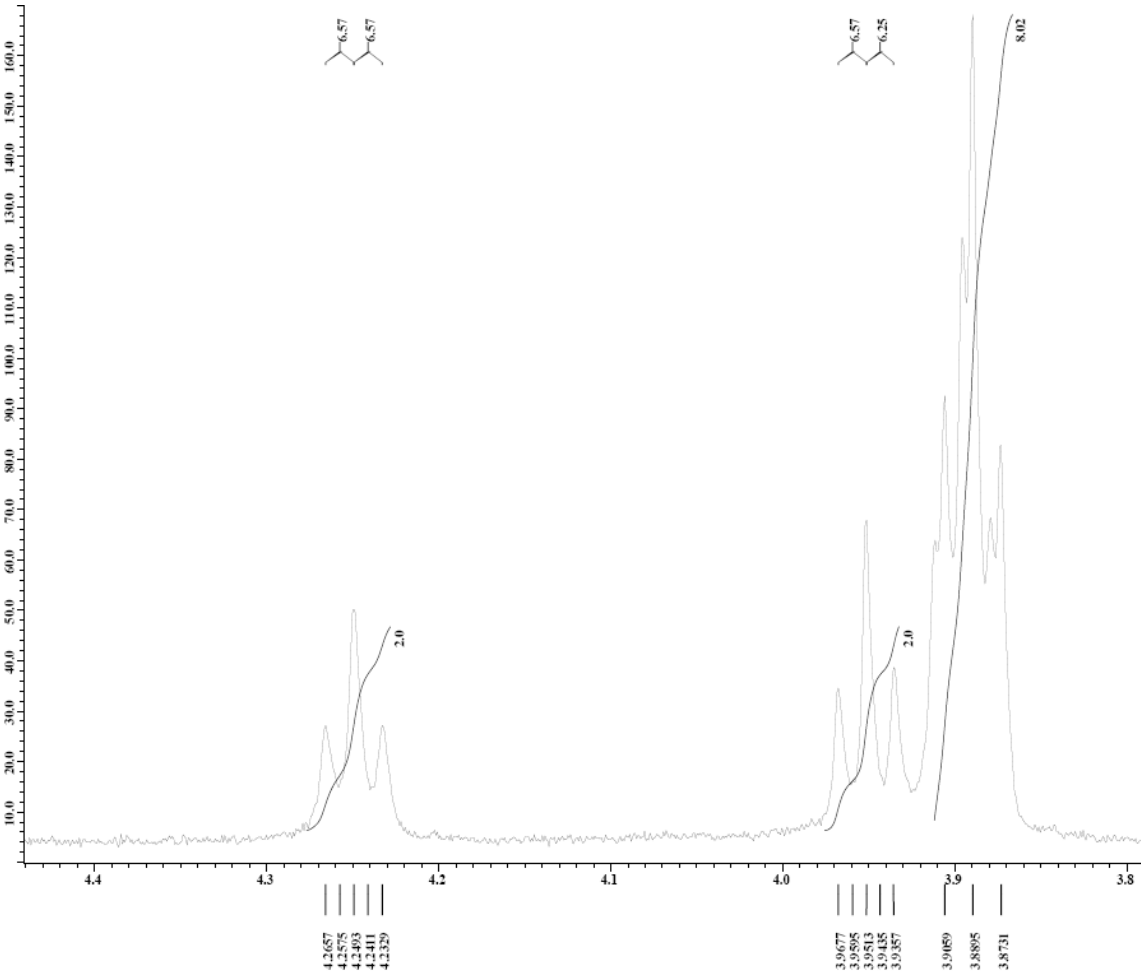

Figure 5. 11: ^{1}H-NMR spectrum displaying the methylene units of the C_{11} alkyl chains of 65

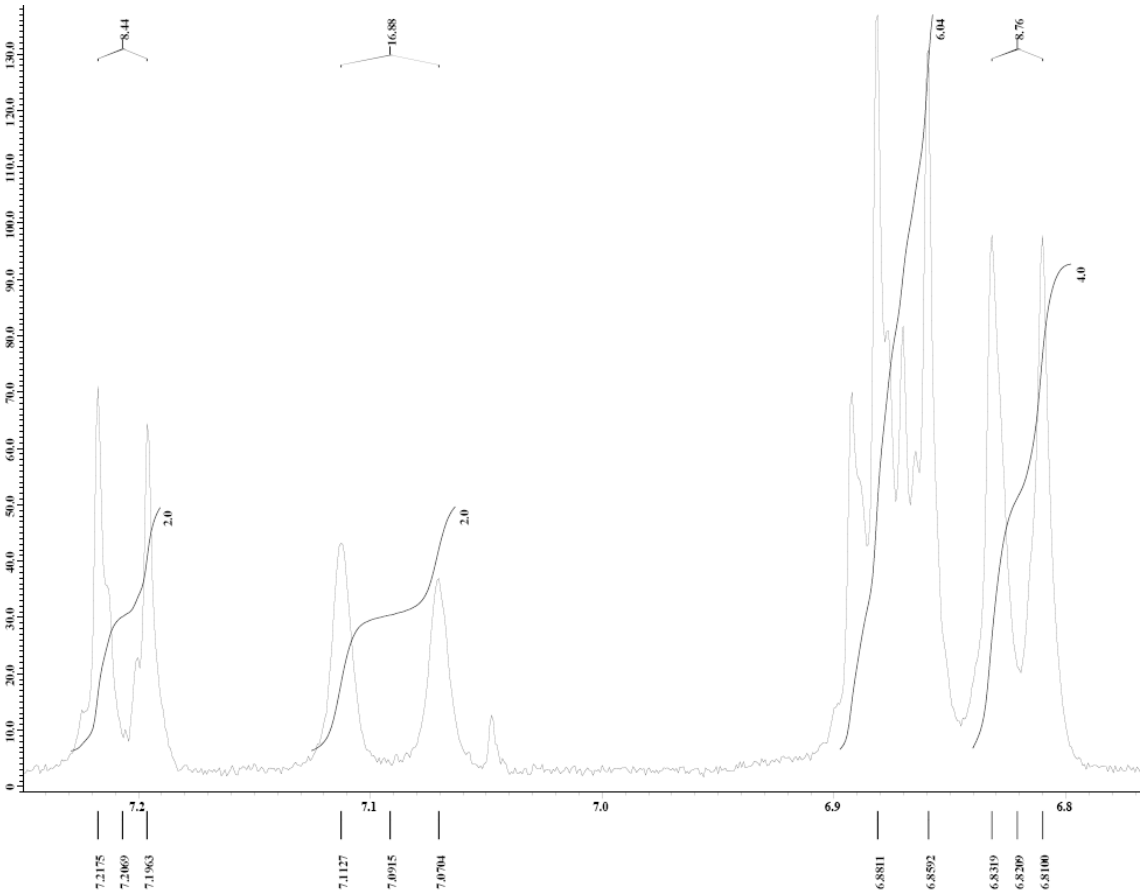

Figure 5. 12: Aromatic region of the ^{1}H-NMR spectrum of 65

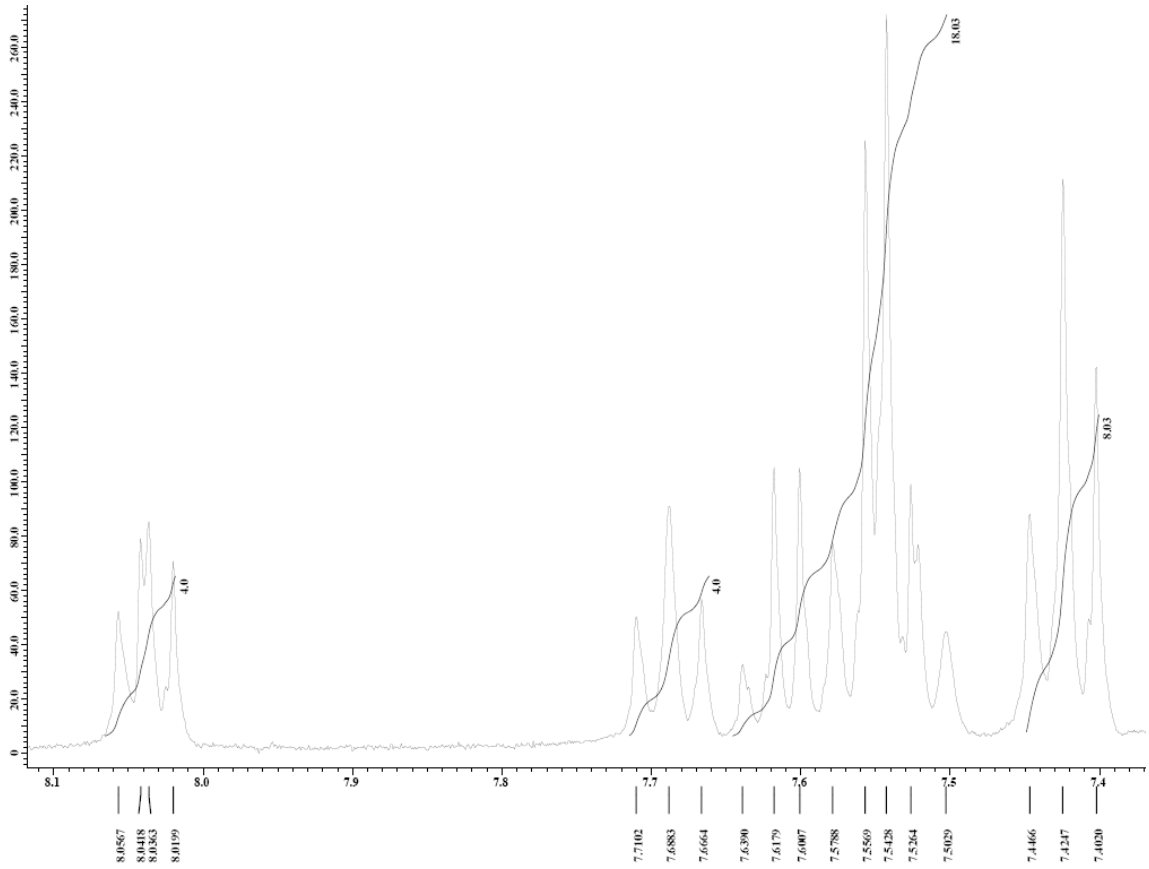

Figure 5. 13: Aromatic region of the ^{1}H-NMR spectrum of 65

5.2.2 Liquid crystal properties

Mesogenic BODIPYs **55-57** exhibited monotropic nematic phases. Mesogenic BODIPYs **52-54** did not display any mesophase formation due to the mesogenic unit not being nematogenic enough to confer liquid crystalline behaviour on the fluorophore. Despite the appearance of the DSC curves, the nematic phases exhibited in compounds **55-57** were monotropic as the mesophase was not observed upon the first heating cycle (Fig. 5.14, 5.15 and 5.16). These compounds display relatively wide nematic ranges compared to the mono-mesogenic BODIPYs due to the presence of an additional mesogenic unit. This additional mesogenic unit causes a stabilisation of the mesophase while also preventing crystallisation with a glass transition being observed instead (shallow peaks on the DSC curves between 55-75°C).

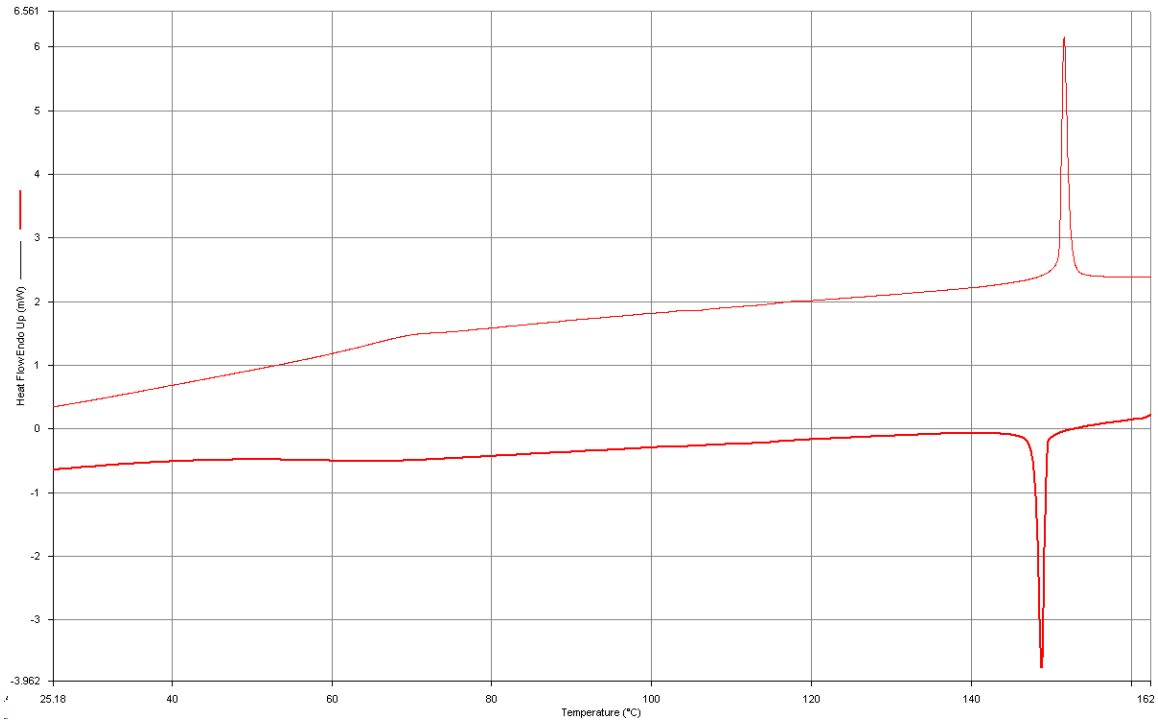

Figure 5. 14: DSC thermogram of 55; showing second heat (top line) and second cool (bottom line)

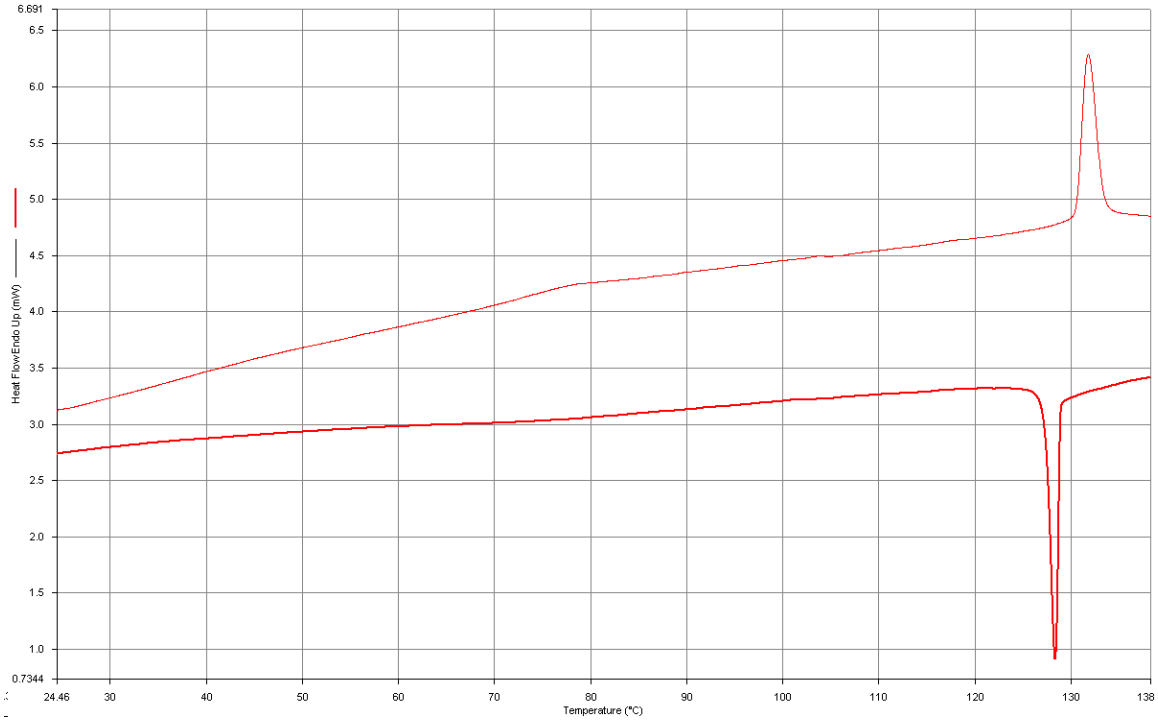

Figure 5. 15: DSC thermogram of 56; showing second heat (top line) and second cool (bottom line)

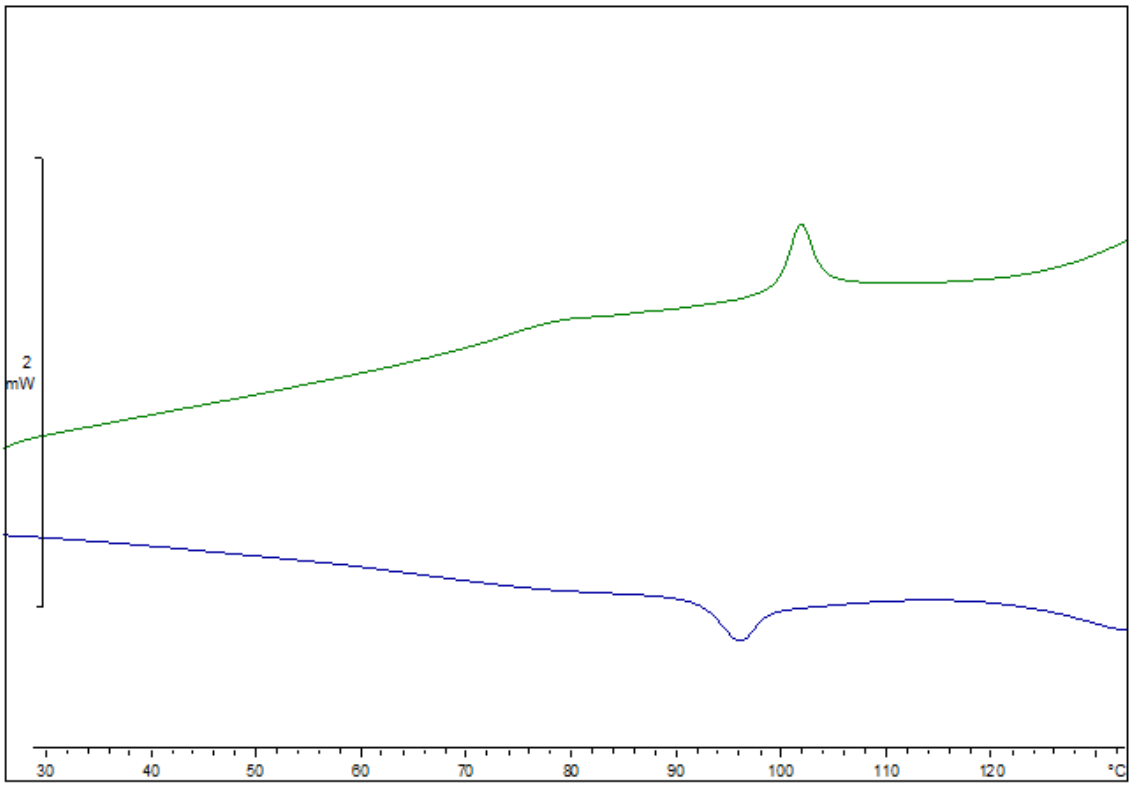

Figure 5. 16: DSC thermogram of 57; showing second heat (top line) and second cool (bottom line)

The OPM images for compounds **55** and **56** display a Schlieren texture which formed very slowly due to the high viscosity of the compounds in the isotropic liquid and nematic phases. Initially, the phase was observed as droplets of nematic texture showing four-brush disclinations (Fig. 5.17). After annealing the texture was less droplet-like and was more easily visible (Fig. 5.18). As in the mono-mesogenic BODIPYs, the orange colour is due to the colour of the compounds themselves and not due to a birefringent effect.

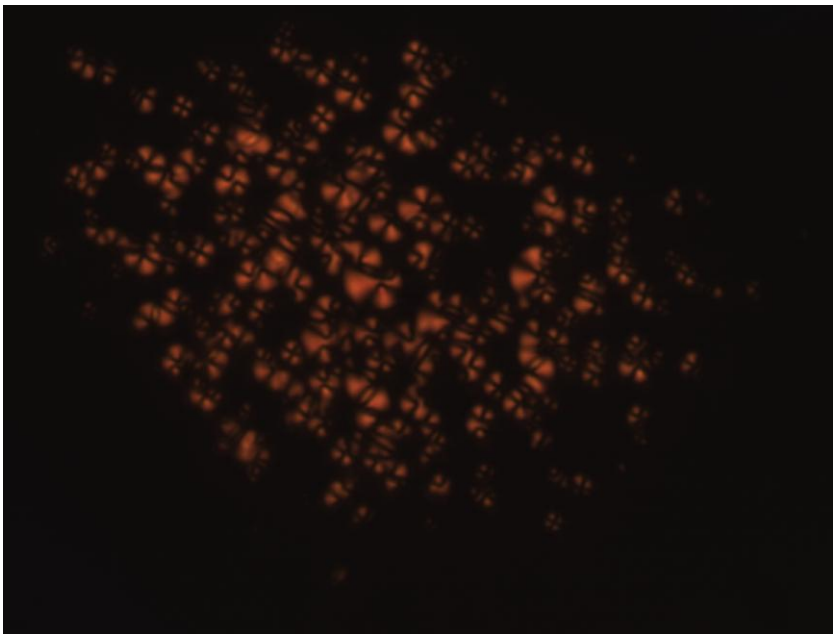

Figure 5. 17: OPM image of 55 in the nematic phase at 138.4°C

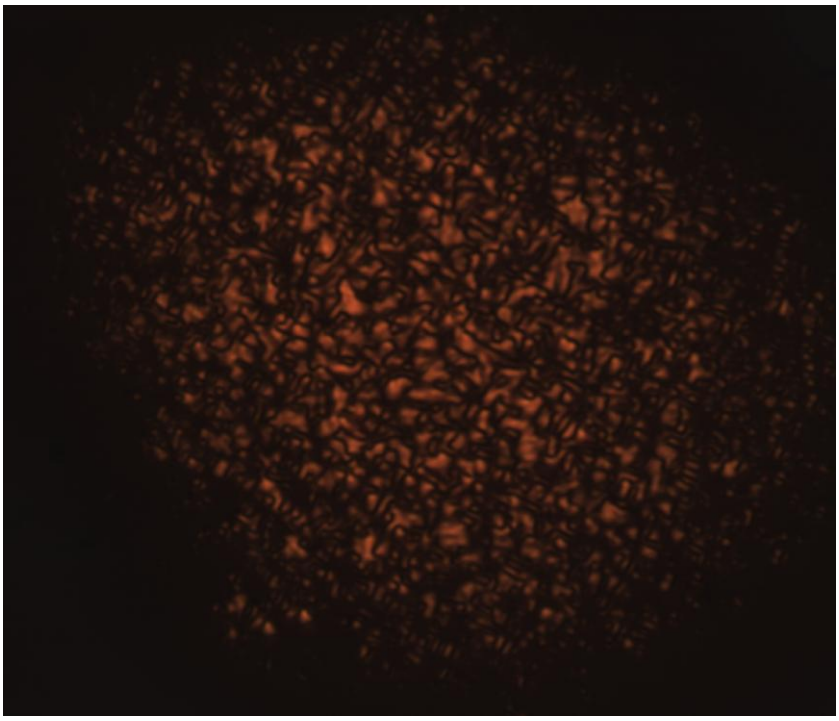

Figure 5. 18: OPM image of 56 in the nematic phase at 124.7°C

A similar texture was observed for compound **57** in the nematic phase. The nematic texture was observed as droplets (Fig. 5.19 and 5.20) but unlike compound 55 did not coalesce into a texture like that observed in Figure 5.16. The two- and four-brush

disclinations are clearly visible in the droplets. As can be seen from Figures 5.17-20, more of the nematic texture becomes visible after longer periods of annealing. A typical nematic texture was not detected for compound **57** despite a large amount of birefringence being observed (Fig. 5.21).

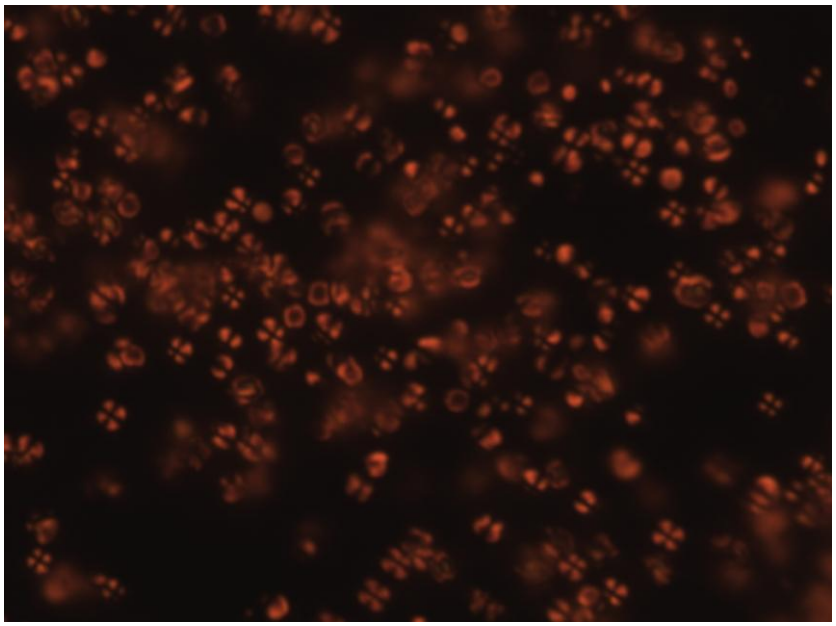

Figure 5. 19: OPM image of 56 in the nematic phase after 1hr annealing at 118.7°C

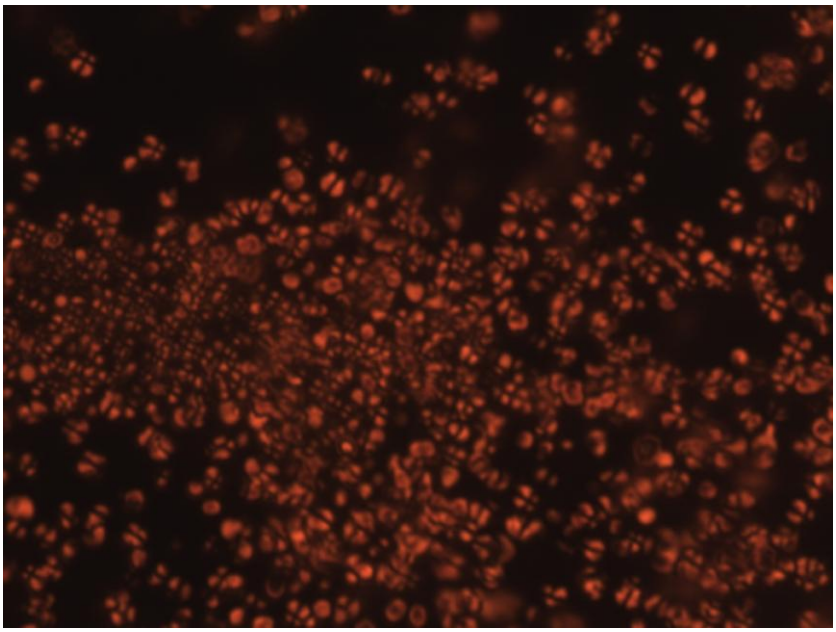

Figure 5. 20: OPM image of 56 in the nematic phase after 3hrs annealing at 118.7°C

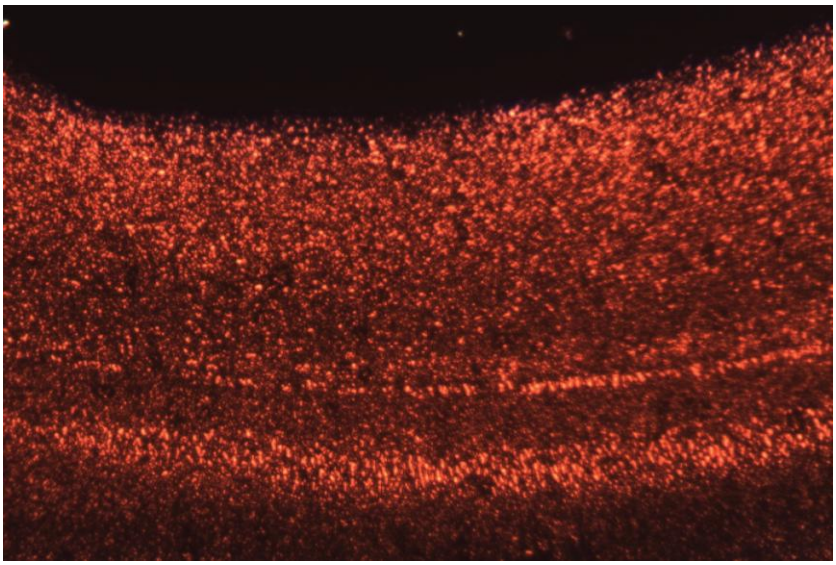

Figure 5. 21: OPM image of 57 in the nematic phase at 89.0°C

Compound	LC transitions (°C)	Nematic range (°C)	ΔH (kJ mol^{-1}) (Iso-N transition)	ΔS_{mol} / R (Iso-N transition)	(ΔS_{mol} / R) / *n* (Iso-N transition)
52	m.p. 78-79	-	-	-	-
53	m.p. 73-74	-	-	-	-
54	m.p. 87-88	-	-	-	-
55	T_g 57 N 149 I	92	5.40	1.54	0.77
56	T_g 65 N 129 I	64	5.71	1.71	0.85
57	T_g 73 N 99 I	26	2.32	0.75	0.37

Table 5. 1: Liquid crystal transitions, nematic ranges, Iso-N enthalpies and Iso-N reduced entropies for compounds 52-57; (ΔS/R) / *n* corresponding to the entropy contribution per mesogen

The nematic range of compound **55** was found to be 92°C, which is the widest of the several series of compounds synthesised. This is attributed to the additional mesogenic unit promoting nematic phase formation, while the lack of alkyl substituents on the fluorophore limits the disruption of the molecular packing. The nematic range of compound **55** is significantly wider than that of compound **23**, indicating that the two mesogenic units linked by the BODIPY 8-phenyl ring form the long molecular axis, with the fluorophore attached laterally. A gradual increase in T_g-N transition along with a

decrease in the clearing point is observed with increasing alkyl substitution resulting in a shortening of the nematic range. With each incremental increase in the number of alkyl groups on the BODIPY core, the glass transition increases by 8°C while the N-Iso transition decreases by 20°C from **55** to **56** and by 30°C from **56** to **57**. This indicates that the ethyl groups have a greater effect on the self-assembly behaviour than the methyl groups. This is to be expected as they are larger and are positioned on the widest point of the fluorophore. The isotropic-to-nematic transition enthalpies and ΔS/R values for compounds **55** and **56** were calculated to be relatively similar, with compound **56** being slightly higher (0.77 for **55** and 0.85 for **56** for the reduced entropies), while the values for compound **57** were calculated to be significantly lower (0.37 reduced entropy). It is interesting to note is that the tetramethyl analogue (**56**) has a lower melting point than the unsubstituted compound (**55**) unlike in the previous series of mono-mesogenic BODIPYs where the incorporation of four methyl groups on the bipyrrolic core caused a significant increase in the melting point. This is presumably due to the fluorophore being attached laterally to the long molecular axis formed by the two mesogenic units.

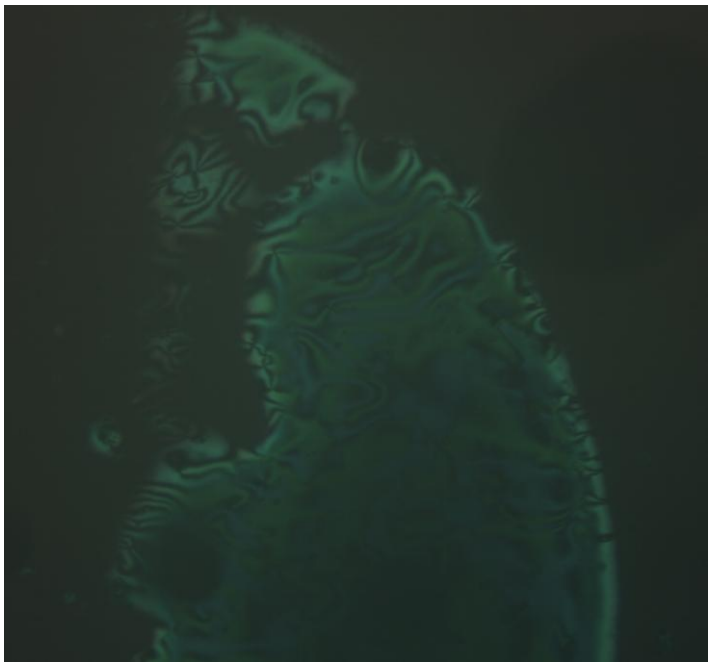

Figure 5. 22: OPM image of 65 at 212.0°C

As can be seen from Fig. 5.22, a Schlieren texture was observed for compound **65** when viewed under crossed polarisers (Fig. 5.22) but the nematic phase transition could not be identified from the DSC thermogram. The DSC thermogram (Fig. 5.23) appeared to show crystal-crystal transitions which were evidenced by the large transition enthalpies of the first peak on the heat cycle (calculated to be 9.54 kJ mol^{-1}). This indicates that the nematic phase can be adopted when the material is sheared as a thin film under a microscope but not when resting in a DSC pan due to this lack of alignment.

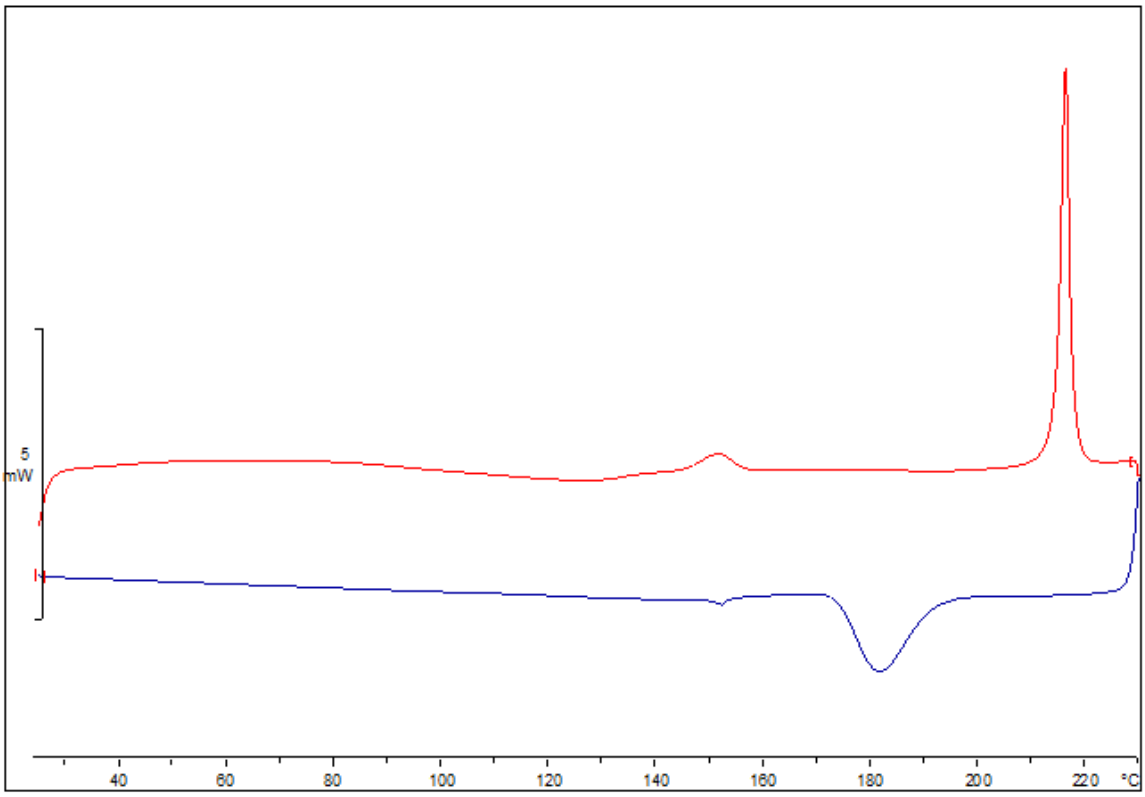

Figure 5. 23: DSC thermogram of 65; showing second heat (top line) and second cool (bottom line)

5.2.3 Fluorescence

The liquid crystalline BODIPYs (**55-57**) were chosen as representative examples of the dimesogenic BODIPY series due to structural similarities with compounds **52-54**. As with the previous series of mesogenic BODIPYs, an increase in fluorescence quantum yield was observed with increasing alkyl substitution. The fluorescence quantum yields for compounds **55-57** were noticeably higher than the mono-mesogenic BODIPYs due to

further restriction of the rotation of the 8-phenyl ring by the two large phenyl units on the 3- and 5-positions (of the 8-phenyl ring). This leads to compound **57** having an almost quantitative fluorescence quantum yield (Φ_F = 0.96). Similar to the mono-mesogenic BODIPYs, the fully alkylated BODIPY (**57**) exhibits slightly red-shifted fluorescence compared to **55** and **56**. The attachment of two phenyl rings to the BODIPY 8-phenyl ring does not appear to have a significant effect on the absorption, emission, absorption coefficient and fluorescence lifetime when compared to the mono-mesogenic analogues (Fig. 5.24).

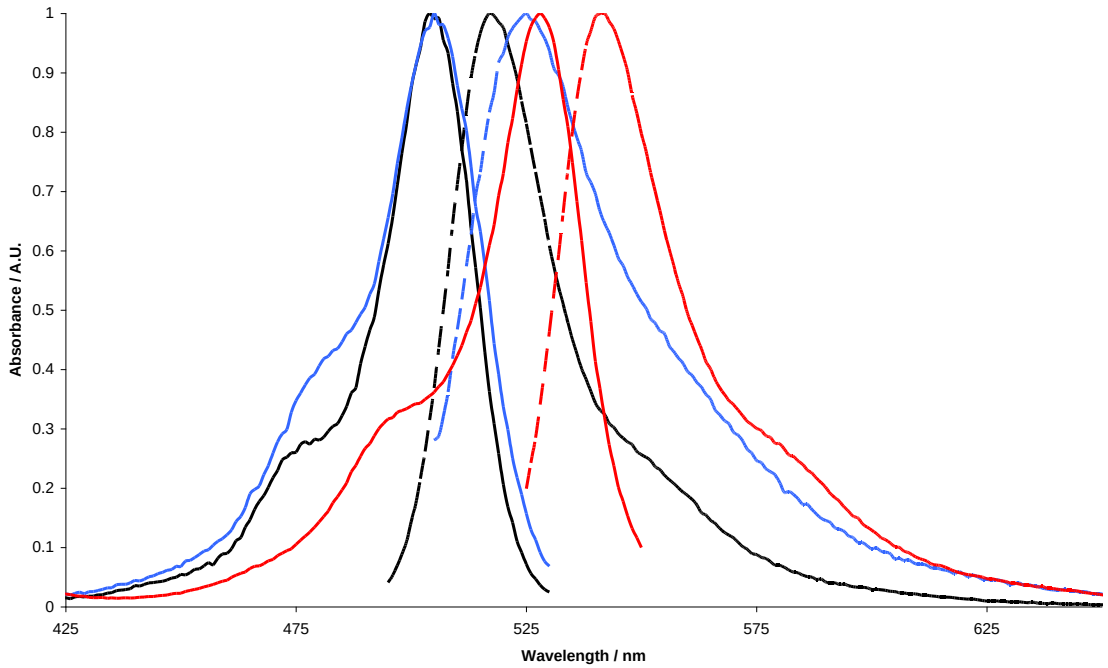

Figure 5. 24: Excitation (solid line) and emission (dashed line) of 55 (blue), 56 (black) and 57 (red); measured in toluene at 298K

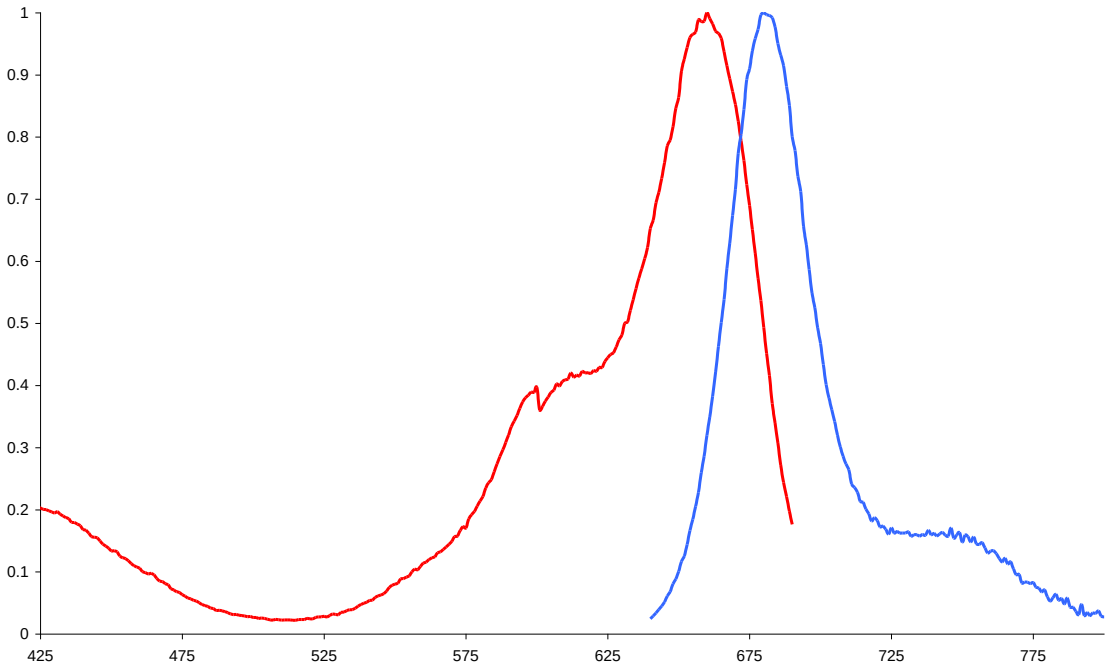

Figure 5. 25: Excitation (red) and emission (blue) of 65; measured in toluene at 298K

Compound	λ_{ex} (nm)	λ_{em} (nm)	Φ_F	ε (M^{-1} cm^{-1})	ΔS (nm)	k_r (10^8 s^{-1})	k_{nr} (10^8 s^{-1})	τ_{fl} (ns)
55	505	525	0.087	55000	20	1.6	17	0.53
56	505	518	0.82	82000	13	1.7	0.38	4.7
57	528	542	0.96	63000	14	1.7	0.71	5.6
65	660	681	0.57	84000	21	1.3	0.98	4.4

Table 5. 2: Photophysical data for 55-57 and 65; measured in toluene or CH_2Cl_2 at 298K

As can be seen, compound **65** displays significantly red-shifted absorption and emission compared to the other BODIPYs due to the extended π-conjugate system (Fig. 5.25). Despite the presence of methyl and ethyl groups, the fluorescence quantum yield is not as high as the previous fully substituted BODIPYs. This was attributed to the slightly flexible styryl units attached directly to the BODIPY core. Compound **65** also displays a pronounced shoulder on the absorption profile corresponding to the vibrational bands.

5.2.4 Structure-property relationship between liquid crystallinity and fluorescence intensity

The presence of two mesogenic units on the BODIPY causes a high preference for the adoption of the nematic phase, albeit monotropically. The two phenyl rings by which the mesogens are attached to the fluorophore have been shown to cause a moderate increase in the fluorescence quantum yield of the resulting compounds due to increased rotational restriction of the 8-phenyl ring of the BODIPY.

Compound	LC transitions (°C)	Nematic range (°C)	Φ_F
55	T_g 57 N 149 I	92	0.087
56	T_g 65 N 129 I	64	0.82
57	T_g 73 N 99 I	26	0.96

Table 5. 3: Structure-property relationship between liquid crystallinity and fluorescence intensity for 55-57

Alongside the increase in fluorescence intensity caused by the phenyl rings, the alkyl groups attached directly to the fluorophore have the greatest effect on the fluorescence and liquid crystallinity (Table 5.3). The lack of any alkyl groups (compound **55**) results in a wide nematic range but weak fluorescence (although more intense than the analogous mono-mesogenic compounds **23** and **30**). The incorporation of four methyl units (compound **56**) causes an increase in the glass transition temperature and a decrease in the melting point, resulting in a shortening of the nematic range with a concurrent increase in fluorescence intensity. This increase in fluorescence intensity is quite dramatic while the reduction in nematic range is only moderate causing the nematic range to remain reasonably wide. Upon the addition of two ethyl groups (compound **57**), the reduction in nematic range becomes more pronounced, while the subsequent increase in fluorescence intensity is smaller. Despite the reduction in nematic range to 26°C, compound **57** displays the widest nematic phase range of all the mono-mesogenic BODIPYs and the highest fluorescence quantum yield of all the compounds synthesised.

5.2.5 Temperature-dependant fluorescence measurements and BODIPY-doped nematic liquid crystal fluorescence

Temperature dependant measurements were performed on compounds **55** and **56** due to their wide nematic ranges and widely different fluorescence quantum yields. Compound **57** was not investigated due to a much smaller increase in fluorescence intensity when compared to compound **56** and shorter nematic range, meaning fewer measurements could be taken when in the nematic phase. As observed for compound **23**, a gradual increase in fluorescence intensity is observed with decreasing temperature (Fig. 5.26 and 5.27). The peak at 572 nm shows emission from the BODIPY which is gradually red-shifted with decreasing temperature due to the formation of *J*-dimers. A similar effect is observed for compound **56**; however, an additional peak at 726 nm also becomes more intense. This peak is also present in the isotropic liquid although less pronounced. A larger increase in the intensity of the peak at 726 nm is observed as the nematic phase begins to form at approximately 130°C. A similar, much shallower, peak is observed for compound **55** at a similar wavelength, appearing as a shoulder on the emission peak. These peaks are also presumably caused by aggregation of the molecules which would occur even in the isotropic liquid due to the high viscosity of the materials.

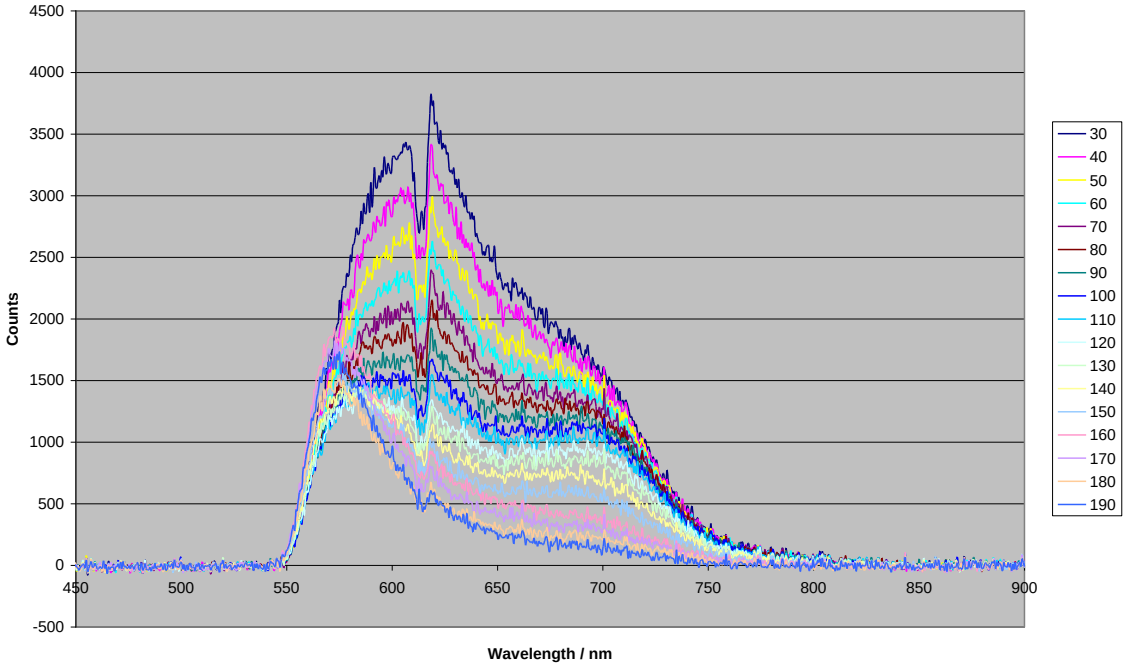

Figure 5. 26: Temperature dependant fluorescence measuerments of 55 at 10°C intervals (heated to 190°C and cooling down to 30°C - see legend); excited with a Nd:YAG laser with heating on a Mettler hot-stage

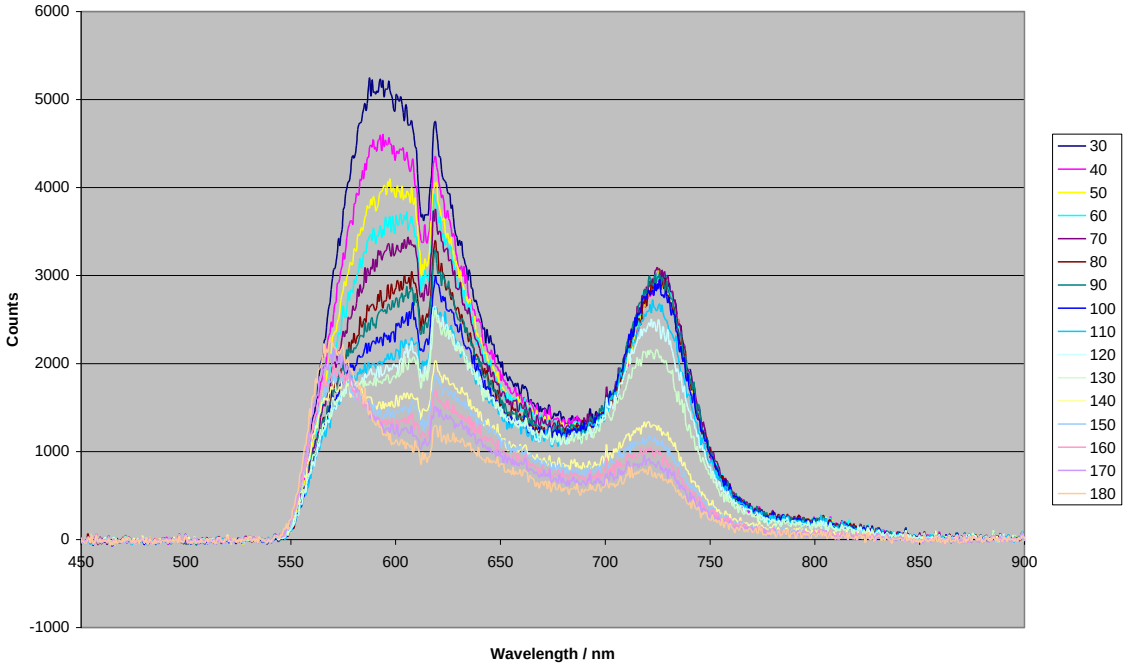

Figure 5. 27: Temeprature dependant fluorescence measurements of 56 at 10°C intervals (heated to 180°C and cooling down to 30°C - see legend); excited with a Nd:YAG laser with heating on a Mettler hot-stage

A mixture of compound **57** in BL024 was incorporated into a twisted nematic cell and the fluorescence intensity measured when an electric field was applied (Fig. 5.28). While initially the observed fluorescence decreased when the electric field was applied, this effect was not seen when it was applied for a second time. The results of this study do not provide conclusive evidence of how the mesogenic BODIPY interacts with the host material, but due to its large size and non-linear shape it would presumably not align to a large degree.

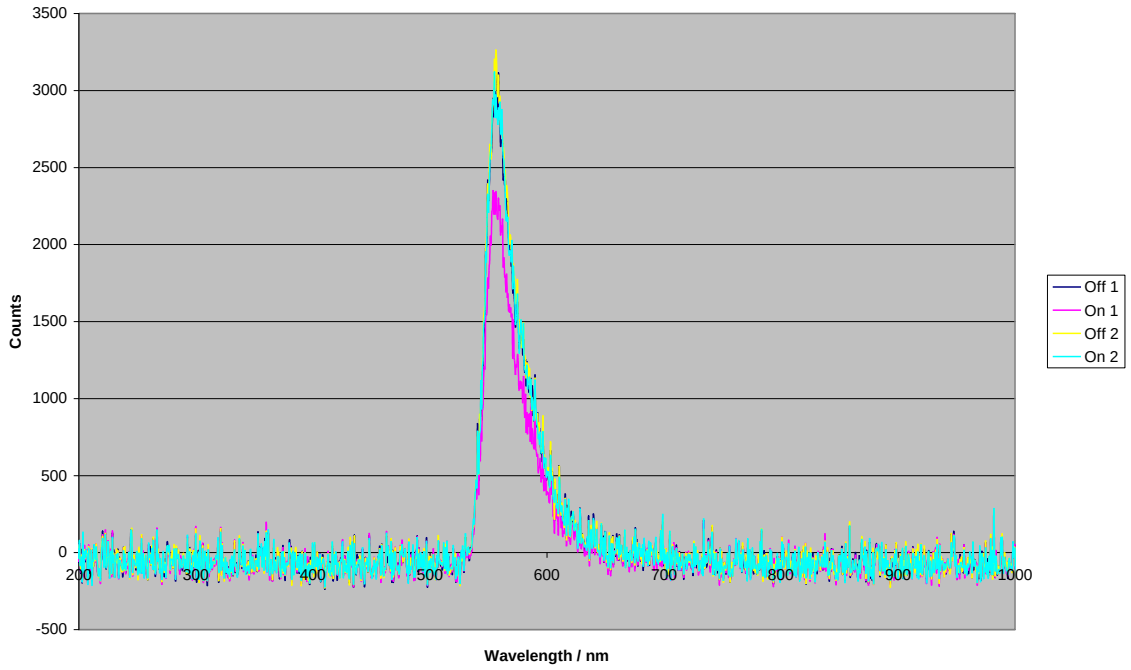

Figure 5. 28: Fluorescence intensity of 57 dissolved in BL024 in a twisted nematic cell (two measurements taken with an electric field applied (On) and two without an electric field applied (Off) - see legend)

5.3 Conclusions

The compounds prepared in these series' show that the palladium-catalyzed coupling reactions developed in the previous chapter can be applied to different BODIPYs, allowing the incorporation of two mesogenic units onto the fluorophore. The yields and purification procedures for these compounds were found to be similar to the mono-mesogenic BODIPYs. It was also found that, despite the use of two mesogens, a more

extended liquid crystalline moiety was still required to induce nematic phase behaviour onto the fluorophore. The nematic phases induced on the BODIPYs are relatively wide when compared to the mono-mesogenic BODIPYs due to the two mesogens providing a high preference for self-assembly.

A mesogenic BODIPY with red-shifted fluorescence was also prepared by the extension of the π-conjugate system (compound **65**). Initially, an aza-BODIPY was prepared to facilitate this but was found to either be difficult to purify or unreactive to the desired functional group. The π-system extension was achieved by the attachment of styryl groups, to which mesogenic units were attached before a third mesogen was attached *via* a Suzuki coupling. This was found to display a Schlieren texture when viewed under crossed polarisers but the DSC thermogram did not show the adoption of a nematic phase. The large size of the molecule could cause the nematic phase to be adopted very slowly, so perhaps analysis *via* DSC employing a much slower heating and cooling rate would enable the characterisation of any potential mesophases.

Temperature dependant fluorescence measurements were carried out on compounds **55** and **56** which showed similar behaviour to the mono-mesogenic compound **23** upon the reduction of the applied temperature. Large peaks attributed to aggregates were observed at lower temperatures with a slightly red-shifted fluorescence compared to the non-aggregated mesogenic BODIPYs observed at higher temperatures. Compound **57** was used to dope BL024 and incorporated into a twisted nematic cell but the fluorescence measurements recorded when an electric field was applied did not yield any information about the orientations of the mesogenic BODIPY molecules relative to the host material.

Chapter 6: Final conclusions

The fluorescent properties of BODIPYs are promoting their use in materials applications including liquid crystals.[224, 228-230, 232] Initially, BODIPYs with the mesogenic units attached to the pyrrolic position were prepared but were found to be non-liquid crystalline. The synthetic routes employed to prepare these compounds also promoted the formation of a large number of pyrrolic side-products making purification difficult and yields low.

The difficult syntheses and lack of liquid crystalline behaviour were overcome with the relocation of the mesogenic unit onto the BODIPY 8-phenyl ring. By synthesising the BODIPYs using halide-bearing benzaldehydes or acid chlorides, palladium-catalyzed couplings could be used to attach the mesogenic units to the fluorophore. This was then extended to prepare ethynyl-bearing BODIPYs which could undergo Sonogashira couplings and copper-catalyzed Huisgen couplings ('click' chemistry). Due to the large size of the mesogen, conventional heating was found to result in a very slow reaction so microwave heating was employed which drastically decreased the reaction time, leading to the formation of fewer side-products and higher yields. Attachment of the mesogens to the BODIPY 8-phenyl ring caused the resulting mesogenic BODIPYs to have a more rod-like shape, thus promoting liquid crystal phase behaviour.

Three of the mono-mesogenic BODIPYs (two from Suzuki couplings and one from Sonogashira coupling) displayed monotropic nematic phase behaviour. However, a strong nematogen was required due to the fluorophores' preference for aggregation and crystalline behaviour. The extension of the long molecular axis by inclusion of an ethynyl linker group caused a reduction in the nematic range compared to the non-ethynyl containing analogue from the Suzuki coupling. A clear inverse relationship between the nematic range of the mesogenic BODIPYs and their fluorescence intensities (controlled by varying the degree of alkyl substitution on the BODIPY core) was observed. By increasing the number of alkyl groups on the BODIPY core, the fluorescence intensity increased due to the reduced rotational mobility when compared to the unsubstituted

systems. In turn, the increased size of the fluorophore caused disruption in the molecular packing which either narrowed or completely eliminated the nematic phase. Four of the mono-mesogenic BODIPYs were dissolved in a commercial liquid crystal (BL024) and incorporated into a twisted nematic cell. The fluorescence intensity was then measured when an electric field was applied and it was found that the compounds containing the bulkier fluorophores displayed an increased fluorescence when the electric field was applied compared to when no electric field was applied. The changes in fluorescence intensity were attributed to changes in the relative alignment of the mesogenic BODIPYs to the incident beam. Changes in the alignment of the mesogenic BODIPY molecules were primarily affected by how efficiently they align with the host material. Temperature dependant fluorescence measurements were taken that showed a gradual increase in fluorescence with decreasing temperature with a noticeably larger increase when the crystalline phase was adopted but no significant difference when the nematic phase was adopted from the isotropic liquid.

In order to produce mesogenic BODIPYs with more stable nematic phase behaviour, an additional mesogenic unit was attached. This was achieved *via* the microwave-assisted Suzuki coupling method developed for the mono-mesogenic BODIPYs in moderate yields. Despite the addition of a mesogenic unit, a relatively powerful nematogen was still required to induce liquid crystallinity. While still monotropic, the nematic phases produced were relatively wide compared to those of the mono-mesogenic BODIPYs resulting in the mesophase being exhibited even when the most bulky fluorophore was attached. The size of these compounds also caused a high viscosity in the nematic and isotropic liquid phases, causing the nematic texture to develop slowly when viewed under crossed polarisers. These compounds also displayed an inverse relationship between fluorescence intensity and nematic range as well as possessing consistently higher fluorescence quantum yields than their respective mono-mesogenic analogues. Temperature dependant measurements were carried out on two of the di-mesogenic BODIPYs but no significant difference in fluorescence intensity was observed in each of the phase transitions.

While these compounds showed that fluorescence intensity could be manipulated with predictable effects on the self-assembly behaviour, each of the mesogenic BODIPYs were shown to fluoresce at similar wavelengths. In order to produce a mesogenic BODIPY with a red-shifted fluorescence, several methods of extending the π-conjugate system were investigated with styryl groups being found to produce the desired wavelength shift and functional groups for mesogen attachment. Two cyanobiphenyl mesogens were attached *via* Williamson ether syntheses and a third mesogen was attached *via* microwave-assisted Suzuki coupling analogous to the previous Suzuki couplings. It was found that this compound exhibited a Schlieren texture when viewed under crossed polarisers but the DSC thermogram did not show the adoption of the nematic phase. This indicates that this compound could adopt the nematic phase as a thin film with shearing but not when resting in a DSC pan with nothing to align the molecules. This could be due to the large size of the molecules causing a very slow adoption of the nematic phase. Also, as three mesogenic units were attached with the long molecular axis of each unit lying in three different directions, adoption of the nematic phase could be slowed down as a result of the different flexible portions of the molecules aligning.

Experimental results indicate that BODIPYs seem to have a preference for aggregation, a feature that needs to be addressed in order for liquid crystallinity to be displayed. The difficulties in introducing liquid crystalline behaviour on BODIPYs can be demonstrated by comparing them to other simpler borondifluoro-containing fluorophores in which the mesophases are more stable.[273] The other disadvantage caused by this is that aggregation does not occur to the same extent as porphyrins which promote the formation of columnar phases[274-276] meaning more complex mesogens must be employed to promote self-assembly. Due to the relatively small amount of research carried out in this particular area, the optimum properties for inducing self-assembly onto BODIPYs are not yet fully understood. However, with the work presented herein, one particular factor, the steric bulk around the fluorophore, affecting both the liquid crystallinity and the fluorescence intensity of BODIPYs has been observed. Additionally, some initial investigations have been made into the potential liquid crystalline properties of BODIPYs with

bathochromically shifted fluorescence despite the marked differences in molecular size and shape of these compounds.

Due to the relative ease of inducing a bathochromic shift in the fluorescence of BODIPY fluorophores, future work should be directed towards inducing liquid crystalline behaviour on BODIPYs with extended π-conjugate systems. The work presented herein, as well as that previously reported,[224, 225, 229, 232] is primarily concerned with altering the liquid crystal properties of the prepared BODIPY compounds instead of the fluorescence properties. This is unsurprising as extensive research into the self-assembly behaviour of BODIPYs is yet to be carried out. However, if practical applications for liquid crystalline BODIPYs are to be realised, methods by which to control both the self-assembly and fluorescence behaviour simultaneously must be established. As inducing a bathochromic shift in BODIPY fluorescence requires the incorporation of relatively bulky conjugated substituents, careful choice of the mesogenic substituent, as well as the number of mesogens and position of attachment would be required.

Chapter 7: Experimental procedures

Instrumentation and chemicals

All chemicals were purchased from Sigma Aldrich (Sigma Aldrich Company Ltd., The Old Brickyard, New Road, Gillingham, Dorset, SP8 4XT) or Alfa Aesar (Alfa Aesar, A Jonson-Matthey Company, Shore Road, Port of Heysham Industrial Park, Heysham, Lancashire, LA3 2XY) with the exception of the palladium catalysts, which were purchased from Strem (Strem Chemicals UK, Ltd., 41 Hills Road, Cambridge, England, CB2 1NT), the boronic esters, which were purchased from Frontier Scientific (Frontier Scientific Europe, Carnforth, Lancashire, LA6 1DE), and 2,4-dimethylpyrrole, 2,4-dimethyl-3-ethylpyrrole and 4-iodobenzoyl chloride, which were purchased from Acros Organics (Fisher Scientific UK, Bishop Meadows Road, Loughborough, Leicestershire, LE11 5RG). All chemicals were used as received with the exception of pyrrole which was distilled before use. All solvents were purchased from Fisher Scientific (Fisher Scientific UK, Bishop Meadows Road, Loughborough, Leicestershire, LE11 5RG) with the exception of *N,N'*-dimethylformamide which was purchased from Acros Organics (Fisher Scientific UK, Bishop Meadows Road, Loughborough, Leicestershire, LE11 5RG). All deuterated solvents were purchased from Fisher Scientific (Fisher Scientific UK, Bishop Meadows Road, Loughborough, Leicestershire, LE11 5RG) and used as received.

Thin-layer chromatography (TLC) was performed using Merck aluminium plates coated with silica gel 60 F_{254} and visualised under UV light (254 nm or 372 nm), potassium permanganate solution or bromine vapour. Column chromatography was performed using MP Silica 32-63, 60 Å. All solvent mixtures are given in v/v ratios.

Microwave-assisted reactions were carried out in a CEM Discover System.

NMR spectroscopy

NMR spectra were recorded on a Jeol JNM ECP400 spectrometer, with TMS $\delta_H = 0$ as the internal standard or residual protic solvent. [$CDCl_3$, $\delta_H = 7.26$; $(CD_3)_2SO$, $\delta_H = 2.50$; CD_3OD, $\delta_H = 3.30$]. Chemical shifts are given in ppm (δ) and coupling constants (J) are given in Hertz (Hz). ^{1}H-NMR were recorded at 400 MHz; ^{13}C-NMR recorded at 100.5 MHz; ^{11}B-NMR recorded at 128.3 MHz; ^{19}F-NMR recorded at 376.83MHz. ^{11}B-NMR experiments were spin decoupled.

Mass spectrometry

ESI-MS and MALDI-TOF-MS were carried out by the EPSRC National Mass Spectrometry Service Centre in Swansea.

Photophysical measurements

UV-visible spectra were measured on a Varian Cary 50 Bio UV-visible Spectrophotometer and an ATI Unicam UV2-100 spectrometer. Fluorescence spectra were measured using a Jobin-Yvon Horiba Fluorolog 3-22 Tau-3 spectrofluorometer with a right angle illumination method. All measurements were carried out in a 4-sided quartz cuvette of 10mm diameter. Lifetime measurements were obtained via the time-correlated single photon counting technique. Samples were excited by a Ti:Saph laser (at an excitation wavelength of 300 nm). Emission was collected at 90° to the source of excitation. The emission wavelength was selected by a monochromator (Jobin Yvon Triax 190). All measurements were performed in a four-sided cuvette using an absorbance value of 0.1, which was measured and checked using the Unicam spectrometer. The Fluorescence lifetime values were quoted to 1 decimal place. Fluorescence quantum yields with an absorbance at the maximum typically below 0.2 were determined by use of an integrating sphere with a HORIBA Jobin-Yvon Fluorolog FL3-22 Tau-3, following a method described in the literature.[277] All measurements, unless stated, were obtained at 298 K and aerated.

DSC and optical polarising microscopy

Transition temperatures and enthalpies were determined using a Mettler DSC822e differential scanning calorimeter with STARe software, under nitrogen/helium, at a rate of 10°C/min, calibrated with indium (156.6°C, 28.45J g^{-1}) and using an aluminium reference. Optical studies were carried out using an Olympus BH-2 optical polarising microscope equipped with a Mettler FP82 HT hot stage and a Mettler FP90 central processor. Photographic images of the mesophases were taken using a JVC digital video camera connected to a PC. Software Studio Capture, supplied by Studio86Designs, was used for image capturing.

4-(Methoxycarbonylacetyl)-3,5-dimethyl-2-ethoxycarbonylpyrrole (1):

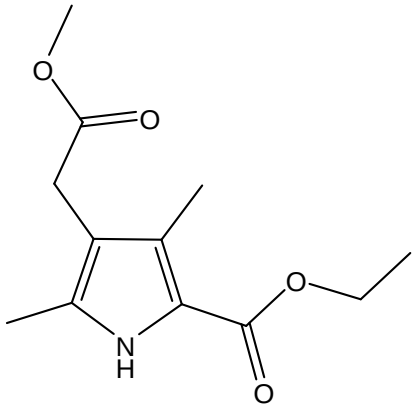

2,4-Pentanedione (10.01g, 0.10mol), methyl bromoacetate (15g, 0.10mol) and anhydrous potassium carbonate (13.82g, 0.10mol) were heated at reflux temperature in dry acetone (15ml) for 16hrs. The solid was then filtered off and the solvent removed from the filtrate to yield an orange/brown oil.

Ethyl acetoacetate (11.71g, 0.09mol) was dissolved in glacial acetic acid (45ml) and cooled to 0°C. Sodium nitrite (6.21g, 0.09mol) dissolved in 10ml of water was then added with stirring to the cooled solution dropwise over 20 minutes. The solution was stirred at r.t. for 1hr. To this solution was added the oil from the first step and sodium acetate (11.48g, 0.14mol). A mixture of zinc dust (15.69g, 0.24mol) and sodium acetate (4.43g, 0.054mol) was added to the mixture in portions over 30 minutes, while maintaining the temperature at 70°C. Once addition was complete, an additional 45ml of glacial acetic acid was added to maintain the solution and the mixture was stirred at reflux for 3hrs. While still hot the mixture was then poured into 300ml cold water. This mixture was stirred at r.t. for 1hr allowing an off-white solid to precipitate. The solid was then filtered off, washed with water and recrystallized from ethanol to yield a light tan solid (10.63g, 49%), m.p. 118-119°C, (lit. 122.5-124°C[259]).

^{1}H-NMR [400MHz, $CDCl_3$] δ 1.36 (3H, t, CH_3, *J* = 7.19), 2.24 (3H, s, CH_3), 2.28 (3H, s, CH_3), 3.39 (2H, s, CH_2), 3.68 (3H, s, CH_3), 4.29 (2H, q, CH_2, *J* = 7.19), 7.86 (1H, bs, NH).

^{13}C-NMR [100MHz, $CDCl_3$] δ 10.6, 11.6, 14.5, 18.4, 30.0, 51.9, 58.5, 59.8, 114.4, 130.8, 161.7, 172.3.

MS (ESI) m/z 239.3 (M^+).

Ethyl 4-carboxymethyl-3,5-dimethyl-1*H*-pyrrole-2-carboxylate:

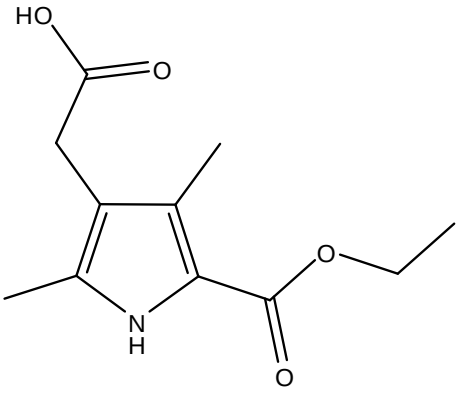

3,5-Dimethyl-2-ethoxycarbonyl-1*H*-pyrrole-4-acetic acid ethyl ester (3g, 13mmol), sodium hydroxide (0.56g, 14mmol), ethanol (60ml) and water (6.25ml) were mixed together and stirred at r.t. for 22hrs. The ethanol was then removed *in vacuo* and water (90ml) was added to the residue. The solution turned cloudy upon addition of the water as some product started to precipitate out. The mixture was acidified with 30% hydrochloric acid to precipitate the remaining product. The solid was filtered off, washed with water and dried *in vacuo* to yield the monoacid (2.14g, 73%), m.p. 197-198°C (lit. 198-199°C[278]).

^{1}H-NMR [400MHz, $CDCl_3$] δ 1.34 (3H, t, -CH_2CH_3, *J* = 7.19), 2.24 (3H, s, Me), 2.28 (3H, s, Me), 3.42 (2H, s, CH_2CO), 4.29 (2H, q, CH_2CH_3, *J* = 7.19), 8.86 (1H, bs, NH), 9.10 (1H, bs, OH).

^{13}C-NMR [100MHz, $CDCl_3$] δ 10.6, 11.4, 14.5, 29.7, 60.0, 114.2, 117.2, 127.6, 131.0, 161.8, 176.4.

MS (ESI) m/z 225.3 (M^+).

2,4-Dimethyl-3-pyrroleacetic acid (2):

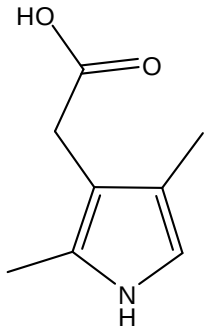

4-(Methoxycarbonylacetyl)-3,5-dimethyl-2-ethoxycarbonylpyrrole (10.63g, 0.044mol) and sodium hydroxide (7.20g, 0.18mol) were dissolved in ethanol (135ml) and stirred at reflux for 16hrs. As the reaction proceeded a tan solid precipitated out. Once the reaction was complete the reaction mixture was acidified with glacial acetic acid, concentrated then filtered and washed with ethanol to yield a fine tan powder (5.33g, 79%), m.p. 60-61°C (lit. 59.5-60.5°C[259]).

^{1}H-NMR [400MHz, MeOD] δ 2.02 (3H, s, CH_3), 2.05 (3H, s, CH_3), 3.15 (2H, s, CH_2), 4.70 (1H, s, Py-H).

^{13}C-NMR [100MHz, MeOD] δ 9.8, 10.1, 116.3, 122.2, 123.4, 126.2, 180.2.

MS (ESI) m/z 176.2 ($M + Na^+$).

2-Formylpyrrole (3):

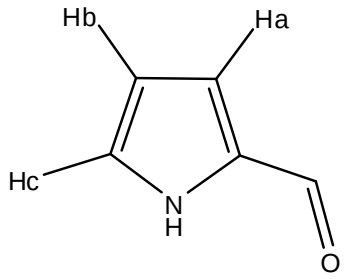

Dry DMF (12.34ml, 0.16mol) was placed in a round bottomed flask and cooled to 0°C. To this was added phosphoryl chloride (14.91ml, 0.16mol) dropwise. Once the addition was complete the orange solution was stirred at r.t. for 15 minutes. The reaction mixture was then cooled to 0°C again and 1,2-DCE (25ml) was added followed by freshly distilled pyrrole (10ml, 0.144mol) in 1,2-DCE (25ml) over a period of 30 minutes *via* a dropping funnel. Once the addition was complete the reaction mixture was refluxed for 15 minutes then allowed to cool to room temperature. To this was added sodium acetate (65g, 0.79mol) in 90ml water (slowly at first but then as quickly as possible) and the reaction mixture was refluxed again for a further 15 minutes then allowed to cool to room temperature. Diethyl ether was added to the mixture and the organic layer was separated. The aqueous layer was washed with ether and the solvent removed from the organic layer to yield a dark oil. This was then purified by column chromatography (20% hexane: CH_2Cl_2) to yield an orange oil which slowly crystallized at room temperature to yield orange/brown needles (8.99g, 66%) m.p. 44-46°C (lit. 45-46°C[279]).

^{1}H-NMR [400MHz, $CDCl_3$] δ 6.35-6.37 (1H, m, Py-Hb), 7.01-7.03 (1H, m, Py-Hc), 7.18-7.20 (1H, m, Py-Ha), 9.51 (1H, s, CHO), 10.50 (1H, bs, NH).

^{13}C-NMR [100MHz, $CDCl_3$] δ 111.3, 121.9, 127.0, 132.8, 179.5.

MS (ESI) m/z 95.1 (M^+).

1,3-Dimethyl-2-acetoxycarbonyl-(4-hydroxy-4'-undecylbiphenyl)-BODIPY (4):

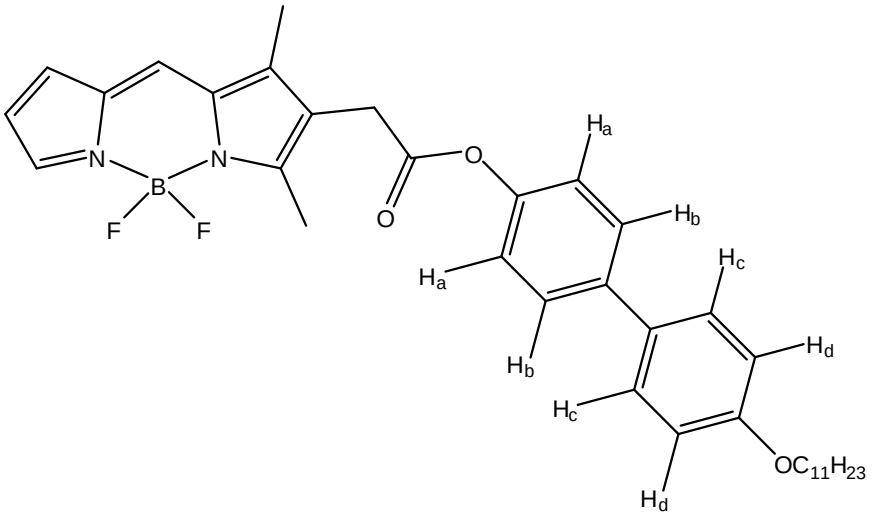

2,4-Dimethyl-3-pyrroleacetic acid (0.4g, 2.61mmol) and 2-formylpyrrole (0.25g, 2.61mmol) were suspended in glacial acetic acid (30ml). 45% Hydrobromic acid in glacial acetic acid (1.5ml) was then added and the mixture was stirred with heating for 3hrs. During this time the solution turned a very dark yellow/brown. The mixture was then cooled to r.t. and the acetic acid removed *in vacuo* to yield a dark solid. This solid was dissolved in CH_2Cl_2 and to this solution was added triethylamine (1.10ml, 7.83mmol) followed by boron trifluoride diethyletherate (1.65ml, 13.05mmol) and the solution was stirred under nitrogen overnight. The mixture was then filtered and the solvent removed from the filtrate and the crude product was purified by column chromatography (10% methanol: CH_2Cl_2) to yield the BODIPY carboxylic acid as a bright red solid (0.1g, 14% (impure)). The BODIPY free acid (0.1g, 0.38mmol), 4-hydroxy-4'-undecylbiphenyl (0.26g, 0.75mmol) and 4-dimethylaminopyridine (90mg, 7.5mmol) were dissolved in THF (10ml) and stirred under nitrogen and protected from light for 10 minutes. To this was added N,N'-dicyclohexylcarbodiimide (90mg, 0.45mmol) and the mixture was stirred at r.t. under nitrogen and protected from light overnight. The mixture was then filtered and the solvent removed *in vacuo*. The residue was redissolved in dichloromethane and purified by column chromatography (3:7 hexane: CH_2Cl_2) to yield the product as a bright orange solid (48 mg, 3% overall), m.p. 133.27°C (determined by DSC), R_f = 0.46 (3:7 hexane:CH_2Cl_2).

^{1}H-NMR [400MHz, $CDCl_3$] δ 0.88 (3H, t, $CH_2C\mathbf{H_3}$, *J* = 6.65), 1.27 (12H, m, CH_2), 1.46 (2H, m, CH_2), 1.80 (4H, m, CH_2), 2.33 (3H, s, 4-Me), 2.68 (3H, s, 2-Me), 3.69 (2H, s, CH_2CO), 3.99 (2H, t, O-CH_2, *J* = 6.41), 6.46 (1H, m, Py-H), 6.95 (2H, d, Ph-H_d, *J* = 8.76), 6.98 (1H, m, Py-H), 7.11 (2H, d, Ph-H_c, *J* = 8.76), 7.25 (1H, s, 5-H), 7.47 (2H, d, Ph-H_b, *J* = 8.76), 7.53 (2H, d, Ph-H_a, *J* = 8.44), 7.68 (1H, m, Py-H).

^{13}C-NMR [100MHz, $CDCl_3$] δ 10.1, 13.6, 14.2, 22.8, 25.0, 26.1, 29.36, 29.42, 29.49, 29.7, 30.4, 32.0, 68.2, 114.9, 116.7, 121.6, 124.2, 125.2, 127.1, 127.8, 132.6, 132.9, 135.5, 139.2, 140.0, 143.2, 149.4, 158.9, 161.8, 168.8. (2 peaks unobserved due to overlap of the alkyl peaks).

^{11}B-NMR [128.3MHz, $CDCl_3$] δ -0.31.

MS (ESI) m/z 600.5 (M^+).

1,3-Dimethyl-2-acetoxycarbonyl-(4'-octyloxybiphenyl-4-nitrile)-BODIPY (5):

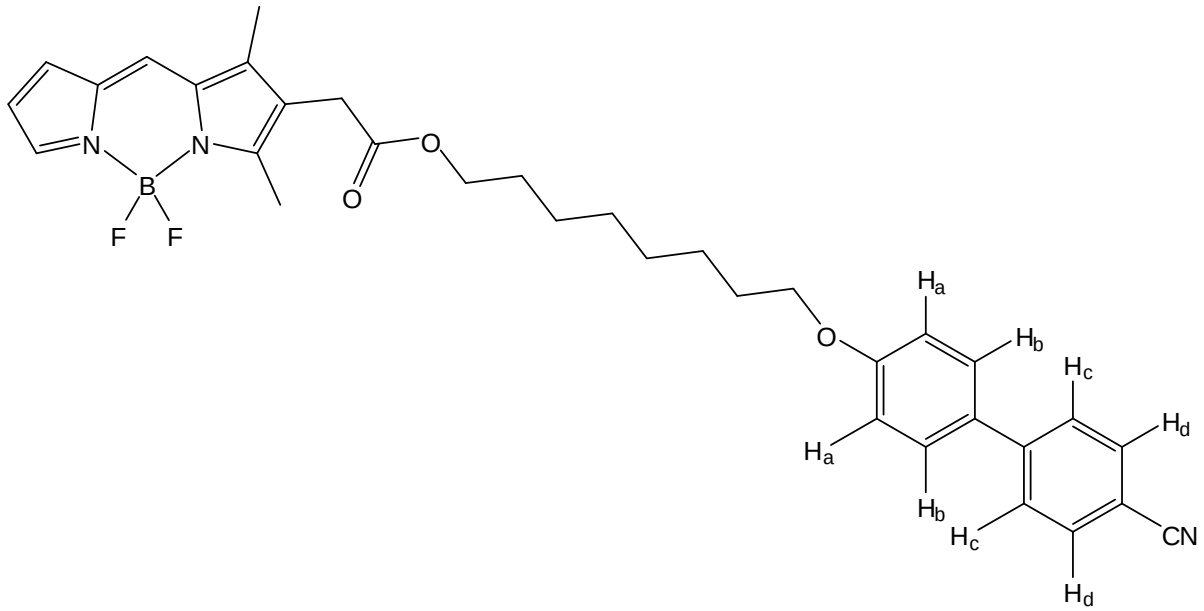

2,4-Dimethyl-3-pyrroleacetic acid (0.4g, 2.61mmol) and 2-formylpyrrole (0.25g, 2.61mmol) were suspended in glacial acetic acid (30ml). 45% Hydrobromic acid in glacial acetic acid (1.5ml) was then added and the mixture was stirred with heating for 3hrs. During this time the solution turned a very dark yellow/brown. The mixture was then cooled to r.t. and the acetic acid removed *in vacuo* to yield a dark solid. This solid was dissolved in CH_2Cl_2 and to this solution was added triethylamine (1.10ml, 7.83mmol) followed by boron trifluoride diethyletherate (1.65ml, 13.05mmol) and the solution was stirred under nitrogen overnight. The mixture was then filtered and the solvent removed from the filtrate and the crude product was purified by column chromatography (10% methanol: CH_2Cl_2) to yield the BODIPY carboxylic acid as a bright red solid (0.151g, 21% (impure)). BODIPY free acid (151mg, 0.54mmol), 4'-(8-hydroxyoctyl)-biphenyl-4-carbonitrile (0.35g, 1.09mmol) and 4-dimethylaminopyridine (0.13g, 1.09mmol) were dissolved in THF (15ml) and stirred under nitrogen and protected from light for 10 minutes. To this was added N,N'-dicyclohexylcarbodiimide (0.13g, 0.65mmol) and the mixture was stirred at r.t. under nitrogen and protected from light overnight. The mixture was then filtered and the solvent removed *in vacuo*. The residue was redissolved in dichloromethane and purified by column chromatography

(40% hexane:CH_2Cl_2) to yield the product as a bright orange solid (152 mg, 10% overall), R_f = 0.35 (4:6 hexane:CH_2Cl_2). Unclear melting point.

^{1}H-NMR [400MHz, $CDCl_3$] δ 1.34 (8H, m, CH_2), 1.63 (2H, m, CH_2), 1.79 (2H, m, CH_2), 2.24 (3H, s, 4-Me), 2.58 (3H, s, 2-Me), 3.41 (2H, s, CH_2CO), 3.99 (2H, t, O-CH_2), 4.09 (2H, t, CO_2CH_2), 6.43 (1H, m, Py-H), 6.93 (1H, d, Py-H), 6.99 (2H, d, Ph-H_a, J = 8.76), 7.20 (1H, s, 5-H), 7.53 (2H, d, Ph-H_b, J = 8.76), 7.63 (2H, d, Ph-H_c, J = 8.44), 7.64 (1H, m, Py-H), 7.66 (2H, d, Ph-H_d, J = 8.44).

^{13}C-NMR [100MHz, $CDCl_3$] δ 10.0, 13.5, 25.0, 25.7, 25.9, 26.0, 28.6, 29.3, 30.4, 34.0, 49.3, 65.4, 68.2, 110.2, 116.2, 116.5, 119.2, 124.8, 125.1, 126.7, 127.2, 128.4, 131.4, 132.7, 132.8, 135.6, 139.5, 142.9, 145.4, 159.9, 162.3, 170.2.

^{11}B-NMR [128.3MHz, $CDCl_3$] δ -0.37.

MS (ESI) m/z 583.5 (M^+).

1,3-Dimethyl-2-acetoxycarbonyl-(4'-undecyloxybiphenyl-4-nitrile)-BODIPY (6):

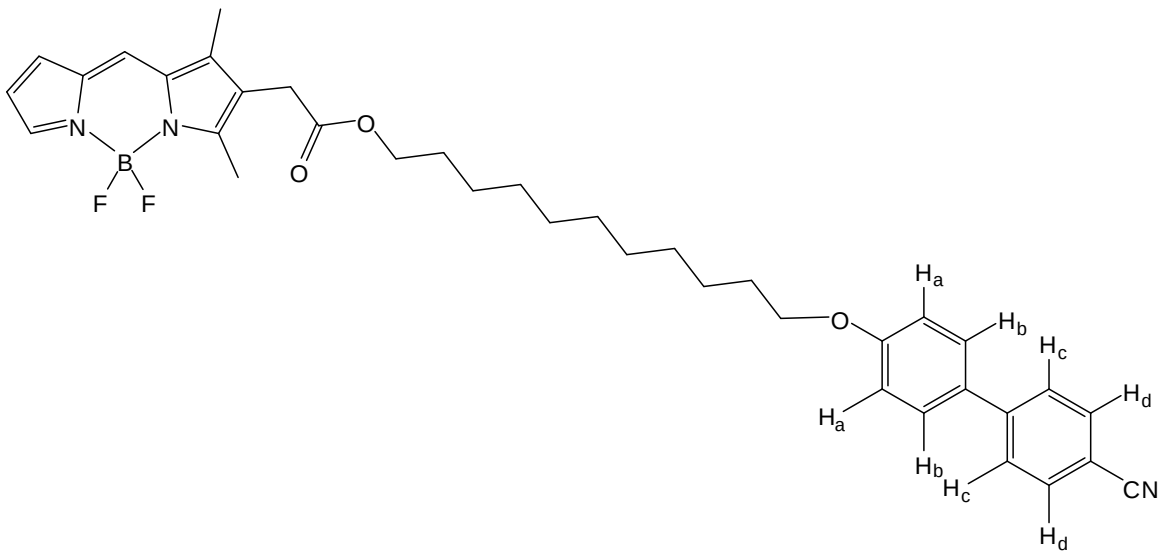

2,4-Dimethyl-3-pyrroleacetic acid (0.4g, 2.61mmol) and 2-formylpyrrole (0.25g, 2.61mmol) were suspended in glacial acetic acid (30ml). 45% Hydrobromic acid in glacial acetic acid (1.5ml) was then added and the mixture was stirred with heating for 3hrs. During this time the solution turned a very dark yellow/brown. The mixture was then cooled to r.t. and the acetic acid removed *in vacuo* to yield a dark solid. This solid was dissolved in CH_2Cl_2 and to this solution was added triethylamine (1.10ml, 7.83mmol) followed by boron trifluoride diethyletherate (1.65ml, 13.05mmol) and the solution was stirred under nitrogen overnight. The mixture was then filtered and the solvent removed from the filtrate and the crude product was purified by column chromatography (10% methanol: CH_2Cl_2) to yield the BODIPY carboxylic acid as a bright red solid (0.25g, 34% (impure)). The BODIPY free acid (0.25g, 0.899mmol), 4'-(8-hydroxyundecyl)-biphenyl-4-carbonitrile (2eq., 0.66g, 1.80mmol) and 4-dimethylaminopyridine (2eq., 0.22g, 1.80mmol) were dissolved in THF (30ml) and stirred under nitrogen and protected from light for 10 minutes. To this was added N, N'-dicyclohexylcarbodiimide (1.2eq., 0.22g, 1.08mmol) and the mixture was stirred at r.t. under nitrogen and protected from light overnight. The mixture was then filtered and the solvent removed *in vacuo*. The residue was redissolved in dichloromethane and purified

by column chromatography (4:6 hexane:CH_2Cl_2) to yield the product as a bright orange solid (220 mg, 13%), R_f = 0.36 (4:6 hexane:CH_2Cl_2). Unclear melting point.

^{1}H-NMR [400MHz, $CDCl_3$] δ 1.26 (12H, m, CH_2), 1.46 (2H, m, CH_2), 1.61 (2H, m, CH_2), 1.80 (2H, m, CH_2), 2.24 (3H, s, Py-4-Me), 2.58 (3H, s, Py-2-Me), 3.41 (2H, s, CH_2CO), 4.00 (2H, t, CH_2-O-Ph, J = 6.57), 4.08 (2H, t, CO_2CH_2, J = 6.73), 6.43 (1H, m, Py-H), 6.93 (1H, m, Py-H), 6.99 (2H, d, Ph-H_a, J = 8.76), 7.21 (1H, s, 5-H), 7.53 (2H, d, Ph-H_b, J = 8.76), 7.64 (2H, d, Ph-H_c, J = 8.44), 7.64 (1H, s, Py-H), 7.69 (2H, d, Ph-H_d, J = 8.44).

^{13}C-NMR [100MHz, $CDCl_3$] δ 10.0, 13.5, 25.9, 26.1, 28.6, 29.25, 29.30, 29.4, 29.5, 30.4, 65.5, 68.2, 110.1, 115.2, 116.5, 119.2, 124.8, 125.1, 126.6, 127.2, 128.4, 131.3, 132.7, 135.6, 139.5, 143.0, 145.4, 159.9, 162.3, 170.2. (3 peaks unobserved due to overlap of the alkyl and aromatic peaks).

^{11}B-NMR [128.3MHz, $CDCl_3$] δ -0.37.

HRMS (ESI) = calc. 643.5939, found 643.5942 ($M + NH_4^+$).

3,5-Dimethyl-2-ethoxycarbonyl-4-(2-hydroxyethyl)-1*H*-pyrrole (7):

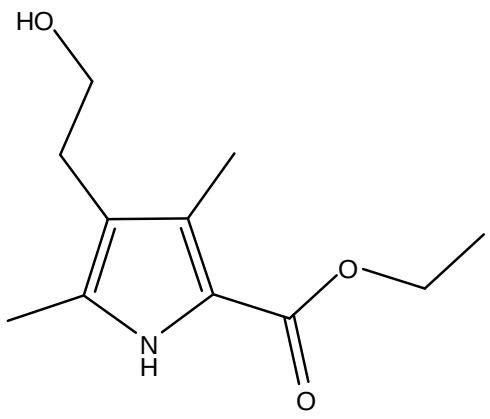

Sodium borohydride (5.04g, 0.13mol) was mixed in THF (20ml) in a 3-necked flask. To this was connected a second 3-necked flask containing 4-(methoxycarbonylacetyl)-3,5-dimethyl-2-ethoxycarbonylpyrrole (3g, 0.013mol) in THF (30ml). Nitrogen was passed through both flasks and bubbled through the pyrrole solution in the second flask. To the mixture of sodium borohydride in THF was added boron trifluoride diethyl etherate (25.2ml, 0.21mol) over a period of 3hrs. This generated diborane which was carried on the nitrogen flow from the first flask through the solution in the second flask. After addition was complete, the pyrrole solution was stirred at r.t. for an additional 14hrs. The reaction mixture was then quenched by the careful addition of methanol. The solvent was then removed to yield an oil which was triturated from hexane to yield an off-white solid (2.56g, 93%), m.p. 121-122°C (lit. 121-123°C[280]).

^{1}H-NMR [400MHz, $CDCl_3$] δ 1.35 (3H, t, -CH_2CH_3, *J* = 7.19), 2.24 (3H, s, CH_3), 2.29 (3H, s, CH_3), 2.66 (2H, t, CH_2CH_2OH, *J* = 6.73), 3.68 (2H, t, CH_2CH_2OH, *J* = 6.73), 4.29 (2H, q, CH_2CH_3, *J* = 7.09), 8.62 (1H, bs, NH).

^{13}C-NMR [100MHz, $CDCl_3$] δ 10.6, 11.7, 14.7, 27.6, 59.9, 62.8, 117.3, 117.6, 127.5, 130.6, 161.7.

MS (ESI) m/z 211.3 (M^+).

Ethyl 3,5-dimethyl-4-(2-*p*-toluenesulphonyloxyethyl)-1*H*-pyrrole-2-carboxylate (8):

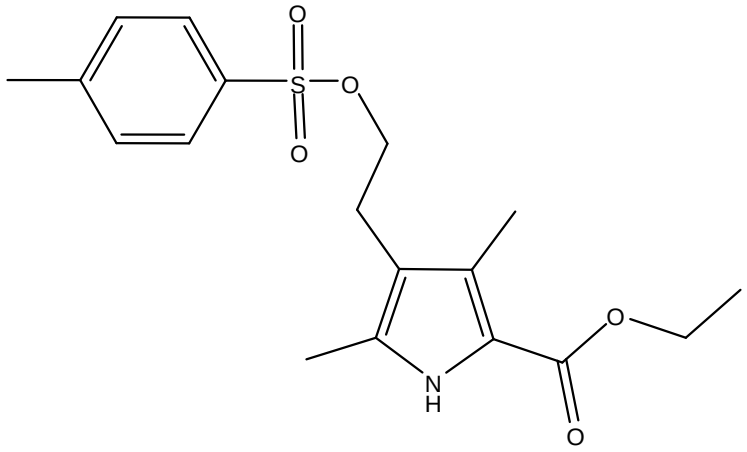

3,5-Dimethyl-2-ethoxycarbonyl-4-(2-hydroxyethyl)-1*H*-pyrrole (1.3g, 6.15mmol) and triethylamine (1.67ml, 12mmol) were dissolved in dry CH_2Cl_2 (40ml) and cooled to 0°C. To this solution was added *p*-toluenesulphonyl chloride (1.76g, 9.23mmol) over a 1hr period. The reaction mixture was then stirred at 0°C for 1hr and then allowed to warm to r.t. and stirred for 16hrs. The reaction mixture was then diluted with CH_2Cl_2 (40ml) and washed with dilute aqueous citric acid (30ml) and water (4 x 30ml), dried over anhydrous Na_2SO_4 and filtered. The solvent was then removed *in vacuo* to yield a brown oil which was triturated with hexane to yield an off-white solid (1.83g, 81%), m.p. 128-129°C (lit. 129-130°C[280]).

^{1}H-NMR [400MHz, $CDCl_3$] δ 1.35 (3H, t, CH_2CH_3, J = 7.51), 2.11 (3H, s, CH_3), 2.14 (3H, s, CH_3), 2.42 (3H, s, *p*-CH_3), 2.71 (2H, t, CH_2CH_2OH, J = 7.19), 3.99 (2H, t, CH_2OH, J = 7.19), 4.28 (2H, q, CH_2CH_3, J = 7.09), 7.26 (2H, d, Ph-H, J = 7.82), 7.66 (2H, d, Ph-H, J = 7.82), 8.63 (1H, bs, NH).

^{13}C-NMR [100MHz, $CDCl_3$] δ 10.4, 11.5, 14.7, 21.6, 24.2, 59.8, 69.9, 115.7, 117.2, 127.1, 127.8, 129.7, 130.63, 132.9, 144.6, 161.6.

MS (ESI) m/z 365.4 (M^+).

Benzyl 4-[(methoxycarbonyl)methyl]-3-acetoxymethylene-5-methylpyrrole-2-carboxylate (9):

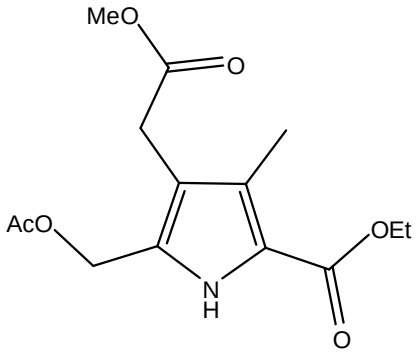

4-(Methoxycarbonylacetyl)-3,5-dimethyl-2-ethoxycarbonylpyrrole (1g, 4.18mmol) was dissolved in glacial acetic acid (10ml) and lead (IV) acetate (1.85g, 4.18mmol) was added in portions over 20mins. The mixture was then stirred at r.t. for 3hrs before water was added until the solution became cloudy. The suspension was stirred for 5mins before additional water was added to complete precipitation and the solid was filtered off. The solid was recrystallized from 60-80 petroleum ether to yield the pure product as a white solid (0.34g, 27%), m.p. 120-121°C.

^{1}H-NMR [$CDCl_3$, 400MHz] δ 1.35 (3H, t, C**H$_3$**CH_2, *J* = 9.14Hz), 2.07 (3H, s, CH_3), 2.28 (3H, s, CH_3), 3.50 (2H, s, CH_2CO_2), 3.68 (3H, s, CH_3), 4.32 (2H, q, C**H$_2$**CH_3, *J* = 7.09Hz), 5.07 (2H, s, CH_2OAc), 9.11 (1H, bs, NH).

^{13}C-NMR [$CDCl_3$, 100MHz] δ 10.4, 14.6, 20.9, 29.8, 52.2, 56.9, 60.2, 117.0, 126.8, 128.2, 154.3, 161.4, 171.6, 171.9.

MS (ESI) m/z 297.3 (M^+).

2,8-Diethoxycarbonyl-3,7-dimethyl-4,6-di(methoxycarbonylmethyl)-dipyrromethane (10):

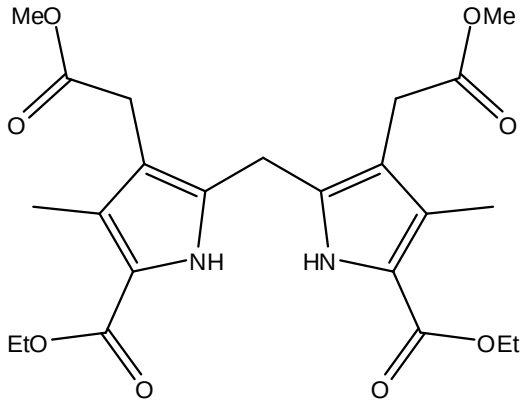

Benzyl 4-[(methoxycarbonyl)methyl]-3-acetoxymethylene-5-methylpyrrole-2-carboxylate (0.34g, 1.14mmol) was mixed in 4:1 HOAc:H_2O (4ml) and heated for 1hr. The mixture was then cooled to r.t. and diluted with water to precipitate the crude product as a white solid. The solid was recrystallized from ethanol to yield the pure product as an off-white solid (0.1g, 38%), m.p. 168-169°C.

^{1}H-NMR [$CDCl_3$, 400MHz] δ 1.33 (6H, t, 2 x C**H$_3$**CH_2, *J* = 7.20Hz), 2.29 (6H, s, 2 x CH_3), 3.53 (4H, s, 2 x CH_2CO_2), 3.79 (6H, s, 2 x CH_3), 3.87 (2H, s, *meso*-H's), 4.25 (4H, q, C**H$_2$**CH_3, *J* = 7.09Hz), 10.01 (2H, bs, 2 x NH).

Product too insoluble to acquire adequate ^{13}C-NMR.

MS (ESI) m/z 463.5 (M^+).

2,4,6,8-Tetramethyl-3,7-di[(carboxy)methyl]-dipyrromethene hydrobromide:

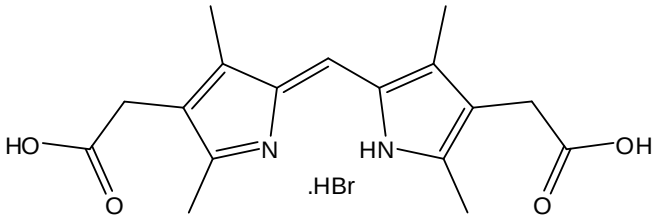

Ethyl 4-carboxymethyl-3,5-dimethyl-1*H*-pyrrole-2-carboxylate (3g, 0.013mol) and 90% formic acid (5ml) were heated to reflux then 45% hydrobromic acid (3.4ml) was added and the mixture was heated for 4hrs. The deep red mixture was then cooled to r.t. and filtered to yield the product dipyrromethene salt as a bright red solid (1.31g, 51%) m.p. >250°C.

^{1}H-NMR [400MHz, CD_3OD] δ 2.37 (6H, s, 2 x Me), 2.51 (6H, s, 2 x Me), 3.55 (4H, s, 2 x CH_2CO), 7.53 (1H, s, *meso*-H), 8.08 (1H, s, HBr).

^{13}C-NMR [100MHz, CD_3OD] δ 8.9, 11.5, 28.9, 121.6, 122.9, 127.4, 144.9, 154.2, 172.7.

HRMS (ESI) = calc. 317.1496, found. 317.1498 ($M - HBr + H^+$).

1,3,5,7-Tetramethyl-2,6-bis[acetoxycarbonyl-(4'-(8-hydroxyoctyloxy)-biphenyl-4-carbonitrile)]-BODIPY (11):

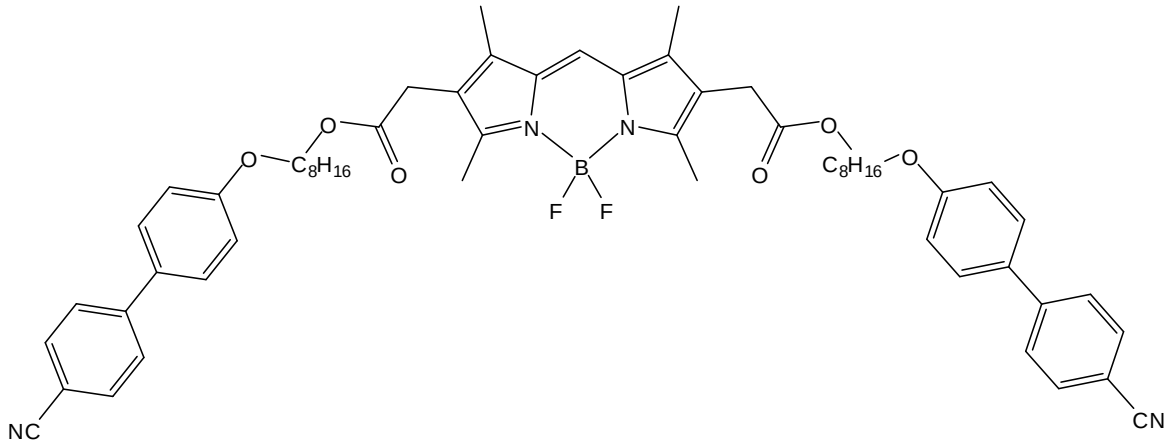

1,3,6,8-Tetramethyl-2,7-di[(carboxy)methyl]-dipyrromethene hydrobromide (0.4g, 1.01mmol) was suspended in dry dichloromethane (350ml) under a nitrogen atmosphere. DIEA (1.76ml, 10.1mmol) was then added and the mixture stirred under nitrogen for 10mins. Boron trifluoride diethyl etherate (1.26ml, 10.1mmol) was then added and the mixture was refluxed under nitrogen and protected from light for 18hrs. The solution was then cooled to r.t. before being washed with 2% $HCl_{(aq)}$ (75ml), dried over $MgSO_4$, filtered and evaporated to give the crude BODIPY dicarboxylic acid which was used without further purification. The BODIPY was then dissolved in dry THF (100ml) and DCC (0.46g, 2.22mmol) and DMAP (0.049g, 0.40mmol) were then added and the mixture was stirred for 10mins under nitrogen. 4'-(8-Hydroxyoctyl)-biphenyl-4-carbonitrile (0.72g, 2.22mmol) was then added and the solution was stirred under nitrogen and protected from light for 20hrs. The THF was then evaporated *in vacuo* and the residue redissolved in dichloromethane (100ml). This solution was washed with 2% $HCl_{(aq)}$ (50ml), brine (50ml) and water (2 x 75ml), dried over anhydrous $MgSO_4$, filtered and evaporated *in vacuo*. The residue was purified by column chromatography eluting with 1:4 hexane:dichloromethane to yield the pure product as a bright orange solid (50 mg, 5% from starting dipyrrin), R_f = 0.41 (1:4 hexane:CH_2Cl_2). Unclear melting point.

^{1}H-NMR [400MHz, $CDCl_3$] δ 1.33 (12H, m, CH_2's), 1.46 (6H, m, CH_2's), 1.61 (6H, m, CH_2's), 2.22 (6H, s, 2 x Me), 2.52 (6H, s, 2 x Me), 3.37 (4H, s, 2 x CH_2CO), 3.99 (4H, t, CH_2OCO, *J* = 6.60Hz), 4.07 (4H, t, CH_2OPh, *J* = 6.60Hz), 6.98 (4H, d, Ph-H, *J* = 8.80Hz), 7.05 (1H, s, *Meso*-H), 7.52 (4H, d, Ph-H, *J* = 8.61Hz), 7.64 (4H, d, Ph-H, *J* = 8.25Hz), 7.69 (4H, d, Ph-H, *J* = 8.25Hz).

^{13}C-NMR [100MHz, $CDCl_3$] δ 9.9, 12.9, 25.9, 26.0, 28.6, 29.18, 29.24, 29.30, 30.4, 65.2, 68.1, 110.1, 115.2, 119.2, 120.1, 127.2, 128.4, 131.4, 132.58, 132.65, 139.0, 145.3, 159.9, 170.8. (2 peaks unobserved due to overlap of the alkyl and aromatic peaks).

^{11}B-NMR [128.3MHz, $CDCl_3$] δ 0.00

HRMS (ESI) = calc. 992.5313, found. 992.5310 ($M + NH_4^+$).

Fluorescence absorption maximum: 525 nm; fluorescence emission maximum: 533 nm.

Benzyl 4-[(methoxycarbonyl)methyl]-3,5-dimethylpyrrole-2-carboxylate (12):

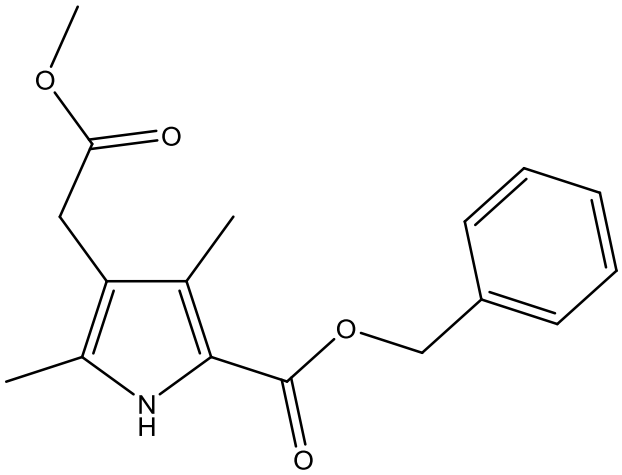

2,4-Pentanedione (9ml, 0.088mol), methyl chloroacetate (7.71ml, 0.088mol), potassium carbonate (12.16g, 0.088mol) and potassium iodide (2.66g, 0.016mol) were mixed in butanone (45ml) and stirred at reflux for 18hrs. The mixture was then cooled to r.t., filtered and the solvent was removed to give an orange oil which was distilled under reduced pressure to yield a light yellow oil (9.01g, 0.052mol) which was kept aside for the pyrrole synthesis.

Benzyl acetoacetate (9ml, 0.052mol) was then dissolved in glacial acetic acid (15ml) and cooled in an ice-bath. To this cooled mixture was added a solution of sodium nitrite (3.77g, 0.055mol) in water (13ml) dropwise with stirring. Once addition was complete the mixture was allowed to warm to r.t. and stirred for a further 1hr. After stirring was complete the product from the first step was added to the solution of the oxime along with an additional 10ml glacial acetic acid. To this was added a mixture of zinc powder (9.18g, 0.14mol) and sodium acetate (9.38g, 0.11mol) in portions maintaining the temperature of the mixture around 70°C. Once the addition was complete the mixture was heated at reflux for a further 3hrs. While still hot the mixture was poured into 250ml cold water. The product was then extracted with dichloromethane which was then dried over anhydrous magnesium sulphate, filtered and the solvent removed to yield a yellow oil. To the oil was added a 1:1 mixture of water:methanol (50ml) and the mixture left to stand for

10mins during which time the product began to precipitate. Full precipitation was achieved by the dilution of the water:methanol solution with water. The product was then filtered off and twice recrystallised from methanol to yield the pure product as an off-white solid (7.08g, 45%), m.p.: 93-94°C (lit. 93-94°C[281]).

^{1}H-NMR [400MHz, $CDCl_3$] δ 2.22 (3H, s, Me), 2.29 (3H, s, Me), 3.38 (2H, s, CH_2CO), 3H, s, OMe), 5.29 (2H, s, CH_2Ph), 7.37 (5H, m, Bn), 8.74 (1H, bs, NH).

^{13}C-NMR [100MHz, $CDCl_3$] δ 10.8, 11.7, 30.0, 52.0, 65.6, 114.7, 116.8, 128.18, 128.22, 128.6, 131.1, 136.5, 172.2.

MS (ESI) m/z 301.3 (M^+).

Benzyl-4-carboxymethyl-3,5-dimethylpyrrole-2-carboxylate (13):

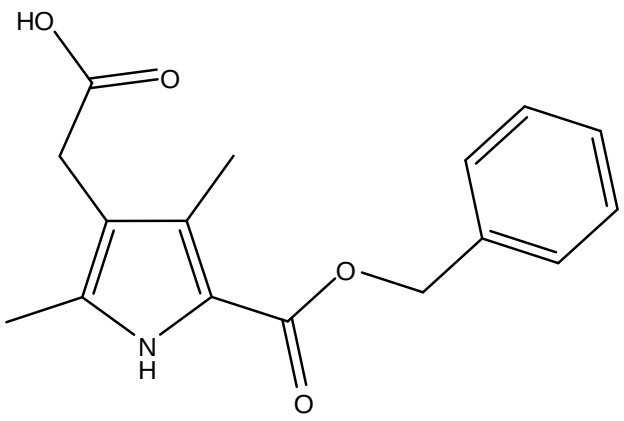

Benzyl 4-[(methoxycarbonyl)methyl]-3,5-dimethylpyrrole-2-carboxylate (1g, 3.32mmol) in ethanol (20ml) and sodium hydroxide (0.15g, 3.65mmol) in water (2.5ml) were mixed together and stirred at r.t. for 18hrs. An additional 5ml water was added and the ethanol removed *in vacuo*. The residue was further diluted with water (45ml) and acidified with hydrochloric acid which caused the product to precipitate. The solid was filtered and washed with water and dried *in vacuo* to yield the pure product as a tan solid (0.67g, 71%), m.p.: 192-194°C (lit. 193-194°C[282]).

^{1}H-NMR [400MHz, $CDCl_3$] δ 2.23 (3H, s, Me), 2.30 (3H, s, Me), 3.42 (2H, s, CH_2CO), 5.29 (2H, s, CH_2Ph), 7.37 (5H, m, Bn), 8.74 (1H, bs, NH).

^{13}C-NMR [100MHz, $CDCl_3$] δ 10.7, 11.6, 29.6, 65.6, 114.0, 116.9, 128.1, 128.2, 128.5, 131.3, 136.4, 176.0.

MS (ESI) m/z 310.3 ($M + Na^+$).

Benzyl 4-[(Methoxycarbonyl)-4-(11-hydroxyundecyloxy)-phenyl-4'-cyano-4-biphenylcarboxylate]-3,5-dimethylpyrrole-2-carboxylate (14):

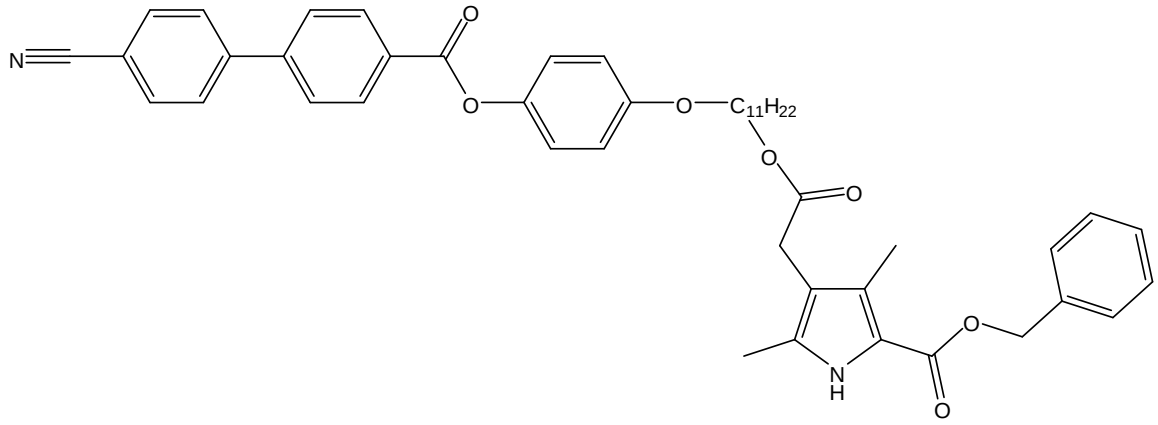

Benzyl-4-carboxymethyl-3,5-dimethylpyrrole-2-carboxylate (0.5g, 1.74mmol) and 4-(11-hydroxyundecyloxy)-phenyl-4'-cyano-4-biphenyl carboxylate (0.86g, 1.77mmol) were dissolved in dry dichloromethane (40ml). DCC (0.61g, 0.03mol) and DMAP (0.22g, 1.79mmol) were then added and the mixture stirred under nitrogen for 20hrs. The mixture was then filtered and the filtrate washed with 2% $HCl_{(aq)}$ (40ml), sat. $Na_2CO_{3(aq)}$ (40ml) and water (2 x 40ml), dried over anhydrous Na_2SO_4, filtered and evaporated *in vacuo*. The crude product was purified by column chromatography eluting with dichloromethane followed by recrystallisation from ethanol to yield the product as a pale yellow solid (0.59g, 45%), R_f = 0.61 (CH_2Cl_2).

^{1}H-NMR [400MHz, $CDCl_3$] δ 1.21 (12H, m, CH_2's), 1.41 (4H, m, CH_2's), 1.76 (2H, m, CH_2), 2.16 (3H, s, Me), 2.23 (3H, s, Me), 3.29 (2H, s, CH_2CO), 3.98 (4H, 2 x t, CH_2OCO + CH_2OPh, J = 6.78Hz), 5.22 (2H, s, CH_2Ph), 6.91 (2H, d, Ph-H, J = 8.80Hz), 7.25 (2H, d, Ph-H, J = 8.80Hz), 7.32 (5H, m, Bn-H), 7.57 (2H, d, Ph-H, J = 8.43Hz), 7.61 (2H, d, Ph-H, J = 8.43Hz), 7.66 (2H, d, Ph-H, J = 8.61Hz), 8.10 (2H, d, Ph-H, J = 8.80Hz), 8.54 (1H, bs, NH).

^{13}C-NMR [100MHz, $CDCl_3$] δ 10.7, 11.6, 25.8, 29.45, 29.47, 29.49, 64.9, 65.5, 68.3, 76.7, 77.0, 77.3, 111.0, 114.4, 114.8, 116.7, 118.9, 121.2, 122.6, 127.7, 128.1, 128.3, 128.5, 132.3, 132.7, 144.9, 151.6, 163.7, 164.9, 171.8. (9 peaks unobserved due to overlap of the alkyl and aromatic peaks).

HRMS (ESI) = calc. 772.3956, found. 772.3958 ($M + NH_4^+$).

4-(11-Hydroxyundecyloxy)-benzoic acid (15):

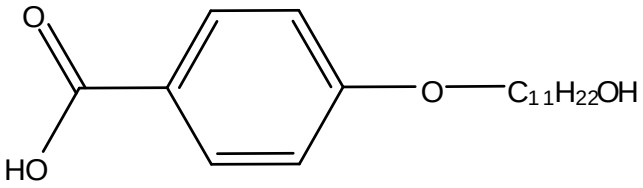

4-Hydroxybenzoic acid (6g, 0.043mol) and sodium hydroxide (3.44g in 21ml water) was dissolved in ethanol (100ml) and heated to reflux. 11-Bromoundecanol (8.25g, 0.033mol) in ethanol (25ml) was then added dropwise. Once addition was complete, the mixture was refluxed for 16hrs. The mixture was then cooled to r.t. and the ethanol was removed by evaporation *in vacuo*. Water (150ml) was then added and the solution acidified with conc. $HCl_{(aq)}$ and the resulting precipitate filtered off and recrystallized from isopropanol to yield a white solid (7.28g, 72%) m.p. 108-110°C (lit. 110°C[283]).

^{1}H-NMR [CD_3OD, 400MHz] δ 1.32 (12H, m, CH_2's), 1.50 (4H, m, CH_2's) 1.78 (2H, m, CH_2), 3.53 (2H, t, CH_2OH, *J* = 6.57Hz), 4.03 (2H, t, CH_2O, *J* = 6.57Hz), 6.96 (2H, d, Ph-H, *J* = 9.07Hz), 7.95 (2H, d, Ph-H, *J* = 9.07Hz).

^{13}C-NMR [CD_3OD, 100MHz] δ 26.9, 30.59, 30.64, 30.68, 33.7, 63.0, 69.3, 115.1, 123.8, 132.8, 164.6, 169.9. (4 peaks unobserved due to overlap of the alkyl peaks).

HRMS (ESI) = calc. 309.2060, found. 309.2063 ($M + H^+$).

4-(11-Hydroxyundecyloxy)-phenyl-4'-cyano-4-biphenyl carboxylate (16):

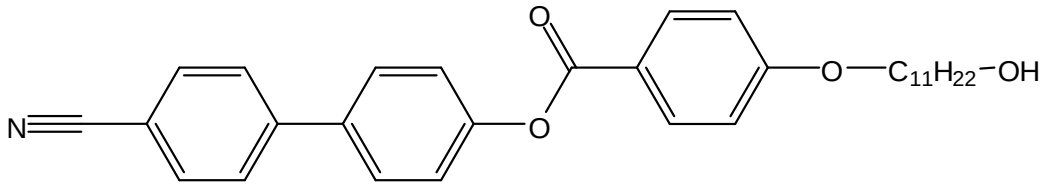

4-(11-Hydroxyundecyloxy)benzoic acid (2g, 6.48mmol) and 4'-(11-hydroxyundecyl)-biphenyl-4-carbonitrile (1.29g, 6.61mmol) were dissolved in dry dichloromethane (80ml). DCC (2.27g, 0.088mol) and DMAP (0.82g, 6.68mmol) were then added and the mixture was stirred under nitrogen for 20hrs. The mixture was then filtered and the filtrate washed with 2% $HCl_{(aq)}$ (50ml), sat. $Na_2CO_{3(aq)}$ (50ml) and water (2 x 50ml), dried over anhydrous $MgSO_4$, filtered and evaporated *in vacuo*. The residue was recrystallized from ethyl acetate to yield the product as a white solid (2.11g, 67%), Cr 125 N 175 I.

^{1}H-NMR [$CDCl_3$, 400MHz] δ 1.29 (12H, m, CH_2), 1.46 (4H, m, CH_2), 1.81 (2H, m, CH_2), 3.63 (2H, t, CH_2OH, *J* = 6.72Hz), 4.03 (2H, t, CH_2OPh, *J* = 6.72Hz), 6.96 (2H, d, Ph-H, *J* = 9.07Hz), 7.31 (2H, d, Ph-H, *J* = 8.76Hz), 7.62 (2H, d, Ph-H, *J* = 8.76Hz), 7.68 (2H, d, Ph-H, *J* = 8.44Hz), 7.71 (2H, d, Ph-H, *J* = 8.76Hz), 8.14 (2H, d, Ph-H, *J* = 8.76Hz).

^{13}C-NMR [$CDCl_3$, 100MHz] δ 25.7, 29.47, 29.50, 29.55, 32.8, 63.1, 68.3, 111.0, 114.4, 118.9, 121.2, 122.6, 127.7, 128.3, 132.3, 132.6, 136.7, 144.9, 151.6, 163.7, 164.8. (4 peaks unobserved due to overlap of the alkyl and aromatic peaks).

HRMS (ESI) = calc. 503.2904, found. 503.2899 ($M + NH_4^+$).

8-(4-Bromophenyl)-BODIPY (17):

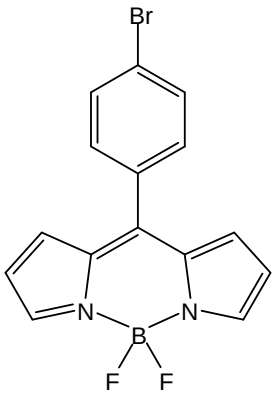

4-Bromobenzaldehyde (5g, 0.027mol) was dissolved in pyrrole (75ml) and the solution was degassed with nitrogen for 20mins. TFA (0.2ml) was then added and the mixture was stirred for 20mins. The pyrrole was removed *in vacuo* and dichloromethane (100ml) was then added and the solution was washed with sat. $Na_2CO_{3(aq)}$ (50ml) and water (2 x 50ml), dried over $MgSO_4$ and evaporated. The residue was redissolved in dichloromethane (100ml) and chloranil (6.64g, 0.027mol) was added and the mixture was stirred for 16hrs. Diisopropylethylamine (25.87ml, 0.15mol) was then added followed by boron trifluoride diethyl etherate (24.99ml, 0.024mol) and the mixture was stirred under nitrogen for 16hrs. The solution was then washed with 2% $HCl_{(aq)}$ (75ml) and water (3 x 75ml), dried over anhydrous $MgSO_4$ and evaporated *in vacuo*. The residue was purified by column chromatography eluting with 4:6 hexane:CH_2Cl_2 to yield the product as a red solid (0.52g, 6%), m.p. 202-203°C, lit. 202-203°C[264].

^{1}H-NMR [400MHz, $CDCl_3$] δ 6.56 (2H, m, Py-H), 6.91 (2H, m, Py-H), 7.45 (2H, d, Ph-H, *J* = 8.61Hz), 7.67 (2H, d, Ph-H, *J* = 8.61Hz), 7.96 (2H, m, Py-H).

^{13}C-NMR [100MHz, $CDCl_3$] δ 118.8, 125.5, 131.3, 131.8, 132.7, 134.7, 144.6, 145.8.

^{11}B-NMR [128.3MHz, $CDCl_3$] δ -0.49.

HRMS (ESI) = calc. 368.9981 and 370.9960, found. 368.9984 and 370.9963 ($M + Na^+$).

5-(4-Iodophenyl)-dipyrromethane:

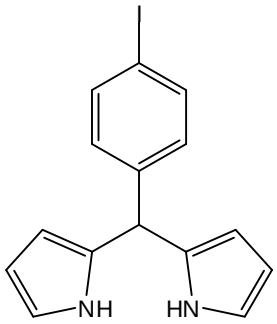

4-Iodobenzaldehyde (6.29g, 0.027mol) was dissolved in freshly distilled pyrrole (75ml, 1.08mol) and degassed with nitrogen for 15mins. TFA (0.1ml) was then added and the solution stirred at r.t. under nitrogen for 20mins. The excess pyrrole was then removed by evaporation *in vacuo* and the oily residue was purified by column chromatography eluting with 1:4 EtOAc:CH_2Cl_2 to give a tan oil which crystallized on standing to yield a tan solid. The resulting solid was recrystallized from EtOH to yield the pure product as a brown solid (5.27g, 56%), m.p. 144-146°C (lit. 145-146°C[284]).

^{1}H-NMR [400MHz, $CDCl_3$] δ 5.40 (1H, s, *meso*-H), 5.87 (2H, m, Py-H), 6.13 (2H, m, Py-H), 6.69 (2H, m, Py-H), 6.94 (2H, d, Ph-H), 7.61 (2H, d, Ph-H), 7.90 (2H, bs, NH).

^{13}C-NMR [100MHz, $CDCl_3$] δ 43.6, 107.4, 108.2, 108.6, 117.5, 117.7, 130.2, 130.3, 130.4, 137.4, 137.6, 137.7.

MS (ESI) m/z 348.2 (M^+).

8-(4-Iodophenyl)-BODIPY (18):

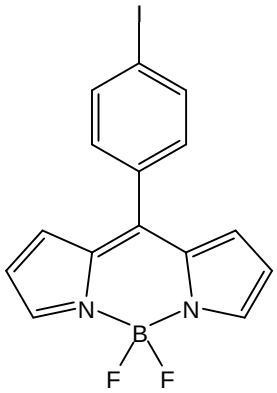

5-(4-Iodophenyl)-dipyrromethane (2g, 5.74mmol) was dissolved in THF (70ml) and to this solution was added DDQ (1.30g, 5.74mmol) and the solution was stirred at r.t. for 4hrs. The THF was then removed *in vacuo* and dichloromethane (150ml) was added to the residue. The mixture was sonicated and filtered to remove the reduced DDQ and the dichloromethane removed *in vacuo*. The residue was redissolved in dichloromethane (100ml) and purged with nitrogen. Diisopropylethylamine (5.05ml, 29mmol) was then added followed by boron trifluoride diethyl etherate (4.36ml, 34mmol) and the solution was stirred at r.t. under nitrogen for 16hrs. The mixture was then filtered through celite and washed with water (3 x 50ml), dried over anhydrous $MgSO_4$ and evaporated *in vacuo*. The residue was purified by column chromatography eluting with 1:1 hexane:CH_2Cl_2 to yield the pure product as a red solid (416 mg, 18%), m.p. 231-232°C.

^{1}H-NMR [400MHz, $CDCl_3$] δ 6.56 (2H, m, Py-H), 6.91 (2H, m, Py-H), 7.31 (2H, d, Ph-H, *J* = 8.43Hz), 7.89 (2H, d, Ph-H, *J* = 8.43Hz), 7.96 (2H, m, Py-H).

^{13}C-NMR [100MHz, $CDCl_3$] δ 97.5, 118.8, 131.3, 131.9, 133.2, 134.6, 137.8, 144.6, 145.9.

^{11}B-NMR [128.3MHz, $CDCl_3$] δ -0.4891.

MS (ESI) = 394.0 (M^-).

8-(4-Iodophenyl)-1,3,5,7-tetramethyl-BODIPY (19):

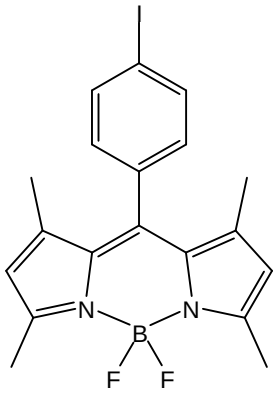

4-Iodobenzoyl chloride (2g, 7.51mmol) and 2,4-dimethylpyrrole (1.55ml, 15.2mmol) were dissolved in dry dichloromethane (60ml) and the solution was refluxed under nitrogen for 3hrs. The solution was cooled to r.t. and triethylamine (4.88ml, 35mmol) was then added followed by boron trifluoride diethyl etherate (5.01ml, 39.5mmol) and the solution was stirred at r.t. for 16hrs. The solution was then washed with water (3 x 50ml) and dried over anhydrous $MgSO_4$ and evaporated *in vacuo*. The residue was purified by column chromatography eluting with 1:1 hexane:$CHCl_3$ to yield the pure product as a bright orange solid (1.18g, 35%), m.p. 213-214°C, lit. 213-215°C[35].

^{1}H-NMR [400MHz, $CDCl_3$] δ 1.42 (6H, s, 2 x CH_3), 2.55 (6H, s, 2 x CH_3), 5.99 (2H, s, Py-H), 7.04 (2H, d, Ph-H, *J* = 8.43Hz), 7.85 (2H, d, Ph-H, *J* = 8.43Hz).

^{13}C-NMR [100MHz, $CDCl_3$] δ 14.59, 14.65, 94.7, 121.4, 129.9, 131.1, 134.6, 138.3, 142.9, 155.9.

^{11}B-NMR [128.3MHz, $CDCl_3$] δ -0.2446.

HRMS (ESI) = calc. 451.0649, found 451.0650 ($M + H^+$).

8-(4-Iodophenyl)-1,3,5,7-tetramethyl-2,6-diethyl-BODIPY (20):

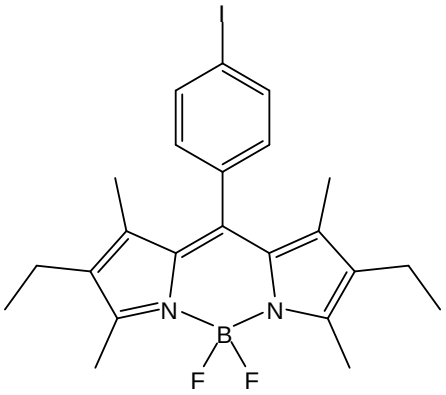

4-Iodobenzoyl chloride (2g, 7.51mmol) and kryptopyrrole (2.03ml, 15.02mmol) were dissolved in dry dichloromethane (60ml) and the solution was heated at reflux under nitrogen for 3hrs. The solution was cooled to r.t. and triethylamine (4.88ml, 35.0mmol) was then added followed by boron trifluoride diethyl etherate (5.01ml, 39.5mmol) and the solution was stirred under nitrogen for 18hrs. The solution was then washed with water (4 x 50ml), dried over anhydrous $MgSO_4$ and evaporated *in vacuo*. The residue was passed through a short silica column eluting with 1:4 hexane:toluene and evaporated *in vacuo*. The crude product was purified by column chromatography eluting with 1:4 CH_2Cl_2:hexane after dry loading to yield the pure product as a bright red solid (1.36g, 36%), m.p. 290°C (decomp.).

^{1}H-NMR [400MHz, $CDCl_3$] δ 0.98 (6H, t, 2 x C**H$_3$**CH_2, *J* = 7.52Hz), 1.31 (6H, s, 2 x CH_3), 2.29 (4H, q, 2 x C**H$_2$**CH_3, *J* = 7.57Hz), 2.52 (6H, s, 2 x CH_3), 7.04 (2H, d, Ph-H, *J* = 7.88Hz), 7.83 (2H, d, Ph-H, *J* = 7.88Hz).

^{13}C-NMR [100MHz, $CDCl_3$] δ 11.9, 12.5, 14.6, 17.1, 94.4, 130.3, 133.0, 135.4, 138.2, 154.1.

^{11}B-NMR [128.3MHz, $CDCl_3$] δ 0.0000.

HRMS (ESI) = calc. 507.1279, found 507.1269 $(M + H)^+$.

4-(11-[4-Boronpinacolatephenylcarboxy]undecyloxy)-phenyl-4'-cyano-4-biphenyl carboxylate (21):

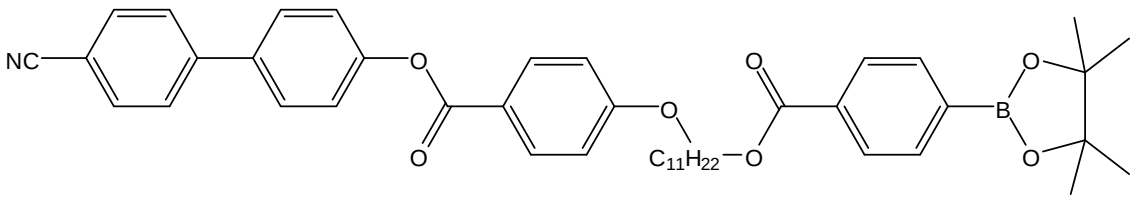

4-(11-Hydroxyundecyloxy)-phenyl-4'-cyano-4-biphenyl carboxylate (0.80g, 1.64mmol), 4-carboxyphenylboronic acid pinacol ester (0.40g, 1.61mmol), DCC (0.56g, 2.74mmol) and DMAP (0.20g, 1.66mmol) were dissolved in dry dichloromethane (50ml) and the solution was stirred at r.t. for 16hrs. The precipitate was then filtered off and the filtrate was washed with 2% $HCl_{(aq)}$ (40ml) and water (2 x 40ml), dried over anhydrous $MgSO_4$ and evaporated *in vacuo*. The residue was then recrystallized from ethyl acetate to yield the pure product as a white crystalline solid (0.80g, 78%).

^{1}H-NMR [400MHz, $CDCl_3$] δ 1.33 (10H, m, CH_2's), 1.36 (12H, s, 4 x CH_3), 1.47 (4H, m, CH_2's), 1.80 (4H, m, CH_2's), 4.06 (2H, t, CH_2OPh, *J* = 6.51Hz), 4.33 (2H, t, CH_2O, *J* = 6.78Hz), 6.99 (2H, d, Ph-H, *J* = 8.98Hz), 7.34 (2H, d, Ph-H, *J* = 8.61Hz), 7.65 (2H, d, Ph-H, *J* = 8.80Hz), 7.70 (2H, d, Ph-H, *J* = 8.61Hz), 7.75 (2H, d, Ph-H, *J* = 8.61Hz), 7.87 (2H, d, Ph-H, *J* = 8.43Hz), 8.03 (2H, d, Ph-H, *J* = 8.43Hz), 8.16 (2H, d, Ph-H, *J* = 8.98Hz).

^{13}C-NMR [100MHz, $CDCl_3$] δ 24.9, 26.0, 28.7, 29.1, 29.2, 29.3, 29.5, 65.2, 68.4, 84.2, 111.0, 114.4, 118.9, 121.2, 122.6, 127.7, 128.3, 128.5, 132.3, 132.6, 132.7, 134.6, 136.7, 144.9, 151.6, 163.7, 164.8, 166.7. (5 peaks unobserved due to overlap of the alkyl and aromatic peaks).

^{11}B-NMR [128.3MHz, $CDCl_3$] δ 29.74.

HRMS (ESI) = calc. 733.4026, found 733.4011 ($M + NH_4^+$).

8-(4-[4-Carboxyphenyl]phenyl)-BODIPY (22):

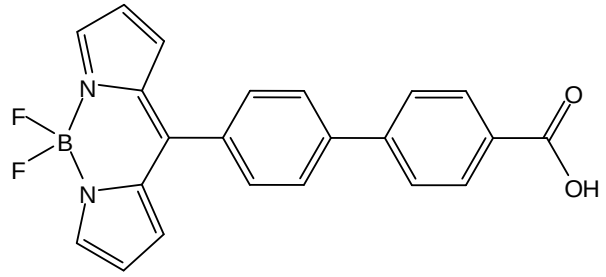

5-(4-Iodophenyl)-BODIPY (200 mg, 0.51mmol), palladium acetate (34 mg, 0.15mmol), triphenyl arsine (62 mg, 0.20mmol) and potassium fluoride (88 mg, 1.52mmol) were dissolved in THF (15ml) and degassed with argon for 30mins. 4-Carboxyphenylboronic acid (151 mg, 0.91mmol) dissolved in THF (5ml) was then added and the solution was heated at 50°C for 50hrs. The THF was then removed *in vacuo* and the residue was purified by column chromatography eluting with 0-10% MeOH in dichloromethane to yield the pure product as a red solid (96 mg, 49%), m.p. 257-258°C.

^{1}H-NMR [400MHz, $CDCl_3$] δ 6.59 (2H, m, Py-H), 7.02 (2H, m, Py-H), 7.69 (2H, d, Ph-H, *J* = 8.13Hz), 7.34 (2H, d, Ph-H, *J* = 8.13Hz), 7.81 (2H, d, Ph-H, *J* = 8.13Hz), 7.96 (2H, m, Py-H), 8.19 (2H, d, Ph-H, *J* = 8.13Hz).

^{13}C-NMR [100MHz, $CDCl_3$] δ 118.5, 126.9, 127.1, 127.2, 130.4, 130.5, 131.0, 131.4, 133.2, 134.7, 142.6, 143.6, 144.0, 168.1.

^{11}B-NMR [128.3MHz, $CDCl_3$] δ -0.4891.

HRMS (ESI) = calc. 388.1189, found 388.1203 (M^+).

8-(4-[11-Carboxyphenylundecyloxy-phenyl-4'-cyano-4-biphenyl-carboxylate]-phenyl)-BODIPY (23):

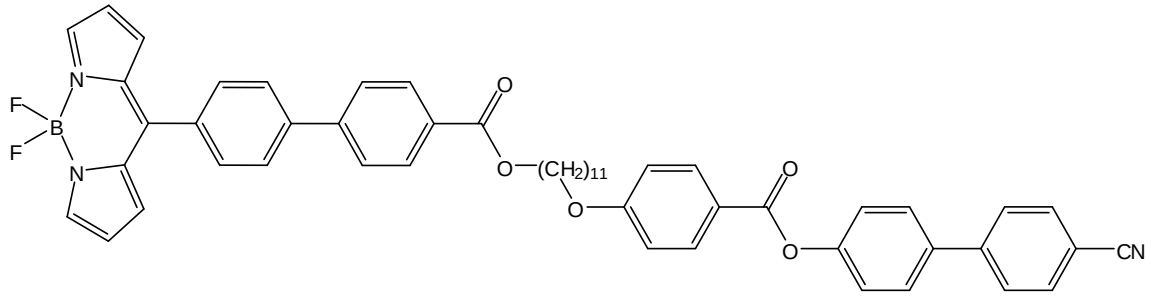

8-(4-Iodophenyl)-BODIPY (50 mg, 0.144mmol), 4-(11-[4-boronpinacolatephenylcarboxy]undecyloxy)-phenyl-4'-cyano-4-biphenyl carboxylate (109 mg, 0.173mmol), palladium (II) acetate (9.7 mg, 43.2μmol), (2-biphenyl)di-*tert*-butylphosphine (17 mg, 57.6μmol) and sodium carbonate (46 mg, 0.432mmol) were mixed in DMF (6ml) and degassed with argon for 30mins. The mixture was then heated in a microwave for 5mins at 65°C (75W). The DMF was then removed *in vacuo* and the residue was purified by column chromatography eluting with 1:1 hexane:CH_2Cl_2 to yield the pure product as a red solid (24 mg, 20%), R_f = 0.61 (CH_2Cl_2), LC transitions: Cr (N 159) 162 I.

^{1}H-NMR [400MHz, $CDCl_3$] δ 1.33 (10H, m, CH_2's), 1.48 (4H, m, CH_2's), 1.81 (4H, m, CH_2's), 4.04 (2H, t, CH_2OPh, *J* = 6.60Hz), 4.36 (2H, t, CH_2O, *J* = 6.78Hz), 6.56 (2H, m, Py-H), 6.98 (4H, m, Py-H + Ph-H), 7.31 (2H, d, Ph-H, *J* = 8.61Hz), 7.63 (2H, d, Ph-H, *J* = 8.61Hz), 7.67 (4H, d, Ph-H, *J* = 8.43Hz), 7.73 (4H, 2 x d, Ph-H), 7.78 (2H, d, Ph-H, *J* = 8.43Hz), 7.96 (2H, m, Py-H), 8.16 (4H, 2 x d, Ph-H).

^{13}C-NMR [100MHz, $CDCl_3$] δ 25.98, 26.03, 28.7, 29.1, 29.27, 29.33, 29.5, 65.3, 68.3, 111.0, 114.3, 118.7, 121.2, 122.6, 127.1, 127.3, 127.7, 128.3, 130.3, 131.2, 131.5, 132.3, 132.7, 133.5, 134.9, 136.7, 144.3, 144.9, 151.6, 163.7, 166.4. (8 peaks unobserved due to overlap of the alkyl and aromatic peaks).

^{11}B-NMR [128.3MHz, $CDCl_3$] δ -0.4891.

HRMS (ESI) = calc. 873.4002, found. 873.4003 ($M + NH_4^+$).

HPLC retention time (80:20 MeCN:DCM): 3.47 mins.

Fluorescence absorption maximum: 505 nm; fluorescence emission maximum: 526 nm.

8-(4-[11-Carboxyphenylundecyloxy-phenyl-4'-cyano-4-biphenyl-carboxylate]-phenyl)-1,3,5,7-tetramethyl-BODIPY (24):

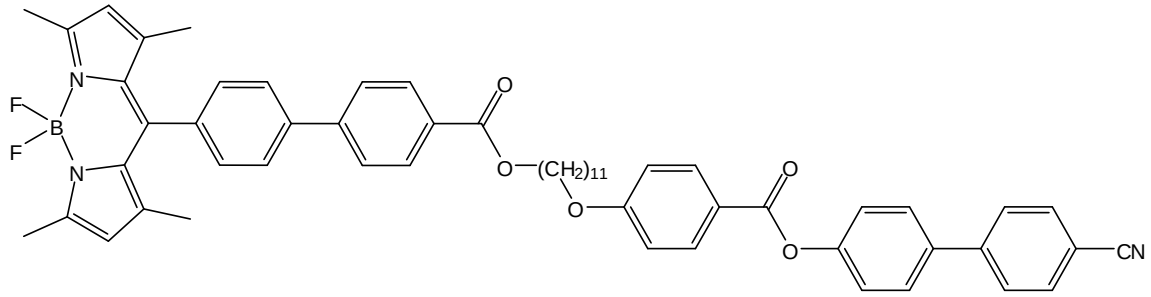

8-(4-Iodophenyl)-2,4,6,8-tetramethyl-BODIPY (60 mg, 0.133mmol), 4-(11-[4-boronpinacolatephenylcarboxy]undecyloxy)-phenyl-4'-cyano-4-biphenyl carboxylate (101 mg, 0.160mmol), dibenzylideneacetone palladium (II) (36 mg, 39.5μmol), (2-biphenyl)di-*tert*-butylphosphine (16 mg, 53.2μmol) and potassium carbonate (55 mg, 0.399mmol) were mixed in DMF (6ml) and degassed with argon for 30mins. The mixture was then heated in a microwave for 5mins at 65°C (75W). The DMF was then removed *in vacuo* and the residue was subjected column chromatography eluting with 0.5:99.5 EtOAc:toluene. The residue was precipitated from CH_2Cl_2 with cold MeOH to yield the pure product as a bright orange solid (59 mg, 49%), R_f = 0.21 (toluene), LC transitions: Cr (N 153) 211 I.

^{1}H-NMR [400MHz, $CDCl_3$] δ 1.34 (10H, m, CH_2's), 1.44 (6H, s, 2 x CH_3), 1.49 (4H, m, CH_2's), 1.81 (4H, m, CH_2's), 2.57 (6H, s, 2 x CH_3), 4.05 (2H, t, CH_2OPh, J = 6.57Hz), 4.36 (2H, t, CH_2O, J = 6.72Hz), 6.00 (2H, s, Py-H), 6.98 (2H, d, Ph-H, J = 8.76Hz), 7.32 (2H, d, Ph-H, J = 8.76Hz), 7.39 (2H, d, Ph-H, J = 8.13Hz), 7.63 (2H, d, Ph-H, J = 8.76Hz), 7.69 (2H, d, Ph-H, J = 8.44Hz), 7.75 (6H, m, Ph-H), 8.15 (4H, dd, Ph-H).

^{13}C-NMR [100MHz, $CDCl_3$] δ 14.6, 26.00, 26.05, 28.8, 29.1, 29.3, 29.4, 29.5, 53.4, 65.3, 68.4, 111.0, 114.4, 118.9, 121.2, 121.3, 122.6, 127.0, 127.7, 127.8, 128.4, 128.8, 129.8, 130.2, 132.4, 132.7, 134.9, 136.7, 140.6, 143.0, 144.3, 151.6, 155.7, 163.7, 164.8, 166.4. (5 peaks unobserved due to overlap of the alkyl and aromatic peaks).

^{11}B-NMR [128.3MHz, $CDCl_3$] δ -0.1836

HRMS (ESI) = calc. 892.4301, found. 892.4274 ($M - F^-$).

HPLC retention time (80:20 MeCN:DCM): 7.52 mins.

Fluorescence absorption maximum: 505 nm; fluorescence emission maximum: 517 nm.

8-(4-[11-Carboxyphenylundecyloxy-phenyl-4'-cyano-4-biphenyl-carboxylate]-phenyl)-1,3,5,7-tetramethyl-2,6-diethyl-BODIPY (25):

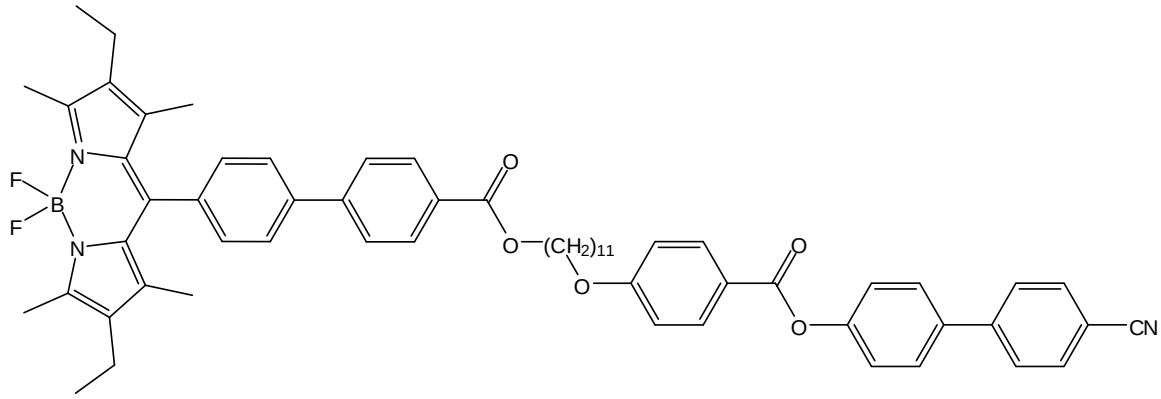

8-(4-Iodophenyl)-2,4,6,8-tetramethyl-3,7-diethyl-BODIPY (60 mg, 0.119mmol), 4-(11-[4-boronpinacolatephenylcarboxy]undecyloxy)-phenyl-4'-cyano-4-biphenyl carboxylate (90 mg, 0.143mmol), dibenzylideneacetone palladium (II) (33 mg, 35.7μmol), (2-biphenyl)di-*tert*-butylphosphine (14 mg, 47.6μmol) and potassium carbonate (49 mg, 0.357mmol) were mixed in DMF (6ml) and degassed with argon for 30mins. The mixture was then heated in a microwave for 5mins at 65°C (75W). The DMF was then removed *in vacuo* and the residue was subjected to column chromatography eluting with 2:98 EtOAc:toluene. The residue was precipitated from CH_2Cl_2 with cold MeOH to yield the pure product as a bright red solid (48 mg, 42%), m.p. 192-194°C, R_f = 0.19 (toluene).

^{1}H-NMR [400MHz, $CDCl_3$] δ 0.97 (6H, t, 2 x C**H$_3$**CH$_2$, *J* = 7.50Hz), 1.33 (16H, m, CH_2's + 2 x CH_3), 1.48 (4H, m, CH_2's), 1.80 (4H, m, CH_2's), 2.29 (4H, q, C**H$_2$**CH$_3$, *J* = 7.50Hz), 2.53 (6H, s, 2 x CH_3), 4.04 (2H, t, CH_2OPh, *J* = 6.57Hz), 4.35 (2H, t, CH_2O, *J* = 6.73Hz), 6.97 (2H, d, Ph-H, *J* = 8.76Hz), 7.31 (2H, d, Ph-H, *J* = 8.44Hz), 7.38 (2H, d, Ph-H, *J* = 8.44Hz), 7.62 (2H, d, Ph-H, *J* = 8.76Hz), 7.67 (2H, d, Ph-H, *J* = 8.44Hz), 7.73 (6H, m, Ph-H), 8.14 (4H, 2 x d, Ph-H).

^{13}C-NMR [100MHz, $CDCl_3$] δ 11.9, 12.5, 14.6, 17.1, 26.00, 26.03, 28.7, 29.2, 29.3, 29.5, 65.2, 68.4, 114.4, 121.2, 122.6, 127.0, 127.7, 128.3, 129.1, 130.2, 132.4, 132.7, 136.6, 138.3, 140.3, 144.4, 144.8, 151.6, 153.9, 163.7. (10 peaks unobserved due to overlap of the alkyl and aromatic peaks).

^{11}B-NMR [128.3MHz, $CDCl_3$] δ 0.0000

HRMS (ESI) = calc. 990.4809, found. 900.4798 ($M + Na^+$).

HPLC retention time (80:20 MeCN:DCM): 10.93 mins.

Fluorescence absorption maximum: 528 nm; fluorescence emission maximum: 543 nm.

8-(4-Trimethylsilylethynylphenyl)-BODIPY:

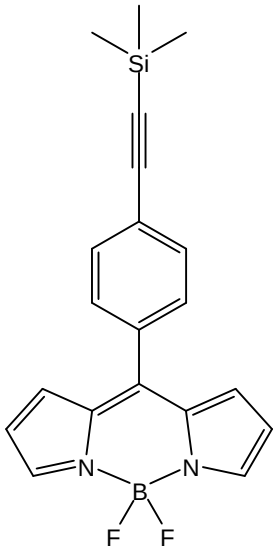

4-[(Trimethylsilyl)ethynyl]benzaldehyde (2g, 9.89mmol) was dissolved in freshly distilled pyrrole (17.2ml, 0.25mol) and the mixture was degassed with argon for 15mins. TFA (0.1ml) was then added and the mixture was stirred at r.t. under argon for 15mins. The excess pyrrole was then distilled off under reduced pressure. The oily residue was then passed through a short silica plug eluting with dichloromethane to remove the pyrrolic by-products. The solvent was removed and redissolved in dry dichloromethane (50ml) and chloranil (2.43g, 9.89mmol) was then added and the mixture was stirred at r.t. for 15hrs. Diisopropylethylamine (18.95ml, 0.11mol) was then added followed by boron trifluoride diethyl etherate (18.79ml, 0.15mol). The solution was then stirred at r.t. for 16hrs. The solution was then filtered through a pad of celite and the filtrate was washed with water (4 x 75ml), dried over anhydrous $MgSO_4$, filtered and evaporated *in vacuo*. The residue was purified by column chromatography eluting with 5:95 EtOAc:CH_2Cl_2 to yield the product as dark red needles (494 mg, 14%), m.p. 140-141°C.

^{1}H-NMR [400MHz, $CDCl_3$] δ 0.22 (9H, s, $Si(CH_3)_3$), 6.48 (2H, m, Py-H), 6.83 (2H, m, Py-H), 7.45 (2H, d, Ph-H, *J* = 8.43Hz), 7.55 (2H, d, Ph-H, *J* = 8.43Hz), 7.88 (2H, m, Py-H).

^{13}C-NMR [100MHz, $CDCl_3$] δ 97.8, 103.9, 118.8, 126.1, 130.5, 131.5, 132.1, 132.8, 144.5.

^{11}B-NMR [128.3MHz, $CDCl_3$] δ -0.49.

HRMS (ESI) = calc. 365.1452, found. 365.1458 ($M + H^+$).

8-(4-Ethynylphenyl)-BODIPY (26):

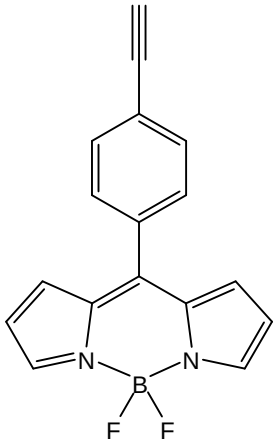

8-(4-Trimethylsilylethynylphenyl)-BODIPY (390 mg, 1.07mmol) was dissolved in THF (30ml) and TBAF (0.48g, 2.14mmol) was then added and the solution was stirred at r.t. for 15hrs. The THF was then removed *in vacuo* and the residue dissolved in dichloromethane (50ml) and washed with 2% $HCl_{(aq)}$ (30ml) and water (2 x 30ml) followed by drying over anhydrous $MgSO_4$, filtration and evaporation *in vacuo*. The residue was purified by column chromatography eluting with 1:1 CH_2Cl_2:hexane to yield the product as a bright red solid (185 mg, 59%), m.p. 182-183°C.

^{1}H-NMR [400MHz, $CDCl_3$] δ 3.19 (1H, s, H-C≡C), 6.49 (2H, m, Py-H), 6.84 (2H, m, Py-H), 7.47 (2H, d, Ph-H, *J* = 8.44Hz), 7.58 (2H, d, Ph-H, *J* = 8.44Hz), 7.89 (2H, m, Py-H).

^{13}C-NMR [100MHz, $CDCl_3$] δ 77.0, 79.7, 115.9, 122.0, 127.5, 128.5, 129.3, 131.2, 131.8, 141.6.

^{11}B-NMR [128.3MHz, $CDCl_3$] δ -0.73

MS (ESI) = 292.0 (M^-).

8-(4-Trimethylsilylethynylphenyl)-1,3,5,7-tetramethyl-BODIPY:

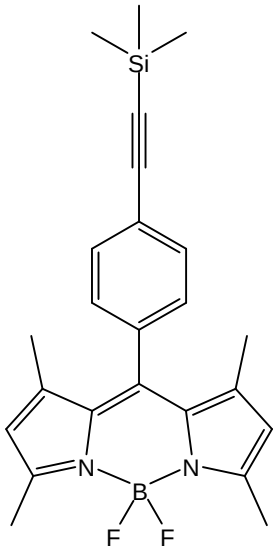

4-[Trimethylsilyl]ethynylbenzaldehyde (1.4g, 6.92mmol) and 2,4-dimethylpyrrole (1.43ml, 13.8mmol) were dissolved in dry dichloromethane (70ml) and degassed with argon for 20mins. TFA (0.1ml) was then added and the solution was stirred at r.t. under nitrogen for 16hrs. DDQ (1.57g, 6.92mmol) was then added and the solution was stirred at r.t. for 5hrs. Triethylamine (4.82ml, 34.6mmol) and boron trifluoride diethyl etherate (5.70ml, 45.0mmol) were then added and the solution was stirred at r.t. for 16hrs. The solution was then washed with water (4 x 50ml), dried over anhydrous $MgSO_4$ and evaporated *in vacuo*. The residue was then passed through a short silica column eluting with 1:1 hexane:CH_2Cl_2 and evaporated *in vacuo*. The residue was then purified by column chromatography eluting with 3:2 hexane:CH_2Cl_2 to yield the pure product as a bright red solid (299 mg, 10%), m.p. 214-215°C.

^{1}H-NMR [400MHz, $CDCl_3$] δ 0.21 (9H, s, Me_3Si), 1.32 (6H, s, 2 x CH_3), 2.48 (6H, s, 2 x CH_3), 5.91 (2H, s, Py-H), 7.17 (2H, d, Ph-H, *J* = 8.44Hz), 7.53 (2H, d, Ph-H, *J* = 8.44Hz).

^{13}C-NMR [100MHz, $CDCl_3$] δ 14.7, 95.9, 104.3, 121.5, 124.0, 128.2, 132.8, 135.3, 143.1, 155.9.

^{11}B-NMR [128.3MHz, $CDCl_3$] δ -0.3060.

HRMS (ESI) = calc. 365.1452, found. 365.1458 ($M + H^+$).

8-(4-Ethynylphenyl)-1,3,5,7-tetramethyl-BODIPY (27):

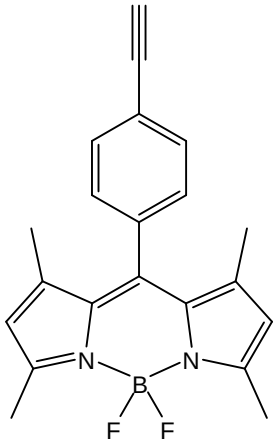

5-(4-Trimethylsilylethynylphenyl)-2,4,6,8-tetramethyl-BODIPY (250 mg, 0.595mmol) was dissolved in methanol (20ml) and anhydrous potassium carbonate (8 mg, 59.5μmol) was added and the mixture was stirred at r.t. for 16hrs. Dichloromethane (80ml) was then added and the mixture was washed with water (3 x 50ml), dried over anhydrous $MgSO_4$ and evaporated *in vacuo*. The residue was purified by column chromatography eluting with 3:2 hexane:CH_2Cl_2 to yield the pure product as a bright red solid (137 mg, 66%), m.p. 252-253°C, lit. 251-252°C, lit. 252-254°C[285].

^{1}H-NMR [400MHz, $CDCl_3$] δ 1.40 (6H, s, 2 x CH_3), 2.55 (6H, s, 2 x CH_3), 3.18 (1H, s, C≡CH), 5.99 (2H, s, Py-H), 7.27 (2H, d, Ph-H, *J* = 8.13Hz), 7.63 (2H, d, Ph-H, *J* = 8.44Hz).

^{13}C-NMR [100MHz, $CDCl_3$] δ 13.0, 77.0, 81.3, 119.8, 121.4, 126.7, 131.3, 134.0, 135.6, 141.4, 154.3.

^{11}B-NMR [128.3MHz, $CDCl_3$] δ -0.2205.

HRMS (ESI) = calc. 349.1682, found 349.1688 (M^+).

8-(4-Ethynylphenyl)-1,3,5,7-tetramethyl-2,6-diethyl-BODIPY (28):

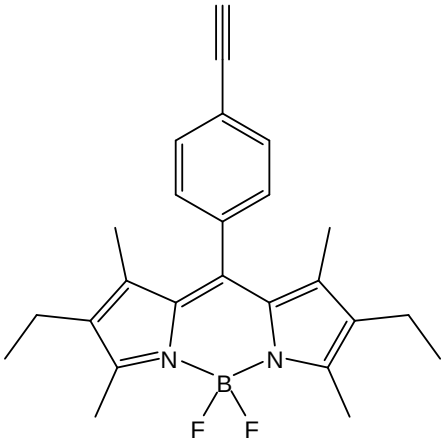

4-[(Trimethylsilyl)ethynyl]benzaldehyde (2g, 9.89mmol) and kryptopyrrole (2.74ml, 20.3mmol) were dissolved in dry dichloromethane (100ml) and degassed with argon for 15mins. TFA (0.1ml) was then added and the solution was stirred at r.t. under argon for 16hrs. Chloranil (2.43g, 9.89mmol) was then added and the mixture stirred at r.t. for 4hrs. Triethylamine (6.89ml, 49.6mmol) was then added, followed by boron trifluoride diethyl etherate (3.66ml, 29.7mmol) and the solution stirred at r.t. under argon for 17hrs. The solution was then washed with water (4 x 80ml), dried over anhydrous $MgSO_4$, filtered and evaporated *in vacuo*. The residue was passed through a short silica column eluting with 2:3 CH_2Cl_2:hexane to remove the pyrrolic by-products. The collected fractions were then dissolved in methanol (15ml) and anhydrous potassium carbonate (15mg, cat.) was added to the solution which was then stirred at r.t. for 16hrs. The methanol was evaporated *in vacuo* and the residue was purified by column chromatography eluting with 1:1 CH_2Cl_2:hexane to yield the pure product as a red solid (309mg, 10%), m.p. 249-250°C, lit. 250°C[26].

^{1}H-NMR [400MHz, $CDCl_3$] δ 0.97 (6H, t, C**H$_3$**CH_2, *J* = 7.61Hz), 1.29 (6H, s, 2 x Me), 2.29 (4H, q, CH_3C**H$_2$**, *J* = 7.51Hz), 2.52 (6H, s, 2 x Me), 3.18 (1H, s, HCC-Ph), 7.26 (2H, d, Ph-H, *J* = 8.43Hz), 7.61 (2H, d, Ph-H, *J* – 8.43Hz).

^{13}C-NMR [100MHz, $CDCl_3$] δ 10.5, 11.1, 13.2, 15.7, 19.4, 119.3, 121.3, 127.1, 131.4, 131.6, 135.1, 136.8, 152.7.

^{11}B-NMR [128.3MHz, $CDCl_3$] δ -0.1224.

HRMS (ESI) = calc. 405.2308, found. 405.2311 ($M + H^+$).

4-(11-[4-Iodophenylcarboxy]undecyloxy)-phenyl-4'-cyano-4-biphenyl carboxylate (29):

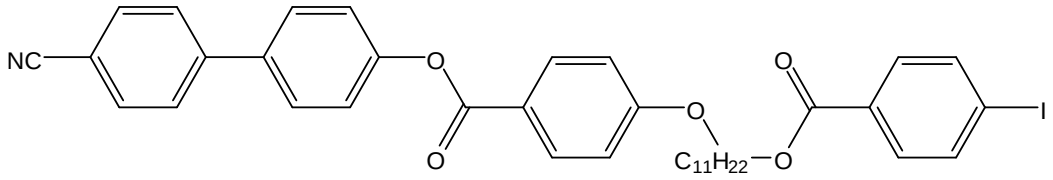

4-Iodobenzoic acid (0.32g, 1.29mmol) and 4-(11-hydroxyundecyloxy)-phenyl-4'-cyano-4-biphenyl carboxylate (0.63g, 1.31mmol) were dissolved in dry dichloromethane (75ml). DCC (0.45g, 2.19mmol) and DMAP (0.16g, 1.33mmol) were then added and the solution was stirred under nitrogen for 16hrs. The mixture was then filtered and the filtrate was washed with 2% $HCl_{(aq)}$ (50ml) and water (2 x 50ml), dried over anhydrous $MgSO_4$ and evaporated *in vacuo*. The residue was then recrystallized from ethyl acetate to yield the pure product as a white solid (0.65g, 71%).

^{1}H-NMR [400MHz, $CDCl_3$] δ 1.30 (10H, m, CH_2's), 1.73 (8H, m, CH_2's), 4.04 (2H, t, CH_2OPh, *J* = 6.57Hz), 4.29 (2H, t, CH_2O, *J* = 6.72Hz), 6.97 (2H, d, Ph-H, *J* = 9.07Hz), 7.31 (2H, d, Ph-H, *J* = 8.76Hz), 7.62 (2H, d, Ph-H, *J* = 8.76Hz), 7.67 (2H, d, Ph-H, *J* = 8.44Hz), 7.73 (4H, d, Ph-H, *J* = 8.76Hz), 7.77 (2H, d, Ph-H, *J* = 8.76Hz), 8.14 (2H, d, Ph-H, *J* = 8.76Hz).

^{13}C-NMR [100MHz, $CDCl_3$] δ 26.0, 29.01, 29.08, 29.2, 29.5, 65.4, 68.4, 111.0, 114.4, 118.9, 121.2, 122.6, 127.7, 128.3, 131.0, 132.3, 132.6, 137.7, 144.9, 151.6, 163.7, 164.9.

HRMS (ESI) = calc. 733.2133, found. 733.2132 ($M + NH_4^+$).

8-(4-[11-Carboxyphenylundecyloxy-phenyl-4'-cyano-4-biphenyl-carboxylate]-ethynylphenyl)-BODIPY (30):

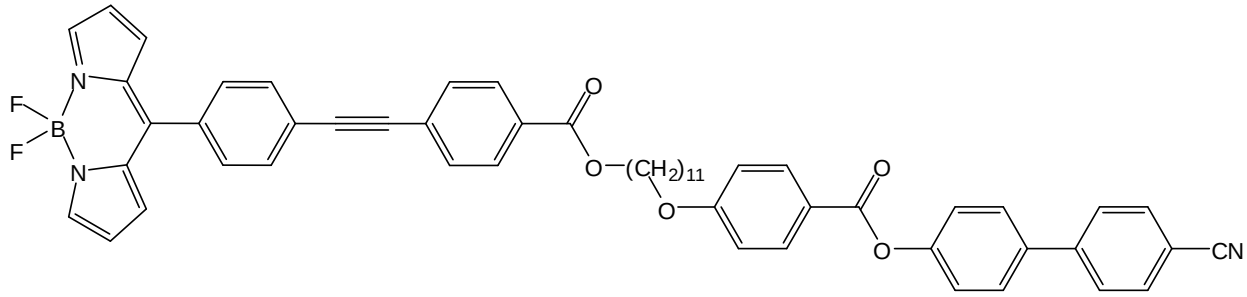

4-(11-[4-Iodophenylcarboxy]undecyloxy)-phenyl-4'-cyano-4-biphenyl carboxylate (101 mg, 0.141mmol), $Pd(PPh_3)_2Cl_2$ (29 mg, 41μmol), Cu(I)I (8 mg, 41μmol) and triethylamine (1ml) were mixed in DMF (4ml) and the mixture was degassed with argon for 30mins. 8-(4-Ethynylphenyl)-BODIPY (40 mg, 0.137mmol) in DMF (1.5ml) was added to the initial mixture and the resulting mixture was then heated in a microwave at 65°C (75W) for 5mins. The DMF was then removed *in vacuo* and the residue subjected to column chromatography eluting with 2:98 EtOAc:toluene to yield an orange solid which was then precipitated from dichloromethane with cold methanol to yield the pure product as a bright orange solid (44 mg, 36%), R_f = 0.11 (toluene), LC transitions: Cr (N 166) 183 I.

^{1}H-NMR [400MHz, $CDCl_3$] δ 1.33 (10H, m, CH_2's), 1.45 (4H, m, CH_2's), 1.82 (4H, m, CH_2's), 4.06 (2H, t, CH_2OPh, J = 6.57Hz), 4.34 (2H, t, CH_2O, J = 6.72Hz), 6.57 (2H, m, Py-H), 6.94 (2H, m, Py-H), 6.98 (2H, d, Ph-H, J = 8.76Hz), 7.32 (2H, d, Ph-H, J = 8.76Hz), 7.58 (2H, d, Ph-H, J = 8.44Hz), 7.63 (4H, d, Ph-H, J = 8.44Hz), 7.70 (6H, m, Ph-H), 7.96 (2H, m, Py-H), 8.06 (2H, d, Ph-H, J = 8.76Hz), 8.15 (2H, d, Ph-H, J = 9.07Hz).

^{13}C-NMR [100MHz, $CDCl_3$] δ 26.00, 26.03, 28.7, 29.3, 29.4, 29.5, 65.4, 68.4, 91.0, 91.3, 111.0, 114.4, 118.8, 121.2, 122.6, 127.2, 127.7, 128.4, 129.6, 130.4, 130.6, 131.4, 131.6, 131.7, 132.4, 132.7, 134.0, 144.5, 144.9, 151.6, 163.7, 164.8, 166.0. (9 peaks unobserved due to overlap of the alkyl and aromatic peaks).

^{11}B-NMR [128.3MHz, $CDCl_3$] δ -0.67.

HRMS (ESI) = calc. 897.4002, found. 897.4001 ($M + NH_4^+$).

HPLC retention time (80:20 MeCN:DCM): 3.70 mins.

Fluorescence absorption maximum: 508 nm; fluorescence emission maximum: 533 nm.

8-(4-[11-Carboxyphenylundecyloxy-phenyl-4'-cyano-4-biphenyl-carboxylate]-ethynylphenyl)-1,3,5,7-tetramethyl-BODIPY (31):

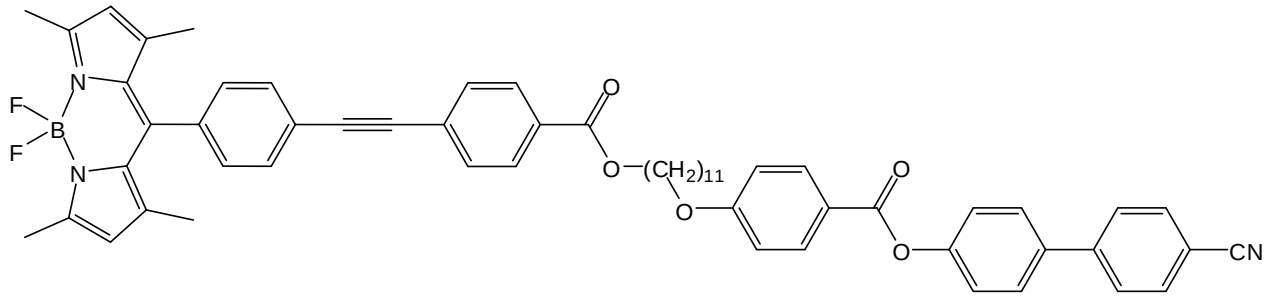

4-(11-[4-Iodophenylcarboxy]undecyloxy)-phenyl-4'-cyano-4-biphenyl carboxylate (106 mg, 0.148mmol), $Pd(PPh_3)_2Cl_2$ (30 mg, 43.2μmol), Cu(I)I (8 mg, 43.2μmol) and triethylamine (1ml) were mixed in DMF (4ml) and the mixture was degassed with argon for 30mins. 8-(4-Ethynylphenyl)-1,3,5,7-tetramethyl-BODIPY (50 mg, 0.144mmol) in DMF (1.5ml) was added to the initial mixture and the resulting mixture was then heated in a microwave at 65°C (75W) for 5mins. The DMF was then removed *in vacuo* and the residue subjected to column chromatography eluting with 1:99 EtOAc:toluene to yield an orange solid which was then precipitated from dichloromethane with cold methanol to yield the pure product as a bright orange solid (51 mg, 38%), m.p. 199-200°C, R_f = 0.47 (5:95 EtOAc:toluene).

^{1}H-NMR [400MHz, $CDCl_3$] δ 1.33 (10H, m, CH_2's), 1.43 (6H, s, 2 x CH_3), 1.46 (4H, m, CH_2's), 1.80 (4H, m, CH_2's), 2.56 (6H, s, 2 x CH_3), 4.05 (2H, t, CH_2OPh, *J* = 6.51Hz), 4.34 (2H, t, CH_2O, *J* = 6.69Hz), 5.99 (2H, s, Py-H), 6.99 (2H, d, Ph-H, *J* = 8.80Hz), 7.32 (4H, m, Ph-H), 7.63 (4H, m, Ph-H), 7.68 (4H, 2 x d, Ph-H), 7.74 (2H, d, Ph-H, *J* = 8.25Hz), 8.01 (2H, d, Ph-H, *J* = 8.06Hz), 8.16 (2H, d, Ph-H, *J* = 8.80Hz).

^{13}C-NMR [100MHz, $CDCl_3$] δ 14.6, 25.97, 26.01, 28.7, 29.2, 29.3, 29.5, 65.4, 68.3, 90.0, 91.4, 110.9, 114.3, 118.9, 121.2, 121.4, 122.6, 123.5, 127.4, 127.7, 128.3, 129.6, 130.2, 131.5, 132.3, 132.4, 132.7, 136.7, 142.9, 144.9, 151.6, 155.8, 163.7, 166.0. (12 peaks unobserved due to overlap of the alkyl and aromatic peaks).

^{11}B-NMR [128.3MHz, $CDCl_3$] δ -0.2446.

HRMS (ESI) = calc. 958.4183, found, 958.4174 ($M + Na^+$).

HPLC retention time (80:20 MeCN:DCM): 4.78 mins.

Fluorescence absorption maximum: 506 nm; fluorescence emission maximum: 519 nm.

8-(4-[11-Carboxyphenylundecyloxy-phenyl-4'-cyano-4-biphenyl-carboxylate]-ethynylphenyl)-1,3,5,7-tetramethyl-2,6-diethyl-BODIPY (32):

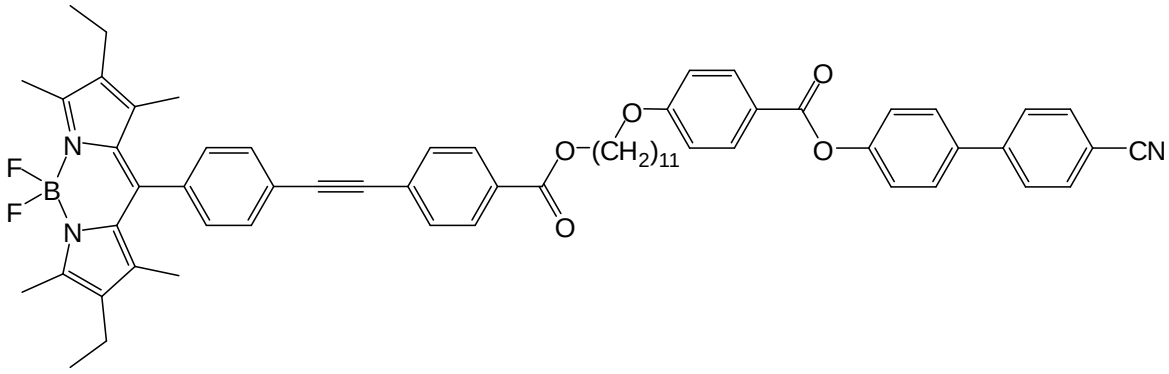

4-(11-[4-Iodophenylcarboxy]undecyloxy)-phenyl-4'-cyano-4-biphenyl carboxylate (88 mg, 0.128mmol), $Pd(PPh_3)_2Cl_2$ (26 mg, 37.2μmol), Cu(I)I (7.2 mg, 37.2μmol) and triethylamine (1ml) were mixed in DMF (4ml) and degassed with argon for 30mins. 8-(4-Ethynylphenyl)-1,3,5,7-tetramethyl-2,6-diethyl-BODIPY (50 mg, 0.124mmol) in DMF (1ml) was then added to this solution and the mixture was then heated in a microwave at 65°C (75W) for 5mins. The DMF was then removed *in vacuo* and the residue subjected to column chromatography eluting with 0-2% EtOAc:toluene to yield an orange solid which was then precipitated from dichloromethane with cold methanol to yield the pure product as a bright red solid (45 mg, 38%), m.p. 184-185°C, R_f = 0.4 (toluene).

^{1}H-NMR [400MHz, $CDCl_3$] δ 0.96 (6H, t, C**H$_3$**CH_2, *J* = 7.51Hz), 1.31 (16H, m, CH_2's + 2 x CH_3), 1.44 (4H, m, CH_2's), 1.79 (4H, m, CH_2's), 2.27 (4H, q, C**H$_2$**CH_3, *J* = 7.50Hz), 2.52 (6H, s, 2 x CH_3), 4.03 (4H, t, CH_2OPh, *J* = 6.57Hz), 4.32 (4H, t, CH_2O, *J* = 6.73Hz), 6.97 (2H, d, Ph-H, *J* = 9.07Hz), 7.30 (4H, m, Ph-H), 7.63 (8H, m, Ph-H), 7.71 (2H, d, Ph-H, *J* = 8.76Hz), 8.03 (2H, d, Ph-H, *J* = 8.76Hz), 8.14 (2H, d, Ph-H, *J* = 9.07Hz).

^{13}C-NMR [100MHz, $CDCl_3$] δ 11.2, 11.9, 13.9, 16.4, 25.3, 28.0, 28.0, 28.4, 28.6, 28.7, 28.8, 64.7, 67.7, 89.2, 90.8, 110.3, 113.7, 120.5, 121.9, 122.7, 127.0, 127.7, 128.0, 128.9, 129.5, 130.9, 131.7, 132.0, 132.3, 135.7, 137.5, 150.9, 163.1, 164.2, 165.3. (13 peaks unobserved due to overlap of the alkyl and aromatic peaks).

^{11}B-NMR [128.3MHz, $CDCl_3$] δ -0.1836.

HRMS (ESI) = calc. 1009.5256, found. 1009.5259 ($M + NH_4^+$).

HPLC retention time (90:10 MeCN:DCM): 12.44 mins.

Fluorescence absorption maximum: 529 nm; fluorescence emission maximum: 544 nm.

8-(4-[11-carboxyphenylundecyloxybiphenyl-4-carbonitrile]-ethynylphenyl)-BODIPY (33):

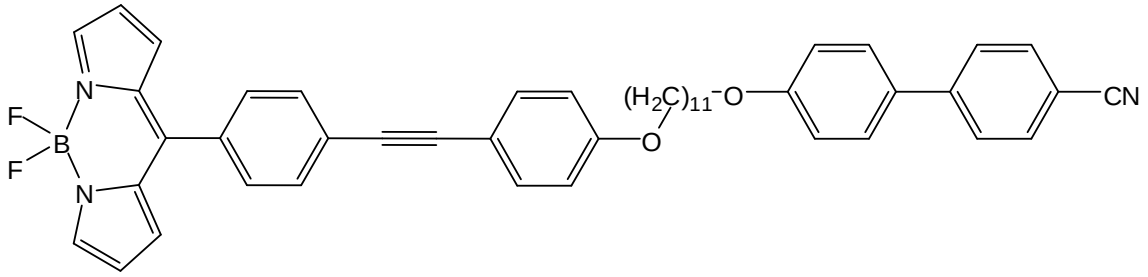

4'-(11-[4-Iodophenylcarboxy]undecyl)-biphenyl-4-carbonitrile (80 mg, 0.144mmol), $Pd(PPh_3)_2Cl_2$ (29 mg, 0.041mmol, 30mol%), copper (I) iodide (8 mg, 0.041mmol, 30mol%) and triethylamine (1ml) were mixed in DMF (4ml) and degassed with argon for 30 mins. 8-(4-Ethynylphenyl)-BODIPY (40 mg, 0.138mmol) in DMF (1.5ml) was then added to the solution which was then heated in a microwave at 65°C (75W) for 5 mins. The DMF was then removed *in vacuo* and the residue subjected to column chromatography eluting with toluene to yield a red solid which was then precipitated from dichloromethane with cold methanol to yield the pure product as a bright red/orange solid which was filtered and dried *in vacuo* (23 mg, 23%), m.p. 143-144°C, R_f = 0.13 (toluene).

^{1}H-NMR [400MHz, $CDCl_3$] δ 1.33 (10H, m, CH_2's), 1.47 (4H, m, CH_2's), 1.80 (4H, m, CH_2's), 4.01 (4H, m, 2 x CH_2), 6.56 (2H, m, Py-H), 6.89 (2H, d, Ph-H), 6.95 (2H, m, Py-H), 7.00 (2H, d, Ph-H), 7.52 (6H, m, Ph-H), 7.66 (6H, m, Ph-H), 7.95 (2H, m, Py-H).

^{13}C-NMR [100MHz, $CDCl_3$] δ 26.0, 28.6, 29.1, 29.2, 29.3, 29.5, 32.2, 65.4, 68.4, 111.0, 114.4, 118.9, 121.2, 122.6, 127.7, 128.3, 131.0, 132.3, 132.6, 137.7, 144.9, 151.6, 163.7, 164.9. (13 peaks unobserved due to overlap of the alkyl and aromatic peaks).

^{11}B-NMR [128.3MHz, $CDCl_3$] δ -0.49.

HRMS (ESI) = calc. 749.3841, found. 749.3838 ($M + NH_4^+$).

4'-(11-Hydroxyundecyloxy)-biphenyl-4-carbonitrile (34):

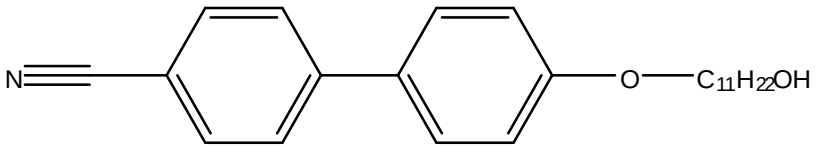

4-Hydroxy-4'-cyanobiphenyl (7g, 0.036mol), 11-bromoundecanol (9.50g, 0.038mol), anhydrous potassium carbonate (7.46g, 0.054mol) and potassium iodide (0.60g, 0.0036mol) were added to acetone (150ml) and refluxed for 18hrs. The mixture was then cooled to r.t. and filtered. The solvent was removed by evaporation *in vacuo* and the residue redissolved in dichloromethane (100ml). This solution was washed with 2% $HCl_{(aq)}$ (50ml) and water (2 x 50ml), dried over anhydrous $MgSO_4$, filtered and evaporated. The residue was recrystallized from ethanol to yield the product as an off-white solid (11.84g, 90%). Liquid crystal transitions: Cr 90 N 92 I (lit. Cr 89.8 N 92 I[286]).

^{1}H-NMR [$CDCl_3$, 400MHz] δ 1.29 (12H, m, CH_2's), 1.46 (4H, m, CH_2's), 1.79 (2H, m, CH_2), 3.63 (2H, t, CH_2OH, *J* = 6.72Hz), 3.99 (2H, t, CH_2O, *J* = 6.57Hz), 6.98 (2H, d, Ph-H, *J* = 8.76Hz), 7.51 (2H, d, Ph-H, *J* = 8.44Hz), 7.62 (2H, d, Ph-H, *J* = 8.13Hz), 7.68 (2H, d, Ph-H, *J* = 8.44Hz).

^{13}C-NMR [$CDCl_3$, 100MHz] δ 25.7, 29.35, 29.40, 29.52, 29.56, 32.8, 63.1, 68.2, 110.0, 115.1, 119.1, 127.1, 128.3, 131.2, 132.6, 145.3, 159.8. (7 peaks unobserved due to overlap of the alkyl and aromatic peaks).

HRMS (ESI) = calc. 383.2693, found. 383.2698 ($M + NH_4^+$).

4'-(11-Mesityloxyundecyloxy)-biphenyl-4-carbonitrile (35):

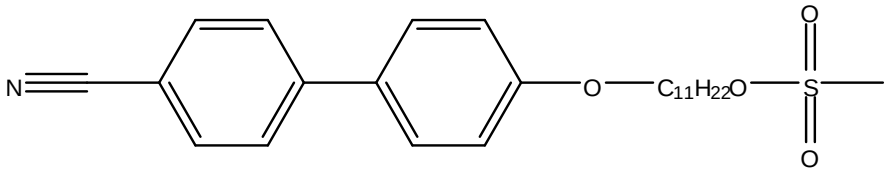

4-(11-Hydroxyundecyloxy)-biphenyl-4-carbonitrile (2g, 5.47mmol), triethylamine (0.91ml, 6.56mmol) and *N,N'*-dimethylaminopyridine (5 mg) were dissolved in dry dichloromethane (50ml) and cooled to 0°C under nitrogen. Methanesulfonyl chloride (0.44ml, 5.74mmol) was then added dropwise. The solution was allowed to warm to r.t. and then stirred for 16hrs. The solution was then washed with brine (50ml) and water (2 x 50ml) and dried over anhydrous sodium sulphate. Removal of solvent by evaporation *in vacuo* yielded a white solid which was then recrystallized from ethanol to yield the product as white needles (2.09g, 86%).

^{1}H-NMR [$CDCl_3$, 400MHz] δ 1.30 (12H, m, CH_2), 1.47 (2H, m, CH_2), 1.75 (2H, m, CH_2), 1.83 (2H, m, CH_2), 3.00 (3H, s, S-Me), 4.01 (2H, t, CH_2OPh, *J* = 6.41Hz), 4.22 (2H, t, CH_2OMs, *J* = 6.57Hz), 6.99 (2H, d, Ph-H, *J* = 8.76Hz), 7.53 (2H, d, Ph-H, *J* = 9.07Hz), 7.64 (2H, d, Ph-H, *J* = 8.13Hz), 7.69 (2H, d, Ph-H, *J* = 8.44Hz).

^{13}C-NMR [$CDCl_3$, 100MHz] δ 25.2, 26.0, 29.12, 29.34, 29.38, 29.41, 37.4, 68.2, 70.2, 110.0, 115.1, 119.1, 127.1, 128.3, 131.2, 132.6, 145.2, 159.8. (7 peaks unobserved due to overlap of the alkyl and aromatic peaks).

HRMS (ESI) = calc. 461.2469, found. 461.2468 ($M + NH_4^+$).

4'-(11-Azidoundecyloxy)-biphenyl-4-carbonitrile (36):

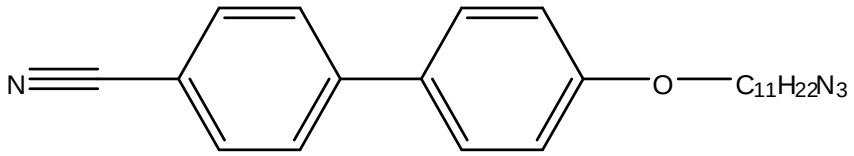

11-(Mesityloxyundecyloxy)-biphenyl-4-carbonitrile (1g, 2.25 mmol) was dissolved in DMSO (25 ml), sodium azide (0.22g, 3.38 mmol) was added and the solution was stirred at 60°C for 16 hrs. The solution was then poured into water and the product extracted with dichloromethane. The organic layer was then washed thoroughly with water, dried over anhydrous magnesium sulphate and evaporated *in vacuo* to yield a yellow oil which crystallized upon standing. The resulting solid was recrystallized from ethanol to yield the product as a pale yellow solid (0.72g, 82%).

^{1}H-NMR [$CDCl_3$, 400MHz] δ 1.30 (12H, m, CH_2), 1.48 (2H, m, CH_2), 1.60 (2H, m, CH_2), 1.81 (2H, m, CH_2), 3.26 (2H, t, CH_2N_3, *J* = 6.88Hz), 4.01 (2H, t, CH_2OPh, *J* = 6.88Hz), 6.99 (2H, d, Ph-H, *J* = 8.76Hz), 7.53 (2H, d, Ph-H, *J* = 8.44Hz), 7.64 (2H, d, Ph-H, *J* = 8.44Hz), 7.69 (2H, d, Ph-H, *J* = 8.44Hz).

^{13}C-NMR [$CDCl_3$, 100MHz] δ 26.0, 26.7, 29.12, 29.34, 29.38, 29.43, 51.5, 68.2, 115.1, 127.1, 128.3, 132.6, 159.8. (11 peaks unobserved due to overlap of the alkyl and aromatic peaks).

HRMS (ESI) = calc. 408.2758, found. 408.2759 ($M + NH_4^+$).

8-(4-Triazol-1-[11-carboxyphenylundecyloxybiphenyl-4-carbonitrile]-yl-phenyl)-BODIPY (37):

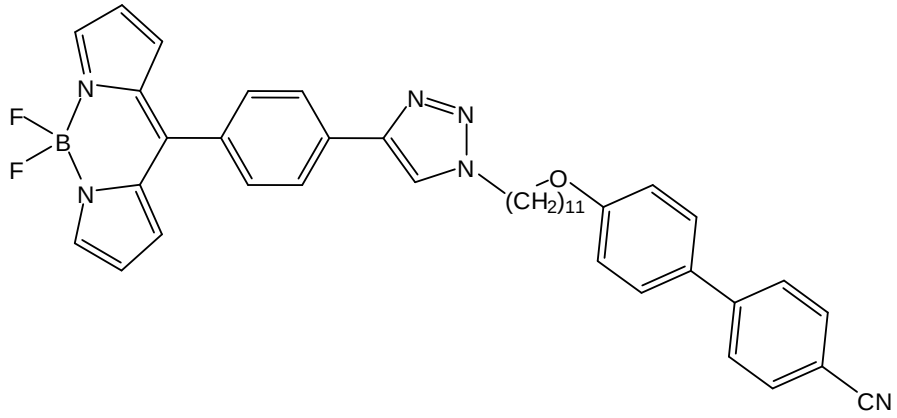

8-(4-Ethynylphenyl)-BODIPY (40 mg, 0.137 mmol), 4'-(11-azidoundecyl)-biphenyl-4-carbonitrile (54 mg, 0.137 mmol), $CuSO_4.5H_2O$ (7 mg, 27.4 μmol), copper nanopowder (9 mg, 0.137 mmol) and sodium ascorbate (14 mg, 68.5 μmol) were mixed in 3:1 THF:H_2O (20 ml) and the mixture was heated at 50°C for 20 hrs. The solvent was removed *in vacuo* and the residue was purified by column chromatography eluting with 2:98 EtOAc:toluene to yield the pure product as a red solid (33 mg, 36%), m.p. 158-160°C, R_f = 0.14 (toluene).

^{1}H-NMR [400MHz, $CDCl_3$] δ 1.31 (12H, m, CH_2's), 1.47 (2H, m, CH_2), 1.81 (2H, m, CH_2), 1.99 (2H, m, CH_2), 4.00 (2H, t, CH_2OPh, J = 6.60Hz), 4.45 (2H, t, CH_2N, J = 7.15Hz), 6.56 (2H, m, Py-H), 6.99 (4H, m, Ph-H + Py-H), 7.53 (2H, d, Ph-H, J = 8.80Hz), 7.64 (4H, m, Ph-H), 7.69 (2H, d, Ph-H, J = 8.80Hz), 7.86 (1H, s, CH-N), 7.96 (2H, m, Py-H), 8.01 (2H, d, Ph-H, J = 8.25Hz).

^{13}C-NMR [100MHz, $CDCl_3$] δ 26.1, 26.8, 29.2, 29.3, 29.4, 29.5, 30.6, 50.6, 68.1, 110.0, 115.0, 118.6, 119.1, 120.1, 125.6, 127.0, 128.3, 131.2, 131.3, 132.5, 133.3, 134.9, 144.1, 145.2, 146.5, 146.8, 159.7. (7 peaks unobserved due to overlap of the alkyl and aromatic peaks).

^{11}B-NMR [128.3MHz, $CDCl_3$] δ -0.4891.

HRMS (ESI) = calc. 683.3483, found. 683.3479 ($M + H^+$).

HPLC retention time (MeCN): 4.20 mins.

Fluorescence absorption maximum: 504 nm; fluorescence emission maximum: 523 nm.

4-(11-Mesityloxyundecyloxy)-phenyl-4'-cyano-4-biphenyl carboxylate (38):

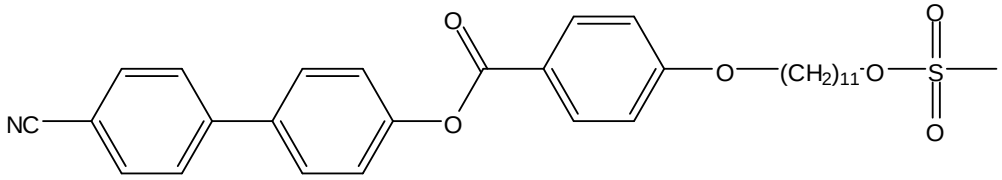

4-(11-Hydroxyundecyloxy)-phenyl-4'-cyano-4-biphenyl carboxylate (1.19g, 2.45 mmol) was dissolved in dry dichloromethane (50 ml) and triethylamine (1.88 ml, 2.94 mmol) was added. Methanesulfonyl chloride (0.95 ml, 2.57 mmol) was then added and the solution stirred at r.t. under nitrogen for 18 hrs. The solution was then washed with brine (50 ml) and water (2 x 50 ml) and dried over anhydrous sodium sulphate and evaporated *in vacuo*. The residue was recrystallized from ethyl acetate to yield the product as an off-white solid (0.84g, 61%), Cr 140 SmA 140 N 155 I.

^{1}H-NMR [$CDCl_3$, 400MHz] δ 1.31 (12H, m, CH_2), 1.39 (2H, m, CH_2), 1.74 (2H, m, CH_2), 1.83 (2H, m, CH_2), 3.01 (3H, s, S-Me), 4.06 (2H, t, CH_2-OPh, *J* = 6.57Hz), 4.23 (2H, t, CH_2-OMs, *J* = 6.72Hz), 6.99 (2H, d, Ph-H, *J* = 8.44Hz), 7.33 (2H, d, Ph-H, *J* = 8.13Hz), 7.64 (2H, d, Ph-H, *J* = 8.13Hz), 7.69 (2H, d, Ph-H, *J* = 8.13Hz), 7.74 (2H, d, Ph-H, *J* = 8.13Hz), 8.16 (2H, d, Ph-H, *J* = 8.44Hz).

^{13}C-NMR [$CDCl_3$, 100MHz] δ 25.4, 26.0, 29.0, 29.1, 29.3, 29.40, 29.42, 29.49, 37.4, 68.4, 70.2, 111.0, 114.4, 118.9, 121.2, 122.6, 127.7, 128.4, 132.4, 132.7, 136.7, 144.9, 151.6, 163.7, 164.9. (6 peaks unobserved due to overlap of the alkyl and aromatic peaks).

HRMS (ESI) = calc. 581.2680, found. 581.2677 ($M + NH_4^+$).

4-(11-Mesityloxyundecyloxy)-benzoic acid (39):

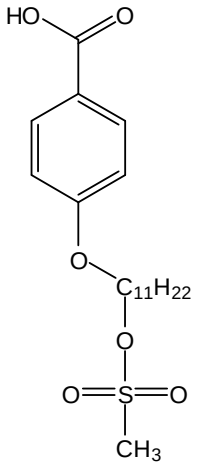

4-(11-Hydroxyundecyloxy)-benzoic acid (1.5g, 4.86 mmol) and DMAP (cat., 5 mg) were dissolved in dry dichloromethane (50 ml) and triethylamine (1.63 ml, 11.7 mmol) was added and the solution was cooled to 0°C in an ice-bath and placed under a nitrogen atmosphere. Methanesulphonyl chloride (0.79 ml, 10.2 mmol) was then added dropwise. Once addition was complete, the solution was allowed to warm to r.t. and then stirred under nitrogen for 16 hrs. The solution was then washed with 2% $HCl_{(aq)}$ (40 ml) and water (2 x 50 ml), dried over anhydrous $MgSO_4$, filtered and evaporated *in vacuo* to yield the pure product as a white solid (1.77g, 94%).

^{1}H-NMR [400MHz, $CDCl_3$] δ 1.28 (12H, m, CH_2's), 1.45 (2H, m, CH_2), 1.73 (2H, m, CH_2), 1.80 (2H, m, CH_2), 2.98 (3H, s, CH_3), 4.01 (2H, t, CH_2OPh, *J* = 6.41Hz), 4.21 (2H, t, CH_2OMs, *J* = 6.37Hz), 6.94 (2H, d, Ph-H, *J* = 8.76Hz), 8.06 (2H, d, Ph-H, *J* = 8.76Hz).

MS (ESI) m/z 408.5 (M + Na^+).

5-(4-Ethynylphenyl)-dipyrromethane (40):

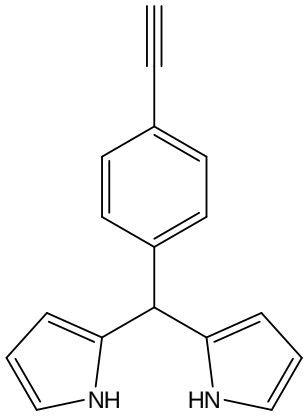

4-[Trimethylsilyl]acetylenebenzaldehyde (3g, 0.015 mol) was dissolved in pyrrole (42 ml, 0.6 mol) and the solution was degassed with nitrogen for 15 mins. Trifluoroacetic acid (0.1 ml) was then added to the solution and the mixture was stirred for 18hrs under nitrogen and protected from light. The excess pyrrole was then removed by evaporation *in vacuo* and the residue was redissolved in dichloromethane (100 ml) and washed with brine (50 ml) and water (2 x 50 ml), dried over anhydrous magnesium sulphate and the dichloromethane removed. The residue was purified by column chromatography eluting with dichloromethane to give a tan oil.

This oil was dissolved in THF/methanol (4:1) and anhydrous potassium carbonate (2.07g) was added to the solution. The mixture was stirred for 4hrs then filtered and the solvent removed *in vacuo*. The residue was purified by column chromatography eluting with 1:1 dichloromethane:hexane to yield the product as an off-white solid (1.35g, 36%), m.p. 109-111°C (lit. 109-110°C[21]).

^{1}H-NMR [400MHz, $CDCl_3$] δ 3.06 (1H, s, H-CC), 5.47 (1H, s, 5-position H), 5.89 (2H, m, Py-H), 6.16 (2H, m, Py-H), 6.71 (2H, m, Py-H), 7.17 (2H, d, Ph-H, *J* = 8.13Hz), 7.44 (2H, d, Ph-H, *J* = 8.44Hz), 7.92 (2H, bs, NH).

^{13}C-NMR [100MHz, $CDCl_3$] δ 43.8, 77.2, 83.4, 107.4, 108.5, 117.4, 120.7, 128.4, 131.8, 132.4, 142.9.

MS (ESI) = *m/z* 246.0 (M^+).

5-(4-Triazol-1-[11-hydroxyundecyl]-yl-phenyl)-dipyrromethane (41):

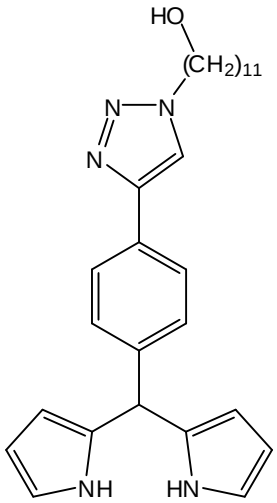

5-(4-Ethynylphenyl)dipyrromethane (0.5g, 2.03 mmol), 11-azidoundecan-1-ol (0.43g, 2.03 mmol), $CuSO_4.5H_2O$ (51 mg, 0.203 mmol) and sodium ascorbate (0.20 g, 1.02 mmol) were mixed in DMF (15 ml) and stirred at r.t. under nitrogen for 16 hrs. Dichloromethane (50 ml) was then added and the solution was washed thoroughly with water (5 x 50ml), dried over anhydrous $MgSO_4$, filtered and evaporated. The residue was passed through a short silica column to yield the product as a yellow/brown oil that crystallized upon standing to yield a yellow/brown solid (0.45g, 48%), m.p. 78-79°C.

^{1}H-NMR [400MHz, DMSO-D_6] δ 1.25 (14H, m, CH_2's), 1.40 (2H, m, CH_2), 1.87 (2H, m, CH_2), 3.37 (2H, m, CH_2), 4.37 (2H, m, CH_2), 5.39 (1H, s, *meso*-H), 5.70 (2H, m, Py-H), 5.93 (2H, m, Py-H), 6.64 (2H, m, Py-H), 7.24 (2H, d, Ph-H, *J* = 8.25Hz), 7.76 (2H, d, Ph-H, *J* = 8.43Hz), 8.54 (1H, s, triazole-H), 10.61 (2H, bs, NH).

Compound too insoluble to carry out accurate ^{13}C-NMR.

HRMS (ESI) = calc. 460.3071, found. 460.3067 ($M + NH_4^+$).

5-(4-Triazol-1-[11-mesityloxyundecyl]-yl-phenyl)-dipyrromethane (42):

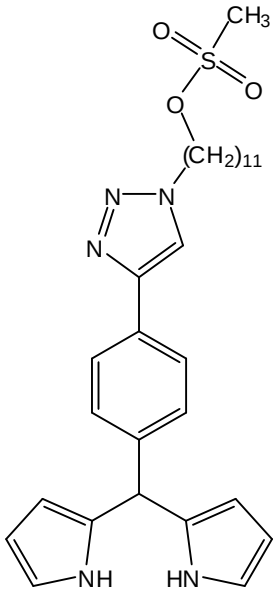

5-(4-Triazol-1-[11-hydroxyundecyl]-yl-phenyl)-dipyrromethane (0.45g, 0.979 mmol) and DMAP (cat., 5 mg) were dissolved in dry dichloromethane (50ml) and triethylamine (0.27 ml, 1.96 mmol) was added and the mixture was cooled to 0°C in an ice-bath and placed under a nitrogen atmosphere. Methanesulphonyl chloride (0.11 ml, 1.47 mmol) was then added dropwise. Once addition of the methanesulphonyl chloride was complete the solution was allowed to warm up to r.t. and then stirred under nitrogen for 16 hrs. The solution was then washed with 2% $HCl_{(aq)}$ (40 ml) and water (2 x 50 ml), dried over anhydrous $MgSO_4$, filtered and evaporated *in vacuo* to yield the pure product as a brown oil (quantitative yield).

^{1}H-NMR [400MHz, $CDCl_3$] δ 1.26 (14H, m, CH_2's), 1.72 (2H, m, CH_2), 1.93 (2H, m, CH_2), 2.99 (3H, s, CH_3), 4.20 (2H, t, CH_2OMs, *J* = 6.51Hz), 4.38 (2H, t, CH_2N, *J* = 7.15Hz), 5.51 (1H, s, 5-position H), 5.93 (2H, m, Py-H), 6.16 (2H, m, Py-H), 6.71 (2H, m, Py-H), 7.28 (2H, d, Ph-H, *J* = 6.14Hz), 7.71 (1H, s, triazole H), 7.77 (2H, d, Ph-H, *J* = 8.43Hz), 8.00 (2H, bs, NH's).

^{13}C-NMR [100MHz, $CDCl_3$] δ 8.6, 25.3, 26.4, 28.9, 29.1, 29.3, 37.4, 43.8, 45.8, 50.5, 70.2, 107.3, 108.2, 108.5, 117.3, 126.0, 128.9. (6 peaks unobserved due to overlap of the alkyl peaks).

MS (ESI) m/z 538.7 (M^+).

5-(4-Triazol-1-[11-carboxyphenylundecyloxybiphenyl-4-carbonitrile]-yl-phenyl)-dipyrromethane (43):

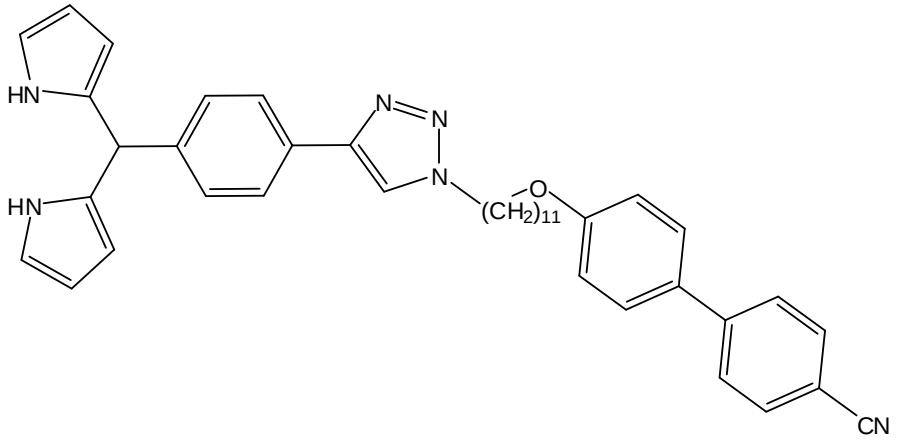

4'-(11-Azidoundecyl)-biphenyl-4-carbonitrile (0.67g, 1.79 mmol), 5-(4-ethynylphenyl)dipyrromethane (0.44g, 1.79 mmol), $CuSO_4.5H_2O$ (45 mg, 0.179 mmol) and sodium ascorbate (71 mg, 0.358 mmol) were mixed in a 12:1:1 mixture of $CHCl_3$:EtOH:H_2O (28 ml) and stirred at r.t. under nitrogen for 18 hrs. Chloroform (40 ml) and water (50 ml) added and the aqueous layer was extracted twice with chloroform. The combined organic extracts were then washed with water (2 x 50 ml), dried over anhydrous $MgSO_4$, filtered and evaporated *in vacuo*. The residue was purified by column chromatography eluting with 1:9 EtOAc:CH_2Cl_2 to yield the product as a light brown solid (0.56g, 49%), m.p. 131-132°C, R_f = 0.59 (1:9 EtOAc:CH_2Cl_2).

^{1}H-NMR [400MHz, DMSO-D_6] δ 1.23 (12H, m, CH_2's), 1.38 (2H, m, CH_2), 1.79 (2H, m, CH_2), 1.83 (2H, m, CH_2), 3.99 (2H, t, CH_2OPh, *J* = 6.41Hz), 4.34 (2H, t, CH_2N, *J* = 6.88Hz), 5.34 (1H, s, 5-position H), 5.65 (2H, m, Py-H), 5.88 (2H, m, Py-H), 6.59 (2H, m, Py-H), 7.02 (2H, d, Ph-H, *J* = 9.07Hz), 7.20 (2H, d, Ph-H, *J* = 8.13Hz), 7.68 (2H, d, Ph-H, *J* = 8.76Hz), 7.70 (2H, d, Ph-H, *J* = 8.44Hz), 7.81 (2H, d, Ph-H, *J* = 8.44Hz), 7.86 (2H, d, Ph-H, *J* = 8.44Hz), 8.50 (1H, s, triazole-H), 10.56 (2H, bs, NH's).

^{13}C-NMR [100MHz, DMSO-D_6] δ 23.62, 23.65, 23.7, 23.8, 25.4, 25.8, 28.7, 28.8, 49.5, 54.9, 67.5, 106.1, 106.9, 115.1, 116.9, 119.0, 120.9, 124.8, 126.8, 128.3, 128.5, 132.8, 132.9, 159.3. (11 peaks unobserved due to overlap of the alkyl and aromatic peaks).

HRMS (ESI) = calc. 637.3649, found. 637.3645 ($M + NH_4^+$).

5-(4-Triazol-1-[11-carboxyphenylundecyloxybiphenyl-4-carbonitrile]-yl-phenyl)-dipyrromethene (44):

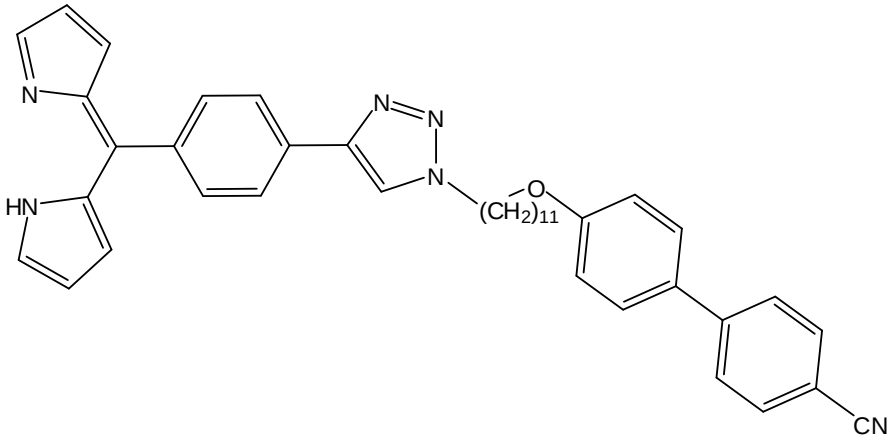

5-(4-Triazol-1-[11-carboxyphenylundecyloxybiphenyl-4-carbonitrile]-yl-phenyl)-dipyrromethane (0.56g, 0.879 mmol) was dissolved in dry dichloromethane (50 ml) then DDQ (0.20g, 0.879 mmol) was added and the mixture stirred at r.t. for 4 hrs. The solution was then washed with water (3 x 50 ml), dried over anhydrous $MgSO_4$, filtered and evaporated *in vacuo*. The residue was purified by column chromatography eluting with 1:9 EtOAc:CH_2Cl_2 to yield an orange/yellow solid (39 mg, 7%), m.p. 98-100°C, R_f = 0.47 (1:9 EtOAc:CH_2Cl_2).

^{1}H-NMR [400MHz, $CDCl_3$] δ 1.29 (12H, m, CH_2's), 1.40 (2H, m, CH_2), 1.73 (2H, m, CH_2), 1.91 (2H, m, CH_2), 3.93 (2H, t, CH_2OPh, *J* = 6.57Hz), 4. 37 (2H, t, CH_2N, *J* = 7.20Hz), 6.39 (2H, m, Py-H), 6.63 (2H, m, Py-H), 6.91 (2H, d, Ph-H, *J* = 8.76Hz), 7.45 (2H, d, Ph-H, *J* = 8.76Hz), 7.48 (2H, d, Ph-H, *J* = 8.13Hz), 7.56 (2H, d, Ph-H, *J* = 8.44Hz), 7.62 (2H, d, Ph-H, *J* = 8.44Hz), 7.71 (2H, m, Py-H), 7.77 (1H, s, triazole-H), 7.86 (2H, d, Ph-H, *J* = 8.44Hz). NH peak not observed.

^{13}C-NMR [100MHz, $CDCl_3$] δ 26.0, 29.35, 29.41, 29.5, 50.5, 68.1, 110.0, 115.1, 117.5, 119.9, 124.9, 127.0, 128.3, 131.3, 131.7, 132.6, 143.7, 145.2, 146.9, 159.8. (15 peaks unobserved due to overlap of the alkyl and aromatic peaks).

HRMS (ESI) = calc. 635.3493, found. 635.3485 ($M + NH_4^+$).

Bis[5-(4-Triazol-1-[11-carboxyphenylundecyloxybiphenyl-4-carbonitrile]-yl-phenyl)-dipyrrinato]-nickel (45):

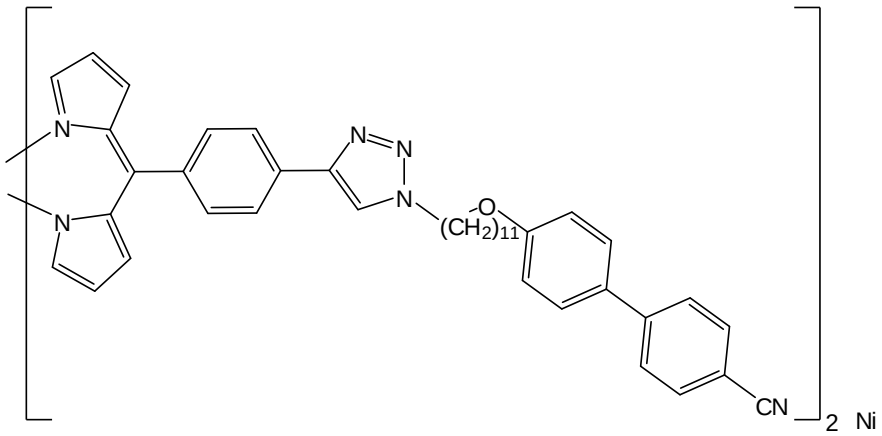

5-(4-Triazol-1-[11-carboxyphenylundecyloxybiphenyl-4-carbonitrile]-yl-phenyl)-dipyrromethene (37 mg, 6.12×10^{-5} mol) was dissolved in dichloromethane (5 ml). To this solution was added nickel (II) acetate (0.22g, 1.53 mmol) in methanol (5 ml) dropwise and the solution was stirred at r.t. for 15 hrs. The solvent was removed and the residue dissolved in dichloromethane and washed with water (2 x 30 ml) and brine (30 ml), dried over anhydrous $MgSO_4$, filtered and evaporated *in vacuo*. The residue was passed through a short silica column eluting with 1:9 EtOAc:CH_2Cl_2 to yield a red/brown solid (20 mg, 49%), m.p. 186-188°C, R_f = 0.68 (1:9 EtOAc:CH_2Cl_2).

^{1}H-NMR [400MHz, $CDCl_3$] δ 1.23 (24H, m, CH_2's), 1.40 (4H, m, CH_2), 1.73 (4H, m, CH_2), 1.91 (4H, m, CH_2), 3.92 (4H, t, CH_2OPh), 4.37 (4H, t, CH_2N), 6.44 (4H, m, Py-H), 6.69 (4H, m, Py-H), 6.91 (4H, d, Ph-H), 7.45 (4H, d, Ph-H), 7.56 (4H, d, Ph-H), 7.61 (4H, d, Ph-H), 7.79 (4H, d, Ph-H), 7.87 (4H, m, Py-H), 9.31 (2H, s, triazole-H).

^{13}C-NMR [100MHz, $CDCl_3$] δ 19.9, 26.1, 26.6, 29.1, 29.3, 29.4, 29.5, 29.6, 30.4, 50.6, 68.2, 110.1, 115.2, 119.3, 119.7, 119.9, 124.9, 127.2, 128.4, 131.4, 131.7, 132.7, 145.4, 159.9. (11 peaks unobserved due to overlap of the alkyl and aromatic peaks).

MS (MALDI) = calc. 1324.6, found. 1324.6 (M^+).

7-(4-Bromophenyl)-6,8-dimethyl-diindolylmethane (46):

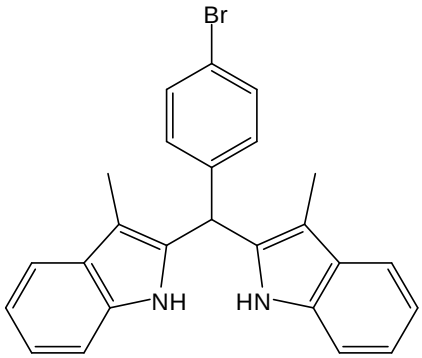

3-Methylindole (1.5g, 11.5 mmol) and 4-bromobenzaldehyde (1.05g, 5.7 mmol) were dissolved in methanol (100 ml) and 60% $HCl_{(aq)}$ (0.47ml, 5.6 mmol) was added over 5mins. The solution was then stirred for 3.5 hrs at r.t. before being neutralized with $NaOH_{(aq)}$ soln. Water (~50 ml) was then added and the mixture was stirred for 1 hr before the precipitate was filtered off and washed with water to yield the pure product as a white solid (282 mg, 12%), m.p. 133-134°C.

^{1}H-NMR [400MHz, $CDCl_3$] δ 2.16 (6H, 2 x CH_3), 5.95 (1H, s, *meso*-H), 7.06 (2H, d, Ph-H, *J* = 8.44Hz), 7.15 (4H, m, Ph-H), 7.24 (2H, d, Ph-H), 7.46 (2H, d, Ph-H, *J* = 8.44Hz), 7.55 (4H, m, Ph-H + NH).

^{13}C-NMR [100MHz, $CDCl_3$] δ 8.5, 40.4, 109.0, 110.9, 118.6, 119.6, 121.3, 121.9, 129.5, 130.2, 132.1, 132.7, 135.3, 139.1.

MS (ESI) m/z 428.4 and 430.4 (M^+).

8-(3,5-Dibromophenyl)-BODIPY (47):

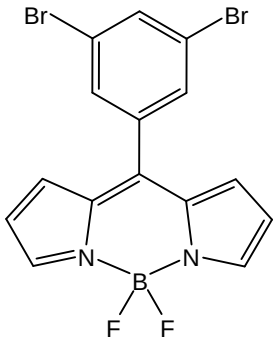

3,5-Dibromobenzaldehyde (1.5g, 5.68 mmol) was dissolved in freshly distilled pyrrole (15.8ml, 0.23 mol) and the solution was degassed with argon for 20 mins. TFA (0.1 ml) was then added and the mixture stirred at r.t. under argon and protected from light for 15 mins. The excess pyrrole was then removed *in vacuo* and the oily residue was passed through a short silica column eluting with 1:4 hexane:CH_2Cl_2 and evaporated *in vacuo*. The residue was dissolved in THF (50 ml) and chloranil (1.40g, 5.68 mmol) was added. The mixture was stirred at r.t. for 16 hrs. The THF was then removed *in vacuo* and the residue redissolved in dichloromethane before filtering to remove the quinine species. The dichloromethane solution was concentrated *in vacuo* to 50 ml before diisopropylethylamine (4.61 ml, 26.5 mmol) was added followed by boron trifluoride diethyl etherate (3.79 ml, 29.9 mmol) and the solution was stirred under nitrogen for 18 hrs. The solution was then filtered through Celite then washed with water (6 x 50 ml), dried over anhydrous $MgSO_4$ and evaporated *in vacuo*. The residue was purified by column chromatography eluting with 1:4 hexane:toluene to yield the pure product as a shiny red solid (0.7g, 29%), m.p. 178-179°C, lit. 179°C[287].

^{1}H-NMR [400MHz, $CDCl_3$] δ 6.58 (2H, d, Py-H), 6.90 (2H, d, Py-H), 7.64 (2H, m, Ph-H), 7.89 (1H, m, Ph-H), 7.97 (2H, m, Py-H).

^{13}C-NMR [100MHz, $CDCl_3$] δ 119.2, 123.1, 131.2, 131.6, 134.5, 136.0, 136.8, 143.0, 145.36.

^{11}B-NMR [128.3MHz, $CDCl_3$] δ -0.7337.

HRMS (ESI) = calc. 424.9266, 426.9246 and 428.9226, found. 424.9263, 426.9242 and 428.9220 ($M + H^+$).

8-(3,5-Dibromophenyl)-1,3,5,7-tetramethyl-BODIPY (48):

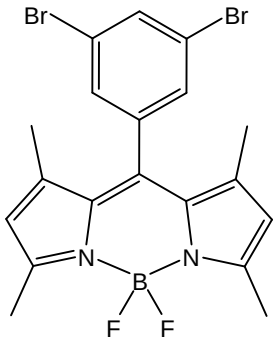

3,5-Dibromobenzaldehyde (1.5g, 5.68 mmol) and 2,4-dimethylpyrrole (1.17 ml, 11.36 mmol) were dissolved in dry dichloromethane (70 ml) and degassed with argon for 20mins. TFA (0.1 ml) was then added and the solution was stirred at r.t. under argon for 16hrs. DDQ (1.29g, 5.68 mmol) was then added and the mixture was stirred for 6 hrs. Triethylamine (3.69 ml, 26.5 mmol) was then added followed by boron trifluoride diethyl etherate (3.79 ml, 29.9 mmol) and the solution was stirred under argon for 18 hrs. The mixture was then filtered and washed with water (6 x 60 ml), dried over anhydrous $MgSO_4$ and evaporated *in vacuo*. The residue was purified by column chromatography eluting with 1:1 hexane:CH_2Cl_2 to yield the pure product as a bright red solid (186 mg, 7%), m.p. 257-258°C (decomp.).

^{1}H-NMR [400MHz, $CDCl_3$] δ 1.47 (6H, s, 2 x CH_3), 2.53 (6H, s, 2 x CH_3), 6.00 (2H, s, Py-H), 7.42 (2H, m, Ph-H), 7.80 (1H, m, Ph-H).

^{13}C-NMR [100MHz, $CDCl_3$] δ 14.6, 14.9, 121.7, 123.6, 130.1, 130.9, 134.7, 137.4, 138.4, 142.7, 156.5.

^{11}B-NMR [128.3MHz, $CDCl_3$] δ -0.4891.

HRMS (ESI) = calc. 480.9896, 482.9876 and 484.9852, found. 480.9887, 482.9867 and 484.9845 ($M + H^+$).

8-(3,5-Dibromophenyl)-1,3,5,7-tetramethyl-2,6-diethyl-BODIPY (49):

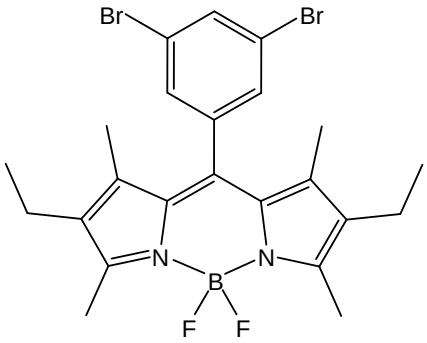

3,5-Dibromobenzaldehyde (1.5g, 5.68 mmol) and kryptopyrrole (1.53 ml, 11.36 mmol) were dissolved in dry dichloromethane (40 ml) and degassed with argon for 20 mins. TFA (0.1 ml) was then added and the solution was stirred at r.t. under argon for 16 hrs. DDQ (1.29g, 5.68 mmol) was then added and the mixture was stirred for 6 hrs. Triethylamine (3.69 ml, 26.5 mmol) was then added followed by boron trifluoride diethyl etherate (3.79 ml, 29.9 mmol) and the solution was stirred under argon for 18 hrs. The mixture was then filtered and washed with water (6 x 60 ml), dried over anhydrous $MgSO_4$ and evaporated *in vacuo*. The residue was purified by column chromatography eluting with 3:2 toluene:hexane to yield the pure product as a bright red solid (384 mg, 13%), m.p. 241-242°C.

^{1}H-NMR [400MHz, $CDCl_3$] δ 0.99 (6H, t, C**H$_3$**CH$_2$, *J* = 7.50Hz), 1.39 (6H, s, 2 x CH_3), 2.31 (4H, q, C**H$_2$**CH$_3$, *J* = 7.50Hz), 2.53 (6H, s, 2 x CH_3), 7.44 (2H, d, Ph-H), 7.81 (1H, t, Ph-H).

^{13}C-NMR [100MHz, $CDCl_3$] δ 12.2, 12.6, 14.6, 17.1, 123.5, 130.4, 133.4, 134.5, 135.9, 137.8, 139.3, 154.8.

^{11}B-NMR [128.3MHz, $CDCl_3$] δ -0.2446.

HRMS (ESI) = calc. 537.0523, 539.0503 and 541.0479, found 537.0515, 539.0495 and 541.0472 ($M + H^+$).

4'-(11-[4-Boronpinacolatephenylcarboxy]undecyloxy)-biphenyl-4-carbonitrile (50):

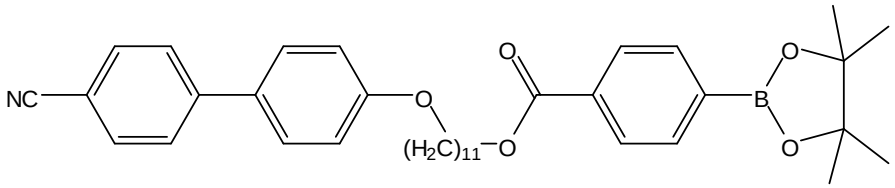

4'-(11-Hydroxyundecyl)-biphenyl-4-carbonitrile (0.90g, 2.47 mmol) and 4-carboxyphenylboronic acid pinacol ester (0.60g, 2.42 mmol) were mixed in dry dichloromethane (50 ml). DMAP (0.30g, 2.49 mmol) was then added followed by DCC (0.85g, 4.11 mmol) and the mixture was stirred at r.t. for 18 hrs. The mixture was then filtered and the filtrate washed with 2% $HCl_{(aq)}$ (50 ml) and water (3 x 50 ml), dried over anhydrous $MgSO_4$ and evaporated *in vacuo*. The residue was recrystallized from EtOAc to yield the pure product as a white solid (0.99g, 69%).

^{1}H-NMR [400MHz, $CDCl_3$] δ 1.31 (10H, m, CH_2's), 1.35 (12H, s, 4 x CH_3), 1.45 (4H, m, CH_2's), 1.78 (4H, m, CH_2's), 4.00 (2H, t, CH_2OPh, *J* = 6.60Hz), 4.31 (2H, t, CH_2O, *J* = 6.69Hz), 6.99 (2H, d, Ph-H, *J* = 8.80Hz), 7.52 (2H, d, Ph-H, *J* = 8.80Hz), 7.63 (2H, d, Ph-H, *J* = 8.80Hz), 7.69 (2H, d, Ph-H, *J* = 8.61Hz), 7.86 (2H, d, Ph-H, *J* = 8.25Hz), 8.01 (2H, d, Ph-H, *J* = 8.43Hz).

^{13}C-NMR [100MHz, $CDCl_3$] δ 24.9, 26.0, 28.7, 29.2, 29.3, 29.5, 29.5, 65.2, 68.2, 84.2, 110.0, 115.1, 119.1, 127.1, 128.3, 128.5, 131.2, 132.6, 132.7, 134.6, 145.3, 159.8, 166.7. (11 peaks unobserved due to overlap of the alkyl and aromatic peaks).

^{11}B-NMR [128.3MHz, $CDCl_3$] δ 29.5926.

HRMS (ESI) = calc. 596.3524, found. 596.3548 $(M - H)^+$.

4'-(11-[4-Bromophenylcarboxy]undecyl)-biphenyl-4-carbonitrile:

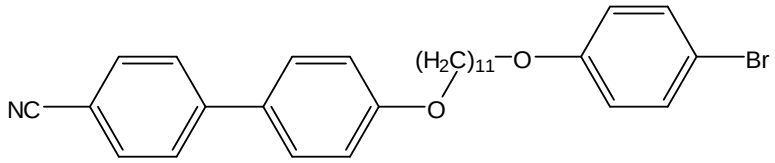

4'-(11-Mesityloxyundecyl)-biphenyl-4-carbonitrile (1.90g, 4.28 mmol), 4-bromophenol (0.84g, 4.84mmol) and anhydrous potassium carbonate (1.54g, 11.1 mmol) were mixed in butanone (100 ml) and refluxed for 16 hrs. The mixture was then cooled to r.t. and concentrated *in vacuo*. Ethyl acetate (80 ml) was then added and the mixture was washed with water (2 x 70 ml), dried over anhydrous $MgSO_4$, filtered and evaporated *in vacuo*. The residue was recrystallized from 1:1 EtOH:CH_2Cl_2 to yield the pure product as a white powder (1.37g, 61%), Cr 92 N 100 I, lit. Cr 92.2 N 99.5 I[286].

^{1}H-NMR [400MHz, $CDCl_3$] δ 1.30 (12H, m, CH_2's), 1.43 (4H, m, CH_2's), 1.76 (4H, m, CH_2), 3.89 (2H, t, CH_2OPh, *J* = 6.56Hz), 3.98 (2H, t, CH_2OPh, *J* = 6.56Hz), 6.75 (2H, d, Ph-H, *J* = 9.07Hz), 6.97 (2H, d, Ph-H, *J* = 8.44Hz), 7.33 (2H, d, Ph-H, *J* = 8.76Hz), 7.50 (2H, d, Ph-H, *J* = 8.76Hz), 7.64 (4H, dd, Ph-H).

^{13}C-NMR [100MHz, $CDCl_3$] δ 26.9, 29.2, 29.3, 29.47, 29.50, 68.17, 68.24, 110.0, 112.6, 115.1, 116.3, 119.1, 127.1, 128.3, 131.3, 132.2, 132.6, 145.3, 158.2, 159.8. (10 peaks unobserved due to overlap of the alkyl and aromatic peaks).

HRMS (ESI) = calc. 537.2111 and 539.2092, found 537.2109 and 539.2089 (M + NH_4^+).

4'-(11-[4-Iodophenylcarboxy]undecyl)-biphenyl-4-carbonitrile:

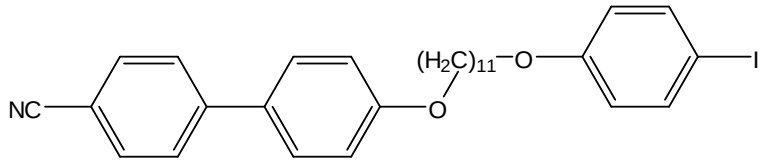

4'-(11-Mesityloxyundecyl)-biphenyl-4-carbonitrile (1.07g, 2.41 mmol), 4-iodophenol (0.69g, 3.13mmol) and anhydrous potassium carbonate (0.87g, 6.27 mmol) were mixed in DMF (30 ml) and refluxed for 16 hrs. The DMF was then removed *in vacuo* and water added to the residue which was then extracted with dichloromethane (2 x 40 ml). The combined organic extracts were then washed with water (2 x 50 ml), dried over anhydrous Na_2SO_4, filtered and evaporated *in vacuo*. The residue was then recrystallized from ethyl acetate to yield the pure product as an off-white solid (1.21g, 88%), m.p. 114-115°C, lit. 114-116°C[288].

^{1}H-NMR [400MHz, $CDCl_3$] δ 1.30 (10H, m, CH_2's), 1.44 (4H, m, CH_2's), 1.77 (4H, m, CH_2's), 3.89 (2H, t, CH_2OPh, *J* = 6.57Hz), 3.99 (2H, t, CH_2OPh, *J* = 6.57Hz), 6.65 (2H, d, Ph-H, *J* = 9.07Hz), 6.97 (2H, d, Ph-H, *J* = 8.76Hz), 7.51 (4H, m, Ph-H), 7.62 (2H, d, Ph-H, *J* = 8.44Hz), 7.67 (2H, d, Ph-H, *J* = 8.44Hz).

^{13}C-NMR [100MHz, $CDCl_3$] δ 26.0, 29.1, 29.3, 29.5, 68.1, 82.4, 110.1, 115.1, 116.9, 119.1, 127.1, 128.3, 131.3, 132.6, 138.1, 145.3, 159.0, 159.8. (12 peaks unobserved due to overlap of the alkyl and aromatic peaks).

HRMS (ESI) = calc. 585.1972, found 585.1970 ($M + NH_4^+$).

8-(3,5-Bis[11-carboxyphenylundecyloxybiphenyl-4-carbonitrile]-phenyl)-BODIPY (52):

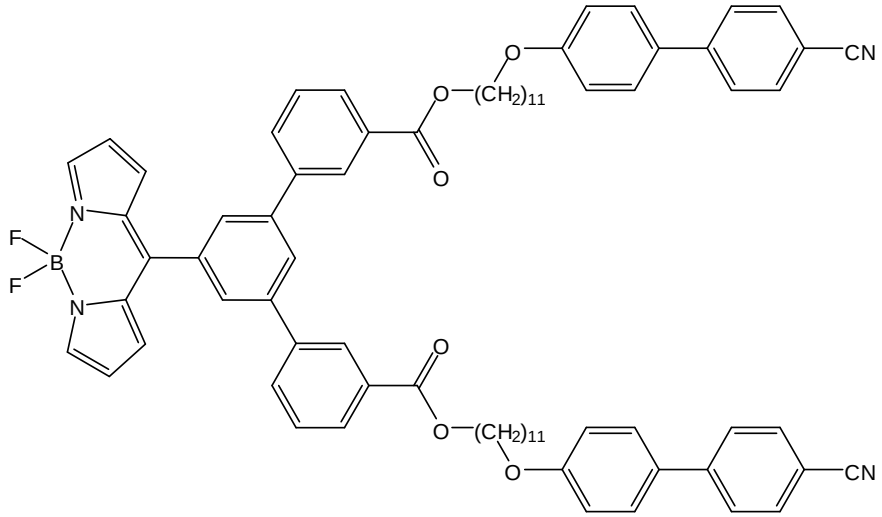

8-(3,5-Dibromophenyl)-BODIPY (40 mg, 93.9 μmol), 4'-(11-[4-boronpinacolatephenylcarboxy]undecyloxy)-biphenyl-4-carbonitrile (134 mg, 0.225 mmol), dibenzylideneacetone palladium (II) (34mg, 37.6μmol), (2-biphenyl)di-*tert*-butylphosphine (14 mg, 47.0 μmol) and potassium carbonate (65 mg, 0.470 mmol) were mixed in DMF (6 ml) and the mixture was degassed with argon for 30 mins. The mixture was then heated in a microwave for 5 mins at 65°C (75W). The DMF was then removed *in vacuo* and the residue subjected to column chromatography eluting with 1:99 EtOAc:toluene. The residue was then precipitated from CH_2Cl_2 with cold MeOH to yield the pure product as a bright red solid (78 mg, 69%), m.p. 78-79°C, R_f = 0.17 (toluene).

^{1}H-NMR [400MHz, $CDCl_3$] δ 1.32 (20H, m, CH_2's), 1.45 (8H, m, CH_2's), 1.80 (8H, m, CH_2's), 4.00 (4H, t, 2 x CH_2OPh, *J* = 6.57Hz), 4.36 (4H, t, 2 x CH_2O, *J* = 6.57Hz), 6.58 (2H, m, Py-H), 6.97 (4H, d, Ph-H, *J* = 8.76Hz), 7.01 (2H, m, Py-H), 7.51 (4H, d, Ph-H, *J* = 8.76Hz), 7.63 (4H, d, Ph-H, *J* = 8.44Hz), 7.68 (4H, d, Ph-H, *J* = 8.44Hz), 7.75 (4H, d, Ph-H, *J* = 8.44Hz), 7.82 (2H, d, Ph-H), 7.99 (2H, m, Py-H), 8.05 (1H, t, Ph-H), 8.18 (4H, d, Ph-H, *J* = 8.44Hz).

^{13}C-NMR [100MHz, $CDCl_3$] δ 26.0, 28.8, 29.2, 29.3, 29.5, 65.4, 68.2, 110.1, 115.1, 118.9, 119.1, 127.1, 127.3, 128.3, 128.5, 130.3, 130.4, 131.2, 131.3, 132.6, 134.9, 135.1, 141.3, 143.8, 144.8, 145.3, 159.8, 166.3. (12 peaks unobserved due to overlap of the alkyl and aromatic peaks).

^{11}B-NMR [128.3MHz, $CDCl_3$] δ -0.4891.

MS (MALDI) = calc. 1202.6, found. 1202.6 (M^+).

HPLC retention time (80:20 MeCN:DCM): 6.26 mins.

8-(3,5-Bis[11-carboxyphenylundecyloxybiphenyl-4-carbonitrile]-phenyl)-1,3,5,7-tetramethyl-BODIPY (53):

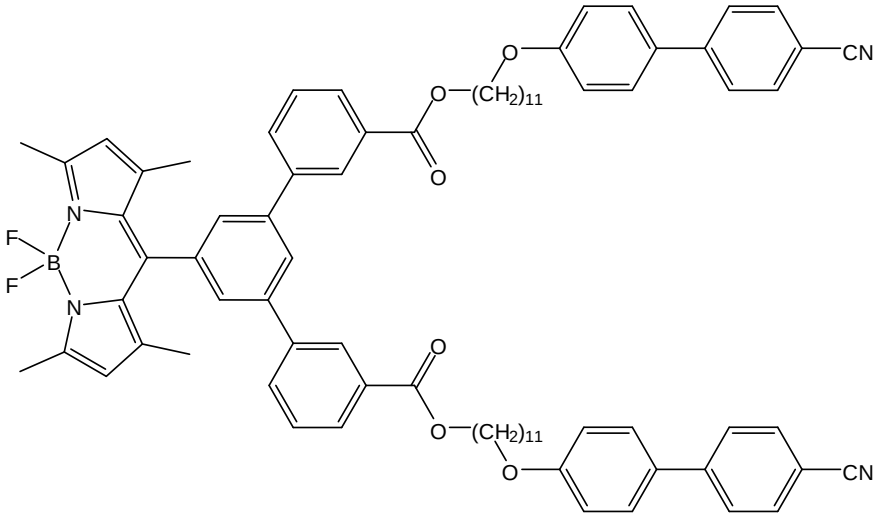

8-(3,5-Dibromophenyl)-1,3,5,7-tetramethyl-BODIPY (45mg, 93.4μmol), 4'-(11-[4-boronpinacolatephenylcarboxy]undecyloxy)-biphenyl-4-carbonitrile (134 mg, 0.224 mmol), dibenzylideneacetone palladium (II) (34 mg, 37.4 μmol), (2-biphenyl)di-*tert*-butylphosphine (14 mg, 46.7 μmol) and potassium carbonate (65 mg, 0.467 mmol) were mixed in DMF (6 ml) and the mixture was degassed with argon for 30 mins. The mixture was then heated in a microwave for 5 mins at 65°C (75W). The DMF was then removed *in vacuo* and the residue subjected to column chromatography eluting with 1:99 EtOAc:toluene. The residue was then precipitated from CH_2Cl_2 with cold MeOH to yield the pure product as a bright red solid (30 mg, 25%), m.p. 73-74°C, R_f = 0.18 (toluene).

^{1}H-NMR [400MHz, $CDCl_3$] δ 1.32 (20H, m, CH_2's), 1.46 (8H, m, CH_2's), 1.50 (6H, s, 2 x CH_3), 1.80 (8H, m, CH_2's), 2.58 (6H, s, 2 x CH_3), 3.99 (4H, t, 2 x CH_2OPh, J = 6.57Hz), 4.35 (4H, t, 2 x CH_2O, J = 6.57Hz), 6.01 (2H, s, Py-H), 6.98 (4H, d, Ph-H, J = 8.76Hz), 7.51 (4H, d, Ph-H, J = 8.76Hz), 7.62 (6H, m, Ph-H), 7.68 (4H, d, Ph-H, J = 8.60Hz), 7.72 (4H, d, Ph-H, J = 8.44Hz), 7.98 (1H, t, Ph-H), 8.14 (4H, d, Ph-H, J = 8.44Hz).

^{13}C-NMR [100MHz, $CDCl_3$] δ 14.6, 14.9, 26.0, 28.7, 29.21, 29.25, 29.4, 29.5, 65.3, 68.2, 110.0, 115.1, 119.1, 121.5, 126.5, 127.0, 127.1, 128.3, 129.3, 130.3, 131.3, 132.6, 141.8, 142.8, 143.9, 145.3, 156.0, 159.8, 166.3. (12 peaks unobserved due to overlap of the alkyl and aromatic peaks).

^{11}B-NMR [128.3MHz, $CDCl_3$] δ 0.0000.

MS (MALDI) = calc. 1258.7, found. 1258.6 (M^+).

HPLC retention time (80:20 MeCN:DCM): 8.92 mins.

8-(3,5-Bis[11-carboxyphenylundecyloxybiphenyl-4-carbonitrile]-phenyl)-1,3,5,7-tetramethyl-2,6-diethyl-BODIPY (54):

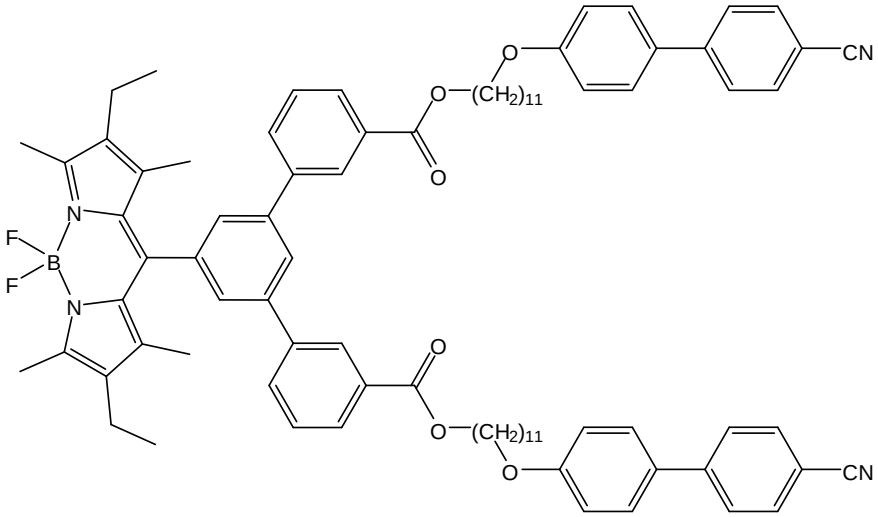

8-(3,5-Dibromophenyl)-1,3,5,7-tetramethyl-2,6-diethyl-BODIPY (50 mg, 92.9 μmol), 4'-(11-[4-boronpinacolatephenylcarboxy]undecyloxy)-biphenyl-4-carbonitrile (133 mg, 0.223 mmol), dibenzylideneacetone palladium (II) (34 mg, 37.2 μmol), (2-biphenyl)di-*tert*-butylphosphine (14 mg, 46.5 μmol) and potassium carbonate (64 mg, 0.465 mmol) were mixed in DMF (6 ml) and the mixture was degassed with argon for 30 mins. The mixture was then heated in a microwave for 5 mins at 65°C (75W). The DMF was then removed *in vacuo* and the residue subjected to column chromatography eluting with 1:99 EtOAc:toluene. The residue was then precipitated from CH_2Cl_2 with cold MeOH to yield the pure product as a bright red solid (56 mg, 46%), m.p. 87-88°C, R_f = 0.18 (toluene).

^{1}H-NMR [400MHz, $CDCl_3$] δ 0.99 (6H, t, 2 x C**H$_3$**CH$_2$, *J* = 7.52Hz), 1.32 (20H, m, CH_2's), 1.40 (6H, s, 2 x CH_3), 1.47 (8H, m, CH_2's), 1.80 (8H, m, CH_2's), 2.30 (4H, q, C**H$_2$**CH$_3$, *J* = 7.50Hz), 2.53 (6H, s, 2 x CH_3), 3.99 (4H, t, 2 x CH_2OPh, *J* = 6.42Hz), 4.35 (4H, t, 2 x CH_2O, *J* = 6.69Hz), 6.98 (4H, d, Ph-H, *J* = 8.80Hz), 7.52 (4H, d, Ph-H, *J* = 8.61Hz), 7.62 (6H, m, Ph-H), 7.69 (4H, d, Ph-H, *J* = 8.06Hz), 7.74 (4H, d, Ph-H, *J* = 8.43Hz), 7.98 (1H, t, Ph-H), 8.15 (4H, d, Ph-H, *J* = 8.25Hz).

^{13}C-NMR [100MHz, $CDCl_3$] δ 12.2, 12.6, 14.6, 17.1, 26.0, 28.7, 29.21, 29.25, 29.4, 29.5, 65.3, 68.2, 110.0, 115.1, 119.1, 126.8, 127.0, 127.1, 127.2, 128.3, 130.0, 130.3, 131.3, 132.5, 133.1, 137.3, 141.7, 144.0, 145.3, 154.3, 159.8, 166.3. (11 peaks unobserved due to overlap of the alkyl and aromatic peaks).

^{11}B-NMR [128.3MHz, $CDCl_3$] δ 0.0000.

MS (MALDI) = calc. 1314.7, found. 1314.6 (M^+).

8-(3,5-Bis[11-carboxyphenylundecyloxy-phenyl-4'-cyano-4-biphenyl-carboxylate]-phenyl)-BODIPY (55):

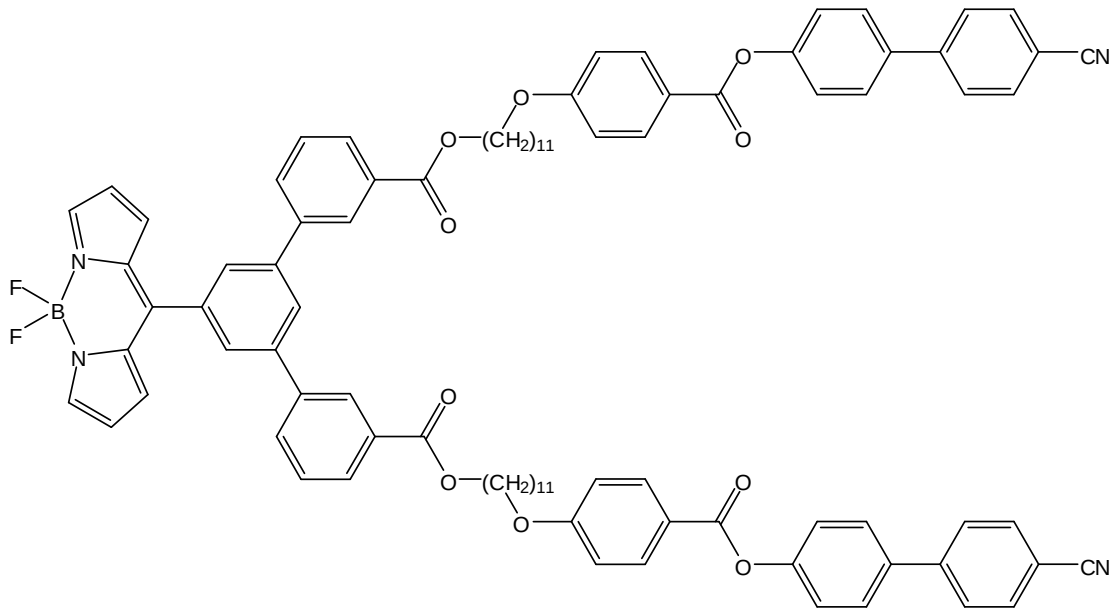

8-(3,5-Dibromophenyl)-BODIPY (35 mg, 82.2 μmol), 4-(11-[4-boronpinacolatephenylcarboxy]undecyloxy)-phenyl-4'-cyano-4-biphenyl carboxylate (125 mg, 0.197 mmol), dibenzylideneacetone palladium (II) (30 mg, 32.9 μmol), (2-biphenyl)di-*tert*-butylphosphine (12 mg, 41.1 μmol) and potassium carbonate (57 mg, 0.411 mmol) were mixed in DMF (6 ml) and the mixture was degassed with argon for 30 mins. The mixture was then heated in a microwave for 5 mins at 65°C (75W). The DMF was then removed *in vacuo* and the residue subjected to column chromatography eluting with 1:99 EtOAc:toluene. The residue was then precipitated from CH_2Cl_2 with cold MeOH to yield the pure product as a bright red solid (56 mg, 47%), R_f = 0.19 (toluene), LC transitions: T_g 57 N 149 I.

^{1}H-NMR [400MHz, $CDCl_3$] δ 1.33 (20H, m, CH_2's), 1.47 (8H, m, CH_2's), 1.80 (8H, m, CH_2's), 4.04 (4H, t, 2 x CH_2OPh, J = 6.57Hz), 4.36 (4H, t, 2 x CH_2O, J = 6.72Hz), 6.58 (2H, m, Py-H), 6.97 (4H, d, Ph-H, J = 9.07Hz), 7.01 (2H, m, Py-H), 7.32 (4H, d, Ph-H, J = 8.76Hz), 7.63 (4H, d, Ph-H, J = 8.76Hz), 7.68 (4H, d, Ph-H, J = 8.44Hz), 7.74 (8H, m, Ph-H), 7.82 (2H, d, Ph-H), 7.99 (2H, m, Py-H), 8.05 (1H, t, Ph-H), 8.16 (8H, m, Ph-H).

^{13}C-NMR [100MHz, $CDCl_3$] δ 25.99, 26.04, 28.7, 29.1, 29.3, 29.4, 29.5, 65.4, 68.4, 111.0, 114.4, 118.9, 121.2, 122.6, 127.3, 127.7, 128.4, 130.3, 130.4, 131.5, 132.4, 132.7, 135.0, 135.3, 136.7, 141.3, 143.7, 144.7, 144.8, 151.5, 163.7, 164.8, 166.3. (14 peaks unobserved due to overlap of the alkyl and aromatic peaks).

^{11}B-NMR [128.3MHz, $CDCl_3$] δ -0.6732.

MS (MALDI) = calc. 1465.6, found. 1465.7 ($M + Na^+$).

HPLC retention time (80:20 MeCN:DCM): 5.79 mins.

Fluorescence absorption maximum: 505 nm; fluorescence emission maximum: 525 nm.

8-(3,5-Bis[11-carboxyphenylundecyloxy-phenyl-4'-cyano-4-biphenyl-carboxylate]-phenyl)-1,3,5,7-tetramethyl-BODIPY (56):

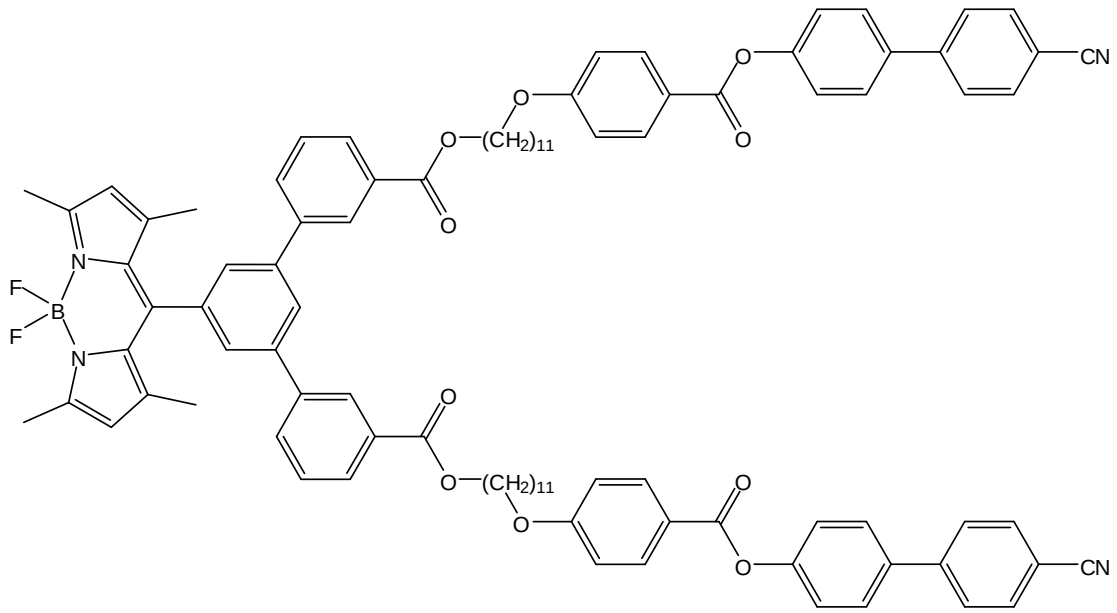

8-(3,5-Dibromophenyl)-1,3,5,7-tetramethyl-BODIPY (40 mg, 82.2 μmol), 4-(11-[4-boronpinacolatephenylcarboxy]undecyloxy)-phenyl-4'-cyano-4-biphenyl carboxylate (125 mg, 0.197 mmol), dibenzylideneacetone palladium (II) (30 mg, 32.9 μmol), (2-biphenyl)di-*tert*-butylphosphine (12 mg, 41.1 μmol) and potassium carbonate (57mg, 0.411 mmol) were mixed in DMF (6 ml) and the mixture was degassed with argon for 30 mins. The mixture was then heated in a microwave for 5 mins at 65°C (75W). The DMF was then removed *in vacuo* and the residue subjected to column chromatography eluting with 1:99 EtOAc:toluene. The residue was then precipitated from CH_2Cl_2 with cold MeOH to yield the pure product as a bright red solid (36 mg, 29%), R_f = 0.52 (15:85 EtOAc:toluene), LC transitions: T_g 65 N 129 I.

^{1}H-NMR [400MHz, $CDCl_3$] δ 1.31 (24H, m, CH_2's), 1.44 (8H, m, CH_2's), 1.49 (6H, s, 2 x CH_3), 1.78 (8H, m, CH_2's), 2.56 (6H, s, 2 x CH_3), 4.02 (4H, t, 2 x CH_2OPh, J = 6.57Hz), 4.33 (4H, t, 2 x CH_2O, J = 6.73Hz), 6.00 (2H, s, Py-H), 6.95 (4H, d, Ph-H, J = 8.76Hz), 7.30 (4H, d, Ph-H, J = 8.44Hz), 7.61 (6H, m, Ph-H), 7.67 (4H, d, Ph-H, J = 8.44Hz), 7.71 (8H, m, Ph-H), 7.96 (1H, t, Ph-H), 8.13 (8H, d, Ph-H, J = 8.76Hz).

^{13}C-NMR [100MHz, $CDCl_3$] δ 14.9, 26.0, 28.7, 29.1, 29.26, 29.34, 29.5, 65.3, 68.4, 114.4, 118.9, 122.6, 127.0, 127.7, 128.3, 130.2, 130.3, 132.3, 132.7, 136.7, 143.9, 144.9, 151.6, 163.6, 164.8, 166.3. (20 peaks unobserved due to overlap of the alkyl and aromatic peaks).

^{11}B-NMR [128.3MHz, $CDCl_3$] δ -0.2446.

MS (MALDI) = calc. 1498.7, found. 1498.7 (M^+).

HPLC retention times (80:20 MeCN:DCM): 7.78 mins.

Fluorescence absorption maximum: 505 nm; fluorescence emission maximum: 518 nm.

8-(3,5-Bis[11-carboxyphenylundecyloxy-phenyl-4'-cyano-4-biphenyl-carboxylate]-phenyl)-1,3,5,7-tetramethyl-2,6-diethyl-BODIPY (57):

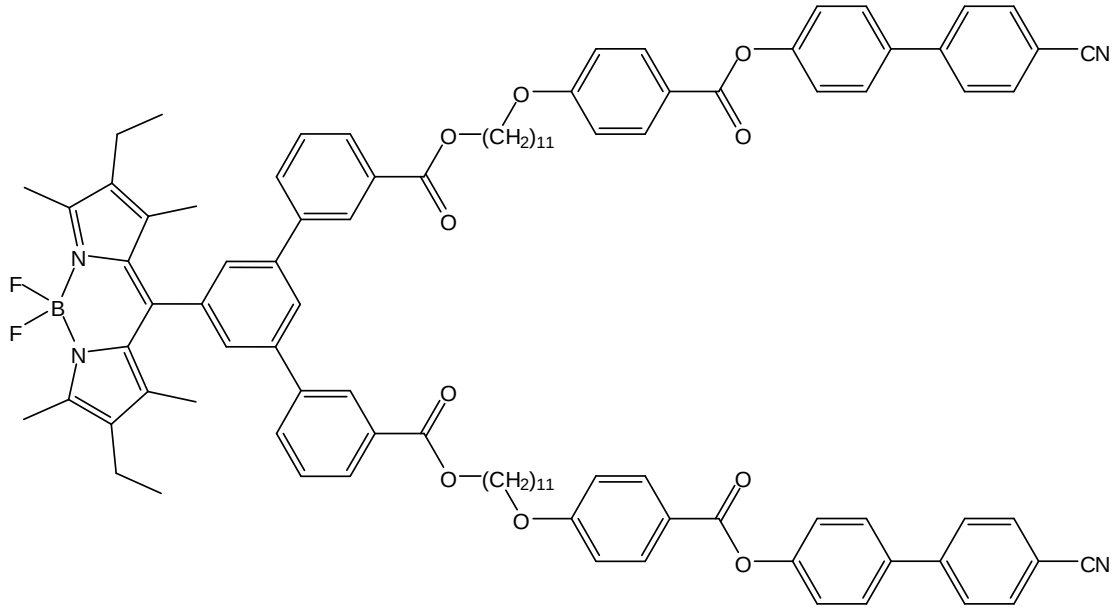

8-(3,5-Dibromophenyl)-1,3,5,7-tetramethyl-2,6-diethyl-BODIPY (44 mg, 82.2 μmol), 4-(11-[4-boronpinacolatephenylcarboxy]undecyloxy)-phenyl-4'-cyano-4-biphenyl carboxylate (125 mg, 0.197 mmol), dibenzylideneacetone palladium (II) (30 mg, 32.9 μmol), (2-biphenyl)di-*tert*-butylphosphine (12 mg, 41.1 μmol) and potassium carbonate (57 mg, 0.411 mmol) were mixed in DMF (6 ml) and the mixture was degassed with argon for 30 mins. The mixture was then heated in a microwave for 5 mins at 65°C (75W). The DMF was then removed *in vacuo* and the residue subjected to column chromatography eluting with 2:98 EtOAc:toluene. The residue was then precipitated from CH_2Cl_2 with cold MeOH to yield the pure product as a bright red solid (57 mg, 45%), R_f = 0.63 (1:9 EtOAc:toluene), LC transitions: T_g 73 N 99 I.

^{1}H-NMR [400MHz, $CDCl_3$] δ 0.99 (6H, t, 2 x C**H$_3$**CH_2, *J* = 7.66Hz), 1.33 (20H, m, CH_2's), 1.41 (6H, s, 2 x CH_3), 1.46 (8H, m, CH_2's), 1.80 (8H, m, CH_2's), 2.30 (4H, q, 2 x C**H$_2$**CH_3, *J* = 7.50Hz), 2.55 (6H, s, 2 x CH_3), 4.04 (4H, t, 2 x CH_2OPh, *J* = 6.57Hz), 4.35 (4H, t, 2 x CH_2O, *J* = 6.73Hz), 6.98 (4H, d, Ph-H, *J* = 8.76Hz), 7.32 (4H, d, Ph-H, *J* = 8.76Hz), 7.63 (6H, m, Ph-H), 7.68 (4H, d, Ph-H, *J* = 8.44Hz), 7.74 (8H, d, Ph-H, *J* = 8.44Hz), 7.99 (1H, t, Ph-H), 8.15 (8H, d, Ph-H, *J* = 8.76Hz).

^{13}C-NMR [100MHz, $CDCl_3$] δ 12.2, 12.6, 14.6, 17.1, 26.00, 26.03, 28.7, 29.1, 29.3, 29.4, 29.5, 53.4, 65.3, 68.4, 111.0, 114.4, 118.9, 121.2, 122.6, 126.8, 127.0, 127.7, 128.4, 130.1, 132.4, 132.7, 133.1, 136.7, 138.0, 141.7, 144.1, 144.9, 151.6, 154.3, 163.7, 164.8, 166.3. (13 peaks unobserved due to overlap of the alkyl and aromatic peaks).

^{11}B-NMR [128.3MHz, $CDCl_3$] δ 0.0000.

MS (MALDI) = calc. 1555.6, found. 1553.8 ($M - H^+$).

HPLC retention times (80:20 MeCN:DCM): 10.40 mins.

Fluorescence absorption maximum: 528 nm; fluorescence emission maximum: 542 nm.

(*E*)-1-(4-Bromophenyl)-3-phenylprop-2-ene-1-one (58):

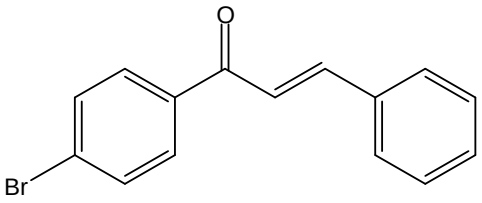

4-Bromoacetophenone (10g, 0.05 mol) and benzaldehyde (5.09 ml, 0.05 mol) were dissolved in 85:15 EtOH/H_2O (100 ml). To this mixture was added potassium hydroxide (84 mg, 1.5 mmol) and the mixture stirred at r.t. for 16 hrs. The precipitate was then filtered and washed with water followed by recrystallisation from ethanol to yield the pure product as an off-white solid (9.62g, 67%), m.p. 99-100°C (lit. 100-101°C).

^{1}H-NMR [400MHz, $CDCl_3$] δ 7.41 (3H, m, *o*- and *p*-H's), 7.46 (1H, d, CHCO, *J* = 15.63Hz), 7.63 (4H, m, Ph-H), 7.80 (1H, d, C**H**CH, *J* = 15.63Hz), 7.87 (2H, d, Ph-H).

^{13}C-NMR [100MHz, $CDCl_3$] δ 121.5, 127.9, 128.5, 129.0, 130.0, 130.8, 131.9, 134.7, 136.9, 145.4, 189.4.

MS (ESI) m/z 286.2 and 288.2 (M^+).

1-(4-Bromophenyl)-3-phenyl-4-nitrobutan-1-one (59):

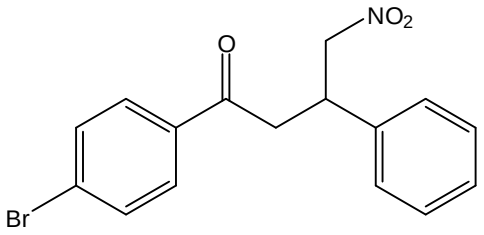

(*E*)-1-(4-Bromophenyl)-3-phenylprop-2-ene-1-one (4g, 14 mmol), nitromethane (3.7 ml, 70 mmol) and diethylamine (4.86 ml, 70 mmol) were dissolved in methanol (115ml) and refluxed for 16 hrs. The solution was then acidified with conc. $HCl_{(aq)}$ and concentrated *in vacuo*. Ethyl acetate (70 ml) was then added and the solution was washed with water (3 x 50 ml), dried over anhydrous $MgSO_4$, filtered and evaporated to give a tan oil which was triturated with methanol to give a tan solid. This was recrystallized from methanol to yield the pure product as a tan solid (3.35g, 69%), m.p. 110-111°C.

^{1}H-NMR [400MHz, $CDCl_3$] δ 3.42 (2H, dd, CH_2CO), 4.21 (1H, m, CH-Ph), 4.69 (1H, dd, CH_a-NO_2), 4.81 (1H, quintet, CH_b-NO_2), 7.30 (5H, m, Ph-H), 7.60 (2H, d, Ph-H, J = 8.76Hz), 7.77 (2H, d, Ph-H, J = 8.76Hz).

^{13}C-NMR [100MHz, $CDCl_3$] δ 36.8, 39.0, 78.2, 124.9, 125.5, 126.4, 126.7, 127.0, 129.6, 132.7, 136.4, 193.4.

MS (ESI) m/z 347.3 and 349.3 (M^+).

(*E*)-1-(4-Bromophenyl)-3-(4-bromophenyl)prop-2-ene-1-one:

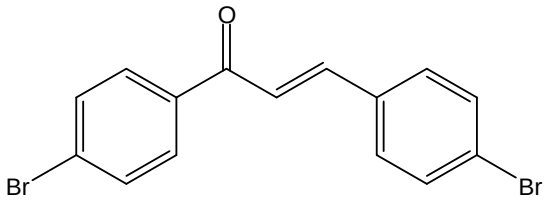

4-Bromoacetophenone (10g, 0.05 mol) and 4-bromobenzaldehyde (9.25g, 0.05 mol) were dissolved in 85:15 EtOH:H_2O (100 ml). To this mixture was added potassium hydroxide (84 mg, 1.5 mmol) and the mixture was stirred at r.t. for 16 hrs. The precipitate was then filtered, washed with water and dried *in vacuo* and was used without further purification (17.20g, 94%), m.p. 176-178°C.

^{1}H-NMR [400MHz, $CDCl_3$] δ 7.46 (1H, d, CHCO, *J* = 15.63Hz), 7.50 (2H, d, Ph-H, *J* = 8.44Hz), 7.56 (2H, d, Ph-H, *J* = 8.44Hz), 7.65 (2H, d, Ph-H, *J* = 8.76Hz), 7.74 (1H, d, C**H**=CH, *J* = 15.63Hz) 7.88 (2H, d, Ph-H, *J* = 8.76Hz).

^{13}C-NMR [100MHz, $CDCl_3$] δ 121.9, 125.1, 128.1, 129.8, 130.0, 132.0, 132.3, 133.6, 136.7, 143.9, 189.1.

MS (ESI) m/z 364.2, 366.2 and 368.2 (M^+).

(*E*)-1-(4-Iodophenyl)-3-phenylprop-2-ene-1-one:

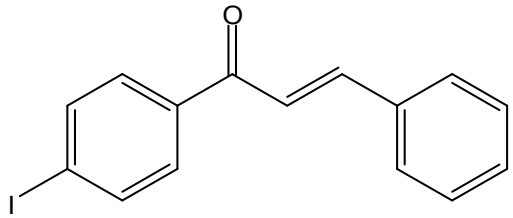

4-Iodoacetophenone (5g, 0.02 mol) and benzaldehyde (2.04 ml, 0.02 mol) were dissolved in 85:15 EtOH/H_2O (40 ml). Potassium hydroxide (34 mg, 0.6 mmol) was then added and the mixture was stirred at r.t. for 16 hrs. The resulting precipitate was then filtered and washed with water followed by recrystallisation from ethanol to yield the pure product as a flaky tan solid (5.61g, 84%), m.p. 109-110°C.

^{1}H-NMR [400MHz, $CDCl_3$] δ 7.41 (4H, m, Ph-H), 7.61 (2H, m, Ph-H + C**H**CH), 7.71 (2H, d, Ph-H, *J* = 8.44Hz), 7.80 (1H, d, COCH, *J* = 15.63Hz), 7.85 (2H, d, Ph-H, *J* = 8.44Hz).

^{13}C-NMR [100MHz, $CDCl_3$] δ 100.6, 121.5, 128.5, 129.0, 129.9, 130.8, 134.7, 137.5, 137.9, 145.4, 189.7.

MS (ESI) m/z 335.2 (M^+).

1-(4-Iodophenyl)-3-phenyl-4-nitrobutan-1-one:

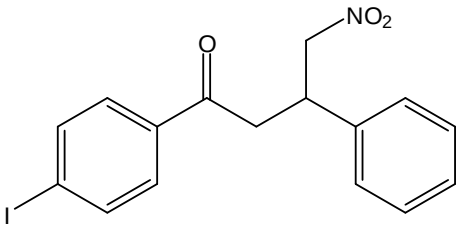

(*E*)-1-(4-Iodophenyl)-3-phenylprop-2-ene-1-one (4g, 0.012 mol), nitromethane (3.22 ml, 0.06 mol) and diethylamine (6.20 ml, 0.06 mol) were dissolved in methanol (100 ml) and refluxed for 15 hrs. The solution was then cooled to r.t. and acidified with conc. $HCl_{(aq)}$ and concentrated by evaporation *in vacuo*. Ethyl acetate (80 ml) was then added and the solution was washed with water (2 x 50 ml), dried over anhydrous Na_2SO_4, filtered and evaporated to give a tan oil. The resulting oil was then triturated with cold methanol and filtered to yield the pure product as a tan solid (3.93g, 83%), m.p. 121-122°C.

^{1}H-NMR [400MHz, $CDCl_3$] δ 3.34 (2H, dd, CH_2NO_2), 4.13 (1H, quintet, CH-Ph), 4.61 (1H, dd, CHCO), 4.74 (1H, dd, CHCO), 7.23 (5H, m, Ph-H), 7.55 (2H, d, Ph-H, *J* = 8.44Hz), 7.75 (2H, d, Ph-H, *J* = 8.44Hz).

^{13}C-NMR [100MHz, $CDCl_3$] δ 36.7, 38.9, 99.2, 124.9, 125.5, 126.7, 126.9, 135.6, 136.4, 193.7.

MS (ESI) m/z 418.2 ($M + Na^+$).

(*E*)-1-Phenyl-3-(4-hydroxyphenyl)prop-2-ene-1-one (60):

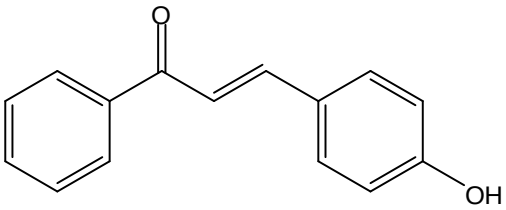

4-Hydroxybenzaldehyde (9.23g, 76 mmol) and acetophenone (7.35 ml, 63 mmol) were dissolved in methanol (70 ml) and to this solution conc. sulphuric acid was added (0.34 ml) and the solution was refluxed for 16hrs. The mixture was cooled and neutralized with $NaOH_{(aq)}$ and the resulting precipitate was filtered off and recrystallized from EtOH to yield the pure product as tan flakes (8.06g, 57%), m.p.186-187°C.

^{1}H-NMR [400MHz, CD_3OD] δ 6.83 (2H, d, Ph-H), 7.52 (2H, m, Ph-H), 7.60 (4H, m, Ph-H), 7.74 (1H, d, CHCO, *J* = 15.22Hz), 8.03 (2H, m, Ph-H).

^{13}C-NMR [100MHz, CD_3OD] δ 117.0, 119.7, 127.7, 129.5, 129.8, 131.9, 133.9, 139.7, 147.0, 161.8, 192.7.

MS (ESI) m/z 242.3 ($M + NH_4^+$).

1,7-Diphenyl-3,5-di(4-hydroxyphenyl)-azadipyrromethene (61):

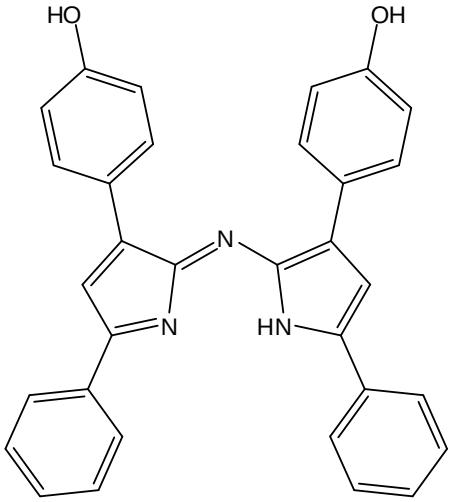

(*E*)-1-Phenyl-3-(4-hydroxyphenyl)prop-2-ene-1-one (4g, 18 mmol), nitromethane (4.83 ml, 90 mmol) and diethylamine (9.35 ml, 90 mmol) were dissolved in methanol and refluxed for 16hrs. The solution was then cooled to r.t. and acidified with conc. $HCl_{(aq)}$ and evaporated. The resulting oil was then dissolved in butan-1-ol (150 ml) and ammonium acetate (37.77g, 0.49 mol) was then added to the solution which was refluxed for 20hrs. The mixture was then cooled to r.t. followed by cooling in an ice-bath before the mixture was filtered to yield the pure product as a shiny dark brown solid (0.98g, 14%), m.p. >300°C.

^{1}H-NMR [400MHz, DMSO-D_6] δ 6.85 (4H, d, Ph-H, *J* = 8.76Hz), 7.49 (2H, s, Py-H), 7.52 (2H, m, Ph-H), 7.60 (4H, t, Ph-H), 7.95 (4H, d, Ph-H, *J* = 8.76Hz), 8.04 (4H, d, Ph-H, *J* = 7.19Hz), 9.78 (1H, bs, NH).

Compound too insoluble to acquire adequate ^{13}C-NMR.

1,7-Diphenyl-3,5-di(4-hydroxyphenyl)-aza-BODIPY (62):

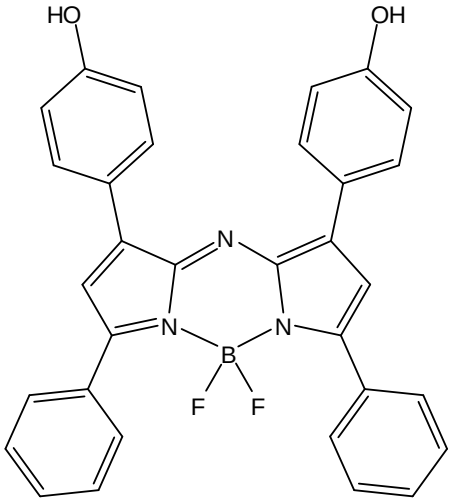

2,8-Diphenyl-4,6-di(4-hydroxyphenyl)-azadipyrromethene (0.6 g, 1.23 mmol) was dissolved in dry dichloromethane (150 ml) and purged with nitrogen. Diisopropylethylamine (2.14ml, 12.3mmol) was then added followed by boron trifluoride diethyl etherate (2.18 ml, 17.2 mmol) and the solution was then stirred at r.t. under nitrogen for 17hrs. The solution was then washed with water, dried over anhydrous $MgSO_4$ and evaporated *in vacuo*. The residue was then purified by column chromatography eluting with 4:1 CH_2Cl_2:EtOAc to yield the pure product as a coppery solid (0.36 g, 55%), m.p. 266-269°C (decomp.).

^{1}H-NMR [400MHz, $CDCl_3$] δ 6.89 (2H, s, Py-H), 6.96 (4H, d, Ph-H, *J* = 8.76Hz), 7.46 (6H, m, Ph-H), 8.01 (8H, m, Ph-H).

^{13}C-NMR [100MHz, $CDCl_3$] δ 116.0, 116.9, 124.1, 128.5, 129.4, 130.5, 131.1, 132.0, 159.2.

^{11}B-NMR [128.3MHz, $CDCl_3$] δ 0.00.

^{19}F-NMR [376.17MHz, $CDCl_3$] δ -130.54 (2F, dd, BF_2).

HRMS (ESI) = calc. 530.1852, found. 530.1839 ($M + H^+$).

8-(4-Iodophenyl)-1,7-bis(4-hydroxystyryl)-3,5-dimethyl-2,6-diethyl-BODIPY (63):

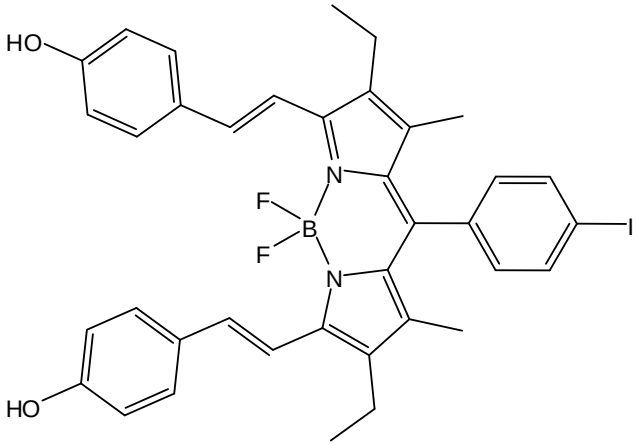

8-(4-Iodophenyl)-1,3,5,7-tetramethyl-2,6-diethyl-BODIPY (753 mg, 1.49 mmol) and 4-iodobenzaldehyde (910 mg, 7.45 mmol) were dissolved in dry toluene (100 ml) over flame-dried molecular sieves. Glacial acetic acid (2.22 ml, 38.7 mmol), piperidine (2.65 ml, 26.8 mmol) and magnesium perchlorate (cat., 5 mg) were then added to the solution which was refluxed under nitrogen for 90 hrs. After cooling to r.t., the mixture was filtered and evaporated *in vacuo*. The residue was subjected to column chromatography eluting with 1:9 EtOAc:CH_2Cl_2. The collected fraction was evaporated and the residue was washed out with cold hexane and filtered off to yield the pure product as a coppery solid (315 mg, 30%), m.p. > 300°C, R_f = 0.5 (15:85 EtOAc:CH_2Cl_2).

^{1}H-NMR [400MHz, DMSO-D_6] δ 1.09 (6H, t, 2 x C**H$_3$**CH_2, *J* = 7.51Hz), 1.34 (6H, s, 2 x CH_3), 2.59 (4H, q, 2 x C**H$_2$**CH_3, *J* = 7.30Hz), 6.87 (4H, d, Ph-H, *J* = 8.44Hz), 7.23 (4H, dd, Ph-H), 7.42 (2H, d, C**H**=CH, *J* = 16.88Hz), 7.47 (4H, d, Ph-H, *J* = 8.76Hz), 7.95 (2H, d, Ph-C**H**=CH, *J* = 8.13Hz), 9.94 (2H, bs, 2 x OH).

^{13}C-NMR [100MHz, DMSO-D_6] δ 11.4, 13.9, 17.7, 24.2, 24.8, 26.2, 45.7, 95.6, 116.0, 127.8, 128.8, 130.8, 131.8, 133.4, 136.1, 136.4, 138.0, 138.2, 149.8, 158.8.

^{11}B-NMR [128.3MHz, DMSO-D_6] δ 0.2446.

Unable to identify relevant mass isotope from ionisation methods used.

8-(4-Iodophenyl)-1,7-bis(4-[11-carboxyphenylundecyloxybiphenyl-4-carbonitrile]-styryl)-3,5-dimethyl-2,6-diethyl-BODIPY (64):

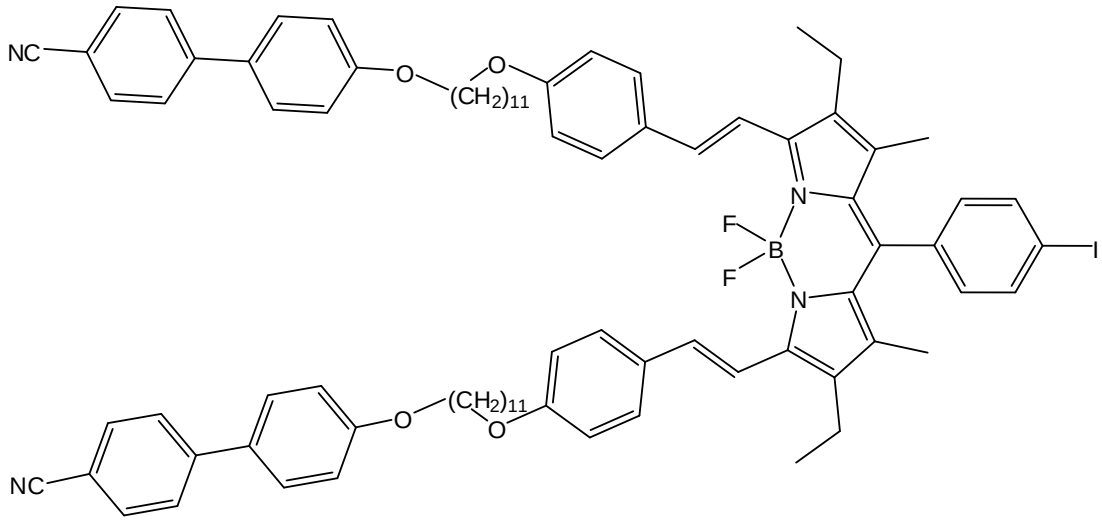

8-(4-Iodophenyl)-1,7-bis(4-hydroxystyryl)-3,5-dimethyl-2,6-diethyl-BODIPY (310 mg, 0.434 mmol), 4'-(11-mesityloxyundecyl)-biphenyl-4-carbonitrile (539 mg, 1.22 mmol) and potassium carbonate (240 mg, 1.74 mmol) were mixed in butanone (80 ml) and the mixture was refluxed for 48 hrs. The mixture was cooled to r.t. and washed with water (3 x 60 ml), dried over anhydrous $MgSO_4$ and evaporated *in vacuo*. The residue was subjected to column chromatography eluting with 1:1 THF:hexane and the collected fraction was evaporated. The residue was then washed sequentially with cold acetone, hexane and MeOH and filtered to yield the pure product as a green solid (268 mg, 44%), R_f = 0.71 (3:7 hexane:CH_2Cl_2). Broad melting point.

^{1}H-NMR [400MHz, $CDCl_3$] δ 1.15 (6H, t, 2 x C**H**$_3$CH$_2$, *J* = 7.50Hz), 1.33 (26H, m, CH_2's + 2 x CH_3), 1.48 (8H, m, CH_2's), 1.79 (8H, m, CH_2's), 2.60 (4H, q, 2 x C**H**$_2$CH$_3$, *J* = 7.40Hz), 4.00 (8H, t, 4 x CH_2O, *J* = 6.41Hz), 6.92 (4H, d, Ph-H, *J* = 8.76Hz), 6.98 (4H, d, Ph-H, *J* = 8.76Hz), 7.08 (2H, d, Ph-H, *J* = 8.13Hz), 7.20 (2H, d, 2 x C**H**=CH, *J* = 16.57Hz), 7.51 (4H, d, Ph-H, *J* = 8.76Hz), 7.55 (4H, d, Ph-H, *J* = 8.76Hz), 7.62 (4H, d, Ph-H, *J* = 8.44Hz), 7.68 (6H, m, Ph-H + 2 x C**H**=CH), 7.85 (2H, d, Ph-H, *J* = 8.44Hz).

^{13}C-NMR [100MHz, $CDCl_3$] δ 11.8, 14.1, 18.4, 26.0, 29.2, 29.36, 29.46, 29.52, 68.1, 68.2, 110.0, 114.8, 115.1, 117.9, 119.1, 127.1, 128.3, 128.8, 130.1, 130.8, 131.3, 132.6, 133.8, 135.7, 138.3, 138.4, 145.3, 150.8, 159.8. (13 peaks unobserved due to overlap of alkyl and aromatic peaks).

^{11}B-NMR [128.3MHz, $CDCl_3$] δ 0.2446.

MS (MALDI) = calc. 1408.6, found. 1408.6 (M^+).

8-(4-[11-Carboxyphenylundecyloxy-phenyl-4'-cyano-4-biphenyl-carboxylate]-phenyl)-1,7-bis(4-[11-carboxyphenylundecyloxybiphenyl-4-carbonitrile]-styryl)-3,5-dimethyl-2,6-diethyl-BODIPY (65):

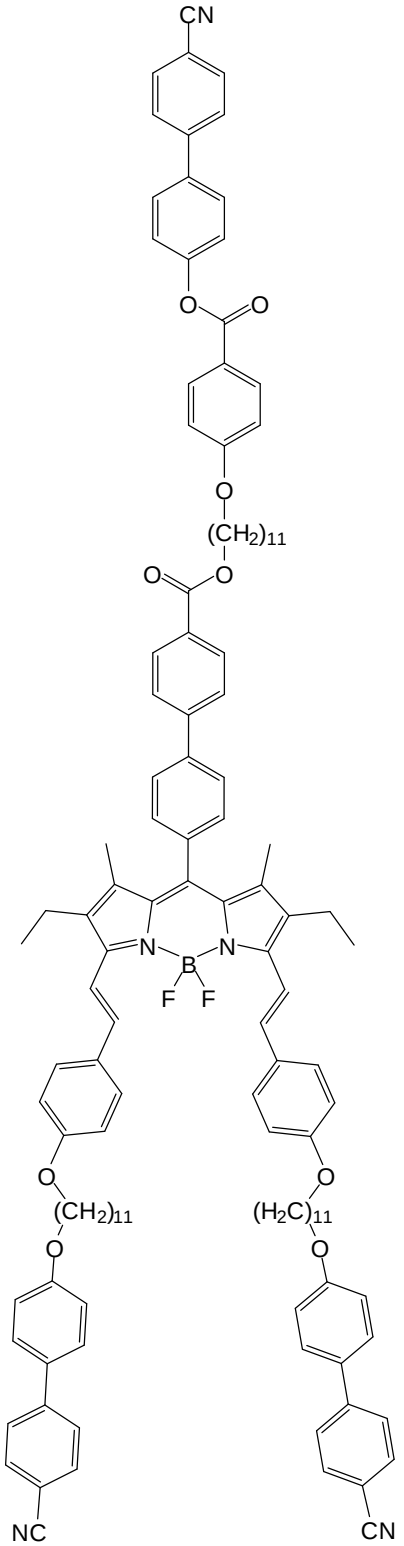

8-(4-Iodophenyl)-1,7-bis(4-[11-carboxyphenylundecyloxybiphenyl-4-carbonitrile]styryl)-3,5-dimethyl-2,6-diethyl-BODIPY (100 mg, 71.0 μmol), 4-(11-[4-boronpinacolatephenylcarboxy]undecyloxy)-phenyl-4'-cyano-4-biphenyl carboxylate (61 mg, 85.2 μmol), bis(triphenylphosphine)palladium (II) chloride (15 mg, 21.3 μmol), (2-biphenyl)di-*tert*-butylphosphine (8.5 mg, 28.4 μmol) and anhydrous potassium carbonate (29 mg, 0.213 mmol) were mixed in DMF (6 ml) and the mixture was degassed with argon for 30mins. The mixture was then heated in a microwave for 10mins at 65°C (75W). The DMF was then removed *in vacuo* and the residue subjected to column chromatography eluting with 3:7 hexane:CH_2Cl_2. The residue was then precipitated from CH_2Cl_2 with cold MeOH and filtered and the solid was washed with cold MeOH and hexane to yield the pure product as a green/blue solid (58 mg, 44%), R_f = 0.21 (1:4 hexane:CH_2Cl_2). Unclear whether compound exhibited a mesophase.

^{1}H-NMR [400MHz, $CDCl_3$] δ 1.04 (6H, t, 2 x C**H$_3$**CH_2, *J* = 7.50Hz), 1.23 (36H, m, CH_2's + 2 x CH_3), 1.37 (12H, m, CH_2's), 1.69 (12H, m, CH_2's), 3.89 (8H, m, 4 x CH_2O), 3.95 (2H, t, CH_2OPh, *J* = 6.41Hz), 4.25 (2H, t, CH_2O, *J* = 6.57Hz), 6.82 (4H, d, Ph-H, *J* = 8.76Hz), 6.88 (6H, m, Ph-H), 7.09 (2H, d, 2 x C**H**=CH, *J* = 16.88Hz), 7.21 (2H, d, Ph-H, *J* = 8.44Hz), 7.42 (8H, m, Ph-H), 7.58 (18H, m, Ph-H), 7.69 (4H, m, Ph-H), 8.03 (4H, m, Ph-H).

Compound too insoluble to acquire adequate ^{13}C-NMR spectrum.

^{11}B-NMR [128.3MHz, $CDCl_3$] δ 0.0000.

MS (MALDI) = calc. 1871.0, found. 1871.0 (M^+).

HPLC retention time (70:30 MeCN:DCM): 8.12 mins.

Fluorescence absorption maximum: 660 nm; fluorescence emission maximum: 681 nm.

References

1. Fischer, H.; Orth, H., *Die Chemie des Pyrrols*. 1937, Leipzig: Akademische Verlagsgesellschaft.

2. Eaton, S. S.; Eaton, G. R.; Chang, C. K., Synthesis and Geometry Determination of Cofacial Diporphyrins - Electron-Paramagnetic-Res Spectroscopy of Dicopper Diporphyrins in Frozen Solution. *J. Am. Chem. Soc.* **1985,** 107, (11), 3177-3184.

3. Rumyantsev, E. V.; Guseva, G. B.; Antina, E. V.; Berezin, M. B.; Sheinin, V. B.; V'Yugin, A. I., Correlation of the basicity of dipyrrolylmethenes biladienes-a,c with the thermal and kinetic stability of their salts. *Russ. J. Gen. Chem.* **2006,** 76, (1), 141-147.

4. Sazanovich, I. V.; Kirmaier, C.; Hindin, E.; Yu, L.; Bocian, D. F.; Lindsey, J. S.; Holten, D., Structural Control of the Excited-State Dynamics of Bis(dipyrrinato)zinc Complexes: Self-Assembling Chromophores for Light-Harvesting Architectures. *J. Am. Chem. Soc.* **2004,** 126, (9), 2664-2665.

5. Sutton, J. M.; Rogerson, E.; Wilson, C. J.; Sparke, A. E.; Archibald, S. J.; Boyle, R. W., Synthesis and structural characterisation of novel bimetallic dipyrromethene complexes: rotational locking of the 5-aryl group. *Chem. Commun.* **2004**, (11), 1328-1329.

6. Falk, H.; Leodolter, A.; Schade, G., On the chemistry of pyrrole pigments, XIX.: The electrochemical oxidation of pyrromethenones and pyrromethenes (bile pigment partial structures). *Beitrage zur Chemie der Pyrrolpigmente, 19. Mitt.: Die elektrochemische Oxidation von Pyrromethenonen und Pyrromethenen (Gallenpigment-Partialstrukturen)* **1978,** 109, (1), 183-192.

7. Tabba, H. D.; Cavaleiro, J. A. S.; Jeyakumar, D.; Neves, M. G. P. M. S.; Smith, K. M., Electrochemical study of the nonaqueous oxidation of dipyrrolic compounds. *J. Org. Chem.* **1989,** 54, (8), 1943-1948.

8. Brőring, M.; Brandt, C. D.; Lex, J.; Humpf, H. U.; Bley-Escrich, J.; Gisselbrecht, J. P., Molecular and electronic structure of (2,2'-bidipyrrinato)nickel(II) complexes. *Eur. J. Inorg. Chem.* **2001**, (10), 2549-2556.

9. Gill, H. S.; Finger, I.; Bozidarevic, I.; Szydlo, F.; Scott, M. J., Preparation of α,β-unsubstituted meso-arylbidipyrrins via metal-templated, oxidative coupling of dipyrrins. *New J. Chem.* **2005,** 29, (1), 68-71.

10. Brőring, M.; Brandt, C. D.; Bley-Escrich, J.; Gisselbrecht, J. P., Structural and spectroelectrochemical studies on (2,2'-bidipyrrinato)copper(II) and -palladium(II) complexes. *Eur. J. Inorg. Chem.* **2002**, (4), 910-917.

11. Vankoeveringe, J. A.; Lugtenburg, J., Novel Pyrromethenes 1-Oxygen and 1-Sulfur Analogs - Evidence for Photochemical Z-E Isomerization. *Recl. Trav. Chim. Pays-Bas* **1977,** 96, (2), 55-58.

12. Kollmannsberger, M.; Gareis, T.; Heinl, S.; Breu, J.; Daub, J., Electrogenerated chemiluminescence and proton-dependent switching of fluorescence: Functionalized difluoroboradiaza-s-indacenes. *Angew. Chem. Int. Ed.* **1997,** 36, (12), 1333-1335.

13. Paine, J. B., *The Porphyrins*, ed. Dolphin, D. Vol. 1. 1978, New York: Academic Press.

14. Arsenault, G. P.; Bullock, E.; MacDonald, S. F., Pyrromethanes and porphyrins therefrom. *J. Am. Chem. Soc.* **1960,** 82, (16), 4384-4389.

15. Wan, C. W.; Burghart, A.; Chen, J.; Bergstrőm, F.; Johansson, L. B. A.; Wolford, M. F.; Kim, T. G.; Topp, M. R.; Hochstrasser, R. M.; Burgess, K., Anthracene - BODIPY cassettes: Syntheses and energy transfer. *Chem. Eur. J.* **2003,** 9, (18), 4430-4441.

16. Ali, A. A. S.; Cipot-Wechsler, J.; Cameron, T. S.; Thompson, A., Formation of vinylic dipyrroles by the deprotonation of meso-alkyl and meso-benzyl dipyrrin HCl salts. *J. Org. Chem.* **2009,** 74, (7), 2866-2869.

17. Lash, T. D.; Chen, S. H., Syntheses of per-N-15 labeled etioporphyrins I-IV and a related tetrahydrobenzoporphyrin for applications in organic geochemistry and vibrational spectroscopy. *Tetrahedron* **2005,** 61, (49), 11577-11600.

18. Clausen, C.; Gryko, D. T.; Yasseri, A. A.; Diers, J. R.; Bocian, D. F.; Kuhr, W. G.; Lindsey, J. S., Investigation of tightly coupled porphyrin arrays comprised of identical monomers for multibit information storage. *J. Org. Chem.* **2000,** 65, (22), 7371-7378.

19. Gryko, D.; Lindsey, J. S., Rational synthesis of meso-substituted porphyrins bearing one nitrogen heterocyclic group. *J. Org. Chem.* **2000,** 65, (7), 2249-2252.

20. Littler, B. J.; Miller, M. A.; Hung, C. H.; Wagner, R. W.; O'Shea, D. F.; Boyle, P. D.; Lindsey, J. S., Refined synthesis of 5-substituted dipyrromethanes. *J. Org. Chem.* **1999,** 64, (4), 1391-1396.

21. Rao, P. D.; Dhanalekshmi, S.; Littler, B. J.; Lindsey, J. S., Rational syntheses of porphyrins bearing up to four different meso substituents. *J. Org. Chem.* **2000,** 65, (22), 7323-7344.

22. Boyle, R. W.; Bruckner, C.; Posakony, J.; James, B. R.; Dolphin, D., 5-Phenyldipyrromethane and 5,15-diphenylporphyrin. *Org. Synth.* **1999,** 76, 287-293.

23. Wagner, R. W.; Lindsey, J. S., A molecular photonic wire. *J. Am. Chem. Soc.* **1994,** 116, (21), 9759-9760.

24. Turfan, B.; Akkaya, E. U., Modulation of boradiazaindacene emission by cation-mediated oxidative PET. *Org. Lett.* **2002,** 4, (17), 2857-2859.

25. Goze, C.; Ulrich, G.; Charbonniere, L.; Cesario, M.; Prange, T.; Ziessel, R., Cation sensors based on terpyridine-functionalized boradiazaindacene. *Chem. Eur. J.* **2003,** 9, (16), 3748-3755.

26. Ulrich, G.; Ziessel, R., Convenient and Efficient Synthesis of Functionalized Oligopyridine Ligands Bearing Accessory Pyrromethene-BF2 Fluorophores. *J. Org. Chem.* **2004,** 69, (6), 2070-2083.

27. Ulrich, G.; Ziessel, R., Functional dyes: Bipyridines and bipyrimidine based boradiazaindacene. *Tet. Lett.* **2004,** 45, (9), 1949-1953.

28. Ziessel, R.; Bonardi, L.; Retailleau, P.; Ulrich, G., Isocyanate-, isothiocyanate-, urea-, and thiourea-substituted boron dipyrromethene dyes as fluorescent probes. *J. Org. Chem.* **2006,** 71, (8), 3093-3102.

29. Yu, L.; Muthukumaran, K.; Sazanovich, I. V.; Kirmaier, C.; Hindin, E.; Diers, J. R.; Boyle, P. D.; Bocian, D. F.; Holten, D.; Lindsey, J. S., Excited-State Energy-Transfer Dynamics in Self-Assembled Triads Composed of Two Porphyrins and an Intervening Bis(dipyrrinato)metal Complex. *Inorg. Chem.* **2003,** 42, (21), 6629-6647.

30. Treibs, A.; Kreuzer, F.-H., Difluorboryl-Komplexe von Di- und Tripyrrylmethenen. *Just. Lieb. Ann. Chem.* **1968,** 718, (1), 208-223.

31. Yamada, K.; Toyota, T.; Takakura, K.; Ishimaru, M.; Sugawara, T., Preparation of BODIPY probes for multicolor fluorescence imaging studies of membrane dynamics. *New J. Chem.* **2001,** 25, (5), 667-669.

32. Haugland, R. P., *Handbook of Fluorescent Probes and Research Chemicals*. 6th ed. Molecular Probes. 1996, Eugene, OR: Molecular Probes.

33. Yee, M. C.; Fas, S. C.; Stohlmeyer, M. M.; Wandless, T. J.; Cimprich, K. A., A cell-permeable, activity-based probe for protein and lipid kinases. *J. Biol. Chem.* **2005,** 280, (32), 29053-29059.

34. Fa, M.; Bergstrom, F.; Hagglof, P.; Wilczynska, M.; Johansson, L. B. A.; Ny, T., The structure of a serpin-protease complex revealed by intramolecular distance measurements using donor-donor energy migration and mapping of interaction sites. *Structure* **2000,** 8, (4), 397-405.

35. Golovkova, T. A.; Kozlov, D. V.; Neckers, D. C., Synthesis and properties of novel fluorescent switches. *J. Org. Chem.* **2005,** 70, (14), 5545-5549.

36. Trieflinger, C.; Rurack, K.; Daub, J., "Turn ON/OFF your LOV light": Borondipyrromethene-flavin dyads as biomimetic switches derived from the LOV domain. *Angew. Chem. Int. Ed.* **2005,** 44, (15), 2288-2291.

37. Zhang, X.; Wang, H.; Li, J. S.; Zhang, H. S., Development of a fluorescent probe for nitric oxide detection based on difluoroboradiaza-s-indacene fluorophore. *Anal. Chim. Act.* **2003,** 481, (1), 101-108.

38. Rurack, K.; Kollmannsberger, M.; Daub, J., Molecular switching in the near infrared (NIR) with a functionalized boron-dipyrromethene dye. *Angew. Chem. Int. Ed.* **2001,** 40, (2), 385-387.

39. Baki, C. N.; Akkaya, E. U., Boradiazaindacene-appended calix[4]arene: Fluorescence sensing of pH near neutrality. *J. Org. Chem.* **2001,** 66, (4), 1512-1513.

40. Gabe, Y.; Urano, Y.; Kikuchi, K.; Kojima, H.; Nagano, T., Highly Sensitive Fluorescence Probes for Nitric Oxide Based on Boron Dipyrromethene Chromophore - Rational Design of Potentially Useful Bioimaging Fluorescence Probe. *J. Am. Chem. Soc.* **2004,** 126, (10), 3357-3367.

41. Arbeloa, T. L.; Arbeloa, F. L.; Arbeloa, I. L.; Garcia-Moreno, I.; Costela, A.; Sastre, R.; Amat-Guerri, F., Correlations between photophysics and lasing properties of dipyrromethene-BF2 dyes in solution. *Chem. Phys. Lett.* **1999,** 299, (3-4), 315-321.

42. Tram, K.; Yan, H.; Jenkins, H. A.; Vassiliev, S.; Bruce, D., The synthesis and crystal structure of unsubstituted 4,4-difluoro-4-bora-3a,4a-diaza-s-indacene (BODIPY). *Dyes and Pigments* **2009,** 82, (3), 392-395.

43. Schmitt, A.; Hinkeldey, B.; Wild, M.; Jung, G., Synthesis of the Core Compound of the BODIPY Dye Class: 4,4-Difluoro-4-bora-(3a,4a)-diaza-s-indacene. *J. Fluor.* **2008**, 1-4.

44. Wael, E. V. d.; Pardoen, J. A.; Koeveringe, J. A. V.; Lugtenburg, J., *Recl. Trav. Chim. Pays-Bas* **1977,** 96, 306.

45. Bandichhor, R.; Thivierge, C.; Bhuvanesh, N. S. P.; Burgess, K., 4,4-Difluoro-1,3,5,7-tetramethyl-4-bora-3a,4a-diaza-s-indacene. *Acta Cryst. Section E: Structure Reports Online* **2006,** 62, (10), o4310-o4311.

46. Alamiry, M. A. H.; Benniston, A. C.; Copley, G.; Elliott, K. J.; Harriman, A.; Stewart, B.; Zhi, Y. G., A molecular rotor based on an unhindered boron dipyrromethane (Bodipy) dye. *Chem. Mater.* **2008,** 20, (12), 4024-4032.

47. Kuimova, M. K.; Yahioglu, G.; Levitt, J. A.; Suhling, K., Molecular rotor measures viscosity of live cells via fluorescence lifetime imaging. *J. Am. Chem. Soc.* **2008,** 130, (21), 6672-6673.

48. Umezawa, K.; Matsui, A.; Nakamura, Y.; Citterio, D.; Suzuki, K., Bright, color-tunable fluorescent dyes in the Vis/NIR region: Establishment of new "tailor-made" multicolor fluorophores based on borondipyrromethene. *Chem. Eur. J.* **2009,** 15, (5), 1096-1106.

49. Thoresen, L. H.; Kim, H.; Welch, M. B.; Burghart, A.; Burgess, K., Synthesis of 3,5-diaryl-4,4-difluoro-4-bora-3a,4a-diaza-s-indacene (BODIPY®) dyes. *Synlett* **1998**, (11), 1276-1278.

50. Burghart, A.; Kim, H.; Welch, M. B.; Thoresen, L. H.; Reibenspies, J.; Burgess, K.; Bergstrom, F.; Johansson, L. B., 3,5-diaryl-4,4-difluoro-4-bora-3a,4a-diaza-s-indacene (BODIPY) dyes: Synthesis, spectroscopic, electrochemical, and structural properties. *J. Org. Chem.* **1999,** 64, (21), 7813-7819.

51. Rettig, W., Charge Separation in Excited States of Decoupled Systems - TICT Compounds and Implications Regarding the Development of New Laser Dyes and the Primary Process of Vision and Photosynthesis. *Angew. Chem. Int. Ed.* **1986,** 25, (11), 971-988.

52. Mikhalyov, I.; Gretskaya, N.; Bergstrom, F.; Johansson, L. B., Electronic ground and excited state properties of dipyrromethene boron difluoride (BODIPY): Dimers with application to biosciences. *Phys. Chem. Chem. Phys.* **2002,** 4, (22), 5663-5670.

53. BergstroÌˆm, F.; Mikhalyov, I.; HaÌˆggloÌˆf, P.; Wortmann, R.; Ny, T.; Johansson, L. B. A., Dimers of dipyrromethene boron difluoride (BODIPY) with light spectroscopic applications in chemistry and biology. *J. Am. Chem. Soc.* **2002,** 124, (2), 196-204.

54. Marushchak, D.; Kalinin, S.; Mikhalyov, I.; Gretskaya, N.; Johansson, L. B., Pyrromethene dyes (BODIPY) can form ground state homo and hetero dimers: Photophysics and spectral properties. *Spectro. Acta A* **2006,** 65, (1), 113-122.

55. Trofimov, B. A., Preparation of Pyrroles from Ketoximes and Actylenes. In *Adv. Hetero. Chem.*, Katritzky, A. R., Ed. Elsevier: 1990; Vol. 51, pp 177-290.

56. Li, Z.; Mintzer, E.; Bittman, R., First synthesis of free cholesterol-BODIPY conjugates. *J. Org. Chem.* **2006,** 71, (4), 1718-1721.

57. Goud, T. V.; Tutar, A.; Biellmann, J. F., Synthesis of 8-heteroatom-substituted 4,4-difluoro-4-bora-3a,4a-diaza-s-indacene dyes (BODIPY). *Tetrahedron* **2006,** 62, (21), 5084-5091.

58. Nicolaou, K. C.; Claremon, D. A.; Papahatjis, D. P., A mild method for the synthesis of 2-ketopyrroles from carboxylic acids. *Tet. Lett.* **1981,** 22, (46), 4647-4650.

59. Tahtaoui, C.; Thomas, C.; Rohmer, F.; Klotz, P.; Duportail, G.; Mely, Y.; Bonnet, D.; Hibert, M., Convenient method to access new 4,4-dialkoxy- and 4,4-diaryloxy-diaza-s- indacene dyes: Synthesis and spectroscopic evaluation. *J. Org. Chem.* **2007,** 72, (1), 269-272.

60. Li, M.; Wang, H.; Zhang, X.; Zhang, H. S., Development of a new fluorescent probe: 1,3,5,7-tetramethyl-8-(4'-aminophenyl)-4,4-difluoro-4-bora-3a, 4a-diaza-s-indacence for the determination of trace nitrite. *Spectro. Acta A* **2004,** 60, (4), 987-993.

61. Zhang, X.; Zhang, H. S., Design, synthesis and characterization of a novel fluorescent probe for nitric oxide based on difluoroboradiaza-s-indacene fluorophore. *Spectro. Acta A* **2005,** 61, (6), 1045-1049.

62. Oleynik, P.; Ishihara, Y.; Cosa, G., Design and synthesis of a BODIPY-α-tocopherol adduct for use as an off/on fluorescent antioxidant indicator. *J. Am. Chem. Soc.* **2007,** 129, (7), 1842-1843.

63. Bricks, J. L.; Kovalchuk, A.; Trieflinger, C.; Nofz, M.; Baschel, M.; Tolmachev, A. I.; Daub, J.; Rurack, K., On the development of sensor molecules that display FeIII-amplified fluorescence. *J. Am. Chem. Soc.* **2005,** 127, (39), 13522-13529.

64. Qi, X.; Jun, E. J.; Xu, L.; Kim, S. J.; Hong, J. S. J.; Yoon, Y. J.; Yoon, J., New BODIPY derivatives as OFF-ON fluorescent chemosensor and fluorescent chemodosimeter for Cu2+: Cooperative selectivity enhancement toward Cu2+. *J. Org. Chem.* **2006,** 71, (7), 2881-2884.

65. Wu, Y.; Peng, X.; Guo, B.; Fan, J.; Zhang, Z.; Wang, J.; Cui, A.; Gao, Y., Boron dipyrromethene fluorophore based fluorescence sensor for the selective imaging of Zn(II) in living cells. *Org. Biomol. Chem.* **2005,** 3, (8), 1387-1392.

66. Martin, V. V.; Rothe, A.; Gee, K. R., Fluorescent metal ion indicators based on benzoannelated crown systems: A green fluorescent indicator for intracellular sodium ions. *Bioorg. Med. Chem. Lett.* **2005,** 15, (7), 1851-1855.

67. Rurack, K.; Kollmannsberger, M.; Resch-Genger, U.; Daub, J., A selective and sensitive fluoroionophore for Hg(II), Ag(I), and Cu(I) with virtually decoupled fluorophore and receptor units [10]. *J. Am. Chem. Soc.* **2000,** 122, (5), 968-969.

68. Wang, J.; Qian, X., A series of polyamide receptor based PET fluorescent sensor molecules: Positively cooperative Hg2+ ion binding with high sensitivity. *Org. Lett.* **2006,** 8, (17), 3721-3724.

69. Mei, Y.; Bentley, P. A.; Wang, W., A selective and sensitive chemosensor for Cu2+ based on 8-hydroxyquinoline. *Tet. Lett.* **2006,** 47, (14), 2447-2449.

70. Kim, H. J.; Kim, J. S., BODIPY appended cone-calix[4]arene: selective fluorescence changes upon Ca2+ binding. *Tet. Lett.* **2006,** 47, (39), 7051-7055.

71. BasaricÌ • , N.; Baruah, M.; Qin, W.; Metten, B.; Smet, M.; Dehaen, W.; Boens, N., Synthesis and spectroscopic characterisation of BODIPY® based fluorescent off-on indicators with low affinity for calcium. *Org. Biomol. Chem.* **2005,** 3, (15), 2755-2761.

72. DiCesare, N.; Lakowicz, J. R., Fluorescent probe for monosaccharides based on a functionalized boron-dipyrromethene with a boronic acid group. *Tet. Lett.* **2001,** 42, (52), 9105-9108.

73. Li, J. S.; Wang, H.; Huang, K. J.; Zhang, H. S., Determination of biogenic amines in apples and wine with 8-phenyl-(4-oxy-acetic acid N-hydroxysuccinimide ester)-4, 4-difluoro-1,3,5,7-tetramethyl-4-bora-3a,4a-diaza-s-indacene by high performance liquid chromatography. *Anal. Chim. Acta* **2006,** 575, (2), 255-261.

74. Matsui, M.; Funabiki, K.; Nakaya, K. I., Application of chiral pyrromethene-BF2 complex dye as a fluorescent labeling reagent. *Bull. Chem. Soc. Jpn.* **2005,** 78, (3), 464-467.

75. De Silva, A. P.; Gunaratne, H. Q. N.; Gunnlaugsson, T.; Huxley, A. J. M.; McCoy, C. P.; Rademacher, J. T.; Rice, T. E., Signaling recognition events with fluorescent sensors and switches. *Chem. Rev.* **1997,** 97, (5), 1515-1566.

76. Tanaka, K.; Miura, T.; Umezawa, N.; Urano, Y.; Kikuchi, K.; Higuchi, T.; Nagano, T., Rational design of fluorescein-based fluorescence probes. Mechanism-based design of a maximum fluorescence probe for singlet oxygen. *J. Am. Chem. Soc.* **2001,** 123, (11), 2530-2536.

77. Ueno, T.; Urano, Y.; Setsukinai, K. I.; Takakusa, H.; Kojima, H.; Kikuchi, K.; Ohkubo, K.; Fukuzumi, S.; Nagano, T., Rational principles for modulating fluorescence properties of fluorescein. *J. Am. Chem. Soc.* **2004,** 126, (43), 14079-14085.

78. Sunahara, H.; Urano, Y.; Kojima, H.; Nagano, T., Design and synthesis of a library of BODIPY-based environmental polarity sensors utilizing photoinduced electron-

transfer-controlled fluorescence ON/OFF switching. *J. Am. Chem. Soc.* **2007,** 129, (17), 5597-5604.

79. Rehm, D.; Weller, A., Kinetics of Fluorescence Quenching by Electron and H-Atom Transfer. *Isr. J. Chem.* **1970,** 8, (2), 259-&.

80. Koutaka, H.; Kosuge, J. I.; Fukasaku, N.; Hirano, T.; Kikuchi, K.; Urano, Y.; Kojima, H.; Nagano, T., A novel fluorescent probe for zinc ion based on boron dipyrromethene (BODIPY) chromophore. *Chem. Pharma. Bull.* **2004,** 52, (6), 700-703.

81. Ueno, T.; Urano, Y.; Kojima, H.; Nagano, T., Mechanism-based molecular design of highly selective fluorescence probes for nitrative stress. *J. Am. Chem. Soc.* **2006,** 128, (33), 10640-10641.

82. Jacob, M.; Schmitt, A.; Jung, G., Disabling Photoinduced Electron Transfer in 4,4-Difluoro-8(-4'- hydroxyphenyl)-1,3,5,7-tetramethyl-4-bora-3a,4a-diaza-s-indacene by Phosphorylation. *J. Fluor.* **2008,** 18, (3-4), 639-644.

83. Rohand, T.; Qin, W.; Boens, N.; Dehaen, W., Palladium-catalyzed coupling reactions for the functionalization of BODIPY dyes with fluorescence spanning the visible spectrum. *Eur. J. Org. Chem.* **2006**, (20), 4658-4663.

84. Thivierge, C.; Bandichhor, R.; Burgess, K., Spectral dispersion and water solubilization of BODIPY dyes via palladium-catalyzed C-H functionalization. *Org. Lett.* **2007,** 9, (11), 2135-2138.

85. Chen, J.; Mizumura, M.; Shinokubo, H.; Osuka, A., Functionalization of boron dipyrrin (BODIPY) dyes through iridium and rhodium catalysis: A complementary approach to α-and β-Substituted BODIPYs. *Chem. Eur. J.* **2009,** 15, (24), 5942-5949.

86. Han, J.; Gonzalez, O.; Aguilar-Aguilar, A.; Peña-Cabrera, E.; Burgess, K., 3- and 5-Functionalized BODIPYs via the Liebeskind-Srogl reaction. *Org. Biomol. Chem.* **2009,** 7, (1), 34-36.

87. Rurack, K.; Kollmannsberger, M.; Daub, J., A highly efficient sensor molecule emitting in the near infrared (NIR): 3,5-distyryl-8-(p-dimethylaminophenyl)-difluoroboradiaza-s-indacene. *New J. Chem.* **2001,** 25, (2), 289-292.

88. Coskun, A.; Akkaya, E. U., Difluorobora-s-diazaindacene dyes as highly selective dosimetric reagents for fluoride anions. *Tet. Lett.* **2004,** 45, (25), 4947-4949.

89. Dost, Z.; Atilgan, S.; Akkaya, E. U., Distyryl-boradiazaindacenes: facile synthesis of novel near IR emitting fluorophores. *Tetrahedron* **2006,** 62, (36), 8484-8488.

90. Yu, Y. H.; Descalzo, A. B.; Shen, Z.; Rohr, H.; Liu, Q.; Wang, Y. W.; Spieles, M.; Li, Y. Z.; Rurack, K.; You, X. Z., Mono- and di(dimethylamino)styryl-substituted borondipyrromethene and borondiindomethene dyes with intense near-infrared fluorescence. *Chem.- Asian J.* **2006,** 1, (1-2), 176-187.

91. Coskun, A.; Deniz, E.; Akkaya, E. U., Effective PET and ICT switching of boradiazaindacene emission: A unimolecular, emission-mode, molecular half-subtractor with reconfigurable logic gates. *Org. Lett.* **2005,** 7, (23), 5187-5189.

92. Barin, G.; Yilmaz, M. D.; Akkaya, E. U., Boradiazaindacene (Bodipy)-based building blocks for the construction of energy transfer cassettes. *Tet. Lett.* **2009,** 50, (15), 1738-1740.

93. Deniz, E.; Isbasar, G. C.; Bozdemir, O. A.; Yildirim, L. T.; Siemiarczuk, A.; Akkaya, E. U., Bidirectional switching of near IR emitting boradiazaindacene fluorophores. *Org. Lett.* **2008,** 10, (16), 3401-3403.

94. Liu, J. Y.; Yeung, H. S.; Xu, W.; Li, X.; Ng, D. K. P., Highly efficient energy transfer in subphthalocyanine - BODIPY conjugates. *Org. Lett.* **2008,** 10, (23), 5421-5424.

95. Zhang, X.; Xiao, Y.; Qian, X., Highyl Efficient Energy Transfer in the Light Harvesting System Composed of Three Kinds of Boron-Dipyrromethene Derivatives. *Org. Lett.* **2008,** 10, (1), 29-32.

96. Rogers, M. A. T., 156. 2 : 4-Diarylpyrroles. Part I. Synthesis of 2 : 4-diarylpyrroles and 2 : 2 : 4 : 4-tetra-arylazadipyrromethines. *J. Chem. Soc.* **1943**, 590-596.

97. Davies, W. H.; Rogers, M. A. T., 46. 2 : 4-Diarylpyrroles. Part IV. The formation of acylated 5-amino-2 : 4-diphenylpyrroles from β-benzoly-α-phenylpropionitrile and some notes on the Leuckart reaction. *J. Chem. Soc.* **1944**, 126-131.

98. Knott, E. B., 225. β-Cycloylpropionitriles. Part II. Conversion into bis-2-(5-cyclylpyrrole)azamethin salts. *J. Chem. Soc.* **1947**, 1196-1201.

99. Toomas H. Allik, R. E. H., Govindarao Sathyamoorthi, and Joseph H. Boyer, Spectroscopy and laser performance of new BF2-complex dyes in solution. *Proc. SPIE Int. Soc. Opt. Eng.* **1994,** 2115, 240-248.

100. McDonnell, S. O.; O'Shea, D. F., Near-infrared sensing properties of dimethlyamino-substituted BF 2-azadipyrromethenes. *Org. Lett.* **2006,** 8, (16), 3493-3496.

101. Gorman, A.; Killoran, J.; O'Shea, C.; Kenna, T.; Gallagher, W. M.; O'Shea, D. F., In vitro demonstration of the heavy-atom effect for photodynamic therapy. *J. Am. Chem. Soc.* **2004,** 126, (34), 10619-10631.

102. Gallagher, W. M.; Allen, L. T.; O'Shea, C.; Kenna, T.; Hall, M.; Gorman, A.; Killoran, J.; O'Shea, D. F., A potent nonporphyrin class of photodynamic therapeutic agent: Cellular localisation, cytotoxic potential and influence of hypoxia. *Brit. J. Canc.* **2005,** 92, (9), 1702-1710.

103. Killoran, J.; O'Shea, D. F., Impact of a conformationally restricted receptor on the BF2 chelated azadipyrromethene fluorosensing platform. *Chem. Commun.* **2006**, (14), 1503-1505.

104. Hall, M. J.; Allen, L. T.; O'Shea, D. F., PET modulated fluorescent sensing from the BF2 chelated azadipyrromethene platform. *Org. Biomol. Chem.* **2006,** 4, (5), 776-780.

105. McDonnell, S. O.; Hall, M. J.; Allen, L. T.; Byrne, A.; Gallagher, W. M.; O'Shea, D. F., Supramolecular photonic therapeutic agents. *J. Am. Chem. Soc.* **2005,** 127, (47), 16360-16361.

106. Coskun, A.; Yilmaz, M. D.; Akkaya, E. U., Bis(2-pyridyl)-Substituted Boratriazaindacene as an NIR-Emitting Chemosensor for Hg(II). *Org. Lett.* **2007,** 9, (4), 607-609.

107. Gawley, R. E.; Mao, H.; Haque, M. M.; Thorne, J. B.; Pharr, J. S., Visible fluorescence chemosensor for saxitoxin. *J. Org. Chem.* **2007,** 72, (6), 2187-2191.

108. Shiragami, T.; Tanaka, K.; Andou, Y.; Tsunami, S. I.; Matsumoto, J.; Luo, H.; Araki, Y.; Ito, O.; Inoue, H.; Yasuda, M., Synthesis and spectroscopic analysis of tetraphenylporphyrinatoantimony(V) complexes linked to boron-dipyrrin chromophore on axial ligands. *J. Phtochem. Photobiol. A* **2005,** 170, (3), 287-297.

109. Liu, J. Y.; Ermilov, E. A.; Roder, B.; Ng, D. K. P., Switching the photo-induced energy and electron-transfer processes in BODIPY-phthalocyanine conjugates. *Chem. Commun.* **2009**, (12), 1517-1519.

110. Paul, D.; Wytko, J. A.; Koepf, M.; Weiss, J., Design and synthesis of a self-assembled photochemical dyad based on selective imidazole recognition. *Inorg. Chem.* **2002,** 41, (14), 3699-3704.

111. Koepf, M.; Trabolsi, A.; Elhabiri, M.; Wytko, J. A.; Paul, D.; Albrecht-Gary, A. M.; Weiss, J., Building blocks for self-assembled porphyrinic photonic wires. *Org. Lett.* **2005,** 7, (7), 1279-1282.

112. Maligaspe, E.; Tkachenko, N. V.; Subbaiyan, N. K.; Chitta, R.; Zandler, M. E.; Lemmetyinen, H.; D'Souza, F., Photosynthetic antenna-reaction center mimicry: Sequential energy- and electron transfer in a self-assembled supramolecular triad composed of boron dipyrrin, zinc porphyrin and fullerene. *J. Phys. Chem. A* **2009,** 113, (30), 8478-8489.

113. Maligaspe, E.; Kumpulainen, T.; Subbaiyan, N. K.; Zandler, M. E.; Lemmetyinen, H.; Tkachenko, N. V.; D'Souza, F., Electronic energy harvesting multi BODIPY-zinc porphyrin dyads accommodating fullerene as photosynthetic composite of antenna-reaction center. *Phys. Chem. Chem. Phys.* **2010,** 12, (27), 7434-7444.

114. Ziessel, R.; Allen, B. D.; Rewinska, D. B.; Harriman, A., Selective triplet-state formation during charge recombination in a fullerene/Bodipy molecular dyad (Bodipy = borondipyrromethene). *Chem. Eur. J.* **2009,** 15, (30), 7382-7393.

115. Yilmaz, M. D.; Bozdemir, O. A.; Akkaya, E. U., Light Harvesting and Efficient Energy Transfer in a Boron-dipyrrin (BODIPY) Functionalized Perylenediimide Derivative. *Org. Lett.* **2006,** 8, (13), 2871-2873.

116. Bozdemir, O. A.; Yilmaz, M. D.; Buyukcakir, O.; Siemiarczuk, A.; Tutas, M.; Akkaya, E. U., Convergent synthesis and light harvesting properties of dendritic boradiazaindacene (BODIPY) appended perylenediimide dyes. *New J. Chem.* **2010,** 34, 151-155.

117. Holten, D.; Bocian, D. F.; Lindsey, J. S., Probing electronic communication in covalently linked multiporphyrin arrays. A guide to the rational design of molecular photonic devices. *Acc. Chem. Res.* **2002,** 35, (1), 57-69.

118. Wagner, R. W.; Lindsey, J. S.; Seth, J.; Palaniappan, V.; Bocian, D. F., Molecular optoelectronic gates. *J. Am. Chem. Soc.* **1996,** 118, (16), 3996-3997.

119. Li, F.; Yang, S. I.; Ciringh, Y.; Seth, J.; Martin Ii, C. H.; Singh, D. L.; Kim, D.; Birge, R. R.; Bocian, D. F.; Holten, D.; Lindsey, J. S., Design, synthesis, and photodynamics of light-harvesting arrays comprised of a porphyrin and one, two, or eight boron-dipyrrin accessory pigments. *J. Am. Chem. Soc.* **1998,** 120, (39), 10001-10017.

120. Ravikanth, M.; Agarwal, N.; Kumaresan, D., Synthesis of energy donors appended dithiaporphyrin systems. *Chem. Lett.* **2000**, (7), 836-837.

121. Kumaresan, D.; Agarwal, N.; Gupta, I.; Ravikanth, M., Synthesis of 21-thia and 21-oxaporphyrin building blocks and boron-dipyrrin appended systems. *Tetrahedron* **2002,** 58, (26), 5347-5356.

122. Kumaresan, D.; Gupta, I.; Ravikanth, M., Synthesis of 21-oxoporphyrin building blocks and energy donor appended systems. *Tet. Lett.* **2001,** 42, (48), 8547-8550.

123. Lee, C. Y.; Jang, J. K.; Kim, C. H.; Jung, J.; Park, B. K.; Park, J.; Choi, W.; Han, Y. K.; Joo, T.; Park, J. T., Remarkably efficient photocurrent generation based on a [60] fullerence-triosmium cluster/Zn-porphyrin/boron-dipyrrin triad SAM. *Chem. Eur. J.* **2010,** 16, (19), 5586-5599.

124. Ulrich, G.; Ziessel, R., Highly Luminescent Probes from Terpyridine, Phenanthroline, and Pyrromethene·BF2 Auxiliaries. *Synlett* **2004**, (3), 439-444.

125. Galletta, M.; Campagna, S.; Quesada, M.; Ulrich, G.; Ziessel, R., The elusive phosphorescence of pyrromethene-BF2 dyes revealed in new multicomponent species containing Ru(II)-terpyridine subunits. *Chem. Commun.* **2005**, (33), 4222-4224.

126. Galletta, M.; Puntoriero, F.; Campagna, S.; Chiorboli, C.; Quesada, M.; Goeb, S.; Ziessel, R., Absorption spectra, photophysical properties, and redox behavior of ruthenium(II) polypyridine complexes containing accessory dipyrromethene-BF 2 chromophores. *J. Phys. Chem. A* **2006,** 110, (13), 4348-4358.

127. Odobel, F.; Zabri, H., Preparations and characterizations of bichromophoric systems composed of a ruthenium polypyridine complex connected to a difluoroborazaindacene or a zinc phthalocyanine chromophore. *Inorg. Chem.* **2005,** 44, (16), 5600-5611.

128. Harriman, A.; Rostron, J. P.; Cesario, M.; Ulrich, G.; Ziessel, R., Electron transfer in self-assembled orthogonal structures. *J. Phys. Chem. A* **2006,** 110, (26), 7994-8002.

129. Nastasi, F.; Puntoriero, F.; Campagna, S.; Diring, S.; Ziessel, R., Photoinduced intercomponent processes in multichromophoric species made of Pt(II)-terpyridine-

acetylide and dipyrromethene-BF2 subunits. *Phys. Chem. Chem. Phys.* **2008,** 10, (27), 3982-3986.

130. Nastasi, F.; Puntoriero, F.; Campagna, S.; Olivier, J. H.; Ziessel, R., Hybrid complexes: Pt(II)-terpyridine linked to various acetylide-bodipy subunits. *Phys. Chem. Chem. Phys.* **2010,** 12, (27), 7392-7402.

131. Yin, X.; Li, Y.; Li, Y.; Zhu, Y.; Tang, X.; Zheng, H.; Zhu, D., Electrochromism based on the charge transfer process in a ferrocene-BODIPY molecule. *Tetrahedron* **2009,** 65, (40), 8373-8377.

132. Rao, M. R.; Kumar, K. V. P.; Ravikanth, M., Synthesis of boron-dipyrromethene-ferrocene conjugates. *J. Organomet. Chem.* **2010,** 695, (6), 863-869.

133. Wijesinghe, C. A.; El-Khouly, M. E.; Blakemore, J. D.; Zandler, M. E.; Fukuzumi, S.; D'Souza, F., Charge stabilization in a closely spaced ferrocene-boron dipyrrin-fullerene triad. *Chem. Commun.* **2010,** 46, (19), 3301-3303.

134. Benniston, A. C.; Harriman, A.; Whittle, V. L.; Zelzer, M.; Harrington, R. W.; Clegg, W., Exciplex-like emission from a closely-spaced, orthogonally-sited anthracenyl-boron dipyrromethene (Bodipy) molecular dyad. *Photochem. Photobiol. Sci.* **2010,** 9, (7), 1009-1017.

135. Harriman, A.; Izzet, G.; Ziessel, R., Rapid energy transfer in cascade-type bodipy dyes. *J. Am. Chem. Soc.* **2006,** 128, (33), 10868-10875.

136. Alamiry, M. A. H.; Harriman, A.; Mallon, L. J.; Ulrich, G.; Ziessel, R., Energy- and charge-transfer processes in a perylene-BODIPY-pyridine tripartite array. *Eur. J. Org. Chem.* **2008**, (16), 2774-2782.

137. Goeb, S.; Ziessel, R., Convenient synthesis of green diisoindolodithienylpyrromethene-dialkynyl borane dyes. *Org. Lett.* **2007,** 9, (5), 737-740.

138. Harriman, A.; Mallon, L.; Ziessel, R., Energy flow in a purpose-built cascade molecule bearing three distinct chromophores attached to the terminal acceptor. *Chem. Eur. J.* **2008,** 14, (36), 11461-11473.

139. Harriman, A.; Mallon, L. J.; Goeb, S.; Ulrich, G.; Ziessel, R., Electronic energy transfer to the S2 level of the acceptor in functionalised boron dipyrromethene dyes. *Chem. Eur. J.* **2009,** 15, (18), 4553-4564.

140. Goeb, S.; Ziessel, R., Synthesis of novel tetrachromophoric cascade-type Bodipy dyes. *Tet. Lett.* **2008,** 49, (16), 2569-2574.

141. Harriman, A.; Mallon, L. J.; Elliot, K. J.; Haefele, A.; Ulrich, G.; Ziessel, R., Length dependence for intramolecular energy transfer in three- and four-color donor-spacer-acceptor arrays. *J. Am. Chem. Soc.* **2009,** 131, (37), 13375-13386.

142. Burghart, A.; Thoresen, L. H.; Chen, J.; Burgess, K.; Bergstrom, F.; Johansson, L. B. A., Energy transfer cassettes based on BODIPY dyes. *Chem. Commun.* **2000**, (22), 2203-2204.

143. Bozdemir, O. A.; Cakmak, Y.; Sozmen, F.; Ozdemir, T.; Siemiarczuk, A.; Akkaya, E. U., Synthesis of symmetrical multichromophoric bodipy dyes and their facile transformation into energy transfer cassettes. *Chem. Eur. J.* **2010,** 16, (21), 6346-6351.

144. Puntoriero, F.; Nastasi, F.; Campagna, S.; Bura, T.; Ziessel, R., Vectorial photoinduced energy transfer between boron-dipyrromethene (bodipy) chromophores across a fluorene bridge. *Chem. Eur. J.* **2010,** 16, (29), 8832-8845.

145. Diring, S.; Puntoriero, F.; Nastasi, F.; Campagna, S.; Ziessel, R., Star-shaped multichromophoric arrays from bodipy dyes grafted on truxene core. *J. Am. Chem. Soc.* **2009,** 131, (17), 6108-6110.

146. Banuelos, J.; Arbeloa, F. L.; Arbeloa, T.; Salleres, S.; Amat-Guerri, F.; Liras, M.; Arbeloa, I. L., Photophysical study of new versatile multichromophoric diads and triads with BODIPY and polyphenylene groups. *J. Phys. Chem. A* **2008,** 112, (43), 10816-10822.

147. Hagfeldt, A.; Gratzel, M., Molecular photovoltaics. *Acc. Chem. Res.* **2000,** 33, (5), 269-277.

148. O'Regan, B.; Gratzel, M., A low-cost, high-efficiency solar cell based on dye-sensitized colloidal TiO2 films. *Nature* **1991,** 353, (6346), 737-740.

149. Erten-Ela, S.; Yilmaz, M. D.; Icli, B.; Dede, Y.; Icli, S.; Akkaya, E. U., A panchromatic boradiazaindacene (BODIPY) sensitizer for dye-sensitized solar cells. *Org. Lett.* **2008,** 10, (15), 3299-3302.

150. Kolemen, S.; Cakmak, Y.; Erten-Ela, S.; Altay, Y.; Brendel, J.; Thelakkat, M.; Akkaya, E. U., Solid-State Dye-Sensitized Solar Cells Using Red and Near-IR Absorbing Bodipy Sensitizers. *Org. Lett.* **2010,** 12, (17), 3812-3815.

151. Kumaresan, D.; Thummel, R. P.; Bura, T.; Ulrich, G.; Ziessel, R., Color tuning in new metal-free organic sensitizers (Bodipys) for dye-sensitized solar cells. *Chem. Eur. J.* **2009,** 15, (26), 6335-6339.

152. Lee, C. Y.; Hupp, J. T., Dye sensitized solar cells: TiO2 sensitization with a bodipy-porphyrin antenna system. *Langmuir* **2010,** 26, (5), 3760-3765.

153. Hall, J. D.; McLean, T. M.; Smalley, S. J.; Waterland, M. R.; Telfer, S. G., Chromophoric dipyrrin complexes capable of binding to TiO2: Synthesis, structure and spectroscopy. *Dalton Tran.* **2010,** 39, (2), 437-445.

154. Peumans, P.; Yakimov, A.; Forrest, S. R., Small molecular weight organic thin-film photodetectors and solar cells. *J. Appl. Phys.* **2003,** 93, (7), 3693-3723.

155. Walzer, K.; Mannig, B.; Pfeiffer, M.; Leo, K., Highly efficient organic devices based on electrically doped transport layers. *Chem. Rev.* **2007,** 107, (4), 1233-1271.

156. Brabec, C. J.; Sariciftci, N. S.; Hummelen, J. C., Plastic solar cells. *Adv. Func. Mater.* **2001,** 11, (1), 15-26.

157. Hummelen, J. C.; Knight, B. W.; Lepeq, F.; Wudl, F.; Yao, J.; Wilkins, C. L., Preparation and characterization of fulleroid and methanofullerene derivatives. *J. Org. Chem.* **1995,** 60, (3), 532-538.

158. Li, G.; Shrotriya, V.; Huang, J.; Yao, Y.; Moriarty, T.; Emery, K.; Yang, Y., High-efficiency solution processable polymer photovoltaic cells by self-organization of polymer blends. *Nature Mater.* **2005,** 4, (11), 864-868.

159. Ma, W.; Yang, C.; Gong, X.; Lee, K.; Heeger, A. J., Thermally stable, efficient polymer solar cells with nanoscale control of the interpenetrating network morphology. *Adv. Func. Mater.* **2005,** 15, (10), 1617-1622.

160. Reyes-Reyes, M.; Kim, K.; Carroll, D. L., High-efficiency photovoltaic devices based on annealed poly(3-hexylthiophene) and 1-(3-methoxycarbonyl)-propyl-1- phenyl-(6,6) C61 blends. *Appl. Phys. Lett.* **2005,** 87, (8), 1-3.

161. Bailey, S. T.; Lokey, G. E.; Hanes, M. S.; Shearer, J. D. M.; McLafferty, J. B.; Beaumont, G. T.; Baseler, T. T.; Layhue, J. M.; Broussard, D. R.; Zhang, Y. Z.; Wittmershaus, B. P., Optimized excitation energy transfer in a three-dye luminescent solar concentrator. *Sol. Ener. Mater. Sol. Cells* **2007,** 91, (1), 67-75.

162. Rousseau, T.; Cravino, A.; Bura, T.; Ulrich, G.; Ziessel, R.; Roncali, J., BODIPY derivatives as donor materials for bulk heterojunction solar cells. *Chem. Commun.* **2009**, (13), 1673-1675.

163. Kronenberg, N. M.; Deppisch, M.; Warthner, F.; Lademann, H. W. A.; Deing, K.; Meerholz, K., Bulk heterojunction organic solar cells based on merocyanine colorants. *Chem. Commun.* **2008**, (48), 6489-6491.

164. Roncali, J.; Leriche, P.; Cravino, A., From one- to three-dimensional organic semiconductors: In search of the organic silicon? *Adv. Mater.* **2007,** 19, (16), 2045-2060.

165. Lloyd, M. T.; Anthony, J. E.; Malliaras, G. G., Photovoltaics from soluble small molecules. *Mater. Today* **2007,** 10, (11), 34-41.

166. Rousseau, T.; Cravino, A.; Bura, T.; Ulrich, G.; Ziessel, R.; Roncali, J., Multi-donor molecular bulk heterojunction solar cells: Improving conversion efficiency by synergistic dye combinations. *J. Mater. Chem.* **2009,** 19, (16), 2298-2300.

167. Rousseau, T.; Cravino, A.; Ripaud, E.; Leriche, P.; Rihn, S.; De Nicola, A.; Ziessel, R.; Roncali, J., A tailored hybrid BODIPY-oligothiophene donor for molecular bulk heterojunction solar cells with improved performances. *Chem. Commun.* **2010,** 46, (28), 5082-5084.

168. Pavlopoulos, T. G.; Boyer, J. H.; Shah, M.; Thangaraj, K.; Soong, M.-L., Laser action from 2,6,8-position trisubstituted 1,3,5,7-tetramethylpyrromethene-BF2 complexes: part 1. *Appl. Opt.* **1990,** 29, (27), 3885-3886.

169. Shah, M.; Thangaraj, K.; Mou-Ling Soong, M. L.; Wolford, L. T.; Boyer, J. H.; Politzer, I. R.; Pavlopoulos, T. G., Pyrromethene–BF2 complexes as laser dyes:1. *Heteroatom. Chem.* **1990,** 1, (5), 389-399.

170. Drexhage, K. H., *Structure and Properties of Laser Dyes*. Topics in Applied Physics, Vol. 1: Dye Lasers, ed. Schafer, F. P. 1990, Berlin: Springer-Verlag. 162.

171. Boyer, J. H.; Haag, A. M.; Sathyomoorthi, G.; Soong, M. L.; Thangaraj, K., Pyrromethene-BF2 Complexes as Laser Dyes: 2. *Heteroatom. Chem.* **1993,** 4, (1), 39-49.

172. Sathyamoorthi, G.; Boyer, J. H.; Allik, T. H.; Chandra, S., Laser Active Cyanopyrromethene-BF2 Complexes. *Heteroatom. Chem.* **1994,** 5, (4), 403-407.

173. Liras, M.; Prieto, J. B.; Pintado-Sierra, M.; Arbeloa, F. L.; Garca-Moreno, I.; Costela, Ã.; Infantes, L.; Sastre, R.; Amat-Guerri, F., Synthesis, photophysical properties, and laser behavior of 3-amino and 3-acetamido BODIPY dyes. *Org. Lett.* **2007,** 9, (21), 4183-4186.

174. Ortiz, M. J.; Garcia-Moreno, I.; Agarrabeitia, A. R.; Duran-Sampedro, G.; Costela, A.; Sastre, R.; Lopez Arbeloa, F.; Baouelos Prieto, J.; Lopez Arbeloa, I., Red-edge-wavelength finely-tunable laser action from new BODIPY dyes. *Phys. Chem. Chem. Phys.* **2010,** 12, (28), 7804-7811.

175. Garcia-Moreno, I.; Zhang, D.; Costela, E.; Martin, V.; Sastre, R.; Xiao, Y., Red-edge laser action from borondipyrromethene dyes. *J. Appl. Phys.* **2010,** 107, (7).

176. Garcia, O.; Sastre, R.; Del Agua, D.; Costela, A.; Garcia-Moreno, I.; Lopez Arbeloa, F.; Baouelos Prieto, J.; Lopez Arbeloa, I., Laser and physical properties of BODIPY chromophores in new fluorinated polymeric materials. *J. Phys. Chem. C* **2007,** 111, (3), 1508-1516.

177. Costela, A.; Garcia-Moreno, I.; Sastre, R.; Lopez Arbeloa, F.; Lopez Arbeloa, T.; Lopez Arbeloa, I., Photophysical and lasing properties of pyrromethene 567 dye in solid poly(trifluoromethyl methacrylate) matrices with different degrees of crosslinking. *Appl. Phys. B* **2001,** 73, (1), 19-24.

178. García, O.; Sastre, R.; Agua, D. d.; Costela, A.; García-Moreno, I.; Roig, A., Efficient optical materials based on fluorinated-polymeric silica aerogels. *Chem. Phys. Lett.* **2006,** 427, (4-6), 375-378.

179. Costela, A.; García-Moreno, I.; Gómez, C.; García, O.; Sastre, R., Enhancement of laser properties of pyrromethene 567 dye incorporated into new organic-inorganic hybrid materials. *Chem. Phys. Lett.* **2003,** 369, (5-6), 656-661.

180. Canva, M.; Georges, P.; Perelgritz, J.-F.; Brum, A.; Chaput, F.; Boilot, J.-P., Perylene- and pyrromethene-doped xerogel for a pulsed laser. *Appl. Opt.* **1995,** 34, (3), 428-431.

181. Faloss, M.; Canva, M.; Georges, P.; Brun, A.; Chaput, F.; Boilot, J. P., Toward millions of laser pulses with pyrromethene- and perylene-doped xerogels. *Appl. Opt.* **1997,** 36, (27), 6760-6763.

182. Rahn, M. D.; King, T. A.; Gorman, A. A.; Hamblett, I., Photostability enhancement of Pyrromethene 567 and Perylene Orange in oxygen-free liquid and solid dye lasers. *Appl. Opt.* **1997,** 36, (24), 5862-5871.

183. Costela, A.; Garcia-Moreno, I.; Gomez, C.; Garcia, O.; Sastre, R., Laser performance of pyrromethene 567 dye in solid polymeric matrices with different cross-linking degrees. *J. Appl. Phys.* **2001,** 90, (7), 3159-3166.

184. Costela, A.; Garcia-Moreno, I.; Pintado-Sierra, M.; Amat-Guerri, F.; Liras, M.; Sastre, R.; Arbeloa, F. L.; Prieto, J. B.; Arbeloa, I. L., New laser dye based on the 3-styryl analog of the BODIPY dye PM567. *J. Photochem. Photobiol. A* **2008,** 198, (2-3), 192-199.

185. Garcia-Moreno, I.; Amat-Guerri, F.; Liras, M.; Costela, A.; Infantes, L.; Sastre, R.; Arbeloa, F. L.; Prieto, J. B.; Arbeloa, A. L., Structural changes in the BODIPY dye PM567 enhancing the laser action in liquid and solid media. *Adv. Func. Mater.* **2007,** 17, (16), 3088-3098.

186. Alvarez, M.; Costela, A.; Garcia-Moreno, I.; Amat-Guerri, F.; Liras, M.; Sastre, R.; Lopez Arbeloa, F.; Baouelos Prieto, J.; Lopez Arbeloa, I., Photophysical and laser emission studies of 8-polyphenylene-substituted BODIPY dyes in liquid solution and in solid polymeric matrices. *Photochem. Photobiol. Sci.* **2008,** 7, (7), 802-813.

187. Garcia-Moreno, I.; Costela, A.; Campo, L.; Sastre, R.; Amat-Guerri, F.; Liras, M.; Lopez Arbeloa, F.; Baouelos Prieto, J.; Lopez Arbeloa, I., 8-Phenyl-Substituted Dipyrromethene·BF2 Complexes as Highly Efficient and Photostable Laser Dyes. *J. Phys. Chem. A* **2004,** 108, (16), 3315-3323.

188. Costela, A.; Garcia-Moreno, I.; Pintado-Sierra, M.; Amat-Guerri, F.; Sastre, R.; Liras, M.; Lopez Arbeloa, F.; Baouelos Prieto, J.; Lopez Arbeloa, I., New analogues of the BODIPY Dye PM597: Photophysical and lasing properties in liquid solutions and in solid polymeric matrices. *J. Phys. Chem. A* **2009,** 113, (28), 8118-8124.

189. Lai, R. Y.; Bard, A. J., Electrogenerated chemiluminescence 71. Photophysical, electrochemical, and electrogenerated chemiluminescent properties of selected dipyrromethene-BF2 dyes. *J. Phys. Chem. B* **2003,** 107, (21), 5036-5042.

190. Strangi, G.; Ferjani, S.; Barna, V.; De Luca, A.; Versace, C.; Scaramuzza, N.; Bartolino, R., Random lasing and weak localization of light in dye-doped nematic liquid crystals. *Opt. Exp.* **2006,** 14, (17), 7737-7744.

191. Veltri, A.; Infusino, M.; Ferjani, S.; Strangi, G., Model for Light Scattering and Lasing in Dye-Doped Nematic Liquid Crystals. *Mol. Cryst. Liq. Cryst.* **2008,** 488, 317-326.

192. Ferjani, S.; Barna, V.; De Luca, A.; Versace, C.; Scaramuzza, N.; Bartolino, R.; Strangi, G., Thermal behavior of random lasing in dye doped nematic liquid crystals. *Appl. Phys. Lett.* **2006,** 89, (12).

193. Ferjani, S.; Barna, V.; De Luca, A.; Versace, C.; Strangi, G., Random lasing in freely suspended dye-doped nematic liquid crystals. *Opt. Lett.* **2008,** 33, (6), 557-559.

194. De Luca, A.; Barna, V.; Ferjani, S.; Caputo, R.; Versace, C.; Scaramuzza, N.; Bartolino, R.; Umeton, C.; Strangi, G., Laser action in dye doped liquid crystals: From periodic structures to random media. *J. Nonlinear Opt. Phys. Mater.* **2009,** 18, (3), 349-365.

195. Zhu, M.; Jiang, L. I.; Yuan, M.; Liu, X.; Ouyang, C.; Zheng, H.; Yin, X.; Zuo, Z.; Liu, H.; Li, Y., Efficient tuning nonlinear optical properties: synthesis and characterization of a series of novel poly(aryleneethynylene)s co-containing BODIPY. *J. Poly. Sci. A* **2008,** 46, (22), 7401-7410.

196. Alemdaroglu, F. E.; Alexander, S. C.; Ji, D.; Prusty, D. K.; Borsch, M.; Herrmann, A., Poly(BODIPY)S: A new class of tunable polymeric dyes. *Macromolecules* **2009,** 42, (17), 6529-6536.

197. Donuru, V. R.; Vegesna, G. K.; Velayudham, S.; Green, S.; Liu, H., Synthesis and optical properties of red and deep-red emissive polymeric and copolymeric BODIPY dyes. *Chem. Mater.* **2009,** 21, (10), 2130-2138.

198. Donuru, V. R.; Vegesna, G. K.; Velayudham, S.; Meng, G.; Liu, H., Deep-red emissive conjugated poly(2,6-BODIPY-ethynylene)s bearing alkyl side chains. *J. Poly. Sci. A* **2009,** 47, (20), 5354-5366.

199. Kim, B.; Ma, B.; Donuru, V. R.; Liu, H.; Frechet, J. M. J., Bodipy-backboned polymers as electron donor in bulk heterojunction solar cells. *Chem. Commun.* **2010,** 46, (23), 4148-4150.

200. Meng, G.; Velayudham, S.; Smith, A.; Luck, R.; Liu, H., Color tuning of polyfluorene emission with BODIPY monomers. *Macromolecules* **2009,** 42, (6), 1995-2001.

201. Huh, J. O.; Do, Y.; Lee, M. H., A BODIPY - Borane dyad for the selective complexation of cyanide ion. *Organometallics* **2008,** 27, (6), 1022-1025.

202. Nagai, A.; Chujo, Y., Aromatic ring-fused BODIPY-based conjugated polymers exhibiting narrow near-infrared emission bands. *Macromolecules* **2010,** 43, (1), 193-200.

203. Nagai, A.; Miyake, J.; Kokado, K.; Nagata, Y.; Chujo, Y., Highly Luminescent BODIPY-Based Organoboron Polymer Exhibiting Supramolecular Self-Assemble Structure. *J. Am. Chem. Soc.* **2008,** 130, (46), 15276-15278.

204. Nagai, A.; Kokado, K.; Miyake, J.; Chujo, Y., Quantum yield and morphology control of BODIPY-based supramolecular self-assembly with a chiral polymer inhibitor. *Polym. J.* **2010,** 42, (1), 37-42.

205. Kajiwara, Y.; Nagai, A.; Chujo, Y., Microwave-assisted preparation of intense luminescent BODIPY-containing hybrids with high photostability and low leachability. *J. Mater. Chem.* **2010,** 20, (15), 2985-2992.

206. Nagai, A.; Kokado, K.; Miyake, J.; Cyujo, Y., Thermoresponsive fluorescent water-soluble copolymers containing BODIPY dye: Inhibition of H-aggregation of the BODIPY units in their copolymers by LCST. *J. Poly. Sci. A* **2010,** 48, (3), 627-634.

207. Nagai, A.; Kokado, K.; Miyake, J.; Chujo, Y., Highly luminescent nanoparticles: Self-assembly of well-defined block copolymers by π-π stacked BODIPY dyes as only a driving force. *Macromolecules* **2009,** 42, (15), 5446-5452.

208. Wang, D.; Miyamoto, R.; Shiraishi, Y.; Hirai, T., BODIPY-conjugated thermoresponsive copolymer as a fluorescent thermometer based on polymer microviscosity. *Langmuir* **2009,** 25, (22), 13176-13182.

209. Bozdemir, O. A.; Bokcakir, O.; Akkaya, E. U., Novel molecular building blocks based on the boradiazaindacene chromophore: Applications in fluorescent metallosupramolecular coordination polymers. *Chem. Eur. J.* **2009,** 15, (15), 3830-3838.

210. Cihaner, A.; Algi, F., A new conducting polymer bearing 4,4-difluoro-4-bora-3a,4a-diaza-s-indacene (BODIPY) subunit: Synthesis and characterization. *Electrochim. Acta* **2008,** 54, (2), 786-792.

211. Algi, F.; Cihaner, A., An ambipolar low band gap material based on BODIPY and EDOT. *Org. Electron.* **2009,** 10, (3), 453-458.

212. Cihaner, A.; Algi, F., Synthesis and properties of 4,4-difluoro-4-bora-3a,4a-diaza-s-indacene (BODIPY)-based conducting copolymers. *React. Func. Polym.* **2009,** 69, (1), 62-67.

213. Lehn, J. M., Toward self-organization and complex matter. *Science* **2002,** 295, (5564), 2400-2403.

214. Sinnokrot, M. O.; Sherrill, C. D., Substituent effects in π-π interactions: Sandwich and t-shaped configurations. *J. Am. Chem. Soc.* **2004,** 126, (24), 7690-7697.

215. Prins, L. J.; Reinhoudt, D. N.; Timmerman, P., Noncovalent synthesis using hydrogen bonding. *Angew. Chem. Int. Ed.* **2001,** 40, (13), 2382-2426.

216. Steinsträsser, R.; Pohl, L., Chemistry and Applications of Liquid Crystals. *Angew. Chem. Int. Ed.* **1973,** 12, (8), 617-630.

217. http://plc.cwru.edu/tutorial/enhanced/files/lc/phase/graphics%5CsmecticA.JPG, In Case Western Reserve University. Date accessed: 30/07/2008.

218. Brown, G. H.; Crooker, P. P., Liquid crystals - A colorful state of matter. *Chem. Eng. News* **1983,** 61, (5), 24-37.

219. http://trappist.elis.ugent.be/ELISgroups/lcd/lc/phase_nematic.jpg, In Universiteit Gent. Date accessed: 20/07/2008.

220. http://upload.wikimedia.org/wikipedia/commons/d/d2/Cholesterinisch.png, Date accessed: 20/07/2008.

221. http://www.csupomona.edu/~jarego/images/e-monoFunk/eMF_DLC_phases.gif, In Cal. Poly. Pamona. Date accessed: 20/07/2008.

222. Chandrasekhar, S.; Sadashiva, B. K.; Suresh, K. A., Liquid crystals of disc-like molecules. *Pramana* **1977,** 9, (5), 471-480.

223. http://fajerpc.magnet.fsu.edu/Education/2010/Lectures/11_Membranes_files/image008.jpg, In Florida State University. Date accessed: 20/07/2008.

224. Camerel, F.; Bonardi, L.; Ulrich, G.; Charbonniare, L.; Donnio, B.; Bourgogne, C.; Guillon, D.; Retailleau, P.; Ziessel, R., Self-assembly of fluorescent amphipathic borondipyrromethene scaffoldings in mesophases and organogels. *Chem. Mater.* **2006,** 18, (21), 5009-5021.

225. Camerel, F.; Bonardi, L.; Schmutz, M.; Ziessel, R., Highly luminescent gels and mesogens based on elaborated borondipyrromethenes. *J. Am. Chem. Soc.* **2006,** 128, (14), 4548-4549.

226. Sartin, M. M.; Camerel, F.; Ziessel, R.; Bard, A. J., Electrogenerated chemiluminescence of B8amide: A BODIPY-based molecule with asymmetric ECL transients. *J. Phys. Chem. C* **2008,** 112, (29), 10833-10841.

227. Ziessel, R.; Bonardi, L.; Retailleau, P.; Camerel, F., New difluoro-boradiazaindacene shaped with gallate platforms. *Compt. Rend. Chim.* **2008,** 11, (6-7), 716-733.

228. Bonardi, L.; Kanaan, H.; Camerel, F.; Jolinat, P.; Retailleau, P.; Ziessel, R., Fine-tuning of yellow or red photo- and electroluminescence of functional difluoro-boradiazaindacene films. *Adv. Func. Mater.* **2008,** 18, (3), 401-413.

229. Wilson, C. J.; James, L.; Mehl, G. H.; Boyle, R. W., Mesogenic dipyrrins—building blocks for the fabrication of fluorescent and metal-containing materials. *Chem. Commun.* **2008**, (38), 4582-4584.

230. Frein, S.; Camerel, F.; Ziessel, R.; Barbera, J.; Deschenaux, R., Highly Fluorescent liquid-crystalline dendrimers based on borondipyrromethene dyes. *Chem. Mater.* **2009,** 21, (17), 3950-3959.

231. Camerel, F.; Ulrich, G.; Barbera, J.; Ziessel, R., Ionic self-assembly of ammonium-based amphiphiles and negatively charged bodipy and porphyrin luminophores. *Chem. Eur. J.* **2007,** 13, (8), 2189-2200.

232. Olivier, J. H.; Camerel, F.; Ulrich, G.; Barbera, J.; Ziessel, R., Luminescent ionic liquid crystals from self-assembled BODIPY disulfonate and imidazolimn frameworks. *Chem. Eur. J.* **2010,** 16, (24), 7134-7142.

233. Higgins, D. A.; Liao, X.; Hall, J. E.; Mei, E., Simultaneous near-field optical birefringence and fluorescence contrast applied to the study of dye-doped polymer-dispersed liquid crystals. *J. Phys. Chem. B* **2001,** 105, (25), 5874-5882.

234. Bozdemir, O. A.; Guliyev, R.; Buyukcakir, O.; Selcuk, S.; Kolemen, S.; Gulseren, G.; Nalbantoglu, T.; Boyaci, H.; Akkaya, E. U., Selective manipulation of ICT and PET processes in styryl-bodipy derivatives: Applications in molecular logic and fluorescence sensing of metal ions. *J. Am. Chem. Soc.* **2010,** 132, (23), 8029-8036.

235. Jiang, J. L.; Lu, H.; Shen, Z., Synthesis, spectroscopic properties and Hg2+ recognition based on a boron dipyrromethene dye (BODIPY). *Chinese J. Inorg. Chem.* **2010,** 26, (6), 1105-1108.

236. Rao, M. R.; Mobin, S. M.; Ravikanth, M., Boron-dipyrromethene based specific chemodosimeter for fluoride ion. *Tetrahedron* **2010,** 66, (9), 1728-1734.

237. Nierth, A.; Kobitski, A. Y.; Ulrich Nienhaus, G.; Jaschke, A., Anthracene-Bodipy dyads as fluorescent sensors for biocatalytic diels alder reactions. *J. Am. Chem. Soc.* **2010,** 132, (8), 2646-2654.

238. Lu, H.; Xiong, L.; Liu, H.; Yu, M.; Shen, Z.; Li, F.; You, X., A highly selective and sensitive fluorescent turn-on sensor for Hg 2+ and its application in live cell imaging. *Org. Biomol. Chem.* **2009,** 7, (12), 2554-2558.

239. Qian, X.; Xiao, Y.; Xu, Y.; Guo, X.; Qian, J.; Zhu, W., "Alive" dyes as fluorescent sensors: Fluorophore, mechanism, receptor and images in living cells. *Chem. Commun.* **2010,** 46, (35), 6418-6436.

240. Domaille, D. W.; Zeng, L.; Chang, C. J., Visualizing ascorbate-triggered release of labile copper within living cells using a ratiometric fluorescent sensor. *J. Am. Chem. Soc.* **2010,** 132, (4), 1194-1195.

241. Saito, R.; Ohno, A.; Ito, E., Synthesis of boradiazaindacene-imidazopyrazinone conjugate as lipophilic and yellow-chemiluminescent chemosensor for superoxide radical anion. *Tetrahedron* **2010,** 66, (3), 583-590.

242. Dodani, S. C.; He, Q.; Chang, C. J., A turn-on fluorescent sensor for detecting nickel in living cells. *J. Am. Chem. Soc.* **2009,** 131, (50), 18020-18021.

243. Jiao, L.; Li, J.; Zhang, S.; Wei, C.; Hao, E.; Vicente, M. G. H., A selective fluorescent sensor for imaging Cu2+ in living cells. *New J. Chem.* **2009,** 33, (9), 1888-1893.

244. Lee, J. S.; Kang, N. Y.; Yun, K. K.; Samanta, A.; Feng, S.; Hyeong, K. K.; Vendrell, M.; Jung, H. P.; Chang, Y. T., Synthesis of a BODIPY library and its application to the development of live cell glucagon imaging probe. *J. Am. Chem. Soc.* **2009,** 131, (29), 10077-10082.

245. Erbas, S.; Gorgulu, A.; Kocakusakogullari, M.; Akkaya, E. U., Non-covalent functionalized SWNTs as delivery agents for novel Bodipy-based potential PDT sensitizers. *Chem. Comm.* **2009**, (33), 4956-4958.

246. Lim, S. H.; Thivierge, C.; Nowak-Sliwinska, P.; Han, J.; Van Den Bergh, H.; Wagniares, G.; Burgess, K.; Lee, H. B., In vitro and in vivo photocytotoxicity of boron dipyrromethene derivatives for photodynamic therapy. *J. Med. Chem.* **2010,** 53, (7), 2865-2874.

247. Yogo, T.; Urano, Y.; Ishitsuka, Y.; Maniwa, F.; Nagano, T., Highly efficient and photostable photosensitizer based on BODIPY chromophore. *J. Am. Chem. Soc.* **2005,** 127, (35), 12162-12163.

248. Zhao, W.; Carreira, E. M., Conformationally restricted aza-bodipy: A highly fluorescent, stable, near-infrared-absorbing dye. *Angew. Chem. Int. Ed.* **2005,** 44, (11), 1677-1679.

249. Ziessel, R.; Ulrich, G.; Harriman, A., The chemistry of Bodipy: A new El Dorado for fluorescence tools. *New J. Chem.* **2007,** 31, (4), 496-501.

250. Loudet, A.; Burgess, K., BODIPY dyes and their derivatives: Syntheses and spectroscopic properties. *Chem. Rev.* **2007,** 107, (11), 4891-4932.

251. Ulrich, G.; Ziessel, R.; Harriman, A., The chemistry of fluorescent bodipy dyes: Versatility unsurpassed. *Angew. Chem. Int. Ed.* **2008,** 47, (7), 1184-1201.

252. Wagner, R. W.; Lindsey, J. S., Boron-dipyrromethene dyes for incorporation in synthetic multi-pigment light-harvesting arrays. *Pure App. Chem.* **1996,** 68, (7), 1373-1380.

253. Chen, T.; Boyer, J. H.; Trudell, M. L., Synthesis of 2,6-diethyl-3methacroyloxymethyl-1,5,7,8tetramethylpyrromethene-BF2 for the preparation of new solid-state laser dyes. *Heteroatom. Chem.* **1997,** 8, (1), 51-54.

254. Ulrich, G.; Goze, C.; Guardigli, M.; Roda, A.; Ziessel, R., Pyrromethene Dialkynyl Borane Complexes for Cascatelle Energy Transfer and Protein Labeling. *Angew. Chem.-Int. Ed.* **2005,** 44, (24), 3694-3698.

255. Atilgan, S.; Ekmekci, Z.; Dogan, A. L.; Guc, D.; Akkaya, E. U., Water soluble distyryl-boradiazaindacenes as efficient photosensitizers for photodynamic therapy. *Chem. Commun.* **2006**, (42), 4398-4400.

256. Brom, J. M.; Langer, J. L., Electroluminescence from pyrromethene dyes in doped polymer hosts. *J. Alloy. Comp.* **2002,** 338, (1-2), 112-115.

257. Hepp, A.; Ulrich, G.; Schmechel, R.; Von Seggern, H.; Ziessel, R., Highly efficient energy transfer to a novel organic dye in OLED devices. *Synth. Met.* **2004,** 146, (1), 11-15.

258. Kato, T.; Mizoshita, N.; Kishimoto, K., Functional liquid-crystalline assemblies: Self-organized soft materials. *Angew. Chem. Int. Ed.* **2006,** 45, (1), 38-68.

259. Paine III, J. B.; Hiom, J.; Dolphin, D., Bromination of dipyrromethenes for porphyrin synthesis. *J. Org. Chem.* **1988,** 53, (12), 2796-2802.

260. Ohta, K.; Takenaka, O.; Hasebe, H.; Morizumi, Y.; Fujimoto, T.; Yamamoto, I., Mesomorphism and Unusual Multiple Melting Behavior via Smectic E Phase in p-n-Alkoxybiphenylbutane-1,3-dione. *Mol. Cryst. Liq. Cryst.* **1991,** 195, 103-121.

261. Mitra, M.; Gupta, S.; Paul, R.; Paul, S., Determination of Orientational Order Parameter from Optical Studies for a Homologous Series of Mesomorphic Compounds. *Mol. Cryst. Liq. Cryst.* **1991,** 199, 257-266.

262. Ratna, B. R.; Shashidhara, R.; Bockb, M.; Goumlbl-wunschb, A.; Heppkeb, G., Effect of Smectic Ordering on the Dielectric Properties of Reentrant Nematic Mixtures. *Mol. Cryst. Liq. Cryst.* **1983,** 99, 285-295.

263. Jain, S. C.; Agnihotry, S. A.; Bhide, V. G., Solid Crystalline Polymorphism in M-24. *Mol. Cryst. Liq. Cryst.* **1982,** 88, 281-294.

264. Pena-Cabrera, E.; Aguilar-Aguilar, A.; Gonzalez-Dominguez, M.; Lager, E.; Zamudio-Vazquez, R.; Godoy-Vargas, J.; Villanueva-Garcia, F., Simple, general, and efficient synthesis of meso-substituted borondipyrromethenes from a single platform. *Org. Lett.* **2007,** 9, (20), 3985-3988.

265. Brűckner, C.; Karunaratne, V.; Rettig, S. J.; Dolphin, D., Synthesis of meso-phenyl-4,6-dipyrrins, preparation of their Cu(II), Ni(II), and Zn(II) chelates, and structural characterization of bis[meso-phenyl-4,6-dipyrrinato]Ni(II). *Can. J. Chem.* **1996,** 74, (11), 2182-2193.

266. Atilgan, S.; Ozdemir, T.; Akkaya, E. U., A sensitive and selective ratiometric near IR fluorescent probe for zinc ions based on the distyryl-bodipy fluorophore. *Org. Lett.* **2008,** 10, (18), 4065-4067.

267. Ekmekci, Z.; Yilmaz, M. D.; Akkaya, E. U., A monostyryl-boradiazaindacene (BODIPY) derivative as colorimetric and fluorescent probe for cyanide ions. *Org. Lett.* **2008,** 10, (3), 461-464.

268. Wang, D.; Shiraishi, Y.; Hirai, T., A distyryl BODIPY derivative as a fluorescent probe for selective detection of chromium(III). *Tet. Lett.* **2010,** 51, (18), 2545-2549.

269. Bellier, Q.; Bouit, P. A.; Kamada, K.; Feneyrou, P.; Malmstrom, E.; Maury, O.; Andraud, C. In *Design of near-infrared dyes for nonlinear optics: Towards optical limiting applications at telecommunication wavelengths*, Proc. SPIE - Int. Soc. Opt. Eng., 2009; 2009.

270. Loudet, A.; Bandichhor, R.; Wu, L.; Burgess, K., Functionalized BF2 chelated azadipyrromethene dyes. *Tetrahedron* **2008,** 64, (17), 3642-3654.

271. Bouit, P. A.; Kamada, K.; Feneyrou, P.; Berginc, G.; Toupet, L.; Maury, O.; Andraud, C., Two-photon absorption-related properties of functionalized bodipy dyes in the infrared range up to telecommunication wavelengths. *Adv. Mater.* **2009,** 21, (10-11), 1151-1154.

272. Zhao, W.; Carreira, E. M., Conformationally restricted aza-BODIPY: Highly fluorescent, stable near-infrared absorbing dyes. *Chem. Eur. J.* **2006,** 12, (27), 7254-7263.

273. Sánchez, I.; Mayoral, M. J.; Ovejero, P.; Campo, J. A.; Heras, J. V.; Cano, M.; Lodeiro, C., Luminescent liquid crystal materials based on unsymmetrical boron difluoride β-diketonate adducts. *New J. Chem.* **2010**, *34*, 2937-2942.

274. Usol'Tseva, N.; Bykova, V.; Zharnikova, N.; Alexandrov, A.; Semeikin, A.; Kazak, A., Influence of meso-substituted porphyrins molecular structure on their mesogenity. *Mol. Cryst. Liq. Cryst.* **2010,** 525, 184-193.

275. Ahsen, A. E.; Segade, A.; Velasco, D.; Aztark, Z. Z., Liquid crystal porphyrins as chemically sensitive coating materials for chemical sensors. *J. Porphyrins Phthalocyanines* **2009,** 13, (11), 1188-1195.

276. Drain, C. M.; Varotto, A.; Radivojevic, I., Self-organized porphyrinic materials. *Chem. Rev.* **2009,** 109, (5), 1630-1658.

277. Porres, L.; Holland, A.; Palsson, L.-O.; Monkman, A. P.; Kemp, C.; Beeby, A., Absolute Measurements of Photoluminescence Quantum Yields of Solutions Using an Integrating Sphere. *J. Fluor.* **2006,** 16, (2), 267-273.

278. Boiadjiev, S. E.; Lightner, D. A., A water-soluble synthetic bilirubin with carboxyl groups replaced by sulfonyl moieties. *Monat. Chem.* **2001,** 132, (10), 1201-1212.

279. Muchowski, J. M.; Solas, D. R., Protecting groups for the pyrrole and indole nitrogen atom. The [2-(trimethylsilyl)ethoxy]methyl moiety. Lithiation of 1-[[2-(trimethylsilyl)ethoxy]methyl]pyrrole. *J. Org. Chem.* **1984,** 49, (1), 203-205.

280. Holmes, D. L.; Lightner, D. A., Synthesis and acidity constants of 13CO2H-labelled mono and dipyrrole carboxylic acids. pK(a) from 13C-NMR. *Tetrahedron* **1995,** 51, (6), 1607-1622.

281. Carr, R. P.; Jackson, A. H.; Kenner, G. W.; Sach, G. S., Pyrroles and related compounds. Part XVI. Synthesis of protoporphyrin-IX by the a- and b-oxobilane routes. *J. Chem Soc. C* **1971**, 487-502.

282. Al-Sheikh-Ali, A.; Cameron, K. S.; Cameron, T. S.; Robertson, K. N.; Thompson, A., Highly diastereoselective templated complexation of dipyrromethenes. *Org. Lett.* **2005,** 7, (21), 4773-4775.

283. Yu, H.; Shishido, A.; Li, J.; Kamata, K.; Iyoda, T.; Ikeda, T., Stable macroscopic nanocylinder arrays in an amphiphilic diblock liquid-crystalline copolymer with successive hydrogen bonds. *J. Mater. Chem.* **2007,** 17, (33), 3485-3488.

284. Lee, C. H.; Lindsey, J. S., One-flask synthesis of meso-substituted dipyrromethanes and their application of the synthesis of trans-substituted porphyrin building blocks. *Tetrahedron* **1994,** 50, (39), 11427-11440.

285. Teki, Y.; Tamekuni, H.; Haruta, K.; Takeuchi, J.; Miura, Y., Design, synthesis, and uniquely electron-spin-polarized quartet photo-excited state of a π-conjugated spin system generated via the ion-pair state. *J. Mater. Chem.* **2008,** 18, (4), 381-391.

286. Cook, A.; Badriya, S.; Greenfield, S.; McKeown, N. B., Styrene-containing mesogens. Part 1: Photopolymerisable nematic liquid crystals. *J. Mater. Chem.* **2002,** 12, (9), 2675-2683.

287. Lager, E.; Liu, J.; Aguilar-Aguilar, A.; Tang, B. Z.; Pena-Cabrera, E., Novel meso-Polyarylamine-BODIPY hybrids: Synthesis and study of their optical properties. *J. Org. Chem.* **2009,** 74, (5), 2053-2058.

288. Nielsen, M. B.; Schreiber, M.; Baek, Y. G.; Seiler, P.; Lecomte, S.; Boudon, C.; Tykwinski, R. R.; Gisselbrecht, J. P.; Gramlich, V.; Skinner, P. J.; Bosshard, C.; Ganter, P.; Gross, M.; Diederich, F., Highly functionalized dimeric tetraethynylethenes and

expanded radialenes: Strong evidence for macrocyclic cross-conjugation. *Chem. Eur. J.* **2001,** 7, (15), 3263-3280.

Appendix 1: HPLC traces

Compound 23:

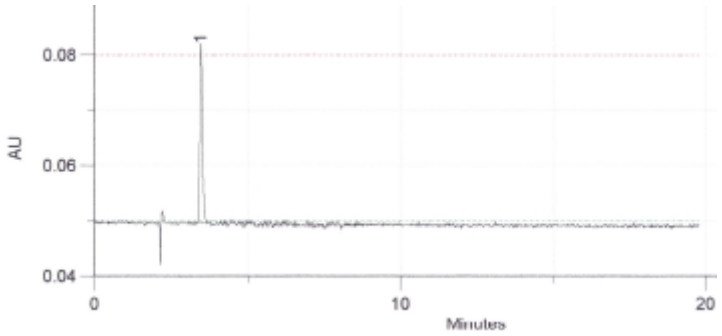

Compound 24:

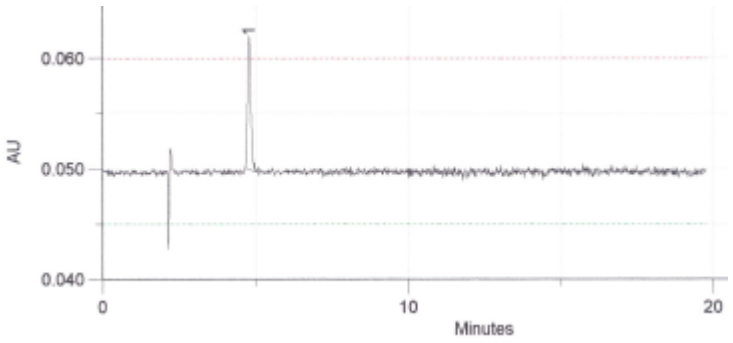

Compound 25:

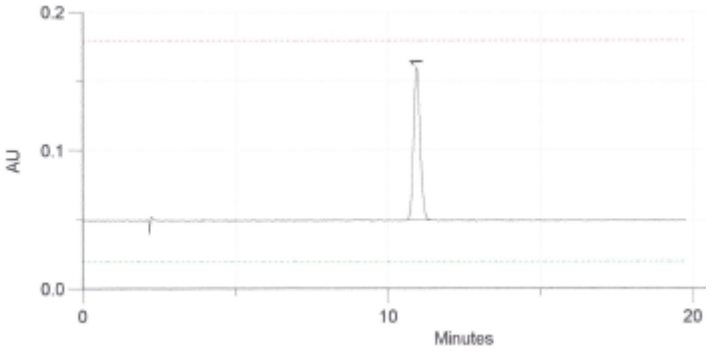

Compound 30:

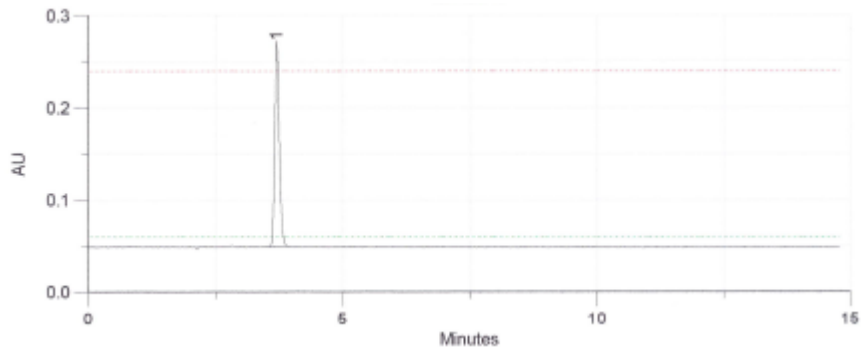

Compound 31:

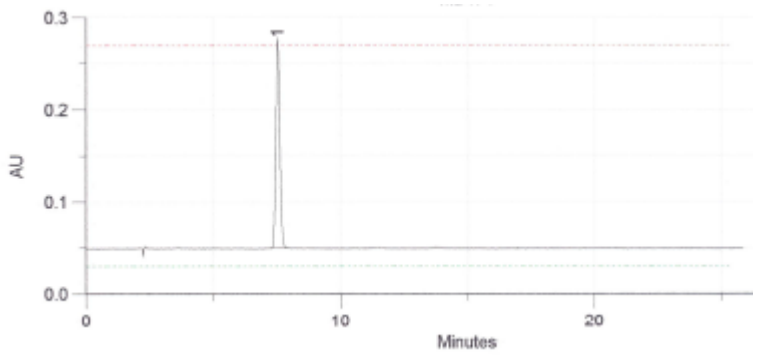

Compound 32:

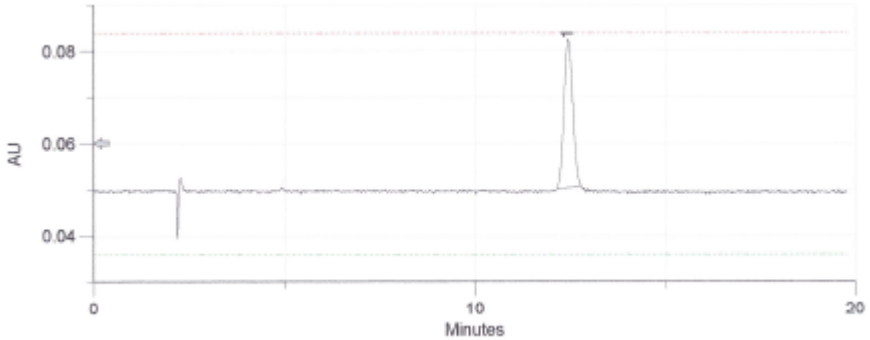

Compound 37:

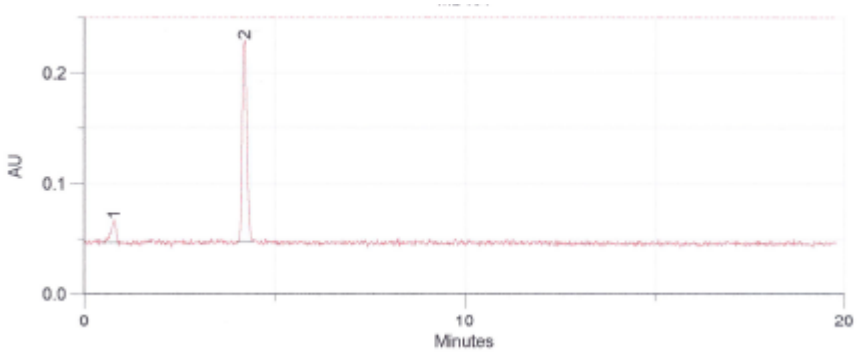

Peak labelled **1** at pump pulse, not impurity.

Compound 52:

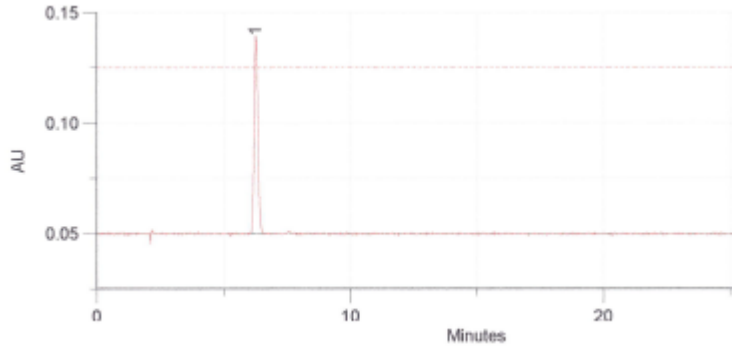

Compound 53:

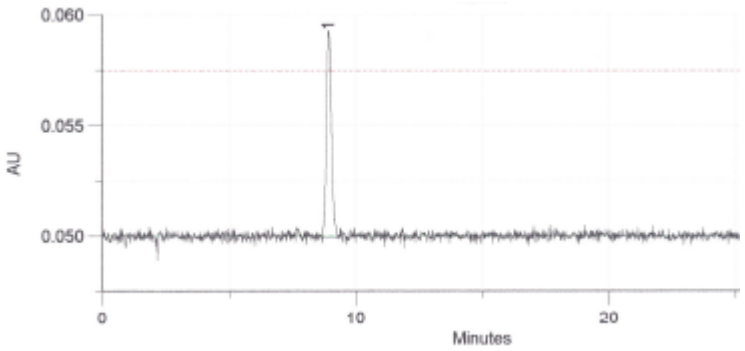

Compound 55:

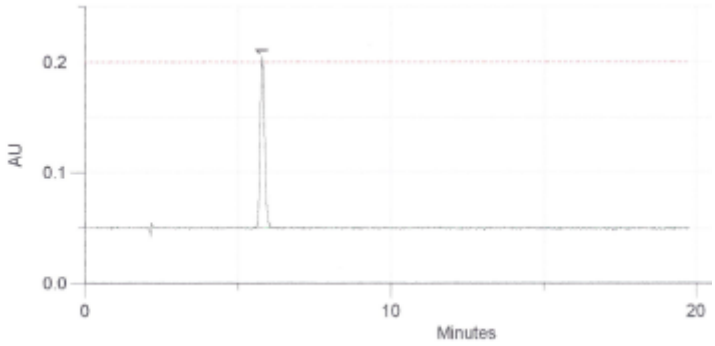

Compound 56:

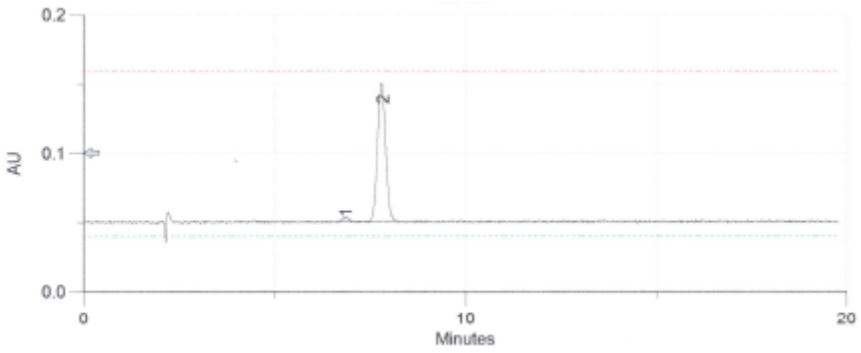

Compound 57:

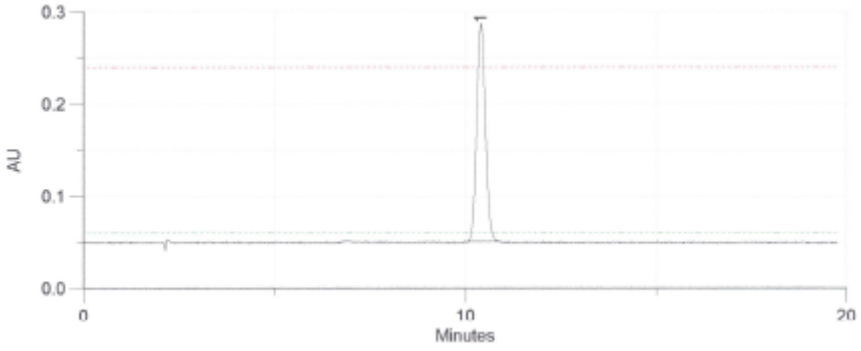

Compound 65:

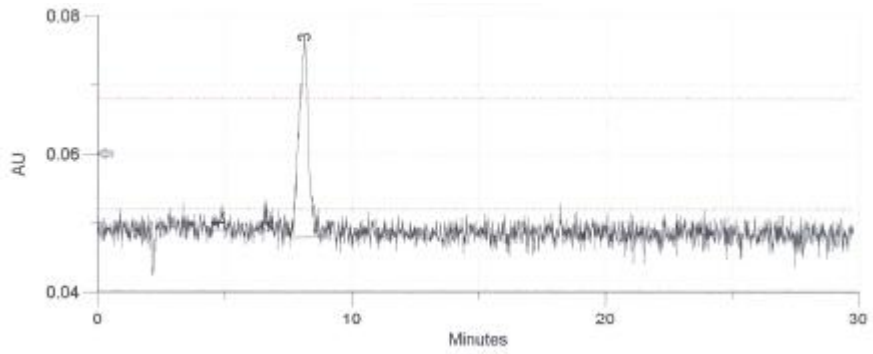

Weak signal due to low solubility of the compound in a 70:30 MeCN:DCM mixture.